Mécanismes moléculaires et cellulaire de l'électrotransfert de plasmides in vitro

Jean-Michel Escoffre

Université de Toulouse

THESE

En vue de l'obtention du

DOCTORAT DE L'UNIVERSITÉ DE TOULOUSE

Délivré par *l'Université Toulouse III - Paul Sabatier*
Discipline ou spécialité : *Biophysique Cellulaire*

Présentée et soutenue par *Jean-Michel ESCOFFRE*
Le *Mardi 23 Mars 2010*

Titre : *MÉCANISMES MOLÉCULAIRE ET CELLULAIRE DE L'ÉLECTROTRANSFERT DE PLASMIDES IN VITRO*

JURY

M. Elmostafa Bahraoui, Professeur, (UPS, Toulouse), Président du jury
Mme Chantal Pichon, Professeur, (Université d'Orléans, Orléans), Rapporteur
M. Bruno Pitard, Directeur de recherche, (CNRS, Nantes), Rapporteur
M. Yves Mély, Professeur, (Université de Strasbourg, Strasbourg), Examinateur
M. Cyril Favard, Ingénieur de recherche, (CNRS, Marseille), Examinateur
M. Justin Teissié, Directeur de recherche, (CNRS, Toulouse), Examinateur
Mme Marie-Pierre Rols, Directrice de recherche, (CNRS, Toulouse), Directrice de thèse

---

Ecole doctorale : *Biologie - Santé - Biotechnologies*
Unité de recherche : *IPBS CNRS - UMR 5089*
Directeur(s) de Thèse : *Mme Marie-Pierre Rols*
Rapporteurs : *Mme Chantal Pichon*
M. Bruno Pitard

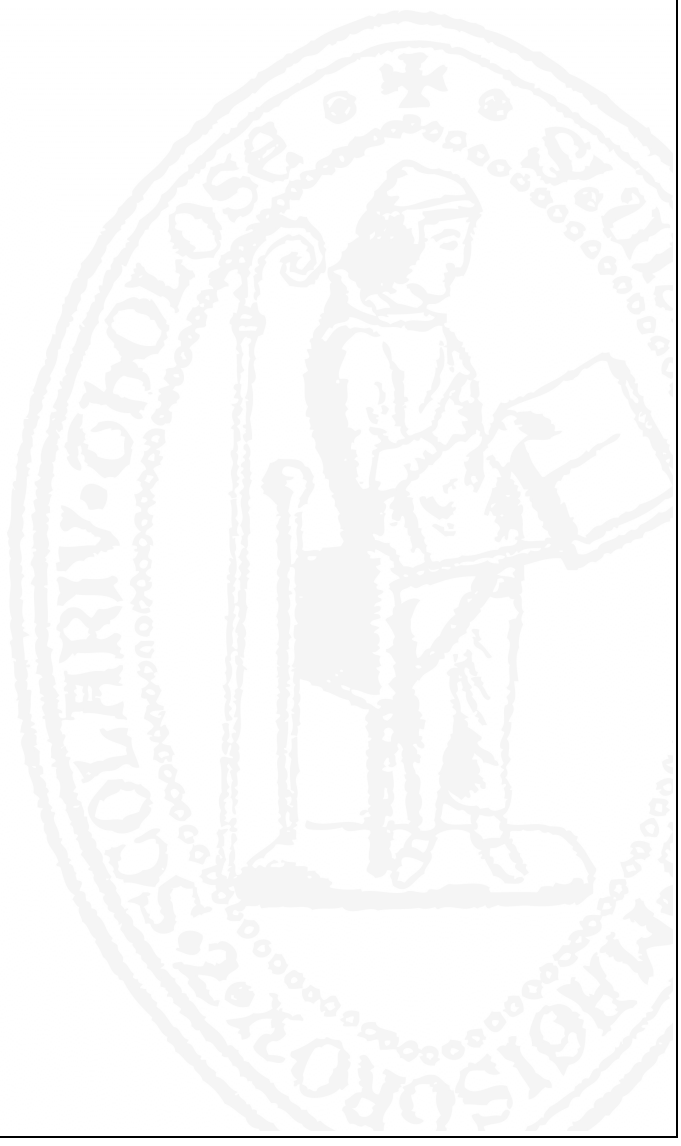

A ma famille passée, présente et future

A mes amis

…

Remerciements

Je remercie les membres du jury d'avoir accepté de juger ce travail. Je souhaite exprimer ma reconnaissance à Madame Chantal Pichon, Professeur à l'Université d'Orléans et à Messieurs Yves Mély, Professeur à l'Université de Strasbourg et Bruno Pitard, Directeur de Recherche au CNRS, pour le soin qu'ils ont apporté à l'examen de ce mémoire et pour toutes les observations et suggestions qu'ils ont formulées pour la correction de ce manuscrit sans oublier leur disponibilité. Je remercie Monsieur Elmostafa Barhaoui, Professeur à l'Université Paul Sabatier de Toulouse, d'avoir accepté de présider ce jury. Je remercie Monsieur Cyril Favard, Ingénieur de Recherche au CNRS d'avoir examiné ce manuscrit. Je souhaite aussi le remercier pour son encadrement dans la partie III de ce travail. Cette collaboration aura été à l'origine de nombreux échanges scientifiques qui ont permis d'enrichir ce travail.

Je souhaite maintenant remercier plus particulièrement les personnes qui ont soutenu scientifiquement ce travail au quotidien. Monsieur Justin Teissié, Directeur de Recherche au CNRS, je vous remercie pour votre accueil au sein de l'équipe de Biophysique Cellulaire à l'IPBS. Je vous remercie pour votre soutien constant et pour l'intérêt que vous avez porté à l'évolution de ce travail. Enfin, grâce à vous et à nos longues discussions matinales ou tardives, analogique ou numériques, les membranes biologiques n'ont plus de secrets pour moi. Je voudrais remercier Madame Marie-Pierre Rols, Directrice de Recherche au CNRS, pour sa direction scientifique. Je te remercie pour ta présence et ton soutien au cours de ce travail de recherche. Merci pour la confiance que tu m'as accordé. Congrès, publications, demande de financements, examen de publication…tu as parfaitement rempli ton rôle et tu m'as donné tous les outils pour devenir un excellent chercheur. Dans quelques années, j'espère transformer l'essai.

Enfin, parce que sans eux, il n'y aurait pas eu de thèse, je voudrais remercier tous mes soutiens financiers à savoir le CNRS, l'Université Paul Sabatier, l'Association Français contre les Myopathies…

Bien entendu, je remercie tous les membres de l'équipe à commencer par ma "maman canard". Muriel (et sa μμ-mobile), je te remercie de m'avoir mis le pied à l'étrier. Merci de m'avoir initié à l'électroperméabilisation, au transfert de gènes, à l'expérimentation animale… Merci pour nos rigolades et nos discussions sur la politique française… Mais chut !!! Big Brother watching you !! Je tiens à rendre hommage à mon grand maître de l'imagerie: Babeth. Le petit scarabée que je suis, te remercie de ta patience, de tes encouragements et de ta disponibilité. Nos petites disputes et tes "va chier" vont me manquer. Aurélie, camarade de jeu de maîtrise, de M2R et de Thèse. Je te remercie pour ta bonne humeur au quotidien. Aurélie, mon très cher alibi sur pattes, qui me permet de faire des pauses clopes alors que je ne fume pas. Je te remercie de ton soutien tout au long de ma thèse, pour les bouffes chez toi… "Mon petit lulu, roi des forêts…" A ton tour mon cher Luc, je te remercie pour tes conseils et ton soutien au cours de mon travail de thèse. Je remercie mes deux physiciens préférés, Chloé et Thomas. Chloé, je te remercie pour nos pauses café/thé et nos petits potins. Certes tu es un excellent professeur mais je suis sûr que tu seras une éminente chercheuse. Mon petit grincheux, Thomas, merci de m'avoir soutenu pendant ma thèse. J'espère que tes premiers pas en biologie resteront de bons souvenirs pour toi. Merci de m'avoir initier à

Latex. Je souhaite aussi remercier les anciens compagnons de paillasse mais qui ont aussi contribué à la bonne humeur dans cette équipe: Julien, Marie, Nicolas, Mario, Mathieu, Louise, Romain, Alaa… Je remercie "Les Garçons" (pardon Caroline !!!): Laurent, Vincent, Grégory, Olivier et Caroline pour votre soutien au cours de ma thèse. Je remercie Claire Millot, Serges Mazères, Stéphanie Dauvilliers et André Lopez, pour votre patience et votre générosité. Je remercie Ayache Bouakaz et Kadija Kaddur pour leur collaboration sur l'électrosonoporation.

Je leur consacre un paragraphe pour eux, les forces vives de nos équipes. Mes très chers stagiaires: Laëtitia, Christelle et Yoann. Vous êtes des personnes de qualité. Certaines parties de ce manuscrit n'auraient pas pu se faire sans votre présence. Laëtitia, je te souhaite de t'épanouir dans ton travail de technicienne. Christelle, tu as dans tes mains tout pour réussir une excellente thèse, c'est tout le mal que je te souhaite. Yoann, tu exportes l'électroperméabilisation en Suisse. Tu es le digne représentant de notre équipe. Je vous souhaite à tous les trois tous mes vœux de réussites personnelle et professionnelle.

Et comme la recherche est aussi internationale, je n'oublie pas Maja, Gregor sénior et junior pour leurs soutiens et leurs conseils. Je remercie également Sasa avec qui j'ai travaillé sur les impulsions brèves. Je tiens à remercier Thomas Vernier pour son écoute, sa disponibilité et nos discussions scientifiques.

Maintenant, parce que la recherche c'est aussi des échanges autour d'un petit café, je voudrais remercier mes voisins de labo et qui sont aussi devenus plus que des voisins. J'espère n'oublier personne. Y'a ceux à qui je dois beaucoup, qui furent les soutiens de tous les jours en M2R et en thèse, quand ça allait et quand ça n'allait pas: Lara, Carolina avec Aurélie (Les 4 mousquetaires: le noyau dur et soudé du M2R et de thèse, soutien psychologique), Roxanne et Gaëlle (nos psychologues de M2R), Marielle (à nous deux, nous sommes les professionnels du KP), Béatrice, Sandrine, Ludivine, Fanny (toujours un sourire, toujours de l'entrain et beaucoup d'humour !!!), Julien, Vanessa (nos collègues parisiens), Anne-Claire, Cécile (pour leurs conseils éclairés).

Parce qu'avant la thèse y'a aussi une vie, les anciens de la fac: Yoann, Patrice, Christelle, Alix, Sébastien, Bernadette, Marlène, Mélanie, Vanessa, Aurélie… Je n'oublie pas non plus Géraldine, présente depuis si longtemps que les années ont finis par souder une amitié durable. Tu es la fidèle parmi la fidèle.

Je voudrais remercier ma famille et plein d'autres vers qui vont mes pensées.

Sur ces dernières paroles, je tire ma révérence et vous souhaite bonne lecture. L'électroperméabilisation n'aura alors presque plus de secret pour vous…

"Notre plus grande gloire n'est pas de ne jamais tomber, mais de nous relever à chaque fois."

Confucius

Résumé

Le transfert de plasmides au sein d'une cellule cible représente un outil clé dans l'étude de fonctions biologiques et dans le développement de nouvelles approches thérapeutiques. Cependant, le transfert de plasmides doit être réalisé avec un minimum d'effets secondaires au niveau de la cellule cible. La technique d'électroperméabilisation est une méthode physique fondée sur la modulation du potentiel électrique transmembranaire natif de la cellule par un champ électrique externe. Cependant, l'utilisation rationnelle de l'électroperméabilisation en pharmacologie et en médecine ne pourra se faire que grâce à une parfaite compréhension des mécanismes impliqués lors de l'électroperméabilisation au niveau membranaire et de ses conséquences cellulaires.

Le mécanisme de l'électrotransfert de plasmides est un processus multi-étapes avec une étape d'interaction plasmide/membrane perméabilisée pendant l'application des impulsions électriques, suivi après ces dernières, d'une étape de translocation du plasmide à travers la membrane plasmique. Ce travail de recherche pluridisciplinaire vise à une meilleure compréhension du mécanisme de l'électrotransfert de plasmides. Il intègre l'étude des conséquences membranaires de l'électrotransfert de plasmide et l'étude de l'interaction plasmide/membrane perméabilisée.

L'application d'impulsions électriques millisecondes et perméabilisantes induit un désordre membranaire et une rapide translocation des phospholipides dans les régions perméabilisées. La translocation électro-induite des phospholipides n'est pas associée à une perte de la viabilité cellulaire.

L'existence du processus multi-étapes de l'électrotransfert de plasmide (perméabilisation membranaire, interaction plasmide/membrane et expression génique) a été confirmé dans différentes lignées cellulaires. Pendant l'application de la première impulsion électrique, les molécules de plasmide migrent par électrophorèse et viennent interagir dans des sites distincts de la région membranaire faisant face à la cathode. L'interaction des molécules de plasmide avec la membrane perméabilisée serait donc un processus rapide (de l'ordre d'une centaine de microsecondes). Les complexes plasmide/membrane se stabilisent en un délai de 200 ms. Un rôle distinct de l'intensité du champ électrique et du nombre d'impulsions électriques a été mis en évidence. Si l'intensité du champ électrique définit la surface membranaire où l'interaction des molécules de plasmide a lieu et de fait, le nombre de spots d'interaction, le nombre d'impulsions électriques définit la quantité de molécules de plasmide présente par complexe. Les complexes plasmide/membrane ainsi formés ne diffusent pas latéralement dans la membrane. Le cytosquelette d'actine n'est pas impliqué dans la formation de ces complexes mais pourrait être impliqué dans le transport intracellulaire des molécules de plasmides.

L'électroperméabilisation et l'interaction plasmide/membrane perturbent la mobilité latérale des protéines membranaire du feuillet externe de la membrane plasmique.

La combinaison de la sonoporation avec l'électroperméabilisation permet d'améliorer l'efficacité de transfection obtenue par l'électroperméabilisation seule. Le transfert de plasmides par électro-sonoporation est une stratégie prometteuse en thérapie génique.

Mots-clés: Electroperméabilisation, membrane, plasmide, transfection, imagerie, fluorescence.

Abstract

Plasmid transfer within a target cell represents a key tool in the study of biological functions and the development of new therapeutic strategies. However, the transfer of plasmids must be carried out with a minimum of side effects on the level of the target cell. The technique of electropermeabilization is a physical method based on the modulation of the native transmembrane electric potential of the cell by an external electric field. However, the rational use of the electropermeabilization in pharmacology and medicine could be done only thanks to one perfect comprehension of the mechanisms involved in the electropermeabilization at the membrane level and its cellular consequences.

The mechanism of the plasmid electrotransfer is a multi-steps process with a step of plasmid/membrane interaction during the application of the electric pulses, followed after these last, of a step of plasmid translocation through the plasma membrane. This multi-disciplinary research task aims at a better comprehension of the mechanism of the plasmid electrotransfer. It integrates the study of the membrane consequences of the electropermeabilization and the study of the plasmid/ membrane interaction.

The application of milliseconds and permeabilizing electric pulses induces a membrane disorder and a fast phospholipid translocation in the permeabilized regions. The electro-induced translocation of phospholipids is not associated with a loss of cell viability.

The existence of the multi-steps process of the plasmid electrotransfer (membrane permeabilization, plasmid/membrane interaction and gene expression) was confirmed in various cell lines. During the application of the first electric pulse, the plasmids migrate by electrophoresis and come to interact in distinct sites from the membrane region facing the cathode. The interaction of plasmids with the permeabilized membrane would be thus a fast process (about a hundred microseconds). The plasmid/membrane complexes are stabilized in a delay of 200 ms. A distinct role from the intensity of the electric field and the number of electric pulses was highlighted. If the intensity of the electric field defines membrane surface where the interaction of the plasmid molecules takes place and in fact, the number of spots of interaction, the number of electric pulses defines the amount of plasmids presents by complex. The plasmid/membrane complexes thus formed do not diffuse laterally in the membrane. The actine cytoskeleton is not involved in the formation of these complexes but could be involved in the intracellular traffic of plasmids.

Electropermeabilization and plasmid/membrane interaction disturbed the lateral mobility of membrane proteins of outer leaflet of plasma membrane.

The combination of the sonoporation with the electropermeabilization makes it possible to improve the effectiveness of transfection obtained by the electropermeabilization alone. The transfer of plasmids by electro-sonoporation is a promising strategy in gene therapy.

Keywords: Electropermeabilization, membrane, plasmid, transfection, imaging, fluorescence.

Table des matières

Abréviations

AAV	"Adéno-associated virus"
ABAE	Cellules endothéliales d'aorte de boeuf
ADN	Acide désoxyribonucléique
ARN	Acide ribonucléique
ATP	Adénosine tri-phosphate
B16F10	Cellules de mélanome murin
CAR	"Coxsackie and adenovirus receptors"
CCD	"Charged coupled device"
CHO	[Cellules d'] ovaire d'hamster chinois
CMV	Cytomégalovirus
CPP	"Cell Penetrating Peptide"
C6-NBD-PC	1-palmitoyl-2-(7-nitrobenz-2-oxa-1,3-diazol-4-yl-hexanoyl)-sn-glycero-3-PC
C2C12	Myoblaste murin
D	Coefficient de diffusion
d	Distance inter-électrodes
DIG	Fraction membranaire enrichie en glycolipides-insoluble aux détergents
DO	Densité optique
DOPC	1,2-dioleoyl-sn-glycero-3-phosphocholine
DRM	Fraction membranaire résistante aux détergents
DTS	"DNA targeting sequence"
E	Amplitude du champ électrique
E. coli	*Escherichia coli*
ECT	Electrochimiothérapie
EDTA	Acide éthylènediaminetétraacétique
Ef	Seuil de fusion
eGFP	"enhanced green fluorescent protein"
EGT	Electrogénothérapie
Ep	Seuil de perméabilisation
EPR	Réassignement des photons
Et	Seuil de transfection
Ext	Extérieur
f	Fréquence des impulsions électriques
F	Constante de Faraday
FCS	"Fluorescence Corrélation Spectroscopy"
FDA	"Food and drug agency"
FGF	"Fibroblast Growth Factor"
FM1-43	N-(3-triethylammoniumpropyl)-4-(4-(dibutylamino)styryl)pyridinium dibromide)
FRAP	"Fluorescence Recovery After Photobleaching"
GDI	"Guanine Di-Phosphate Dissociation Vector"
GEM	Fraction membranaire enrichie en glycolipides
GM-CSF	"Granulocyte macrophage-colony stimulating factor"
GPI	Glycosyl-PhosphatidylInositol
GTPase	"Guanine Triphosphate Hydrolase"
GUV	Vésiculaire uni-lamellaire géante
HA	"Hemagglutinin"
HCT-116	Cellules de carcinome de colon humain
HLV	"Hydrodynamic limb vein"
HSV	"Herpes simplex virus"
HTV	"Hydrodynamic tail vein"
I	Intensité du courant électrique
IF	Intensité de fluorescence
Int	Intérieur
kpb	Kilo paire de base
kDa	Kilo Dalton
LATP	"Latency-Active Promoter"
Lc	Phase liquide cristal

Ld	Phase liquide désordonnée
Lo	Phase liquide ordonnée
LUV	Large vésicule uni-lamellaires
MEM	Milieu minimum d'Eagle
MLV	Vésicule multi-lamellaire
MoMLV	"Moloney Murine Leukemia Virus"
msPEF	Millisecond Pulsed Electric Field
μ	Coefficient de migration électrophorétique
N	Nombre d'impulsions électriques
NBD	N-4-nitrobenzo-2-oxa1,3-diazole
NLS	"Nuclear Localization Sequence"
nsPEF	Nanosecond Pulsed Electric Field
PBS	Tampon phosphate salin
PB	Pulsation Buffer
PC	Phosphatidylcholine
PCL	"Packing cell lines"
PE	Phosphatidyléthanolamine
PEI	Polyéthylénimine
PI	Propidium Iodide
PSF	Fonction d'étalement du point
M	Fraction mobile
PS	Phosphatidylsérine
R	Résistance
ROI	Région d'intérêt
SFV	"Semliki Forest Virus"
SHSY5Y	Cellules de neuroblastome humain
SIN	"Sindbis virus"
SM	Sphingomyéline
SNARE	"Soluble N-éthylmaleimide-sensitive factor Attachment Protein Receptors"
So	Phase solide ordonnée
SPT	"Single particle tracking"
SPHV	"Short Pulse and High Voltage"
STP	Structure transitoire de perméation
SUV	Petites vésicules uni-lamellaires
SV40	"Simian virus 40"
T	Durée des impulsions électriques
TAE	Tampon Tris-Acétate-EDTA
Tm	Température de transition de phase
TNF-α	"Tumour necrosis factor-alpha"
TOTO-1	Dimère de benzithiazolium-4-quinolium
TPL	"Total PhosphoLipids"
U	Tension électrique
u.a.	Unité arbitraire
UI	Unité International
VEE	"Venezuelan equine encephalitis virus"
VEGF	"Vascular endothelium growth factor"
VIH-1	Virus d'Immunodéficience Humaine-1
WTT	Wild type Toronto
$\Delta\Psi_0$	Différence de potentiel transmembranaire native
$\Delta\Psi_i$	Différence de potentiel transmembranaire électro-induite
$\lambda_{max(excitation)}$	Longueur d'onde maximale d'excitation
$\lambda_{max(émission)}$	Longueur d'onde maximale d'émission

I. INTRODUCTION

I. Introduction

La **membrane plasmique** est une **barrière physique et sélective** qui empêche la transfert de petites molécules (e.g. médicaments anti-tumoraux) et de macromolécules (e.g. plasmide) hydrophiles et/ou chargées au sein des cellules. Par conséquent, sa déstabilisation transitoire est nécessaire afin d'augmenter sa **perméabilité** à ces divers composés. Une connaissance approfondie des membranes biologiques sur les plans structural, dynamique et fonctionnel est nécessaire à la compréhension des mécanismes de transport de molécules exogènes dans les cellules *(Engelman, 2005; Jacobson et al., 2007)* et la mise en place de stratégies à la fois sûres et efficaces de transfert de molécules.

Ce chapitre bibliographique se décompose en cinq parties:

(1) Structure, dynamique et fonctions des membranes biologiques: Nous décrirons la membrane plasmique comme un assemblage multimoléculaire, structuré, dynamique et fonctionnel.

(2) La perméabilité membranaire: Nous aborderons les forces impliquées dans la cohésion membranaire et les mécanismes impliqués dans le transport des petites molécules et des macromolécules.

(3) La vectorisation de gènes in vitro et in vivo: Nous focaliserons notre attention sur les stratégies mises en place pour un transfert sûr et efficace de molécules de plasmide *in vitro* et *in vivo*.

(4) L'électroperméabilisation: Nous ferons un état lieux de ce qui est connu (ou pas) de l'électroperméabilisation.

(5) L'électrotransfert de plasmide: Nous présenterons l'état de l'art de l'électrotransfert de plasmide: des mécanismes biophysiques impliqués dans le transfert de plasmide à travers de la membrane plasmique aux applications *in vivo*.

PARTIE 1

STRUCTURE, DYNAMIQUE, ET FONCTIONS DES MEMBRANES BIOLOGIQUES

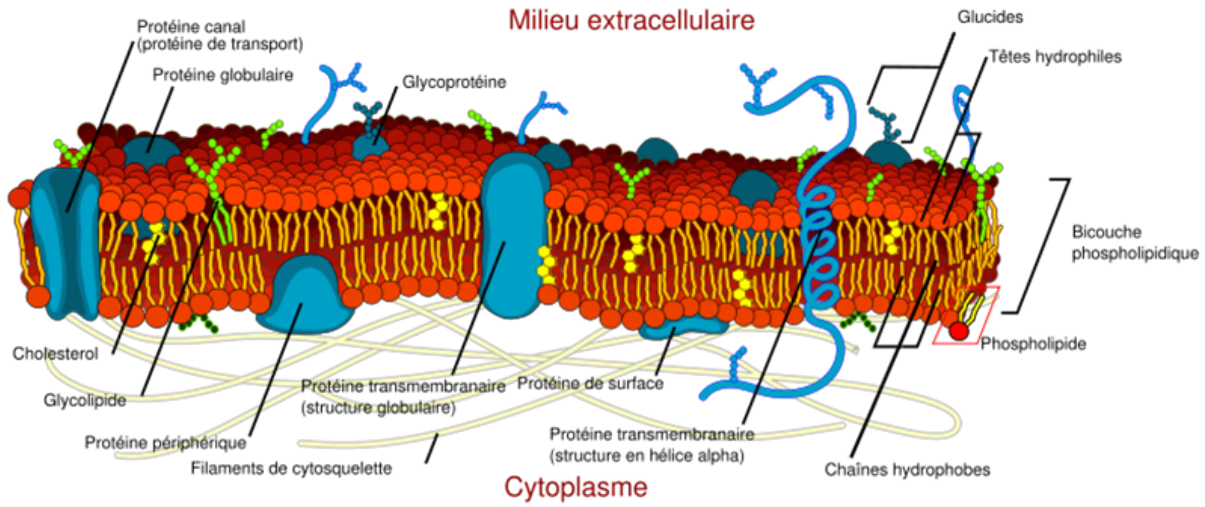

Figure I-1: Modèle de membrane plasmique *(Source: www.wikepedia.fr).*

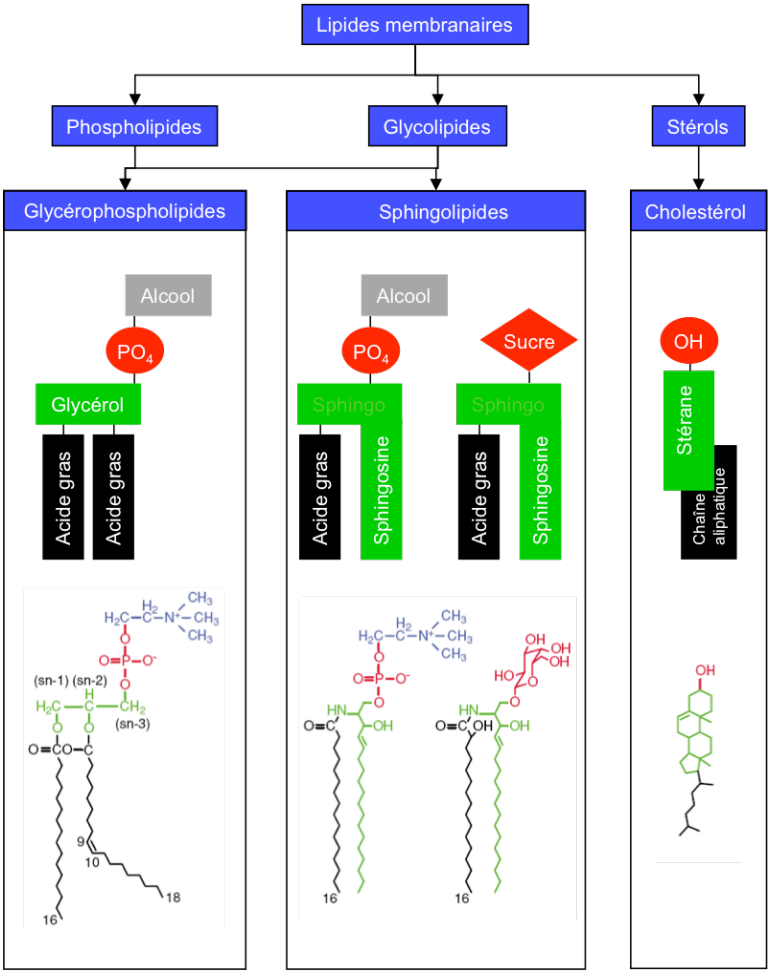

Figure I-2: Classification des phospholipides. Phospholipides PL (glycérophospholipides, sphingolipides) et stérols non estérifiés sont illustrés par des exemples. Les glycérophospholipides sont formés à partir d'un alcool phosphatidyl, du glycérol et deux longues chaînes d'acides gras. La partie polaire (alcool phosphatidyl) et la partie non polaire (acide gras) sont reliées grâce au glycérol. Le squelette des sphingolipides contient, à la place du glycérol, la sphingosine. Les sphingolipides ont pour tête non polaire, la phosphotidylcholine ou la phosphatidyléthanolamine, alors que les glycosphingolipides ont un sucre *(D'après, Fantini et al., 2002)*.

Partie 1. Structure, dynamique et fonctions des membranes biologiques

1. La composition biochimique des membranes biologiques

Les composants majoritaires d'une membrane sont les **lipides** et les **protéines** (Figure I-1). Les **sucres** sont généralement associés aux lipides et aux protéines sous forme de glycolipides et de glycoprotéines. L'**eau** représente 30% du poids sec de la membrane. La composition d'une membrane varie d'un organisme à l'autre, d'un type cellulaire à l'autre et d'une membrane à une autre *(Meer et al. 2008)*.

1.1. Les lipides

La figure I-2 représente les distinctes catégories de lipides selon leur nature chimique *(Fantini et al., 2002)*. Les **lipides** sont des molécules amphiphiles qui donnent lieu à des arrangements supramoléculaires spécifiques en milieu aqueux. Les **glycérophospholipides** et les **sphingolipides** présentent un squelette faisant intervenir, respectivement, le glycérol et la sphingosine. Selon la nature du squelette, différentes liaisons hydrogènes peuvent être établies. La tête polaire des lipides peut leur conférer une charge globalement neutre, ou négative (Figures I-2 & I-3). Les parties hydrophobes des acides gras peuvent présenter des insaturations. En effet, les insaturations C=C de type *cis* diminuent les interactions hydrophobes de Van der Waals entre les parties hydrocarbonées des lipides et augmentent ainsi la fluidité membranaire. Les **stérols** sont une autre classe de lipides qui possède une structure majoritairement hydrophobe. Le **cholestérol** représente 30 - 40% des phospholipides des membranes de cellules animales *(Maxfield and Tabas, 2005)*.

La topographie des lipides membranaires des érythrocytes montre une asymétrie de la distribution des lipides (Figure I-4). En effet, le feuillet externe se compose majoritairement de phosphatidylcholine et sphingomyéline alors que les phosphatidyléthanolamines et les phosphatidylsérines sont préférentiellement localisées sur le feuillet interne *(Rothman and Lenard, 1977 ; Zachowski, 1993)*. Cette **asymétrie membranaire,** produite lors de la synthèse des membranes dans le réticulum endoplasmique, est maintenue par des protéines transportant des lipides (Floppases, aminophospholipides translocases…) ou supprimée par la protéine scramblase *(Yamaji-Hasegawa and Tsujimoto, 2006)*.

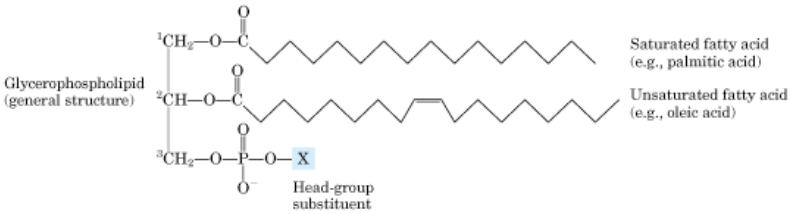

Name of glycerophospholipid	Name of X	Formula of X	Net charge (at pH 7)
Phosphatidic acid	—	—H	−1
Phosphatidylethanolamine	Ethanolamine	$-CH_2-CH_2-\overset{+}{N}H_3$	0
Phosphatidylcholine	Choline	$-CH_2-CH_2-\overset{+}{N}(CH_3)_3$	0
Phosphatidylserine	Serine	$-CH_2-\underset{COO^-}{CH}-\overset{+}{N}H_3$	−1
Phosphatidylglycerol	Glycerol	$-CH_2-\underset{OH}{CH}-CH_2-OH$	−1
Phosphatidylinositol 4,5-bisphosphate	*myo*-Inositol 4,5-bisphosphate	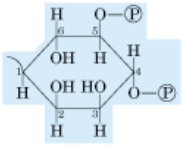	−4
Cardiolipin	Phosphatidyl-glycerol	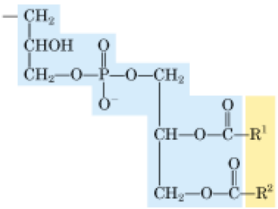	−2

Figure I-3: Glycérophospholipides. Structure des différentes têtes polaires de glycérophospholipides *(Source: www.biochem.arizona.edu).*

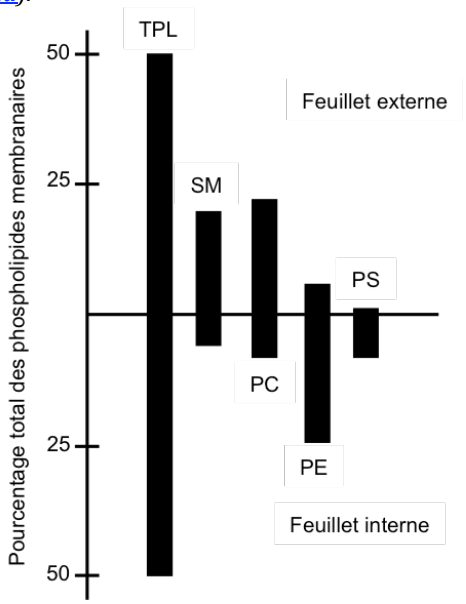

Figure I-4: Topographie des lipides membranaires. La répartition des lipides dans les membranes d'érythrocytes humains est donnée pour la concentration totale en phospholipides (TPL), glycérophospholipides (PC, phosphatidylcholine; PE, phosphatidyléthanolamine; PS phosphatidylsérine) et des sphingolipides de type sphingomyéline (SM), pour chaque feuillet de la membrane plasmique *(D'après, Rothman et al., 1977).*

Cette asymétrie lipidique correspond à un **état d'équilibre** important sur le plan fonctionnel. En effet, la présence d'une charge de surface différente des deux côtés de la membrane est une conséquence de l'asymétrie membranaire. Cette différence de charge participe à la création du **potentiel transmembranaire natif**.

Lorsque l'asymétrie membranaire est rompue, les **phosphatidylsérines** sont rapidement exposées *(Bassé et al., 1993)*. Dès la mise en route du remodelage membranaire, l'influx compensatoire tardif de phosphatidylcholines ou de sphingomyélines, après exposition de phosphatidylsérines et/ou de phosphatidyléthanolamines provoque une surcharge transitoire de phospholipides dans le feuillet externe. Ce déséquilibre crée une augmentation de la courbure de la membrane qui forme des bourgeons à partir desquels des microparticules sont libérées *(Fox et al., 1990)*. L'exposition de la phosphatidylsérine à la surface cellulaire est considérée comme un événement précoce de l'**apoptose**, suivi d'une libération dans le milieu extracellulaire de microparticules porteuses de phosphatidylsérines et de marqueurs protéiques spécifiques de la cellule d'origine qui sont des déterminants pour leur élimination par phagocytose *(Martin et al., 1995)*. L'exposition de phosphatidylsérines est également impliquée dans la **réponse hémostatique**. En effet, elles permettent le recrutement et la concentration des facteurs de la coagulation à la surface membranaire des cellules *(Toti et al., 1996)*. La **phosphatidyléthanolamine**, aminophospholipide majoritaire des membranes plasmiques, est l'unique phospholipide qui ne présente pas une structure en bicouche *(Israelachvili et al., 1980)*. Cette propriété lui confère une importante mobilité transversale et facilite la **fusion membranaire** de systèmes modèles *(Verkleij et al., 1984 ; Ellens et al., 1989)*. Il a été également montré qu'une forte concentration de phosphatidyléthanolamines dans le feuillet externe de la membrane plasmique des myoblastes augmente la fusion de ces derniers pour former les myotubes *(Herwitz, 1981 ; Santini et al., 1990)*.

1.2. Les protéines

Les protéines membranaires jouent des rôles majeurs dans le transfert d'information (récepteurs), le transport de matière (transporteurs et canaux) et la transformation d'énergie. Les protéines peuvent être partiellement insérées dans un des deux feuillets membranaires en gardant une partie hydrophile: ce sont **les protéines extrinsèques** (ou périphériques). Cette insertion membranaire est rendue possible par

la présence d'une partie alkylée hydrophobe, tel qu'un acide gras myristoyl ou palmitoyl. Les **protéines transmembranaires** (ou intégrales, intrinsèques) sont insérées au niveau des deux feuillets par les domaines hydrophobes des protéines (Figure I-1) *(Rothman and Lenard, 1977)*. Les **protéines du cytosquelette** sont en interaction avec la membrane plasmique (Figure I-1). Le cytosquelette d'actine est impliqué dans des processus membranaires telles que l'endocytose *(Pekmans and Helenius, 2002 ; Parton and Richards, 2003)*. Les protéines membranaires diffusent latéralement dans les membranes biologiques. Les protéines membranaires extrinsèques ont un coefficient de diffusion latérale de l'ordre de 1 $\mu m^2/s$ alors que les protéines membranaires intrinsèques ont un coefficient de diffusion latérale compris entre 0,1 et 0,5 $\mu m^2/s$ *(Owen et al., 2009)*.

2. Les systèmes de membranes modèles

Devant la complexité des membranes cellulaires, il est apparu nécessaire de développer des systèmes de membranes modèles. Ces membranes modèles sont des **systèmes simplifiés** par rapport aux membranes biologiques. En effet, ces membranes sont composées d'une quantité connue de 1 ou plusieurs lipides associés ou non à des protéines. Ces systèmes simplifiés apportent de précieuses informations sur les propriétés des membranes et leurs interactions avec l'environnement.

2.1. Les monocouches

Le dépôt de lipides à l'interface air-solvant aqueux conduit à la formation d'une **monocouche** de lipides. Les monocouches sont utilisées pour l'étude de l'interaction et de l'insertion de composés avec les feuillets d'une membrane lipidique *(Mendez et al., 2008 ; Fernandez-Botello et al., 2008)*.

2.2. Les liposomes

Les liposomes sont des vésicules **unilamellaires** ou **multilamellaires** (MLV, multilamellar vesicle). Les vésicules unilamellaires sont constituées d'une seule **bicouche** lipidique fermée alors que les vésicules multilamellaires sont formées de bicouche en pelures d'oignon ou en multiples compartiments (Figure I-5A). En fonction du protocole de formation des liposomes, les feuillets externe et interne peuvent avoir des compositions variables.

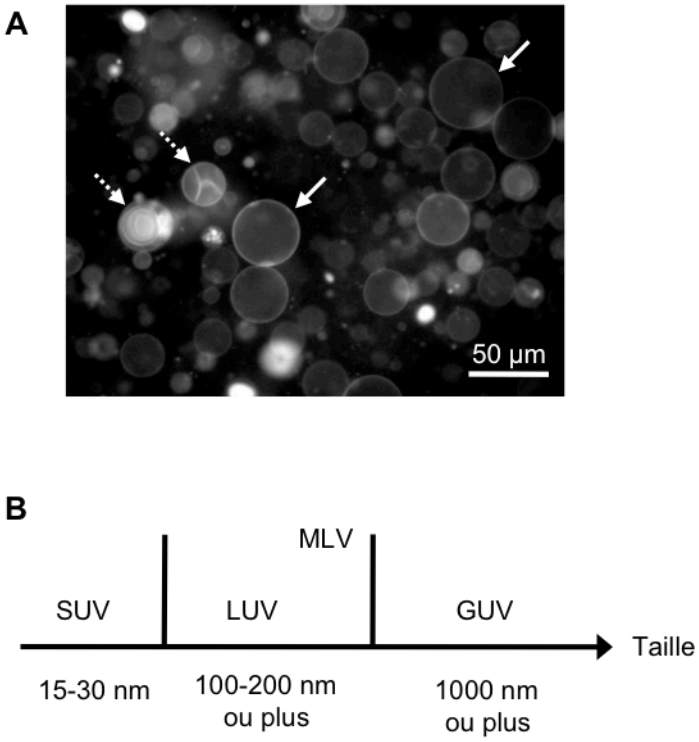

Figure I-5: Les liposomes.
A. Vésicules unilamellaires (flèche continue) et multilamellaires (flèche discontinue) de DOPC.
B. Rayon moyen des différents liposomes.

Contrairement aux SUV (small unilamellar vesicle), le rayon moyen des LUV (large unilamellar vesicle) et des GUV (giant unilamellar vesicle) confère à ces derniers des propriétés mécaniques en terme de rayon de courbure plus proches du rayon moyen des cellules (Figure I-5B) *(Hristova et al., 2002)*. Suivant le type de vésicules unilamellaires utilisées, les interactions entre des molécules et la membrane ou le fonctionnement des protéines membranaires reconstituées peuvent être modifiés. Les LUV sont généralement utilisées pour l'étude des propriétés de diffusion de composés ou la vectorisation de composés actifs *(Teissié, 1987)*. Les GUV constituent un modèle identique en taille et en forme à une cellule en suspension. Parce qu'elles présentent une grande surface membranaire, les GUV sont utilisées dans l'étude des microdomaines membranaires *(de Almeida et al., 2007)*, la vectorisation de macromolécules *(Berezhna et al., 2005)* ou l'étude de fonctions cellulaires *(Khalifat et al., 2008 ; Delatour et al., 2008).*

3. Dynamique structurale et domaines membranaires

3.1. Structure des membranes et lyotropisme des lipides

Les propriétés **amphiphiles** des lipides confèrent à ces derniers la capacité à adopter différentes organisations en milieu aqueux. En effet, le modèle d'**Israelachvili**, permet de prédire les différentes organisations adoptées par les lipides (micelles, bicouches planes ou vésicules) en milieu aqueux par comparaison des volumes occupés par les parties hydrophobes et hydrophiles des lipides. Ces arrangements supramoléculaires ont pour objectif de minimiser les interactions des parties hydrophobes avec l'environnement aqueux et de favoriser les interactions hydrophiles des parties polaires avec celui-ci. Ce **polymorphisme lipidique** est fonction de nombreux paramètres physico-chimiques, tels que la température, la force ionique ou encore le pH *(Israelachvili et al., 1980)*.

Les membranes des cellules forment des **bicouches lipidiques**. Mais ces dernières sont constituées également de phospholipides dits "non bicouches" d'après le modèle d'Israelachvili *(Israelachvili et al., 1980)*. L'existence de ces structures en "non bicouche" (e.g. micelle, phase hexagonale…) au sein de la membrane plasmique est liée à des processus de fusion et de division cellulaires. Ces structures auraient un rôle au voisinage immédiat des protéines transmembranaires dont la partie hydrophobe ne correspondrait pas à la partie hydrophobe d'un feuillet ou de la bicouche (*Piknova et al., 1993)*.

3.2. Mouvements moléculaires des lipides

L'édifice membranaire n'est pas une structure figée mais **dynamique**. En effet, les lipides sont animés de mouvements (Figure I-6). Les chaînes d'acides gras des lipides non stéroïdiens subissent des **changements conformationnels** tels que les rotations des liaisons C-C et les mouvements d'**isomérisation** *cis-trans* (10^{-10} s à 10^{-11} s). Les lipides sont animés de mouvements de **rotation** sur eux-mêmes (10^{-9} s à 10^{-11} s) et de **diffusion latérale** (10^{-8} $cm^2.s^{-1}$ à 10^{-9} $cm^2.s^{-1}$). Enfin, les lipides ont la capacité de passer d'un feuillet membranaire à l'autre (quelques heures à quelques jours). Cette **diffusion transversale** (ou flip-flop) est un phénomène très lent car la tête polaire des lipides se heurte à la barrière énergétique au niveau des parties hydrophobes *(Bevers et al., 1999)*. Les mouvements à courte échelle des lipides attribuent à la membrane une certaine fluidité.

Au sein d'une bicouche composée d'un seul lipide, le **thermotropisme lipidique** se traduit par la transition d'une phase ordonnée gel (solide So) à une phase liquide cristalline (liquide désordonnée L_d ou cristal liquide L_c) lorsque la température est augmentée *(Brown and London, 1998)*. Cette transition de phase a lieu à une certaine température dite **température de transition de phase** du lipide (T_m). Les changements de conformation de chaînes hydrocarbonées induites par la transition de phase, conduisent à une fragilisation des interactions hydrophobes de Van der Waals qui correspond à une augmentation des mouvements moléculaires et de la fluidité membranaire.

L'ensemble de ces notions de dynamique ont donné naissance au concept du modèle membranaire de la **mosaïque fluide** de Singer et Nicholson *(Simons and Ikonen, 1997)*.

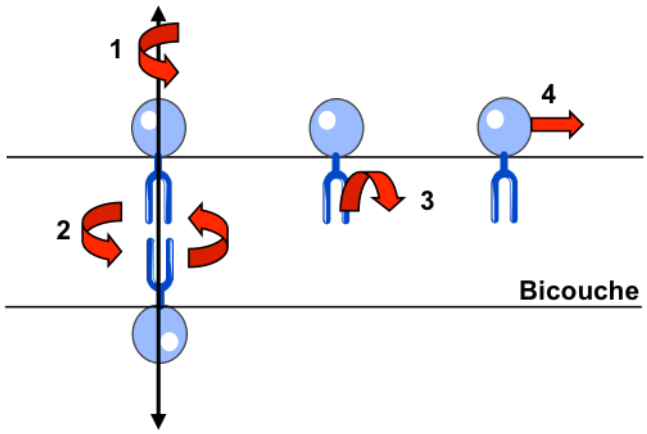

Figure I-6: Les différents mouvements moléculaires des lipides. (1) Rotation des lipides sur eux-mêmes, (2) Flip-Flop des lipides, (3) Changements conformationnels des chaînes d'acides gras de lipides, et (4) Diffusion latérale des lipides *(D'après Shetcher, 2000)* (Illustration réalisée grâce à Servier Medical Art, www.servier.fr).

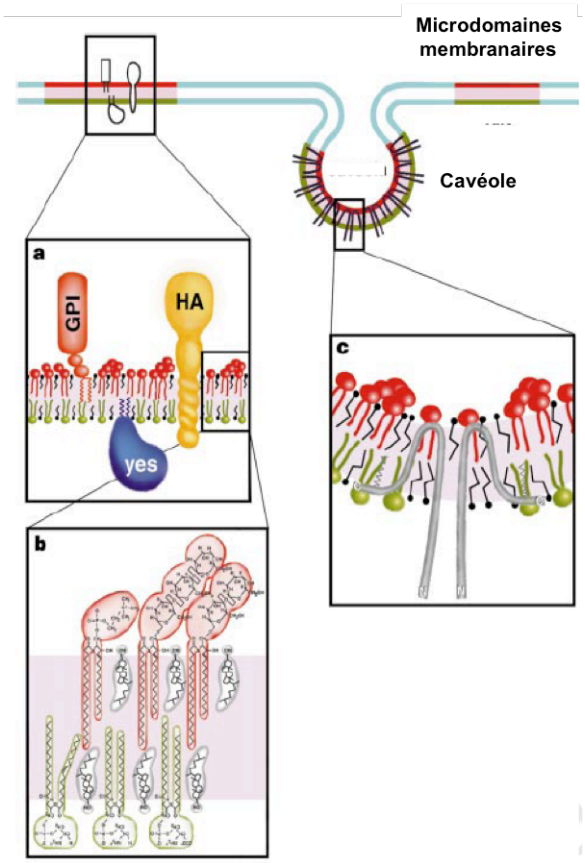

Figure I-7: Représentation schématique du modèle d'organisation des microdomaines membranaires et des cavéoles. a. Les microdomaines contiennent des protéines associées au feuillet externe de la membrane plasmique par leur ancre GPI, des protéines liées au feuillet interne par des groupements acyles (protéine Yes appartenant à la famille des kinases Scr) ou des protéines associées par leurs domaines transmembranaires (HA). **b.** Les microdomaines membranaires sont enrichis en sphingomyélines et les glycosphingolipides (en rouge) sur le feuillet externe et les glycérolipides (phosphatidylsérine et phosphatidyléthanolamine (en vert) sur le feuillet interne. Le cholestérol (en gris) est présent dans les deux feuillets. **c.** Les cavéoles sont formées par l'association aux microdomaines membranaires de molécules de cavéolines *(D'après Simons & Ikonen, 1997).*

3.3. Les microdomaines membranaires

Face à de nombreuses évidences, un consensus scientifique a permis de redéfinir les membranes biologiques comme une structure liquide en deux dimensions **hautement dynamique** et présentant une **hétérogénéité latérale** de ses composants *(Mukherjee and Maxfield, 2004 ; Kusumi and Suzuki, 2005)*. Cette nouvelle définition fait apparaître la notion de **microdomaines membranaires** *(Simons and Vaz, 2004)*.

Des études comparatives de méthodes biophysiques permettant d'étudier la dynamique des membranes biologiques ont permis de mettre en évidence des confinements de molécules au sein de structures définies comme des microdomaines membranaires. Ces complexes condensés sont caractérisés par leur richesse en cholestérol, sphingolipides et protéines à ancre GPI. En terme de dynamique, ces microdomaines correspondent à une **phase liquide ordonnée** (Lo) entourée d'une **phase liquide désordonnée** (Ld) *(Fantini et al., 2002 ; Almeida et al., 2005)*. Deux types de microdomaines particuliers ont été identifiés: les **cavéoles** et les **rafts** (Figure I-7) *(Nabi and Le, 2003)*.

De par leur structure et leur dynamique, ils sont définis comme **résistant aux détergents non ioniques**, tels que le Triton X-100 *(Babiychuk and Draeger, 2006)*. Ces fractions insolubles aux détergents constituent les DRMs (Detergent-resistant membranes), DIGs (Detergent-insoluble glycolipid fractions) ou GEMs (Glycolipid-enriched membranes). Cette approche n'est pas sans artéfacts. En effet, l'addition de détergent non ionique sur les membranes biologiques conduit à une réorganisation des lipides durant la solubilisation (coalescence des microdomaines). Par conséquent, les structures membranaires réfractaires à la solubilisation dans le détergent sont différentes de celles présentes avec l'extraction au détergent. Les microdomaines membranaires seraient des domaines de l'ordre de **50 nm de diamètre**. En conséquence, ils sont trop petits pour être visualisés en microscopie optique. Le développement conjoint de méthodes biophysiques (SPT, FRAP, FCS…) *(Marguet et al., 2006; Haluska et al., 2008)* et de sondes fluorescentes *(Demchenko et al., 2009)* permet de les détecter, d'estimer leur taille et la dynamique des composés qui les constituent.

Les microdomaines membranaires sont impliqués dans le **transport membranaire** (sécrétion, endocytose…) *(Helms and Zurzolo, 2004)* et dans la **signalisation cellulaire** *(Simons and Ikonen, 1997 ; Simons and Toomre, 2000)*. De récents travaux suggèrent que ces microdomaines seraient des voies d'entrée pour les agents pathogènes comme les bactéries *(Wang et al., 2008)* et les virus *(Tang et al., 2008)*.

3.4. Les propriétés mécaniques des membranes

Les membranes biologiques possèdent trois grandes propriétés mécaniques: l'étirement (stretching), la courbure (bending) et le cisaillement (shearing) au sein d'un ou des deux feuillets lipidiques *(MacMahon and Gallop, 2005 ; Janmey and Kinnunen, 2006)*. Ces propriétés sont impliquées dans de nombreux processus biologiques comme la division cellulaire, l'exocytose, et l'endocytose.

4. Les grandes fonctions des membranes biologiques

Les membranes biologiques constituent un caractère omniprésent dans les cellules procaryotes ou eucaryotes. Le rôle fondamental des membranes est d'assurer une **compartimentation** métabolique et chimique en maintenant des compositions et des concentrations différentes dans les milieux que ces dernières délimitent *(Edidin, 2003)*.

Les membranes biologiques ne sont pas des barrières absolues. En effet, l'homéostasie cellulaire nécessite des **échanges continuels** et **contrôlés** de matière (macromolécules, ions…), d'énergie (ATP…) et d'information (hormones, neurotransmetteurs…).

PARTIE 2

LA PERMÉABILITÉ MEMBRANAIRE

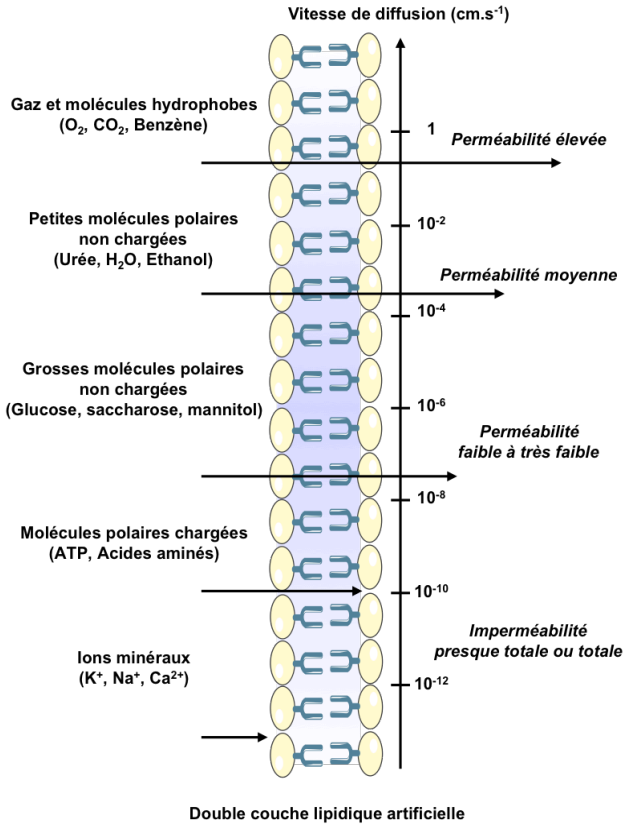

Figure I-8: Perméabilité membranaire de diverses catégories de molécules et d'ions à travers les bicouches lipidiques artificielles *(D'après Shetcher, 2000)* (Illustration réalisée grâce à Servier Medical Art, www.servier.fr).

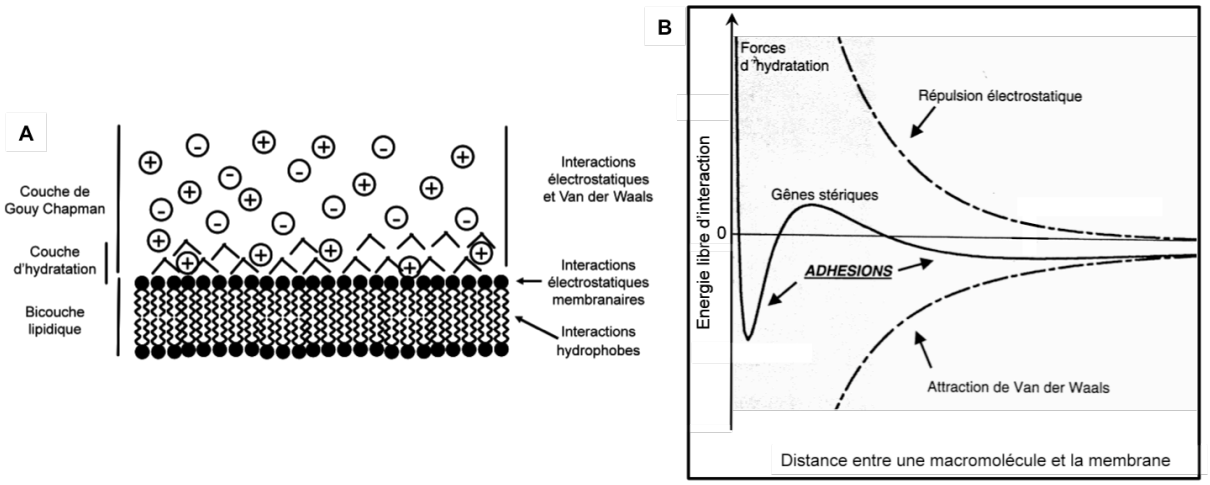

Figure I-9: Diagramme énergétique des forces de cohésion et de stabilisation présentes au voisinage de la membrane plasmique. L'approche des macromolécules au voisinage d'une membrane est régulée par les forces attractives ou répulsives. Les deux minima d'adhésions séparés par une barrière énergétique, permettent l'adhésion des molécules à la membrane plasmique. La déshydratation de la surface membranaire est l'étape ultime à franchir pour une interaction stable macromolécules/membrane plasmique *(Adapté de la thèse de Cécile Faurie).*

Partie 2. La perméabilité membranaire

La première fonction des membranes plasmiques est son rôle de **barrière physique** entre les milieux extracellulaire et intracellulaire. Les membranes biologiques présentent un caractère hydrophobe qui s'oppose à la libre diffusion d'ions, de solutés hydrophiles et de macromolécules. Cette propriété des membranes semble s'opposer au second rôle des membranes, celui d'assurer des **échanges** entre les milieux extracellulaire et intracellulaire. En effet, la survie cellulaire dépend des échanges de matière entre ces deux compartiments: importation de matières premières et exportation des déchets cellulaires. Afin d'assurer ces deux fonctions, la cellule a mis en place un contrôle strict des flux d'eau, d'ions, et de molécules au niveau de la membrane plasmique (Figure I-8): on parle alors de **perméabilité sélective**.

1. La cohésion membranaire

La cohésion membranaire est le minimum requis pour maintenir la compartimentation entre les milieux extérieur et intérieur (Figure I-9). L'organisation en bicouche de la membrane provient de l'existence : (i) de **forces hydrophobes** entre les chaînes aliphatiques des acides gras. L'attraction qui existe entre deux surfaces hydrophobes permet de minimiser ainsi leurs contacts avec des molécules d'eau ; (ii) de **forces de répulsion** de type électrostatique entre les têtes hydratées des phospholipides qui se disposent à l'extérieur et assurent l'interface avec l'eau (Figure I-9).

La stabilité de cet édifice multimoléculaire est assurée par un réseau de forces intermoléculaires qui maintiennent la cohésion membranaire *(Israelachvili, 1993 ; Israelachvili et al., 1980)*:

(i) **Les forces attractives de Van Der Waals**, regroupent toutes les interactions dipôles-dipôles s'exerçant entre deux molécules. Elles dépendent en particulier des propriétés électrostatiques des molécules (polaires, non polaires, ou chargées). L'énergie d'interaction due aux forces de Van Der Waals de longue portée entre deux surfaces s'exerce sur des distances de 3 à 10 nm.

(ii) Les **forces de répulsions électrostatiques** s'exercent à longue portée entre deux surfaces. Si deux surfaces planes portent des charges de même signe, l'énergie d'interaction répulsive électrostatique est due à la répulsion de ces charges. Les cellules

portant une densité surfacique de charges globalement négative, exercent donc une répulsion électrique mutuelle. Les charges de surface sont équilibrées par une couche d'ions de charges opposées (contre ions) distribuée dans la solution sur une petite distance d'après le modèle de Gouy-Chapman *(Tocanne and Teissie, 1990)*. Cette distance est caractérisée par la distance de Debye (K). Les forces de répulsions électrostatiques s'exercent aussi sur une distance de 3 à 10 nm.

(iii) Les **forces répulsives** qui résultent de **l'interaction stérique entre les molécules de surface**. Lorsque deux cellules se rapprochent, la répulsion provient principalement d'interactions stériques des molécules du glycocalix *(Bell et al., 1984)*. Lorsque deux surfaces entrent en contact, les couches de polymères s'interpénètrent et une partie de l'eau est extraite de l'espace intercellulaire. Les forces répulsives résultent donc de la compression stérique des chaînes de polymères et de la pression osmotique dans l'espace intercellulaire. Elles s'exercent à plus faible distance (< 5 nm).

(iv) Les **forces répulsives d'hydratation** sont issues de l'organisation interfaciale des molécules d'eau au voisinage des têtes polaires *(Israelachvili and Wennerstrom, 1996)*. L'interface membranaire est en contact direct avec des phases aqueuses des deux compartiments que la membrane sépare. L'interaction des molécules d'eau avec l'interface est susceptible d'influencer des champs électriques locaux associés aux têtes polaires des phospholipides et est à l'origine des forces d'hydratation. La nature de la tête polaire des phospholipides, leur méthylation, les états physiques des chaînes hydrocarbonées et le mélange de différents lipides affectent l'hydratation de la membrane. Les forces répulsives liées à l'hydratation se manifestent à très courtes distances (<1 nm).

(v) Les **forces d'ondulation** spontanée des membranes dépendent de la contribution de la fluctuation thermique de forces répulsives entre les bicouches. Ce mouvement est relativement de grande amplitude et maintient les bicouches membranaires à une certaine distance. Ces forces de répulsion d'origine entropique, sont donc sous la dépendance de la rigidité des bicouches *(Helfrich, 1978)*. Elles proviennent de la répulsion osmotique entre les groupes de surfaces mobiles et ont la même origine que les forces stériques. Elles ont généralement une faible portée.

A

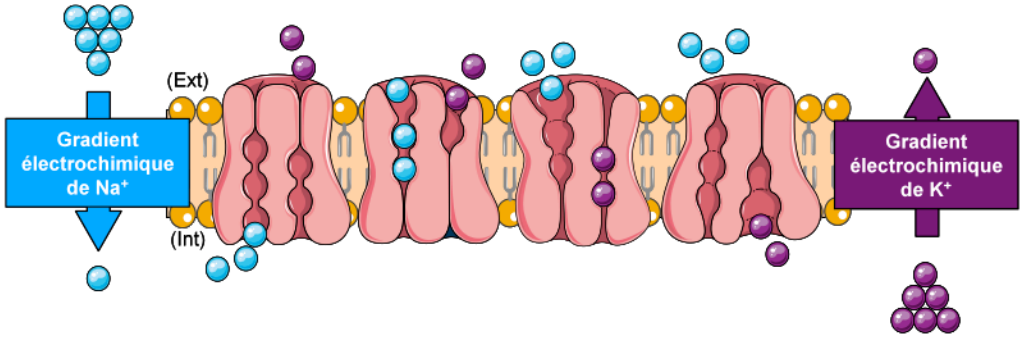

B

Ions	$[Ion]_{intra}$ (mmol.L^{-1})	$[Ion]_{extra}$ (mmol.L^{-1})
K^+	160	4
Na^+	7-12	144
Mg^{2+}	5	1-2
Ca^{2+}	10^{-4}-10^{-5}	2
Cl^-	4-7	120
HCO^-_3	8	26-28

Figure I-10: La Na^+/K^+ ATPase. A. Cette pompe est à l'origine de la différence de concentrations ioniques en K^+ et en Na^+ entre le cytoplasme et le milieu extérieur. Cette séparation de charge et la différence de perméabilité de la membrane aux ions K^+ et Na^+ sont les causes majeures du potentiel capacitif membranaire (Illustration réalisée grâce à Servier Medical Art, www.servier.fr). **B.** Ce tableau présente les concentrations extracellulaires et intracellulaires des principaux ions impliqués dans l'homéostasie cellulaire *(D'après Shetcher, 2000)*.

2. Transport de petites molécules

Les membranes plasmiques sont perméables à des petites molécules et imperméables à des ions organiques ou minéraux. Le transport de ces derniers est assuré par des systèmes de transports protéiques (canaux, pompes, et perméase).

2.1. Molécules non chargées

Dans le cas de molécules non chargées, la loi physique première déterminant le sens du transport est celle de la **diffusion**. Ce mouvement s'effectue selon le **gradient de concentration** de ces molécules neutres et ne nécessite pas d'apport énergétique: il s'agit du **transport passif**. Cependant, les cellules peuvent s'opposer à la diffusion en consommant de l'énergie (hydrolyse de l'ATP): il s'agit du **transport actif**.

2.2. Diffusion d'ions et potentiel transmembranaire

Le mouvement de tout **ion** à travers un pore ou un canal est couplé au **gradient électrochimique** de cet ion ; celui-ci se déplace selon son **gradient de concentration** et **du potentiel transmembranaire**, $\Delta\Psi$.

Le potentiel transmembranaire est la résultante de trois composantes: le potentiel dipolaire, le potentiel de surface et le potentiel capacitif dû à la séparation des charges. Les lipides présentent un moment dipolaire *(Starke-Peterkovic et al., 2006)*. La superposition des lipides au niveau de la membrane selon une direction donnée additionne les moments dipolaires de chaque lipide. Ainsi, un **potentiel dipolaire** global est créé. La membrane plasmique a généralement des charges négatives à sa surface. En effet, 10 à 20% des lipides sont anioniques, en particulier les gangliosides et les protéines peuvent être chargés. Ces charges sont partiellement neutralisées par les contre-ions de la phase aqueuse. Par conséquent, une séparation de charges est induite et un **potentiel de surface** est créé. Enfin, la membrane plasmique est une bicouche lipidique imperméable aux ions (à l'exception de petits ions). Cette propriété fait de la membrane, une **capacité électrique**. Cette charge capacitive est due en majorité à la différence de concentrations des ions K^+ et Na^+ dans le milieu extracellulaire et le cytoplasme, induite par la Na^+/K^+ ATPase (Figure I-10). Par conséquent, ce transporteur est à l'origine de la formation et du maintien de la **différence de potentiel électrique transmembranaire $\Delta\Psi_0$**, nommé aussi potentiel transmembranaire natif ou potentiel

de repos de la cellule. Ainsi, l'équation de Goldman-Hodgkin-Katz relie la différence de potentiel électrique transmembranaire et la concentration des différents ions:

$$\Delta\Psi \approx \frac{RT}{F}\ln\left(\frac{P_{Na}\left[Na^{+}\right]_{e} + P_{K}\left[K^{+}\right]_{e}}{P_{Na}\left[Na^{+}\right]_{i} + P_{K}\left[K^{+}\right]_{i}}\right) \quad (Eq.I-1)$$

Avec R, constante des gaz parfaits: 1,987 cal.°K^{-1}.mol^{-1} ; T, température en Kelvin ; F, Constante de Faraday: 23000 cal.mol^{-1}.V^{-1} ; [ ]$_e$, Concentration externe en ion ; [ ]$_i$, Concentration interne en ion.

Cette équation permet d'apprécier la contribution des différents ions au potentiel électrique transmembranaire. En effet, ce sont les concentrations de l'ion K^+ le plus perméant qui déterminent la valeur de la différence de potentiel électrique. Ainsi, le potentiel de repos tend vers le potentiel de Nernst défini par l'équation 2 (Eq. I-2):

$$\Delta\Psi \approx \frac{RT}{F}\ln\left(\frac{\left[K^{+}\right]_{e}}{\left[K^{+}\right]_{i}}\right) \quad (Eq.I-2)$$

Avec R, constante des gaz parfaits: 1,987 cal.°K^{-1}.mol^{-1} ; T, température en Kelvin ; F, Constante de Faraday: 23000 cal.mol^{-1}.V^{-1} ; $[K^+]_e$, Concentration externe en ion potassium ; $[K^+]_i$, Concentration interne en ion potassium.

Si la perméabilité aux petites molécules repose sur le principe général de la diffusion, celle des macromolécules fait appel à d'autres mécanismes.

3. Transport des macromolécules

Les cellules sont capables également d'absorber et de sécréter des macromolécules (protéines, polysaccharides…). Certaines cellules peuvent ingérer des particules de plus grande taille telles que des bactéries. Les cellules mettent en place des mécanismes de franchissement de la membrane plasmique qui reposent sur la formation de vésicules. Deux grands processus sont à distinguer: **l'exocytose** qui conduit à la libération des macromolécules dans le milieu extracellulaire et **l'endocytose** qui permet l'internalisation des macromolécules *(Gundelfinger et al., 2003)*.

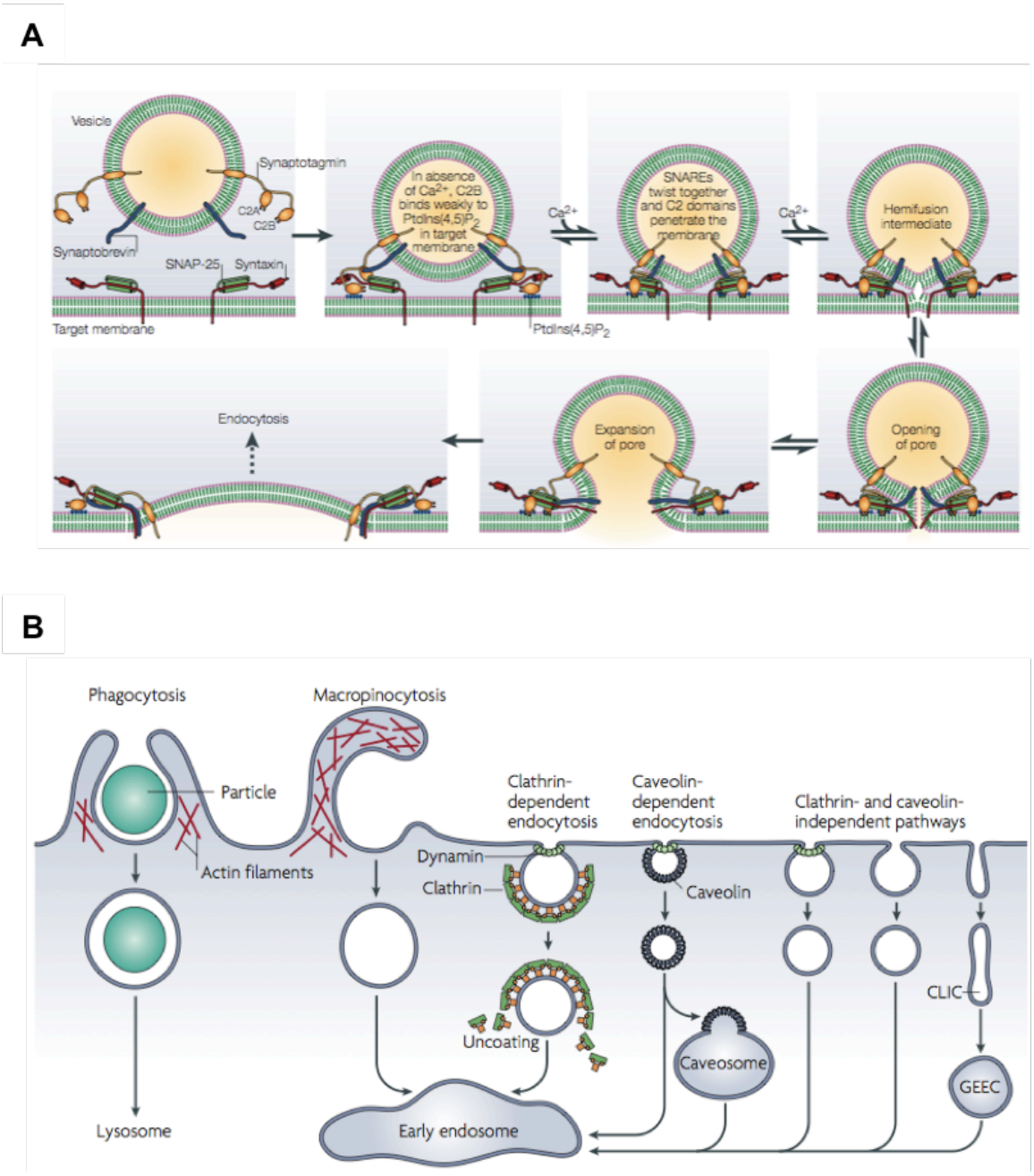

Figure I-11: Le transport de macromolécules. A. L'exocytose *(D'après Chapman, 2002).* **B.** L'endocytose *(D'après Mayor and Pagano, 2007).*

3.1. L'exocytose

L'exocytose est un processus assurant le passage de composés du cytoplasme vers le milieu extracellulaire. Ce mécanisme permet ainsi la libération de substances (hormones, enzymes, neurotransmetteurs…) après fusion de la membrane des vésicules d'exocytose avec la membrane plasmique (Figure I-11a). Il existe deux types d'exocytose: la **voie de sécrétion constitutive** et la **voie de sécrétion provoquée**. La première voie achemine continuellement certaines protéines sécrétées ou membranaires et des phospholipides à la membrane plasmique. Dans la deuxième voie, la fusion avec la membrane plasmique n'est effective que lorsque la cellule a reçu un signal extracellulaire. Les mécanismes régissant le processus d'exocytose font appel à nombreux partenaires protéiques (GTPase, GDI, v-SNARE et t-SNARE…) et restent mal connus *(Gundelfinger et al., 2003)*.

3.2. L'endocytose

L'endocytose est un processus qui permet l'internalisation de substances du milieu extracellulaire vers le cytoplasme: la membrane plasmique s'invagine progressivement au site d'absorption des composés extracellulaires puis une vésicule close se forme et se détache de la membrane. Il existe trois formes d'endocytose: la pinocytose, la phagocytose, l'endocytose (Figure I-11b).

La **pinocytose** est un phénomène constitutif qui a lieu en l'absence de ligand et qui est observé généralement dans toutes les cellules animales *(Kirkham and Parton, 2005)*. Elle est divisée en deux catégories: La **micropinocytose** (vésicules de 0,2-0,4 µm de diamètre) et la **macropinocytose** (vésicules de 1-2 µm de diamètre) permettent l'entrée de substances de tailles variables du milieu extracellulaire. Ce phénomène se traduit par la projection de lamellipodes vers le milieu extérieur puis par la fusion de ces lamellipodes pour former des vésicules de pinocytose (Figure I-11b). La pinocytose peut être induite par la stimulation de facteurs de croissance.

La **phagocytose** est processus par lequel des particules de grande ou très grandes tailles (bactéries, virus, corps apoptotiques…) sont absorbées par des cellules ; les vésicules ainsi formées sont appelées **phagosomes** (1-2 µm de diamètre) (Figure I-11b). Ce processus est induit par une interaction spécifique entre la particule à ingérer et la membrane plasmique *(Haas, 2007)*. Certains types cellulaires, tels que les amibes et les macrophages sont spécialisés dans ce mode d'internalisation.

L'endocytose se décompose en deux voies : l'**endocytose médiée par les récepteurs** qui est un processus d'internalisation très sélectif, efficace et saturable alors que l'**endocytose en phase fluide** est peu sélectif, peu efficace et peu saturable. La combinaison des deux mécanismes représente **l'endocytose totale**. L'endocytose peut avoir lieu au niveau de microdomaines spécifiques: les puits recouverts de **clathrine** et les **cavéoles** (Figure I-11b) *(Pekmans and Helenius, 2002 ; Parton and Richards, 2003)*.

Néanmoins, quelle que soit la voie d'internalisation empruntée, les composés extracellulaires sont piégés dans l'endosome et sont soit **recyclés** à la membrane plasmique, soit **digérés** dans l'endolysosome après fusion de l'endosome tardif avec les lysosomes *(Luzio et al., 2007)*.

La membrane plasmique est un assemblage multimoléculaire, structuré, dynamique et fonctionnel. Son rôle de barrière physique et sélective empêche la délivrance de petites molécules (e.g. cisplatine, bléomycine) et de macromolécules (e.g. protéine, plasmide) hydrophiles et/ou chargées au sein des cellules où se situent leurs cibles intracellulaires. Par conséquent, une déstabilisation de la membrane plasmique est nécessaire afin d'augmenter la perméabilité membranaire à ces divers composés.

PARTIE 3

VECTORISATION DE GÈNES *IN VITRO* ET *IN VIVO*

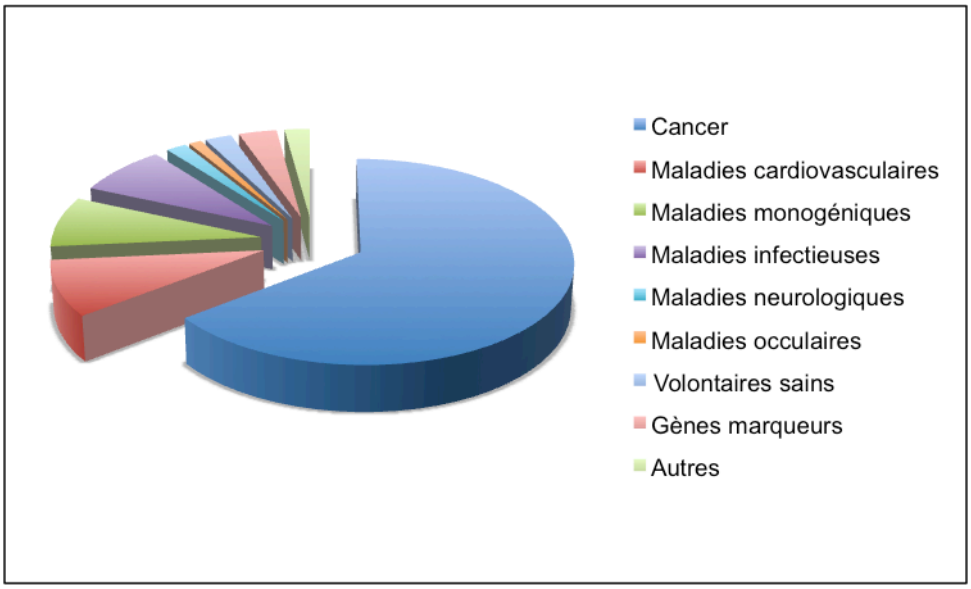

Figure I-12: Maladies traitées dans les protocoles de thérapie génique dans le monde en 2009 *(Source: www.wiley.co.uk/genetherapy).*

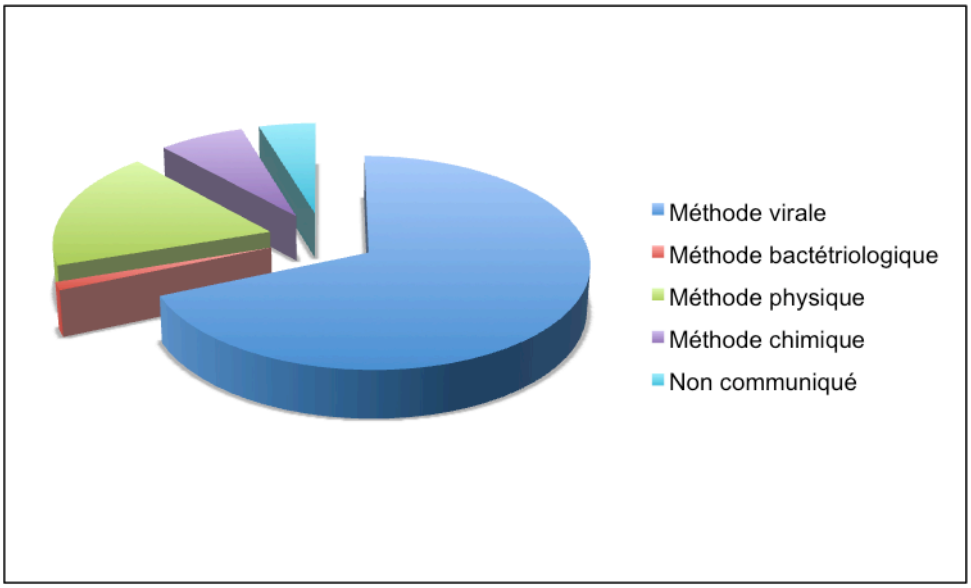

Figure I-13: Méthodes de transfert de gènes utilisées dans les protocoles de thérapie génique dans le monde en 2009 *(Source: www.wiley.co.uk/genetherapy).*

Partie 3. Vectorisation de gènes *in vitro* et *in vivo*

La **vectorisation** de molécules exogènes, comme des protéines (anticorps, peptides antigéniques), des drogues (bléomycine, cisplatine) et des acides nucléiques (gène, siRNA, oligonucléotides anti-sens) *in vitro* et *in vivo* représente un enjeu majeur dans les recherches fondamentale et appliquée. En effet, sur le plan cognitif, le transfert de ces molécules est nécessaire à la compréhension des mécanismes moléculaire et cellulaire d'un contexte physiologique et/ou pathologique. Les applications biomédicales de la vectorisation suscitent un grand intérêt dans le développement de protocoles de **thérapie génique**. La thérapie génique se définit comme l'apport en *trans* d'un **gène thérapeutique** par un **vecteur** au sein de **cellules cibles** d'un organisme entier (thérapie génique *in vivo*) ou de cellules cibles avant greffe de ces dernières dans cet organisme (thérapie génique *ex vivo*). La thérapie génique laisse naître une lueur d'espoir dans la prévention ou le traitement de pathologies où les thérapies actuelles sont soit inexistantes soit inefficaces, comme le cancer, les maladies génétiques, les maladies rares et orphelines (Figure I-12).

Si plus de 1 500 essais cliniques de thérapies géniques ont déjà été réalisés, la grande majorité de ces essais sont au stade préliminaire et ont pour objectif de vérifier la faisabilité et l'innocuité de la technique de transfert plutôt qu'un bénéfice direct pour les patients *(Edelstein et al., 2007)*. Le succès d'une thérapie génique réside dans la combinaison **agent thérapeutique/vecteur/cellule cible**, appropriée à un contexte pathologique donné. Les situations étant extrêmement variables, chaque tentative de thérapie génique est unique. Elle est réussie dès lors que le médicament amène un bénéfice thérapeutique au patient. Actuellement plusieurs types de vecteurs sont utilisés (Figures I-13). Néanmoins, les chercheurs sont confrontés à des problèmes d'efficacité et de sécurité des vecteurs. Le premier évènement indésirable fût le décès de Jesse Gelsinger atteint d'une déficience congénitale du métabolisme qui a eu lieu en 1999 aux Etats-Unis *(Lehrman, 1999)*. Ce décès est attribué à une réaction inflammatoire induite par l'adénovirus, vecteur du gène médicament *(Raper et al., 2003)*. En janvier 2000, la FDA USA ordonne l'arrêt de plusieurs essais cliniques. En février 2005, le département de la justice américaine considère comme responsable l'université de Pennsylvanie et ordonne le paiement d'une amende 570 000 dollars ainsi que des restrictions dans la recherche menée par les médecins, responsable de cet essai clinique *(Couzin et al.,*

2005). Cette tragédie est une véritable onde de choc qui frappe la communauté scientifique américaine. Les espoirs fondés sur la thérapie génique s'amenuisent et un moratoire sur l'ensemble des essais cliniques est instauré *(Zallen, 2000)*.

En France, le professeur Alain Fischer met en place avec succès un essai clinique de thérapie génique pour traiter le syndrome d'immunodéficience sévère lié au chromosome X *(Cavazzana-Calvo et al., 2000 ; Fischer et al., 2000)*. Cependant, trois ans après le traitement par thérapie génique, deux jeunes patients ont développé une prolifération incontrôlée des lymphocytes T matures. Cette anomalie est induite par l'insertion mutationnelle du rétrovirus proche du promoteur du proto-oncogène LMO2 conduisant ainsi à une expression aberrante de ce gène *(Hacein-Bey-Abina et al., 2003a,b)*. Le gouvernement français et la FDA USA stoppent les essais cliniques similaires et les patients sont traités par chimiothérapie. Après révision du protocole clinique, l'essai clinique du professeur Fischer est repris en utilisant de faibles doses de cellules modifiées. Cependant en janvier 2005, un troisième enfant a développé une leucémie impliquant un autre oncogène. Une rémission de la leucémie est observée chez deux enfants mais le troisième décède en octobre 2004. Néanmoins, depuis six ans, d'autres enfants ont bénéficié de cette thérapie et une correction de leur immunodéficience a été observée chez l'ensemble de ces patients. Suite à ces deux effets indésirables, les sociétés américaines et européennes de thérapie génique préconisent l'utilisation de vecteurs rétroviraux SIN (self-inactivating) afin d'augmenter le rapport bénéfice/risque.

Ces premiers essais cliniques nous montrent la nécessité d'allier efficacité avec sécurité. L'association efficacité/sécurité nécessite la connaissance et la maîtrise des mécanismes biologiques mis en jeu lors de la vectorisation et leurs conséquences physiologiques au cours du temps.

Nous présentons ci-dessous les différents vecteurs utilisés dans les essais cliniques de thérapie génique. Face à l'absence ou au faible nombre d'études comparatives des méthodes entre elles en terme d'efficacité et d'innocuité, il s'avère difficile de les comparer.

A

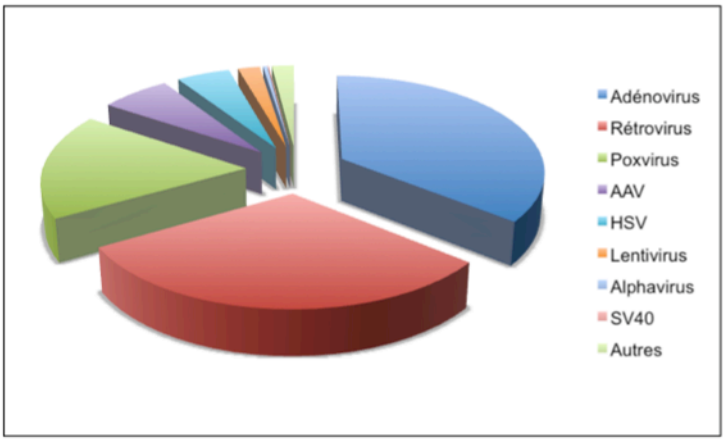

B

Vecteurs Viraux	Expression	Cellules	Caractéristiques
Adénovirus	Transitoire	Quiescentes et en division	Utilisation *ex vivo* et *in vivo* Insert 10 kb-30 kb Immunogène
Rétrovirus	Stable	En division	Utilisation *ex vivo* et *in vivo* Insert 10 kb Intégration chromosomique
Lentivirus	Stable	Quiescentes et en division	Utilisation *ex vivo* et *in vivo* Insert 10 kb
Adeno-Associated Virus	Stable	Quiescentes et en division	Utilisation *ex vivo* et *in vivo* Insert 5 kb
Herpes Simplex Virus	Transitoire	Quiescentes	Utilisation *ex vivo* et *in vivo* Insert 30-40 kb
Simian Virus 40	Stable	Quiescentes et en division	Utilisation *ex vivo* et *in vivo* Insert 5 kb Intégration chromosomique
Poxvirus	Stable	Quiescentes et en division	Utilisation *ex vivo* et *in vivo* Insert Immunogène
Alphavirus	Stable	Quiescentes et en division	Utilisation *ex vivo* et *in vivo* Immunogène

Figure I-14: Vectorisation virale. Principaux vecteurs viraux utilisés dans les protocoles de thérapie génique dans le monde en 2009 (A) et leurs principales caractéristiques (B) *(Source: www.wiley.co.uk/genetherapy).*

1. Vectorisation virale

Les virus introduisent leur ADN dans les cellules infectées avec une grande efficacité. Contrairement aux virus, les vecteurs viraux sont utilisés pour transférer efficacement des gènes thérapeutiques au sein des cellules cibles et sont délétés des gènes viraux impliqués dans la réplication du génome, la virulence et l'infection. Ces délétions rendent les vecteurs viraux plus sûrs mais leur production nécessite l'utilisation de lignées cellulaires d'empaquetage ("Packaging Cell Lines", PCL) qui sont modifiées pour remplacer les fonctions des gènes viraux délétés. Actuellement, plusieurs types de vecteurs viraux sont utilisés (Figure I-14) *(Gardlik et al., 2005)*.

1.1. Les adénovirus

Les adénovirus sont des virus non enveloppés de 70 nm de diamètre et dont leur génome est constitué d'un ADN double brin. Une cinquantaine de sérotypes différents sont connus mais les sérotypes 2 et 5 sont les plus fréquemment utilisés *(Gardlik et al., 2005)*. Les **vecteurs adénoviraux** sont produits *in vitro* à très hautes concentrations (10^{10}-10^{11} particules virales/ mL) et sont facilement utilisables. La capacité d'insertion pour un gène thérapeutique est de **10 kb à 30 kb** pour les vecteurs adénoviraux de dernière génération ("gutless vectors") *(Waehler et al., 2007)*. Les vecteurs adénoviraux possèdent la capacité de transduire efficacement les **cellules quiescentes et en division**. Ils présentent également un large tropisme cellulaire et n'ont pas la capacité de s'intégrer dans le génome de la cellule cible. Ce dernier avantage est aussi une limitation car ils ne permettent qu'une expression transitoire du gène thérapeutique. Une des limitations de ces vecteurs adénoviraux est leur **immunogénéicité** *(Lehrman, 1999)*. Afin de limiter l'immunogénéicité des protéines de la capside, ces dernières peuvent être modifiées à partir de différents sérotypes d'adénovirus. Néanmoins, cette immunogénéicité peut être utilisée dans le cadre d'une thérapie anti-cancéreuse pour stimuler la réponse immunitaire contre les cellules cancéreuses chez le patient *(Bernt et al., 2005)*.

1.2. Les rétrovirus et les lentivirus

Les rétrovirus sont des virus à ARN dont les particules virales ont une taille de 100 nm de diamètre. Pour la construction de **vecteurs rétroviraux**, les gènes *gag* (capside), *pol* (reverse transcriptase) ou *env* (glycoprotéine de l'enveloppe) sont délétés

et remplacés par le gène thérapeutique (capacité d'insertion, **10 kb**). Le transfert ciblé de gène peut être obtenu par fusion du gène *env* avec une séquence codant un ligand reconnu par un récepteur porté par les cellules cibles *(Gardlik et al., 2005 ; Waehler et al., 2007)*. La majorité de vecteurs rétroviraux est basée sur le MoMLV (Moloney murine leukemia virus). Ce virus possède la capacité naturelle de s'intégrer dans le génome de l'hôte. Cette propriété est un avantage dans le traitement des pathologies héréditaires et chroniques. Mais cette propriété constitue un risque de **mutations insertionnelles** et de toxicité basée sur la surexpression du gène thérapeutique *(Hacein-Bey-Abina et al., 2003a,b)*. Les vecteurs rétroviraux présentent deux autres limitations: (i) titre viral modéré 10^{10} particules virales/mL et (ii) l'incapacité de transduire les **cellules quiescentes**. En dépit de ces limitations, les vecteurs rétroviraux sont les plus utilisés dans les essais cliniques de thérapie génique. Pour surmonter ces limitations, des vecteurs sont dérivés des lentivirus. Les **lentivirus** (e.g. Virus d'immunodéficience humain de type I, VIH-1) sont un groupe de rétrovirus capables d'infecter les **cellules quiescentes et en division**. Les vecteurs lentiviraux assurent un transfert efficace du gène thérapeutique sans induction de réponses inflammatoires. De plus, ils permettent une expression à long terme de l'expression du transgène *(Gardlik et al., 2005 ; Waehler et al., 2007)*.

1.3. Les "adeno-associated virus" (AAV)

Les AAV sont des virus non enveloppés dont le génome est constitué d'un ADN simple brin de 4,5 kb. La majorité des vecteurs AAV sont dérivés de l'AAV de sérotype 2 *(Gardlik et al., 2003)*. Les **vecteurs AAV** sont générés par insertion du gène thérapeutique entre les deux ITRs (Inverted Terminal Repeats) remplaçant ainsi séquences codantes telles que les gènes *cap* et *rep*. La capacité d'insertion des vecteurs AAV est de **4-5 kb**. La production des particules virales nécessite des PCLs contenant les gènes *cap* et *rep* ainsi que les gènes adénoviraux E2A, E4 et VA. Les vecteurs AAV permettent une expression à long terme du gène thérapeutique. De plus, les vecteurs AAV présentent de nombreux avantages comme leur stabilité, leur sécurité, leur efficacité de transduction, leur résistance à l'inactivation par la chaleur et leur large tropisme cellulaire. Le transfert ciblé de gène peut être obtenu par remplacement du gène cap de l'AAV-2 par celui d'un autre sérotype *(Bartoli et al., 2007 ; Goyenvalle et al.,*

2004) ou par fusion du gène *cap* avec une séquence codant un ligand reconnu par un récepteur porté par les cellules cibles *(Waehler et al., 2007)*.

1.4. Les "Herpes Simplex Virus" (HSV)

Les virus HSV sont des virus enveloppés dont le génome est composé d'un ADN double brin d'une taille de 150 kb *(Gardlik et al., 2003)*. Les vecteurs HSV sont dérivés du sérotype 1. Ils sont produits par clonage du gène thérapeutique dans un plasmide codant l'origine HSV et le signal d'empaquetage *(Kennedy, 1997)*. Mais, ils peuvent être également produits par clonage du gène thérapeutique dans un plasmide encadré par des séquences spécifiques de HSV (recombinaison homologue). Ces plasmides sont transfectés dans des cellules transduites par un virus helper HSV. La délétion des gènes impliqués dans la réplication et l'encapsidation est nécessaire à la production de particules virales sûres. Le principal avantage des vecteurs HSV est leur grande capacité d'insertion pour les gènes thérapeutiques (**30-40 kb**). L'entrée en phase de latence du vecteur HSV induit une extinction de l'expression du gène thérapeutique. Mais cette limitation peut être surmontée en plaçant le gène thérapeutique sous le contrôle des promoteurs LATP1 ou LATP2 qui sont actifs en phase de latence. La sécurité et l'efficacité de transduction des cellules quiescentes ouvrent d'intéressantes perspectives dans le traitement de neuropathologie *(Kennedy, 1997)*.

1.5. Le virus SV40 (Simian Virus 40)

Le virus **SV40** est un virus non enveloppé constitué d'une capside icosaédrique. Son génome est constitué d'un ADN double brin *(Vera and Portes, 2004)*. Les vecteurs dérivés des SV40 sont obtenus par délétion du gène Tag afin de les rendre déficient pour la réplication, non oncogène et non immunologique. Les vecteurs SV40 possèdent un large tropisme cellulaire et peuvent transduire les **cellules quiescentes et en division**. Ils offrent le grand avantage de ne pas être immunogène permettant ainsi des administrations répétées *in vivo (Cordelier and Strayer, 2006 ; Cordelier et al., 2007)*. Les vecteurs SV40 sont produits à des hauts titres viraux 10^{12} UI/mL. Néanmoins, ils présentent un risque de mutations insertionnelles et leur capacité d'insertion d'un gène thérapeutique est limitée à 2,5 kb. Afin de surmonter cet obstacle, une nouvelle génération de vecteurs SV40 dit "gutless" a été développée. Ces vecteurs sont délétés des gènes Tag et des protéines de la capside. Ainsi la capacité d'insertion d'un gène

thérapeutique est repoussée à **5 kb**. La production de vecteurs SV40 nécessite l'utilisation de PCLs qui fournissent en *trans* les protéines Tag et de la capside.

1.6. Les poxvirus et les alphavirus

Les vecteurs poxvirus dérivés de **vaccinia virus** sont obtenus par introduction directe du gène thérapeutique dans le génome de vaccinia virus sans délétions antérieures *(Gardlik et al., 2005)*. Ces vecteurs présentent une large capacité d'insertion et ne s'intègrent pas le génome de l'hôte mais conservent leur capacité de réplication qui peut causer des effets secondaires telles que des réponses immunitaires *(Triozzi et al., 2005 ; Kaufman et al., 2005)*.

Les **alphavirus** sont des virus enveloppés dont le génome est constitué d'un RNA simple brin. Les vecteurs alphaviraux sont incompétents pour la réplication. La production de vecteurs alphaviraux nécessite une PCL qui amène en *trans* les gènes structuraux *(Gardlik et al., 2005)*. Cependant, leur large tropisme cellulaire, leur haute toxicité cellulaire (apoptose) et leur compétence pour la réplication confèrent aux vecteurs alphaviraux un grand avenir dans le traitement des cancers et le développement de vaccins par thérapie génique *(Vaha-Koskela et al., 2007 ; Lyons et al., 2007 ; Leslie et al., 2007)*.

Les vecteurs viraux utilisent les propriétés infectieuses des virus dont ils dérivent afin d'introduire le gène thérapeutique dans la cellule cible. Leurs efficacités de transfection sont proches de 100% in vitro. Les vecteurs viraux sont largement utilisés in vivo. Ils représentent plus de 70% des protocoles autorisés en essais cliniques (Figure I-13). Néanmoins, ils peuvent induire des évènements indésirables telles qu'une réponse immunitaire (Marshall, 1999) ou une mutation insertionnelle (Hacein-Bey-Abina et al., 2003a).

2. L'ADN plasmidique

Dans le cas des vecteurs viraux, le gène thérapeutique est inséré dans le génome des vecteurs viraux. En ce qui concerne la vectorisation de ce gène par des approches bactériologique ou physico-chimique, le gène thérapeutique est porté par un **ADN plasmidique**. L'ADN plasmidique ou plasmide est une molécule circulaire et fermée, constituée d'un ADN double brin. Contrairement aux particules virales, l'ADN plasmidique est facile à manipuler et à produire en grande quantité. De plus, il n'est pas

immunogène (i.e. absence d'anticorps anti-ADN) et sa probabilité d'insertion dans le génome de l'hôte est très faible. Par conséquent, il devient une molécule très attractive pour une délivrance de gènes thérapeutiques en toute sécurité *(Gill et al., 2009)*. Néanmoins, la vectorisation de gènes thérapeutiques par ces vecteurs est inefficace. Cependant, l'efficacité de ces derniers peut être augmentée en les associant à des méthodes de vectorisation bactériologiques, chimiques ou physiques *(Wells, 2004 ; Palffy et al., 2006).*

3. Vectorisation bactériologique

3.1. La bactofection

La **bactofection** consiste en la vectorisation directe de plasmide contenant un gène thérapeutique par des souches bactériennes au sein de cellules cibles (Figure I-15A). La principale limitation de cette approche est les effets secondaires induits par l'interaction hôte-bactéries. De plus, le système immunitaire peut provoquer une clearance rapide des bactéries ou des réactions auto-immunes. Afin de réduire ces effets secondaires, les souches bactériennes sont génétiquement modifiées pour les rendre non pathologiques et elles contiennent un gène suicide pour faciliter l'élimination de ces dernières. Les souches bactériennes franchissent la membrane plasmique par des différents mécanismes d'**endocytose**. Lors de la destruction des bactéries, les plasmides sont libérés et délivrés dans le noyau. Les principaux avantages de la bactofection sont la facilité de mise en œuvre et le tropisme cellulaire de certaines souches bactériennes *(Palffy et al., 2006)*.

3.2. La thérapie génique alternative

Dans le cadre de la **thérapie génique alternative**, les bactéries ne sont pas utilisées pour leur capacité à transfecter les plasmides mais pour leur capacité à persister dans les tissus cibles (Figure I-15B). Ces bactéries contiennent un plasmide qui permet la production ***in situ*** d'une protéine thérapeutique. En comparaison avec la bactofection, cette approche offre de nombreuses possibilités en matière de régulation de l'expression de gènes, notamment l'utilisation d'inducteurs d'expression de faibles poids moléculaires qui permettent un contrôle fin de la production de la protéine thérapeutique. Cette production peut être sécurisée par l'utilisation d'antibiotiques ou de gènes suicides (e.g. thymidine kinase). Bien que la bactofection et la thérapie génique

alternative partagent de nombreuses caractéristiques tels que les effets secondaires qu'elles peuvent induire, le seul élément qui les différencie réside dans l'expression du gène thérapeutique. En effet dans le cadre de la bactofection, l'expression du gène thérapeutique est assurée par la cellule hôte eucaryote alors que dans celui de la thérapie génique alternative les bactéries sont le siège de la production de la protéine thérapeutique *(Palffy et al., 2006)*.

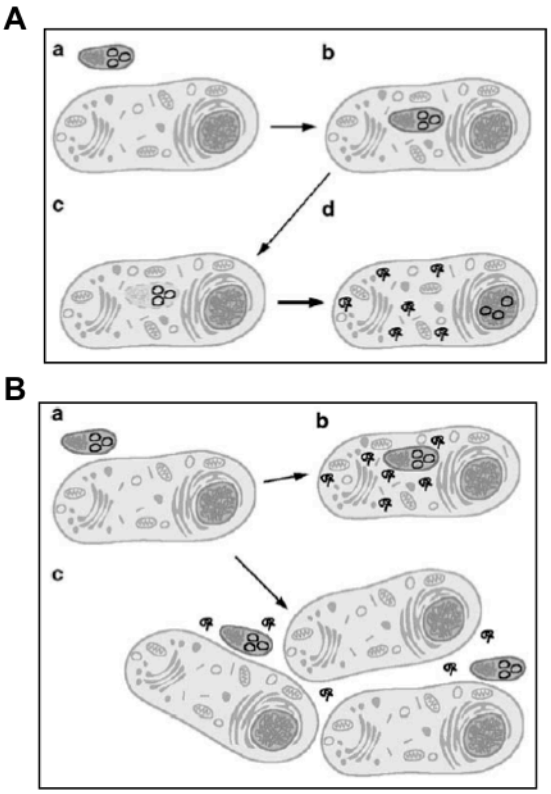

C

Vecteurs bactériologiques	Expression	Cellules	Caractéristiques
Bactofection	Transitoire Stable	Quiescentes et en division	Utilisation *ex vivo* et *in vivo* Endocytose
Thérapie génique alternative	Transitoire Stable	Quiescentes et en division	Utilisation *ex vivo* et *in vivo* Endocytose

Figure I-15: Vectorisation bactériologique: A. Bactofection: (a) Les bactéries contenant le plasmide porteur du gène thérapeutique sont injectées dans le tissu cible. (b) Les bactéries pénètrent dans les cellules (en division ou quiescentes). (c) Les vecteurs sont détruits ou subissent une lyse induite par leur présence dans le cytoplasme. (d) Les plasmides sont libérés dans le noyau et l'expression du gène thérapeutique est assurée par la cellule hôte. **B. Thérapie génique alternative:** (a) Les bactéries contenant le plasmide porteur du gène thérapeutique sont injectées dans le tissu cible. Les bactéries pénètrent dans les cellules ou restent dans la matrice extracellulaire. (b) Après leur entrée dans les cellules, l'expression du gène thérapeutique est assurée par les bactéries. (c) Les bactéries restent dans l'espace intercellulaire où sont sécrétées les protéines thérapeutiques. **C.** Principales caractéristiques de la bactofection et de la thérapie génique alternative *(D'après, Palffy et al., 2006)*.

3.3. Les souches bactériennes

De nombreuses souches bactériennes sont utilisées dans ces deux approches et elles peuvent être classifiées selon leur localisation dans l'hôte. Les bactéries peuvent être localisées dans le cytoplasme (*Listeria, Shigella*), dans les vacuoles (*Salmonella, Yersinia*) ou dans l'espace extracellulaire (*Agrobacterium*). Seulement les souches bactériennes les plus utilisées dans ces deux approches sont présentées.

Escherichia coli est un organisme modèle très bien décrit et utilisé en bactofection *(Larsen et al., 2008)* et en thérapie génique alternative *(Celec et al., 2005)*. Les souches *E. coli* utilisées en bactofection sont génétiquement modifiées pour augmenter leurs capacités à franchir la membrane plasmique et à libérer le plasmide dans le cytoplasme des cellules hôtes. Ces souches portent les gènes *inv* de *Yersinia pseudotuberculosis* qui code l'invasine et *hly* de *Listeria monocytogene* qui code la listeriolysin O. L'invasine permet à *E. coli* de pénétrer dans les cellules exprimant les intégrines β1 à leur surface (e.g. cellules épithéliales pulmonaires). La protéine listeriolysin O induit la lyse des lysosomes après phagocytose des bactéries *(Palffy et al., 2006)*.

L. monocytogenes est une souche bactérienne préférentiellement utilisée en bactofection *(Shen et al., 2004)*. La souche est génétiquement modifiée pour porter le gène *ply118* qui code la lysine qui est responsable de la lyse bactérienne et la libération du plasmide dans la cellule hôte. Les séquences de régulation de *ply118* contiennent le promoteur Pact qui est préférentiellement activé après que la bactérie soit entrée dans le cytoplasme de la cellule hôte. Cette lyse bactérienne est restreinte au cytoplasme de la cellule hôte.

Bifidobacterium longum est une bactérie anaérobique facultative utilisée en thérapie génique alternative. Après son injection systémique, la croissance de B. longum est limitée dans des aires hypoxiques telles que le tissu des tumeurs solides *(Fu et al., 2005)*. Comme *B. longum*, *Salmonella typhimurium* est utilisée en bactofection *(Niethammer et al., 2002)* et en thérapie génique alternative *(Nemunaitis et al., 2003)* dans le traitement des cancers. Cette souche bactérienne est atténuée par délétions des gènes *aroA*, *aroC* (synthèse des acides aminés aromatiques), *ssaV* (appareil de sécrétion) et *sifA* (résidence dans l'endosome). De plus, la production de TNF-α (marqueur de l'inflammation) est réduite par l'inhibition de la production du lipide A ou lipopolysaccharide qui est obtenue par délétion du gène *msbB*. Le ciblage de *S.*

typhimurium dans les tumeurs est obtenu par la délétion du gène *purI*. Ces mutants sont dépendants de sources exogènes d'adénine. Les tissus tumoraux représentent une source d'adénine à cause du renouvellement accru des cellules.

Les vecteurs bactériologiques utilisent leurs propriétés infectieuses pour introduire le gène thérapeutique dans la cellule cible (Figure I-15C). Leurs efficacités de transfection sont comparables à celles des vecteurs physiques et chimiques. Cependant, cette approche n'est utilisée que dans 1% des essais cliniques de thérapie génique dans le monde en 2009. En effet, les souches bactériennes peuvent induire une forte réponse immunitaire et d'autres effets secondaires liés à l'interaction hôte/vecteur bactériologique (Palffy et al., 2006).

4. Vectorisation chimique

Les méthodes chimiques utilisent des molécules chimiques pour complexer les plasmides. La formation de ces complexes repose sur des **interactions électrostatiques** entres les plasmides chargés négativement et des composés chimiques chargés positivement (Figure I-16).

4.1. Les liposomes et les lipoplexes

De nombreux **liposomes** ont été développés à partir de dérivés de cholestérol, de diacylglycérol et de lipopolyamines *(Pitard, 2002; Barteau et al., 2008)*. La complexation des lipides cationiques avec le plasmide conduit à la formation de particules chargées positivement appelées **lipoplexes,** qui peuvent ainsi s'associer avec les composés membranaires chargés négativement tels que les protéoglycans *(Kopatz et al., 2004)* (Figure I-16A). En plus de moduler la charge du plasmide, les lipides cationiques compactent le plasmide dans des petites particules qui facilitent son entrée dans les cellules cibles et le protègent de l'action des nucléases. Après leur association à la membrane, les lipoplexes pénètrent dans la cellule par **endocytose** induite par un récepteur. Des ligands spécifiques de récepteurs peuvent être conjugués sur les liposomes afin de cibler spécifiquement le transfert de gènes *(Carrière et al., 2004)*. Une fois dans l'endosome, l'un des composants des lipoplexes doit induire la lyse de ce dernier afin de permettre la libération du plasmide. Ensuite, le plasmide franchit l'enveloppe nucléaire et l'expression du transgène a lieu.

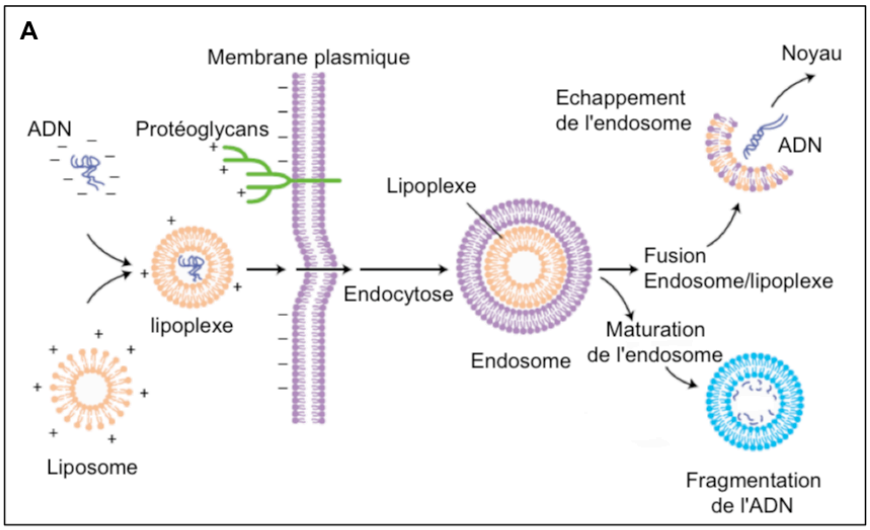

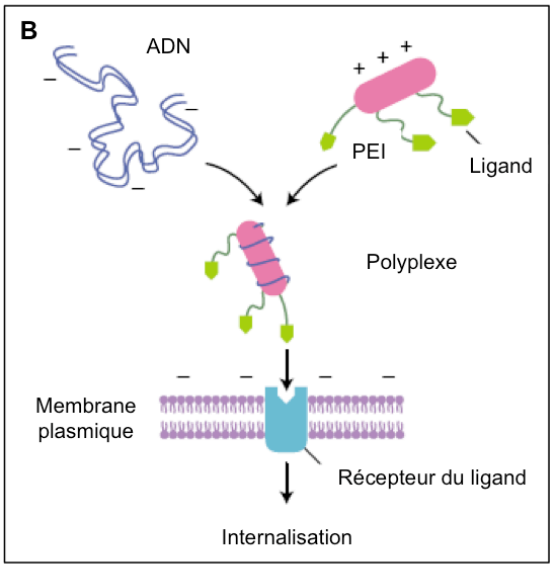

C

Vecteurs chimiques	Expression	Cellules	Caractéristiques
Liposomes Lipoplexes	Transitoire Stable	Quiescentes et en division	Utilisation *ex vivo* et *in vivo* Endocytose
Polycations Polyplexes	Transitoire Stable	Quiescentes et en division	Utilisation *ex vivo* et *in vivo* Endocytose
Vecteurs peptidiques	Transitoire Stable	Quiescentes et en division	Utilisation *ex vivo* et *in vivo* Endocytose

Figure I-16: A. Lipoplexe: Les lipides cationiques se complexent avec le plasmide. Le lipoplexe est internalisé par endocytose. Si la maturation de l'endosome et sa fusion au lysosome ont lieu, le plasmide est dégradé par les enzymes dans l'endolysosome. En revanche, si un des composants du lipoplexe induit une lyse de l'endosome, le plasmide est libéré dans le cytoplasme et il peut potentiellement atteindre le noyau, où l'expression génique a lieu. **B. Polyplexe:** Le plasmide se complexe avec un polymère cationique (PEI, poly-éthylène-imine) qui est conjugué à un ligand spécifique qui cible un type cellulaire. L'interaction ligand/récepteur permet une internalisation du polyplexe par endocytose et une expression génique cellule spécifique. **C. Vectorisation chimique:** Principaux vecteurs chimiques utilisés dans le transfert de gènes et leurs principales caractéristiques *(D'après, Parker et al., 2003)*.

4.2. Les polycations et les polyplexes

Les **polycations** synthétiques sont semblables aux liposomes tant sur le plan du principe de la méthode que sur celui du mécanisme de vectorisation du transgène (Figure I-16B). Les polycations principalement utilisés sont la poly-L-lysine, la poly-L-ornithine, la polyéthylénimine (PEI), le chitosan et les dendrimères *(Park et al., 2006)*. Les polycations condensent le plasmide en des particules de moins de 200 nm, appelées **polyplexes**, facilitant ainsi le franchissement de la membrane plasmique et induisent la lyse des endosomes (Figure I-16B). Comme pour les liposomes, des ligands peuvent être associés aux polyplexes afin d'augmenter la spécificité du ciblage du transfert de gènes *(Kim et al., 2006)*.

4.3. Les peptides

Certaines protéines et peptides possèdent la capacité de franchir la membrane plasmique et d'atteindre le cytoplasme. Il s'agit de facteurs de transcription qui appartiennent à la famille des protéines à homéodomaine, tels que la protéine Anetennapedia de *Drosophila melanogaster*, la protéine Tat du HIV-1 et les facteurs de croissances FGF-1 et FGF-2. Les peptides dérivés de ces protéines (Antp, Tat peptide) sont identifiés comme des **domaines de transduction protéique** (PTD). A partir de l'étude physico-chimique de ces peptides, d'autres peptides ont été créés comme les peptides nona-arginine, poly-histidine et les peptides amphipathiques (KALA, MAP…) *(Pichon et al., 2001 ; Deshayes et al., 2005)*. Ces peptides sont nommés "Cell-Penetrating Peptides" (CPPs). Ils ont comme propriétés communes d'être de courts peptides (30 résidus) de charge nette positive qui permet une association avec les plasmides. Les complexes ainsi formés pénètrent dans les cellules par des mécanismes dépendant ou indépendant de l'endocytose *(Duchardt et al., 2007)*. Afin d'améliorer le ciblage du transfert de gène, des ligands spécifiques de récepteurs peuvent être associés au complexe (Figure I-16).

Cependant, les vecteurs chimiques ont pour limitation le fait que le plasmide ne diffuse pas au sein du cytoplasme et noyau *(Lukacs et al., 2000)*. Par conséquent, le franchissement de l'enveloppe nucléaire ne peut être réalisé qu'au moment de la division cellulaire (limitant ainsi l'utilisation de ces méthodes au transfert de gènes dans des cellules en division). Cet obstacle peut être levé par l'addition de **séquence de**

localisation nucléaire (NLS) *(Zanta et al., 1999)* ou de **séquence de ciblage de l'ADN** (DTS) *(Vaughan and Dean, 2005 ; Miller and Dean, 2008)*.

De plus, les vecteurs chimiques montrent une certaine toxicité *in vivo* lorsqu'ils sont administrés par voie intraveineuse. Cette toxicité est induite par l'interaction de ces vecteurs avec les érythrocytes et les composants du sang chargés négativement, tels que l'albumine, qui peut induire une embolie. Néanmoins, cette toxicité peut être significativement réduite par l'ajout de composés hydrophiles aux complexes, tels que le **polyéthylèneglycol** *(Huang et al., 2007)*.

Afin d'introduire le gène thérapeutique dans la cellule cible, les processus d'endocytose sont exploités par les vecteurs chimiques. Malgré leur innocuité, ces méthodes moins efficaces que les méthodes virales ne représentent seulement que 7% des protocoles autorisés en essais cliniques en 2009 (Figure I-13).

5. Vectorisation physique

Les méthodes physiques sont basées sur une perturbation mécanique ou physique qui induit une déstabilisation de la membrane plasmique pour permettre l'accessibilité des plasmides dans le cytoplasme ou le noyau (Figure I-17).

5.1. La micro-injection

La micro-injection directe de plasmides consiste à injecter des plasmides dans le noyau d'une cellule à l'aide d'une micropipette. Cette méthode nécessite une grande adresse et un dispositif coûteux. Si les taux de transfection sont proches de 100%, le nombre de cellules traitées reste néanmoins très faible *(Chemet et al., 2009)*. Cette technique est principalement utilisée pour l'obtention d'**animaux transgéniques** *(Murphy, 2008).*

Vecteurs physiques	Expression	Cellules	Caractéristiques
Micro-injection	Transitoire Stable	Quiescentes et en division	Utilisation *ex vivo* Accès direct
Injection directe	Transitoire Stable	Quiescentes et en division	Utilisation *in vivo* Endocytose?
Injection hydrodynamique	Transitoire Stable	Quiescentes et en division	Utilisation *in vivo* Pores
Laser	Transitoire Stable	Quiescentes et en division	Utilisation *ex vivo* et *in vivo* Perforation
Ultrasons	Transitoire Stable	Quiescentes et en division	Utilisation *ex vivo* et *in vivo* Pores
Champs magnétique	Transitoire Stable	Quiescentes et en division	Utilisation *ex vivo* et *in vivo* Endocytose? Pores?
Biolistique	Transitoire Stable	Quiescentes et en division	Utilisation *ex vivo* et *in vivo* Performation
Electroperméabilisation	Transitoire Stable	Quiescentes et en division	Utilisation *ex vivo* et *in vivo* Pores?

Figure I-17: Vectorisation physique. Principaux vecteurs physiques utilisés dans le transfert de gènes et leurs principales caractéristiques.

5.2. L'injection directe

L'une des plus simples méthodes de vectorisation du plasmide est l'injection directe de ce dernier dans le tissu cible ou par voie systémique. De nombreux tissus ont été ainsi transfectés par cette méthode tels que le muscle squelettique, le foie, la peau, les tumeurs… L'injection par voie systémique est une administration conventionnelle pour l'injection de plasmides. Cependant, la rapide dégradation du plasmide par les nucléases du sérum et sa clearance par les phagocytes mononucléaires induisent une **faible efficacité de transfection**. Cette efficacité de transfection peut être améliorée en associant cette méthode avec d'autres méthodes physiques *(Ohlfest et al., 2005)*.

5.3. L'injection hydrodynamique

L'injection hydrodynamique est une méthode **simple** et **efficace** de vectorisation de plasmide nu dans le foie et le muscle squelettique de petits rongeurs *(Suda and Liu, 2007)*. Le transfert de plasmide nu dans le foie d'une souris de 20 g est réalisé par une injection rapide dans la veine caudale (HTV, Hydrodynamic Tail Vein) de 5 µg de plasmide en 5 ou 8 s dans 2 mL de solution saline *(Herweijer et Wolff, 2007)*. Dans ces conditions de vectorisation, l'expression du transgène est détectée à 90% dans le foie. Pour comprendre l'internalisation de plasmide nu dans le foie, il faut savoir que cet organe est richement vascularisé et que ses vaisseaux contiennent de nombreux et larges **pores** (ou fenestrae). L'injection hydrodynamique induit une augmentation de la pression intravasculaire conduisant ainsi à l'ouverture des pores hépatiques et au chargement du plasmide nu par les hépatocytes (**Hydroporation**) *(Zhang et al., 2004)*. Cette méthode physique est envisagée dans le traitement de pathologies hépatiques *(Takehara et al., 2007)* and hématologiques *(De Meyer et al., 2008)*. En effet, cette méthode permet un transfert efficace du gène codant le facteur de von Willebrand dans le foie de souris. Cette expression restaure la formation du clou plaquettaire dans les modèles murins du syndrome de von Willebrand *(De Meyer et al., 2008).*

Le transfert de plasmide nu dans le muscle squelettique est effectué par une injection rapide dans la veine irrigant le tissu musculaire (HLV, Hydrodynamic Limb Vein). De plus, la vectorisation est facilitée par la mise en place de garrots qui permettent d'augmenter transitoirement la pression intravasculaire. Cependant, seuls les muscles du membre isolé par les garrots sont transfectés (10-40% des fibres musculaires sont transfectées) *(Liang et al., 2004)*. Le récent développement de la

procédure HLV offre une méthode sûre et efficace dans la délivrance de gènes thérapeutiques en clinique humaine *(Herweijer et Wolff, 2007)*.

5.4. Le laser

Zeira et collaborateurs montrent la preuve de concept selon laquelle le transfert de plasmide dans les muscles peut être augmenté par l'application d'un **laser infra-rouge femtoseconde** (5 s à 30 mW). Le mécanisme par lequel le laser augmente l'efficacité de transfection serait la formation de **pores** dans la membrane plasmique *(Kurata et al., 1986)*. *In vitro*, cette méthode induit des efficacités de transfection comparable à celles obtenues par micro-injection *(Tao et al., 1987)*. Une des limitations de cette méthode est la profondeur à laquelle est focalisé le faisceau laser. En effet, dans ce travail, le laser est focalisé à 2 mm en dessous de la peau de la souris. La transposition de cette méthode en clinique humaine nécessite un dispositif moins contraignant et un pouvoir de pénétration plus important du faisceau laser *(Zeira et al., 2003)*. Le laser induit des efficacités de transfection comparable à celles obtenus avec l'électroperméabilisation dans le muscle squelettique. Cependant, contrairement à l'électroperméabilisation, le laser n'induit pas d'inflammation sévère du tissu musculaire *(Zeira et al., 2003)*. Néanmoins, ce groupe a également démontré l'application de cette méthode physique dans le domaine de la vaccination génétique intradermique contre l'antigène de surface du virus de l'hépatite B *(Zeira et al., 2007)*.

5.5. Les ultrasons

Les ultrasons sont généralement utilisés à des fins thérapeutiques et diagnostiques. Des ultrasons de faibles intensités sont utilisés dans le diagnostic par imagerie alors que des ondes de chocs ultrasonores sont utilisées dans le traitement de pathologies rénales et dans la destruction thermique de tumeurs. L'exposition d'ultrasons en présence de **microbulles** (agents de contraste utilisés en imagerie ultrasonore) augmente de plusieurs ordres de grandeur l'efficacité de transfection de plasmides *in vitro (Mehier-Humbert et al., 2005a ; Duvshani-Eshet et al., 2006).* Associé avec le cavitation acoustique, la formation de **pores** de 100 nm de diamètre avec une durée de vie de quelques secondes au sein de la membrane plasmique serait le mécanisme prédominant de pénétration des plasmides (**Sonoporation**) *(Mehier-Humbert et al., 2005b)*. *In vivo*, les muscles squelettiques et cardiaques *(Li et al., 2003 ;*

Chen et al., 2003), le foie *(Miao et al., 2005)* et le cerveau *(Hynynen et al., 2003)* ont été traités avec succès avec cette méthode de transfert *(Newman et Bettinger, 2007)*.

5.6. Les champs magnétiques

L'utilisation de champs magnétiques intenses fournit une source d'énergie suffisante pour le transfert de plasmides couplés à des **nanoparticules paramagnétiques** par l'intermédiaire de vecteurs chimiques (PEI, Lipofectamine…) *(Scherer et al., 2002)*. Une injection locale de nanoparticules (**Magnétofection**) suivie d'une application de champs magnétiques augmente l'efficacité de transfection *in vitro (Kamau et al., 2006 ; Chorny et al., 2007)* et *in vivo (Xenariou et al., 2006)*. Actuellement, le franchissement de la membrane plasmique des nanoparticules n'est pas décrit dans la littérature. Nous pouvons supposer que les champs magnétiques et/ou les nanoparticules induisent une perturbation physique et/ou mécanique de la membrane plasmique. Néanmoins, Chorny et collaborateurs ont pu démontrer que l'utilisation de nanoparticules de 375 nm de diamètre permettait d'échapper à la voie lysosomiale et d'augmenter l'efficacité de transfection *(Chorny et al., 2007).* Cependant, l'amélioration du transfert de plasmides associée avec les champs magnétiques n'apparaîtrait pas aussi importante que celle induite par l'injection hydrodynamique ou l'électroperméabilisation, bien que des comparaisons directes n'ont pas été réalisées. L'une des limitations de cette méthode est son dispositif très contraignant et qui requiert une miniaturisation *(Kamau et al., 2006 ; Chorny et al., 2007)*. Le magnétotransfert intradermique du gène VEGF permet le traitement de l'ischémie de la peau *(Holzbach et al., 2008)*. Dans le cadre d'un essai clinique (phase I), Huttinger et al., montrent que le transfert du gène GM-CSF par magnétofection dans les fibrosarcomes félins induit l'éradication de ces derniers *(Huttinger et al., 2008)*.

5.7. La biolistique

Le bombardement de microparticules ou la biolistique permet un transfert direct de plasmides dans les cellules et les tissus. Le bombardement de **particules d'or ou de tungstène** couplées à des plasmides permet une pénétration directe, à travers la membrane plasmique, dans le cytoplasme puis le noyau en échappant à la voie endosomiale. *In vitro*, cette méthode induit des efficacités de transfection comparable à celles obtenues par électroperméabilisation *(Murphy and Messer, 2001)*. Durant ces cinq dernières années, le bombardement de microparticules a été utilisé dans le

développement de stratégies de vaccination génétique et d'immunothérapie au niveau de la peau *(Ghochikyan et al., 2003 ; Dietrich et al., 2006)*. Cependant, une des limitations de cette méthode est la faible pénétration des plasmides dans le tissu, limitant ainsi son utilisation dans la délivrance de plasmides dans la peau. Néanmoins, Dileo et collaborateurs ont mis au point un nouveau protocole qui permet l'injection sous haute pression des microparticules. Ainsi, les tissus sous-cutanés tels que les muscles et les tumeurs peuvent être transfectés *(Dileo et al., 2003)*. De récents travaux ont démontré l'utilisation de cette méthode en thérapie génique contre des pathologies oculaires *(Zagon et al., 2006)* et uro-génitales *(Chuang et al., 2003).*

5.8. L'électroperméabilisation

L'électroperméabilisation permet le transfert de plasmides dans de nombreux types cellulaires ou des tissus par application d'un champ électrique externe. Ce dernier facilite la pénétration des plasmides en augmentant la perméabilité membranaire. Cette technique est **simple**, **rapide** et **peu onéreuse** *(Golzio et al., 2004).* Depuis ces quinze dernières années, cette méthode non virale connaît un grand succès *in vivo* dans la vectorisation de plasmides dans de nombreux tissus (physiologiques ou pathologiques) tels que la peau *(Titomirov et al., 1991; Vandermeulen et al., 2007; Heller et al., 2007)*, le muscle *(Aihara et Miyazaki, 1998; Mir et al., 1999; Bloquel et al., 2006)*, le cerveau *(Saito et Nakatsuji, 2001; Akaneya et al., 2005)*, le foie *(Heller et al., 1996; Liu et Huang, 2002; Jaichandran et al., 2006)*, les articulations *(Grossin et al., 2003)*, les poumons *(Pringle et al., 2007),* les tumeurs *(Rols et al., 1998b)*… Cette méthode offre de nombreuses perspectives dans le développement de protocoles de vaccination génétique *(Peng et al., 2007)* et d'immunothérapie anti-cancéreuse *(Ugen et al., 2006).*

Les méthodes physiques sont basées sur une action mécanique ou physique qui va déstabiliser la membrane plasmique pour permettre l'accessibilité des plasmides dans le cytoplasme ou le noyau. Ces méthodes, moins efficaces que les méthodes virales, restent équivalentes aux méthodes chimiques. Néanmoins, de part leurs possibilités accrues de ciblage, les méthodes physiques se développent et deviennent de plus en plus sûres. En 2009, les méthodes physiques représentent 18% des essais de protocoles cliniques autorisés dont 2 essais cliniques par électroperméabilisation (Daud et al., 2008) (Figure I-13).

PARTIE 4

L'ÉLECTROPERMÉABLISATION

Partie 4. L'électroperméabilisation

1. Introduction

L'application d'un champ électrique externe sur des cellules induit une perméabilisation transitoire de la membrane plasmique *(Teissié et al., 2005)*. Ce phénomène connu sous le nom d'électroperméabilisation ou d'électroporation confère de nouvelles propriétés à la membrane plasmique : cette dernière devient **perméable**, **fusogénique** et permet l'**insertion de protéines membranaires**. L'utilisation raisonnée d'un champ électrique externe (paramètres électriques optimisés: intensité du champ électrique, durée et nombre d'impulsions électriques) permet un transfert sûr et efficace de molécules non-perméantes (acides nucléiques, protéines, composés anti-tumoraux…) *in vitro* et *in vivo* dans le cadre d'applications cliniques *(Daud et al., 2008; Sersa et al., 2008)* et biotechnologiques *(Hui et Yuan, 2008; Zimmermann et al., 2006)*. Des applications dans le domaine des industries agroalimentaires et environnementales (e.g. stérilisation) ont également été reportées *(Mosqueda-Melgar et al., 2007; Larkin et al., 2007)*. Cependant, malgré son utilisation croissante, sa maîtrise nécessite également une meilleure compréhension des mécanismes physico-chimiques impliqués dans la réorganisation de la membrane plasmique.

La revue publiée dans *European Biophysics Journal* se concentre sur les questions liées aux mécanismes biophysiques responsables de l'électroperméabilisation de la membrane plasmique. Les récents résultats utilisant des simulations de dynamique moléculaire aussi bien que des études expérimentales sur les effets des impulsions électriques sur les composants membranaires sont discutés au sein de cette revue.

2. La revue

Eur Biophys J (2007) 36:973–983
DOI 10.1007/s00249-007-0194-7

REVIEW

Membrane perturbation by an external electric field: a mechanism to permit molecular uptake

J.-M. Escoffre · D. S. Dean · M. Hubert · M.-P. Rols · C. Favard

Received: 15 February 2007 / Revised: 9 May 2007 / Accepted: 15 May 2007 / Published online: 19 June 2007

Abstract Electropermeabilisation is a well established physical method, based on the application of electric pulses, which induces the transient permeabilisation of the cell membrane. External molecules, otherwise nonpermeant, can enter the cell. Electropermeabilisation is now in use for the delivery of a large variety of molecules, as drugs and nucleic acids. Therefore, the method has great potential in the fields of cancer treatment and gene therapy. However many open questions about the underlying physical mechanisms involved remain to be answered or fully elucidated. In particular, the induced changes by the effects of the applied field on the membrane structure are still far from being fully understood. The present review focuses on questions related to the current theories, i.e. the basic physical processes responsible for the electropermeabilisation of lipid membranes. It also addresses recent findings using molecular dynamics simulations as well as experimental studies of the effect of the field on membrane components.

Presented at the joint biannual meeting of the SFB-GEIMM-GRIP, Anglet France, 14–19 October, 2006.

J.-M. Escoffre · M. Hubert · M.-P. Rols (✉) · C. Favard
Institut de Pharmacologie et de Biologie Structurale - CNRS UMR 5089, 205 route de Narbonne, 31077 Toulouse Cedex 4, France
e-mail: rols@ipbs.fr

D. S. Dean
Laboratoire de Physique Théorique - CNRS UMR 5152, IRSAMC, Université Paul Sabatier, 118 Route de Narbonne, 31062 Toulouse Cedex 4, France

Present Address:
C. Favard (✉)
Institut Fresnel - CNRS UMR 6133, Campus de Saint Jérôme, av. Escadrille Normandie, 13397 Marseille Cedex 20, France
e-mail: cyril.favard@fresnel.fr

Abbreviations

PC	Phosphatidyl-Choline
PS	Phosphatidyl-Serine
PE	Phosphatidyl-Ethanolamine
SM	Sphingomyelin
DOPC	1,2-Dioleoyl-sn-Glycero-3-Phosphocholine
DOPS	1,2-Dioleoyl-sn-Glycero-3-Phosphoethanolamine
NBD	7-Nitrobenz-2-oxa-1,3-diazol-4-yl

Introduction

The cell membrane acts as a barrier that hinders the free entrance of most hydrophilic molecules into the cell. Their permeability can however be transiently increased by applying an electric field. This process, called electropermeabilisation and also named electroporation, has received increasing attention, particularly as an elegant and convenient means to gain access to the cytoplasm (Neumann 1989; Teissie et al. 2002; Weaver 1995). The phenomenon of electropermeabilisation has been observed for decades. Early reports were related with the death of cells caused by the irreversible permeabilisation of the cell membranes (Sale and Hamilton 1968). Studies in the 1970s revealed that short electric pulses in the μs and kV/cm range could induce transient vesicle as well as cell membrane permeabilisation leading to the transport of small molecules. Studies in the 1980s and 1990s showed that cells submitted

to longer electric pulses, i.e. in the ms range, can be transfected (Rols 2006; Teissie et al. 2005). Recent studies, coming from new technologies, concerns nanosecond pulsed electric fields, indicate that very short (10–300 ns) but high pulses (up to 300 kV/cm) induce effects that primarily affect intracellular structures and functions (Beebe et al. 2003). Therefore, the use of electric pulses to deliver therapeutic molecules has been rapidly developed over the last decade. This technology is relevant in a variety of researches and clinical settings including cancer therapy, modulation of pathogenic immune responses, delivery of therapeutic proteins and drugs (Gehl et al. 1999; Gilbert et al. 1997; Miklavcic et al. 2000; Rols 2006; Bigey et al. 2002). Electrochemotherapy, a new cancer treatment modality, has emerged (Belehradek et al. 1993; Mir et al. 1991a, b) and beside drugs, many other potentially therapeutic agents such as DNA can be electrotransfered (for review see Favard et al. 2007).

Whatever is the potentiality of this technique, there is a general agreement that very little is known about the underlying mechanisms brought into play in the cell and its membranes, following electropermeabilisation. Understanding these mechanisms is of vital importance, first to enhance the efficiency in in vitro use and secondly in order to optimise the safety of the method in its in vivo use. The major technical difficulties in the study of electropermeabilisation arise from the extreme complexity of the cell membrane and the lack of techniques available to study molecular phenomenon in living cells. The aim of this paper is to review current understanding of permeabilisation phenomena, i.e. the basic physical processes on lipid membranes. We will describe the classical electromagnetic theory behind the phenomenon and point out its limitations in its ability to give a full description of electroporation. The basic idea behind the semi-phenomenological theory for the formation of electropores is discussed, recent results coming from numerical simulations and effects of the external electric field at the molecular level are also reviewed.

The theory of electropermeabilisation

In developing a theory, it is helpful to start from a simplified model of cell membranes. In what follows, the term vesicle will be use for any kind of object constituted of an external medium and an internal medium separated by a lipid membrane (containing or not proteins) as depicted in Fig. 1.

Transmembrane electric potential modification

Most analytical theories of electropermeabilisation are based on a continuum point of view and do not take into account the precise details of the system at a molecular level. Here we will review the basic electrical theory of these systems and point out some of the underlying assumptions behind it.

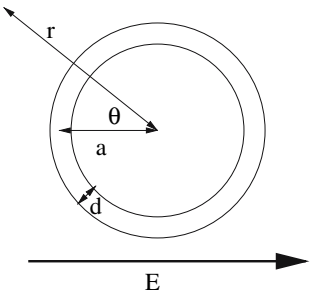

Fig. 1 Vesicle of radius a with membrane thickness d in an externally applied field $\mathbf{E}$ (direction of field indicated). r is the distance from the center of the vesicle

At the simplest level, the interaction of a vesicle with the applied electric field can be modelled by associating macroscopic electric properties with, in the simplest case, the three underlying materials of the system: the medium exterior to the vesicle, the vesicle membrane and the vesicle interior. Assuming that these components are homogeneous and have linear electromagnetic responses to applied fields the relevant electrical properties of a component are λ the electrical conductivity and ϵ the dielectric constant. In what follows we will denote the corresponding quantities by the subscripts e (exterior), m (membrane) and i (interior). The relevant Maxwell equation to compute the electrostatic potential for this system is (see for example Landau and Lifshitz 1975)

$$\nabla \cdot \left(\epsilon \frac{\partial}{\partial t} \nabla \phi + \lambda \nabla \phi \right) = 0 \tag{1}$$

and the boundary conditions are fixed away from the vesicle by the externally applied field. The local electric field $\mathbf{E}$ and current density $\mathbf{j}$ are then given by:

$$\mathbf{E} = -\nabla \phi \, ; \quad \mathbf{j} = \lambda \mathbf{E} \tag{2}$$

The second equation is simply Ohm's law and assumes a linear relationship between the induced current density and the local electric field. In most studies the local conductivity is taken to be a scalar but in principle for anisotropic systems such as a membrane it should be a tensor, there being a clear difference in the direction perpendicular to the membrane and that transverse in the membrane. The dielectric properties of the membrane are also anisotropic, we recall that the dielectric response of a material is due to the distribution and properties of its component dipoles and we thus expect different properties depending on whether we are in the region of the hydrophilic heads or the hydrophobic tail region within the bilayer. Another

important point is that the phenomenon of electropermeabilisation indicates a change in membrane structure at sufficiently high electric fields, this implies that the assumption of linear electrical response breaks down at this point and that nonlinear effects become important. However we can assume that up to this point the above set of equations gives a reasonable description of the electrical properties of the system.

The steady state equation in the presence of an applied field is the Laplace equation:

$$\nabla \cdot (\lambda \nabla \phi_s) = 0 \tag{3}$$

This equation is difficult to solve for an arbitrary geometry due to the spatial variation of λ but can be analysed in certain geometries and limits (Bernhardt and Pauly 1973; Cartree 1992; Neumann et al. 1989; Schwann 1957; Zimmermann 1974). For a planar membrane it is easily solved. If E is the applied field outside a flat membrane, the field within (perpendicular to its surface) the membrane is given by the continuity equation for the normal (in this case the only non-zero) component of the electric field

$$E_m = \frac{\lambda_e}{\lambda_m} E \tag{4}$$

This is a very simple result but has far reaching consequences. The external conductivity λ_e (which is for example of the order of 5 S/m for a weak electrolyte) is much greater than that of the membrane—typically the order of 10^{-6} S/m. This leads to a huge magnification effect with respect to the applied field. It is the creation of this large electric field within the membrane which is the basic reason for the electropermeabilisation phenomenon.

Another example which can be treated analytically is for a spherical vesicle placed in a uniform field [the case of an ellipsoidal vesicles can also be treated analytically (Bernhardt and Pauly 1973; Kotnik and Miklavcic 2000)]. The geometry is shown in Fig. 1, we denote by r the distance from the centre of the vesicle (the origin), by a the radius of the vesicle (distance from the centre of the vesicle to the middle of the membrane) and by d the thickness of the membrane. The angle θ at a given point is the angle between the position of that point from the origin and the direction of the applied field. The Laplace equation can be solved in this geometry and we find that the steady state jump in the electric potential, in the normal direction, across the membrane is given by

$$\Delta\phi_s(\theta) = \frac{3}{2} gaE\cos(\theta) \tag{5}$$

where g is a so called form factor dependent on a, d and the three electrical conductivities. In the limit where $d \ll a$, g is given by Neumann et al. (1989)

$$g = \frac{2\lambda_i\lambda_e\frac{d}{a}}{\lambda_m(\lambda_i + 2\lambda_e) + 2\frac{d}{a}(\lambda_i - \lambda_m)(\lambda_e - \lambda_m)} \tag{6}$$

In the limit where the membrane has an extremely low conductivity with respect to the other conductivities, the dielectric limit, we find that $g = 1$ and from (6) we see that the average electric field across the membrane is amplified, with respect to the applied field E by the factor a/d and its magnitude is maximal at the faces of the vesicle opposite the electrodes. Indeed it has been established for some time that it is in these electrode facing regions that the membrane becomes permeabilised. It is widely accepted that beyond a certain critical threshold $\Delta\phi_c$ permeabilisation occurs. This value of $\Delta\phi_c$ is found to be typically of the order of 100 mV (see later).

Experimentally, the vesicle or the cell is not permanently submitted to the external electric field. Therefore the variation of the transmembrane potential depends on the time t after which the pulse is applied. For a constant pulse the time dependent solution for the spherical vesicle gives the potential drop across the membrane to be

$$\Delta\phi(\theta, t) = \Delta\phi_s(\theta)\left(1 - \exp\left(-\frac{t}{\tau_m}\right)\right) \tag{7}$$

where $\Delta\phi_s$ is the steady state potential given by (5) and τ_m is the charging time of the membrane given by

$$\tau_m = aC_m\left(\frac{\lambda_i + 2\lambda_e}{2\lambda_i\lambda_e + \frac{a}{d}\lambda_m(\lambda_i + 2\lambda_e)}\right) \tag{8}$$

where C_m is the membrane capacitance per unit area. If the membrane is purely dielectric, $\lambda_m = 0$, the charging time is maximal and increases as the radius a is increased.

In order to achieve the steady state in potential drop, the external field should be applied for a time longer than τ_m. As an example, conventional electropermeabilisation protocols involve pulses of 0.1–1 kV/cm longer than 100 μs. Typically these pulses durations are much higher than the charging time constant of the outer membrane, i.e. $t_{\text{pulse}} \gg \tau_m$ (with $\tau_m \sim 1$ μs).

As stated above, when a critical value of $\Delta\phi$ is achieved across the membrane it has been observed that the lipid membrane becomes permeable (Hibino et al. 1993; Kotnik and Miklavcic 2000). The critical value has been experimentally determined to be of the order of 200–300 mV for cells (Gabriel and Teissie 1997; Teissie and Rols 1993). Clearly this critical value may be achieved before the system reaches its steady state. Thus intense but short pulses can induce the permeabilisation of the vesicle without reaching the steady state in the induced potential. For instance, recent technology authorise the use of nanosecond pulsed electric fields (nsPEFs), used in

so-called supra-electroporation, which consist in large external electric fields, i.e. 10–300 kV/cm applied in pulses shorter than 1 μs. As a confirmation of what is expected above when nsPEFs are applied to cell suspensions, they induce conduction currents in the cytoplasm exponentially decreasing with the charging time constant of the outer membrane. They also induce a corresponding displacement current through inner vesicular membrane structures (Gowrishankar et al. 2006; Vernier et al. 2004, 2006b) . For pulse durations shorter than or equal to the charging time of the outer membrane (i.e. $t_{\text{pulse}} \leq \tau_m$), a transient cytosolic field can develop membrane voltages across intracellular organelles and vesicles in excess of their critical transmembrane potential (Tekle et al. 2005; Beebe and Schoenbach 2005; Kolb et al. 2006).

The case where an electric field is applied across a suspension of cells or a tissue is more difficult to analyse, the electric field seen by a single cell is modified, with respect to the single cell case, by the presence of the others. This problem can be studied numerically and analytically using effective medium approximations (Susil et al. 1998; Pavlin et al. 2002; Yurong et al. 2005). The spirit of the effective medium approximation is that the presence of the other cells modifies the conductivity of the effective medium seen by a given cell. However for nearly dielectric membranes the potential difference generated is only weakly dependent on the conductivity of the external medium and thus the effect is not too drastic and the size the induced potential drop is not significantly changed.

In this section we have considered the effect on a vesicle of the distribution of the electric field. Of course the vesicle should be expected to react to the field at some point. Later we will discuss the theory of pore formation and it is interesting to consider how the field across a vesicle changes when pores are formed. Shown in Fig. 2 (bottom) is a spherical vesicle placed in a uniform field (from left to right) with a membrane conductivity one hundred time smaller than that of the external and internal media $\lambda_m = \lambda_e/100$. The colours on the figure (obtained by numerical solution of the Laplace equation) show the magnitude of the local electric field $|\mathbf{E}|$. We see clearly that the magnitude of the electric field is maximal at the two faces opposite the electrodes. In Fig. 2 (top) is the same vesicle but with two holes cut out at the poles opposite the electrodes. We see that the magnitude of the field within the pore regions collapses to the order of the applied field and that the maximal potential drop is across the membrane around the pore edges, however this potential drop is significantly lower than the initial drop at the poles for the membrane without holes. From these figures we see that the permeabilisation of one region of the membrane will prevent the permeabilisation of other regions by lowering the strength of the local electric field in these regions.

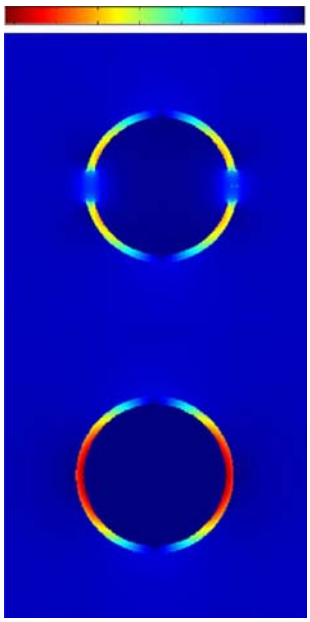

Fig. 2 Vesicles without (*bottom*) and with (*top*) pores, placed in a uniform electric field (applied horizontally), shown is the magnitude of the field $|\mathbf{E}|$ (*red high*, *blue low*)

Electromechanical effects on membranes—continuum description

Varying the different parameters of the applied electric field (value, duration, number and delay between pulses) can lead to different effects such as a slight increase in membrane conductivity, reversible electrical breakdown or irreversible breakdown leading to vesicle destruction. This latter phenomenon is often happening in systems subjected to extremely large applied electric field and was first observed in the early 1970s (Crowley 1973; Neumann and Rosenheck 1972). The electrically generated forces on the membrane can be calculated using the Maxwell stress tensor (see for instance Landau and Lifshitz 1975) and these forces will be balanced by the elastic and bending forces generated by the membrane. Deformations of the membrane are therefore determined by its mechanical properties. The elastic behaviour of a lipid membrane is generally characterised by a bending modulus and a stretching modulus. Typically bending a lipid membrane involves energy of the order of 1–10 k_BT while stretching requires much larger energy.

The first class of theories to explain electropermeabilisation were based on a continuum electrostatic and elastic description of the membrane (Crowley 1973). A perfectly flat dielectric membrane in a field is subject to an electrostatic compression. The field polarises the membrane and leads to a negative/positive polarisations charge on the surface of the membrane. The electrostatic compression

can be thought of as being generated by the attraction of these two surface charges across the membrane and this compression leads to an elastic response of the membrane. If the elasticity of the membrane (and its dielectric constant) are assumed to be independent on the thickness there is a critical field strength beyond which no equilibrium between the electrical and elastic forces is possible. This critical field strength only indicates that the model needs to be modified at high field strengths or becomes unphysical. It is however an indication that some new physics comes into play but does not tell us what it is. This model has a number of other drawbacks, the field necessary for the breakdown is too large with the experimentally observed permeabilisation threshold. Also a high degree of compression is predicted before the breakdown (40% compression), however this means that the membrane capacitance should vary up to the breakdown point but this is not observed.

For curved membranes the situation is however quite different, the stresses on spherical vesicles have been studied (Isambert 1998) and the resulting asymmetry leads to net lateral forces (which in the flat case above cancel exactly) and an increase in the surface tension Γ which is of the order

$$\Delta\Gamma \sim \frac{9\epsilon_m}{8d} E^2 a^2 \tag{9}$$

This increased surface tension is a result of the curved and closed geometry of the vesicle. In a planar membrane any local curvature, for example due to thermal fluctuations, induced asymmetry between the two sides and lead to net lateral stresses which can induced undulation instabilities beyond a critical field strength and these instabilities are again associated with an unspecified breakdown but not necessarily permeabilisation (Sens and Isambert 2002). We should however note that the lateral stress in this case leads to a negative contribution to the surface tension.

There seems to be a number of scenarios under which a membrane model can be destabilised by the application of an electric field. This destabilisation could be identified as the onset of electropermeabilisation. A common criticism made of this point of view is that this approach predicts an instability at a well defined field strength, however experimental evidence strongly suggests that there is a stochastic component in electropermeabilisation. Permeabilisation is seen to be achieved with a certain probability or after a certain time dependent on the applied field and other factors.

The creation of pores

When a membrane cannot be compressed or deformed it will need another way to minimise the electric stress. One solution is to become permeable, the defaults (or holes or pores) created in the membrane decrease the area of the membrane and strongly increase the membrane conductivity.

The theory of electroporation for cell membranes is similar to the theory of soap film rupture (Derjaguin and Gutop 1961). If one imagines a membrane with surface tension Γ_0 and then one cuts a circular hole in it of radius r, the energy change in the system due to the hole is

$$W(r) = -\Gamma_0 \pi r^2 + 2\pi\gamma_0 r \tag{10}$$

where γ_0 is a line tension associated with the pore, where the hydrophobic membrane interior is in contact with the water in the pore. Strictly speaking γ_0 should be r dependent as for large pores the hydrophilic lipid heads can line the pore interior and the energy cost is more associated with a bending one than a hydrophobic one. For pore radii smaller than $r_c = \gamma_0/\Gamma_0$ the effective force on the pore tries to close it while for $r > r_c$ the pore expands indefinitely—this scenario is associated with membrane rupture. In this simple model, pore formation in the membrane is clearly favoured by increasing the membrane surface tension Γ_0. In fact membrane pore formation has been observed in vesicles when the surface tension is increased by applying mechanical stress or even using intense light (Sandre et al. 1999). In these experiments the pore formation was seen to be temporary, pores open until leak-out of internal fluid relaxes the tension and the pores close. In order to slow down the time scale of this process to one over which it is observable the vesicles were immersed in a viscous environment. The line tension γ_0 in giant vesicles has been experimentally measured to be 10^{-11} N (Zhelev and Needham 1993). The energy function $W(r)$ can be interpreted as the energy of a particle at position r and in the limit where inertial and hydrodynamic effects can be neglected one can write a Smoluchowski equation for the number density of pores of radius r, denoted by $n(r)$ (Pastushenko et al. 1979; Powell and Weaver 1986)

$$\frac{\partial n}{\partial t} = \frac{\partial}{\partial r}\left[D\left(\frac{\partial n}{\partial r} + \frac{n}{k_B T}\frac{\partial W}{\partial r}\right)\right] \tag{11}$$

where D is the pore radius diffusion constant. This equation, although some what idealised, can be used to compute properties such as the number of pores $\int n(r)\,\mathrm{d}r$ and the area occupied by the pores $\int n(r) r^2\,\mathrm{d}r$. This is by no means a unique model for pore dynamics (although it is certainly the most popular) and versions dominated by inertial effects and hydrodynamics have also been studied (Wilhem et al. 1993; Karatekin et al. 2003).

The key point in electroporation theory is to quantify the dependence of the pore energy function $W(r)$ as a function

of r and also how to distinguish between small hydrophobic pores and larger hydrophilic pores. In most models the pores are taken to be nonconducting (Abidor et al. 1979; Barnett and Weaver 1991) and the energy change is taken into account by considering the change of the pores specific capacitance as water replaces lipid in a cylindrical region of radius r through the membrane thickness. This then gives a pore energy which depends on the potential drop across the membrane $\Delta\phi$ and effectively increases the surface tension term Γ to $\Gamma(\Delta\phi)$ which is given by

$$\Gamma(\Delta\phi) = \Gamma_0 + \frac{1}{2}\frac{\epsilon_m}{d}\left(\frac{\epsilon_e}{\epsilon_m} - 1\right)\Delta\phi^2 \tag{12}$$

where ϵ_e is the dielectric constant of the external medium, water or salt solution. The typical values of these dielectric constants are $\epsilon_e = 80\epsilon_0$ and $\epsilon_m = 2\epsilon_0$, where ϵ_0 is the vacuum permittivity. This increase in the effective surface tension then lowers the energy barrier for pore formation and also decreases the critical radius r_c beyond which the pore becomes unstable.

However the situation when the pores are considered to be conductive is quite different (Wilhelm 1993; Winterhalter and Helfrich 1987). Here the effect of the field decreases the surface tension (thus inhibits pore formation), however it decreases the line tension γ thus favouring the formation of pores for small radii. Explicitly it was shown

$$\Gamma(\Delta\phi) = \Gamma_0 - \frac{1}{2}\epsilon_m\frac{\Delta\phi^2}{d} \tag{13}$$

$$\gamma(\Delta\phi) = \gamma_0 - \frac{1}{2}\epsilon_e\frac{\Delta\phi^2}{\pi} \tag{14}$$

This means that conductive pores favour the early stage of pore formation but tend to stabilise larger pores and so the behaviour of conductive and non-conductive pores is quite different. It seems that a model reconciling these two limits is still to be proposed. Clearly we expect that the dielectric description is most relevant for small pores but beyond a certain radius conductive effects become dominant.

Equations of the form (10) describe hydrophilic pores where the lipid head groups are assumed to line the pore interior. These head groups will tend to repel each other due to steric and/or electrostatic interactions. These effects can be taken into account by including an interaction term of the pore with itself $W_{\text{int}}(r) = C/r^4$ where C is positive (Barnett and Weaver 1991). This repulsive interaction stabilises hydrophilic pores (gives a local minimum of W at $r \neq 0$). This modified potential cannot be valid at very small r as we know that the state with no pores exists. Thus there is a critical value R_* below which W must take another form. This is the radius below which there is no space to line the pores with the hydrophilic heads and thus the pore is hydrophobic. The simplest model for a hydrophobic pore is just to take $W(r) = \frac{1}{2}\kappa r^2$ for $r < r_*$. This form can be derived from microscopic modelling (Glaser et al. 1988) but in physics this simple harmonic oscillator form for the energy about a stable point is rather generic. The coefficients of the model can be taken to assure that W is continuous at r_* and that the minimum in the potential of W for $r > r_*$ occurs before r_* thus giving (meta-)stable hydrophilic pores.

The exposition above is applicable for single pores and does not take into account their interaction. Even without an applied field the pores should be coupled by the membrane tension, as a pore opens up it relaxes the tension of the others. This tension coupling can be taken into account in terms of A_p the total area occupied by the pores in a model proposed by Neu and Krassowska (2003). Apart from this the effective potential drop $\Delta\phi$ should also be modified by the presence of pores and the electrostatic energy for a hydrophilic toroidal pore is also different to that of a cylinder (Neu et al. 2003).

Despite some impressive success in describing experimental results the above theories still need to be tested at a molecular level, for instance by molecular dynamics simulations. While they have more microscopic details than continuum models they still rely on certain continuum concepts such as line and surface tensions.

Molecular dynamics simulation

Advantages and limitations

Biophysical and biological methods used to study the electropermeabilisation process present kinetics and sensitivities which, respectively, permit only millisecond and micrometre scale resolution of post-pulse membrane modifications. Moreover, these methods are rather indirect and only permit the visualisation of the consequences of permeabilisation such as the entrance or efflux of molecules. Therefore, they can not be used to visualise molecular phenomena with nanosecond resolution. Recently (for instance see the review by Tieleman 2006) these small distance and short time aspects has however been studied using molecular dynamics simulations. Nevertheless, molecular simulations present some limitations. Indeed, the complexity (one or two lipids components) and size of the simulations systems are still rather limited and certain quantitative aspects found in these simulations, for instance the critical permeabilisation field threshold, do not agree with experimental data. However these simulations give vital insight into the permeabilisation process and we may

have some confidence in the qualitative results of such simulations. In addition simulations can also be used to test the validity of theoretical models of pore formation by evaluating the energy change associated with a pore (Leontiadou et al. 2004; Wohlert et al. 2006).

Pore formation under applied tension

In a typical atomistic molecular dynamics simulation the system consists of 500 lipids in the bilayer and there are 20 or so water molecules in the system for each lipid. Before examining the effect of an electric field on these bilayers it is interesting to examine the effect of membrane surface tension on pore formation. In these systems a negative surface tension is applied, this can be achieved by choosing the area occupied per lipid be less than the equilibrium one (Leontiadou et al. 2004; Wohlert et al. 2006). For instance imposing an area per lipid of 0.60 nm^2 rather than the simulation equilibrium one of 0.62 nm^2 imposes a surface tension of about −10 mN/m (Wohlert et al. 2006). It is found that beyond a critical lateral pressure (–50 to –10 bar) pores form in the simulations and are stable over the life time of the simulations. The pores that are formed in these simulations are hydrophilic : when a hole is formed through the hydrophobic chains of the lipids, the lipid head groups reorientate in order to face the water entering the membrane. In Leontiadou et al. (2004) the line tension γ of (10) is estimated to be 3×10^{-11} N, and is the same order of magnitude as the experimental estimate mentioned in Sect. ''Creation of pores''.

Electropermeabilisation

Simulations involving electric fields across a membrane is a heavy computational task in molecular dynamics simulations as the field must be calculated from the charge distribution and acts not only on charged components of the system but also on the dipole moments of the system, and in particular the solvent water. The force acting on a dipole of moment **d** is given by

$$\mathbf{f} = \mathbf{d} \cdot \nabla \mathbf{E} \tag{15}$$

and is zero in a constant field. However where the field varies strongly the dipole is subjected to strong forces. In the simulations of Tieleman (2004), on phospholipid bilayers, it was shown that the initial step in the electroporation process is quite different to that of electroporation under an applied lateral tension. The field applied were of the order of 0.5 V/nm and the poration proceeds by penetration of water molecules into the lipid bilayer due to the strong electrical forces acting on their dipole moments. As the water molecules penetrate the bilayer the local variations of the electric field in these defects lead to further forces on the dipoles, thus accelerating the process of pore formation. In this initial step of pore formation the pores are hydrophobic but eventually are lined with the phospholipid head groups and thus become hydrophilic. The presence or absence of salt is found to have little effect on the initial process of pore formation. Indeed simulations on an octane layer in water, with no charged head groups or salt, shows exactly the same behaviour. Similar results were found in the simulations of Tarek (2005), where wire-like chains of water were seen to penetrate the bilayer. The pores are then again stabilised by a lining of lipid head groups.

Vernier et al. (2004) showed that when an electric field of 0.45 V/nm is applied on DOPC-DOPS bilayer, the poration is observed on time scales shorter than 5 ns and PS translocation occurred only along pore walls (see Fig. 3). PS lipids do not facilitate water pore formation, consistent with the idea that interactions in the hydrophobic interior of the membrane govern the relative ease of spread of water column into the bilayer (Tieleman 2004). When the field polarity is changed, PS translocation is reversed. This result suggested that pulse-driven PS externalisation appears to be an electrophoretic transport of PS head groups through hydrophilic pores (Vernier et al. 2006a).

Gene electrotransfer

DNA is an anionic and hydrophilic molecule which under normal circumstances can not cross the plasma membrane. However, electropermeabilisation allows an increased membrane permeability with respect to DNA. The molecular basis behind this process of gene electrotransfer is highly debated. Indeed, there are two hypotheses: the first suggests that DNA is transported through large stable pores that form without significant interaction with DNA molecules and then reseal. Krassowska's theoretical model and Tieleman's molecular simulation back up this hypothesis

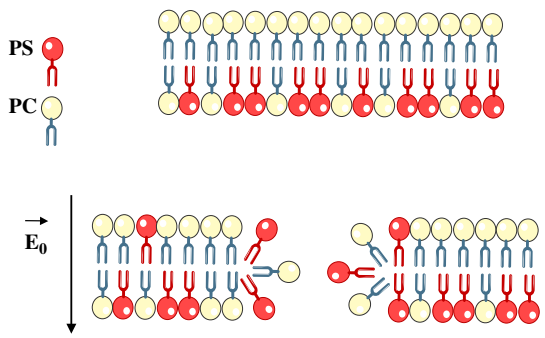

Fig. 3 Phosphatidylserine translocation: pulse-driven PS externalisation appears to be an electrophoretic transport of PS headgroups through hydrophilic pores

(Krassowska and Filev 2007; Smith et al. 2004; Tieleman 2004). The second hypothesis, which is more widely supported, is as follows. Experimental investigations (Golzio et al. 2002; Sukharev et al. 1992) and molecular simulations suggest that DNA molecules migrate into cells by direct interaction with lipids and by forming intermediates that involve lipid/DNA complexes. In this hypothesis, electric field application induces many pores of a diameter which is too small to allow DNA transport (steric, entropic and image charge forces prevent the passage). However, when the electric field is switched off, structural modifications can assure DNA translocation into the cytoplasm. Indeed, plasma membrane is a dynamic and functional assembly which consists of several molecules and presents heterogeneity of lateral and transversal distribution of these molecules. Consequently, one can suggest that such induced-electric field perturbations on membrane components distribution could promote DNA translocation.

Electric field effect on membrane components

We have previously seen how analytical theories and molecular simulation can predict the existence of pores in idealised or simplified vesicles. Nevertheless, in order to fully understand the effect of electric field on membranes, it is necessary to analyse its effects on the membrane components.

Transbilayer mobility

Phospholipid distribution in two leafs of plasma membrane is asymmetric. Indeed, PE and PS phospholipids are presents in the inner leaf whereas PC phospholipids set in the outer leaf of plasma membrane. Transmembrane asymmetry is supported by proteins like flippases and floppases (Janmey and Kinnunen 2006). Some investigations showed that this transmembrane asymmetry is lost when electric field is applied in cells (Dressler et al. 1983; Haest et al. 1997). Haest et al. (1997) described that the passive transbilayer mobility of fluorescently labeled (using NBD) lipids in erythrocytes increase with the strength, the duration and the number of field pulses (Fig. 3). Moreover, this study revealed that the enhanced mobilities induced by electropermeabilisation differ for the NBD-lipids used (the following mobility ordering is observed: SM $\ll$ PS $<$ PC $<$ PE). These enhanced transbilayer mobilities of the phospholipid probes do not return to their normal values even during the prolonged resealing of field-pulse-treated cells (24–27 h at 37°C, Haest et al. 1997). Moreover, ATP-dependent components of the flip-flop of lipid probes are suppressed in electroporated and resealed cells. This inhibition is partly due to loss of cellular Mg^{2+} during the electropermeabilisation. Indeed, the electropermeabilisation induces the entry and the exit of, respectively, water and ATP. Translocated lipids contribute to the stabilisation of water channels (Kotulska et al. 2007; Tarek 2005). Moreover, Devaux showed that membrane lipids translocation can induce microvesicles formation (100–200 nm) (Devaux 2000). Consequently, one can suppose that electro-translocated lipids play also a role in endocytosis mediated by electric field. Such electroendocytosis process has been observed on cells several hours after the electropermeabilisation (Mahrour et al. 2005; Antov et al. 2005). The key point in these investigations is that if the electropermeabilisation phenomenon is very fast (induced at the nanoseconds to milliseconds time range of order) its consequences can persist for a long time (from minutes to hours).

Lateral diffusion

Several investigations have suggested that when low electric fields (LEFs) are applied on cells, electrophoretic segregation of charged lipids and proteins occurs in the plane of the cell membrane (McLaughlin and Poo 1981). Indeed, the tangential electric field (E_θ) in the cell membrane is a driving force which induces electromigration towards the anode or cathode sides of the cell, either by electrophoretic mobility of charged components or by electrophoresis (Fig. 4). For weakly conducting membranes this tangential components is given by

$$E_\theta = \frac{3}{2} E \sin(\theta). \tag{16}$$

An asymmetric distribution of acetylcholine receptors in embryonic muscle cells or Concanavalin A receptors in

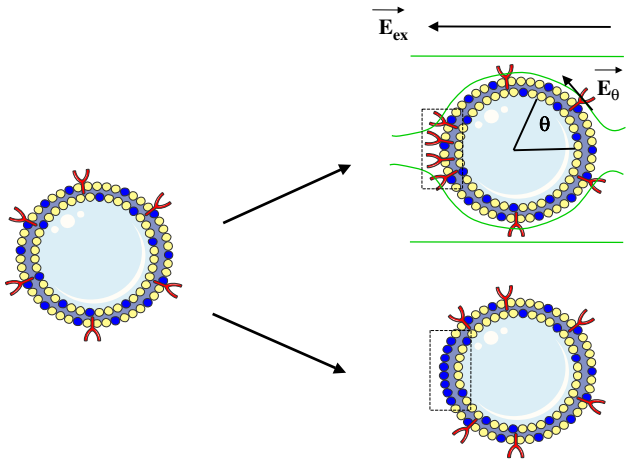

Fig. 4 Proteins and lipids electromigration: the external E_{ex} and tangential electric field, E_θ, is a driving force which induce electrophoretic mobility of proteins and/or lipids toward cathodic sides of the cell. *Green lines* represent electric field lines

Xenopus myoblasts, is induced when a DC electric field of 10 V/cm is applied for 45 min up to 3 h (Lin-Liu et al. 1984; McLaughlin and Poo 1981). McLaughlin and Poo 1981 have described that the the additional exposure of Xenopus myoblasts to the same strength of field but with opposite polarity for 10 min completely reverses the asymmetric accumulation of Con A receptors towards other side of the cell. Moreover, the lateral electromigration of epidermal growth factor receptors on corneal epithelial cells (Zhao et al. 1999) and $F_{c\epsilon}$ receptors on rat basophilic leukaemia cells toward the cathodic sides of the cell occurs when a DC electric field of 1.5 V/cm is applied for 12 h and when a 10 V/cm field is applied for 30 min to 1 h. The common point made in these investigations is that protein electromigration occurs only when electric fields of these orders are applied over a relatively long period of time. Consequently, one can speculate that low electric field application during short time scale causes limited electrophoretic motility which induces limited and reversible protein aggregation, as opposed to what happens for long exposure times. These results may have direct consequences on subsequent transport process across the membrane. Antov et al. (2005) have suggested that the electrophoretic segregation of charged components (e.g., glycolipids and glycoproteins) in the outer leaflet on the cell membrane is responsible for both enhanced adsorption and stimulated uptake via changes in the membrane elastic properties that enhance budding and fission processes. This phenomenon is called *electroendocytosis*.

Protein conformations

Several investigations have suggested that membrane proteins (i.e. voltage-sensors in skeletal muscle fibers) may undergo some structural and functional damage during the electric injury (Teissie and Tsong 1980; Chen and Lee 1994). Membrane proteins consist of amino acids which carry electrical charges (Tsuji and Neumann 1983) and each peptide unit is an electric dipole with a moment of about 3.5 Debyes. The major functional structure of the membrane protein is α-helical. In this structure, many peptide dipoles are aligned to form larger dipoles of the order of 120 Debyes across the plasma membrane (Hol 1985). In response to physiological membrane potential changes, these electric dipoles are perturbed in voltage-dependent membrane proteins (i.e. channel proteins, voltage sensors). An external electric field will strongly affect the electric dipoles in membrane proteins and this may cause conformational and functional damage (Chen 2005). Indeed, a 4 ms transmembrane potential pulse of –600 mV results in a reduction of both Na^+ and K^+ channel conductivities, and a reduction of ionic selectivity of the K^+ channels against Na^+ ions. This phenomenon induces a depolarisation of the membrane resting potential in frog skeletal muscle membrane. The kinetics of the spontaneous reversal of the electroconformational damage of channel proteins was found to be dependent on the magnitude of imposed membrane potential pulse (Chen and Lee 1994).

Conclusion

The current state of our theoretical understanding of membrane permeabilisation due to electromagnetic fields, and the associated transport of molecules, is some what incomplete and limited. Certain effects of the electric field parameters on membrane permeabilisation, and the associated transport of molecules, are well established but a great deal of what happens at the molecular level remains speculative. Molecular dynamics simulations are now giving interesting new insight into the process. However, a cell membrane is highly complex and can not be considered as the simple assembly of one or two classes of lipids. Electroinduced destabilisation of the membrane includes both lateral and transverse redistribution of lipids and proteins, leading to mechanical and electrical modifications which are not yet fully understood. One may suggest that such modifications can be involved in the subsequent transport of molecules interacting with them such as the DNA molecules. Experimental verification of the basic mechanisms leading to the electropermeabilisation and other changes in the membrane remain a priority given the importance of these phenomena for processes in cell biology and in medical applications.

Acknowledgments This work was supported by the *Association Française contre les Myopathies*.

References

Abidor IG, Arakelyan VB, Chernomordik LV, Chizmadzhev YA, Pastushenko VF, Tarasevich (1979) Electric breakdown of bilayer membranes I: the main experimental facts and their qualitative description. Bioelectrochem Bioenerg 6:37–52

Antov Y, Barbul A, Mantsur H, Korenstein R (2005) Electroendocytosis: exposure of cells to pulsed low electric fields enhances adsorption and uptake of macromolecules. Biophys J 88:2206–2223

Barnett A, Weaver JC (1991) Electroporation: a unified, quantitative theory of reversible electrical breakdown and mechanical rupture in artificial planar bilayer membranes. Biolectrochem Bioenerg 25:163–182

Beebe SJ, Schoenbach KH (2005) Nanosecond pulsed electric fields: a new stimulus to activate intracellular signalling. J Biomed Biotechnol 4:297–300

Beebe SJ, White J, Blackmore PF, Deng Y, Somers K and Schoenbach KH (2003) Diverse effects of nanosecond pulsed electric fields on cells and tissues. DNA Cell Biol 22:785–796

Belehradek M, Domenge C, Luboinski B, Orlowski S, Belehradek J Jr, Mir LM (1993) Electrochemotherapy, a new antitumor treatment. First Clin Phase I-II Trial Cancer 72:3694–700

Bernhardt J, Pauly H (1973) On the generation of potential difference across the membrane of ellipsoidal cells in an alternating electric field. Biophysik 10:89–98

Bigey P, Bureau MF, Scherman D (2002) In vivo plasmid DNA electrotransfer. Curr Opin Biotechnol 13:443–447

Cartee LA, Plonsey R (1992) The transient subthreshold response of spherical and cylindrical cell models to extracellular stimulation. IEEE Trans Biomed Eng 39:76–85

Chen W (2005) Electroconformational denaturation of membrane proteins. Ann N Y Acad Sci 1066:92–105

Chen W, Lee RC (1994) Altered ion channel conductance and ionic selectivity induced by large imposed membrane potential pulse. Biophys J 67:603–612

Crowley JM (1973) Electrical breakdown of bimolecular lipid membranes as an electromechanical instability. Biophys J 13:711–24

Derjaguin BV, Gutop YV (1961) Theory of the breakdown (rupture) of free films. Kolloidn Zh 24:370–374

Devaux PF (2000) Is lipid translocation involved during endo-exocytosis? Biochimie 82:497–509

Dressler V, Schwister K, Haest CW, Deuticke B (1983) Dielectric breakdown of the erythrocyte membrane enhances transbilayer mobility of phospholipids. Biochim Biophys Acta 732:304–307

Favard C, Dean DS, Rols MP (2007) Electrotransfer as a non viral method of gene delivery. Curr Gene Ther 7:67–77

Gabriel B, Teissie J (1997) Direct observation in the millisecond time range of fluorescent molecule asymmetrical interaction with the electropermeabilized cell membrane. Biophys J 73:2630–2637

Gehl J, Sorensen TH, Nielsen K, Raskmark P, Nielsen SL, Skovsgaard T, Mir LM (1999) In vivo electroporation of skeletal muscle: threshold, efficacy and relation to electric field distribution. Biochim Biophys Acta 1428:233–240

Gilbert RA, Jaroszeski MJ, Heller R (1997) Novel electrode designs for electrochemotherapy. Biochim Biophys Acta 1334:9–14

Glaser RW, Leikin SL, Chernomordik LV, Pastushenko VF, Sokirko AI (1988) Reversible electrical breakdown of lipid bilayers and formation and evolution of pores. Biochem Biophys Acta 940:275–287

Golzio M, Teissie J, Rols MP (2002) Direct visualization at the single-cell level of electrically mediated gene delivery. Proc Natl Acad Sci U S A 99:1292–1297

Gowrishankar TR, Esser AT, Vasilkoski Z, Smith KC, Weaver JC (2006) Microdosimetry for conventional and supra-electroporation in cells with organelles. Biochem Biophys Res Comm 341:1266–1276

Haest CWM, Kamp D, Deuticke B (1997) Transbilayer reorientation of phospholipids probes in the human erythrocytes membrane. Lessons from studies on electroporated and resealed cells. Biochim Biophys Acta 1325:17–33

Hibino M, Itoh H, Kinosita K, (1993) Time courses of cell electroporation as revealed by submicrosecond imaging of transmembrane potential. Biophys J 64:1789–1800

Hol WGJ (1985) Effects of the alpha-helix dipole upon the functioning and structure of proteins and peptides. Adv Biophys 19:133–165

Isambert H (1998) Understanding the electroporation of cells and artificial bilayer membranes. Phys Rev Lett 80:3404–3407

Janmey PA and Kinnunen PKJ (2006) Biophysical properties of lipids and dynamics membranes. Trends Cell Biol 16:538–546

Karateki E, Sandre O, Guitouni H, Borghi N, Puech P-H, Brochard-Wyart F (2003) Cascades of transient pores in giant vesicles: Line tension and transport. Biophys J 84:1734–1749

Kolb JF, Kono S, Schoenbach KH (2006) Nanosecond pulsed electric field generators for the study of subcellular effects. Bioelectromagnetics 27:172–187

Kotnik T, Miklavcic D (2000) Analytical description of transmembrane voltage induced by electric field on spheroidal cells. Biophys J 79:670–679

Kotulska M, Kubica K, Koronkiewicz S, Kalinowski S (2007) Modeling of the induction of lipid membrane electropermeabilization. Bioelectrochemistry 70:64–70

Krassowka W, Filev PD (2007) Modeling electroporation in a single cell. Biophys J 92:404–417

Landau LD, Lifshitz EM (1975) Electrodynamics of continuous media. Pergamon Press, Oxford

Leontiadou H, Mark AE, Marrink SJ (2004) Molecular dynamics simulations of hydrophilic pores in lipid bilayers. Biophys J 86:2156–2164

Lin-Liu R, Adey WR, Poo MM (1984) Migration of cell surface concanavalin A receptors in pulsed electric fields. Biophys J 45:1211–1217

Mahrour N, Pologea-Moraru R, Moisescu MG, Orlowski S, Levêque P, Mir LM (2005) In vitro increase of the fluid-phase endocytosis induced by pulsed radiofrequency electromagnetic fields: importance of the electric field component. Biochem Biophys Acta 1668:126–137

McLaughlin S, Poo MM (1981) The role of electro-osmosis in the electric-field-induced movement of charged macromolecules on the surfaces of cells. Biophys J 34:85–93

Miklavcic D, Semrov D, Mekid H, Mir LM (2000) A validated model of in vivo electric field distribution in tissues for electrochemotherapy and for DNA electrotransfer for gene therapy. Biochim Biophys Acta 1523:73–83

Mir LM, Belehradek M, Domenge C, Orlowski S, Poddevin B, Belehradek J Jr, Schwaab G, Luboinski B, Paoletti C (1991a) Electrochemotherapy, a new antitumor treatment: first clinical trial. C R Acad Sci III 313:613–618

Mir LM, Orlowski S, Belehradek J Jr, Paoletti C (1991b) Electrochemotherapy potentiation of antitumour effect of bleomycin by local electric pulses. Eur J Cancer 27:68–72

Neu JC, Krassowska W (2003) Modeling postshock evolution of large electropores. Phys Rev E 67:021915–021926

Neu JC, Smith KC, Krassowska W (2003) Electrical energy required to form large conducting pores. Bioelectrochem Bioenerg 60:107–114

Neumann E, Rosenheck K (1972) Permeability changes induced by electric impulses in vesicular membranes. J Membr Biol 10:279–290

Neumann E, Sowers AE, Jordan CA (1989), Electroporation and electrofusion in cell biology. Plenum, New York

Pastushenko VF, Chizmadzhev YA, Arekelyan VB (1979) Electric breakdown of bilayer membranes II. Calculation of the membrane lifetime in the steady-state diffusion approximation. Bioelectrochem Bioenerg 6:53–62

Pavlin M, Pavselj, Miklavcic D (2002) Dependence of induced transmembrane potential on cll density, arrangement, and cell position inside a cell system. IEEE Trans Biomed Eng 49:605–612

Powell KT, Weaver JC (1986) Transient aqueous pores in bilayer membranes: a statistical theory. Bioelectrochem Bioenerg 15:211–227

Rols MP (2006) Electropermeabilization, a physical method for the delivery of therapeutic molecules into cells. Biochim Biophys Acta 1758:423–428

Sale AJ, Hamilton WA (1968) Effects of high electric fields on micro-organisms. 3. Lysis of erythrocytes and protoplasts. Biochim Biophys Acta 163:37–43

Sandre O, Moreaux L, Brochard-Wyart F (1999) Dynamics of transient pores in stretched membranes. Proc Nat Acad Sci USA 96:10591–10596

Schwan HP (1957) Electrical properties of tissue and cell suspensions. Adv Biol Med Phys 5:147–209

Sens P, Isambert H (2002) Undulation instability of lipid membranes under an electric field. Phys Rev Lett 88:128102–128105

Smith KC, Neu JC, Krassowska W (2004) Model of creation and evolution of stable electropores for DNA delivery. Biophys J 86:2813–2826

Sukharev SI, Klenchin VA, Serov SM, Chernomordik LV, Chizmadzhev Yu A (1992) Electroporation and electrophoretic DNA transfer into cells. The effect of DNA interaction with electropores. Biophys J 63:1320–1327

Susil R, Semerov D, Miklavcic (1998) Electric field-induced transmembrane potential depends on cell density and organization. Electro-Magnetobiol 17:391–399

Tarek M (2005) Membrane electroporation: a molecular dynamics simulation. Biophys J 88:4015–4053

Teissie J, Rols MP (1993) An experimental evaluation of the critical potential difference inducing cell membrane electropermeabilization. Biophys J 65:409–413

Teissie J, Tsong TY (1980) Evidence of voltage-induced channel opening in Na/K ATPase of human erythrocyte membrane. J Membr Biol 55:133–140

Teissie J, Eynard N, Vernhes MC, Benichou A, Ganeva V, Galutzov B, Cabanes PA (2002) Recent biotechnological developments of electropulsation. A prospective review. Bioelectrochemistry 55:107–112

Teissie J, Golzio M, Rols MP (2005) Mechanisms of cell membrane electropermeabilization: a minireview of our present (lack of ?) knowledge. Biochim Biophys Acta 1724:270–280

Tekle E, Oubrahim H, Dzekunov SM, Kolb JF, Schoenbach KH, Chock PB (2005) Selective field effects on intracellular vacuoles and vesicle membranes with nanosecond electric pulses. Biophys J 89:274–284

Tieleman DP (2004) The molecular basis of electroporation. BMC Biochem 5:10

Tieleman DP (2006) Computer simulations of transport through membranes:passive diffusion, pores, channels and transporters. Clin Exp Pharm Phys 33:893–903

Tsuji K, Neumann E (1983) Conformational flexibility of membrane proteins in electric fields I. Ultraviolet absorbance and light scattering of bacteriorhodopsin in purple membranes. Biophys Chem 17:153–163

Vernier PT, Sun Y, Marcu L, Craft CM, Gundersen MA (2004) Nanoelectropulse-induced phosphatidylserine translocation. Biophys J 86:4040–4048

Vernier PT, Ziegler MJ, Sun Y, Gundersen MA, Tieleman DP (2006a) Nanopore-facilitated, voltage-driven phosphatidylserine translocation in lipid bilayers-in cells and in silico. Phys Biol 3:233–247

Vernier PT, Sun Y, Gundersen MA (2006b) Nanoelectropulse-driven membrane perturbation and small molecule permeabilization. BMC Cell Biol 7:1–16

Weaver JC (1995) Electroporation theory. Concepts and mechanisms. Methods Mol Biol 55:3–28

Wilhelm C, Winterhalter M, Zimmermann U, Benz R (1993) Kinetics of pore size during irreversible electric breakdown of lipid bilayer membranes. Biophys J 64:121–128

Winterhalter M, Helfrich W (1987) Effect of voltage on pores in membranes. Phys Rev A 36:5874–5876

Wohlert J, den Otter WK, Edholm O, Briels WJ (2006) Free energy of a trans-membrane pore calculated from atomist molecular dynamics simulations. J Chem Phys 124:154905–154914

Yurong Q, Shengli L, Yuehua J, Taicheng Y, Jie W (2005) Transmembrane voltage induced on a cell membrane in suspensions exposed to an alternating field: a theoretical analysis. Bioelectrochemistry 67:57–65

Zhao M, Dick A, Forrester JV and McCaig CD (1999) Electric field-directed cell motility involves up-regulated expression and asymmetric redistribution of the epidermal growth factor receptors and is enhanced by fibronectin and laminin. Mol Biol 10:1259–1276

Zhelev DV, Needham D (1993) Tension stablized pores in giant vesciles: determination of pore size and pore line tensions. Biophys Acta 1147:89–104

Zimmermann U, Pilwat G, Riemann F (1974) Dielectric breakdown of cell membranes. Biophys J 14:881–899

3. Les conclusions

L'état actuel de nos connaissances sur les mécanismes biophysiques de l'électroperméabilisation de la membrane plasmique et le transport de molécules associé, est limité *(Teissié et al., 2005)*. Certains effets des paramètres des impulsions électriques sur la perméabilisation membranaire, et le transport de molécules, sont bien établis mais peu d'éléments à l'échelle moléculaire sont connus. Les études de **dynamique moléculaire** donnent aujourd'hui des perspectives prometteuses dans la compréhension des mécanismes de l'électroperméabilisation à l'échelle moléculaire. Cependant, une membrane plasmique est très complexe et ne peut pas être considérée comme un ensemble simple d'une ou de deux classes de lipides. La déstabilisation électrique de la membrane inclut une **redistribution latérale et transversale des lipides et des protéines**, menant à des modifications mécaniques et électriques qui ne sont pas encore entièrement comprises. De telles modifications peuvent être impliquées dans la perméabilisation membranaire et dans le transport de molécules telles que les molécules de plasmide. La vérification expérimentale des mécanismes de base conduisant à l'électroperméabilisation et à d'autres changements de la membrane demeure une priorité étant donnée l'importance de ces phénomènes dans les processus en biologie cellulaire et dans des applications médicales.

PARTIE 5

L'ÉLECTROTRANSFERT DE PLASMIDE

Partie 5. L'électrotransfert de plasmide

1. Etat des lieux

Le principe de base de l'électrotransfert de plasmide *in vitro* consiste à l'application contrôlée d'un champ électrique externe sur des cellules en présence d'un plasmide. L'expression du gène est détectée quelques heures après la remise en culture des cellules transfectées et persiste pendant plusieurs jours. L'efficacité de transfection dépend du type cellulaire et de l'état physiologique des cellules *(Golzio et al., 2004)*. En raison des potentialités cliniques de cette méthode, la compréhension des mécanismes devient un enjeu majeur.

La revue publiée dans *Molecular Biotechnology* décrit les différents aspects connus des mécanismes impliqués dans l'électrotransfert et les limites actuelles du transfert de molécules de plasmide dans les cellules.

1.2. La revue

Mol Biotechnol (2009) 41:286–295
DOI 10.1007/s12033-008-9121-0

REVIEW

What is (Still not) Known of the Mechanism by Which Electroporation Mediates Gene Transfer and Expression in Cells and Tissues

Jean-Michel Escoffre · Thomas Portet · Luc Wasungu · Justin Teissié · David Dean · Marie-Pierre Rols

Published online: 18 November 2008

Abstract Cell membranes can be transiently permeabilized under application of electric pulses. This treatment allows hydrophilic therapeutic molecules, such as anticancer drugs and DNA, to enter into cells and tissues. This process, called *electropermeabilization* or *electroporation*, has been rapidly developed over the last decade to deliver genes to tissues and organs, but there is a general agreement that very little is known about what is really occurring during membrane electropermeabilization. It is well accepted that the entry of small molecules, such as anticancer drugs, occurs mostly through simple diffusion after the pulse while the entry of macromolecules, such as DNA, occurs through a multistep mechanism involving the electrophoretically driven interaction of the DNA molecule with the destabilized membrane during the pulse and then its passage across the membrane. Therefore, successful DNA electrotransfer into cells depends not only on cell permeabilization but also on the way plasmid DNA interacts with the plasma membrane and, once into the cytoplasm, migrates towards the nucleus. The focus of this review is to describe the different aspects of what is known of the mechanism of membrane permeabilization and associated gene transfer and, by doing so, what are the actual limits of the DNA delivery into cells.

Keywords Gene transfer · Gene expression · Membrane · Electric field · Electroporation · Electropermeabilization

Introduction

The administration of naked nucleic acids into cells and tissues can be considered as the simplest and safest method for gene delivery [1]. However, one drawback of the method for gene therapy is the low efficiency of gene expression. Therefore, different strategies have been developed for years in this field, based on the use of virus as biological vectors and on the development of chemical or physical methods. The common aspect of these methods is to transfer DNA into cells via cell membrane modification. Virus and chemical vectors fuse with the plasma membrane and/or are endocytosed. Physical approaches transiently destabilize the membrane creating leaky structures or "pores". One of the most successful, but indeed the only one, clinical trials of gene therapy has been obtained with virus for the treatment of severe combined immunodeficiency disease, but this clinical trial had to be suspended because the virus caused leukaemia due to the insertion of the gene near an oncogene [2–4]. Therefore, there is still nowadays a challenging need to develop an efficient and safe method for gene transfer.

The use of electric pulses as a safe tool to deliver therapeutic molecules to tissues and organs has been

Jean-Michel Escoffre and Thomas Portet have contributed equally to this work.

J.-M. Escoffre · T. Portet · L. Wasungu · J. Teissié · M.-P. Rols (✉)
CNRS, IPBS (Institut de Pharmacologie et de Biologie Structurale), 205, Route de Narbonne, 31077 Toulouse, France
e-mail: rols@ipbs.fr

J.-M. Escoffre · T. Portet · L. Wasungu · J. Teissié · M.-P. Rols
Université de Toulouse, UPS, IPBS, 31077 Toulouse, France

T. Portet · D. Dean
Laboratoire de Physique Théorique - CNRS UMR 5152, IRSAMC, Université Paul Sabatier, 118 Route de Narbonne, 31062 Toulouse cedex 4, France

rapidly developed over the last decade. The method refers to the transient increase in the permeability of cell membranes when submitted to electric field pulses. This process is commonly known as *electropermeabilization* or *electroporation* [5]. Hydrophilic molecules that are otherwise non-permeant, such as the highly toxic drug bleomycin, can gain direct access to the cytosol of cells. A cancer treatment modality, *electrochemotherapy (ECT)*, has emerged [6–8]. It is successfully used in clinical trials for cancer treatment [9–12]. Beside drugs, electropermeabilization can be used to deliver a wide range of potentially therapeutic agents including proteins, oligonucleotides, RNA and DNA [13]. Nowadays, it represents one of the most widespread techniques used in molecular genetics. In vivo gene electrotransfer is of special interest since it is the most efficient non-viral strategy for gene delivery and also because of its low cost, easiness of realization and safety. The most widely targeted tissue is skeletal muscle. The strategy is not only promising for the treatment of muscle disorders, but also for the systemic secretion of therapeutic proteins. Vaccination and oncological gene therapy are other fields of application [14]. *Electrogenetherapy (EGT)* is relevant in a variety of researches and clinical settings including cancer therapy, modulation of pathogenic immune responses, delivery of therapeutic proteins and drugs [15]. This, together with the capacity to deliver large DNA constructs, greatly expands the research and clinical applications of in vivo DNA electrotransfer [16–22].

However, the mechanisms underlying cell membrane permeabilization and associated gene transfer are not completely understood. This is of high importance for in vitro use in terms of efficiency but also for in vivo use in terms of security. The successful electrotransfer of plasmid DNA into cells depends on the way the cell membrane has been permeabilized, reversibly or not, and on the way DNA interacts with the membrane and is transported from the plasma membrane towards the nuclear envelope. The focus of this review is to describe the different aspects of what is known (and still not known) on the mechanism of membrane electropermeabilization and associated gene transfer and by doing so, reviewing what are the actual limits for DNA delivery into cells.

Basics of Cell Membrane Electropermeabilization

Membrane Electropermeabilization or Membrane Electroporation?

As its name suggests, the basic theory of *electroporation* is that the electric field causes the formation of pores in the membrane [23, 24]. Theoretical models have been proposed to explain the mechanism of this reversible membrane electropermeabilization and its potentiality to allow the access of non-permeant molecules inside the cells [25]. The formation of pores is supported by a thermodynamic approach because it allows the reduction of the electrostatic energy of the system. It is hindered by the line tension needed to create the associated transbilayer hole (assumed to be a cylinder). It is thus only at a critical value of the field strength (energy threshold) that their formation is possible. Roughly speaking, the poration process is an activated one, similar to nucleation, where the surface tension term favours pores formation while the line tension tends to suppress it. The effect of the electric field is to effectively increase the surface tension and thus lower the activation barrier [26].

It is widely accepted however that the standard theory of electroporation has limits [27]. These pores have never been observed. Large post pulse pores, arising from primary pores have indeed been detected in red blood cells pulsed under hypoosmotic conditions [28]. An alternative theory, which is less familiar because of conflicts with experimental results, is based on an electromechanical instability where the electric field compresses the membrane. Molecular dynamics and coarse grain simulations are the newest approaches. Computer simulations at the microscopic length scale are becoming possible, however the complexity and more importantly the size of the system that can be simulated are still rather limited [29]. Molecular dynamics has suggested that electropores (in fact water leaks) could be generated but they have been obtained only under field conditions larger than those experimentally required to induce reversible membrane permeabilization [30]. The geometry of the membrane and its mechanical properties such as surface to volume ratio, rigidity and composition, for example the role played by microdomains, must be taken into account as well as the surface tension and line tension associated with the pores. Indeed, only a few experimental data concerning the molecular changes involved in membrane electropermeabilization have been reported. ^{31}P NMR studies performed both on model membranes and on mammalian cells suggested a reorganization of the polar head group region of the phospholipids leading to a weakening of the hydration layer [31, 32]. Transbilayer reorientation of phospholipid probes has been reported in the human erythrocyte membrane suggesting an increase in the flip-flop of phospholipids as a direct consequence of electropermeabilization [33].

Altogether, and even if the term electroporation is commonly used among biologists, the term electropermeabilization should be preferred in order to prevent any molecular description of the phenomenon.

Membrane Electropermeabilization is Controlled by the Transmembrane Voltage

It has been known for more than 30 years that, as far as membrane permeabilization is concerned, the key effect of electric field on cells is a position-dependent change in the resting transmembrane potential difference $\Delta\Psi_o$ of their plasma membrane. If we model the cell membrane as a thin spherical dielectric shell, the electrically induced potential difference $\Delta\Psi_E$, which is the difference between the potential inside the cell Ψ_{in} and the potential outside the cell Ψ_{out}, at a point M on the cell surface is given by:

$$\Delta\Psi_E(t) = \Psi_{in} - \Psi_{out} = -g(\lambda)rE\cos\theta(M)\left[1 - e^{-t/\tau}\right] \quad (1)$$

where t is the time after the onset of the electric pulse, g depends on the conductivities λ of the membrane, of the cytoplasm and of the extracellular medium, r is the radius of the cell, E the field strength, θ(M) the angle between the normal to the membrane at the position M and the direction of the field and τ is the membrane charging time [34]. The field-induced potential difference is added to the resting potential [35, 36]

$$\Delta\Psi = \Delta\Psi_o + \Delta\Psi_E. \quad (2)$$

Being dependent on the angular parameter θ, the field effect is position-dependent on the cell surface. Therefore, the side of the cell facing the anode is going to be hyperpolarized while the side of the cell facing the cathode is depolarized (Fig. 1a). This theoretical prediction has been experimentally validated by using a voltage-sensitive fluorescent dye [37]. The transmembrane potential difference of a cell exposed to an electric field is therefore a critical parameter for successful cell permeabilization, whatever the size of the cell, its shape or orientation [38, 39]. It defines the sites (location, extend) where molecules uptake can take place.

Membrane Electropermeabilization is Controlled by Electric Field Parameters

Permeabilization indeed occurs only on the part of the cell membrane where potential difference has been brought at its critical value [36, 40]. This value has been evaluated in the order of 200–300 mV independently of the cell type [41, 42]. Permeabilization is therefore controlled by the field strength. This means that field intensity E larger than a critical value, Ep, must be applied. E_p is dependent on the size of the target cells. It ranges from values close to 200 V/cm in the case of large cells such as myotubes to 1–2 kV/cm in the case of bacteria [41]. Large cells are therefore more sensitive to lower field strengths than smaller ones. Electric field values have therefore to be adapted to each cell line in order not to affect their viability. The field strength triggers permeabilization: when E is larger than E_p, it controls the area of the cell surface which is affected [43]. From Eq. 1, it is clear that for field intensities close to E_p, permeabilization is only present for θ values close to 0 or π. Under that condition, only the localized parts of the membrane surface facing the electrodes are affected. However, within these permeabilized cell caps, the extent of permeabilization is not a function of the field strength [42, 44, 45], whereas, it is controlled by the number and duration of electric pulses [45]. So, membrane permeabilization only occurs for electric field values E higher than the threshold value E_p, whatever the pulse number and the pulse duration. Increasing E, above

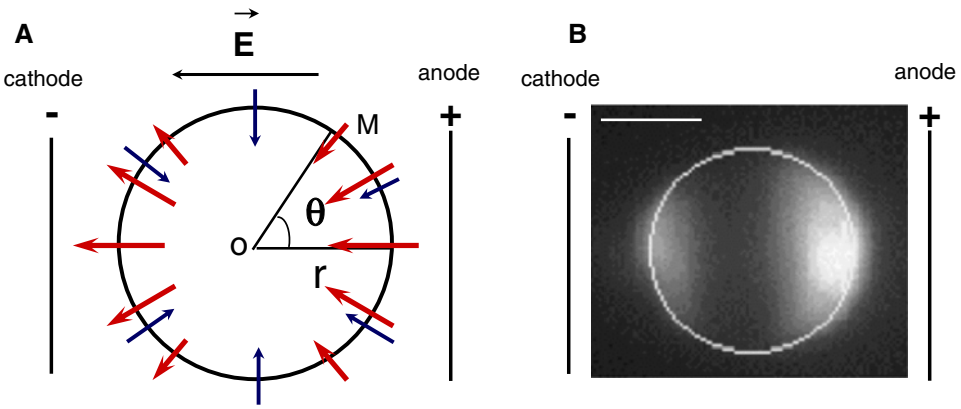

Fig. 1 Physical principle of electropermeabilization. **a** The plasma membrane is the site of native transmembrane potential difference, $\Delta\Psi 0$ (*Blue arrow*). If we consider the cell like a sphere and the plasma membrane like a dielectric spherical shell, when we apply an electric pulse, an induced transmembrane voltage $\Delta\Psi E$ is created (*Red arrow*). Being dependent on the angular parameter θ, the $\Delta\Psi E$ effect is position-dependent on the cell surface; therefore, the side of the cell facing the anode is hyperpolarized while the side of the cell facing the cathode is depolarized. **b** The localization and asymmetry of electropermeabilization can be detected by propidium iodide uptake in a CHO cell submitted to a train of 10 pulses, 5 ms, 1 Hz at 0.7 kV/cm. Scale bar: 10 μm

E_p, leads to an increase in the area where permeabilization takes place and, in that particular area, the extent of permeabilization is determined by the number and duration of electric pulses.

This electro-induced permeabilization of the cell membrane can be quantified in terms of the flow F_S of molecules S diffusing through the plasma membrane. Fick's law and experimental data obtained in the case of the release of ATP from mammalian cells allowed to establish that:

$$F_S(t) = P_S x(N,T) A/2\left(1 - E_p/E\right)\Delta S\, e^{-k(N,T)t} \quad (3)$$

where P_S is the permeation coefficient of the molecule S across the membrane, x is a function which depends on the pulse number N and the pulse duration T, it represents the probability of permeabilization ($0 < x < 1$), A is the cell surface, E is the applied electric field intensity, E_p the threshold for permeabilization, ΔS is the concentration difference of S between cell and external medium, k is the time constant of the resealing process and t is the time after the pulse [44]. Such a concept leads to the notion of *membrane domains* involved in electropermeabilization: *macrodomains* where permeabilization can take place, which area is determined by the pulse intensity according to: $A/2\ (1 - E_p/E)$, and, within that macrodomains, *microdomains (defects, permeant structures)* where permeabilization actually takes place, which density depends on the pulse number and on the pulse duration according to the x function. The molecular characteristics of these domains in terms of lipid and proteins composition, structures and dynamics remain an open question.

Membrane Electropermeabilization is a Fast and Localized Process

The use of videomicroscopy allowed visualization of the permeabilization phenomenon at the single cell level. Propidium iodide, a fluorescent non-permeant molecule, can be used as a probe for small molecules. Its uptake in the cytoplasm is a fast process that can be detected during the seconds following electric pulses application. In less than 1 min, it appears at the nucleus level. Moreover, exchange across the pulsed cell membrane is not homogeneous on the whole cell membrane. It occurs at the sides of the cells facing the electrodes on an asymmetrical way (Fig. 1a). It is more pronounced at the anode-facing side of the cells than at the cathode one, i.e. in the hyperpolarized area than in the depolarized one [46], in agreement with the above theoretical considerations and Eqs. 1 and 2.

Electropermeabilization can therefore be described as a 3-step process in respect with electric field (EF):

(i) Before EF: membrane acts as a barrier that prevents the free exchange of hydrophilic molecules between cell cytoplasm and external medium.
(ii) During EF: when reaching a threshold value, the transmembrane potential increase induces the formation of local *Transient Permeable Structures* facing the electrodes that allow the exchange of molecules.
(iii) After EF: resealing is occurring. Membrane permeability to small molecules is present with a lifetime ranging from seconds to minutes depending on EF conditions and on the temperature [44, 47]. After resealing, the uptaken solutes are sequestered inside the treated cell.

However, in the case of larger molecules (MW above 4 kDa), direct transfer to the cytoplasm is only observed if macromolecules (proteins, DNA) are present during the electric pulse. Proteins added after the permeabilizing electric field can indeed enter the cell by macropinocytosis [48, 49]. Gene expression is only obtained when DNA is present during application of the pulses. Therefore, the mechanism of macromolecules uptake is different from the one observed for small molecules.

Basics of Plasmid DNA Electrotransfer and Expression

Theoretical Considerations

Although the first pioneering report on plasmid DNA electrotransfer in cells has been published more than 20 years ago by E. Neumann [23], the mechanisms that mediate DNA electrotransfer remain to be elucidated. Different scenario can be proposed [50]. The simplest one is that the membrane is permeabilized, then the DNA is pushed through the *putative electropores* by the electrophoretic effect, which may be necessary to overcome the problem of passing a charge into the relatively low dielectric medium of the membrane. Another possibility is that the electric field leads to an aggregation of ion pumps which open and permit the passage of the DNA. Finally, another scenario is that the DNA forms a charged vesicle which is internalized by the cell in an endocytic process.

IIn the context of studies on model membranes, DNA interactions with lipid bilayers have indeed been studied. DNA injection by a micropipette, to a part of a giant unilamellar vesicle, resulted in membrane topology transformations which can be monitored using phase contrast microscope [51, 52]. DNA-induced endocytosis was observed in the absence of any electric field. A possible mechanism for DNA/lipid membrane interaction is DNA encapsulation within an inverted micelle included in the lipid membrane. High-molecular mass DNA that was

efficiently taken up by large unilamellar vesicles exposed to a short pulse of electric field (0.1–1 ms) with an intensity as high as 12.5 kV/cm indicated that DNA was taken up as a result of the electrostimulated formation of endosome-like vesicles rather than via field-induced membrane pores [53]. Other data report that electrotransfer of DNA through lipid bilayer could be mediated by transient complexes between DNA and the lipids in the pore edges of elongated, electropercolated hydrophilic pore zones [54]. Moreover, the association of DNA with a lipid bilayer greatly facilitates the transport of small ions. This suggests a locally conductive DNA/lipid interaction zone where parts of the DNA strand may be transiently inserted in the bilayer, leaving other parts of the DNA probably protruding out from the outer surface of the bilayer. DNA is not only transiently inserted in, but also actually electrophoretically pulled through, the permeabilized zones onto the other membrane side leaving finally the bilayer structure basically intact [55].

DNA Electrotransfer Depends on Membrane Permeabilization but also on DNA Electrophoresis

Electrotransfection, i.e. plasmid DNA electrotransfer into cells and then its expression, is detected for electric field values leading to plasma membrane permeabilization. Millisecond pulses are generally required to obtain efficient gene expression i.e. keeping intact the cell viability, by limiting the electric field intensities required when short pulses are used [47, 56, 57]. Nevertheless electrotransfection can be obtained with short strong pulses [23]. Transfection threshold values are the same as those for cell permeabilization [58].

The transfection efficiency TE obeys the following equation:

$$\mathrm{TE} = KNT^{2.3}\left(1 - E_p/E\right)f(\mathrm{ADN}) \quad (4)$$

where K is a constant. The dependence on the plasmid concentration f(ADN) is rather complex and it is observed that high levels of plasmids are toxic [59]. The effect of pulse duration appears to be crucial. Pulse duration appears to be a key parameter for efficient gene expression in cells and tissues [23, 60].

Electrically induced DNA uptake by cells is a vectorial process with the same direction as DNA electrophoresis in an external electric field [61, 62]. The transfection efficiency is significantly higher in cell monolayers facing the cathode compared to those exposed to field pulses of the reverse direction. This is due to contribution of the electrophoresis to the translocation of the polyanionic plasmid DNA across the electropermeabilized cell membrane [63]. The polarity of the electric field has therefore a direct effect on transfection. Adherent cells facing the cathode exhibit much higher transfection yield as well as gene expression than cells facing the anode [63]. This dependance of the transfection efficiency on the direction of the field might be due to the involvement of the electrophoretic force in the translocation of the negatively charged DNA molecule [61]. While cell permeabilization is only slightly affected by reversing the polarity of the electric pulses or by changing the orientation of pulses, transfection level increases are observed. These last effects are due to an increase in the cell membrane area where DNA interacts [64].

The use of a two-pulse technique allowed the separation of the two effects provided by an electric field: membrane electropermeabilization and DNA electrophoresis. The first pulse (high voltage, μs time range duration) creates permeabilization efficiently. The second pulse of much lower amplitude, but substantially longer (ms time range), does not cause permeabilization and transfection by itself but enhances TE in muscles by about one order of magnitude. In vivo, the effect of electrophoresis is not completely understood. A recent publication indicates that electrophoresis may not be instrumental in electro-gene transfer [65]. But several studies from the group of Mir show the benefit of the combination of short high-voltage and long low-voltage pulses allowing to evidence the necessity of association of cell electropermeabilization and convenient electrophoretic transport of DNA towards and/or across the permeabilized membrane within the tissue [66–68]. DNA electrotransfer has indeed been achieved in tibialis cranialis muscles of C57BL/6 mice by using such long but low-intensity pulses [69, 70]. Other data performed in the skin also demonstrate that the combination of such electric pulses is an efficient protocol to enhance DNA expression [71].

DNA Electrotransfer is a Multistep and Localized Process

Fluorescent plasmids indeed allow to monitor the interaction of nucleic acids with field treated cells. DNA molecules, negatively charged, migrate when submitted to an electric field. In low electric field regime, the DNA simply flows around the membrane towards the anode. However beyond a critical permeabilizing field value ($E_c > E_p$) the DNA interacts with the permeabilized membrane, but only at the pole facing the cathode (as opposed to the case for small molecules that are observed to enter the cells through both poles) [46]. Clusters or aggregates of DNA are formed, but once the field is turned off the growth of these clusters is stopped. The DNA/membrane interaction is not homogeneously distributed on the permeabilized areas facing the cathode (macrodomains) but is present into membrane *competent sites* whose size

range from 0.1 to 0.5 μm. These observations are consistent with a process where plasmids interact with electropermeabilized part of the cell surface, following their interfacial electrophoretically driven insertion [5, 72]. Due to the good correlation between visualization of DNA insertion in the membrane and gene expression, these results are consistent with a multistep process of DNA electrotransfer (Fig. 2):

(i) Before EF: membrane acts as a barrier that prevents the entrance of plasmid DNA into the cell.
(ii) During EF, the plasma membrane is permeabilized on the sides of the cell facing the electrodes and the negatively charged DNA migrates electrophoretically towards the plasma membrane on the cathode side where it is inserted in particular domains.
(iii) After EF, a translocation of the plasmid to the cytoplasm takes place leading to gene expression. This second step, including plasmid DNA diffusion in the cytosol and its passage through the nuclear pores, remains rather poorly understood.

New directions of research are needed to characterize membranes domains involved in molecule electrotransfer. DNA transfer occurs through *competent domains* present in the electropermeabilized cell membrane. Their size is in the same range of order than the so-called rafts domains. Lipid rafts are plasma membrane microdomains enriched in sphingolipids and cholesterol. These domains have been suggested to serve as platforms for various cellular events, such as signalling and membrane trafficking [73, 74]. One can wonder if they are involved in DNA electrotransfer.

DNA Expression from DNA Electrotransfer is Hindered by Internal Membrane

If the first steps of gene electrotransfection, i.e. migration of the plasmid DNA towards the electropermeabilized plasma membrane and its interaction with it, are starting to be described and therefore represent guidelines to improve gene electrotransfer, the successful expression of the plasmid depends on its subsequent migration into the cell. Therefore, diffusional properties of plasmid DNA, metabolic instability of plasmid DNA in cells and tissues as well as plasmid DNA nuclear translocation represent cell limiting factors that have to be considered [75].

The cytoplasm is composed of a network of microfilament and microtubule systems, and a variety of subcellular organelles bathing in the cytosol. The mesh-like structure of the cytoskeleton, the presence of organelles and the high protein concentration impose an intensive molecular crowding of the cytoplasm which limits the diffusion of large sized macromolecules. The translational mobility of macromolecule smaller than 500–750 kDa is only 3–4 fold slower than in water, but it is markedly impeded for larger molecules [76]. Mobility of plasmid DNA is negligible in the cytoplasm of microinjected myotubes [77]. But, successful in vivo DNA expression can be obtained by electric fields. These discordant results might be explained by the disassembly of the cytoskeleton network that may occur

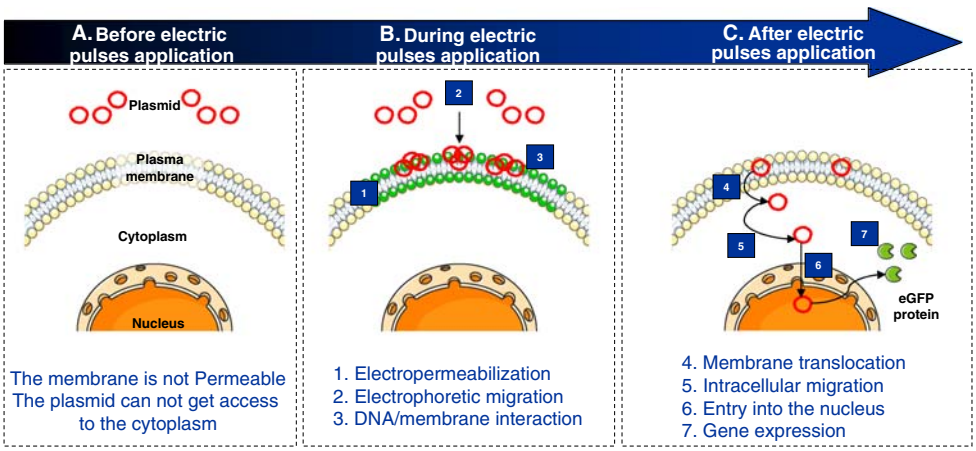

Fig. 2 DNA electrotransfection: Electrotransfection mechanism is a multistep process. **a** Before electric pulses application: DNA molecules are labelled with fluorescent marker, rhodamine. DNA molecules are incubated with CHO cells. No natural adsorption of DNA molecules on plasma membrane is observed. **b** During electric pulses application: Plasma membrane is electropermeabilized (step 1; in *green*). DNA molecules undergo the electrophoretic migration (step 2) and interact with permeabilized membrane. DNA aggregates are formed (step 3). This interaction takes place only on the membrane facing the cathode. **c** After electric pulses application: DNA translocation into the cytoplasm occurs 30 min after application of electric pulses (step 4). Then, DNA molecules migrate into the cytoplasm (step 5). About 2 h after electric pulses application, DNA molecules are present at nucleus level (step 6). Finally, 24 h after electrotransfection, eGFP expression is detected under fluorescence microscopy (step 7)

during electropermeabilization [78] and reinforces the idea that the cytoplasm constitutes a diffusional barrier to gene transfer.

Stability of plasmid DNA can be quantitatively assessed by microinjection. Such experiments revealed that 50% of the DNA is eliminated in 12 h from HeLa and COS cells and in 4 h from myotubes [79]. Cytosolic elimination of plasmid DNA cannot be attributed to the only cell division, since degradation is observed in cell cycle arrested cells. In the case of tissues, radiolabelled plasmid indeed progressively leave muscles and is degraded as soon as 5 min after plasmid injection, with or without electrotransfer. While a major part of plasmid DNA is rapidly cleared and degraded, the electrotransferable pool of plasmid DNA represents a very small part of the amount injected and belongs to another compartment where it is protected from endogenous DNAses [80].

Finally, beside cytoskeleton, the nuclear envelope represents the last physical obstacle to the expression of the plasmid DNA. The inefficient nuclear uptake of plasmid DNA from the cytoplasm was recognized more than 20 years ago. While molecules smaller than 40 kDa can diffuse through the nuclear pore complexes, larger molecules must carry a specific targeting signal, the nuclear localization sequence to traverse. The significant size of plasmid DNA (2–10 MDa) makes it unlikely that the nuclear entry occurs by passive diffusion. Dividing cells are highly transfectable compared to quiescent ones, suggesting that DNA enter the nucleus upon the disassembly of the nuclear envelope during mitosis. Cell synchronization indeed affects gene delivery by electric field [81–83], reinforcing the statement that the melting of the nuclear membrane facilitates direct access of plasmid DNA to the nucleus.

Therefore, clear limits of efficient gene expression by electric pulses are due to cytoplasm crowding and transfer through nuclear envelope. New challenges are to overcome these limiting steps. The dense latticework of the cytoskeleton impedes free diffusion of DNA. However, since transfections do work, there must be mechanisms by which DNA circumvents cytoplasmic obstacles. One possibility is that plasmids become cargo on cytoskeletal motors, much like viruses do, and move to the nucleus in a directed fashion. Electrotransfered plasmid DNA, containing specific sequences, like most viruses, could then utilize the microtubule network and its associated motor proteins to traffic through the cytoplasm to the nucleus [84, 85].

Another alternative could come from nanosecond pulsed electric fields. New findings indeed indicate that very short (10–300 ns) but high pulses (up to 300 kV/cm) extend classical electropermeabilization to include events that primarily affect intracellular structures and functions. As the pulse duration is decreased below the plasma membrane charging time constant (see Eq. 1), plasma membrane effects decrease and intracellular effects predominate [86, 87]. When used in conjugation with classical electropermeabilization, nanopulses can increase gene expression. The idea is to perform classical membrane permeabilization allowing plasmid DNA electrotransfer, and then 30 min later to permeabilize specifically the nuclear envelope by using short nano pulse EF. By this way, it will become possible not only to electropermeabilize cells but also to electromanipulate them.

Conclusions

Clear differences of processes by which molecules of different sizes translocate across the electropermeabilized membrane have been observed. While small soluble molecules could rather freely cross the permeabilized membrane for a time much longer than the duration of the electric pulse application, DNA transfer involves complex steps including interaction with the permeabilized membrane and migration into the cytosol. If the effects of the electric field parameters are about to be elucidated (pulse strength higher than a threshold value, long pulse duration for efficient gene expression), the associated destabilization of the membrane which is a stress for the cells and may affect the cell viability has still to be clearly described. Moreover, it becomes evident that extracellular as well as intracellular barriers compromise the transfection efficiency. Clearly, DNA electrotransfer through an electropermeabilized cell membrane is much more complex than the passage of a thread through the eye of a needle. The challenge for electro-mediated gene therapy is to pinpoint the rate limiting steps in this complex process and implement strategies to overcome the barriers encountered by therapeutic plasmid DNA.

Acknowledgements Many thanks are due to the financial supports from the CNRS, the French ANR PCV programme, the Association Française sur les Myopathies, the Region Midi Pyrénées and the Fondation pour la Recherche Médicale.

References

1. Wolff, J. A., & Budker, V. (2005). The mechanism of naked DNA uptake and expression. *Advances in Genetics, 54*, 3–20.
2. Hacein-Bey-Abina, S., Von Kalle, C., Schmidt, M., McCormack, M. P., Wulffraat, N., Leboulch, P., et al. (2003). LMO2-associated clonal T cell proliferation in two patients after gene therapy for SCID-X1. *Science, 302*, 415–419.
3. Hacein-Bey-Abina, S., Le Deist, F., Carlier, F., Bouneaud, C., Hue, C., De Villartay, J. P., et al. (2002). Sustained correction of X-linked severe combined immunodeficiency by ex vivo gene therapy. *New England Journal of Medicine, 346*, 1185–1193.

4. Bester, A.C., Schwartz, M., Schmidt, M., Garrigue, A., Hacein-Bey-Abina, S., Cavazzana-Calvo, M., Ben-Porat, N., Von Kalle, C., Fischer, A., & Kerem, B. (2006). Fragile sites are preferential targets for integrations of MLV vectors in gene therapy. *Gene Therapy, 13*, 1057–1059.
5. Rols, M. P. (2006). Electropermeabilization, a physical method for the delivery of therapeutic molecules into cells. *Biochimica et Biophysica Acta, 1758*, 423–428.
6. Mir, L. M., Belehradek, M., Domenge, C., Orlowski, S., Poddevin, B., Belehradek, J., Jr., et al. (1991). Electrochemotherapy, a new antitumor treatment: First clinical trial. *Comptes Rendus de l'Academie des Sciences. Serie III, Sciences de la Vie, 313*, 613–618.
7. Mir, L. M., Orlowski, S., Belehradek, J., Jr., & Paoletti, C. (1991). Electrochemotherapy potentiation of antitumour effect of bleomycin by local electric pulses. *European Journal of Cancer, 27*, 68–72.
8. Belehradek, M., Domenge, C., Luboinski, B., Orlowski, S., Belehradek, J., Jr., & Mir, L. M. (1993). Electrochemotherapy, a new antitumor treatment. First clinical phase I-II trial. *Cancer, 72*, 3694–3700.
9. Gehl, J. (2003). Electroporation: Theory and methods, perspectives for drug delivery, gene therapy and research. *Acta Physiologica Scandinavica, 177*, 437–447.
10. Gothelf, A., Mir, L. M., & Gehl, J. (2003). Electrochemotherapy: Results of cancer treatment using enhanced delivery of bleomycin by electroporation. *Cancer Treatment Reviews, 29*, 371–387.
11. Mir, L. M., Glass, L. F., Sersa, G., Teissie, J., Domenge, C., Miklavcic, D., et al. (1998). Effective treatment of cutaneous and subcutaneous malignant tumours by electrochemotherapy. *British Journal of Cancer, 77*, 2336–2342.
12. Sersa, G., Miklavcic, D., Cemazar, M., Rudolf, Z., Pucihar, G., & Snoj, M. (2008). Electrochemotherapy in treatment of tumours. *European Journal of Surgical Oncology, 34*, 232–240.
13. Golzio, M., Rols, M. P., & Teissie, J. (2004). In vitro and in vivo electric field-mediated permeabilization, gene transfer, and expression. *Methods, 33*, 126–135.
14. Scherman, D., Bigey, P., & Bureau, M. F. (2002). Applications of plasmid electrotransfer. *Technology in Cancer Research and Treatment, 1*, 351–354.
15. Bloquel, C., Fabre, E., Bureau, M. F., & Scherman, D. (2004). Plasmid DNA electrotransfer for intracellular and secreted proteins expression: New methodological developments and applications. *The Journal of Gene Medicine, 6*(Suppl 1), S11–S23.
16. Trezise, A. E., Buchwald, M., & Higgins, C. F. (1993). Testis-specific, alternative splicing of rodent CFTR mRNA. *Human Molecular Genetics, 2*, 801–802.
17. Miklavcic, D., Semrov, D., Mekid, H., & Mir, L. M. (2000). A validated model of in vivo electric field distribution in tissues for electrochemotherapy and for DNA electrotransfer for gene therapy. *Biochimica et Biophysica Acta, 1523*, 73–83.
18. Gehl, J., Sorensen, T. H., Nielsen, K., Raskmark, P., Nielsen, S. L., Skovsgaard, T., et al. (1999). In vivo electroporation of skeletal muscle: Threshold, efficacy and relation to electric field distribution. *Biochimica et Biophysica Acta, 1428*, 233–240.
19. Gilbert, R. A., Jaroszeski, M. J., & Heller, R. (1997). Novel electrode designs for electrochemotherapy. *Biochimica et Biophysica Acta, 1334*, 9–14.
20. Gehl, J. (2008). Electroporation for drug and gene delivery in the clinic: Doctors go electric. *Methods in Molecular Biology, 423*, 351–359.
21. Mir, L. M. (2008). Application of electroporation gene therapy: Past, current, and future. *Methods in Molecular Biology, 423*, 3–17.
22. Hirao, L. A., Wu, L., Khan, A. S., Hokey, D. A., Yan, J., Dai, A., et al. (2008). Combined effects of IL-12 and electroporation enhances the potency of DNA vaccination in macaques. *Vaccine, 26*, 3112–3120.
23. Neumann, E., Schaefer-Ridder, M., Wang, Y., & Hofschneider, P. H. (1982). Gene transfer into mouse lyoma cells by electroporation in high electric fields. *EMBO Journal, 1*, 841–845.
24. Neumann, E., Sowers, A. E., & Jordan, C. A. (1989). *Electroporation and electrofusion in cell biology*. New York: Plenum.
25. Escoffre, J.M., Dean, D.S., Hubert, M., Rols, M.P. and Favard, C. (2007). Membrane perturbation by an external electric field: A mechanism to permit molecular uptake. *European Biophysics Journal, 36*, 973–983.
26. Weaver, J. C. (1995). Electroporation theory. Concepts and mechanisms. *Methods in Molecular Biology, 55*, 3–28.
27. Teissie, J., Golzio, M., & Rols, M. P. (2005). Mechanisms of cell membrane electropermeabilization: A minireview of our present (lack of ?) knowledge. *Biochimica et Biophysica Acta, 1724*, 270–280.
28. Chang, D. C., & Reese, T. S. (1990). Changes in membrane structure induced by electroporation as revealed by rapid-freezing electron microscopy. *Biophysical Journal, 58*, 1–12.
29. Tarek, M. (2005). Membrane electroporation: A molecular dynamics simulation. *Biophysical Journal, 88*, 4045–4053.
30. Tieleman, D. P. (2004). The molecular basis of electroporation. *BMC Biochem, 5*, 10.
31. Stulen, G. (1981). Electric field effects on lipid membrane structure. *Biochimica et Biophysica Acta, 640*, 621–627.
32. Lopez, A., Rols, M. P., & Teissie, J. (1988). 31P NMR analysis of membrane phospholipid organization in viable, reversibly electropermeabilized Chinese hamster ovary cells. *Biochemistry, 27*, 1222–1228.
33. Haest, C. W., Kamp, D., & Deuticke, B. (1997). Transbilayer reorientation of phospholipid probes in the human erythrocyte membrane. Lessons from studies on electroporated and resealed cells. *Biochimica et Biophysica Acta, 1325*, 17–33.
34. Bernhardt, J., & Pauly, H. (1973). On the generation of potential differences across the membranes of ellipsoidal cells in an alternating electrical field. *Biophysik, 10*, 89–98.
35. Mehrle, W., Hampp, R., & Zimmermann, U. (1989). Electric pulse induced membrane permeabilization. Spatial orientation and kinetics of solute efflux in freely suspended and dielectrophoretically aligned plant mesophyll protoplasts. *Biochimica et Biophysica Acta, 978*, 267–275.
36. Kotnik, T., & Miklavcic, D. (2000). Analytical description of transmembrane voltage induced by electric fields on spheroidal cells. *Biophysical Journal, 79*, 670–679.
37. Hibino, M., Itoh, H., & Kinosita, K., Jr. (1993). Time courses of cell electroporation as revealed by submicrosecond imaging of transmembrane potential. *Biophysical Journal, 64*, 1789–1800.
38. Valic, B., Golzio, M., Pavlin, M., Schatz, A., Faurie, C., Gabriel, B., et al. (2003). Effect of electric field induced transmembrane potential on spheroidal cells: Theory and experiment. *European Biophysics Journal, 32*, 519–528.
39. Pucihar, G., Kotnik, T., Valic, B., & Miklavcic, D. (2006). Numerical determination of transmembrane voltage induced on irregularly shaped cells. *Annals of Biomedical Engineering, 34*, 642–652.
40. Hibino, M., Shigemori, M., Itoh, H., Nagayama, K., & Kinosita, K., Jr. (1991). Membrane conductance of an electroporated cell analyzed by submicrosecond imaging of transmembrane potential. *Biophysical Journal, 59*, 209–220.
41. Teissie, J., & Rols, M. P. (1993). An experimental evaluation of the critical potential difference inducing cell membrane electropermeabilization. *Biophysical Journal, 65*, 409–413.

42. Gabriel, B., & Teissie, J. (1997). Direct observation in the millisecond time range of fluorescent molecule asymmetrical interaction with the electropermeabilized cell membrane. *Biophysical Journal, 73*, 2630–2637.
43. Schwister, K., & Deuticke, B. (1985). Formation and properties of aqueous leaks induced in human erythrocytes by electrical breakdown. *Biochimica et Biophysica Acta, 816*, 332–348.
44. Rols, M. P., & Teissie, J. (1990). Electropermeabilization of mammalian cells. Quantitative analysis of the phenomenon. *Biophysical Journal, 58*, 1089–1098.
45. Gabriel, B., & Teissie, J. (1999). Time courses of mammalian cell electropermeabilization observed by millisecond imaging of membrane property changes during the pulse. *Biophysical Journal, 76*, 2158–2165.
46. Golzio, M., Teissie, J., & Rols, M. P. (2002). Direct visualization at the single-cell level of electrically mediated gene delivery. *Proceedings of the National Academic Sciences of the United Sciences of America, 99*, 1292–1297.
47. Rols, M. P., & Teissie, J. (1998). Electropermeabilization of mammalian cells to macromolecules: Control by pulse duration. *Biophysical Journal, 75*, 1415–1423.
48. Glogauer, M., Lee, W., & McCulloch, C. A. (1993). Induced endocytosis in human fibroblasts by electrical fields. *Experimental Cell Research, 208*, 232–240.
49. Rols, M. P., Femenia, P., & Teissie, J. (1995). Long-lived macropinocytosis takes place in electropermeabilized mammalian cells. *Biochemical and Biophysical Research Communications, 208*, 26–35.
50. Favard, C., Dean, D. S., & Rols, M. P. (2007). Electrotransfer as a non viral method of gene delivery. *Current Gene Therapy, 7*, 67–77.
51. Angelova, M. I., & Tsoneva, I. (1999). Interactions of DNA with giant liposomes. *Chemistry and Physics of Lipids, 101*, 123–137.
52. Angelova, M. I., Hristova, N., & Tsoneva, I. (1999). DNA-induced endocytosis upon local microinjection to giant unilamellar cationic vesicles. *European Biophysics Journal, 28*, 142–150.
53. Chernomordik, L. V., Sokolov, A. V., & Budker, V. G. (1990). Electrostimulated uptake of DNA by liposomes. *Biochimica et Biophysica Acta, 1024*, 179–183.
54. Hristova, N. I., Tsoneva, I., & Neumann, E. (1997). Sphingosine-mediated electroporative DNA transfer through lipid bilayers. *FEBS Letters, 415*, 81–86.
55. Spassova, M., Tsoneva, I., Petrov, A. G., Petkova, J. I., & Neumann, E. (1994). Dip patch clamp currents suggest electrodiffusive transport of the polyelectrolyte DNA through lipid bilayers. *Biophysical Chemistry, 52*, 267–274.
56. Kubiniec, R. T., Liang, H., & Hui, S. W. (1990). Effects of pulse length and pulse strength on transfection by electroporation. *Biotechniques, 8*, 16–20.
57. Liang, H., Purucker, W. J., Stenger, D. A., Kubiniec, R. T., & Hui, S. W. (1988). Uptake of fluorescence-labeled dextrans by 10T 1/2 fibroblasts following permeation by rectangular and exponential-decay electric field pulses. *Biotechniques, 6*, 550–552, 554, 556–558.
58. Wolf, H., Rols, M. P., Boldt, E., Neumann, E., & Teissie, J. (1994). Control by pulse parameters of electric field-mediated gene transfer in mammalian cells. *Biophysical Journal, 66*, 524–531.
59. Rols, M. P., Coulet, D., & Teissie, J. (1992). Highly efficient transfection of mammalian cells by electric field pulses. Application to large volumes of cell culture by using a flow system. *European Journal of Biochemistry, 206*, 115–121.
60. Heller, R., Jaroszeski, M., Atkin, A., Moradpour, D., Gilbert, R., Wands, J., et al. (1996). In vivo gene electroinjection and expression in rat liver. *FEBS Letters, 389*, 225–228.
61. Klenchin, V. A., Sukharev, S. I., Serov, S. M., Chernomordik, L. V., & Chizmadzhev Yu, A. (1991). Electrically induced DNA uptake by cells is a fast process involving DNA electrophoresis. *Biophysical Journal, 60*, 804–811.
62. Sukharev, S. I., Klenchin, V. A., Serov, S. M., Chernomordik, L. V., & Chizmadzhev Yu, A. (1992). Electroporation and electrophoretic DNA transfer into cells. The effect of DNA interaction with electropores. *Biophysical Journal, 63*, 1320–1327.
63. Muller, K. J., Horbaschek, M., Lucas, K., Zimmermann, U., & Sukhorukov, V. L. (2003). Electrotransfection of anchorage-dependent mammalian cells. *Experimental Cell Research, 288*, 344–353.
64. Faurie, C., Phez, E., Golzio, M., Vossen, C., Lesbordes, J. C., Delteil, C., et al. (2004). Effect of electric field vectoriality on electrically mediated gene delivery in mammalian cells. *Biochimica et Biophysica Acta, 1665*, 92–100.
65. Liu, F., Heston, S., Shollenberger, L. M., Sun, B., Mickle, M., Lovell, M., et al. (2006). Mechanism of in vivo DNA transport into cells by electroporation: Electrophoresis across the plasma membrane may not be involved. *The Journal of Gene Medicine, 8*, 353–361.
66. Satkauskas, S., Bureau, M. F., Puc, M., Mahfoudi, A., Scherman, D., Miklavcic, D., et al. (2002). Mechanisms of in vivo DNA electrotransfer: Respective contributions of cell electropermeabilization and DNA electrophoresis. *Mol Ther, 5*, 133–140.
67. Satkauskas, S., Andre, F., Bureau, M. F., Scherman, D., Miklavcic, D., & Mir, L. M. (2005). Electrophoretic component of electric pulses determines the efficacy of in vivo DNA electrotransfer. *Human Gene Therapy, 16*, 1194–1201.
68. Bureau, M. F., Gehl, J., Deleuze, V., Mir, L. M., & Scherman, D. (2000). Importance of association between permeabilization and electrophoretic forces for intramuscular DNA electrotransfer. *Biochimica et Biophysica Acta, 1474*, 353–359.
69. Mir, L. M., Bureau, M. F., Gehl, J., Rangara, R., Rouy, D., Caillaud, J. M., et al. (1999). High-efficiency gene transfer into skeletal muscle mediated by electric pulses. *Proceedings of the National Academic Sciences of the United Sciences of America, 96*, 4262–4267.
70. Aihara, H., & Miyazaki, J. (1998). Gene transfer into muscle by electroporation in vivo. *Nature Biotechnology, 16*, 867–870.
71. Pavselj, N., & Preat, V. (2005). DNA electrotransfer into the skin using a combination of one high- and one low-voltage pulse. *Journal of Controlled Release, 106*, 407–415.
72. Phez, E., Faurie, C., Golzio, M., Teissie, J., & Rols, M. P. (2005). New insights in the visualization of membrane permeabilization and DNA/membrane interaction of cells submitted to electric pulses. *Biochimica et Biophysica Acta, 1724*, 248–254.
73. Brown, D. A., & London, E. (2000). Structure and function of sphingolipid- and cholesterol-rich membrane rafts. *Journal of Biological Chemistry, 275*, 17221–17224.
74. Brown, D. A., & London, E. (1998). Functions of lipid rafts in biological membranes. *Annual Review of Cell and Developmental Biology, 14*, 111–136.
75. Lechardeur, D., & Lukacs, G. L. (2002). Intracellular barriers to non-viral gene transfer. *Current Gene Therapy, 2*, 183–194.
76. Seksek, O., Biwersi, J., & Verkman, A. S. (1997). Translational diffusion of macromolecule-sized solutes in cytoplasm and nucleus. *Journal of Cell Biology, 138*, 131–142.
77. Dowty, M. E., Williams, P., Zhang, G., Hagstrom, J. E., & Wolff, J. A. (1995). Plasmid DNA entry into postmitotic nuclei of primary rat myotubes. *Proceedings of the National Academic Sciences of the United Sciences of America, 92*, 4572–4576.
78. Rols, M. P., & Teissie, J. (1992). Experimental evidence for the involvement of the cytoskeleton in mammalian cell electropermeabilization. *Biochimica et Biophysica Acta, 1111*, 45–50.

79. Lechardeur, D., Sohn, K. J., Haardt, M., Joshi, P. B., Monck, M., Graham, R. W., et al. (1999). Metabolic instability of plasmid DNA in the cytosol: A potential barrier to gene transfer. *Gene Therapy, 6*, 482–497.
80. Bureau, M. F., Naimi, S., Torero Ibad, R., Seguin, J., Georger, C., Arnould, E., et al. (2004). Intramuscular plasmid DNA electrotransfer: Biodistribution and degradation. *Biochimica et Biophysica Acta, 1676*, 138–148.
81. Takahashi, M., Furukawa, T., Nikkuni, K., Aoki, A., Nomoto, N., Koike, T., et al. (1991). Efficient introduction of a gene into hematopoietic cells in S-phase by electroporation. *Experimental Hematology, 19*, 343–346.
82. Schwachtgen, J. L., Ferreira, V., Meyer, D., & Kerbiriou-Nabias, D. (1994). Optimization of the transfection of human endothelial cells by electroporation. *Biotechniques, 17*, 882–887.
83. Golzio, M., Teissie, J., & Rols, M. P. (2002). Cell synchronization effect on mammalian cell permeabilization and gene delivery by electric field. *Biochimica et Biophysica Acta, 1563*, 23–28.
84. Vaughan, E. E., & Dean, D. A. (2006). Intracellular trafficking of plasmids during transfection is mediated by microtubules. *Molecular Therapy, 13*, 422–428.
85. Vaughan, E. E., Geiger, R. C., Miller, A. M., Loh-Marley, P. L., Suzuki, T., Miyata, N., & Dean, D. A. (2008). Microtubule acetylation through HDAC6 inhibition results in increased transfection efficiency. *Molecular Therapy, 16*, 1841–1847.
86. Schoenbach, K. H., Beebe, S. J., & Buescher, E. S. (2001). Intracellular effect of ultrashort electrical pulses. *Bioelectromagnetics, 22*, 440–448.
87. Beebe, S. J., White, J., Blackmore, P. F., Deng, Y., Somers, K., & Schoenbach, K. H. (2003). Diverse effects of nanosecond pulsed electric fields on cells and tissues. *DNA and Cell Biology, 22*, 785–796.

1.3. Conclusions

Les mécanismes impliqués dans le transfert de petites molécules (<4 kDa) et de macromolécules (>4 kDa) sont clairement différents. Alors que les petites molécules peuvent franchir librement la membrane perméabilisée pendant et après l'application des impulsions électriques, le transfert de molécules de plasmide est un **processus multi-étapes** *(Golzio et al., 2002)*. La transfection est détectée à partir d'une valeur seuil supérieure ou égale au seuil de perméabilisation, i.e. $\mathbf{E_t \geq E_p}$, et pour des durées d'impulsions électriques de l'ordre de la milliseconde. La **perméabilisation** de la membrane plasmique et la **migration électrophorétique** sont nécessaires à la transfection des cellules. Le transfert de plasmides a lieu dans les zones membranaires perméabilisées par les impulsions électriques. L'efficacité de transfection dépend de l'intensité, du nombre, de la durée et de la fréquence des impulsions électriques dans la mesure où la viabilité cellulaire n'est pas affectée. La présence du plasmide pendant l'application des impulsions électriques est nécessaire à l'obtention d'une expression génique.

Les lois physiques de l'électroperméabilisation démontrent que toutes les cellules sont perméabilisables et potentiellement transfectables. Néanmoins, les données de la littérature montrent que les approches expérimentales sont très souvent différentes et les résultats contradictoires. Chaque type cellulaire a sa propre réponse vis-à-vis des impulsions électriques, du transfert du plasmide et de son expression. Les lois physiques de l'électrotransfert de plasmide se heurtent à la réalité biologique du système étudié (cellules, tissus…) et de son organisation (matrice extracellulaire, cytoplasme…) *(Mesojednik et al., 2007; Henshaw et Yuan, 2008)*. Par conséquent, il est difficile d'émettre des conclusions générales concernant la vectorisation de plasmide par l'application d'impulsions électriques.

2. Les mécanismes biophysiques *in vitro*

Le mécanisme de l'électrotransfert de plasmide est un processus multi-étapes: (1) perméabilisation de la membrane plasmique, (2) migration électrophorétique du plasmide, (3) interaction avec la membrane électroperméabilisée, (4) translocation de la membrane plasmique, (5) migration cytoplasmique, (6) passage de l'enveloppe nucléaire et (7) expression génique *(Golzio et al., 2002)*. La majorité des modèles proposés ne décrit que l'étape de translocation de la membrane plasmique. Néanmoins,

il apparaît clairement que le processus est dépendant de deux facteurs. Un **facteur physique**, au niveau de la membrane plasmique, qui permet la perméabilisation, l'interaction et la translocation du plasmide et qui correspond à une réponse à court terme. Un **facteur physiologique** de la cellule qui permet la migration cytoplasmique, le passage de l'enveloppe nucléaire, l'expression génique et la survie cellulaire et qui correspond à une réponse à long terme.

La présente revue publiée dans *Biophysical Reviews* se concentre sur les mécanismes biophysiques impliqués dans l'électrotransfert de plasmide *in vitro*. Dans la première partie, les évènements qui ont lieu avant, pendant et après l'application des impulsions électriques en présence de molécules de plasmides, sont décrits à l'échelle de la cellule. Dans une deuxième partie, les différentes théories sur les structures membranaires impliquées dans le transfert de molécules de plasmide seront discutées.

2.1. La revue

Biophys Rev (2009) 1:177–184
DOI 10.1007/s12551-009-0022-7

REVIEW

Gene electrotransfer: from biophysical mechanisms to in vivo applications

Part 1- Biophysical mechanisms

Jean-Michel Escoffre · Chloé Mauroy · Thomas Portet · Luc Wasungu · Chrystelle Rosazza · Yoann Gilbart · Laetitia Mallet · Elisabeth Bellard · Muriel Golzio · Marie-Pierre Rols · Justin Teissié

Received: 13 August 2009 / Accepted: 29 October 2009 / Published online: 17 November 2009

Abstract Electropulsation is one of the nonviral methods successfully used to deliver genes into living cells in vitro and in vivo. This approach shows promise in the field of gene and cellular therapies. The present review focuses on the processes supporting gene electrotransfer in vitro. In the first part, we will report the events occurring before, during, and after pulse application in the specific field of plasmid DNA electrotransfer at the cell level. A critical discussion of the present theoretical considerations about membrane electropermeabilization and the transient structures involved in the plasmid uptake follows in a second part.

Keywords Electropermeabilization · Electroporation · Gene electrotransfer · Biophysical mechanisms · Membranes

Introduction

Electropermeabilization results from a controlled application of electric pulses to cells, leading to their transient and reversible membrane permeabilization (Neumann et al. 1989; Teissié et al. 2005; Escoffre et al. 2007). This process brings new properties to the cell plasma membrane, which, besides being permeabilized, becomes fusogenic and allows exogenous proteins to be inserted in it. Electropermeabilization is used to introduce a large variety of molecules into many different cells in vitro (Orlowski and Mir 1993; Eynard et al. 1997). Clinical applications of the method are now under development as results of the EU Cliniporator and ESOPE programs. A local anti-tumoral drug delivery to patients (a method called electrochemotherapy) is in clinical trials in tens of hospitals through Europe (Mir et al. 1995; Cemazar and Sersa, 2007; Sersa et al. 2008; Mir et al. 1998, 2006). The most frequent application of electric field-induced membrane permeabilization is the transfer and expression of genes into mammalian cells. However, this application not only involves the introduction of DNA into cells, but also depends on subsequent cellular processes (Weaver and Chizmadzhev 1996). The transfer of naked DNA plasmid and the expression of the gene of interest are enhanced by electropulsation into different tissues, including the skeletal muscle (Aihara and Miyazaki 1998; Mir et al. 1999), liver (Heller et al. 1996; Liu and Huang 2002), skin (Titomirov et al. 1991; Vandermeulen et al. 2007), and tumors (Rols et al. 1998a). The transfection efficiency of this physical method in vivo is still low compared to the viral vectors. However, due to the ease with which it is performed and its speed, reproducibility, and safety, gene electrotransfer holds a great potential for clinical application.

One of main limits of the widespread use of electropermeabilization is that very little is known about the biophysical mechanisms supporting the reorganization of the cell membrane (pore, electropore, defects?). The

J.-M. Escoffre and C. Mauroy have contributed equally to this work.

J.-M. Escoffre · C. Mauroy · T. Portet · L. Wasungu · C. Rosazza · Y. Gilbart · L. Mallet · E. Bellard · M. Golzio · M.-P. Rols (✉) · J. Teissié (✉)
CNRS, IPBS (Institut de Pharmacologie et de Biologie Structurale),
205 route de Narbonne,
31077 Toulouse, France
e-mail: rols@ipbs.fr
e-mail: Justin.Teissie@ipbs.fr

J.-M. Escoffre · C. Mauroy · T. Portet · L. Wasungu · C. Rosazza · Y. Gilbart · L. Mallet · E. Bellard · M. Golzio · M.-P. Rols · J. Teissié
Université de Toulouse UPS, IPBS,
31077 Toulouse, France

molecular target of the field effect remains unclear (Teissié et al. 2005). The other main limit in gene electrotransfer comes from the transfer inside the nucleus. In nondividing cells, the nuclear envelope is an especially problematic hurdle to gene transfer, which should take place through the nuclear pore complex (Van der Aa et al. 2006, 2007; Pouton et al. 2007). No direct biophysical method to alter the nuclear envelope or pore has been reported (yet). A successful approach is in modifying plasmid (pDNA) vectors to enhance nuclear import through the NPC (Miller and Dean 2009).

The present review focuses on the processes supporting gene electrotransfer in vitro. The events occurring before, during, and after pulse application leading to gene electrotransfer will be described. Theoretical considerations about membrane structures involved in the plasmid uptake will be described in a (very) critical manner. In a companion paper, in vivo gene electrotransfer and its clinical applications will be addressed.

Biophysical mechanisms

In vitro biophysical considerations

Gene electrotransfer to mammalian cells is obtained by mixing cells and plasmids in a biocompatible buffer (control of pH, osmolarity, conductivity), then by applying a well-controlled electric field pulse train (shape of pulses, choice of field strength, pulse duration, number of pulses, delay between pulses) and finally bringing the mixture into a culture medium. Expression of the coded activity can be detected after a couple of hours but reaches a high level after 24 h (Golzio et al. 2004). Transfer of a large polyelectrolyte across the membrane requires a transient loss of cohesion of the proteolipidic assembly. This dramatic event should nevertheless preserve the cell viability to observe the expression of the activity coded by the plasmid.

Experimental facts: events before, during, and after electropulsation

The plasma membrane is not permeable to hydrophilic molecules such as nucleic acids. Plasmid molecules, due to their negative charge, cannot interact with the cell plasma membrane that bears the same charge. DNA molecules therefore cannot get access to the cytoplasm. No transfected cells are detected in the absence of plasmid or when plasmid is added after the electropulsation. The prepulse incubation time is not very important but to avoid a negative effect of exogenous nucleases should be kept short and processed at a low temperature (Rols et al. 1994). Indeed, gene expression is obtained after applying electric pulses to plasmid/cell mixture after a short incubation (Neumann et al. 1982; Klenchin et al. 1991; Wolf et al. 1994). These results are the same whatever the cell types (bacteria, yeast, and mammalian cells) (Golzio et al. 1998; Eynard et al. 1992; Ganeva et al. 1995). Preadsorption of DNA on the mammalian cell surface is not requested and was indeed reported to prevent expression (Neumann et al. 1982).

Gene electrotransfer is only detected for electric field values leading to membrane permeabilization ($E_c > E_p$). Transfection threshold values are the same as the ones for cell permeabilization when millisecond pulses are applied (Rols and Teissié 1998). Field strength is observed to have a critical role. Plasmid molecules, negatively charged, migrate when submitted to an electric field (Wolf et al. 1994; Neumann et al. 1992). In the "low" electric field regime (i.e., $E_c < E_p$), plasmid simply electrophoretically flows along the cell membrane towards the anode. It can be trapped when divalent ions are present (Frantescu et al. 2005; Xie and Tsong 1993).

However, beyond a critical permeabilizing field value ($E_c > E_p$), two main processes occur: (1) plasma membrane is permeabilized (at the microsecond scale); (2) plasmid undergoes the electrophoretic migration (at the millisecond scale) *and* interacts with permeabilized membrane (Golzio et al. 2002). Metastable plasmids/membrane complexes are formed and grow as local aggregates (at the millisecond scale). But once the field is turned off, the growth of the plasmid aggregates is stopped. The plasmid/membrane interaction is not homogeneously distributed on the permeabilized areas but is detected in association with membrane competent-like sites whose sizes range from 0.1 to 0.5 μm. This interaction takes place only when the plasma membrane is under permeabilization (a field over Ec must be present) (Golzio et al. 2002). It does not occur if the plasmid molecules are added after electropermeabilizing cells (Neumann et al. 1982; Tsong 1991; Klenchin et al. 1991). Recent works on electric field vectoriality show that the plasmid/membrane interaction is not a simple accumulation of plasmid at the membrane surface level, but a plasmid "irreversible" insertion occurs into the permeabilized membrane. No free plasmid diffusion into the cytoplasm is detected as was proposed in older works (Klenchin et al. 1991).

Under permeabilizing field conditions, the pulse duration plays a critical role in the formation of the plasmid/membrane complexes. These complexes are easily detected when the pulse duration is at least 1 ms, but highly sensitive technologies show that they are formed with shorter pulses (unpublished data). This suggests that the density of defects is critical in the plasmid/membrane interaction. Furthermore, this interpretation is supported by the observation

that the plasmid content in the complex is under the control of the field strength (E), the number of successive pulses (N), and the pulse duration (T) (Golzio et al. 2002). The time for reaction with the membrane of the plasmid dragged against permeabilized membrane under the electrophoretic migration is increased by long pulse durations. This again is involved in the positive role of the pulse duration in gene electrotransfer. This contribution of the pulse duration to the plasmid/membrane interaction has already been illustrated by a complex dependence of the gene expression (Wolf et al. 1994). The associated gene expression Expr is shown to obey the following equation:

$$Expr = KNT^{2.3}\left(1 - \frac{E_p}{E}\right)f(DNA)$$

as long as the cell viability is not affected to a large extent by the pulse duration (Golzio et al. 2002). All parameters are as described above, with K being a constant and N, the number of electric pulses. Its dependence on the plasmid concentration is rather complex, as high levels of plasmids appear to be toxic (Rols et al. 1992). The practical conclusion is that in vitro an effective transfer is obtained by using long pulses in order to drive the plasmid towards the permeabilized membrane but with low field strength to preserve the cell viability (Rols and Teissié 1998; Kubiniec et al. 1990). Nevertheless, the gene transfection was obtained with short long pulses in the pioneering experiments (Neumann et al 1982), in a very recent report (Kanduser et al. 2009), and with stem cells (Ferreira et al. 2008).

Plasmid/membrane complex remains accessible to DNase I, up to 60 s after the pulsation in the case of CHO cells. The plasmid aggregates, which are anchored in the membrane after the electric field application, remain sensitive to the degrading action of the nucleases that were added externally post-pulse, which are known not to cross the membrane (Eynard et al. 1997). Nevertheless, the opposite observation, reported as a protective effect against DNAse, was detected when using a different protocol (Klenchin et al. 1991). More than 2 s appears to be needed to get a stable plasmid/membrane complex after a 5 ms pulse (Phez et al. 2005). Several minutes after the electropulsation, plasmids are still present on/in the cell surface. The biophysical structure of the membrane plasmid complex has to be explained. Plasmids leave the complex and diffuse in the cytoplasm. Then, plasmids are present at the nucleus surface, but only a small fraction cross the nuclear envelope to be expressed a few hours after the electropulsation (Golzio et al. 2002). These intracellular steps remain rather poorly understood as already mentioned. A positive effect of working at 37°C in all these post-pulse steps was observed (Rols et al. 1994). Hypo-osmolar buffers gave an increase in expression (Golzio et al. 1998). Starving cells prevented expression, suggesting an active contribution of the cell metabolism in transfer and/or expression (Rols et al. 1998b) (Table 1).

Theories of DNA plasmid electroentry

Although the first pioneering report on gene electrotransfer in cells was published more than 25 years ago by E. Neumann, the molecular basis behind the process of gene electrotransfer is highly debated. Different scenarios have been proposed (Fig. 1):

(i) Krassowska's model supports the simplest mechanism, in which plasmid enters the 5 nm thick membrane through stable macropores (i.e., 20 to 200 nm Ø) (Smith et al. 2004; Krassowska and Filev 2007). The electrically induced defects result from the field-associated membrane potential changes. Their model relies on tension-coupled pores that do not bring membrane rupture [a dramatic feature of the classical Chizmadzhev model (Weaver and Chizmadzhev 1996)]. It predicts a post-pulse growth of macropores on the seconds time scale fairly consistent with experimental evidence (Neu and Krassowska 2003). This model predicts pores large enough to permit the plasmid uptake, even in its circular or supercoiled conformation (Blackburn and Gait 1996). These pores remain open for the entire duration of electropulsation providing adequate time for the plasmid to enter the cell (Sukharev et al. 1994).

Table 1 Steps in gene electrotransfer. The central column describes the events that occur before, during, and after the electropulsation. The right column reports their time scale

Steps	Events	Time scale
Before electropulsation	Plasma membrane is not permeable. Plasmid cannot get access to the cytoplasm.	
During electropulsation	Electropermeabilization takes place.	Microseconds
	Plasmid molecules are electrophoretically driven into contact with the cell surface.	Milliseconds
	Metastable complexes are formed between plasmid molecules and the localized electropermeabilized part of cell membrane.	Milliseconds
After electropulsation	Stable complexes result.	Seconds
	Plasmids leave the complexes and diffuse in the cytoplasm.	Minutes
	A small fraction of the plasmid molecules cross the nuclear envelope to be expressed.	Hours
	Gene expression occurs.	Days

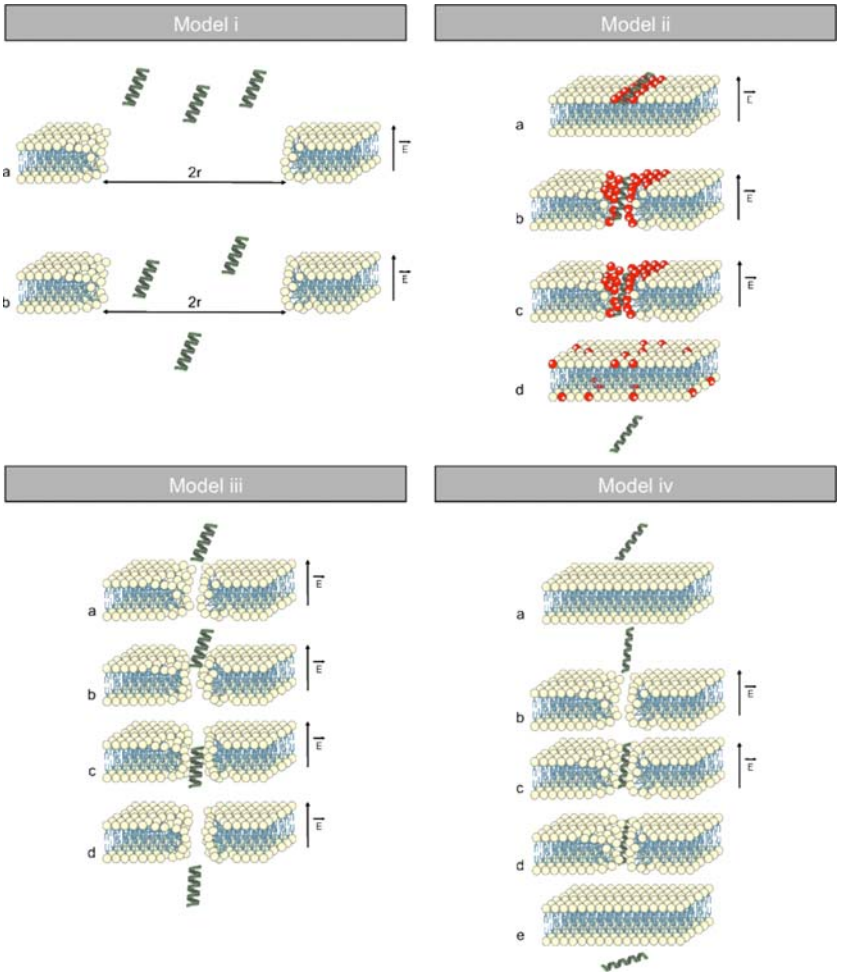

Fig. 1 Differents models of gene electrotransfer. *Model i*: *a* The electric pulse induces a macrodefect (2r>20 nm) and an electrophoretically mediated DNA accumulation. *b* After the pulse, a free diffusion of DNA takes place across the long-lived macropore. *Model ii*: *a* DNA is preadsorbed with the plasma membrane by an interaction with cationic lipids, sphingosines. *b* DNA is transiently inserted in plasma membrane. *c* DNA is electrophoretically pulled through the permeabilized zones. *d* DNA leaves the membrane and enters into the cell. *Model iii*: *a* The electric pulses induce the membrane permeabilization. *b* DNA is concentrated near the membrane surface and pushed through the putative electropores by electrophoretic forces. *c* The mechanical interaction between the pores and the DNA driven by electrophoretic forces induces an adjustment of pore sizes. *c* DNA enters into the cell. *Model iv*: *a* DNA remains at the interfacial region when no pore is present. *b* Under high electric field, the DNA diffuses towards the interior of the bilayer after a pore is created beneath it. *c* Diffusion of the strand toward the interior of the membrane leads to a complex DNA/lipid in which the lipid head groups encapsulate the DNA. *d* After the electric field pulse, the DNA is translocated. *e* DNA enters into the cell

This model remains an attractive model in spite of the existence of many experimental contradictions. Indeed, until now, no study made it possible to visualize these membrane pores. This validation appears impossible (Weaver and Chizmadzhev 1996). Moreover, the resealing time of pores appears to be shorter in this model than in experiments (e.g., seconds rather than minutes) (Bier et al. 1999; Golzio et al. 1998; Satkauskas et al. 2002; Tekle et al. 1991). In addition, in the case of CHO cells, plasmid accessibility to DNAase I in the minute following the end of electropulsation shows that the plasmid transfer inside the cell occurs after the electropulsation (Eynard et al. 1997). Of course, no selectivity of the macropore is predicted meaning that DNAases have free access. To date, theoretical models could predict stable pores of only a few nanometers in radius; larger pores are unstable (Freeman et al. 1994; Joshi and Schoenbach 2000) These models are confirmed by some experiments in which high-voltage, short pulses are used that must have created a large number of pores with radii of about 1 nm (Glaser et al. 1988; Kakorin and Neumann 2002; Schwister and Deuticke 1985). To reconcile these results with the experimental evidence of plasmid translocation after electropulsation, some researchers postulated that plasmid entry into cells relies on the plasmid/membrane interactions, which may be facilitated by a coalescence of many small, 1 nm pores

(Neumann et al. 1996; Rols and Teissié 1998; Rols et al 1998b; Sukharev et al 1992, 1994). The slow transport of DNA across the electropermeabilized membrane reflects a highly interactive electrotransfer, where many small pores coalesced into large pores that were transiently occluded by DNA (Neumann et al. 1999).

(ii) Other data report that gene electrotransfer through lipid bilayer could be mediated by transient complexes between plasmid and the lipids in the pore edges of elongated, electropercolated hydrophilic pore zones (Hristova et al. 1997). This is present with specific lipids. Moreover, the plasmid association with a lipid bilayer greatly facilitates the transport of small ions. This suggests a locally conductive plasmid/lipid interaction zone where parts of the plasmid may be inserted in the bilayer, leaving other parts of the plasmid probably protruding out from the outer surface of the bilayer. Plasmid is not only transiently inserted in, but also actually electrophoretically pulled through the permeabilized zones onto the other membrane side ultimately leaving the bilayer structure basically intact (Spassova et al. 1994). With such a model, in the case of mammalian cells, the resting potential difference should be the driving force for plasmid translocation after the pulse-induced insertion. This has not been checked yet.

(iii) Previous works suggested that electric pulses induce the membrane permeabilization, then plasmid molecules are concentrated near the membrane surface and pushed through the putative electropores by electrophoretic forces (Winterbourne et al. 1988; Klenchin et al. 1991; Sukharev et al. 1992; Tekle et al. 1994). The mechanical interaction between the pores and the plasmid driven by electrophoretic forces induces an adjustment of pore sizes and/or lifetimes to allow plasmid entry in the cell. The plasmid may interact with the electropermeabilized membrane in three possible ways: (1) The plasmid coil is aligned in an electric field, and at the appropriate pulse polarity it moves toward the permeabilized membrane. The plasmid may interact with a single membrane defect; it becomes enhanced upon plasmid interaction by the action of electrophoretic forces. (2) The passage of the (linearized) plasmid coil can be initiated by penetration of one end of the thread, which then leads the whole molecule through one pore. (3) The plasmid molecule can be involved in two pores (or more) and moving with electrophoretic forces, it cuts the membrane between these pores as a sharp thread can do (Sukharev et al. 1992). Transfer is dependent on electrophoretic forces and is complete at the end of the pulse. Interestingly, hypothesis (1) suggests a deformation of the electric field distribution close to the membrane. The large membrane defect is associated with enhanced membrane conductivity. The electric field lines will focus on the defect carrying more plasmids to it. This is in agreement with the formation of the experimentally detected plasmid aggregates (Golzio et al. 2002).

If the electrophoretic forces are the only driving forces of the plasmid transfer into the cell, similar transfection efficiencies should be obtained for equal *ET* values (i.e., *E*, field strength and *T*, pulse duration). However, in the case of HeLa cells, the number of transfected clones as a function of *ET* values is different according to whether short or long electric pulses are used (Hui 1995). Then, when the *ENT* value is constant, transfection rate depends preferentially on *T* (Rols and Teissié 1998). Therefore, the electrophoretic migration cannot be the only driving force of the plasmid transfer into the cells but clearly supports the formation of aggregates.

(iv) A molecular dynamic approach gives a mechanism by which plasmids do not translocate across the membrane during the electropulsation (Tarek 2005). The DNA/lipid system simulation was undertaken starting from a well-equilibrated 12 bp DNA duplex placed near a model POPC bilayer. The perturbation of the system under a 1.0 V nm^{-1} transverse electric field is followed for 2 ns. Under this high electric field, the DNA duplex diffuses towards the interior of the bilayer only *after* the creation of a pore beneath it, and within the same timescale, it remains at the interfacial region when no pore is present. Diffusion of the strand toward the interior of the membrane leads to a DNA/lipid complex in which the lipid head groups encapsulate the strand. The partial charges carried by the zwitterionic phosphatidylcholine groups of the lipids are known to be efficient for neutralizing the charges carried by the DNA (Bandyopadhyay et al. 1999). Such interactions between the plasmid and the lipids contribute to the effective screening of DNA charges and therefore to the stabilization of the complex.

The process described herein provides support to the gene delivery model by Golzio and collaborators (Golzio et al. 2002), in which it is proposed that only localized parts of the cell membrane brought to the permeabilized state are competent for transfer and that the proper transfer of plasmid—that does not require that the electric pulse be maintained—is preceded by an "anchoring step," connecting the plasmid to the permeabilized membrane, which takes place during the pulse. One should not forget that electropulsation-mediated gene delivery concerns much

larger supercoiled plasmids than the 12 bp construct considered here. Transfer of such plasmids is certainly a complex process and all aspects may not be addressed by simulations (Tarek 2005). Nevertheless this model shows that the plasmid is stabilized in the membrane core after electropulsation in agreement with the overall experimentally observed process of DNA translocation. DNA migration from the outer side of the cell membrane to the cytoplasm is beyond this simulation study, and no calculation was carried out to follow the resealing process.

Conclusions

The molecular mechanisms involved in the phenomenon of gene electrotransfer remain poorly understood. The study of the mechanisms of gene electrotransfer shows that permeabilization is necessary but that the mechanism of the transfer of the DNA molecules is different from that of the small molecules (Table 1) (Teissié et al. 2005). The current models described in this review are sometimes contradictory and do not always fit the experimental facts (Fig. 1). Indeed, experimental observations showed that the electrotransfer is a slow mechanism. This is in contradiction with the prediction of models i and iii. Models iii and iv are in agreement with a localized plasmid/membrane interaction (so-called competent membrane sites). These sites appear to be created by the electropermeabilization process by altering the field distribution (Freeman et al. 1994). This occurs through the perturbation of the transmembrane voltage by a conducting defect. A spatially inhomogeneous electric field is expected within the outer buffer near electrodefects (Pastushenko and Chizmadzhev 1982; Powell and Weaver 1986; Barnett and Weaver 1991 ; Weaver 1993). This brings a nonzero component of the electric field parallel to the membrane surface, i.e., the equipotentials near the membrane have significant, nonlinear gradients. For this reason, the current flowing through a membrane electrodefect not only results in a potential drop within the membrane, but also in the buffer near the defects (Weaver and Chizmadzhev 1996). Model ii suggests a putative method for transmembrane transfer and needs further investigations. One major problem with these theoretical models is that they consider only the lipid assembly description of a membrane while the presence of membrane proteins may affect the electropermeabilization of lipid bilayers by changing their mechanical properties (Troiano et al. 1999).

The knowledge and the control of the biophysical mechanisms of gene electrotransfer are necessary to evaluate their consequences in biological and physiological terms and their effectiveness for the development of clinical and biotechnological protocols.

Acknowledgments This work was supported by the CNRS, the AFM (Association Française pour les Myopathies), the ANR Cemirbio, and the région Midi-Pyrénées.

References

Aihara H, Miyazaki JI (1998) Gene transfer into muscle by electroporation in vivo. Nature Biotechnol 16:867–870

Bandyopadhyay S, Tarek M, Klein ML (1999) Molecular dynamics study of lipid-DNA complexes. J Phys Chem B 103:10075–10080

Barnett A, Weaver JC (1991) Electroporation: a unified, quantitative theory of reversible electrical breakdown and rupture. Bioelectrochem Bioenerg 25:163182

Bier M, Hammer SM, Canaday DJ, Lee RC (1999) Kinetics of resealing for transient electropores in isolated mammalian skeletal muscle cells. Bioelectromagnetics 20:194–201

Blackburn GM, Gait MJ (1996) Nucleic acids in chemistry and biology. Oxford University Press, Oxford

Cemazar M, Sersa G (2007) Electrotransfer of therapeutics molecules into tissues. Curr Opin Mol Ther 9:554–562

Escoffre JM, Hubert M, Dean DS, Rols MP, Favard C (2007) Membrane perturbation by an external electric field: a mechanism to permit molecular uptake. Eur Biophys J 36:973–983

Eynard N, Sixou S, Duran N, Teissié J (1992) Fast kinetics studies of *Escherichia coli* electrotransformation. Eur J Biochem 209:431–436

Eynard N, Rols MP, Ganeva V, Galutzov B, Sabri N, Teissié J (1997) Electrotransformation pathways of prokaryotic and eukaryotic cells: recents developments. Bioelectrochem Bioenerg 44:103–110

Ferreira E, Potier E, Logeart-Avramoglou D, Salomskaite-Davalgiene S, Mir LM, Petite H (2008) Optimization of a gene electrotransfer method for mesenchymal stem cell transfection. Gene Ther 15:537–544

Frantescu A, Kakorin S, Toensing K, Neumann E (2005) Adsorption of DNA and electric fields decrease the rigidity of lipid vesicle membranes. Phys Chem Chem Phys 7:4126–4131

Freeman SA, Wang MA, Weaver JC (1994) Theory of electroporation of planar bilayer membranes: predictions of the aqueous area, change in capacitance, and pore-pore separation. Biophys J 67:42–56

Ganeva V, Galutzov B, Teissié J (1995) Fast kinetics studies of plasmid DNA transfer in intact yeast cells mediated by electropulsation. Biochem Biophys Res Commun 214:825–832

Glaser RW, Leikin SL, Chernomordik LV, Pastushenko VF, Sokirko AI (1988) Reversible electrical breakdown of lipid bilayer: formation and evolution of pores. Biochim Biophys Acta 940:275–287

Golzio M, Mora MP, Raynaud C, Delteil C, Teissié J, Rols MP (1998) Control by osmotic pressure of voltage-induced permeabilization and gene transfer in mammalian cells. Biophys J 74:3015–3022

Golzio M, Teissié J, Rols MP (2002) Direct visualization at the single-cell level of electrically mediated gene delivery. Proc Natl Acad Sci USA 99:1292–1297

Golzio M, Rols MP, Teissié J (2004) In vitro and in vivo electric-field-mediated permeabilization, gene transfer, and expression. Methods 33:126–135

Heller R, Jaroszeski M, Atkin A, Moradpour D, Gilbert R, Wands J, Nicolau C (1996) In vivo gene electroinjection and expression in rat liver. FEBS Lett 389:225–228

Hristova NI, Tsoneva I, Neumann E (1997) Sphingosine-mediated electroporative DNA transfer through lipid bilayers. FEBS Lett 415:81–86

Hui SW (1995) Effects of pulse length and strength on electroporation efficiency. Methods Mol Biol 55:29–40

Joshi RP, Schoenbach KH (2000) Electroporation dynamics in biological cells subjected to ultrafast electrical pulses: a numerical simulation study. Phys Rev E 62:1025–1033

Kakorin S, Neumann E (2002) Ionic conductivity of electroporated lipid bilayer membranes. Bioelectrochem 56:163–166

Kanduser M, Miklavcic D, Pavlin M (2009) Mechanisms involved in gene electrotransfer using high- and low-voltage pulse—an in vitro study. Bioelectrochem 74:265–271

Klenchin VA, Sukharev SI, Serov SM, Chernomordik LV, Chizmadzev YuA (1991) Electrically induced DNA uptake by cells is a fast process involving DNA electrophoresis. Biophys J 60:804–811

Krassowska W, Filev PD (2007) Modeling electroporation in a single cell. Biophys J 92:404–417

Kubiniec RT, Liang H, Hui SW (1990) Effects of pulse length andpulse strength on transfection by electroporation. BioTechniques8:16 –20

Liu F, Huang L (2002) Electric gene transfer to the liver following systemic administration of plasmid DNA. Gene Ther 9:1116–1119

Miller AM, Dean DA (2009) Tissue-specific and transcription factor-mediated nuclear entry of DNA. Adv Drug Deliv Rev 61:603–613

Mir LM, Roth C, Orlowski S, Quintin Colonna F, Fradelizi D et al (1995) Systemic antitumor effects of electrochemotherapy combined with histocompatible cells secreting interleukin-2. J Immunother Emphasis Tumor Immunol 17:30–38

Mir LM, Glass LF, Sersa G, Teissié J, Domenge C, Miklavcic D et al (1998) Effective treatment of cutaneous and subcutaneous malignant tumours by electrochemotherapy. Br J Cancer 77:2336–2342

Mir LM, Bureau MF, Gehl J, Rangara R, Rouy D, Caillaud JM, Delaere P, Branellec D, Schwartz B, Scherman D (1999) High-efficiency gene transfer into skeletal muscle mediated by electric pulses. Proc Natl Acad Sci USA 96:4262–4267

Mir LM, Gehl J, Sersa G, Collins CG, Garbay JR, Billard V et al (2006) Standard operating procedures of the electrochemotherapy: instructions for the use of bleomycin or cisplatin administered either systemically or locally and electric pulses delivered by the CliniporatorTM by means of invasive or non-invasive electrodes. Eur J Cancer 42(suppl 4):14–25

Neu JC, Krassowska W (2003) Modeling postshock evolution of large electropores. Phys Rev E Stat Nonlin Soft Matter Phys 67:021915

Neumann E, Shaefer-Ridder M, Wang Y, Hofschneider PH (1982) Gene transfer into mouse lyoma cells by electroporation in high electric fields. EMBO J 1:841–845

Neumann E, Sowers AE, Jordan CA (1989) Electroporation and electrofusion in cell biology. Plenum, New York

Neumann E, Werner E, Sprafke A, Kruger K (1992) Electroporation phenomena. Electrooptics of plasmid DNA and of lipid bilayer vesicles. In: Jennings BR, Stoylov SP (eds) Colloid and molecular electro-optics. IOP, Bristol, pp 197–206

Neumann E, Kakorin S, Tsoneva I, Nikolova B, Tomov T (1996) Calcium-mediated DNA adsorption to yeast cells and kinetics of cell transformation by electroporation. Biophys J 71:868–877

Neumann E, Kakorin S, Toensing K (1999) Fundamentals of electroporative delivery of drugs and genes. Bioelectrochem Bioenerg 48:3–16

Orlowski S, Mir LM (1993) Cell electropermeabilization: a new tool for biochemical and pharmacological studies. Biochim Biophys Acta 1154:51–63

Pastushenko VF, Chizmadzhev YAQ (1982) Stabilization of conducting pores in BLM by electric current. Gen Physiol Biophys 1:43–52

Phez E, Faurie C, Golzio M, Teissié J, Rols MP (2005) New insights in the visualization of membrane permeabilization and DNA/membrane interaction of cells submitted to electric pulses. Biochim Biophys Acta 1724:248–254

Pouton CW, Wagstaff KM, Roth DM, Moseley GW, Jans DA (2007) Targeted delivery to the nucleus. Adv Drug Deliv Rev 59:698–717

Powell KT, Weaver JC (1986) Transient aqueous pores in bilayer membranes: a statistical theory. Bioelectrochem Bioenerg 15:211–227

Rols MP, Teissié J (1998) Electropermeabilization of mammalian cells to macromolecules: control by pulse duration. Biophys J 75:1415–1423

Rols MP, Coulet D, Teissié J (1992) Highly efficient transfection of mammalian cells by electric field pulses. Application to large volumes of cell culture by using a flow system. Eur J Biochem 206:115–121

Rols MP, Delteil C, Serin G, Teissié J (1994) Temperature effects on electrotransfection of mammalian cells. Nucleic Acid Res 22:540

Rols MP, Delteil C, Golzio M, Dumond P, Cros S, Teissié J (1998a) In vivo electrically mediated protein and gene transfer in murine melanoma. Nat Biotechnol 16:168–171

Rols MP, Delteil C, Teissié J (1998b) Control by ATP and ADP of voltage-induced mammalian-cell-membrane permeabilization, gene transfer and resulting expression. Eur J Biochem 254:382–388

Satkauskas S, Bureau MF, Puc M, Mahfoudi A, Scherman D, Miklavcic D, Mir LM (2002) Mechanisms of in vivo DNA electrotransfer: respective contributions of cell electropermeabilization and DNA electrophoresis. Mol Ther 5:133–140

Schwister K, Deuticke B (1985) Formation and properties of aqueous leaks induced in human erythrocytes by electrical breakdown. Biochim Biophys Acta 816:332–348

Sersa G, Miklavcic D, Cemazar M, Rudolf Z, Pucihar G, Snoj M (2008) Electrochemotherapy in treatment of tumours. Eur J Surg Oncol 34:232–240

Smith KC, Neu JC, Krassowska W (2004) Model of creation and evolution of stables electropores for DNA delivery. Biophys J 86:2813–2826

Spassova M, Tsoneva I, Petrov AG, Petkova JI, Neumann E (1994) Dip patch clamp currents suggest electrodiffusive transport of the polyelectrolyte DNA through lipid bilayers. Biophys Chem 52:267–274

Sukharev SI, Klenchin VA, Serov SM, Chernomordik LV, Chizmadzhev YuA (1992) Electroporation and electrophoretic DNA transfer into cells. The effect of DNA interaction with electropores. Biophys J 63:1320–1327

Sukharev SI, Titomirov AV, Klenchin VA (1994) Electrically induced DNA transfer into cells. Electroporation in vivo. In: Wolff JA (ed) Gene therapeutics: methods and applications of direct gene transfer. Birkhäuser, Boston, pp 210–232

Tarek M (2005) Membrane electroporation: a molecular dynamics simulation. Biophys J 88:4015–4053

Teissié J, Golzio M, Rols MP (2005) Mechanisms of cell membrane electropermeabilization: a minireview of our present (lack of?) knowledge. Biochim Biophys Acta 1724:270–280

Tekle E, Astumian RD, Chock PB (1991) Electroporation by using bipolar oscillating electric field: an improved method for DNA transfection of NIH 3T3 cells. Proc Natl Acad Sci USA 88:4230–4234

Tekle E, Astumian RD, Chock PB (1994) Selective and asymmetric molecular transport across electroporated cell membranes. Proc Natl Acad Sci USA 91:11512–11516

Titomirov AV, Sukharev S, Kistanova E (1991) In vivo electroporation and stable transformation of skin cells of newborn mice by plasmid DNA. Biochim Biophys Acta Rep 1088:131–134

Troiano GC, Stebe KJ, Raphael RM, Tung L (1999) The effects of gramicidin on electroporation of lipid bilayers. Biophys J 76:3150–3157

Tsong TY (1991) Electroporation of cell membranes. Biophys J 60:297–306

Van der Aa MA, Mastrobattista E, Oosting RS, Hennik WE, Koning GA, Crommelin DJ (2006) The nuclear pore complex: the gateway to successful nonviral gene delivery. Pharm Res 23:447–459

Van der Aa MA, Mastrobattista E, Oosting RS, Hennink WE, Koning GA, Crommelin DJ (2007) The nuclear pore complex: the gateway to successful nonviral gene delivery. Adv Drug Deliv Rev 59:698–717

Vandermeulen G, Staes E, Vanderhaeghen ML, Bureau MF, Scherman D, Préat V (2007) Optimisation of intradermal DNA electrotransfer for immunisation. J Control Res 124:81–87

Weaver JC (1993) Electroporation: a general phenomenon for manipulating cells and tissues. J Cell Biochem 51:426–435

Weaver JC, Chizmadzhev YA (1996) Theory of electroporation: a review. Bioelectrochem Bioenerg 41:135–160

Winterbourne DJ, Thomas S, Hermon-Taylor J, Hussain I, Johnstone AP (1988) Electric-shock-mediated transfection of cells. Biochem J 251:427–434

Wolf H, Rols MP, Boldt E, Neumann E, Teissié J (1994) Control by pulse parameters of electric field-mediated gene transfer in mammalian cells. Biophys J 66:524–531

Xie TD, Tsong TY (1993) Study of mechanisms of electric field-induced DNA transfection. V. Effects of DNA topology on surface binding, cell uptake, expression, and integration into host chromosomes of DNA in the mammalian cell. Biophys J 65:1684–1689

2.2. Conclusions

Les modèles moléculaires proposés sont parfois contradictoire et ne sont pas toujours en accord avec les données expérimentales. En effet, les observations expérimentales montrent que l'électrotransfert de plasmide est **un mécanisme complexe et lent**. Ces observations sont en contradiction avec les modèles i *(Smith et al., 2004; Krassowska et al., 2007)* et iii. Le modèle ii nécessite d'autres investigations *(Hristova et al., 2002)*. En revanche, les modèles iii *(Winterbourne et al., 1988; Klenchin et al., 1991; Sukharev et al., 1992; Tekle et al., 1994)* et iv *(Tarek, 2005)* sont en accord avec l'existence d'une interaction localisée entre les molécules de plasmide et la membrane perméabilisée. Le problème majeur avec les différents modèles proposés est qu'ils considèrent la membrane comme un assemblage purement lipidique alors que la membrane plasmique des cellules est un assemblage hautement structuré et dynamique, composé de lipides et de protéines. Ces dernières peuvent être impliquées dans l'électroperméabilisation des membranes en modifiant les propriétés mécaniques de ces dernières.

La membrane plasmique serait un partenaire actif des premières étapes du mécanisme.

La connaissance et le contrôle des mécanismes de l'électrotransfert de plasmide sont nécessaires pour évaluer leurs conséquences biologiques et physiologiques et leur efficacité pour le développement de protocoles cliniques et biotechnologiques.

3. Les applications *in vivo*

L'électrotransfert de plasmide est une méthode couramment utilisée *in vitro* et dont les applications *in vivo* sont de plus en plus nombreuses depuis ces dix dernières. De plus, quelques essais cliniques ont été maintenant approuvés. *In vivo*, l'électrotransfert de plasmide se heurte aux problèmes liés à l'organisation du tissu (i.e. contacts des cellules entre elles) sur la distribution du champ électrique et des molécules de plasmide.

La première partie de la revue publiée dans *Biophysical Reviews* se concentre sur les mécanismes biophysiques impliqués dans l'électrotransfert de plasmide *in vivo*. Dans

une deuxième partie, les procédures et les applications d'électrotransfert de plasmide *in vivo* seront discutées.

3.1. La revue

Biophys Rev (2009) 1:185–191
DOI 10.1007/s12551-009-0019-2

REVIEW

Gene electrotransfer: from biophysical mechanisms to in vivo applications

Part 2 - In vivo developments and present clinical applications

Jean-Michel Escoffre · Chloé Mauroy · Thomas Portet · Luc Wasungu · Aurelie Paganin-Gioanni · Muriel Golzio · Justin Teissié · Marie-Pierre Rols

Received: 13 August 2009 / Accepted: 19 October 2009 / Published online: 10 November 2009

Abstract Gene electrotransfer can be obtained not just on single cells in diluted suspension. For more than 10 years, this is a quasi routine strategy in tissue on the living animal and a few clinical trials have now been approved. New problems have been brought by the close contacts of cells in tissue both on the local field distribution and on the access of DNA to target cells. They need to be solved to provide a further improvement in the efficacy and safety of protein expression. There is a competition between gene transfer and cell destruction. Nevertheless, present results are indicative that electrotransfer is a promising approach for gene therapy. High level and long-lived expression of proteins can be obtained in muscles. This is used for a successful method of electrovaccination.

Keywords Electropermeabilization · Electroporation · Gene electrotransfer · In vivo applications

Introduction

Although the applications of tissue electropermeabilization are compelling, success has been limited by a poor understanding of the differences between electropermeabilization of single cells and intact tissues. In simple systems, such as isolated cells in suspension, plasmid transport into cells has been shown to be under control of electrical parameters. More than two decades of studies have provided theoretical models of electropermeabilization at the membrane level and largely phenomenological understanding at the cellular level. This was summarized in the companion paper. But relatively little basic approach has been done at the tissue level. Because there are different physical barriers and heterogeneous geometries within tissue, in vitro pseudo-tissue models such as dense cell suspensions (Pucihar et al. 2007) and multi-cellular tumor spheroid (Wasungu et al. 2009; Canatella et al. 2004) have been developed to understand the biophysical processes of electropermeabilization and gene transfer in tissues. These studies showed a perturbation of local electrical field on dense cell suspensions (Pucihar et al. 2007) and a limitation of gene delivery (Wasungu et al. 2009) related to the self-organization of cells in pseudo-tissues. Indeed, close contacts between cells and extracellular matrix may: (1) modify the electric field distribution, and (2) act as physical barriers that limit the diffusion of DNA plasmid (steric hindrance) and therefore its access to cells present in the core of the tissue. The systematic comparison of biophysical studies from isolated cells to 3D spheroid model allows the development and the optimization of in vivo gene electrotransfer procedures. In vivo biophysical mechanisms and applications of gene electrotransfer can now be addressed (Gehl 2008).

In vivo biophysical considerations

Plasmids are injected in the tissue and electric field pulses are generated in situ by an electrode system (so-called

Jean-Michel Escoffre and Chloé Mauroy have contributed equally to this work.

J.-M. Escoffre · C. Mauroy · T. Portet · L. Wasungu · A. Paganin-Gioanni · M. Golzio · J. Teissié (✉) · M.-P. Rols (✉)
CNRS, IPBS (Institut de Pharmacologie et de Biologie Structurale), Université de Toulouse UPS,
205 route de Narbonne,
31077 Toulouse, France
e-mail: justin.teissie@ipbs.fr
e-mail: rols@ipbs.fr

applicators) (Luxembourg et al. 2007). Expression is obtained when suitable electrical parameters are applied. The in vivo mechanism is still to be elucidated. However, most results bring evidence that in vivo gene electrotransfer is a multi-step process where plasmid distribution, cell permeabilization and plasmid electrophoresis act synergically as predicted from experiments at the single cell level (Golzio et al. 2002).

In vitro studies showed that electropermeabilization and electrophoretic forces are involved in the process of gene electrotransfer. As a consequence, Mir and collaborators proposed the combination of short intense pulses (termed HV pulses for high-voltage pulses) and low long pulses (termed LV for low-voltage pulses) for gene delivery (Satkauskas et al. 2002, 2005; Andre et al. 2008). The current data suggest that the HV+LV pulse combination does not bring significant improvement to gene delivery in vitro (Kanduser et al. 2009), whereas it is able to boost gene transfer into skeletal muscle (Satkauskas et al. 2005). Indeed, they showed that, under appropriate pulses conditions, the HV permeabilize the cells and the LV, which cannot permeabilize the muscle fibers, are supporting the migration of plasmid towards or across the permeabilized membrane of muscle fibers. The HV+LV combination was extended to other tissues such as liver and skin in rodent models (André et al. 2008). Striking differences between the different tissues were found, likely related to cell size and tissue organization (Hojman et al. 2008). This study has revealed differences in the electrical parameters needed to ensure efficient gene electrotransfer in various tissues. In each tissue, transfection efficiency depends on the plasmid distribution and electric field distribution within the tissue. In particular, plasmid distribution is different in different types of tissue (Andre et al. 2006; Mesojednik et al. 2007). Plasmids distribute easily in muscle; in small rodents, plasmids are dispersed all across the whole muscle. In liver, on the other hand, they found it necessary to perform intravenous injection in order to avoid the hydrodynamic effect of the injection of fluid directly in the tissue (Liu et al. 1999). Moreover, in agreement with the theory of electropermeabilization, higher HV field strengths are required to permeabilize small cells like tumor and skin cells compared to large cells like muscle fibers (Valic et al. 2003). However, no HV is necessary to obtain efficient gene transfer in the liver. Hepatocytes are electrically connected through gap junctions. These junctions permit viewing a cluster of hepatocytes as one large cell, such that the electric potential drop induced by the external field involves a large amplification factor. In consequence, small external field strengths might become effective in electropermeabilizing the hepatocyte membrane. Nevertheless, LV parameters must be adapted in each case to the specific tissue. Optimal gene expression with the HV and LV pulse combination in muscle and skin is obtained with a rather large range of field intensities for the HV pulses. Because the transfection efficiency appears to be due largely to the electrophoretic displacement during LV pulse, this pulse combination is less susceptible to the lack of homogeneity in the field distribution. In fact, in a large part of the tissue, the local electric field intensity of the HV pulse will remain within the window of efficiency over a wide range of field strengths. Thus, using the HV and LV pulse combination allows manipulation over a range of therapeutic field strengths. Moreover, Hojman and collaborators showed that slight cell disturbances occur with the HV+LV combination used for gene transfer. This is highly important, as minimal perturbation of cell physiology is essential for efficient transgene expression (Hojman et al. 2008).

A key parameter of gene electrotransfer is the local electric field strength. As the field results from a voltage applied between two electrodes, the electrode configuration is obviously controlling the field distribution and transfection efficiency (Gehl and Mir 1999). Electrode configurations for therapeutic purposes are parallel plates and wire and contact plate electrodes as well as needle electrodes and arrays (Jaroszeski et al. 1997; Ramirez et al. 1998; Gilbert et al. 1997; Mazères et al. 2009). Electrode configuration controls electric field distribution in tissue. However, due to its anatomy and its electrical properties, tissue reacts to the applied external electric field. If the applied external electric field is high enough, local permeabilization of the tissue occurs, i.e., electric field distribution strongly controls permeabilization (Miklavcic et al. 1998). If the local electric field is too high, an irreversible alteration in cell membrane occurs. This may result in local burns. In gene therapy, it is very important to obtain a large volume of permeabilized tissue, covering whole tissue being subjected to electropulsation and preserving cell viability. Therefore, it is necessary to choose optimal electrode configuration and pulse parameters for particular target tissue. A safe approach is to compute in advance the electric field distribution in tissues by means of numerical modeling. Modeling of electric field distribution in tissue is difficult due to heterogeneous material properties of tissue and its shape (Mossop et al. 2006). Numerical modeling has been successfully used and is also validated by comparison of computed and measured consequences of electric field distribution (Miklavcic et al. 1998, 2000). Tissue electrical heterogeneity was never taken into account in the simulation, since tissues were always considered as an amorphous (ohmic) conducting gel (Gowrishankar and Weaver 2003). Electropermeabilization induces a membrane conductance change as previously described (Kinosita and Tsong 1979; Abidor et al. 1994) and observed in tissue (Miklavcic et al. 2000). Due to the swelling, the volume fraction is affected (Deng et al. 2003). Such a geometrical change should affect

the field distribution in tissue and the value of the field at the cell level in the tissue (Pavlin et al. 2002). A precise simulation of the time dependent field distribution in the tissue is clearly needed for different electrode geometries to optimize this electro-technical aspect of the biological treatment (Pucihar et al. 2009).

Plate parallel electrodes and needle arrays are the most popular electrodes to in vivo gene electrotransfer. Plate electrodes offer the advantages that electric pulses can be applied transcutaneously and that electric field between the electrodes is quite homogeneous (Gehl et al. 1999). The two main limitations are (1) the small gap between the electrodes, which is limited by the electrical power of electropulsators, and (2) high field at the contact of the electrode with the skin, which can induce burns. The needle electrodes enable deeper penetration of the electric field into the tissue. However, the electric field distribution is not as homogenous resulting in higher field intensity around the needles. This may lead to local tissue necrosis. The heterogeneous field distribution is under the control of the diameter of each electrode. As a consequence, new electrodes have been designed and tested to minimize tissue damages (Dona et al. 2003; Babiuk et al. 2003).

The various biophysical studies of in vitro and in vivo gene electrotransfer processes allowed the development and the optimization of protocols for routine clinical applications.

In vivo gene electrotransfer

The use of electropulsation for introducing naked DNA plasmid in vivo is a growing field. Several works report the gene electrotransfer into the skeletal (Aihara and Miyazaki 1998; Mir et al. 1999) and cardiac muscle (Dean 2005; Harrison et al. 1998), liver (Heller et al. 1996; Liu and Huang 2002), skin (Titomirov et al. 1991; Vandermeulen et al. 2007), tumors (Rols et al. 1998), spleen (Tupin et al. 2003), kidney (Isaka et al. 2005), lung (Zhou et al. 2007), brain (Saito and Nakatsuji 2001), and joints (Khoury et al. 2006). The feasibility of electropulsation as a nucleic acid delivery method was demonstrated using reporter or therapeutic genes into specific tissues in vivo (Mir et al. 2005).

Gene electrotransfer procedure

Endotoxin-free plasmid solutions are injected in the target tissue localized between the electrodes, where electric pulses are applied. Gene expression depends on the amount of injected plasmid (range of plasmid amount: 20–100 μg) (Mir et al. 1999; Mathiesen 1999) and on the volume of injection (Dupuis et al. 2000). For clinical applications, different routes of injection are defined on the target: intramuscular (i.m.), intradermal (i.d.), intratumoral (i.t.), and intravenous (i.v.) (Lucas et al. 2002). The volume of injection is limited by the size of the target to avoid a dramatic and damaging swelling. The injection speed is seldom taken into account. But a recent work suggested that the injection speed is a key parameter to gene delivery into skeletal muscle and liver (André et al. 2006). In case of mice skeletal muscle, injection speed of 1.5 μL/s is associated with a high level expression (Golzio et al. 2004).

The delay between injection and electropulsation depends on the tissue. In the case of murine B16 melanoma tumors, a short delay (<1 min) leads to a high level of transfection (Rols et al. 1998). Whereas, in murine skeletal muscle, a delay between a few seconds and 4 h does not change the transfection efficiency (Satkauskas et al. 2001).

The electric pulse parameter used in gene electrotransfer varied between the studies (Mir et al. 1999; Cemazar et al. 2009). Gene expression is detected only when an overcritical voltage to electrode distance is applied bringing about electropermeabilization. This threshold is dependent on the target tissues (Heller et al. 1996; Rols et al. 1998). In the case of skeletal muscle, lowest values are found. As explained, the geometry of electrodes technically controls this threshold. It is higher with contact electrodes than with needle electrodes (Gehl et al. 1999). Electric pulse duration must be adjusted with the origin of the tissue. Indeed, an efficient transfection into skeletal muscles and tumors required the application of limited number of long pulses (several ms) at a low frequency (1 Hz). But, a very high number of repetitive short but stronger pulses (several μs) at a high frequency (kHz) give a high level of gene expression into the same tissues (Lucas et al. 2002; Vicat et al. 2000; Rizzuto et al. 1999; Mir et al. 1999; Durieux et al. 2002). A suitable protocol using a short high voltage pulse (kV/cm, μs) followed by several longer low voltage pulses (V/cm, ms) at a low frequency (1 Hz) has been proposed to aid gene delivery into skeletal muscle (Bureau et al. 2000). The first pulses permeabilize the tissue while the other ones act on plasmid electrophoresis (Satkauskas et al. 2002). In the case of liver, low numbers of short (several μs) stronger pulses at a low frequency (1 Hz) efficiently transfect this tissue (Heller et al. 1996).

Electropulsation on live animals may cause side effects such as reversible inflammation (Hartikka et al. 2001), burns of the skin (Lee et al. 2000), vasocontrictory reflex (Gehl et al. 2002), or tissue destruction depending on the type of electrodes and electric field parameters.

Optimization of the experimental procedures is clearly needed. An empirical approach may be used (Molnar et al. 2004). A more systematic investigation of physical as well as biochemical parameters may bring a more rational evaluation.

In vivo applications

Secreted therapeutic proteins

The skeletal muscle is the most transfected tissue by gene electrotransfer. Indeed, the skeletal muscle has interesting physiological properties such as multi-nucleated (i.e., high number of expression machineries) and long-lived fibers (i.e., long-lasting gene expression), which open several applications in gene therapy (Aihara and Miyazaki 1998; Mir et al. 1999). This organ is composed of long-lived fibers, which allow long-lasting gene expression. Moreover, its rich vascularization makes it a secreting organ of therapeutic proteins (Trollet et al. 2008). Indeed, the i.m. electrotransfer of plasmid-encoding erythropoietin (EPO) induces the production of EPO therapeutic doses in order to treat the anemia related to kidney diseases (Rizzuto et al. 1999; Hojman et al. 2007) or β-thalassemy (Payen et al. 2001). In the same way, TGFR-β2 receptor and VEGF-164 factor expressions treat respectively, the lung injury and fibrosis (Yamada et al. 2007) and diabetic neuropathy (Murakami et al. 2006).

Gene electrotransfer allowed the development of anti-tumoral immunotherapies. Indeed, electrotransfer of plasmid-encoding suicide gene (e.g., ePNP/fludarabine) (Deharvengt et al. 2007), cytokines (e.g., IL-12) (Daud et al. 2008), anti-angiogenesis factors (e.g., vasostatin) (Jazowiecka-Rakus et al. 2006), tumor suppressors (e.g., p53) (Kusumanto et al. 2007) into skeletal muscle or tumors stimulated or activated the immune responses against the tumours. This immuno-therapy induced a decrease of tumor growth and limited the tumor recovery and metastasis progression in the case of melanoma, hepato-carcinoma, and colon and mammary carcinoma.

Electrovaccination

Gene electrotransfer allowed the development of genetic electrovaccination. Genetic vaccination rests on the principle of direct injection of plasmid encoding vaccinal protein into the muscle or the skin (Wolff et al. 1990; Rice et al. 2008). This protein induces host response and activates the immune system. Compared to the gene therapy, genetic vaccination requires only low and transient gene expressions in few cells (Rice et al. 2008). Several works showed that the gene electrotransfer increase the immune response against the antigen compared to the injection alone (Dupuis et al. 2000; Widera et al. 2000; Babiuk et al. 2002; Dayball et al. 2003). The electrovaccination allowed the development of genetic vaccines against bacterial infections such as *Mycobacterium tuberculosis* (Zhang et al. 2007) and viral infections such as HIV (Hirao et al. 2008). Recently, electrovaccination showed its efficiency to induce immune response against tumors such as melanoma, and colon and mammary carcinoma (Kalat et al. 2002; Buchan et al. 2005; Curcio et al. 2008).

RNA interference

In the last 10 years, RNA interference (RNAi) has rapidly become an important tool for studying gene functions and holds promise for the development of therapeutic gene silencing (Cheng et al. 2003). RNAi is a post-transcriptionnal process triggered by the delivery of plasmid encoding short hairpin RNA (shRNA) that induces genes silencing in a sequence-specific manner (Takahashi et al. 2009). Recently, Escoffre et al. (2008). demonstrated that the electrotransfer of plasmid encoding shRNA induces a long-lasting reporter gene silencing into mice muscle. Moreover, this strategy induces an efficient silencing of endogenous genes such as myostatin and TLR-4 involved in the myopathies and inflammatory diseases (Magee et al. 2006; Eefting et al. 2007).

Conclusions

Electropulsation, a biophysical approach, is one of the non-viral methods successfully used to transfer plasmid DNA into living cells in vitro and in vivo. It has the main advantages of being easy to perform, fast, reproducible and safe (Golzio et al. 2004). Currently, it is described by an empirical model supported by direct experimental evidences in which gene electrotransfer appears as a multistep process (see the companion paper). Its further development need a better understanding of the basic effects induced at the membrane, cellular and tissue levels by electrical events and the plasmid entry in the cell. Gene electrotransfer appears promising for gene and cell therapies (Daud et al. 2008). But if the effects of the electric field parameters are under control (electric pulse strength higher than a threshold value, millisecond pulse duration for efficient gene expression), the associated membrane destabilization, which is a stress for the cells and may affect the cell viability, has still to be clearly described (see the companion paper). Moreover, it becomes evident that extracellular barriers, e.g., extracellular matrix and exogenous nucleases, and intracellular barriers, e.g., cytoplasm crowding, endogenous nucleases, and nuclear envelope, compromise the transfection efficiency. Studies will also be necessary to understand the cascade of events triggered by electropermeabilization at the tissue levels where new constraints coming from tissue organizations are present, such as the inhomogeneity of the electric field strength and the intercellular distribution of plasmid DNA.

Acknowledgements This work was supported by the CNRS, the AFM (Association Française pour les Myopathies) and the region Midi-Pyrénées.

References

Abidor IG, Li LH, Hui SW (1994) Studies of cell pellets: II. Osmotic properties, electroporation, and related phenomena: membrane interactions. Biophys J 67:427–435

Aihara H, Miyazaki JI (1998) Gene transfer into muscle by electroporation in vivo. Nature Biotechnol 16:867–870

André FM, Cournil-Henrionnet C, Vernerey D, Opolon P, Mir LM (2006) Variability of naked DNA expression after direct local injection: the influence of the injection speed. Gene Ther 13:1619–1627

André FM, Gehl J, Sersa G, Préat V, Hojman P, Eriksen J, Golzio M, Cemazar M, Pavselj N, Rols MP, Miklavcic D, Neumann E, Teissié J, Mir LM (2008) Efficiency of high- and low-voltage pulse combinations for gene electrotransfer in muscle, liver, tumor and skin. Hum Gene Ther 19:1261–1271

Babiuk S, Baca-Estrada ME, Foldvari M, Storms M, Rabussay D, Widera G, Babiuk LA (2002) Electroporation improves the efficacy of DNA vaccines in large animals. Vaccine 20:3399–3408

Babiuk S, Baca-Estrada ME, Foldvari M, Baizer L, Stout R, Storms M et al (2003) Needle-free topical electroporation improves gene expression from plasmids administrated in porcine skin. Mol Ther 8:992–998

Buchan S, Gronevik E, Mathiesen I, King CA, Stevenson FK, Rice J (2005) Electroporation as a "prime/boost" strategy for naked DNA vaccination against a tumor antigen. J Immunol 174:6292–6298

Bureau FM, Gehl J, Deleuze V, Mir LM, Scherman D (2000) Importance of association between permeabilization and electrophoretic forces for intramuscular DNA electrotransfer. Biochim Biophys Acta 1474:353–359

Canatella PJ, Black MM, Bonnichsen DM, Mckenna C, Prausnitz MR (2004) Tissue electroporation: quantification and analysis of heterogenous transport in multicellular environments. Biophys J 86:3260–3268

Cemazar M, Golzio M, Sersa G, Hojman P, Kranjc S, Mesojednik S, Rols MP, Teissie J (2009) Control by pulse parameters of DNA electrotransfer into solid tumors in mice. Gene Ther 16:635–644

Cheng JC, Moore TB, Sakamoto KM (2003) RNA interference and human disease. Mol Gen Metabol 80:121–128

Curcio C, Khan AS, Spadaro M, Quaglino E, Cavallo F, Forni G, Draghia-Akli R (2008) DNA immunization using constant-current electroporation affords long-term protection from autochthonous mammary carcinomas in cancer-prone transgenic mice. Cancer Gene Ther 15:108–114

Daud AI, DeConti RC, Andrews S, Urbas P, Riker AI, Sondak VK, Munster PN, Sullivan DM, Ugen KE, Messina JL, Heller R (2008) Phase I trial of interleukin-12 plasmid electroporation in patients with metastatic melanoma. J Clin Oncol 26:5896–58903

Dayball K, Millar J, Miller M, Wan YH, Bramson J (2003) Electroporation enables plasmid vaccines to elicit CD8+ T cell responses in the absence of CD4+ T cells. J Immunol 171:3379–3384

Dean DA (2005) Nonviral gene transfer to skeletal, smooth, and cardiac muscle in living animals. Am J Physiol Cell Physiol 285: C233–C245

Deharvengt S, Rejuba S, Wack S, Aprahamian M, Hajri A (2007) Efficient electrogene therapy for pancreatic adenocarcinoma treatment using the bacterial purine nucleoside phosphorylase suicide gene with fludarabine. Int J Oncol 30:1397–1406

Deng J, Schoenbach KH, Buescher ES, Hair PS, Fox PM, Beebe SJ (2003) The effects of intense submicrosecond electrical pulses on cells. Biophys J 84:2709–2714

Dona M, Sandri M, Rossini K, Dell'Aica I, Podhorska-Okolow M, Carraro U (2003) Functional in vivo gene transfer into the myofibers of adult skeletal muscle. Biochem Biophys Res Commun 312:1132–1138

Dupuis M, Denis-Mize K, Woo C, Goldbeck C, Selby MJ, Chen M, Otten GR, Ulmer JB, Donnelly JJ, Ott G, McDonald DM (2000) Distribution of DNA vaccines determines their immunogenicity after intramuscular injection in mice. J Immunol 165:2850–2858

Durieux AC, Bonnefoy R, Manissolle C, Freyssenet D (2002) High-efficiency gene electrotransfer into skeletal muscle: description and physiological applicability of a new pulse generator. Biochem Biophys Res Comm 296:443–450

Eefting D, Grimbergen JM, de Vries MR, van Weel V, Kaijzel EL, Que L, Moon RT, Lowik CW, van Bockel JH, Quax PH (2007) Prolonged in vivo gene silencing by electroporation-mediated plasmid delivery of small interfering RNA. Hum Gene Ther 18:861–869

Escoffre JM, Debin A, Reynes JP, Drocourt D, Tiraby G, Hellaudais L, Teissié J, Golzio M (2008) Long-lasting in vivo gene silencing by electrotransfer of shRNA expressing plasmid. Tech Cancer Res Treat 7:1–8

Gehl J (2008) Electroporation for drug and gene delivery in the clinic: doctors go electric. Methods Mol Biol 433:351–359

Gehl J, Mir LM (1999) Determination of optimal parameters for in vivo gene transfer by electroporation, using a rapid in vivo test for cell permeabilization. Biochem Biophys Res Commun 261:377–380

Gehl J, Sorensen TH, Nielsen K, Raskmark P, Nielsen SL, Skovsgaard T, Mir LM (1999) In vivo electroporation of skeletal muscle: threshold, efficacy and relation to electric field distribution. Biophys Biochim Acta 1428:233–240

Gehl J, Skovsgaard T, Mir LM (2002) Vacular reactions to in vivo electroporation: characterization and consequences for drug and gene delivery. Biochim Biophys Acta 1569:51–58

Gilbert RA, Jaroszeski MJ, Heller R (1997) Novel electrode designs for electrochemotherapy. Biochim Biophys Acta 1334:9–14

Golzio M, Teissié J, Rols MP (2002) Direct visualization at the single-cell level of electrically mediated gene delivery. Proc Natl Acad Sci USA 99:1292–1297

Golzio M, Rols MP, Teissié J (2004) In vitro and in vivo electric field-mediated permeabilization, gene transfer, and expression. Methods 33:126–135

Gowrishankar TR, Weaver JC (2003) An approach to electrical modelling of single and multiple cells. Proc Natl Acad Sci USA 100:3203–3208

Harrison RL, Byrne BJ, Tung L (1998) Electroporation-mediated gene transfer in cardiac tissue. FEBS Lett 435:1–5

Hartikka J, Sukhu L, Buchner C, Hazard D, Bozoukova V, Margalith M, Nishioka WK, Wheeler CJ, Manthorp M, Sawdey M (2001) Electroporation-facilitated delivery of plasmid DNA in skeletal muscle: plasmid dependence of muscle damage and effect of poloxamer 188. Mol Ther 4:407–415

Heller R, Jaroszeski M, Atkin A, Moradpour D, Gilbert R, Wands J, Nicolau C (1996) In vivo gene electroinjection and expression in rat liver. FEBS Lett 389:225–228

Hirao LA, Wu L, Khan AS, Satishchandran A, Draghia-Akli R, Weiner DB (2008) Intradermal/cutaneous immunization by electroporation improves plasmid vaccine delivery and potency in pigs a rhesus macaques. Vaccine 26:440–448

Hojman J, Gissel H, Gehl J (2007) Sensitive and precise regulation of haemoglobin after gene transfer of erythropoietin to muscle tissue using electroporation. Gene Ther 14:950–959

Hojman P, Gissel H, Andre FM, Cournil-Henrionnet C, Erisken J, Gehl J, Mir LM (2008) Physiological effects of high- and low-voltage pulse combinations for gene electrotransfer in muscle. Hum Gene Ther 19:1249–1260

Isaka Y, Yamada K, Takabatake Y, Mizui M, Miura-Tsujie M, Ichimaru N, Yazawa K, Utsugi R, Okuyama A, Hori M, Imai E, Takahara S (2005) Electroporation-mediated HGF gene transduction protected the kidney against graft injury. Gene Ther 12:815–820

Jaroszeski MJ, Gilbert RA, Heller R (1997) In vivo antitumor effects of electrochemotherapy in a hepatoma model. Biochim Biophys Acta 1334:15–18

Jazowiecka-Rakus J, Jarosz M, Szala S (2006) Combination of vasostatin gene therapy with cyclophosphamide inhibits growth of B16(F10) melanoma tumours. Acta Biochim Pol 53:199–202

Kalat M, Kupcu Z, Schuller S, Zalusky D, Zehetner M, Paster W, Schweighoffer T (2002) In vivo plasmid electroporation induces tumor antigen-specific CD8+ T-cell responses and delays tumor growth in a syngeneic mouse melanoma model. Cancer Res 62:5489–5494

Kanduser M, Miklavcic D, Pavlin M (2009) Mechanisms involved in gene electrotransfer using high- and low-voltage pulses—an in vitro study. Bioelectrochemistry 74:265–271

Khoury M, Bigey P, Louis-Plence P, Noel D, Rhinn H, Scherman D, Jorgensen C, Apparailly F (2006) A comparative study on intra-articular versus systemic electrotransfer in experimental arthritis. J Gene Med 8:1027–1036

Kinosita K Jr, Tsong TY (1979) Voltage-induced conductance in human erythrocyte membranes. Biochim Biophys Acta 554:479–497

Kusumanto YH, Mulder NH, Dam WA, Losen M, De Baets MH, Meijer C, Hospers GA (2007) Improvement of in vivo transfer of plasmid DNA in muscle: Comparison of electroporation versus ultrasound. Drug Deliv 14:273–277

Lee RC, Zhang D, Hannig J (2000) Biophysical injury mechanisms in electrical shock trauma. Annu Rev Biomed Eng 2:477–509

Liu F, Huang L (2002) Electric gene transfer to the liver following systemic administration of plasmid DNA. Gene Ther 9:1116–1119

Liu F, Song Y, Liu D (1999) Hydrodynamics-based transfection in animals by systemic administration of plasmid DNA. Gene Ther 6:1258–1266

Lucas ML, Heller L, Coppola D, Heller R (2002) IL-12 plasmid delivery by in vivo electroporation for the successful treatment of established subcutaneaous B16.F10 melanoma. Mol Ther 5:668–675

Luxembourg A, Evans CF, Hannaman D (2007) Electroporation-based DNA immunization: translation to the clinic. Expert Opin Biol Ther 7:1647–1664

Magee TR, Artaza JN, Ferrini MG, Vernet D, Zurriga FI, Cantini L, Reusz-Porszasz S, Rajfer J, Gonzalez-Cadavid NF (2006) Myostatin short interfering hairpin RNA gene transfer increases skeletal muscle mass. J Gene Med 8:1171–1181

Mathiesen I (1999) Electropermeabilization of skeletal muscle enhances gene transfer in vivo. Gene Ther 6:508–514

Mazères S, Sel D, Golzio M, Pucihar G, Tamzali Y,Miklavcic D, Teissié J (2009) Non invasive contact electrodes for in vivo localized cutaneous electropulsation andassociated drug and nucleic acid delivery. J. Control. Release 134:125–131

Mesojednik S, Pavlin D, Sersa G, Coer A, Kranjc S, Grosel A, Tevz G, Cemazar M (2007) The effect of the histological properties of tumors on transfection efficiency of electrically assisted gene delivery to solid tumors in mice. Gene Ther 14:1261–1269

Miklavcic D, Beravs K, Semrov D, Cemazar M, Demsar F, Sersa G (1998) The importance of electric field distribution for effective in vivo electroporation of tissues. Biophys J 74:2152–2158

Miklavcic D, Semrov D, Mekid H, Mir LM (2000) A validated model of in vivo electric field distribution in tissues for electrochemotherapy and for DNA electrotransfer for gene therapy. Biochim Biophys Acta 1523:73–83

Mir LM, Bureau MF, Gehl J, Rangara R, Rouy D, Caillaud JM, Delaere P, Branellec D, Schwartz B, Scherman D (1999) High-efficiency gene transfer into skeletal muscle mediated by electric pulses. Proc Natl Acad Sci USA 96:4262–4267

Mir LM, Moller PH, André F, Gehl J (2005) Electric pulse-mediated gene delivery to various animal tissues. Adv Genet 54:83–114

Molnar MJ, Gilbert R, Lu Y, Liu AB, Guo A, Larochelle N et al (2004) Factors influencing the efficacy, longevity, and safety of electroporation-assisted plasmid-based gene transfer into mouse muscles. Mol Ther 10:447–455

Mossop BJ, Barr RC, Henshaw JW, Zaharoff DA, Yuan F (2006) Electric fields in tumors exposed to external voltage sources: implication for electric field-mediated drug and gene delivery. Ann Biomed Eng 34:1564–1572

Murakami T, Arai M, Sunada Y, Nakamura A (2006) VEGF 164 gene transfer by electroporation improves diabetic sensory neuropathy in mice. J Gene Med 8:773–781

Pavlin M, Pavselj N, Miklavcic D (2002) Dependence of induced transmembrane potential on cell density, arrangement, and cell position inside a cell system. IEEE Trans Biomed Eng 49:605–612

Payen E, Bettan M, Rouyer-Fessard P, Beuzard Y, Scherman D (2001) Improvement of mouse β-thalassemia by electrotransfer of erythropoietin cDNA. Exp Hematol 29:295–300

Pucihar G, Kotnik T, Teissié J, Miklavcic D (2007) Electropermeabilization of dense cell suspensions. Eur Biophys J 36:173–185

Pucihar G, Miklavcic D, Kotnik T (2009) A time-dependent numerical model of transmembrane voltage inducement and electroporation of irregularly shaped cells. IEEE Trans Biomed Eng 56:1491–14501

Ramirez LH, Orlowski S, An D, Bindoula H, Dzodic R, Ardouin P et al (1998) Electrochemotherapy on liver tumours in rabbits. Br J Cancer 77:2104–2111

Rice J, Ottensmeier CH, Stevenson FK (2008) DNA vaccines: precision tools for activating effective immunity against cancer. Nature Rev Cancer 8:108–120

Rizzuto G, Cappelletti M, Malone D, Savino R, Lazzaro D, Costa P, Mathiesen I, Cortese R, Ciliberto G, Laufer R, La Monica N, Fattori E (1999) Efficient and regulated erythropoietin production by naked DNA injection and muscle electroporation. Proc Natl Acad Sci USA 96:6417–6422

Rols MP, Delteil C, Golzio M, Dumond P, Cros S, Teissie J (1998) In vivo electrically mediated protein and gene transfer in murine melanoma. Nat Biotechnol 16:168–171

Saito T, Nakatsuji N (2001) Efficient gene transfer into embryonic mouse brain using in vivo electroporation. Dev Biol 240:237–246

Satkauskas S, Bureau MF, Mahfoudi A, Mir LM (2001) Slow accumulation of plasmid in muscle cells: supporting evidence for a mechanism of DNA uptake by receptor-mediated endocytosis. Mol Ther 4:317–323

Satkauskas S, Bureau MF, Puc M, Mahfoudi A, Scherman D, Miklavcic D, Mir LM (2002) Mechanisms of in vivo DNA electrotransfer: respective contributions of cell electropermeabilization and DNA electrophoresis. Mol Ther 5:133–140

Satkauskas S, André F, Bureau MF, Scherman D, Mikkavcic D, Mir LM (2005) Electrophoretic component of electric pulses determines the efficacy of in vivo DNA electrotransfer. Hum Gene Ther 16:1194–1201

Takahashi Y, Nishikawa M, Takakura Y (2009) Nonviral vector-mediated RNA interference: its gene silencing characteristics and important factors to achieve RNAi-based gene therapy. Adv Drug Deliv Rev 61:760–766

Titomirov AV, Sukharev S, Kistanova E (1991) In vivo electroporation and stable transformation of skin cells of newborn mice by plasmid DNA. Biochim Biophys Acta Report 1088:131–134

Trollet C, Scherman D, Bigey P (2008) Delivery of DNA into muscle for treating systemic diseases: advantages and challenges. Methods Mol Biol 423:199–214

Tupin E, Poirier B, Bureau MF, Khallou-Laschet J, Vranckx R, Caligiuri G, Gaston AT, Duong JP, Huyen V, Scherman D, Bariéty J, Michel JB, Nicoletti A (2003) Non-viral gene transfer of murine spleen cells achieved by in vivo electroporation. Gene Ther 10:569–579

Valic B, Golzio M, Pavlin M, Schatz A, Faurie C, Gabriel B, Teissié J, Rols MP, Miklavcic D (2003) Effect of electric field induced transmembrane potential on spheroidal cells: theory and experiment. Eur Biophys J 32:519–528

Vandermeulen G, Staes E, Vanderhaeghen ML, Burea MF, Scherman D, Préat V (2007) Optimisation of intradermal DNA electrotransfer for immunisation. J. Control. Release 124:81–87

Vicat JM, Boisseau S, Jourdes P, Lainé M, Wion D, Bouali-Benazzouz R, Benabid AL, Berger F (2000) Muscle transfection by electroporation with high-voltage and short-pulse currents provides high-level and long-lasting gene expression. Hum Gene Ther 11:909–916

Wasungu L, Escoffre JM, Valette A, Teissie J, Rols MP (2009) A 3D in vitro spheroid model as a way to study the mechanisms of electroporation. Int J Pharm in press

Widera G, Austin M, Rabussay D, Goldbeck C, Barnett SW, Chen M, Leung L, Otten GR, Thudium K, Selby MJ, Ulmer JB (2000) Increased DNA vaccine delivery and immunigenicity by electroporation in vivo. J Immunol 164:4635–4640

Wolff JA, Malone RW, Williams P, Chong W, Acsadi G, Jani A, Felgner PL (1990) Direct gene transfer into mouse muscle in vivo. Science 247:1465–1468

Yamada M, Kuwano K, Maeyama T, Yoshimi M, Hamada N, Fukumoto J, Egashira K, Hiasa K, Takayama K, Nakanishi Y (2007) Gene transfer of soluble transforming growth factor type II receptor by in vivo electroporation attenuates lung injury and fibrosis. J Clin Pathol 60:916–920

Zhang X, Divangahi M, Ngai P, Santosuosso M, Millar J, Zganiacz A, Wang J, Bramson J, Xing Z (2007) Intramuscular immunization with a monogenic plasmid DNA tuberculosis vaccine: Enhanced immunogenicity by electroporation and co-expression of GM-CSF transgène. Vaccine 25:1342–1352

Zhou R, Norton JE, Zhang N, Dean DA (2007) Electroporation-mediated transfer of plasmids to the lung results in reduced TLR9 signaling and inflammation. Gene Ther 14:775–780

3.2. Conclusions

L'électroperméabilisation est une méthode non-virale qui permet un transfert efficace et sûr de molécules de plasmide au sein de cellules et de tissus. Cette méthode est facile à mettre en œuvre, rapide, reproductible et sûre. L'électrotransfert de plasmide est décrit comme un processus multi-étapes. L'électrotransfert de plasmide *in vivo* permet de nombreuses applications dans le domaine de la clinique vétérinaire et humaine, e.g. l'électro-vaccination *(Zhang et al., 2007; Curcio et al., 2008)*, la thérapie génique anti-tumorale (Shibata et al., 2002; Heller et al., 2006), l'ARN interférence *(Magee et al., 2006; Eefting et al., 2007)*.

Son utilisation rationnelle passera par une compréhension du mécanisme à l'échelle de la membrane plasmique, de la cellule et du tissu.

De plus, il devient évident que des barrières extracellulaires (e.g. la matrice extracellulaire, l'organisation intercellulaire dans les tissus) et des barrières intracellulaires (e.g. le cytosquelette et l'enveloppe nucléaire) peuvent compromettre l'efficacité du transfert de plasmides. De futures études seront nécessaires pour comprendre la cascade d'évènements induits par l'électroperméabilisation à l'échelle du tissu où de nouvelles contraintes liées à l'organisation du tissu telles que l'hétérogénéité du champ électrique, la bio-distribution des molécules de plasmide sont présentes.

II. OBJECTIFS

II. Objectifs

Les thérapies géniques et cellulaires représentent un enjeu majeur pour le développement de protocoles à visée préventive ou thérapeutique. Le transfert de molécules thérapeutiques (e.g. plasmide, médicaments anti-cancéreux…) apparaît comme l'élément essentiel de cette approche. Au niveau du transfert de plasmide, de nombreuses méthodes ont été développées pour faciliter la pénétration de plasmide au sein de la cellule. Les méthodes virales, dont l'efficacité est largement supérieure aux autres méthodes, reste généralement la méthode de choix pour la majorité des essais cliniques malgré les risques qui peuvent y être associés. Ainsi le développement de méthodes alternatives demeure indispensable, et notamment la compréhension des mécanismes mis en jeu afin de caractériser les possibles effets délétères. L'électroperméabilisation *in vivo* présente de grandes potentialités d'application aussi bien pour le transfert de plasmide que de petites molécules. Cependant, son utilisation rationnelle nécessite la bonne maîtrise des mécanismes *in vitro* et une parfaite connaissance des contraintes liées à l'*in vivo*.

Les mécanismes biophysiques impliqués dans le phénomène d'électroperméabilisation demeurent mal connus. L'étude des mécanismes étendue aux plasmides montre que la perméabilisation est nécessaire mais que le mécanisme du transfert de plasmide est différent de celui des petites molécules (i.e. <4 kDa). Le mécanisme de l'électrotransfert de plasmide est un processus multi-étapes, nettement plus complexe que celui de l'électroperméabilisation. Le modèle que nous décrivons et dans le cadre duquel se situe ce travail de thèse implique différentes étapes de: (1) perméabilisation de la membrane plasmique, (2) migration électrophorétique du plasmide, (3) interaction avec la membrane électroperméabilisée, (4) translocation de la membrane plasmique, (5) migration cytoplasmique, (6) passage de l'enveloppe nucléaire et (7) expression génique. En revanche, de nombreux points restent encore à élucider.

Les travaux présentés dans ce travail de thèse ont pour objectif l'étude des conséquences membranaires de l'électroperméabilisation et l'étude biophysique du

mécanisme de transfert de plasmide *in vitro*. Ces études ont été réalisées au niveau de la cellule unique avec une bonne résolution spatio-temporelle des phénomènes observés.

La première partie de ce travail a porté sur l'influence de la cohésion membranaire sur le mécanisme de perméabilisation membranaire. L'organisation membranaire est caractérisée par une répartition asymétrique des phospholipides. Nous avons étudié si l'électroperméabilisation pouvait perturber cette organisation membranaire.

La deuxième partie s'est focalisée sur la caractérisation biophysique de l'interaction plasmide/membrane perméabilisée. Cette interaction apparaît comme une étape clé du mécanisme. Pour conforter cette hypothèse, nous avons étudié l'effet des paramètres électriques et de la polarité des impulsions électriques sur cette interaction. Puis, nous avons étudié l'effet de la topologie du plasmide sur l'interaction/membrane perméabilisée. Enfin, nous avons étendu l'étude à d'autres lignées cellulaires.

La troisième partie a consisté à étudier l'influence de la perméabilisation membranaire électro-induite sur la mobilité latérale des protéines membranaires par la technique de FRAP.

La quatrième partie vise à combiner la sonoporation à l'électroperméabilisation afin d'augmenter l'efficacité de transfection.

III. RÉSULTATS

PARTIE I

EFFETS DE L'ÉLECTROPERMÉABILISATION SUR LA COHÉSION MEMBRANAIRE

III. Résultats

Partie I. Effets de l'électroperméabilisation sur la cohésion membranaire

1. Introduction

L'application d'impulsions électriques altère l'organisation et la cohésion de l'édifice membranaire. La membrane plasmique, mise hors équilibre, devient perméable aux petites molécules (<4kDa). Ainsi, la matrice lipidique se retrouve perturbée. Un changements d'orientation des têtes polaires des phospholipides a lieu ; il conduit à un destruction de la couche d'hydratation *(Stulen, 1981; Lopez et al., 1988)*. Ces travaux, bien qu'anciens, sont les seuls travaux expérimentaux relatifs à l'étude du phénomène d'électroperméabilisation cellulaire à l'échelle moléculaire.

La distribution des phospholipides au sein de deux feuillets d'une membrane est asymétrique. Les phospholipides PE et PS sont majoritairement présents sur le feuillet interne, alors que le PC se situe majoritairement sur le feuillet externe de la membrane plasmique. L'asymétrie de la distribution transverse est maintenue par l'intervention de protéines membranaires *(Devaux et al., 2006)*. De précédentes études montrent que l'électroperméabilisation des érythrocytes est un processus qui se décompose en deux étapes: (i) une perméabilisation rapide de la membrane des érythrocytes pendant l'électroperméabilisation et (ii) un gonflement colloïdal des érythrocytes associé à un hémolyse dans les minutes qui suivent l'électroperméabilisation *(Dressler et al., 1983; Chang et Reese, 1990; Haest et al., 1997)*. Dans ces conditions expérimentales, l'électroperméabilisation est corrélée à une augmentation de la mobilité transverse des phospholipides pendant la phase de gonflement colloïdal *(Dressler et al., 1983; Schwister et Deuticke, 1985; Chang et Reese, 1990; Haest et al., 1997; Henszen et al., 1997; Schwarz et al., 1999)*. Il n'y a, à ce jour, aucune corrélation spatiale ni temporelle de l'électroperméabilisation avec l'augmentation de la mobilité transverse des phospholipides. De plus, l'ensemble de ces travaux est limité aux érythrocytes qui correspondent à un modèle de cellule anucléée, avec un cytosquelette très particulier.

L'objectif de ce travail est d'étudier les conséquences membranaires de l'électroperméabilisation au niveau de cellules animales nucléées. Notre stratégie consiste à

travailler à l'échelle de la cellule unique par vidéo-microscopie de fluorescence afin d'obtenir des informations à la fois temporelle et spatiale des phénomènes de mobilité transverse des phospholipides de la membrane plasmique des cellules CHO.

L'ensemble des résultats obtenus dans cette étude fera l'objet d'une publication en 2010.

2. Publication

TRANSVERSE MOVEMENTS OF PHOSPHOLIPIDS IN PLASMA MEMBRANE OF MAMMALIAN CELLS SUBJECTED TO ELECTRIC FIELD PULSES

Jean-Michel Escoffre[§], Cécile Faurie[¶], Sarra C Sébaï[#], Elisabeth Bellard[§], Muriel Golzio[§], Justin Teissié[§] and Marie-Pierre Rols[§*]

[§]CNRS; IPBS (Institut de Pharmacologie et de Biologie Structurale); 205 route de Narbonne, F-31077, Toulouse, France; Université de Toulouse; UPS; IPBS; F-31077, Toulouse, France. [¶]Cancéropole GSO Inserm U563; CHU Purpan BP 3028, 31024 Toulouse Cedex 3, France. [#]Laboratoire de Physico-chimie des polymères et des milieux disperses, ESPCI, CNRS UMR 7615, 10 rue Vauquelin, F-75005 Paris, France.

[*]Correspondence: rols@ipbs.fr

Keywords: Electroporation, electropulsation, lipid asymmetry, phospholipid flip/flop, mammalian cell, fluorescence imaging.

ABSTRACT

Electric field pulses can induce a transient membrane permeabilization, a process called electropulsation (or electroporation). Very little is known about the consequences of the membrane electropulsation at the molecular and cell levels. Progresses in the knowledge of the electropulsation process and on involved molecular mechanisms are a biophysical challenge. As a transient loss of the membrane cohesion must be associated with permeabilization, we investigated the occurrence of enhanced transverse movement of phospholipids under electrical conditions preserving the cell viability. Our main objective was to detect and visualize, at the single cell level, transverse diffusion of phospholipids. We performed studies by using digitized fluorescence microscopy and C6-NBD-PC and FM1-43 as fluorescent probes, to monitor phospholipid translocation. We observed that millisecond permeabilizing electric pulses induced a rapid phospholipid flip/flop within less than 1s strictly restricted to the permeabilized regions according to an ATP-independent process. Our results support the existence of direct interactions between the movement of the membrane phospholipids and the electric field. This movement appears as a direct effect of electric field pulses and not as a secondary one as previously reported in the erythrocytes. While charged phospholipids such as phosphatidylserine are transiently moved to the outer leaflet, this is not associated to apoptosis as usually observed in other flip/flop associated processes.

INTRODUCTION

The cell plasma membrane acts as a physical and selective barrier that hinders the free diffusion of hydrophilic and charged molecules between the external medium and the cytosol (1). Its composition in most healthy mammalian cells is asymmetric (2, 3). Phosphatidylserine (PS) and phosphatidylethanolamine reside in the inner leaflet of plasma membrane, while phosphatidylcholine (PC) and sphingomyelin are found mostly in the outer leaflet. This asymmetry is a stationary state, which is crucial from a functional point of view (4-6). Any process that alters the PS asymmetric distribution usually affects the cell viability, by apoptotic processes. The maintenance of this membrane asymmetry is governed by a balance between active protein-mediated processes and by passive diffusion (i.e. flip/flop) (7). Several studies have shown that specific membrane proteins mediate the ATP-dependent transport of phospholipids across the plasma membrane (8-12). Passive diffusion is assumed to play a minor role in the transverse movement of phospholipids in the plasma membrane. This diffusive process is very slow due to the energy barrier presented by passage of a hydrophilic headgroup across the hydrophobic membrane core. The time taken for a phospholipid to flip/flop is characterized by an average lifetime of several hours to several days (13, 14). When molecular packing defects are present at the phase transition of lipid assemblies, rapid transbilayer movement occurred (10, 15). External electric field pulses can induce packing defects along permeabilization and bring cell death (16-18). However, under controlled conditions, the cell viability can be preserved and the electropulsation can be routinely used for efficient and safe delivery (19).

Older works, performed on erythrocytes, addressed the effect of electric pulses delivery on phospholipid asymmetry (8, 20-25). Erythrocytes electropulsation is a two-step process composed by a rapid membrane permeabilization step leading to ion exchanges, and followed in the minutes following pulse delivery, by a dramatic osmotic swelling. Swelling is accompanied by the haemoglobin leakage leading to an increase in the size of erythrocytes and changes in their shape (21, 22). The induced hemolysis brings to the formation of ghosts and therefore prevents to address the question of cell viability. In these studies, electropulsation has been correlated with an increase of the transverse mobility of phospholipids leading to a perturbation of the phospholipid asymmetry (8, 20-22). Phospholipid flip/flop has not been detected during the application of electric field pulses but along the osmotic swelling (20, 24, 25). This loss in asymmetry is an irreversible process. These previous works are based on data obtained on cell population, a long time

after pulse delivery. No direct observation of what occurs at the plasma membrane level is available. No direct correlation between the phospholipid flip/flop sites and the permeabilized sites could be obtained. Moreover, erythrocytes as a simple and convenient way to study electropulsation process have several limits. These cells, with no nucleus and with a bi-dimensional actin/spectrin cytoskeleton, have a cytoplasmic organization, very different of that of mammalian cells.

A key problem in the electropulsation is indeed the lack of knowledge about structural and dynamical changes induced by the electric field on the plasma membrane (17). Indeed very little is known about what is really occurring in the cell membrane at the molecular level (17). Major structural changes (e.g. villi) and deformations (e.g. blebs) have been observed in the plasma membrane of electropermeabilized cells (26, 27). These alterations, which are taken as evidence for a reorganization of the cytoskeleton, are reversible under controlled conditions (28, 29). After a few minutes, the cells recover their membrane integrity. The electric field alters the organization and cohesion of the plasma membrane. The first effect of the electric pulses is on the lipid matrix (30-32). The proteolipidic matrix is disrupted, and a reorganization of the polar headgroups of phospholipids leads to a destabilization of the hydration layer (30, 31). These previous experimental studies constitute our limited present state of knowledge of cell electropulsation at the molecular level. The bottleneck in such studies is the lack of convenient experimental strategies to visualize molecular processes in such a complex environment that is a living cell. Fluorescence videomicroscopy at the single cell level is now providing a convenient approach (33, 34).

The aim of the present work was to further investigate the consequences of the application of millisecond pulsed electric field (msPEF) on the cell membrane both at molecular and cell levels. Any direct investigation with both spatial and temporal resolutions of the effects of msPEFs on transverse mobility of phospholipids could help to understand mechanisms of electropulsation. Our strategy consisted on monitoring the transverse mobility on Chinese hamster ovary cells (CHO cells). To detect phospholipids internalization and translocation, CHO cells were stained with the fluorescent probes, C6-NBD-PC (i.e. 1-palmitoyl-2-(7-nitrobenz-2-oxa-1,3-diazol-4-yl-hexanoyl)-sn-glycero-3-PC) and FM1-43 (i.e. N-(3-triethylammoniumpropyl)-4-(4-(dibutylamino)styryl)pyridinium dibromide), respectively. This approach provides a direct visualization of transient lipid movement, with spatio-temporal information on the association between the

permeabilization of regions and phospholipids flip/flop sites within them. This physical approach allowed us to address several questions: (i) Did the application of the electric pulses induce an increase of phospholipid flip/flop in viable nucleated cells? (ii) Was there a direct association between the membrane permeabilization regions and the phospholipid flip/flop sites? (iii) Did the electric field play the role either of a direct actor or of a simple catalyst? (iv) To what extent did this process lead to cell death? (v) What could molecular model(s) support the phospholipid translocation induced by msPEFs?

MATERIALS AND METHODS

Cell culture

Chinese hamster ovary cells (Wild Type Toronto clone) were selected for their ability to grow in suspension or plated. They were grown in MEM medium as previously described (34).

Electropulsation apparatus

Electropulsation was operated by using a CNRS cell electropulsator (Jouan, St Herblain, France), which delivered square-wave electric pulses. An oscilloscope (Enertec, St Etienne, France) monitored pulse shape. Stainless steel rods parallel electrodes (diameter 0.5 mm, length 10 mm, inter-electrode distance 7 mm) were connected to the voltage pulse generator (33). CHO cells were electropulsed by application of msPEFs known to induce macromolecules loading into CHO cells. 10 pulses lasting 5 ms at a frequency of 1 Hz were applied under 0.7 kV/cm at room temperature (35, 36).

Electropulsation

Cells were cultured on microscope glass coverslip chamber (Labteck II system, Nunc™) at 0.5 10^6 CHO cells per well 1h before electropulsation to get them attached to the coverslip but keeping their spherical shape. Cells were electropulsed in 1 mL pulsation buffer (PB) (10 mM K_2HPO_4/KH_2PO_4, 1 mM $MgCl_2$, 250 mM sucrose, pH 7.4) containing propidium iodide (PI) (100 µM) (Sigma-Aldrich®, St-Louis, MO). PI uptake was measured only in the regions of the cell chamber where the electric field was homogeneous (37, 38). To determine the value of θp, fluorescence intensity profile is drawn along the cell membrane. A plot of fluorescence intensity as a function of the polar angle is obtained and it reading gives us the value of θp (39).

Cell viability

Cell viability was determined by the ability of cells to grow and divide over a 24h period. Cells were pulsed, kept for 10 min at 30°C and then grown in Petri dishes after adding 1 mL of culture medium for 24h at 37°C in a 5% CO_2 incubator. Viability was measured by monitoring cells growth through a coloration method (40).

ATP depletion of CHO cells

CHO cells were incubated with sodium azide (Sigma-Aldrich®, St-Louis, MO) and 2-deoxy-D-glucose (Sigma-Aldrich®, St-Louis, MO) at 2 mM and 10 mM, respectively, in PBS at 21°C during 15 min. This optimum condition resulted a decrease of ATP content by 75% of its initial value without affecting cell viability as previously described (41).

C6-NBD-PC membrane probe

C6-NBD-PC (Avanti Polar Lipids, Inc. Alabaster, Alabama) is a molecule of phosphocholine where one of the acyl chains is substituted by a fluorescent group, N4-nitrobenzo-2-oxa-1,3-diazole (NBD). Its incorporation into the outer leaflet of the plasma membrane of CHO cells is facilitated by its short acyl chain (only 6 carbon atoms) (42). Fluorescent vesicles were obtained by mixing of 10 µL di-oleoyl-phosphatidylcholine solution (20 mg/mL) and 20 µL C6-NBD-PC solution (1 mg/mL). A mixed lipid film was obtained by chloroform evaporation in a glass vial under nitrogen flow. The vial was placed in a vacuum for one hour. The lipid film was resuspended with a 10 mL PBS-Ca^{2+}/Mg^{2+} buffer at 4°C. The solution was stirred during 1 minute followed by a sonication for 7 min at 60% of 25 W (VibraCell, Bioblock Scientific) (42). Cells were cultured on a microscope glass coverslip chamber with 0.5 10^4 CHO cells per well, 1h before labeling. After 3 washes with a 1 mL PBS-Ca^{2+}/Mg^{2+} buffer at 4°C, CHO cells were incubated with 1 mL of fluorescent vesicle solution for 10 minutes at 4°C to limit endocytosis. After the labeling, CHO cells were washed 3 times with the PB to eliminate the excess of fluorescent vesicles (42).

FM1-43 membrane probe

FM1-43 dye (Molecular Probes, Inc., Eugene, Oregon) is a lipophilic styryl compound used in studies involving the plasma membrane. The water-soluble FM1-43 dye, which is non-toxic for cells and virtually non-fluorescent in aqueous media, is reported to insert into

the outer leaflet of the surface membrane where it becomes highly fluorescent (43, 44). Cells were cultured on a microscope glass coverslip chamber with 0.5 10^4 CHO cells per well, 1h before labeling. CHO cells were washed three times and then mixed with 3 µM FM1-43 in PB for 15 min at 37°C. Cells were directly pulsed in PB with FM1-43, without washing as previously described (45).

Annexin-V

Apoptosis was detected by annexin-V assay (Molecular Probes, Inc., Eugene, Oregon). 1h before electropulsation, cells were cultured on a microscope glass coverslip chamber with 0.5 10^4 CHO cells per well. After electropulsation, CHO cells were washed three times with annexin-V binding buffer and then labeled with 50 µL annexin-V FITC in the PB for 15 min at room temperature in the dark. Cells were analyzed by flow cytometer and fluorescence microscopy (46).

Fluorescence imaging

For microscopic observations, the microscope glass coverslip chamber carrying the electrodes was placed on the stage of an inverted digitized fluorescence videomicroscope (Leica DMIRB, Wetzlar, Germany). Cells were observed with a Leica 100×, 1.30 oil immersion objective. The wavelengths were selected by using the Leica L4 filter block for the C6-NBD-PC and FM1-43 labeled cells and the Leica N2.1 filter block for PI-labeled cells. Images were recorded with a Photometrics cooled CCD camera (Princeton instrument, Inc.) and a computer-controlled excitation light shutter (Leica, EL 6000). This shutter limits photobleaching. Digitized images were processed with a MetaMorph Acquisition software (Version 7.04r4 © 1992-2006 Molecular Devices) run on a DELL computer (Microsoft Windows XP).

Data analysis

To quantify C6-NBD-PC internalization, for each cell, the mean fluorescence intensities of the membrane and of the cytoplasm were determined along a profile line scan as follows. The two maxima of the line scan corresponding to the membrane were detected and their intensity averaged after subtraction of the background. After localization of the maxima, based on a preview of line scans, a shift of 10 pixels from these maxima indexes in direction of the cell enter was established to reach the cytoplasm. Thus, after subtraction of the background, measurement of the mean fluorescence in the cytoplasm along the line scan

is calculated between these two limits. Finally, we calculated the mean fluorescence ratio R between cytoplasm and membrane. This ratio was calculated before and after electropulsation, at 0.5, 5, 10 minutes and values after electropulsation were corrected by subtraction of pre-pulse value.

To quantify charged phospholipid (e.g. PS) translocation, surface plots in pseudo-color of FM1-43 emission were processed by Image J software (48). Then, mean fluorescence intensities of plasma membrane facing the anode (I_A) and the cathode (I_C) between before (n=0) and during (n=10) electropulsation was determined. Mean intensities were corrected from the background fluorescence.

Statistical analysis

We analyzed from 100 cells per assay. This was obtained by a delayed image analysis of the stored files. On each figure of this manuscript, we displayed a representative cell of observed cells. Errors bars represented the standard error of the mean. The statistical significance of differences between the means was evaluated by an unpaired Student's t-test. All statistics tests were sided (NS, not significant; $^{*}P<0.05$; $^{**}P<0.01$; $^{***}P<0.005$).

RESULTS

Theory

The main effect of the application of electric fields on cells is the modulation of their transmembrane potential difference (17, 18). This potential difference, $\Delta\Psi_m$, consists of two major contributions, the resting ($\Delta\Psi_0$) and the electro-induced position dependent ($\Delta\Psi_E$) membrane potential differences. When a cell is described as an insulating spherical shell, the expression of the steady state electro-induced membrane potential differences, $\Delta\Psi_E$, can be written as:

$$\Delta\Psi_E(t) = \Psi_{in} - \Psi_{out} = -g(\lambda) rE\cos(\theta_M)\left[1 - e^{\frac{-t}{\tau}}\right] \quad (1)$$

where t is the time after the onset of the electric pulse, g(λ) designates a complex function of the specific conductivities of the membrane, the pulsation and the cytoplasm, r is the radius of the cell, E the field intensity, θ the angle between the direction of the field and the normal to the membrane at the point M considered on the cell surface and τ is the membrane charging time (≈ µs in our conditions) (Fig. S1A). For CHO cells, the resting membrane potential difference, $\Delta\Psi_0$, is about -40 and -60 mV (49). Consequently, values of the

transmembrane potential difference ($\Delta\Psi_m$) are higher at the pole facing the positive electrode than at the pole facing the negative one. Membrane permeabilization takes place when $\Delta\Psi_m$ reaches threshold closed to:

$$\Delta\Psi_m = \left|\Delta\Psi_0 + \Delta\Psi_E\right| = 0.2 - 0.3V \quad (2)$$

A key consequence of this external field effect is the occurrence of a strong field effect across the membrane (i.e. 0.05 V/nm for 5 nm layer). The electric field modulation of the potential difference (38, 39, 50, 51) across the cell membrane leads to an asymmetrical field distribution. Under msPEFs leading to gene transfer (47), the permeabilization was detected at the membrane regions facing two electrodes (37, 38), the membrane permeabilization facing the anode affecting a larger cap than that in the region facing the cathode (Fig. S1B). These data suggested that transient and permeant structures are created in membrane regions facing the two electrodes (Fig. S1B) (17, 18, 37). Nevertheless, the molecular organization of the support for permeabilization remains unknown (52) and may be different on the two sides of the cell (53, 54). A vectorial character of the transmembrane field effect on the interfacial dipoles appears to be present (55, 56). The torque (consequence of a field on a dipole) gives movements of opposite directions on the two sides of the membrane. On one side, the dipole is pulled in an erected configuration while on the other it is pushed towards the membrane. The transmembrane directions of the electric field are opposite on the two cell caps (57). This results on an erected configuration on the outer layer of one cap and on the sticked one on the other cap.

The first target of the field is on the charged species present in the proteolipidic membrane. In the case of lipid assemblies, lipid headgroup orientation is affected during the field application (30). This appears as one of the steps triggering the electropulsation process (58). But in the case of mammalian cells, this tilt in the polar head orientation remains present after the pulse as long as the cells are permeabilized (31). Molecular dynamics simulation of the kinetics of electropulsation showed that this tilt can be induced with transmembrane fields as low as 0.05 V/nm (52). The relaxation time for this reorientation is of the order of microseconds but in real membranes, this should be even slower. Indeed a stabilizing effect of proteins on phospholipid bilayers was found in

simulations by the decreased typical pore formation times for a protein-free membrane with respect to a gramicidin-lipid system (59). From this simulation study, it appears that low external fields affect the dipole orientation much slowly than compared to case when a strong field is applied. A field-induced asymmetry in lipid dipole distribution is present between the two lipid leaflets. The kinetics of the dipole orientation will not be the same on both sides of the cell. This is observed, when cells are exposed to nanosecond pulsed electric fields (nsPEFs), $\Delta\Psi_m$ value at the anodic pole cell reached values of 1.6 V after 15 ns, almost five times the voltage level generally required for msPEFs. $\Delta\Psi_m$ value on the side facing the cathode reached values of 0.6 V in the same time period, indicating a strong asymmetry in conduction mechanisms in the membranes of the two opposite cell hemispheres (60). Molecular simulations showed that with application of nsPEFs, the dipoles of PC on the outer layer at the anode side reorient leading the defect initiation at the outer membrane surface. No PC translocation is described. However, if "pores" form, the negatively charged lipids (such as PS) begins to drift and diffuse towards the exterior surface (61). Simulations described PS translocation as a nanopore facilitated (i.e. very fast) event, rather than the result of molecular translocation across the transmembrane energy barrier. It appears as a direct effect of the field on the charged group (PS). On a nanosecond time scale, PS translocation does not result in a simultaneous translocation of several phospholipids, described under the term of a periodic lipid block, which may have explained the PC translocation as a by effect (62). Nanosecond PS translocation is the result of an electrophoretic migration of the negatively charged PS headgroup along the surface of nanometer-diameter "electropores" (46). Nevertheless, under nsPEFs, membrane permeabilization and PS translocation are detected for $\Delta\Psi_m$ calculated value of 3.4 V (63), but to be corrected from the direct experiments (60).

One open question is the description of the dipole of PC as it is indeed a hydrated lipid headgroup. Water molecules have been described as highly sensitive to the electric field and able to induce the nanometer membrane defects during the nanosecond pulse (52, 63). This occurs after the tilt of the polar groups (52) and should take place under our experimental conditions (msPEFs). Following the tilt, a collective effect of the water dipoles of the hydrated PC headgroup may induce its translocation.

Strategy

We investigated the effects of msPEFs on transverse mobility of phospholipids by fluorescence videomicroscopy at the single cell level by using two complementary approaches: (i) To visualize the putative phospholipids internalization within the CHO cells subjected to msPEFs, we labeled the cells with C6-NBD-PC (42, 64). Once inserted into the membrane, C6-NBD-PC does not spontaneously translocate from the outer leaflet to inner leaflet. But if transverse movement occurs, C6-NBD-PC can then freely exchange with the phospholipids of intracellular organelles. As consequence, the detection of this probe into the intracellular membrane network, i.e. within the cytoplasm, will be indicative of its internalization (64). (ii) To further investigate phospholipid translocation in the CHO cells after the application of msPEFs, FM1-43 was used to detect the charged phospholipid (e.g. PS) translocation. The common test to detect charged phospholipid translocation, the annexin-V assay was not suitable (65). The main limitations of annexin-V assay for real-time observations at the single cell level are that long incubation and washing are required. In contrast, FM1-43 can be observed directly without any incubation or washing because its fluorescence quantum yield is one thousand times larger in the lipid environment of plasma membrane than it is in the aqueous solvent (44). The membrane insertion of FM1-43 is a fast process due to (i) a decrease of lipid packing (66) and (ii) an electrostatic process where negatively charged phospholipid (e.g. PS) translocation attracts the positive charged FM1-43 from the medium into the plasma membrane. The increase of membrane insertion of FM1-43 induces a fluorescence overshoot at the membrane level (48).

Effects of msPEFs on C6-NDB-PC internalization

In absence of any electric pulses, just after the labeling, the C6-NBD-PC was detected only at the plasma membrane level (Figs. 1A and 1D). The light plot showed that the maximal intensity was measured at the plasma membrane level (Figs. 1A and 1D). After 10 min, the C6-NBD-PC remained localized at the plasma membrane level (Figs. 1A and 1D). No bleaching was present under our experimental protocol. No C6-NBD-PC internalization was observed over time. The application of a non-permeabilizing electric field (i.e. 0.1 kV/cm) on cells exhibited the same probe distribution over time (Table 1). The application of electric field pulses, which did not permeabilize the plasma membrane, did not induce any detectable C6-NBD-PC internalization in CHO cells.

When cells were subjected to a train of 10 electric field pulses (i.e. 0.7 kV/cm, 5 ms, 1 Hz frequency), all the cells were permeabilized as previously observed by our group from the uptake of PI (19). Up to 30 s after application of the first pulse, the C6-NBD-PC localization remained almost unchanged. The radial light plots confirm the membrane localization of the probe. Nevertheless, a slight and diffuse labeling was seen in the cytoplasm of permeabilized cells (Figs. 1B and 1D). Over time, the probe was more present in the organelle membranes, enhancing the detection of intracellular membrane network (Figs. 1B and 1D). At 10 min post-pulse, the light plot showed a decrease of the membrane fluorescence level with an increase in the intracellular fluorescence level (Figs. 1B and 1D). Labeling of the nuclear envelope was observed 10 min after msPEFs application (Fig. 1B Panel C). Total cell fluorescence decreased slightly after electropulsation (Fig. 1B). We got the same results on ATP-depleted CHO cells (Table 1). These results are evidence for electropulsation induced C6-NBD-PC internalization according to an ATP-independent process.

When C6-NBD-PC staining was performed after the application of electric field pulses (i.e. during the membrane resealing), no labeling of the intracellular membrane network could be observed (Figs. 1C and 1D). This result was indicative that the pulse-induced long-lived permeant structures were not associated with PC like phospholipid internalization.

Effects of msPEFs on charged phospholipid translocation

Charged phospholipid translocation and/or phospholipid scrambling were monitored by time-lapse fluorescence microscopy at the single living cell level (Fig. 2). In absence of any electric pulses, or after non-permeabilizing electric pulses (i.e. 0.1 kV/cm), the FM1-43 was only detected at the plasma membrane and intracellular network (Table 1 and Fig. 2A, n = 0) as quantified by the surface plot (Fig. 2B, n = 0). During the application of a permeabilizing electric pulse train, a fast increase of fluorescence intensity appeared at the membrane regions facing the electrodes (Fig. 2, n = 1 to n = 10). This fluorescence intensity increased with the number of electric pulses (Fig. 2). Moreover, the fluorescence increase facing the anode was twice that of the one facing the cathode (Fig. 2C). This fluorescence intensity overshoot decayed 1 min after the application of electric pulses (Figs. 2A and 2B). We got the same results on ATP-depleted CHO cells (Table 1). Little or no entry of the FM1-43 probe inside the cell was observed (Fig. 2). msPEFs induced a rapid charged

phospholipid translocation and/or phospholipid scrambling only in the membrane regions facing the electrodes, where permeabilization took place

Effects of msPEFs on cell viability

The CHO cells were subjected to msPEFs, which allowed their transient and reversible permeabilization. Under such experimental conditions, permeabilization took place facing the electrodes and was shown here to be associated to an increase of transbilayer movements of phospholipids (Fig. S1B). This permeabilization was linked to a 20% decrease in cell viability (measured 24h following electric pulses application) but with no detection of apoptotic cells (less than 5% of the cells being positive to the annexin-V test) (Fig. S2). Moreover, no morphological alterations such as membrane blebs were observed (data not shown).

DISCUSSION

In the present study, the effects of permeabilizing electric field pulses on the transverse mobility of phospholipids were directly addressed on single CHO cells. Electropulsation is a localized process, taking place on the cell caps facing the electrodes (19, 47), under the control of the electric field strength. To determine the biophysical mechanisms involved in this process, we monitored and quantified the pulse-induced transverse mobility of C6-NBD-PC and FM1-43, by non-invasive fluorescence digitized time-lapse videomicroscopy. We wished to answer the following questions: (i) Did the application of the electric pulses induce an increase of phospholipid flip/flop in viable nucleated cells? (ii) Was there a direct association between the membrane permeabilization regions and the phospholipid flip/flop sites? (iii) Did the electric field play the role either of a direct actor or of a simple catalyst? (iv) To what extent did this process lead to cell death? (v) What biophysical molecular model(s) could support the phospholipid translocation induced by millisecond pulsed electric field?

We obtained the following observations and conclusions. (i) Application of msPEFs induces both phospholipid internalization (Fig. 1B) and externalization (Fig. 2). These effects result from the permeabilizing nature of electric pulses because phospholipids flip/flop occurred only when the electric pulses were permeabilizing (Fig. S1 and Table 1). These results showed that the application of electropermeabilizing pulses directly altered

the phospholipid organization of the plasma membrane by increasing the transverse dynamics of phospholipids and according to an ATP-independent process (Table 1). An enhanced transverse dynamics of phospholipids was reported in a previous work on erythrocytes (8). But the present observations were obtained on mammalian cells, where the membrane resealing was present (in contrast to red blood cells where irreversible permeabilization was induced giving ghosts with dramatic changes in shape and cytoskeleton disruption). (ii) In experiments performed with nanosecond electric pulses, charged phospholipid (e.g. PS) translocation and/or phospholipid scrambling was an asymmetric process that was restricted to the membrane areas facing the anode (63, 67, 68). In order to determine whether charged phospholipid translocation and/or phospholipids scrambling was limited to electropermeabilized regions, we measured the experimental value of cap angle θp from electropulsation (assayed by PI uptake) (Fig. S1B) and charged phospholipid translocation (assayed by FM1-43) experiments and compared these two values. For both processes, the experimental values of angle θp were similar (55° ± 5° and 50° ± 5° respectively). These data supported the conclusion that charged phospholipid translocation and/or phospholipid scrambling were strictly restricted to the permeabilized membrane regions (Fig. 2). (iii) The phospholipid flip/flop was a direct consequence of electric field pulses and was not due to the resulting long-lived leaky membrane organization (Fig. 1B-C). Indeed, in the case of C6-NBD-PC internalization, a progressive staining of intracellular membrane network was observed after the application of electric field (Fig. 1B). But, when the C6-NBD-PC staining of cells was performed after the application of msPEFs (i.e. during membrane resealing), no labeling of intracellular membrane network (i.e. probe internalization) was detected (Fig. 1C). Furthermore, the FM1-43 experiments showed that a fluorescence intensity overshoot took place in the permeabilized regions as a direct result of the application of msPEFs (Fig. 2). This fluorescence increase dissipated in the minutes post msPEFs (Fig. 2) that could be explained by lateral diffusion of the dye along the cell plasma membrane or by the membrane resealing. These results support the conclusion that a direct interaction between the external electric field pulse and the phospholipids took place as previously proposed and described under high field ultra-short conditions (61, 67). These previous reports were under more stringent conditions where the organization of interfacial water was strongly affected (69) but are predicted (see the theoretical results) on a slower time scale under our conditions (52). (iv) Permeabilization takes place on cell caps facing the electrodes, areas

shown here to be associated to charged phospholipid translocation and/or phospholipid scrambling. All the cells have been permeabilized under the applied electric field conditions (data not shown). This permeabilization was transient and linked to a 20% decrease in cell viability but with no detection of apoptotic cells. No morphological alterations such as membrane blebs were observed. The location of these molecules in particular domains remained an open question. Cells are not detected as apoptotic cells in opposition to the results described in previous works (70). (v) At a molecular point of view, our data could be interpreted via two possible mechanisms: either (i) membrane defects created by electric pulses provided a new pathway for phospholipids to migrate between the membrane leaflets (8, 20) by creating a lipid continuity between the outer and inner leaflets as postulated by the "electroporation theory" (16) or (ii) electric pulses cause phospholipid translocation by a direct torque on the headgroup dipole (46, 61). In the first model, "electropores" should be created in permeabilized regions (Fig. 2) in agreement with permeabilization results but remained present during the resealing (as long as "pores" were present). However, no transmembrane movement was observed after the pulse as shown by the post addition of the C6-NBD-PC, although permeabilization is still present for 10 minutes. Therefore, this absence of phospholipid flip/flop after the application of msPEFs brought experimental evidences that either the pulse-induced long lived “pores” could not be the pathways of phospholipids exchange between the two membrane leaflets in the permeabilized regions (20, 71); or pulse-induced “defects” present during pulse application were the pathways of phospholipid flip/flop, but the post-pulse “electropores” present during the membrane resealing could not support phospholipid translocation in agreement with previous work (72). The second model suggests a direct interaction between the external electric field and the phospholipids as previously described (52, 61, 68). Phospholipids are the key target of electric field mediated permeabilization (32). In our electrical conditions, the transmembrane field is around 0.05 V/nm (for 5 nm bilayer). This transmembrane field can induce the tilt in the polar head orientation as previously described in molecular dynamics simulations (52) and experimental data (30, 31). Indeed, in the case of PC, the hydrated headgroup contains a dipole with positive charge on choline and negative charge carried by the phosphate group. In absence of external electric field, lipid dipoles present an orientation due to the interfacial charges (61, 73). During the induction step of electropulsation, the electric field could induce membrane defects by tilting the lipid dipoles relative to the surface of the membrane (17, 74). Water molecules

have been described as highly sensitive to the electric field (75) and able to induce membrane defects under electric field (52, 63, 68). Following the tilt of lipid dipoles (52, 76, 77), a collective effect of water dipoles of hydrated PC head-groups should induce their translocation under our experimental conditions (msPEFs) (Fig. 1B). However, if pore form, the negatively charged lipids (PS) begin to drift and diffuse towards the exterior surface (61). Simulations described PS translocation as a nanopore facilitated (i.e. very fast) event, rather than the result of molecular translocation across the transmembrane energy barrier. Therefore, the charged phospholipids translocation can only occur in the permeabilized region facing the anode during the application of electric pulses (Fig. 2). Nevertheless, FM1-43 fluorescence overshoot was detected in the permeabilized region facing the cathode (Fig. 2). This fluorescence overshoot could be interpreted by FM1-43 insertion into a disordered membrane (i.e. decrease of lipid packing) by the electric field (32, 66). This result may indicate that msPEFs induce membrane disorder and phospholipid scrambling in the permeabilized regions facing the electrodes but the charged lipids (PS) translocation is added to the preceeding processes in the permeabilized region facing the anode (43). This putative mechanism supports a direct interaction between the external electric field and the phospholipids (Fig. 3).

Moreover, in the light of earlier studies, the asymmetric nature of the observed fluorescence intensity overshoot could suggest that the structure of the permeabilized membrane at the anode pole is different from that found at the cathode pole (38, 39, 78) as previously shown on lipid vesicles (53). Indeed, previous works on small molecule uptake via electropulsation suggested that “electropores” were created on both caps of the cell facing the electrodes, with smaller “pore” size (but greater in number) on the anode side and larger “pores” (with a lower number) on the cathode side (54). This asymmetrical process was associated to a vectorial effect of the electric field on the plasma membrane (38, 39). Field-driven translocation of phospholipids might also contribute to an asymmetric potential distribution at opposite hemispheres. Depending on their charge, membrane-embedded molecules will either be driven into cell or pulled out into the outer leaflet of the membrane. As a result of a significant change in membrane surface, charges inside and outside the cell will affect the transmembrane voltage (57, 60). The different structures, composition and dynamics of membrane defects induced by the application of msPEFs remain to be elucidated.

ACKNOWLEDGEMENTS

The authors would like to thank P.T. Vernier, S. Orlowski, P.F. Devaux and A. Lopez for fruitful discussions, S. Mazères for his help in C6-NBD-PC labeling, C. Millot for help with the cell culture and D.S. Dean for the proof reading of this manuscript. The Association Française sur les Myopathies (to MPR), the Région Midi-Pyrénées, the Direction Générale des Armées and the Institut National du Cancer (to JT) have supported this work. JM Escoffre is the recipient of an allocation de recherche du Ministère de l'Enseignement Supérieur et de la Recherche.

REFERENCES

1. Stephens, D. J., and R. Pepperkok. 2001. The many ways to cross the plasma membrane. *Proc Natl Acad Sci U S A* 98:4295-4298.
2. Rothman, J. E., and J. Lenard. 1977. Membrane asymmetry. *Science* 195:743-753.
3. Zachowski, A. 1993. Phospholipids in animal eukaryotic membranes: transverse asymmetry and movement. *Biochem J* 294 (Pt 1):1-14.
4. Manno, S., Y. Takakuwa, and N. Mohandas. 2002. Identification of a functional role for lipid asymmetry in biological membranes: Phosphatidylserine-skeletal protein interactions modulate membrane stability. *Proc Natl Acad Sci U S A* 99:1943-1948.
5. Pomorski, T., S. Hrafnsdottir, P. F. Devaux, and G. van Meer. 2001. Lipid distribution and transport across cellular membranes. *Semin Cell Dev Biol* 12:139-148.
6. Balasubramanian, K., and A. J. Schroit. 2003. Aminophospholipid asymmetry: A matter of life and death. *Annu Rev Physiol* 65:701-734.
7. Yamaji-Hasegawa, A., and M. Tsujimoto. 2006. Asymmetric distribution of phospholipids in biomembranes. *Biol Pharm Bull* 29:1547-1553.
8. Haest, C. W., D. Kamp, and B. Deuticke. 1997. Transbilayer reorientation of phospholipid probes in the human erythrocyte membrane. Lessons from studies on electroporated and resealed cells. *Biochim Biophys Acta* 1325:17-33.
9. John, K., J. Kubelt, P. Muller, D. Wustner, and A. Herrmann. 2002. Rapid transbilayer movement of the fluorescent sterol dehydroergosterol in lipid membranes. *Biophys J* 83:1525-1534.

10. John, K., S. Schreiber, J. Kubelt, A. Herrmann, and P. Muller. 2002. Transbilayer movement of phospholipids at the main phase transition of lipid membranes: implications for rapid flip-flop in biological membranes. *Biophys J* 83:3315-3323.
11. Devaux, P. F., I. Lopez-Montero, and S. Bryde. 2006. Proteins involved in lipid translocation in eukaryotic cells. *Chem Phys Lipids* 141:119-132.
12. Devaux, P. F., A. Herrmann, N. Ohlwein, and M. M. Kozlov. 2008. How lipid flippases can modulate membrane structure. *Biochim Biophys Acta* 1778:1591-1600.
13. Kornberg, R. D., and H. M. McConnell. 1971. Inside-outside transitions of phospholipids in vesicle membranes. *Biochemistry* 10:1111-1120.
14. Wimley, W. C., and T. E. Thompson. 1990. Exchange and flip-flop of dimyristoylphosphatidylcholine in liquid-crystalline, gel, and two-component, two-phase large unilamellar vesicles. *Biochemistry* 29:1296-1303.
15. De Kruijff, B., and E. J. Van Zoelen. 1978. Effect of the phase transition on the transbilayer movement of dimyristoyl phosphatidylcholine in unilamellar vesicles. *Biochim Biophys Acta* 511:105-115.
16. Neumann, E., A. E. Sowers, and C. A. Jordan. 1989. Electroporation and Electrofusion in Cell Biology. Plenum.
17. Teissie, J., M. Golzio, and M. P. Rols. 2005. Mechanisms of cell membrane electropulsation: a minireview of our present (lack of ?) knowledge. *Biochim Biophys Acta* 1724:270-280.
18. Escoffre, J. M., D. S. Dean, M. Hubert, M. P. Rols, and C. Favard. 2007. Membrane perturbation by an external electric field: a mechanism to permit molecular uptake. *Eur Biophys J* 36:973-983.
19. Golzio, M., M. P. Rols, and J. Teissie. 2004. In vitro and in vivo electric field-mediated permeabilization, gene transfer, and expression. *Methods* 33:126-135.
20. Dressler, V., K. Schwister, C. W. Haest, and B. Deuticke. 1983. Dielectric breakdown of the erythrocyte membrane enhances transbilayer mobility of phospholipids. *Biochim Biophys Acta* 732:304-307.
21. Henszen, M. M., M. Weske, S. Schwarz, C. W. Haest, and B. Deuticke. 1997. Electric field pulses induce reversible shape transformation of human erythrocytes. *Mol Membr Biol* 14:195-204.

22. Schwarz, S., B. Deuticke, and C. W. Haest. 1999. Passive transmembrane redistributions of phospholipids as a determinant of erythrocyte shape change. Studies on electroporated cells. *Mol Membr Biol* 16:247-255.
23. Kinosita, K., Jr., and T. Y. Tsong. 1977. Formation and resealing of pores of controlled sizes in human erythrocyte membrane. *Nature* 268:438-441.
24. Schwister, K., and B. Deuticke. 1985. Formation and properties of aqueous leaks induced in human erythrocytes by electrical breakdown. *Biochim Biophys Acta* 816:332-348.
25. Chang, D. C., and T. S. Reese. 1990. Changes in membrane structure induced by electroporation as revealed by rapid-freezing electron microscopy. *Biophys J* 58:1-12.
26. Escande-Geraud, M. L., M. P. Rols, M. A. Dupont, N. Gas, and J. Teissie. 1988. Reversible plasma membrane ultrastructural changes correlated with electropulsation in Chinese hamster ovary cells. *Biochim Biophys Acta* 939:247-259.
27. Gass, G. V., and L. V. Chernomordik. 1990. Reversible large-scale deformations in the membranes of electrically-treated cells: electroinduced bleb formation. *Biochim Biophys Acta* 1023:1-11.
28. Rols, M. P., and J. Teissie. 1992. Experimental evidence for the involvement of the cytoskeleton in mammalian cell electropulsation. *Biochim Biophys Acta* 1111:45-50.
29. Teissie, J., and M. P. Rols. 1994. Manipulation of cell cytoskeleton affects the lifetime of cell membrane electropulsation. *Ann N Y Acad Sci* 720:98-110.
30. Stulen, G. 1981. Electric field effects on lipid membrane structure. *Biochim Biophys Acta* 640:621-627.
31. Lopez, A., M. P. Rols, and J. Teissie. 1988. 31P NMR analysis of membrane phospholipid organization in viable, reversibly electropermeabilized Chinese hamster ovary cells. *Biochemistry* 27:1222-1228.
32. Teissie, J., and T. Y. Tsong. 1981. Electric field induced transient pores in phospholipid bilayer vesicles. *Biochemistry* 20:1548-1554.
33. Mazeres, S., D. Sel, M. Golzio, G. Pucihar, Y. Tamzali, D. Miklavcic, and J. Teissie. 2009. Non invasive contact electrodes for in vivo localized cutaneous

electropulsation and associated drug and nucleic acid delivery. *J Control Release* 134:125-131.

34. Rols, M. P., P. Femenia, and J. Teissie. 1995. Long-lived macropinocytosis takes place in electropermeabilized mammalian cells. *Biochem Biophys Res Commun* 208:26-35.
35. Rols, M. P., D. Coulet, and J. Teissie. 1992. Highly efficient transfection of mammalian cells by electric field pulses. Application to large volumes of cell culture by using a flow system. *Eur J Biochem* 206:115-121.
36. Hui, M. 1995. Effects of pulse length and strength on electroporation efficiency. In Animal Cell Electroporation & Electrofusion Protocols. J. A. Nicholoff, editor. Humana Press, Clifton, N.J. 29-40.
37. Gabriel, B., and J. Teissie. 1997. Direct observation in the millisecond time range of fluorescent molecule asymmetrical interaction with the electropermeabilized cell membrane. *Biophys J* 73:2630-2637.
38. Gabriel, B., and J. Teissie. 1998. Mammalian cell electropulsation as revealed by millisecond imaging of fluorescence changes with the electropermeabilized cell membrane. *Bioelectrochemistry* 47:113-118.
39. Gabriel, B., and J. Teissie. 1999. Time courses of mammalian cell electropulsation observed by millisecond imaging of membrane property changes during the pulse. *Biophys J* 76:2158-2165.
40. Gabriel, B., and J. Teissie. 1995. Spatial compartmentation and time resolution of photooxidation of a cell membrane probe in electropermeabilized Chinese hamster ovary cells. *Eur J Biochem* 228:710-718.
41. Rols, M. P., C. Delteil, M. Golzio, and J. Teissie. 1998. Control by ATP and ADP of voltage-induced mammalian-cell-membrane permeabilization, gene transfer and resulting expression. *Eur J Biochem* 254:382-388.
42. Julien, M., J. F. Tournier, and J. F. Tocanne. 1993. Differences in the transbilayer and lateral motions of fluorescent analogs of phosphatidylcholine and phosphatidylethanolamine in the apical plasma membrane of bovine aortic endothelial cells. *Exp Cell Res* 208:387-397.
43. Zweifach, A. 2000. FM1-43 reports plasma membrane phospholipid scrambling in T-lymphocytes. *Biochem J* 349:255-260.

44. Gaffield, M. A., and W. J. Betz. 2006. Imaging synaptic vesicle exocytosis and endocytosis with FM dyes. *Nat Protoc* 1:2916-2921.
45. Vernier, P. T., Y. Sun, and M. A. Gundersen. 2006. Nanoelectropulse-driven membrane perturbation and small molecule permeabilization. *BMC Cell Biol* 7:37.
46. Vernier, P. T., M. J. Ziegler, Y. Sun, M. A. Gundersen, and D. P. Tieleman. 2006. Nanopore-facilitated, voltage-driven phosphatidylserine translocation in lipid bilayers--in cells and in silico. *Phys Biol* 3:233-247.
47. Golzio, M., J. Teissie, and M. P. Rols. 2002. Direct visualization at the single-cell level of electrically mediated gene delivery. *Proc Natl Acad Sci U S A* 99:1292-1297.
48. Sun, Y., P. T. Vernier, M. Behrend, J. Wang, M. M. Thu, M. Gundersen, and L. Marcu. 2006. Fluorescence microscopy imaging of electroperturbation in mammalian cells. *J Biomed Opt* 11:024010.
49. Teissie, J., and M. P. Rols. 1993. An experimental evaluation of the critical potential difference inducing cell membrane electropulsation. *Biophys J* 65:409-413.
50. Hibino, M., H. Itoh, and K. Kinosita, Jr. 1993. Time courses of cell electroporation as revealed by submicrosecond imaging of transmembrane potential. *Biophys J* 64:1789-1800.
51. Tekle, E., R. D. Astumian, and P. B. Chock. 1990. Electro-permeabilization of cell membranes: effect of the resting membrane potential. *Biochem Biophys Res Commun* 172:282-287.
52. Bockmann, R. A., B. L. de Groot, S. Kakorin, E. Neumann, and H. Grubmuller. 2008. Kinetics, statistics, and energetics of lipid membrane electroporation studied by molecular dynamics simulations. *Biophys J* 95:1837-1850.
53. Tekle, E., R. D. Astumian, W. A. Friauf, and P. B. Chock. 2001. Asymmetric pore distribution and loss of membrane lipid in electroporated DOPC vesicles. *Biophys J* 81:960-968.
54. Tekle, E., R. D. Astumian, and P. B. Chock. 1994. Selective and asymmetric molecular transport across electroporated cell membranes. *Proc Natl Acad Sci U S A* 91:11512-11516.
55. Genco, I., A. Gliozzi, A. Relini, M. Robello, and E. Scalas. 1993. Electroporation in symmetric and asymmetric membranes. *Biochim Biophys Acta* 1149:10-18.

56. Diederich, A., Bähr, G., Winterhalter, M.,. 1998. Influence of polylysine on the rupture of negatively charged membrane. *Langmuir* 14:4597-4605.

57. Pakhomov, A. G., A. M. Bowman, B. L. Ibey, F. M. Andre, O. N. Pakhomova, and K. H. Schoenbach. 2009. Lipid nanopores can form a stable, ion channel-like conduction pathway in cell membrane. *Biochem Biophys Res Commun* 385:181-186.

58. Schmeer, M., Seipp, T., Pliquett, U., Kakorin, S. and Neumann, E.,. 2004. Mechanism for the conductivity changes caused by membrane electroporation of CHO cell-pellets. *Phys. Chem. Chem. Phys.,* 6:5564-5574.

59. Siu, S. W., and R. A. Bockmann. 2007. Electric field effects on membranes: gramicidin A as a test ground. *J Struct Biol* 157:545-556.

60. Frey, W., J. A. White, R. O. Price, P. F. Blackmore, R. P. Joshi, R. Nuccitelli, S. J. Beebe, K. H. Schoenbach, and J. F. Kolb. 2006. Plasma membrane voltage changes during nanosecond pulsed electric field exposure. *Biophys J* 90:3608-3615.

61. Hu, Q., R. P. Joshi, and K. H. Schoenbach. 2005. Simulations of nanopore formation and phosphatidylserine externalization in lipid membranes subjected to a high-intensity, ultrashort electric pulse. *Phys Rev E Stat Nonlin Soft Matter Phys* 72:031902.

62. Sugar, I. P., and E. Neumann. 1984. Stochastic model for electric field-induced membrane pores. Electroporation. *Biophys Chem* 19:211-225.

63. Vernier, P. T., M. J. Ziegler, Y. Sun, W. V. Chang, M. A. Gundersen, and D. P. Tieleman. 2006. Nanopore formation and phosphatidylserine externalization in a phospholipid bilayer at high transmembrane potential. *J Am Chem Soc* 128:6288-6289.

64. Devaux, P. F., P. Fellmann, and P. Herve. 2002. Investigation on lipid asymmetry using lipid probes: Comparison between spin-labeled lipids and fluorescent lipids. *Chem Phys Lipids* 116:115-134.

65. van Genderen, H., H. Kenis, P. Lux, L. Ungeth, C. Maassen, N. Deckers, J. Narula, L. Hofstra, and C. Reutelingsperger. 2006. In vitro measurement of cell death with the annexin A5 affinity assay. *Nat Protoc* 1:363-367.

66. Schote, U., and J. Seelig. 1998. Interaction of the neuronal marker dye FM1-43 with lipid membranes. Thermodynamics and lipid ordering. *Biochim Biophys Acta* 1415:135-146.

67. Vernier, P. T., Y. Sun, L. Marcu, C. M. Craft, and M. A. Gundersen. 2004. Nanoelectropulse-induced phosphatidylserine translocation. *Biophys J* 86:4040-4048.

68. Vernier, P. T., and M. J. Ziegler. 2007. Nanosecond field alignment of head group and water dipoles in electroporating phospholipid bilayers. *J Phys Chem B* 111:12993-12996.

69. Pliquett, U., R. P. Joshi, V. Sridhara, and K. H. Schoenbach. 2007. High electrical field effects on cell membranes. *Bioelectrochemistry* 70:275-282.

70. Tekle, E., M. D. Wolfe, H. Oubrahim, and P. B. Chock. 2008. Phagocytic clearance of electric field induced 'apoptosis-mimetic' cells. *Biochem Biophys Res Commun* 376:256-260.

71. Gurtovenko, A. A., and I. Vattulainen. 2007. Lipid transmembrane asymmetry and intrinsic membrane potential: two sides of the same coin. *J Am Chem Soc* 129:5358-5359.

72. Pucihar, G., T. Kotnik, D. Miklavcic, and J. Teissie. 2008. Kinetics of transmembrane transport of small molecules into electropermeabilized cells. *Biophys J* 95:2837-2848.

73. Seelig, J., P. M. Macdonald, and P. G. Scherer. 1987. Phospholipid head groups as sensors of electric charge in membranes. *Biochemistry* 26:7535-7541.

74. Kotulska, M., K. Kubica, S. Koronkiewicz, and S. Kalinowski. 2007. Modeling the induction of lipid membrane electropulsation. *Bioelectrochemistry* 70:64-70.

75. Teissie, J. 2007. Biophysical effects of electric fields on membrane water interfaces: a mini review. *Eur Biophys J* 36:967-972.

76. Tarek, M. 2005. Membrane electroporation: a molecular dynamics simulation. *Biophys J* 88:4045-4053.

77. Tieleman, D. P. 2004. The molecular basis of electroporation. *BMC Biochem* 5:10.

78. Teruel, M. N., and T. Meyer. 1997. Electroporation-induced formation of individual calcium entry sites in the cell body and processes of adherent cells. *Biophys J* 73:1785-1796.

79. Teissie, J., and M. P. Rols. 1986. Fusion of mammalian cells in culture is obtained by creating the contact between cells after their electropulsation. *Biochem Biophys Res Commun* 140:258-266.

80. Abidor, I. G., and A. E. Sowers. 1992. Kinetics and mechanism of cell membrane electrofusion. *Biophys J* 61:1557-1569.

	E < Ep	**E < Ep ATP depletion**	**E > Ep**	**E > Ep ATP depletion**
C6-NBD-PC internalization	No	No	Yes	Yes
Charged phosphoslipid translocation	No	No	Yes	Yes

Table 1: Effect of electric pulses on C6-NDB-PC internalization and charged phospholipid translocation on ATP-depleted and non ATP-depleted CHO cells.

non ATP-depleted (columns 2 & 4) and ATP-depleted (columns 3 & 5) CHO cells were submitted to an electric field pulse sequence under the threshold value (10 pulses lasting 5 ms at a frequency of 1 Hz, at 0.1 kV/cm) or above the threshold value (10 pulses lasting 5 ms at a frequency of 1 Hz, at 0.7 kV/cm). C6-NDB-PC internalization and charged phospholipid translocation were detected at the single cell level under fluorescence microscopy. E and Ep represented the applied electric field value and the threshold value, respectively.

FIGURES

Figure 1: Effect of msPEFs on C6-NBD-PC internalization on CHO cells.

A. C6-NBD-PC distribution of CHO cells before electropulsation. The outer leaflet of plasma membrane is labeled with the probe, C6-NBD-PC. CHO cells were observed at the single cell level over time). Graphs representing the fluorescence profile (yellow line) are drawn crossing the cell along its diameter.

B. C6-NBD-PC distribution on of CHO cells after electropulsation. The outer leaflet of plasma membrane is labeled with the probe, C6-NBD-PC. CHO cells were observed at the single cell level over time after the application of permeabilizing electric pulses (10 pulses lasting 5 ms at a frequency of 1 Hz, at 0.7 kV/cm). Black arrows on graphs show the C6-NBD-PC internalization. Graphs representing the fluorescence profile (yellow line) are drawn parallel to electric field lines at the poles facing the electrodes.

C. C6-NBD-PC staining of CHO cells after electropulsation. CHO cells were electropermeabilized (10 pulses lasting 5 ms at a frequency of 1 Hz, at 0.7 kV/cm). Then, C6-NBD-PC staining was performed 0.5 min, 5 min and 10 min after electropulsation. Graphs representing the fluorescence profile (yellow line) are drawn parallel to electric field lines at the poles facing the electrodes.

D. Quantification of C6-NBD-PC internalization on CHO cells. The mean fluorescence ratio R between cytoplasm and membrane was calculated and multiplied by 100. This ratio was calculated before and after electropulsation, at 0.5, 5, 10 minutes and values after electropulsation were corrected by subtraction of pre-pulse value. Errors bars represented the standard error of the mean. The statistical significance of differences between the means of R for "no electropulsation" condition and for "electropulsation" condition (NS, not significant; $^{*}P<0.05$; $^{**}P<0.01$; $^{***}P<0.005$) and the means of R for "electropulsation" and for "C6-NBD-PC staining after electropulsation" condition (NS, not significant; $^{§}P<0.05$; $^{§§}P<0.01$; $^{§§§}P<0.005$) was evaluated by an unpaired Student's t-test.

Figure 2: Effect of msPEFs on charged phospholipid translocation and/or phospholipid scrambling on CHO cells.

A. CHO cells were labeled with FM1-43. CHO cells were observed at the single cell level by fluorescence videomicroscopy during the electropulsation (10 pulses lasting 5 ms at a frequency of 1 Hz, at 0.7 kV/cm).

B. The surface plot histograms in pseudo-color were determined by Image J software.

C. Quantification of charged phospholipid translocation and/or phospholipid scrambling. The mean fluorescence intensities of membrane facing the electrodes before electropulsation (n=0) and during electropulsation (n=10) were determined and expressed in percentage (R). Errors bars represented the standard error of the mean. The statistical significance of differences between the means of R for the anode and the cathode (NS, not significant; $^{*}P<0.05$; $^{**}P<0.01$; $^{***}P<0.005$) was evaluated by an unpaired Student's t-test.

Figure 3: Pulse-induced transverse movements of phospholipids.

A. In absence of external electric field, lipid dipoles present a random reflecting the electrical properties of the membrane interface (73). A local order of the interfacial water molecules is present.

B. During the induction step of electropulsation, the millisecond pulsed electric field induce a torque on the lipid dipoles and tilt them relative to the surface of the membrane (30, 52). More order is present on the water dipoles. The field effect is amplified by collective effect of water dipoles of hydrated PC headgroups. The effect on water dipoles is opposite on the two layers of the membrane.

C. Following the tilt of lipid dipoles, membrane defects are present supporting lipid translocations.

D. Phospholipid translocation occurred according to a still not known mechanism (17).

E. After electropulsation along the resealing process, PC and PS have been translocated on the inner and outer leaflets, respectively, of a still perturbed membrane (PC, orange phospholipid; PS, blue phospholipid; water molecule, red molecule). A change in the order of the interfacial water molecules is present relative to the distribution present in A as shown by the long lived fusogenic state (79, 80).

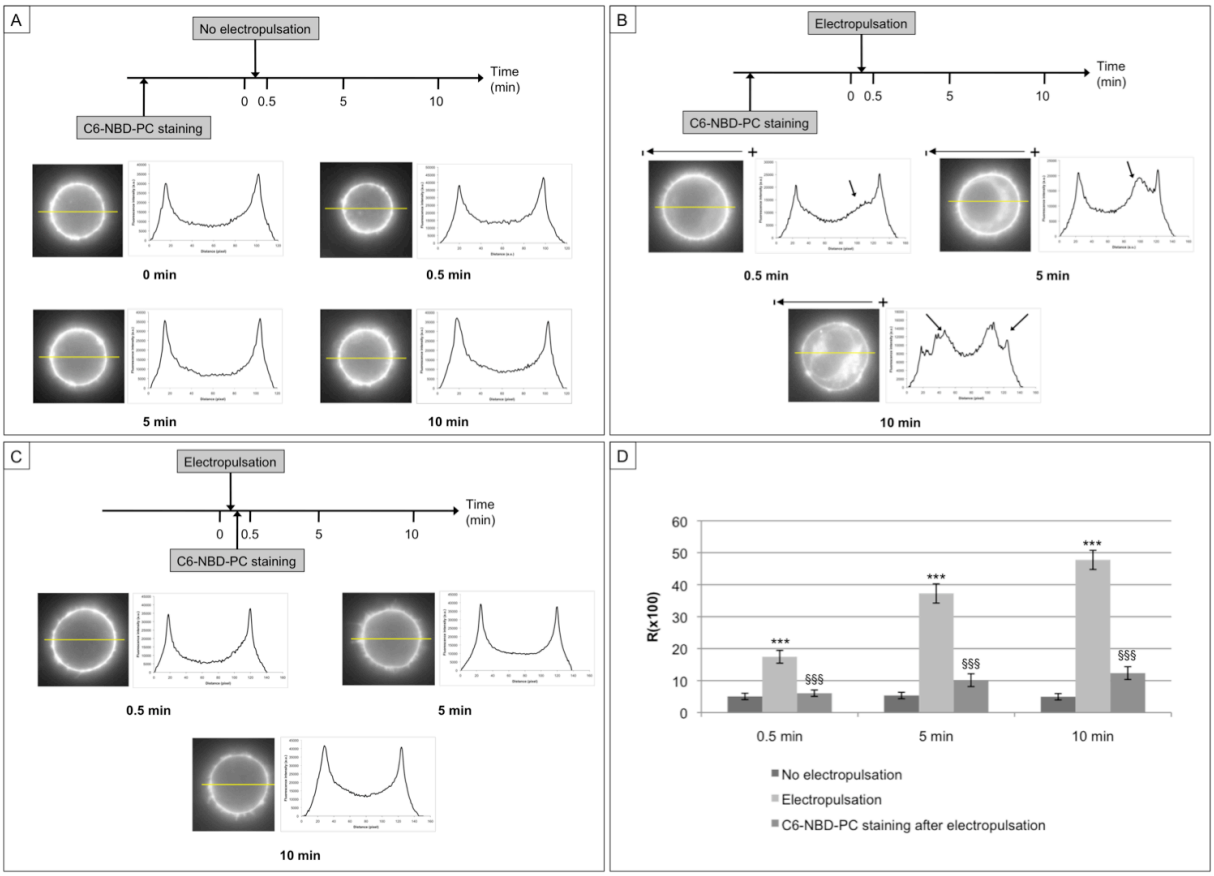
A
No electropulsation
Time (min)
0 0.5 5 10
C6-NBD-PC staining
0 min
0.5 min
5 min
10 min
B
Electropulsation
Time (min)
0 0.5 5 10
C6-NBD-PC staining
0.5 min
5 min
10 min
C
Electropulsation
Time (min)
0 0.5 5 10
C6-NBD-PC staining
0.5 min
5 min
10 min
D
R(x100)
60
50
40
30
20
10
0
***
§§§
0.5 min
5 min
10 min
No electropulsation
Electropulsation
C6-NBD-PC staining after electropulsation

Figure 1

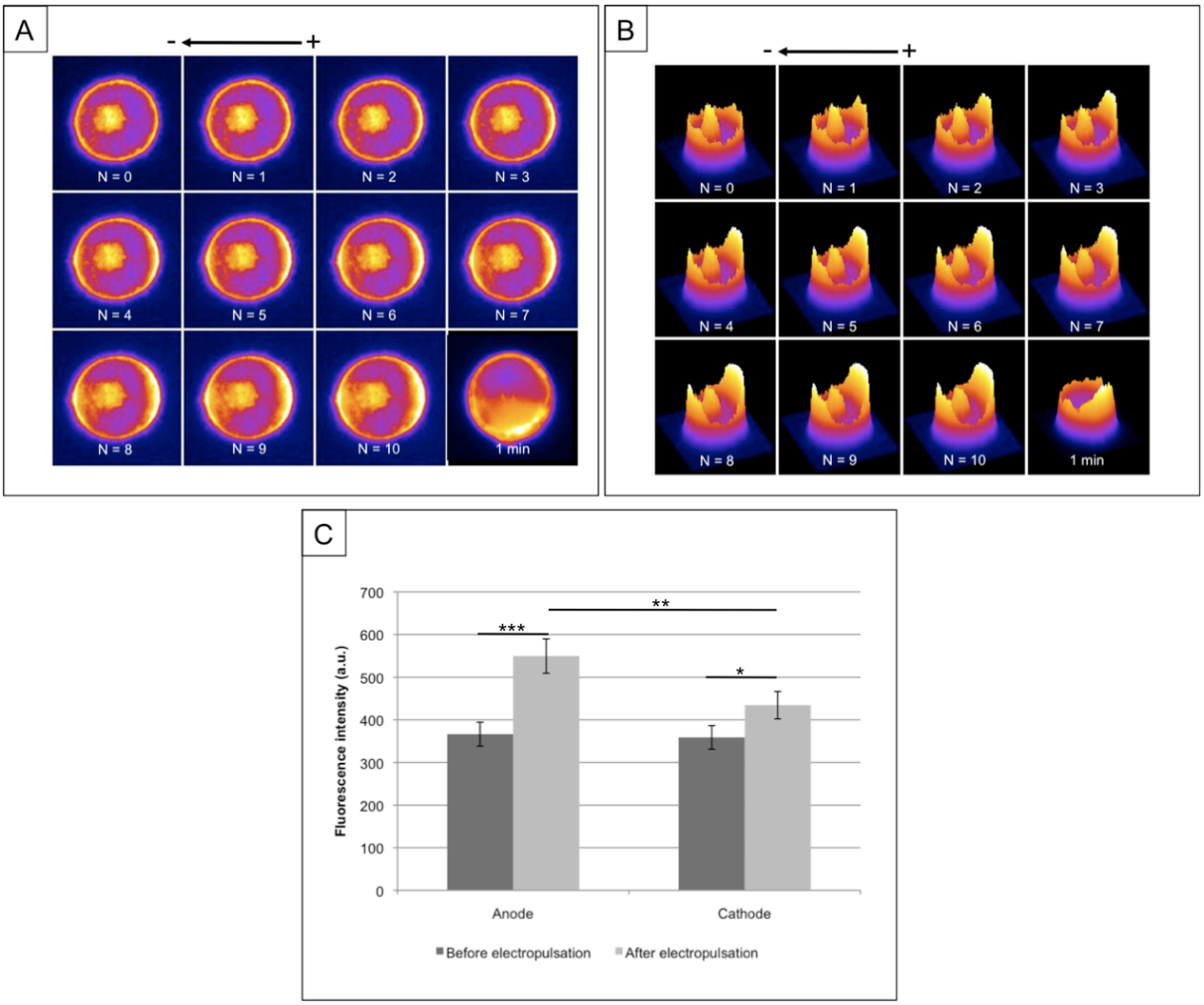
A
- +
N = 0
N = 1
N = 2
N = 3
N = 4
N = 5
N = 6
N = 7
N = 8
N = 9
N = 10
1 min
B
- +
N = 0
N = 1
N = 2
N = 3
N = 4
N = 5
N = 6
N = 7
N = 8
N = 9
N = 10
1 min
C
Fluorescence intensity (a.u.)
700
600
500
400
300
200
100
0
***
**
*
Anode
Cathode
Before electropulsation
After electropulsation

Figure 2

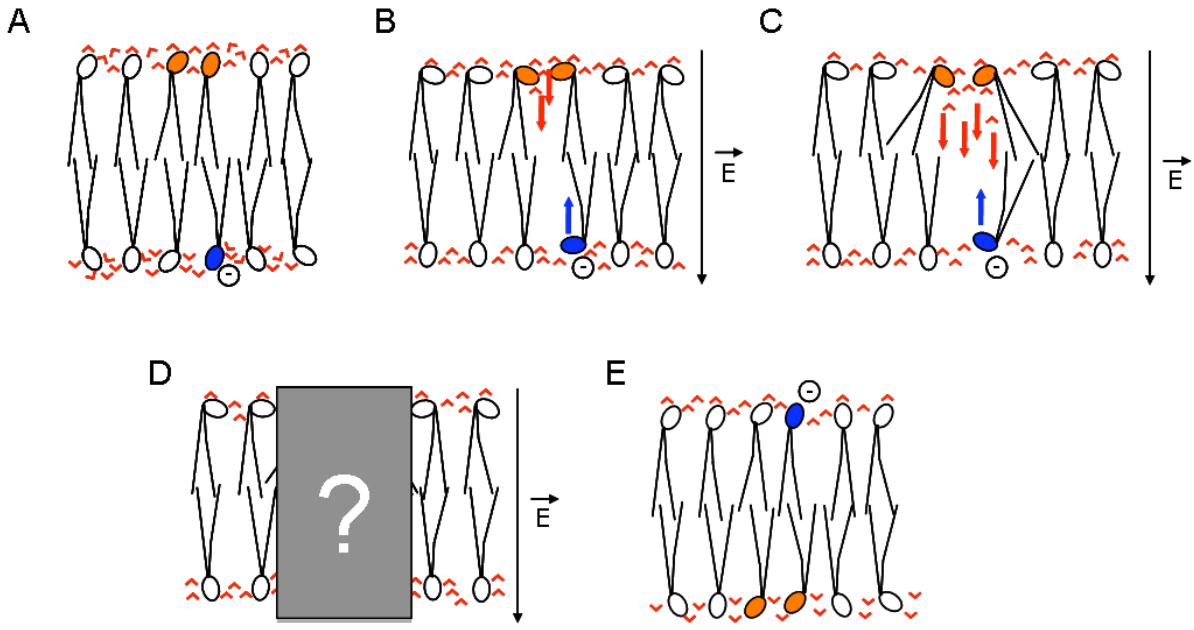

Figure 3

Supporting Material

Transverse movements of phospholipids in plasma membrane of mammalian cells submitted to electric field pulses.

Jean-Michel Escoffre, Cécile Faurie, Sarra C Sébaï, Elisabeth Bellard, Muriel Golzio, Justin Teissié and Marie-Pierre Rols.

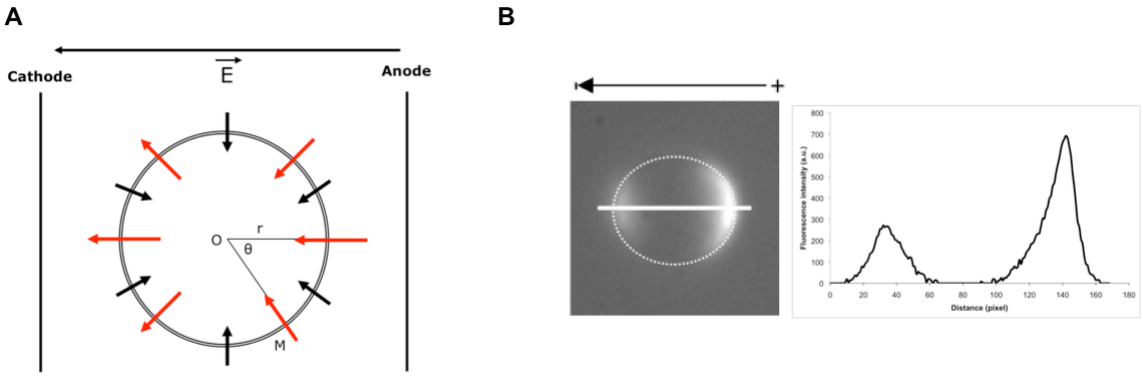

Figure S1: Electropermeabilization. A. Physical principle of electropermeabilization. The plasma membrane is the site of native transmembrane potential difference, $\Delta\Psi_0$ (black arrow). If we consider a cell to be a dielectric spherical shell, when we apply an electric pulse, an induced transmembrane voltage $\Delta\Psi_E$ is created (red arrow). Being dependent on the angular parameter θ, the $\Delta\Psi_E$ effect is position-dependent on the cell surface; therefore, the side of the cell facing the anode is hyperpolarized while the side of the cell facing the cathode is depolarized. B. Electropermeabilization of CHO cells at the single cell level. In presence of 100 µM PI in pulsation buffer, CHO cells were electropermeabilized (10 pulses lasting 5 ms at a frequency of 1 Hz, at 0.7 kV/cm). Light plots represented the fluorescence profile (white line) drawn parallel to the electric field lines at permeabilized sites level. Images were taken 10 seconds after the application of the electropermeabilization pulses. Thirty cells were assayed.

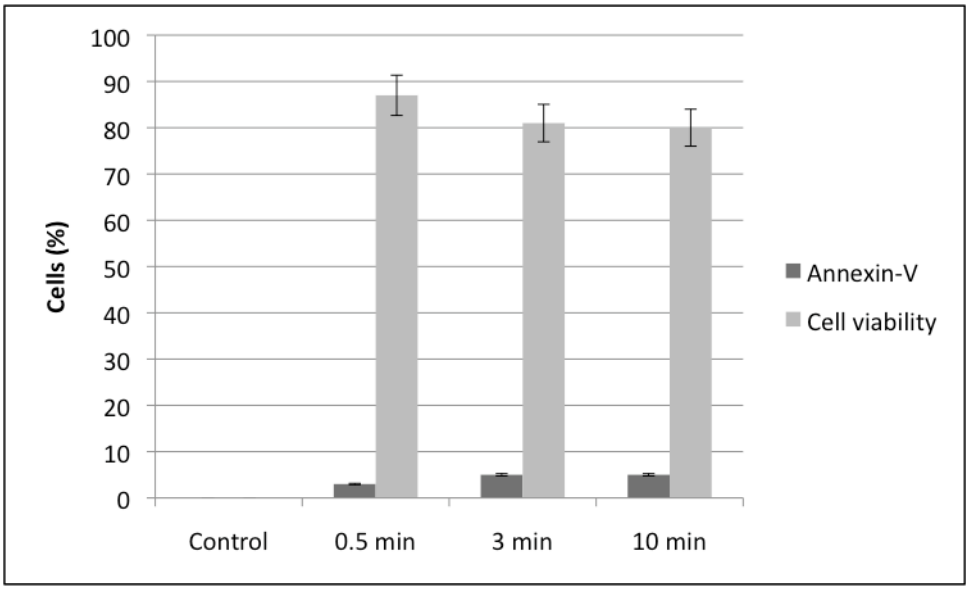

Figure S2: Cell viability and apoptosis. CHO cells were submitted to 10 pulses lasting 5 ms at a frequency of 1 Hz, at 0.7 kV/cm. The cell viability is determined 24h after the electropulsation by colorimetric method. The apoptosis is detected 0.5 min, 3 min and 10 min after the electropulsation by flow cytometer.

3. Discussion et Conclusions

L'application d'impulsions électriques millisecondes et perméabilisantes altère l'organisation des phospholipides de la membrane plasmique en induisant un désordre membranaire et en augmentant leur mobilité transverse entre le feuillet externe et le feuillet interne. Ces observations réalisées sur des cellules animales nucléées confirment les résultats obtenus sur des fantômes d'érythrocytes *(Dressler et al., 1983; Schwister et Deuticke, 1985; Haest et al., 1997; Henszen et al., 1997; Schwarz et al., 1999)*. De plus, ils permettent de montrer que cette perte d'asymétrie transverse électro-induite est un processus rapide (i.e. moins d'une seconde) qui se produit dans les régions membranaires perméabilisées.

D'un point de vue moléculaire, nos résultats peuvent être interprétés selon deux mécanismes possibles: (i) soit les défauts membranaires ou "électropores" créés par les impulsions électriques sont des structures avec une continuité lipidique qui permettent aux phospholipides de migrer d'un feuillet à l'autre *(Haest et al., 1997; Dressler et al., 1983)* en accord avec la théorie de l'électroporation *(Neumann, 1982)*, (ii) soit les impulsions électriques induisent la translocation des phospholipides par une action directe sur les dipôles des têtes des phospholipides *(Hu et al., 2005; Vernier et al., 2006)*. Dans le premier modèle, les "électropores" seraient créés dans les régions perméabilisées en accord avec les résultats de perméabilisation mais resteraient présents durant la phase de retour à l'état non perméable (aussi longtemps que les "pores" sont présents). Cependant, aucune augmentation des mouvements transverses des phospholipides n'est observée pendant cette phase. Par conséquent, ces résultats suggèrent que ces "électropores" à durée de vie longue ne sont pas des structures de passage entre les feuillets membranaires pour les phospholipides *(Dressler et al., 1983; Gurtovenko et Vattulainen, 2007)*; ou que les "électropores" présents pendant l'application des impulsions électriques sont différents de ceux présents pendant la phase de réintégrité membranaire. Donc, seuls les électropores présents pendant l'application des impulsions électriques permettraient la translocation des phospholipides *(Pucihar et al., 2008)*. Le second modèle suggère une interaction directe du champ électrique sur les phospholipides en accord avec de précédentes études *(Hu et al., 2005; Vernier et al., 2007; Bockmann et al., 2008)*. En absence de champ électrique, les dipôles des PC présentent une orientation contrôlée par les charges interfaciales *(Seelig,*

1987; Hu et al., 2005). Pendant la phase d'induction de l'électroperméabilisation, le champ électrique transmembranaire de 0,05 V/nm, généré dans nos conditions expérimentales, pourrait induire l'inclinaison des têtes polaires des phospholipides par rapport à la surface de la membrane *(Stulen, 1981; Lopez et al., 1988; Bockmann et al., 2008)*. Après l'inclinaison des dipôles des PC *(Tieleman, 2004; Tarek, 2005; Bockmann et al., 2008)*, un effet collectif des dipôles des molécules d'eau (très sensibles aux champs électriques *(Teissié, 2007)*) des têtes hydratées des PC pourrait induire la translocation des PC. De précédentes études montrent que la translocation de phospholipides chargés tels que les PS est un événement facilité par la présence de "nanopores" plutôt que le résultat d'une translocation moléculaire à travers une barrière d'énergie transmembranaire *(Hu et al., 2005)*. Par conséquent, la translocation des PS ne peut avoir lieu que dans la région membranaire faisant face à l'anode pendant l'application des impulsions électriques.

A la lumière de précédentes études, nos résultats confirmeraient que les défauts membranaires créés par l'application des impulsions électrique seraient de nature différente face à l'anode et face à la cathode *(Teruel et Meyer, 1997; Gabriel et Teissié, 1998; Gabriel et Teissié, 1999)*. En effet, de précédents travaux suggèrent que de nombreux et petits "électropores" seraient créés dans la région membranaire faisant à l'anode alors que quelques larges "électropores" seraient créés dans la région membranaire faisant à la cathode *(Tekle et al., 1994)*. Cette asymétrie est associée à un effet vectoriel du champ électrique sur la membrane. La translocation électro-induite des phospholipides pourrait contribuer une distribution asymétrique du potentiel aux hémisphères opposés *(Pakhomov et al., 2004; Frey et al., 2006)*.

L'application d'impulsions électriques millisecondes et perméabilisantes induit un désordre membranaire et une rapide translocation des phospholipides dans les régions perméabilisées. Cette translocation semble être induite par un effet direct du champ électrique sur les dipôles des têtes des phospholipides et non pas un effet secondaire comme il a été rapporté dans de précédents travaux sur les érythrocytes. La translocation électro-induite des phospholipides n'est pas associée à une perte de la viabilité cellulaire.

PARTIE II

CARACTÉRISATION DE L'INTERACTION PLASMIDE/MEMBRANE PERMÉABILISÉE

Partie II. Caractérisation de l'interaction plasmide/membrane perméabilisée

1. Etude dynamique de l'interaction plasmide/membrane perméabilisée

1.1. Introduction

Les mécanismes biophysiques impliqués dans l'électrotransfert de molécules de plasmide sont bien plus complexes que ceux impliqués dans l'électrotransfert de petites molécules *(Teissié et al., 2005)*. En effet, l'électrotransfert de petites molécules telles que le PI est induit par un processus de migration électrophorétique pendant l'application des impulsions électriques *(Pucihar et al., 2008)* et par simple diffusion après l'application des impulsions électriques *(Teissié et Rols, 1993; Gabriel et Teissié, 1997)*. En revanche dans le cas de l'électrotransfert de molécules de plasmide, ces dernières viennent interagir avec la membrane plasmique perméabilisée sous la forme d'agrégats localisés *(Golzio et al., 2002)*. La composante dynamique de ce processus n'est pas ou peu connue car les outils biophysiques utilisés présentent une résolution spatiale à l'échelle du micromètre et une résolution temporelle à l'échelle de la seconde.

L'objectif de ce travail vise à étudier l'interaction des molécules de plasmides avec la membrane plasmique avec une résolution temporelle de l'ordre de 2 ms permettant de visualiser ce phénomène pendant sa formation. Nous cherchons à déterminer le processus impliqué dans la création des sites compétents pour la formation de complexes de plasmide et à caractériser sur le plan dynamique ces complexes.

L'ensemble des résultats obtenus dans cette étude fera l'objet d'une publication en 2010.

1.2. Publication

Electromediated formation of DNA nano-complexes on cell membranes and their role in gene delivery

Jean-Michel Escoffre[† a], Thomas Portet[† b,a], Cyril Favard[† c], Christelle Rosazza [a], Justin Teissié [a], David S. Dean [b] and Marie-Pierre Rols [a].

[a] *Institut de Pharmacologie et de biologie structurale, CNRS UMR 5089, Université Paul Sabatier, Toulouse, FRANCE.*
[b] *Laboratoire de Physique Théorique, CNRS UMR 5152, Université Paul Sabatier, Toulouse, FRANCE.*
[c] *Institut Fresnel, CNRS UMR 6133, Universités Aix Marseille, Marseille, FRANCE.*

[†] JME, TP and CF have the same contribution. Corresponding author: MPR.

Abstract

Electroporation is a physical method to induce the uptake of therapeutic drugs and DNA, by eukaryotic cells and tissues. The phenomena behind electro-mediated membrane permeabilization to plasmid DNA have been shown to be significantly more complex than those for small molecules. Small molecules cross the permeabilized membrane by diffusion whereas plasmid DNA first interacts with the electropermeabilized part of the cell surface, forming localized aggregates. The dynamics of this process is still poorly understood because direct observations have been limited to time scales exceeding several seconds. Here, cells are electropermeabilized in the presence of plasmid DNA and monitored with a temporal resolution of 2 ms. This allows us to show that during the first pulse application, plasmid complexes, or aggregates, start to form at distinct sites on the cell membrane. FRAP measurements show that the positions of these sites are remarkably immobile during the application of further pluses. We find that the actin cytoskeleton does not seem to play a role in the initial formation of DNA/membrane interaction sites but it may be important in the subsequent intracellular DNA traffic. A theoretical model is proposed to explain the appearance of distinct interaction sites, the quantitative increase in DNA and also their immobility, leading to a tentative explanation for the success of electro-mediated gene delivery.

Keywords: electroporation; DNA; actin cytoskeleton; membrane biophysics; molecule uptake; fast digital microscopy.

Abbreviations: FRAP, fluorescence recovery after photobleaching; PI, Propidium Iodide; CHO, Chinese Hamster Ovary.

Electropermeabilization is the phenomena by which the application of an electric field across a lipid membrane renders it permeable to the passage of small and even macro molecules such as DNA [1,2]. It is exploited in the clinical context where the permeabilization of cells to a therapeutic agent is required, for example in gene therapy and chemotherapy [3,4,5]. Despite the use of electropermeabilization in medical science, many questions remain open as to the underlying biophysical phenomena which underpin its success. This is especially the case for the permeabilization of membranes to DNA where a number of interesting biological and physical factors remain to be understood. Given the size of the DNA, if the permeabilization is due to pores, as suggested by the standard theory of electroporation [6,7], the pores must be relatively large due to (i) the relatively large size

Email addresses: escoffre@ipbs.fr (Jean-Michel Escoffre[†]), portet@irsamc.ups-tlse.fr (Thomas Portet[†]), favard@fresnel.fr (Cyril Favard[†]), christelle.rosazza@ipbs.fr (Christelle Rosazza), justin.teissie@ipbs.fr (Justin Teissié), dean@irsamc.ups-tlse.fr (David S. Dean), rols@ipbs.fr (Marie-Pierre Rols).

of the DNA and (ii) the large charge of DNA as dielectric exclusion must be overcome [8]. The cell membrane is very heterogeneous and one expects that the location of regions permeabilized to DNA will be determined not only by the local electric field but also by the local membrane composition. In cell membranes, the regions most susceptible to permeabilization may be those containing certain types of transmembrane proteins or at the boundary between differing types of lipid domains [9]. Another key, physical factor is how the field not only modifies the permeability of the membrane, but also influences the movement of the DNA by electrophoresis. While for small molecules, with little electric charge, thermal diffusion dominates the transport, large charged molecules will be strongly advected by the electric field [10]. Experimental study [11] has demonstrated that the physical phenomena involved in electro-mediated membrane permeabilization to plasmid DNA are indeed significantly more complex than those for small molecules. Small molecules cross the permeabilized membrane directly by diffusion whereas plasmid DNA first interacts with the electropermeabilized part of the cell surface resulting in the formation of localized aggregates. However the dynamics of this initial interaction is only partially understood because the direct observations of [11] were limited to time scales exceeding several seconds. In this paper, we have analyzed the interaction between the cell membrane and strongly charged macromolecules (4.7 kbp plasmid DNA) upon the application of a permeabilizing electric field, at a temporal resolution of 2 ms. This enables us to address the following unresolved, and key, questions (i) What is the phenomenon leading to formation of the sites where the DNA aggregates? (ii) What is the underlying dynamics behind their formation? (iii) To what extent are the sites localized in space, and over what time scales? and (iv) What is the mechanism behind this localization? We put forward a model for the transport of charged molecules in the presence of the electric field which provides an interpretation for most of our experimental findings on DNA and whose validity is also tested via additional experiments using the, much smaller, charged molecule Propidium Iodide. Furthermore, we also demonstrate that the actin cytoskeleton has no measurable influence on the formation of the DNA membrane/interaction spots but we find evidence that it may be involved in the subsequent intracellular DNA traffic.

Results

Electropulsation experiments. To study membrane permeabilization by electric fields, and the associated processes of molecular uptake, we used PI and fluorescent plasmid DNA. Membrane permeabilization was induced by applying 20 ms electric pulses of intensity 0.5 kV/cm. This protocol is known to induce both membrane permeabilization and DNA transfer, accompanied by an associated gene expression [11]. Membrane permeabilization was observed at the single cell level at a rate of 500 frames per second. This image acquisition frequency made it possible to monitor the entire process of molecular uptake, both during and after pulse application, with a good spatial resolution using confocal microscopy. Particular attention was paid to the molecular uptake occurring after a single permeabilizing pulse and a series of 10 pulses.

Electropulsation experiments with PI. As shown in Figs. 1A and 1C, and in agreement with previous studies [11], membrane permeabilization, as detected by the uptake of PI, was observed at sites of the cell membrane facing the two electrodes. The influx into the cells of PI, deduced from the associated fluorescence intensity, suggests free transport across the permeabilized regions of the membrane into the cytoplasm (no trapping in the region near the membrane is observed). The uptake of PI into cells started at the moment the pulse was applied and the concentration of PI in the cell increased for up to a minute (Fig. 1E), showing that the permeabilized membrane state, due to defect regions such as metastable pores, persists for some time after the field is cut. Indeed, the majority of molecules which were taken up entered the cell after the pulses. Analyzing the molecular uptake image by image led to the observation that PI uptake was both asymmetric and delayed: it was higher at the anode facing side of the cell and its entrance at the cathode facing side occurred after a 4-5 second delay. This asymmetry can be explained by the fact that PI has a charge +2e in solution and thus the electrophoretic force drives it toward the cathode. The post-pulse diffusion of PI into the cytoplasm of the permeabilized cell can be seen in Movie 1 (published in supporting information).

Electropulsation experiments with DNA. Electro-induced uptake by cells in presence of plasmid DNA showed results that differed considerably from those for cells pulsed in presence of PI. DNA was only observed to interact with the membrane for electric fields greater than a critical value (0.25 kV/cm) which induces their permeabilization, i.e. leading to PI uptake. In the low field regime DNA simply flowed around the cells towards the anode. For permeabilizing fields, plasmid DNA was not observed to enter the cell during pulse application or during the minute that followed. However, DNA was seen to accumulate at distinct sites on the cathode facing side of the permeabilized cell membrane (Fig. 1D). At these sites the DNA appeared to form aggregates, which

became visible as soon as the electric pulse was triggered (Fig. 2A, 2B). Intriguingly, the number and apparent size of these sites did not increase with the number of pulses applied. During the application of a single pulse, the fluorescence of the sites increased linearly in time showing that the quantity of DNA at each site increased linearly (Fig. 1F), but no such fluorescence increase was observed in the absence of the electric field. Therefore the accumulation of DNA at the interaction sites must be principally due to electrophoresis.

The presence of stable sites, where membrane plasmid DNA interaction occurred, was observed across the entire cell population (Fig. 1D) (see Movie 2 in supporting information). The average distance between a site and its nearest neighbor was found to be about 1 μm. The diameter of the individual sites was found to be in the range of 0.2-0.6 μm (lower range limit due to optical diffraction). As shown in Fig. 2C, the total amount of DNA in the membrane region also increased linearly with the number of electric pulses. The final average amount of DNA localized in the membrane region correlated with the amount of DNA reaching the nucleus, as estimated by the rate of GFP expression, between 2 and 24 hours after pulse application (see supporting information).

As shown in Figs. 1E and 1F, part of the DNA interacting with the membrane was observed to be desorbed after the pulses but a large proportion stayed fixed, this could be due to an interaction between the membrane and DNA but also because the DNA forced into the pore electrophoretically is virtually immobile in the cell in the absence of the electric field. This last observation shows that the observed DNA membrane interaction could be, at least partially, due to (i) electrophoretic accumulation along with (ii) reduced mobility of the DNA in the pore region within the cell.

We also studied the mobility of the DNA complexes at the interaction sites. In order to measure the in-membrane or lateral diffusion constant of the complexes, we carried out Fluorescence Recovery After Photobleaching (FRAP) experiments. The FRAP results showed that no exchange between DNA aggregates or with the bulk DNA took place and that the DNA was, on experimental time scales, totally immobile, its lateral diffusion coefficient being less than $10^{-16}\mathrm{m}^2\mathrm{s}^{-1}$. This could be explained by the reduced mobility of individual DNA molecules within the cell or because DNA forms large aggregates which are immobile due to their large size. It is unlikely that this immobility is due to an intrinsic immobility of pores, as the measured diffusion constant is orders of magnitude smaller than the typical values reported in the literature for transmembrane objects, such as proteins.

Experiments on the role of the actin cytoskeleton in DNA uptake. To attempt to understand the origin of the immobility of the DNA in interaction with the membrane, we explored the role of the actin cytoskeleton on the uptake of DNA after its insertion into/ interaction with the permeabilized membrane. We combined two approaches (i) direct – using actin-EGFP expressing CHO cells that can be directly electropulsed under the microscope and give direct access to the kinetics of actin polymerization and (ii) indirect – combining fixation of pulsed cells at various times following electropulsation and their labeling with fluorescent phalloidin to visualize the distribution of polymerized actin. As shown in Figs. 3B and 3E, in the minutes following their electropermeabilization, CHO cells pulsed in absence of DNA did not present any obvious difference in the organization of their cytoskeleton compared to control cells which had not been pulsed (Figs. 3A and 3D). However, when they were electropulsed in the presence of plasmid DNA, actin spot formation was seen (a few minutes after pulsation) in the region of the DNA membrane interaction sites (Figs. 3C and 3F). This result was obtained whichever protocol was used to observe the cytoskeleton. The colocalization of DNA and actin spots is clearly seen in Figs. 3G, 3H and 3I, which respectively show DNA spots (red), actin spots (green), and the superposition of the two acquisition channels (yellow). One could argue that actin polymerization around inserted DNA may be responsible for its immobilization at the membrane level as well as in its subsequent traffic inside the cytoplasm. However, actin cytoskeleton perturbation with Latrunculin A did not seem to modify the features of DNA spot creation, their stability or immobility (see supporting information). This implies that, despite the fact that actin causes a drastic decrease in the mobility of individual large DNA molecules inside cells, the initial formation of DNA spots and their immobility is not caused by the actin network.

Theory

In order to better understand the features of the electro-mediated DNA uptake, we developed a theoretical model that we used to carry out numerical simulations. We assumed that the cell membrane was an infinitesimally thin non-conducting surface. This approximation is valid where the membrane thickness is small compared to all other length scales and the conductivities of the cell interior σ_i and exterior electropulsation solution σ_e are much greater than the conductivity σ_m of the cell membrane. An electric field of magnitude $|\mathbf{E}_0| = E_0$ is applied in the z direction, perpendicular to the electrodes, and the local electric potential ϕ is given, in the steady state regime,

by the solution to Laplace's equation [12]

$$\nabla \cdot \sigma \nabla \phi = 0, \tag{1}$$

with the boundary conditions $\phi = -E_0 z$ as $|z| \to \infty$. In what follows we will assume that the DNA is advected by the field given by the solution of Laplace's equation (1) and will neglect additional fields that would be caused by local accumulation of charge due to the DNA. This is because the applied fields are relatively large and because we expect the DNA to be strongly screened. Once the electric field has been computed the DNA is advected by the field but also diffuses. The local concentration of DNA $c(\mathbf{x}, t)$ obeys the electrodiffusion equation

$$\frac{\partial c}{\partial t} = -\nabla \cdot \mathbf{j} \tag{2}$$

where $\mathbf{j}$ is the thermodynamic current $\mathbf{j} = -D\nabla c + \mu c\mathbf{E}$, with D the local diffusion constant of the DNA, which depends on its environment, and is denoted by D_e outside the cell, D_m in the membrane and D_i in the cell interior. The term μ is the electrophoretic mobility and is defined via the velocity $\mathbf{v}$ of the molecule in a (locally) uniform field $\mathbf{E} = -\nabla\phi$ as

$$\mathbf{v} = \mu\mathbf{E}. \tag{3}$$

As for the diffusion constant, the value of μ will also depend on the local environment as it depends on electrolyte concentration and viscosity. As the electrode system is in contact with a bath of the transported molecule we impose the boundary conditions $\nabla c = 0$ as $c \to \infty$ on equation (2) (note that this is compatible with the Ohmic behavior $\mathbf{j} = \mu c\mathbf{E}$ far from the cell). We assume that D_m and $\mu_m = 0$, which means that DNA cannot move into intact regions of membrane.

Modeling pores. We will assume that when the field is applied, the membrane becomes permeabilized and pores are formed. For the ease of computation we will investigate what happens when a circular pore is formed at each face of the cell facing the electrodes, that facing the anode in the angular region $\theta \in [0, \theta_p]$ and that facing the cathode in the region $\theta \in [\pi - \theta_p, \pi]$. In this region we assume that the conductivity is σ_i and that the diffusion constant is D_i, effectively we have taken away the membrane from these regions and replace it by the cellular interior. We numerically compute the evolution of the concentration of marker molecules as a function of time using the experimental applied field protocols (we assume that the membrane charging process is much quicker that any of the diffusion processes and thus change the electric field instantaneously).

Estimation of theoretical parameters. We were able to follow the fluorescence of the DNA in the buffer solution in a uniform electric field and thus measure its velocity. Using equation (3). we estimated the electrophoretic mobility in solution to be $\mu_e = 10^{-8} m^2 V^{-1} s^{-1}$. This agrees with more precise measurements reported in the literature [13]. The diffusion constant of DNA in aqueous solution is estimated from the literature to be $D_e = 10^{-12} m^2 s^{-1}$[14].

The charge of the PI is taken to be $q = +2e$ and its diffusion constant in aqueous solution is estimated to be $D_e = 10^{-10} m^2 s^{-1}$ (by estimating its effective radius and using the Stokes formula for the diffusion constant of a solid sphere). The electrophoretic mobility for PI is estimated via the Stokes Einstein relation $\mu = \frac{qD}{k_B T}$ where k_B is Boltzmann's constant and T is the temperature.

In the cell interior we estimate that for PI the effective diffusion constants and electrophoretic mobilities are smaller than their external values by a factor of 10 but for the larger DNA molecules they are smaller by a factor of 1 000 (in fact this factor is a lower bound) due largely to the interaction between the DNA and the actin network of the cell interior [14,15]. Finally we took the radius of the spherical vesicle to be $R = 8\ \mu m$ as estimated from the average cell size.

Theoretical results and comparison with experiments. We assume that the marker fluorescence is proportional to the concentration $c(\mathbf{x}, t)$. For the comparison with the experiments we took a pore angle $\theta_p = 3.6^o$ as estimated by the size of the DNA/membrane interaction sites we observed. We computed the average fluorescence intensity inside the cell using $I_{cell} \propto c_{cell}$. In Figs. 1G and 1H we show the predicted behavior for PI fluorescence for one pulse with applied field 0.5 $kV\ cm^{-1}$ applied for 20 ms and see that it compares very well with that measured experimentally (Fig. 1 E). Similarly we see in the same figures the comparison between theory and experiment is also good for DNA (with the same pulse protocol), with the exception that the slight decrease in DNA fluorescence after the pulse has been applied is less pronounced in the theoretical curve of Fig. 1F. However some of the experimentally observed decrease may be due to photo bleaching of the fluorescent marker. Note that although we have only simulated one pore, if we assume that the pores behave independently (as conduction channels in parallel) the overall form of the increase in fluorescence for several pores should be approximately of the same form, up to an overall change in the fluorescence levels, as that for single pore.

In the case of PI, our model also reproduced the other qualitative behavior seen in the experiments. Numerical calculations showed that the PI enters through the anode facing side of the vesicle during the pulse application

and that its entry into the cathode facing side is delayed, as expected from the physical arguments given in the Results section.

For DNA, computations showed that just after the field application there is virtually no uptake of DNA at the anode facing side of the cell, but that at the cathode facing side there is an accumulation of DNA near the surface of the cell in the region where the pore is. In our model the DNA accumulation, apparently, at the surface of the cell, is due to the strong (as compared to the case of PI) electrophoretic force which pushes the DNA into the hole opposite the cathode and then the much reduced mobility of the DNA in this region. For DNA most of the contribution to the total cell fluorescence comes from the region close to the membrane surface, thus justifying our comparison of Figs. 1E, 1F with Figs. 1G, 1H.

Constant number of interaction sites. The experimental results show that after the first interaction sites become visible, no further sites appear during subsequent pulsation. An explanation for this is that the pores formed are conducting and thus the electric field across the membrane is lowered in the non-conducting regions of the membrane. A simple criterion for determining whether a membrane can be locally permeabilized is if the stress caused by the electric field causes the local surface tension to exceed the lysis tension of the membrane. In a simple electric model for the membrane this turns out to be equivalent to the local transmembrane voltage $\Delta\phi$ exceeding a critical value $\Delta\phi_c$, which has values typically between $250-1000\ mV$ [16,17]. To see how the presence of a pore reduces the transmembrane potential elsewhere we consider the simplified case of an infinitesimally thin, non-conducting, infinite flat membrane with a conducting pore of radius a. The potential drop across the membrane at a distance r from the center of the pore is [18] $\Delta\phi(r) = \frac{2\Delta\phi_o}{\pi}\arctan(\frac{\sqrt{r^2-a^2}}{a})$, where $\Delta\phi_o$ is the potential drop far from the pore (or in the absence of the pore) and we assume that $\Delta\phi_o > \Delta\phi_c$. If pores can only be formed in regions where $\Delta\phi > \Delta\phi_c$ one sees that this critical potential drop cannot be exceeded within in a radius $r_c = \frac{a}{\cos\left(\frac{\pi\Delta\phi_c}{2\Delta\phi_o}\right)}$ from the center of the pore. Although a very approximate estimate, this shows that we should expect pores to be separated from each other by a distance of the order of the pore size. This is indeed the case as can be seen in Fig. 2B, where the fluorescence peaks widths are of the same order as the inter-peak distance.

Discussion

Despite the complexity of the system studied here, a number of our experimental observations can be explained qualitatively and to an extent quantitatively on a largely physical basis. According to the standard theory of electropermeabilization, the effect of the electric field is to render the cell membrane permeable to external molecules via the formation of pores. Another effect of the electric field on the DNA is an electrophoretic one, DNA is pushed toward the cathode facing side of the cell and, as our numerical calculations have shown, if a sufficiently large pore is present the DNA can be forced through it. However once the DNA is inside the cell it stays, on experimental time scales, very close to the surface either due to the reduced electrophoretic mobility and diffusion constant of individual DNA molecules caused by the actin cytoskeleton or because it forms aggregates which are immobile due to their large size. Results on cells where the actin cytoskeleton is disrupted also show spot formation and so we conclude that the principal mechanism for spot formation is the formation of aggregates where the DNA molecules are bound together and thus diffuse as a macroscopic object with a very small diffusion constant. A possible mechanism for this aggregation is the presence of multivalent cations induced by the high concentration of DNA in the pore region [19].

In untreated cells the presence of a high concentration of actin filaments close to the DNA spots could be interpreted as a possible first step in the mechanism by which these DNA aggregates enter into the cell. The role of actin has been shown to be important in a number of modes of exogenous molecular uptake (endocytosis, phagocytosis, macropinocytosis) and is also expected to play a role in clathrin or caveolin independent endocytosis [20,21]. Perimembranar actin polymerisation is known to occur when a high amount of PIP2, of high negative charge, is present in the membrane [22]. It is possible that the high local density of negative charge in the DNA spots could trigger a similar response from the actin network. As is the case for extracellular pathogens, membrane invaginations could form due to the DNA spots, without any assistance from the cell machinery [23]. As reported for cationic vectors [24] a growing network of cortical actin may pull the DNA aggregates into the cell. Thus, binding to the membrane and a subsequent connection to the actin network could be a very general means for particle engulfment and transport which could be exploited by both pathogens (bacteria, viruses) and non-viral vectors.

To conclude we have been able to provide a detailed explanation of why gene therapy using electroporation is successful. In principle large aggregates of DNA or vesicles filled with DNA could be too large to pass through the pores formed by electroporation. However individual DNA molecules, while they can pass through electropores, have a limited mobility within the cell and may well be totally degraded before reaching the nucleus. Our results indicate that the actin cytoskeleton reacts to the presence of DNA aggregates and may play an important role in the subsequent intracellular transport, it seems reasonable that only aggregates beyond a certain size can induce this cytoskeletal response and can be transported by the cell. In addition, the fact that the DNA is in aggregate form means that the DNA in the center of the aggregate is relatively protected from degradation by the cellular environment. Therefore, for gene therapy purposes, it is optimal for DNA to enter the cell as single molecules, but the subsequent transport toward the nucleus is, for biological (inducing a response of the actin cytoskeleton) and physical (diminishing enzymatic degradation) reasons, optimized if the DNA is in aggregate form. We thus see that a rather beautiful and subtle, and to an extent fortuitous, combination of biological and physical factors underpin the success of gene therapy via electroporation. As our understanding of these underlying phenomena advances we should be able to refine and optimize the protocols used in electro-mediated gene therapies.

Acknowledgements

Our group belongs to the CNRS consortium Celltiss. This work has benefitted from the financial support of the Association Française contre les Myopathies and the Institut Universitaire de France. We wish to thank Gabor Forgacs for useful discussions on this work.

References

[1] Neumann E, Sowers AE, Jordan CA (1989) *Electroporation and electrofusion in cell biology* (Plenum, New York).
[2] Weaver JC (1995) Electroporation theory. Concepts and mechanisms. *Methods Mol. Biol.* 55:3–28.
[3] Belehradek M, Domenge C, Luboinski B, Orlowski S, Belehradek J, Mir L (1993) Electrochemotherapy, a new antitumor treatment. First clinical phase I-II trial. *Cancer* 72:3694–3700.
[4] Daud AI, DeConti RC, Andrews S, Urbas P, Riker AI, Sondack VK, Munster PN, Sullivan DM, Ugen KE, Messina IJ Heller R (2008) Phase I trial of interleukin-12 plasmid electroporation in patients with metastatic melanoma. *J. Clin. Oncol.* 26:5896–5903.
[5] Rols MP (2006) Electropermeabilization, a physical method for the delivery of therapeutic molecules into cells. *Biochim. Biophys. Acta* 1758:423–428.
[6] Pastushenko VF., Chizmadzhev YA Arekelyan VB (1979) Electric breakdown of bilayer membranes II. Calculation of the membrane lifetime in the steady-state diffusion approximation. *Bioelectrochem. Bioenerg.* 6:53-62.
[7] Powell KT, Weaver JC (1986) Transient aqueous pores in bilayer membranes: a statistical theory. *Bioelectrochem. Bioenerg.* 15 : 211-227.
[8] Parsegian VA (1969) Energy of an ion crossing of a low dielectric membrane: Solutions to four relevant electrostatic problems. *Nature* 221:844–846.
[9] Antonov VF, Petrov W, Molnar AA, Predvoditelev DA, Ivanov AS (1980) Appearance of single-ion channels in unmodifed lipid bilayer-membranes at the phase transition temperature. *Nature* 283:585–586.
[10] Gabriel B, Teissié J (1999) Time courses of mammalian cell electropermeabilization observed by millisecond imaging of membrane property changes during the pulse. *Biophys. J.* 76:2158–2165.
[11] Golzio M, Teissie J, Rols MP (2002) Direct visualization at the single-cell level of electrically mediated gene delivery. *Proc. Natl. Acad. Sci. U S A* 99:1292–1297.
[12] Landau LD, Lifshitz EM (1975) *Electrodynamics of Continuous Media* (Pergamon Press, Oxford).
[13] Stellwagen NC, Gelfi C, Righetti PG (1997) The free solution mobility of DNA. *Biopolymers* 42:687–703.
[14] Lukacs GL,Haggie P, Seksek O, Lechardeur D, Freedman N, Verkman AS (2000) Size-dependent DNA mobility in cytoplasm and nucleus. *J. Biol. Chem.* 275:1625–1629.
[15] Dauty E, Verkman AS (2005) Actin cytoskeleton as the principal determinant of size-dependent DNA mobility in cytoplasm. *J. Biol. Chem.* 280:7823–7828.
[16] Teissié J and Rols MP (1993) An experimental evaluation of the critical potential difference inducing cell membrane electropermeabilization. *Biophys. J.* 65:409–413.
[17] Portet T, Camps Febrer F, Escoffre JM, Favard C, Rols MP, Dean DS (2009), Visualization of membrane loss during the shrinkage of giant vesicles under electropulsation. *Biophys. J.* 96:4109-4121.
[18] Winterhalter M Helfrich W (1987) Effect of voltage on pores in membranes. *Phys. Rev. A* 36:5874-5876.
[19] Bloomfield VA, Crothers DM, Tinoco I (1999) *Nucleic acids: structures, properties and functions* (University Science Books, Sausalito).
[20] Soldati T., Schliwa M.(2006) Powering membrane traffic in endocytosis and recycling. *Nat. Mol. Cell Biol.* 7:897-908.
[21] Smythe E., Ayscough K.R.(2006) Actin regulation in endocytosis. *J. Cell Sci.* 119:4589-4598.

[22] Doherty GJ, McMahon HT (2008) Mediation, modulation and consequences of membrane cytoskeleton interactions. *Ann. Rev. Biophys.* 37:65-95.
[23] Romer, W, Berland, L, Chambon, V et al. (2007) Shiga toxin induces tubular membrane invaginations for its uptake into cells. *Nature* 450:670-676.
[24] Kopatz, I, Remy, JS and Behr, JP (2004) A model for non-viral gene delivery: through syndecan adhesion molecules and powered by actin. *J Gene Medecine* 6:769-776
[25] Rols MP, Coulet D, Teissié J (1992) Highly efficient transfection of mammalian cells by electric field pulses. Application to large volumes of cell culture by using a flow system. *Eur. J. Biochem.* 206:115–121.
[26] Rye HS, Yue S, Wemmer DE, Quesada MA, Haugland RP, Mathies RA, Glazer AN (1992) Stable fluorescent complexes of double-stranded DNA with bis-intercalating asymmetric cyanine dyes: properties and applications. *Nucleic Acids Res.* 20:2803–2812.
[27] Wolf H, Rols MP, Boldt E, Neumann E, Teissié J (1994) Control by pulse parameters of electric field-mediated gene transfer in mammalian cells. *Biophys. J.* 66:524–531.
[28] Golzio M, Mora MP, Raynaud C, Delteil C, Teissié J, Rols MP (1998) Control by osmotic pressure of voltage-induced permeabilization and gene transfer in mammalian cells. *Biophys. J.* 74:3015–3022.
[29] Causeret M, Taulet N, Comunale F, Favard C, Gauthier-Rouviere C (2005) N-cadherin association with lipid rafts regulates its dynamic assembly at cell-cell junctions in C2C12 myoblasts. *Mol. Biol. Cell.* 16:2168–2180.
[30] Sun M., Northup N, Marga F, Huber T, Byfield FJ, Levitan I, Forgacs G (2007) The effect of cellular cholesterol on membrane-cytoskeleton adhesion. *J. Cell Sci.* 120:2223–2231.

Materials and methods

Cells. Chinese hamster ovary (CHO) cells were used. The WTT clone was selected for its ability to grow in suspension or plated on Petri dishes or on a microscope glass coverslip. Cells were grown as previously described [25]. For microscopy experiments, 10^5 cells were put on a Lab-tek chamber 12 hours before electric pulse treatment with 1 ml of culture medium.
DNA staining. A 4.7 kbp plasmid (pEGFP-C1, Clonetech, Palo Alto, CA) carrying the green fluorescent protein gene controlled by the CMV promoter was stained stoechiometrically with the DNA intercalating dye TOTO-1 (or alternatively POPO-3) (Molecular Probes, Eugene, OR) [26]. The plasmid was stained with $2.3\text{x}10^{-4}$ M dye at a DNA concentration of $1\mu g/\mu l$ for 60 minutes on ice. This concentration yields an average base pair to dye ratio of 5. Even if the labeling is not covalent, the equilibrium is dramatically in favor of the linked form. Plasmids were prepared from *E. Coli* transfected bacteria by using Maxiprep DNA purification system (Qiagen, Chatsworth, CA).
Electropermeabilization apparatus. Electropulsation was carried out with a CNRS cell electropulsator (Jouan, St Herblain, France) which delivers square-wave electric pulses. An oscilloscope (Enertec, St. Etienne, France) was used to monitor the pulse shape. The electropulsation chamber was built using two stainless-steel parallel rods (diameter 0.5 mm, length 10 mm, inter-electrode distance 5 mm) placed on a Lab-tek chamber. The electrodes were connected to the voltage generator. A uniform electric field was generated. The chamber was placed on the stage of an inverted digitized videomicroscope (Leica DMIRB, Wetzlar, Germany) or a confocal microscope (Zeiss, LSM 5 life, Germany).
Electropermeabilization. Permeabilization of cells was performed by application of long electric pulses required to transfer genes and to load macromolecules into cells. Cell viability was preserved when using long pulse duration by decreasing the electric field intensity [27,28]. Penetration of PI (100 μM in a low ionic strength pulsing buffer: 10 mM phosphate, 1 mM MgCl2, 250 mM sucrose, pH 7.4) was used to monitor permeabilization. 10 pulses of 20 ms duration and 0.5 kV/cm amplitude were applied at a frequency of 1 Hz at room temperature. For plated cells, the culture medium was removed and replaced by the same buffer described above.
Microscopy. Cells were observed with a Leica 100×, 1.3 numerical aperture oil immersion objective. Images (and optical sections) were recorded with the CELLscan System from Scanalytics (Billerica, MA) fitted with a cooled CCD camera (Princeton Instrument, Trenton, NJ). This digitizing set up allowed a quantitative localized analysis of the fluorescence emission as described previously [11]. This was done along the cell membrane. Images were taken at a 1 Hz frequency. For fast kinetics studies, a Zeiss LSM 5 Live confocal microscope was used. All measurements were performed at room temperature. Image sequences were acquired at a frequency of 500 fps.
FRAP experiments. FRAP experiments were performed on a Zeiss LSM 510 confocal microscope. The 488 nm line of the Arg+ laser was used for excitation of TOTO-1. We used a sequential mode of acquisition with a 63×, 1.4 numerical aperture water immersion lens. After 50 pre-bleach scans, a region of interest (ROI) with a radius $w = 1\mu$m was bleached, and fluorescence recovery was sampled on 150 scans, *i.e.* 40 s [29].
Cytoskeleton experiments. Actin-EGFP expressing CHO cells: CHO cells were transfected by electropulsation with 2 μg of pEGFP-Actin plasmid encoding the human beta actin fused with EGFP protein (Clonetech, Palo Alto,

CA). After electropulsation, cells were cultured at 37^o C. Rhodamine Phalloidin labelling: after electropulsation, CHO cells were washed twice with PBS. Then, cells were fixed in 4% paraformaldehyde solution (InvitroGen) and permeabilized with 0.01% Triton X-100 (Sigma) in PBS for 10 min. Then, cells were washed twice with PBS. To reduce nonspecific background staining, cells were incubated with 1% BSA (Sigma) in PBS for 20 min and labelled with Rhodamine Phalloidin (1U/coverslip) (InvitroGen). Finally, cells were washed twice with PBS and air dried, then mounted in permanent mountant (Moviol, Fluka). Actin cytoskeleton destabilization: cells were incubated at 37^o C for 1 hour with 1 μM Latrunculin A (Sigma) in culture medium. This protocol is known to efficiently disrupt the actin cytoskeleton [30].

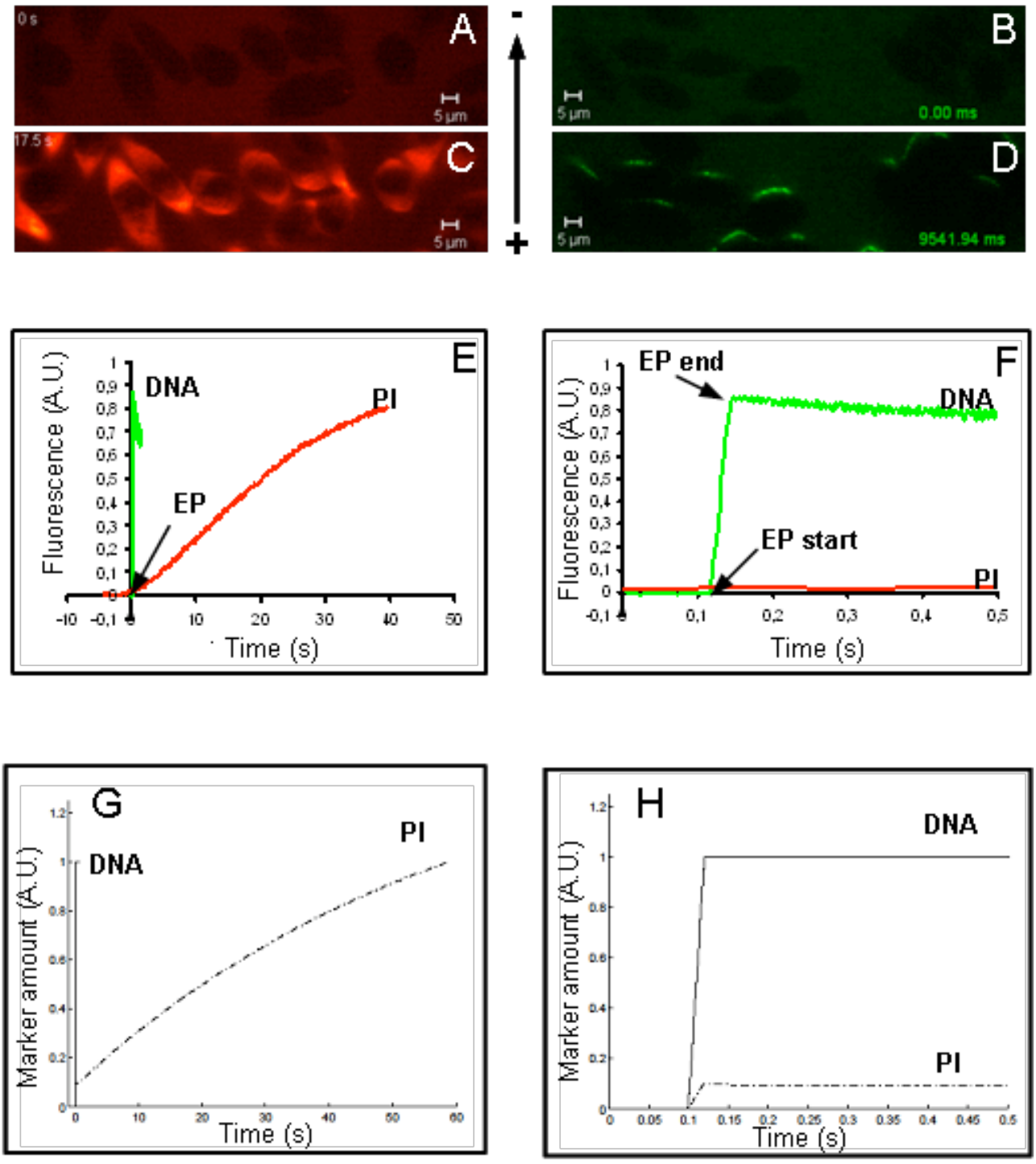

Figure 1. Results and theoretical predictions of uptake of PI and DNA by electropulsed cells. 1A and 1B: cells in the presence of PI and DNA before electropulsation, there is clearly no uptake of either marker. 1C: uptake of PI by cells after being electropulsed. 1D: interaction of DNA and cells after being electropulsed. 1E: long time behavior of PI (red) and DNA (green) uptake measured from the corresponding fluorescence. 1F: same data shown over a shorter time scale. 1G: long term uptake of PI and DNA as predicted by the electrodiffusion model. 1H: corresponding behavior over shorter time scale.

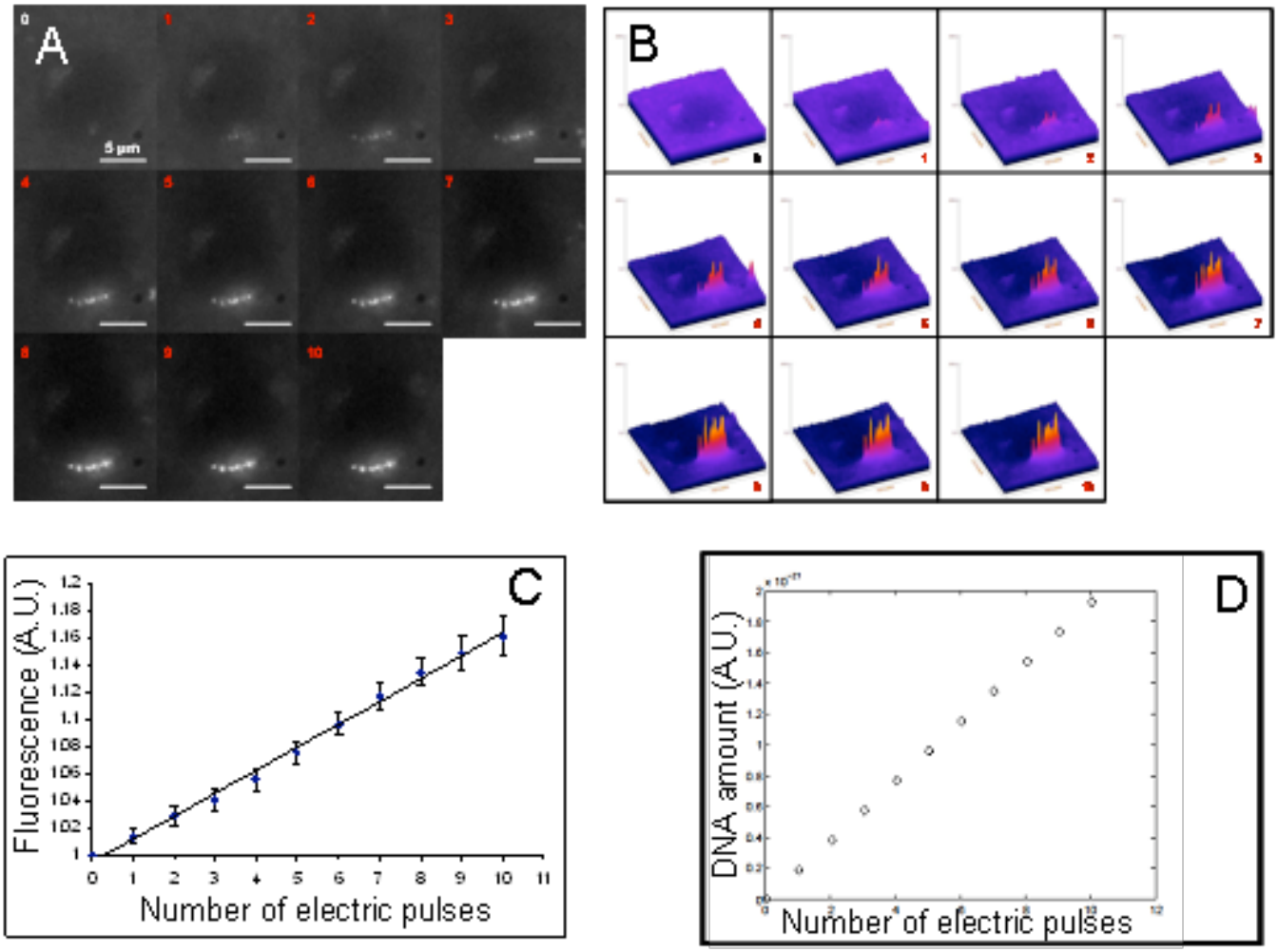

Figure 2. Evolution of DNA fluorescence at interaction sites as a function of the number of electropulses. 2A raw imaging data. 2B: quantified increase in DNA fluorescence based on a digital analysis of 2A. 2C: experimentally measured increase of total fluorescence due to DNA uptake as a function of the number of applied pulses. 2D: increase in DNA fluorescence as a function of the number of pulses as predicted by the electrodiffusion model.

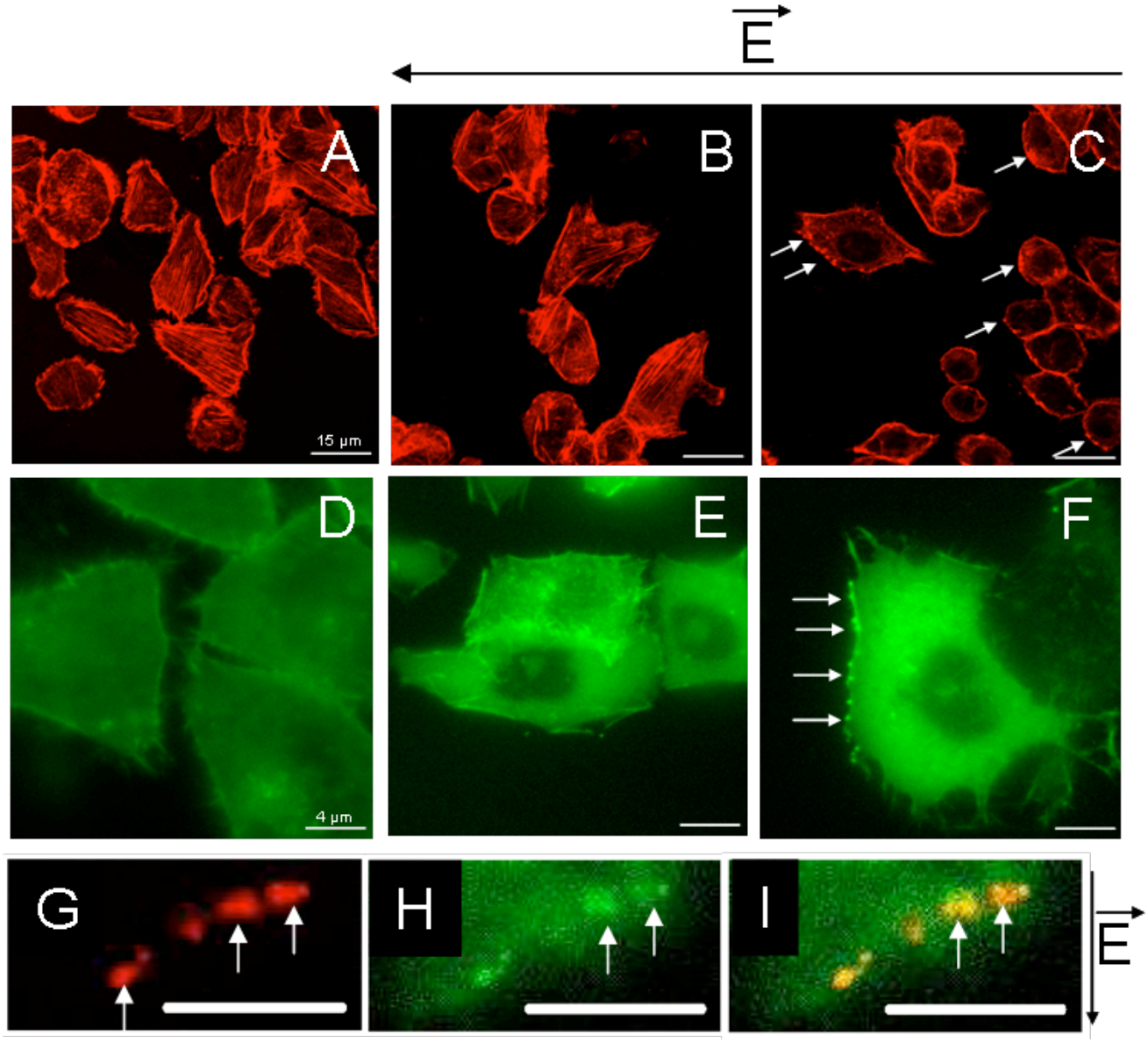

Figure 3. Visualization of actin and DNA spots 10 minutes after electric treatment. A, B and C: Fixed CHO cells, whose cytoskeleton was labeled with Rhodamine Phalloidin. D, E and F: Live CHO cells expressing actin-EGFP. A,D: control cells. B,E: cells pulsed without DNA. C,F: cells pulsed in presence of DNA, actin spots are indicated by white arrows. G: cell showing DNA/POPO aggregates. H: same cell showing actin-EGFP spots. I: superposition of G and H. On frames G, H and I, scalebars are 5 μm.

1.3. Discussion et Conclusions

La pénétration de molécules de PI dans les cellules commence dès l'application des impulsions électriques. La concentration de PI dans les cellules augmente pendant et dans les minutes qui suivent, l'électropulsation. La majorité des molécules de PI pénètre dans les cellules après l'électropulsation. Ces résultats confirment que l'état perméabilisé de la membrane plasmique dû à des défauts membranaires persiste pendant quelques minutes après l'application des impulsions électriques *(Rols et Teissié, 1990a*). La pénétration des molécules de PI dans les cellules est un phénomène asymétrique: en accord avec les lois de physiques, les deux régions membranaires de la cellule qui font face aux électrodes sont électroperméabilisées. Cependant, l'entrée des molécules de PI est plus importante dans la région membranaire faisant face à l'anode. En revanche, son entrée dans la région membranaire située face à la cathode a lieu après 5 s de délai. Cette asymétrie s'explique par le fait que le PI qui présente deux charges positives, pénètre dans les cellules face à la cathode sous l'effet des forces électrophorétiques *(Pucihar et al., 2008)*. En revanche, après l'application des impulsions électriques, sa pénétration dans les cellules est un processus de diffusion *(Teissié et Rols, 1993; Gabriel et Teissié, 1997)*.

La pénétration de molécules de plasmide dans les cellules est un processus plus complexe que celui des petites molécules comme le PI. L'application d'impulsions électriques perméabilisantes ne permet pas une entrée directe des molécules de plasmide dans les cellules. Dès que les impulsions électriques permébilisantes sont appliquées, les molécules de plasmide viennent interagir avec la région membranaire perméabilisée située face à la cathode. Cette interaction plasmide/membrane a lieu dans des sites distincts de la membrane perméabilisée. Ce résultat montre que l'application d'impulsions électriques perméabilisantes induit la formation de sites compétents pour l'interaction plasmide/membrane. La distance moyenne entre ces sites compétents est de l'ordre de 1 µm. Le diamètre de ces complexes plasmide/membrane est de l'ordre de 0,2-0,6 µm *(Golzio et al., 2002)*. De façon surprenante, le fait que l'augmentation du nombre d'impulsions électriques n'entraînent pas une augmentation du nombre de spots fluorescents indique que dans les conditions expérimentales utilisées, les sites compétents pour l'interaction des molécules de plasmide à la membrane plasmique

perméabilisée sont présents dès la première impulsion électrique. En revanche, le nombre d'impulsions électriques définit la quantité de molécules de plasmide présentes dans les complexes plasmide/membrane. Par conséquent, ces résultats montrent que l'insertion des molécules de plasmide dans ces sites doit être principalement due à la migration électrophorétique. Les complexes plasmide/membrane sont particulièrement stables et sont visibles plusieurs minutes après l'application des impulsions électriques. Les résultats de FRAP montrent l'absence d'échanges de molécules de plasmide entre les complexes, et entre les complexes et le milieu extérieur ou le cytoplasme, dans les minutes qui suivent l'électropulsation. De plus, dans nos conditions expérimentales, **ces** complexes apparaissent immobiles ($D<10^{-16}$ m^2s^{-1}). Ce résultat pourrait s'expliquer par le fait que les molécules de plasmides présentent une mobilité réduite dans les cellules liée à la présence du cytosquelette *(Lukacs et al., 2000 ; Dauty et al., 2005)*. Le cytosquelette d'actine ne semble pas être impliqué dans la formation et dans l'immobilité des complexes plasmide/membrane. Néanmoins, l'existence d'une polymérisation de l'actine au niveau des sites compétents pour l'interaction plasmide/membrane dans les 5 à 10 minutes tendrait à montrer que le cytosquelette d'actine pourrait jouer un rôle dans le trafic intracellulaire des molécules de plasmide. En effet, la présence d'agrégats de plasmides fluorescents dans le cytoplasme suggérant la formation de vésicules d'endocytose a déjà été rapportée *(Golzio et al., 2002 ; Jérôme et al., 2009)*.

Pendant l'application de la première impulsion électrique, les molécules de plasmide migrent par électrophorèse et viennent interagir dans des sites distincts de la région membranaire faisant face à la cathode. Les complexes plasmide/membrane ainsi formés ne diffusent pas latéralement dans la membrane. Le cytosquelette d'actine n'est pas impliqué dans la formation de ces complexes mais pourrait être impliqué dans le transport intracellulaire des molécules de plasmides.

2. Effet de l'intensité du champ électrique et du nombre d'impulsions électriques sur l'électrotransfert de plasmide

2.1. Introduction

Dans la majorité des expériences, l'électroperméabilisation est révélée par l'incorporation de composés fluorescents (e.g. iodure de propidium, bromure

d'éthidium…). L'influence des paramètres électriques sur l'efficacité de perméabilisation a été étudiée à l'échelle de la population cellulaire par cytométrie en flux, microscopie ou spectroscopie de fluorescence. L'augmentation de l'intensité, du nombre ou de la durée des impulsions électriques entraînent une augmentation du taux de perméabilisation (i.e. pourcentage de cellules perméabilisées) et de l'efficacité de perméabilisation (i.e. intensité de fluorescence associée) *(Liang et al., 1988; Kwee et al., 1989; Rols et al., 1990c; Rols et Teissié, 1998)*. L'utilisation de la vidéo-microscopie en cinétique rapide a permis de visualiser l'entrée des composés, au niveau membranaire et à l'échelle de la cellule unique. Les molécules pénètrent dans la cellule, pendant l'application des impulsions électriques, au niveau des régions membranaires perméabilisées faisant face aux deux électrodes. L'intensité des impulsions électriques définit la surface membranaire perméabilisée *(Gabriel et Teissié, 1997; 1999)*. La durée des impulsions électriques appliquées ne modifie pas la surface perméabilisée mais influerait sur le nombre et/ou la taille des structures de perméabilisation créées *(Gabriel et Teissié, 1997; Rols et Teissié, 1990)*.

L'électrotransfection est révélée par l'expression de la protéine codée par le plasmide transférée. L'analyse, à l'échelle de la population cellulaire, de l'efficacité de transfection en fonction des paramètres électriques a été étudiée. La transfection n'est détectée qu'au delà de valeurs d'intensités de champ électrique supérieures au seuil de perméabilisation (E_p) *(Wolf et al., 1994)*. L'augmentation de la valeur de E entraîne l'augmentation du taux de transfection, jusqu'à un maximum, puis chute pour des valeurs de champ électriques plus élevées *(Chu et al., 1987; Wolf et al., 1994; Hui, 1995)*. L'optimum de transfection correspond à des valeurs de E pour lesquelles la viabilité est préservée, en général supérieure à 50%. Le taux de transfection dépend également de la durée et du nombre d'impulsions électriques. Pour une intensité de champ électrique donnée, le transfert de plasmide augmente avec la durée de l'impulsion électrique *(Chu et al., 1987; Kubiniec et al., 1990; Wolf et al., 1994; Hui, 1995; Rols et Teissié,1998)*. Dans le cas des cellules CHO, il existe une dépendance linéaire entre le nombre d'impulsions électriques et le taux de transfection *(Wolf et al., 1994)*.

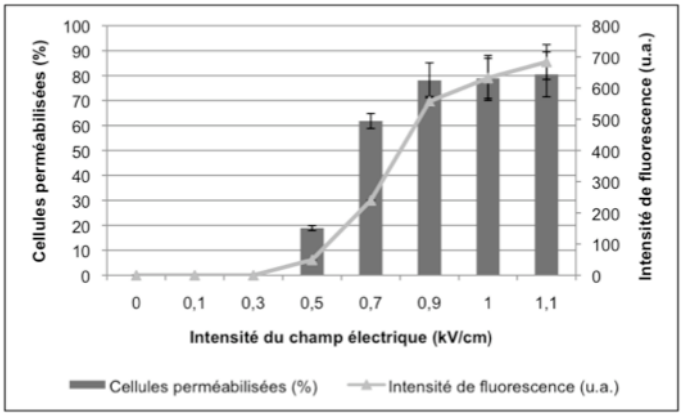

Figure III-1: Effet de l'intensité du champ électrique sur la perméabilisation des cellules CHO. 10 impulsions électriques de 5 ms de 1 Hz ont été appliquées à une suspension cellulaire (1.10^6 cellules/point expérimental) reprise dans du tampon de pulsation contenant 100 µM de PI. Après 10 minutes à 30°C, les cellules sont analysées en cytométrie de flux. Le pourcentage de cellules perméabilisées et l'intensité de fluorescence associée à la perméabilisation sont représentés sur ce graphique. (N=3; moyenne ± SEM).

Le marquage du plasmide par l'intercalation d'une sonde fluorescente, TOTO-1, et l'utilisation de la vidéo-microscopie de fluorescence ont permis de visualiser, à l'échelle de la cellule unique, la première étape de l'électrotransfert: l'interaction du plasmide à la membrane plasmique perméabilisée *(Golzio et al., 2002; Faurie et al., 2004; Phez et al., 2005; Faurie et al., 2010)*. Le plasmide interagit une dizaine de minutes au niveau de la région membranaire perméabilisée face à la cathode et de manière non homogène, sous la forme d'agrégats ou de complexes. Les résultats menés sur le rôle des paramètres électriques sur l'interaction du plasmide avec la membrane plasmique perméabilisée restent préliminaires.

L'influence de l'intensité du champ électrique et du nombre d'impulsions électriques sur la perméabilisation, l'interaction plasmide/membrane et l'électrotransfert de plasmide sont analysés dans cette partie. L'étude est menée sur des cellules CHO en suspension, qui présentent une forme sphérique et donc pour lesquelles les équations théoriques de l'électroperméabilisation peuvent être facilement appliquées.

2.2. Résultats

2.2.1. Effet de l'intensité du champ électrique

Les conditions électriques retenues pour toutes les expériences sont de 10 impulsions électriques de 5 ms à la fréquence de 1 Hz. Ces conditions sont optimales pour le transfert des macromolécules *(Rols et Teissié, 1998)*.

2.2.1.1 Electroperméabilisation

La pénétration de l'iodure de propidium dans les cellules est détectée lorsque l'intensité du champ électrique est supérieure à une valeur seuil (E_p) comprise entre 0,3 et 0,5 kV/cm pour des cellules CHO en suspension (Figure III-1). Au delà de cette valeur seuil, l'augmentation de l'intensité du champ électrique s'accompagne d'une augmentation du pourcentage de cellules perméabilisées (de 19±1% pour 0,5 kV/cm à 81±9% pour 1,1 kV/cm) et de l'intensité de fluorescence associée (de 50± u.a. pour 0,5 kV/cm à 684±56 u.a. pour 1,1 kV/cm), selon un profil sigmoïdal (Figure III-1). L'optimum du pourcentage de cellules perméabilisées et viables (i.e. 70%) est obtenu pour une valeur d'intensité du champ électrique de 0,7 kV/cm.

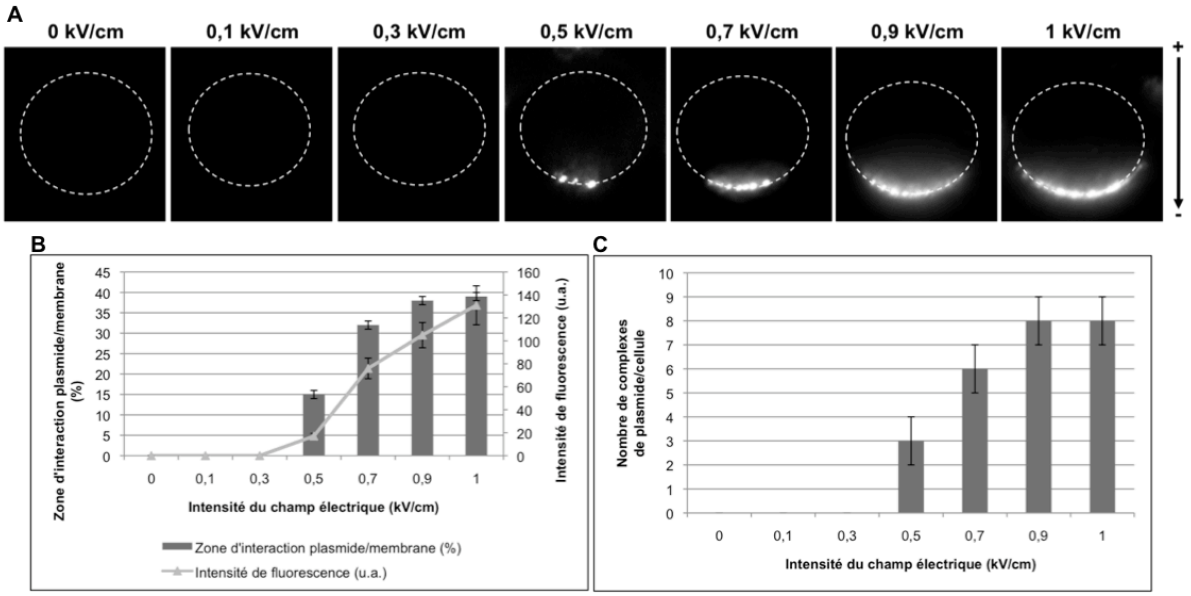

Figure III-2: Effet de l'intensité du champ électrique sur l'interaction plasmide/membrane sur des cellules CHO. 10 impulsions électriques de 5 ms de 1 Hz ont été appliquées à des cellules CHO sphériques (1.10^5 cellules/point expérimental) en présence de 5 µg de plasmide peGFP-C1 marqué au TOTO-1 dans du tampon de pulsation. (A) Les cellules sont observées en microscopie de fluorescence. L'acquisition des images est réalisée à la fin de l'application des impulsions électriques. La flèche noire indique le sens du champ électrique. (B) Le périmètre de la zone d'interaction plasmide/membrane (exprimé en pourcentage du périmètre total de la cellule) et l'intensité de fluorescence totale associée sont déterminés. (C) Le nombre de complexes de plasmide par cellule est déterminé. ($N_{cellules}$=30; moyenne ± SEM).

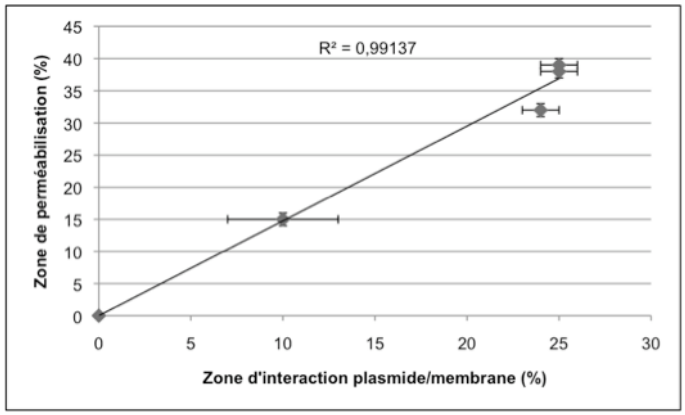

Figure III-3: Corrélation entre la zone perméabilisée et la zone d'interaction plasmide/membrane. 10 impulsions électriques de 5 ms de 1 Hz ont été appliquées à des cellules CHO sphériques (1.10^5 cellules/point expérimental) en présence de 5 µg de plasmide peGFP-C1 marqué au TOTO-1 ou de 100 µM de PI dans du tampon de pulsation. Les cellules sont observées en microscopie de fluorescence. Le périmètre de la zone d'interaction plasmide/membrane ou de la zone de perméabilisation face à la cathode (exprimé en pourcentage du périmètre total de la cellule) est déterminé. ($N_{cellules}$=30; moyenne ± SEM).

2.2.1.2. Interaction plasmide/membrane

L'interaction plasmide/membrane est déterminée par microscopie de fluorescence à l'échelle de la cellule unique. Les clichés sont enregistrés à la fin du train d'impulsions électriques. Des profils de fluorescence sur tout le pourtour des cellules sont tracés. Le périmètre d'interaction du plasmide à la membrane, en pourcentage du périmètre cellulaire total, et l'intensité de fluorescence totale dans la zone d'interaction sont calculés (Figure III-2A).

En absence de champ électrique ou pour des valeurs de champ électrique inférieure à 0,5 kV/cm, aucune interaction du plasmide à la membrane plasmique n'est visualisée (Figure III-2). A 0,5 kV/cm, l'interaction du plasmide à la membrane plasmique est présente sous la forme de 3±1 complexes de plasmides fluorescents face à la cathode (15±1% du périmètre cellulaire total) (Figure III-2B et 2C). A 0,7 kV/cm, 6±1 complexes de plasmides fluorescents sont visualisés à la membrane face à la cathode (Figure III-2C) et le périmètre d'interaction représente 32±1% du périmètre cellulaire total (Figure III-2B). L'interaction du plasmide à la membrane est observée sur l'ensemble des cellules perméabilisées. A 0,9 kV/cm et à 1 kV/cm, l'interaction du plasmide à la membrane perméabilisée se présente sous la forme d'une succession de 8±1 complexes de plasmides fluorescents face à la cathode (Figure III-2C). Le périmètre d'interaction représente alors 40±1% du périmètre cellulaire (Figure III-2B). Ainsi, l'augmentation de l'intensité du champ électrique entraîne une augmentation du périmètre d'interaction du plasmide à la membrane plasmique et une augmentation du nombre de complexes de plasmides fluorescents (Figure III-2). Cette augmentation du périmètre d'interaction plasmide/membrane est corrélée à celle du périmètre de perméabilisation de la membrane plasmique (Figure III-3). La fluorescence totale dans la zone d'interaction, et donc la quantité d'ADN en interaction, augmente avec l'intensité du champ électrique (de 17±3 u.a. pour 0,5 kV/cm à 131±17 u.a.) (Figure III-2B). Cependant, la fluorescence par complexe de plasmides fluorescents semble être indépendante de l'intensité du champ électrique.

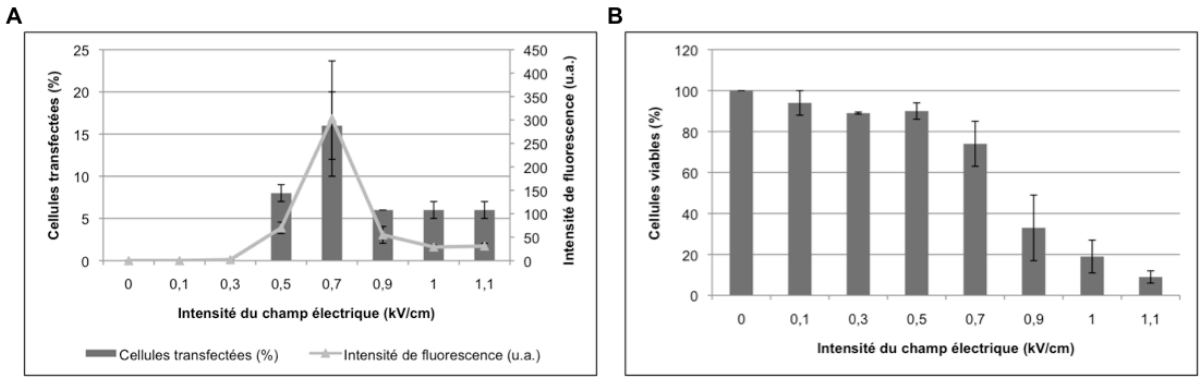

Figure III-4: Effet de l'intensité du champ électrique sur l'électrotransfert de plasmide et sur la viabilité des cellules électrotransfectées. 10 impulsions électriques de 5 ms de 1 Hz ont été appliquées à une suspension cellulaire (1.10^6 cellules/point expérimental) en présence de 5 µg de plasmide peGFP-C1 dans du tampon de pulsation. Après 10 minutes à 30°C, les cellules sont remises en culture. (A) Le pourcentage de cellules transfectées et l'intensité de fluorescence associée sont détectés par cytométrie de flux 24h après électrotransfert. (B) La survie cellulaire est révélée par spectrophotométrie 24h après électrotransfert. (N=3; moyenne ± SEM).

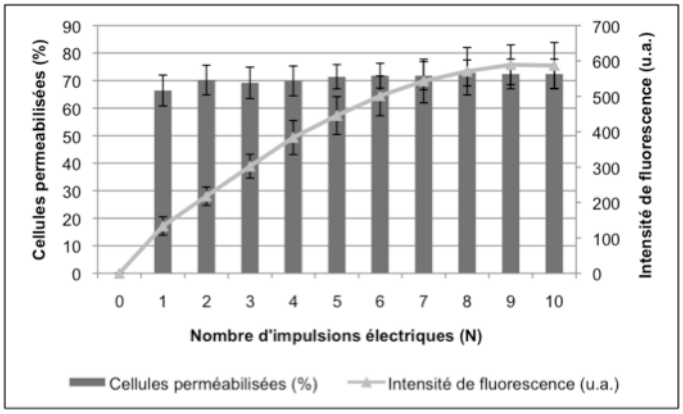

Figure III-5: Effet du nombre d'impulsions électriques sur la perméabilisation des cellules CHO. 1 à 10 impulsions électriques de 5 ms de 1 Hz à 0,7 kV/cm ont été appliquées à une suspension cellulaire (1.10^6 cellules/point expérimental) reprise dans du tampon de pulsation contenant 100 µM de PI. Après 10 minutes à 30°C, les cellules sont analysées en cytométrie de flux. Le pourcentage de cellules perméabilisées et l'intensité de fluorescence associée à la perméabilisation sont représentés sur ce graphique. (N=3; moyenne ± SEM).

2.2.1.3. Electrotransfert de plasmide

Le transfert de plasmide dans les cellules mesuré grâce à son expression qui débute 2 à 3 heures après les impulsions électriques, est maximale au bout de 24 heures. Il est détecté lorsque l'intensité du champ électrique est supérieure à une valeur seuil comprise entre 0,3 et 0,5 kV/cm pour des cellules en suspension (Figure III-4A). Au delà de cette valeur seuil, l'augmentation de l'intensité du champ électrique s'accompagne d'une augmentation du pourcentage de cellules transfectées et de l'intensité de fluorescence associée, puis lorsque la viabilité cellulaire devient inférieure à 50%, le taux et l'efficacité de transfection chutent de façon importante (Figure III-4A et 4B). L'optimum du transfert de plasmide est obtenu pour une intensité de champ électrique de 0,7 kV/cm, pour laquelle le taux de transfection est de 16±4% et l'efficacité de transfection est de 303±123 u.a. avec une viabilité cellulaire de 74±11% (Figure III-4).

Les courbes de viabilité cellulaire en absence de plasmide pEGFP-C1 sont quasi identiques à celles obtenues en présence de plasmide (variabilité comprise entre 5 et 10%). Ce plasmide n'est pas toxique pour les cellules aux concentrations utilisées dans les expériences.

2.2.2. Effet du nombre d'impulsions électriques

2.2.2.1. Electroperméabilisation

Les cellules CHO sont soumises à des trains de 1 à 10 impulsions électriques de 5 ms à une intensité électrique de 0.7 kV/cm et à la fréquence de 1 Hz en présence d'iodure de propidium. Le taux et l'efficacité de perméabilisation sont déterminés par cytométrie de flux.

En absence de champ électrique, aucune perméabilisation membranaire n'est détectée. En revanche, dès la première impulsion électrique, l'optimum du taux de perméabilisation (i.e. 70±5% de cellules perméabilisées) est obtenu (Figure III-5). De plus, le taux de perméabilisation ne varie pas avec l'augmentation du nombre d'impulsions électriques (Figure III-5). Par contre, l'efficacité de perméabilisation (i.e. intensité de fluorescence associée à l'iodure de propidium) augmente quasi linéairement jusqu'à la huitième impulsion électrique (de 134±26 u.a. pour N=1 à 571±67 u.a. pour N=8) pour atteindre un plateau entre la huitième et la dixième impulsions électriques (Figure III-5).

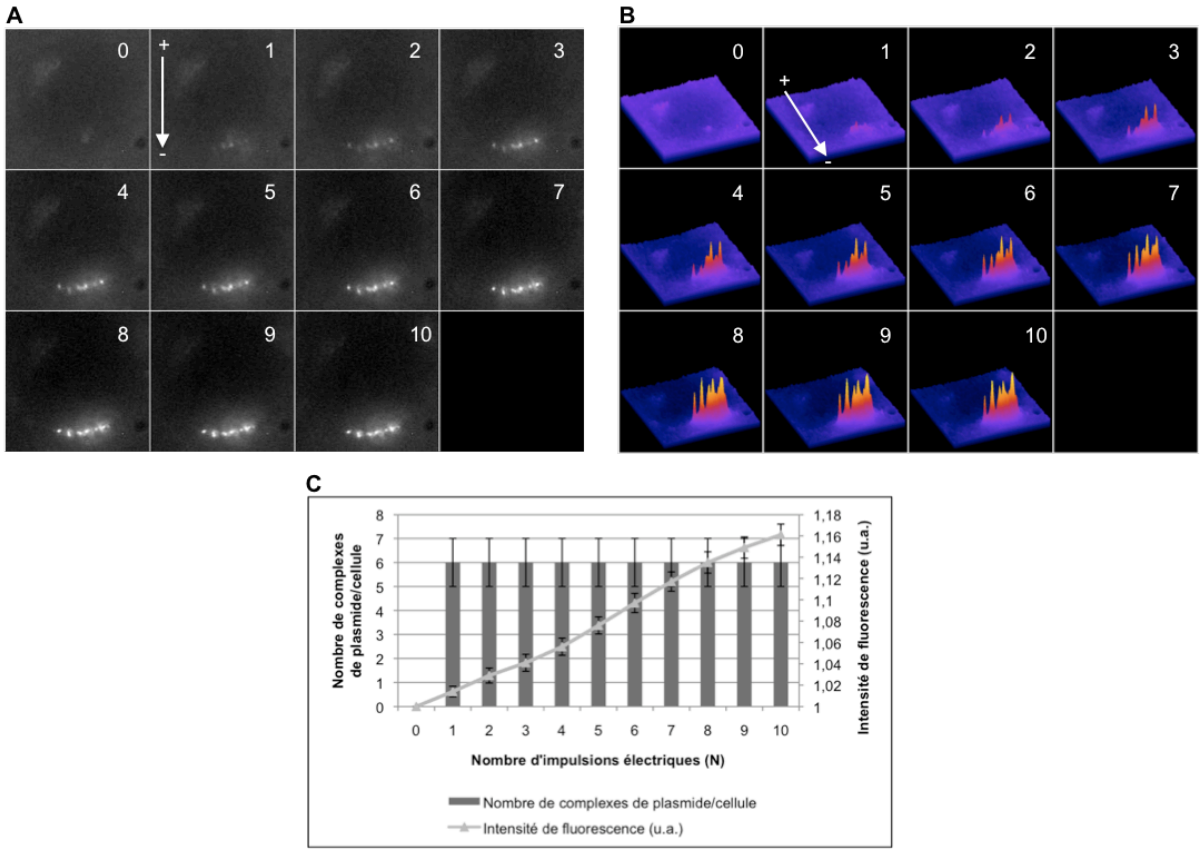

Figure III-6: Effet du nombre d'impulsions électriques sur l'interaction plasmide/membrane sur des cellules CHO. 1 à 10 impulsions électriques de 5 ms de 1 Hz à 0,7 kV/cm ont été appliquées à des cellules CHO sphériques (1.10^5 cellules/point expérimental) en présence de 5 µg de plasmide peGFP-C1 marqué au TOTO-1 dans du tampon de pulsation. (A) Les cellules sont observées en microscopie de fluorescence. L'acquisition des images est réalisée avant (N=0) et pendant (N=1 à N=10) les impulsions électriques. La flèche blanche indique le sens du champ électrique. (B) À partir des images obtenues, des histogrammes de fluorescence sont générés avec le logiciel ImageJ. (C) Le nombre d'agrégats de plasmide par cellule et l'intensité de fluorescence totale associé à l'interaction plasmide/membrane sont déterminés par le logiciel MetaMorph. ($N_{cellules}$=30; moyenne ± SEM).

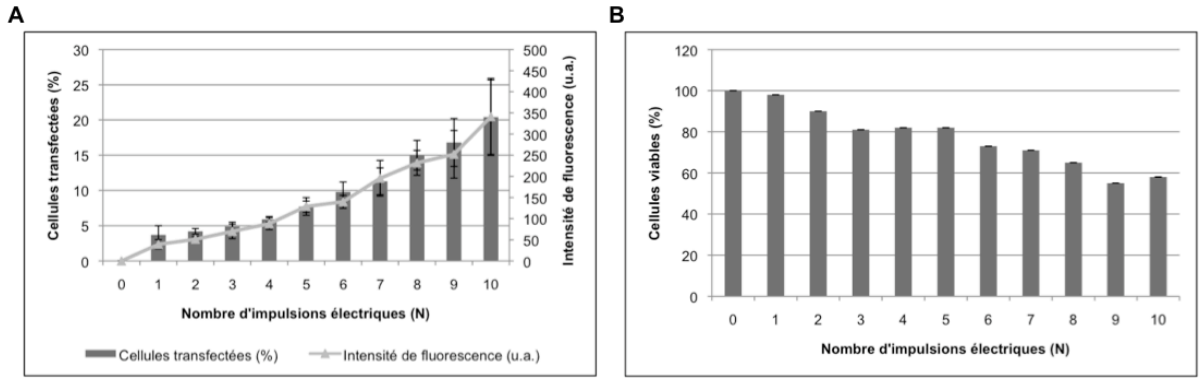

Figure III-7: Effet de du nombre d'impulsions électriques sur l'électrotransfert de plasmide et la viabilité des cellules électrotransfectées. 10 impulsions électriques de 5 ms de 1 Hz à 0,7 kV/cm ont été appliquées à une suspension cellulaire (1.10^6 cellules/point expérimental) en présence de 5 µg de plasmide peGFP-C1 dans du tampon de pulsation. Après 10 minutes à 30°C, les cellules sont remises en culture. (A) Le pourcentage de cellules transfectées et l'intensité de fluorescence associée sont détectés par cytométrie de flux 24h après électrotransfert. (B) La survie cellulaire est révélée par spectrophotométrie 24h après électrotransfert. (N=3; moyenne ± SEM).

2.2.2.2. Interaction plasmide/membrane

10 impulsions électriques de 5 ms à une intensité électrique de 0.7 kV/cm et à la fréquence de 1 Hz sont appliquées sur les cellules CHO en présence de plasmide fluorescent. Des clichés en fluorescence sont enregistrés avant et entre chaque impulsion électrique.

Avant l'application du champ électrique, aucune interaction spontanée du plasmide à la membrane plasmique n'est visualisée (Figure III-6). Dès la première impulsion électrique et pendant le train d'impulsions électriques, le plasmide fluorescent interagit à la membrane perméabilisée face à la cathode sous la forme d'environ 6±1 complexes de plasmides fluorescents (Figure III-6C). Des histogrammes de fluorescence dans la zone d'interaction du plasmide à la membrane perméabilisée sont obtenus. Entre la première et la dixième impulsion électrique, le périmètre d'interaction du plasmide à la membrane plasmique (32±1% du périmètre cellulaire total) et le nombre de complexes de plasmides fluorescents ne varient pas (Figure III-6C). Par contre, la fluorescence totale dans la zone d'interaction et donc la quantité de plasmide interagissant à la membrane plasmique perméabilisée augmentent quasi linéairement avec le nombre d'impulsions électriques (de 1,014±0,005 u.a. pour N=1 à 1,61±0,01 u.a. pour N=10) (Figure III-6C). La quantité de plasmide par complexes fluorescents semble donc contrôlée par le nombre d'impulsions.

2.2.2.3. Electrotransfert de plasmide

Les cellules CHO sont soumises à des trains de 1 à 10 impulsions électriques de 5 ms à une intensité électrique de 0.7 kV/cm et à la fréquence de 1 Hz en présence de plasmide pEGFP-C1. Le taux et l'efficacité de transfection sont déterminés 24 heures après l'électrotransfert de plasmide par cytométrie de flux.

En absence de champ électrique ou de plasmide pEGFP-C1, aucune expression d'EGFP et donc de transfert de plasmide n'est détectée. Le taux (4±1% pour N=1 à 20±5% pour N=10) et l'efficacité (39±11 u.a. pour N=1 à 341±91 pour N=10) de transfection augmentent avec le nombre d'impulsions électriques (Figure III-7A). Un optimum de transfection est obtenu pour 10 impulsions électriques (i.e. 20±5% cellules transfectées avec une intensité de fluorescence associée de 341±91 u.a.) (Figure III-7B).

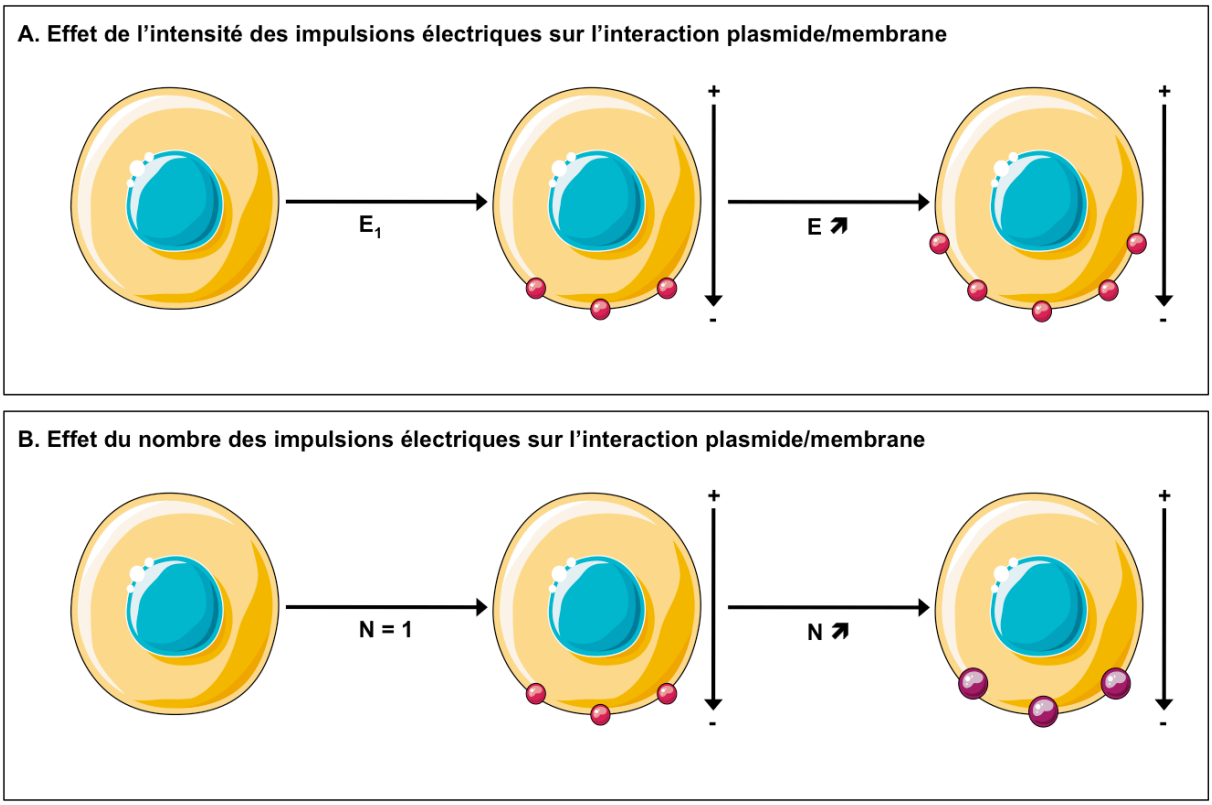

Figure III-8: Représentation schématique de l'effet du nombre et de l'intensité d'impulsions électriques sur l'interaction plasmide/membrane perméabilisée. (A) L'application d'impulsions électriques d'intensité E_1 induit la formation de complexes plasmide/membrane (ici 3). Cette interaction des molécules de plasmides à la membrane perméabilisée est prise comme référence. L'augmentation de l'intensité du champ électrique (E↗) induit une augmentation de la zone membranaire compétente pour l'interaction plasmide/membrane. Par conséquent, le nombre de complexes plasmide/membrane et la quantité de plasmide en interaction avec la membrane perméabilisée augmentent. (B) La première impulsion électrique créée le nombre de sites compétents (ici 3) pour l'interaction plasmide/membrane (ronds rouges). L'augmentation du nombre d'impulsions électriques (N↗) induit une augmentation linéaire de la quantité de molécules de plasmide en interaction avec la membrane plasmique perméabilisée (ronds violets). (Illustration réalisée grâce à Servier Medical Art, www.servier.fr).

En revanche, la viabilité cellulaire diminue progressivement avec l'augmentation du nombre d'impulsions électriques (98% pour N=1 à 58% pour N=10). Néanmoins, la viabilité cellulaire reste supérieure à 50% après l'application de 10 impulsions électriques.

2.3. Discussion et Conclusions

L'application d'impulsions électriques au-delà d'une valeur seuil d'intensité de champ électrique (E_i) permet l'interaction des molécules de plasmide au niveau de la membrane face à la cathode et sous la forme d'agrégats localisés. Pour 10 impulsions électriques, le seuil d'interaction dans le cas des cellules CHO est compris entre 0.3 kV/cm et 0.5 kV/cm. Cette valeur seuil E_i correspond à la valeur seuil de perméabilisation (E_p) et de transfection (E_t). L'augmentation de l'intensité du champ électrique au-delà de ce seuil entraine une augmentation de la surface d'interaction des molécules de plasmide à la membrane perméabilisée et de la quantité de plasmide en interaction (Figure III-8A).

A 0,7 kV/cm et dès la première impulsion, l'interaction de molécules de plasmide est visualisée sous la forme de spots fluorescents à la membrane plasmique face à la cathode. La formation du complexe plasmide/membrane est donc un phénomène rapide comme montré au début de ce chapitre par l'étude dynamique. L'augmentation du nombre d'impulsions électriques ne modifie pas la surface d'interaction des molécules de plasmide à la membrane, ni le nombre de spots formés, mais influe sur la quantité de plasmide en interaction avec la membrane plasmique perméabilisée (Figure III-8B).

Ces résultats mettent en évidence un rôle distinct de l'intensité du champ électrique et du nombre d'impulsions électriques* (Figure III-8)*. Si l'intensité du champ électrique définit la surface membranaire où l'interaction des molécules de plasmide a lieu et de fait, le nombre de spots d'interaction, le nombre d'impulsions électriques définit la quantité de molécules de plasmide présente par complexe. De façon surprenante, le fait que l'augmentation du nombre d'impulsions électriques n'entraîne pas une augmentation du nombre de spots fluorescents indique que dans les conditions expérimentales utilisées, les sites compétents pour l'interaction des molécules de plasmide à la membrane plasmique perméabilisée sont présents dès la première impulsion électrique.

Dans le cas de l'électroperméabilisation, des études par vidéo-microscopie à haute résolution (prise d'image toutes les 3,33 ms) ont permis de déterminer que l'intensité du champ électrique E définit la surface membranaire perméabilisée A_{perm}.

$$A_{perm} = \frac{A_{tot}\left[2 - \frac{E_p}{E} - \frac{E_f}{E}\right]}{2} \quad (Eq.III-1)$$

avec A_{tot}, surface totale de la cellule ; E_p, intensité du champ électrique seuil permettent la perméabilisation de la membrane face à l'anode ; E_f, intensité du champ électrique seuil permettant la perméabilisation de la membrane face à la cathode.

L'intensité du champ électrique joue donc le même rôle sur la perméabilisation et l'interaction des molécules de plasmide à la membrane, en définissant la surface membranaire potentiellement perméabilisable ou compétente pour l'interaction de molécules de plasmide (Figure III-3).

La migration des molécules de plasmide dans un champ électrique est décrite par l'équation suivante:

$$L = \mu ENT \quad (Eq.III-2)$$

avec L, longueur du cylindre dont le contenu est accumulé électrophorétiquement à la surface membranaire ; μ, mobilité électrophorétique de l'ADN (1.5 10^{-4} cm^2/Vs) (Neumann et al., 1982) ; E, intensité du champ électrique ; N, nombre d'impulsions électriques ; T, durée de l'impulsion électrique.

Dans le cas de l'interaction de molécules de plasmide à la membrane, le champ électrique, en plus de moduler la surface des structures membranaires compétentes pour l'interaction, joue un rôle dans l'accumulation électrophorétique des molécules de plasmide à la membrane plasmique. Pour 10 impulsions électriques de 5 ms à 0,7 kV/cm, la valeur est égale à 53 μm, ce qui correspond à un facteur d'accumulation d'environ 50.

L'augmentation de la valeur de l'intensité du champ électrique entraîne une augmentation de l'efficacité de transfection *(Chu et al., 1987; Wolf et al., 1994 ; Hui, 1995)*. Pour une intensité de champ électrique donnée, l'électrotransfert de plasmide augmente également avec le nombre d'impulsions électriques *(Chu et al., 1987 ; Kubiniec et al., 1990 ; Wolf et al., 1994 ; Hui, 1995 ; Rols et Teissié, 1998)*.

La perméabilisation de la membrane plasmique est une condition nécessaire et suffisante pour induire l'interaction de molécules de plasmide avec la membrane plasmique. Les résultats présentés concernant l'influence des paramètres électriques sur l'interaction de molécules de plasmide à la membrane plasmique confirment le rôle clé de cette étape vis-à-vis de l'expression. En revanche, dans nos conditions expérimentales, ces deux étapes (i.e. la perméabilisation membranaire et l'interaction plasmide/membrane) sont nécessaires mais pas suffisantes pour obtenir le transfert du plasmide et donc l'expression génique.

3. Etude comparative des impulsions électriques SPHV et EGT sur l'électrotransfert de plasmide

3.1. Introduction

Sous l'effet d'impulsions électriques perméabilisantes, la durée des impulsions joue un rôle majeur dans l'interaction plasmide/membrane. Cette interaction est classiquement détectée pour des durées d'impulsions électriques de l'ordre de la milliseconde *(Golzio et al., 2002)*. Ceci suggère que outre une migration électrophorétique du plasmide, la densité des défauts membranaires électro-induits est critique dans l'interaction des molécules de plasmide avec la membrane perméabilisée. Sous l'effet d'impulsions électriques perméabilisantes, le transfert de molécules de plasmide augmente fortement avec la durée des impulsions électriques *(Chu et al., 1987; Kubiniec et al., 1990 ; Hui, 1995; Wolf et al., 1994; Rols et Teissié, 1998a)*. Dans le cas des cellules CHO, le logarithme de la transfection (Tr) est une fonction linéaire du logarithme de la durée (T) de l'impulsion (vague carrée).

$$Log(Tr) = A + BLog(T) \quad (Eq.III-3)$$

Le taux de transfection (Tr) est alors décrit mathématiquement par la relation suivant:

$$Tr = C(E)T^{B} \quad (Eq.III-4)$$

Avec C(E), décrit l'effet de l'intensité du champ électrique (surface perméabilisée) et de la concentration en plasmide; B, une constante qui a pour valeur 2,3 (Wolf et al., 1994).

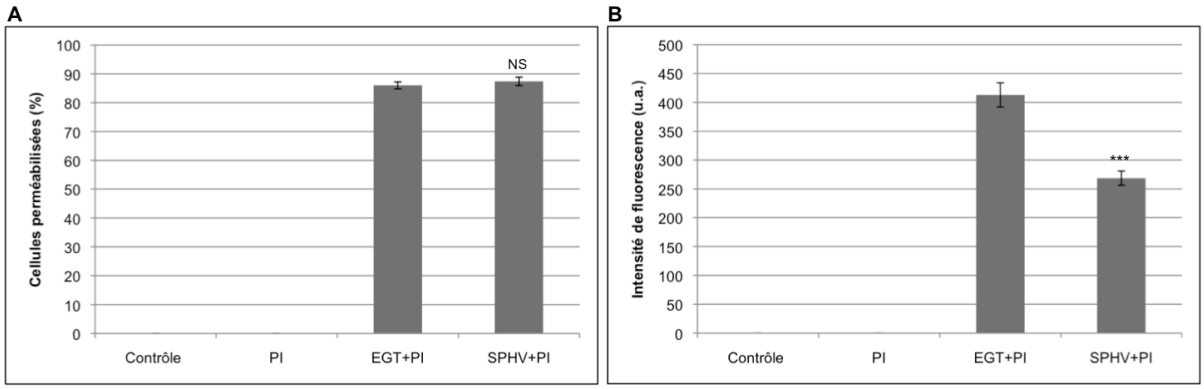

Figure III-9: Etude comparative des conditions électriques SPHV et EGT sur la perméabilisation des cellules CHO. Une suspension cellulaire (1.10^6 cellules/point expérimental) reprise dans du tampon de pulsation contenant 100 µM de PI. Elle est soumise soit aux conditions électriques SPHV: 4x200 µs, 1 Hz à 1,2 kV/cm, soit aux conditions électriques EGT: 8x5 ms, 1 Hz, à 0,7 kV/cm. Après 10 minutes à 30°C, les cellules sont analysées en cytométrie de flux. Le pourcentage de cellules perméabilisées (A) et l'intensité de fluorescence associée à la perméabilisation (B) sont représentés sur ce graphique. (N=3; moyenne ± SEM).

La conclusion pratique est que *in vitro,* un transfert efficace est obtenu en utilisant de longues impulsions électriques pour permettre la migration électrophorétique des molécules de plasmides vers la membrane perméabilisée mais avec de faible intensité de champ électrique pour préserver la viabilité cellulaire. En fait, des protocoles de transfection *in vitro* montrent que l'application d'impulsions électriques de quelques microsecondes avec de fortes intensités (i.e. SPHV, Short Pulse High Voltage) permettent la transfection efficace au sein des cellules *(Neumann et al., 1982; Zerbib et al., 1985; Neil et Zimmermann, 1993; Friedrich et al., 1998; Kanduser et al., 2009)* et en particulier les cellules souches *(Ferreira et al., 2008)*.

Dans cette partie, notre objectif est d'analyser la capacité des impulsions électriques microsecondes de fortes intensités à induire une transfection efficace des cellules. Pour cela, une étude comparative entre les conditions électriques EGT (8 x 5 ms, 1 Hz à 0,7 kV/cm) et SPHV (4 x 200 µs, 1 Hz à 1,2 kV/cm) est entreprise sur des cellules CHO.

3.2. Résultats

3.2.1. Electroperméabilisation

Les cellules CHO en suspension sont soumises soit à des impulsions électriques SPHV (4 x 200 µs, 1 Hz à 1,2 kV/cm), soit à des impulsions électriques EGT (8 x 5 ms, 1 Hz à 0,7 kV/cm) en présence d'iodure de propidium. Le taux et l'efficacité de perméabilisation sont déterminés par cytométrie de flux.

En absence de champ électrique, aucune perméabilisation membranaire n'est détectée. Suite à l'application d'un train d'impulsions électriques, un fort taux de perméabilisation (i.e. 87±1% en conditions SPHV vs 86±1% en conditions EGT) est obtenu (Figure III-9A). Ce taux de perméabilisation est similaire pour les deux types de train d'impulsions électriques appliqué (Figure III-9A). Par contre, l'efficacité de perméabilisation est 1.5 fois plus faible dans les conditions SPHV par rapport aux conditions EGT (i.e. 269±12 u.a. vs 413±21 u.a.) (Figure III-9B).

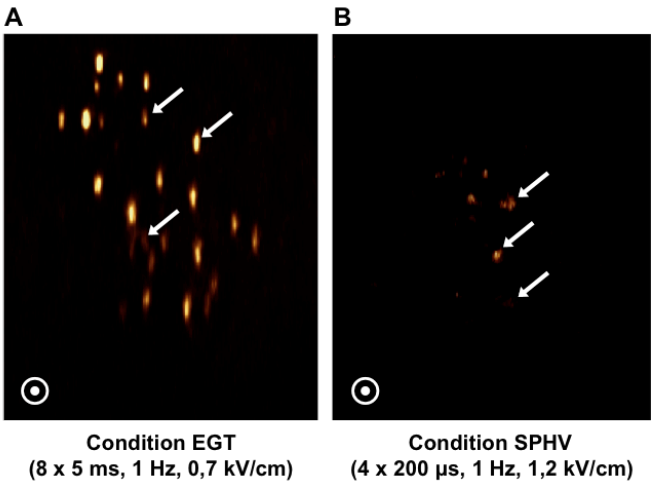

Figure III-10: Etude comparative des conditions électriques SPHV et EGT sur l'interaction plasmide/membrane sur des cellules CHO. Des cellules CHO sphériques (1.10^5 cellules/point expérimental) sont incubées en présence de 2 µg de plasmide peGFP-C1 marqué au TOTO-1 dans du tampon de pulsation. Elles sont soumises soit aux conditions électriques SPHV: 4x200 µs, 1 Hz à 1,2 kV/cm (A), soit aux conditions électriques EGT: 8x5 ms, 1 Hz, à 0,7 kV/cm (B). L'interaction plasmide/membrane est observée dans les secondes qui suivent l'application des impulsions électriques par microscopie de fluorescence après déconvolution et reconstitution en 3D. Le symbole ⊙ signifie que la flèche du champ électrique se dirige vers le lecteur.

3.2.2. Interaction plasmide/membrane

Les conditions électriques SPHV (i.e. 4 x 200 µs, 1 Hz à 1.2 kV/cm) et EGT (i.e. 8 x 5 ms, 1 Hz à 0.7 kV/cm) sont appliquées sur les cellules CHO en présence de 2 µg de plasmide marqué au TOTO-1. Après l'application des impulsions électriques, une acquisition d'un ensemble d'images (x,y) à différents plans en z est réalisée grâce au pilotage par un piezo de la position d'un objectif 100x à immersion. L'obtention d'une série de plans (x,y) permet ainsi une reconstitution 3D de l'objet observé grâce au module de déconvolution par correction de PSF associé au du logiciel MetaMorph (Figure III-10) *(Sibarita, 2005)*.

Avant l'application du champ électrique, aucune interaction spontanée du plasmide à la membrane plasmique n'est visualisée. L'application d'impulsions électriques SPHV conduit à la formation de complexes plasmide/membrane face à la cathode à l'image de ceux obtenus avec des impulsions électriques EGT (Figure III-10) *(Golzio et al., 2002; Faurie et al., 2004; Phez et al., 2005)*. Néanmoins, le nombre de complexes formés dans les conditions SPHV est deux fois plus faible que celui obtenus dans les conditions EGT (i.e. 10±5 u.a. vs 20±5) (Figure III-10). De plus, l'intensité de fluorescence totale associée à ces complexes est 30 fois plus faible dans les conditions SPHV par rapport aux conditions EGT (Figure III-10).

En conclusion, la formation de complexes plasmide/membrane a lieu dans des conditions électriques SPHV (i.e. avec des impulsions électriques de 200 µs) mais avec un nombre de complexes beaucoup moins importants et avec une quantité plus faible de plasmides.

3.2.3. Electrotransfert de plasmide

Les cellules CHO en suspension sont soumises soit à des impulsions électriques SPHV soit à des impulsions électriques EGT en présence 2 µg de plasmide peGFP-C1. 24 heures après l'électrotransfert de plasmide, les cellules transfectées sont observées en microscopie de fluorescence (Figure III-11A). Puis, le taux et l'efficacité de transfection sont déterminés par cytométrie de flux.

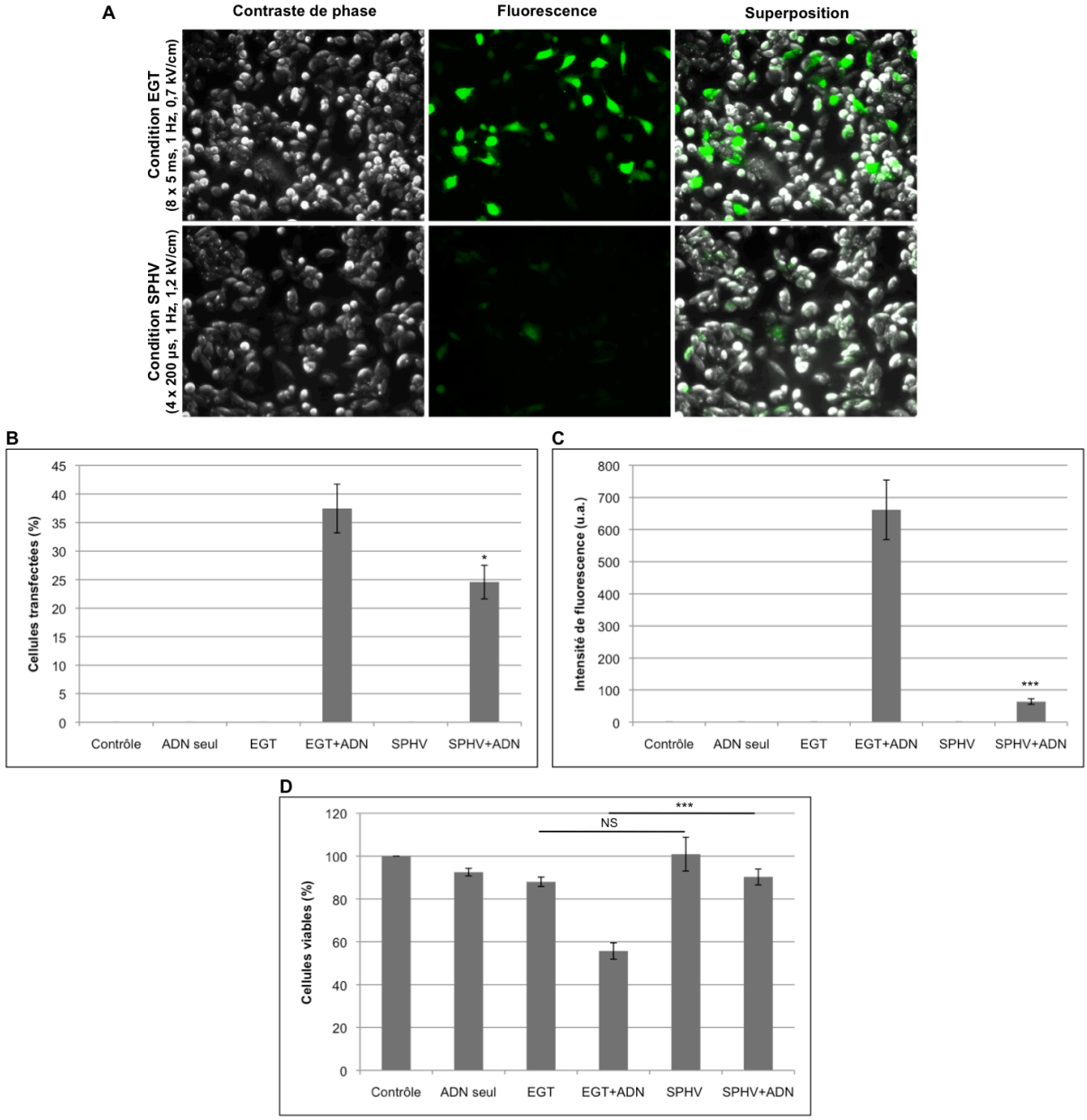

Figure III-11: Etude comparative des conditions électriques SPHV et EGT sur l'électrotransfert de plasmide et la viabilité des cellules électrotransfectées. Une suspension cellulaire (1.10^6 cellules/point expérimental) est incubée en présence de 2 µg de plasmide peGFP-C1 dans du tampon de pulsation. Elles sont soumises soit aux conditions électriques SPHV: 4x200 µs, 1 Hz à 1,2 kV/cm, soit au condition électrique EGT: 8x5 ms, 1 Hz, à 0,7 kV/cm. Après 10 minutes à 30°C, les cellules sont remises en culture. Les cellules transfectées sont observées en microscopie de fluorescence (A). Le pourcentage de cellules transfectées (B) et l'intensité de fluorescence associée (C) sont détectés par cytométrie de flux 24h après électrotransfert. La survie cellulaire (D) est révélée par spectrophotométrie 24h après électrotransfert. (N=3; moyenne ± SEM).

En absence de champ électrique ou de plasmide pEGFP-C1, aucune expression d'EGFP et donc de transfert de plasmide, le cas échéant, n'est détectée. Le taux de transfection est légèrement plus faible dans les conditions SPHV (i.e. 25±3%) par rapport aux conditions EGT (i.e. 37±4%) (Figure III-11B). De plus, dans les conditions SPHV, l'intensité de fluorescence associée à la transfection est 10 fois plus faible par rapport à celle obtenue dans les conditions EGT (64±9 u.a. vs 662±93 u.a.) (Figure III-11C).

En revanche, si la viabilité cellulaire des cellules transfectées est peu affectée dans des conditions électriques SPHV (90±4%), elle est diminuée de 44% dans des conditions EGT (56±4%) (Figure III-11D). Le pourcentage de cellules transfectées est de 22,5% en conditions électriques SPHV contre 21% en conditions électriques EGT, soit des valeurs statistiquement équivalentes. Rappelons que le pourcentage de cellules perméabilisées donc susceptibles d'être transfectées est d'environ 87%. Notons que dans des conditions électriques EGT, la présence de plasmides entraîne une forte chute de viabilité cellulaire. Cela n'est pas le cas dans des conditions électriques SPHV. Ce résultat conduit à poser la question du rôle d'un plasmide électrotransféré sur le devenir cellulaire et en particulier celui de la quantité de plasmide introduite dans la cellule cible *(Li et al., 1999; Shimokawa et al., 2000)*.

3.4. Discussion et Conclusions

L'application d'impulsions électriques SPHV ou EGT induit des taux de perméabilisation comparables. Néanmoins, l'efficacité de perméabilisation est plus faible pour des impulsions électriques SPHV par rapport aux résultats obtenus avec les impulsions électriques EGT (Figure III-9). En accord avec de précédents travaux, nos résultats montrent que la pénétration de molécules hydrophiles est sous le contrôle de la durée des impulsions électriques. En effet, la durée des impulsions électriques contrôle la densité des défauts membranaires et leur durée de vie *(Rols et Teissié, 1998a)*. Nos résultats pourraient s'expliquer par le fait que l'application d'impulsions électriques SPHV induirait un faible nombre de défauts membranaires et/ou de courte de durée de vie par opposition aux impulsions électriques EGT génératrices d'un plus grand nombre de défauts et/ou de longue durée de vie. De plus, de récents travaux montrent que la pénétration du PI est induite par migration électrophorétique pendant l'application des impulsions électriques *(Pucihar et al., 2008; cf. Partie II, p4)*. Nos

résultats sont donc en accord avec le fait que pendant la durée cumulée des impulsions électriques EGT (40 ms), la quantité de PI, qui pénètre dans les cellules par migration électrophorétique, est plus grande que celle pénétrante sous l'effet d'impulsions électriques SPHV (0,8 ms). Cependant, les intensités fluorescence associées à l'entrée de PI ne sont pas d'un rapport 50 (i.e. 40/0,8) car l'entrée du PI a lieu massivement après l'application des impulsions électriques *(Pucihar et al., 2008; cf. Partie II p4).*

L'application d'impulsions électriques SPHV permet l'interaction des molécules de plasmides au niveau de la membrane face à la cathode et sous la forme d'agrégats (Figure III-10). Néanmoins, le nombre de complexes de plasmide par cellule et l'intensité de fluorescence associée sont respectivement 2 et 30 fois plus faibles par rapport aux résultats obtenus avec des impulsions électriques EGT (Figure III-10). La migration des molécules de plasmide dans un champ électrique est décrite par l'équation Eq. III-2. Dans le cas de l'interaction du plasmide avec la membrane perméabilisée, la durée des impulsions électriques joue un rôle sur l'accumulation électrophorétique des molécules de plasmide à la membrane. Pour des impulsions électriques SPHV et EGT, la valeur de L est égale à 1,5 et à 42 respectivement, ce qui correspond à un facteur d'accumulation de 2 et de 40 respectivement. Par conséquent, nous obtenons un rapport de 20 en terme de densité de défauts membranaires électro-induits. Néanmoins, il est nécessaire de corriger ces facteurs d'accumulation par la surface de la membrane susceptible de réagir donc d'être perméabilisée sous le contrôle de l'intensité du champ électrique E, i.e. par $\left(1-\frac{E_p}{E}\right)$ avec E_p=0,3 kV/cm et E=0,7 kV/cm ou 1,2 kV/cm. Par conséquent, en terme de densité de défauts membranaires électro-induits, nous obtenons un rapport de 26. Nous trouvons un facteur 30 dans la quantité de plasmides en interaction avec la membrane, ce qui est globalement en accord avec ces facteurs d'accumulation.

En conclusion, le complexe plasmide/membrane se forme lors d'impulsions électriques brèves. La durée de l'impulsion électrique joue en priorité sur l'accumulation électrophorétique des molécules de plasmide à la membrane perméabilisée.

L'application d'impulsions électrique SPHV permet le transfert et l'expression de molécules de plasmide dans les cellules *in vitro* (Figure III-11). Ce résultat est en accord

avec les résultats pionniers obtenus *in vitro* par Neumann et collaborateurs *(Neumann et al., 1982)* et confirmés par Zerbib et collaborateurs *(Zerbib et al., 1985)*. De plus, ces conditions électriques ont été validées *in vivo* pour le transfert de plasmide *(Heller et al., 1996; Daud et al., 2008)*. Dans les conditions électriques SPHV, le taux de transfection est légèrement plus faible que celui obtenu en condition EGT (Figure III-11B). En revanche, l'efficacité de transfection est 10 fois plus faible en condition SPHV par rapport aux résultats obtenus en condition EGT (Figure III-11C). Ce résultat est parfaitement corrélé avec le fait qu'une quantité beaucoup plus faible de molécules de plasmide vient interagir avec la membrane perméabilisée dans des conditions SPHV. En revanche, dans nos conditions expérimentales, l'application d'impulsions électriques SPHV n'affecte pas ou peu la viabilité des cellules transfectées contrairement aux données de littérature *(Zerbib et al., 1985; Neil et Zimmermann, 1993; Rols et Teissié, 1998; Friedrich et al., 1998)*.

Une des perspectives à ce travail viserait à définir des paramètres électriques intermédiaires entre les impulsions électriques SPHV et EGT afin d'associer l'efficacité de transfection à la viabilité cellulaire.

Nos résultats montrent pour la première fois, que l'application d'impulsions SPHV induit l'interaction de molécules de plasmide avec la membrane plasmique perméabilisée. Cette interaction est corrélée avec le transfert de plasmide et son expression dans les cellules CHO. Néanmoins, en accord avec la littérature et dans nos conditions expérimentales, l'application d'impulsions électriques EGT est plus efficace pour le transfert de plasmide que les impulsions électriques SPHV. Cependant, contrairement à la littérature et dans nos conditions expérimentales, ces dernières sont peu délétères pour les cellules transfectées.

4. Effet de l'application d'impulsions électriques bipolaires asymétriques sur l'électrotransfert de plasmide

4.1. Introduction

La visualisation de l'entrée de composés fluorescents en conditions électriques unipolaire (impulsions électriques dans le même sens et dans la même direction) a révélé une asymétrie de la perméabilisation membranaire: la surface perméabilisée à la membrane face à l'anode est plus importante que celle face à la cathode *(Tekle et al., 1994; Gabriel et Teissié, 1997, 1999)*. Cette asymétrie s'explique par l'effet vectoriel du champ électrique. L'application d'impulsions électriques bipolaires et symétriques entraîne une symétrie de la perméabilisation, ce qui s'accompagne d'une augmentation de l'efficacité de perméabilisation *(Tekle et al., 1991; Kotnik et al., 2001, Faurie et al., 2004)*.

En conditions unipolaires, les molécules de plasmide, chargées négativement, migrent par électrophorèse vers l'anode et interagissent uniquement au niveau de la région membranaire qui fait face à la cathode *(Golzio et al., 2002)*. De récentes études ont montré que l'application d'impulsions électriques bipolaires et symétriques (champ électrique non homogène) induit la perméabilisation et l'interaction plasmide/membrane au niveau des régions membranaires face aux deux électrodes. L'application de ces impulsions augmentent ainsi la surface d'interaction des molécules de plasmides avec la membrane perméabilisée *(Faurie et al., 2004; Phez et al., 2005)*. Ces études ont révélé l'existence de deux classes de plasmide en interaction avec la membrane plasmique: des molécules de plasmide en interaction faible et d'autres en interaction forte *(Phez et al., 2005; Faurie et al., 2010)*.

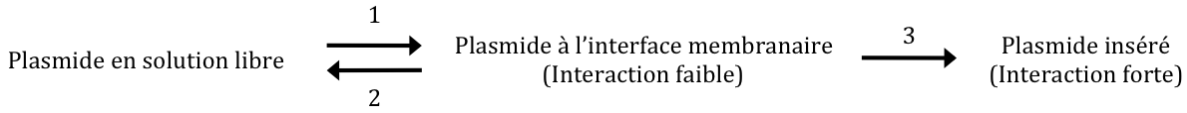

L'application d'impulsions électriques permet l'interaction des molécules de plasmides à la membrane (réactions 1 et 3). L'augmentation de la surface d'interaction plasmide/membrane induite par l'application d'impulsions électriques bipolaires et

symétriques, s'accompagne d'une augmentation du taux et de l'efficacité de transfection sans que la viabilité cellulaire ne soit affectée *(Phez et al., 2005)*. Cependant, en inversion de polarité, au niveau du pôle cellulaire face à l'anode, les molécules de plasmide en interaction faible pourraient retourner dans le milieu extra-cellulaire (réaction 2) *(Phez et al., 2005; Faurie et al., 2010)*. Mais cette métastabilité du complexe plasmide/membrane serait très furtive (≈ 1s).

Dans cette partie, nous avons proposé de déterminer la durée nécessaire à l'établissement d'interactions plasmide/membrane fortes. Notre stratégie a consisté à soumettre les cellules CHO à des impulsions bipolaires et asymétriques (Figure III-12). Cette étude a été rendue possible par le développement sous notre pilotage intellectuel d'une nouvelle classe d'électropulsateurs par la société Betatech (Licence de commercialisation du CNRS). Il devient alors possible d'appliquer des trains d'impulsions électriques avec une inversion très rapide, le cas échéant de la polarité (aussi court que possible 5 µs). Nous disposons d'un contrôle complet et indépendant des paramètres électriques de chaque impulsion. Notons enfin que l'électropulsateur conserve en mémoire les profils de impulsions délivrées. L'un des avantages de ce type de générateurs est de s'affranchir de réactions électrochimiques au niveau des électrodes, processus mis en évidence par Kotnik et collaborateurs *(Kotnik et al., 2001)*. Une étude systématique de ces réactions par analyse directe sous vidéo-microscopie a illustré cet avantage *(Travail post-doctoral de Vanessa Sonois, Ph.D., 2008-2009)*.

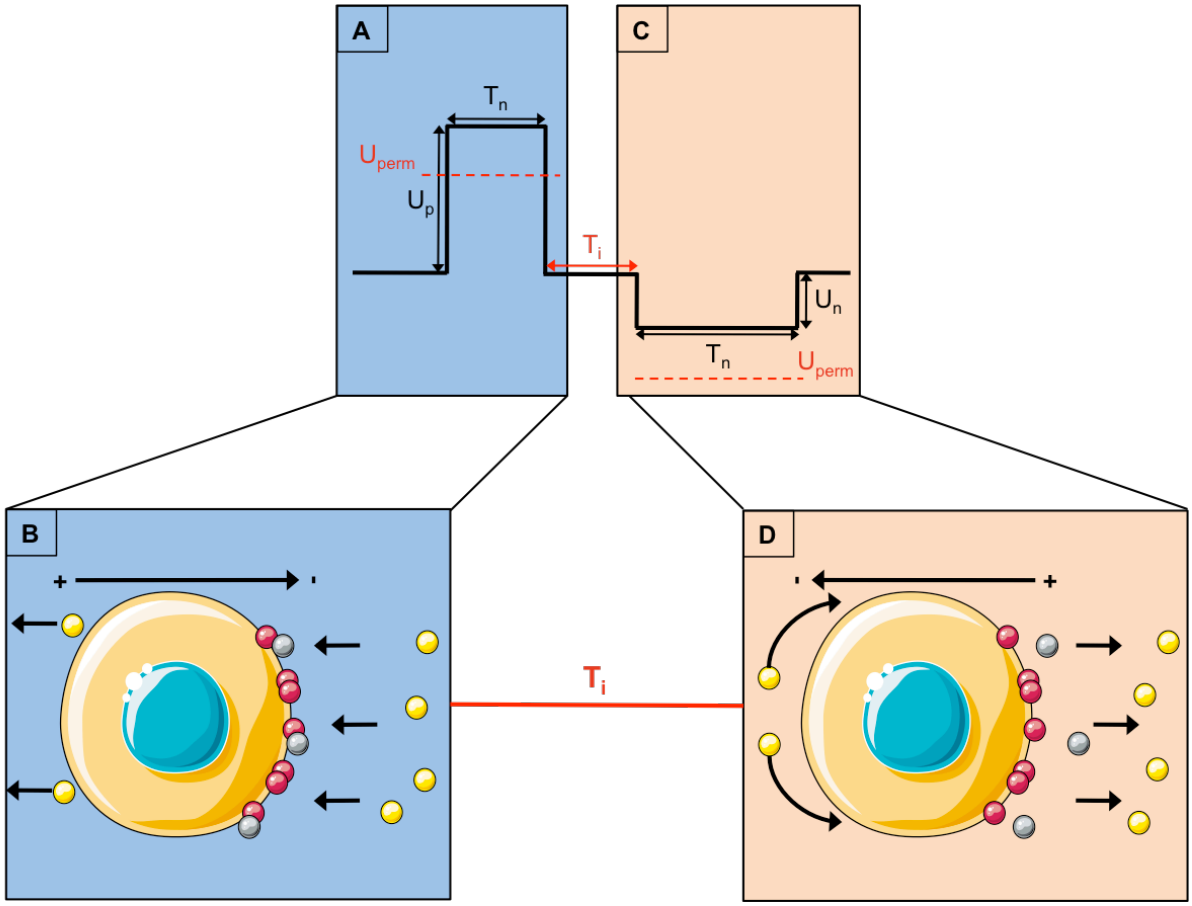

Figure III-12: Impulsions électriques bipolaires et asymétriques. Les impulsions électriques appliquées sur les cellules CHO sont bipolaires et asymétriques. La première partie de l'impulsion électrique (carré bleu A) est une impulsion positive perméabilisante d'une durée de 5 ms (i.e. T_n) et d'intensité électrique 0,7 kV/cm (i.e. U_n). Cette impulsion positive perméabilise la membrane plasmique et induit la migration électrophorétique des molécules de plasmide (rond jaune) jusqu'à la membrane plasmique perméabilisée. Des interactions plasmide/membrane faibles (rond gris) et fortes (rond rouge) sont induites (carré bleu B). La deuxième partie de l'impulsion électrique (carré orange C), est une impulsion négative et non perméabilisante d'une durée de 35 ms (i.e. T_p) et d'intensité électrique de 0,1 kV/cm (i.e. U_p). Cette impulsion électrique ne perméabilise pas la membrane plasmique mais génèrerait des forces électrophorétiques qui pourrait décrocher les molécules de plasmides en interaction faible (rond gris) avec la membrane plasmique (carré orange D). Le nombre et la fréquence de ces impulsions électriques sont respectivement de 10 et de 0,1 Hz. La durée, T_i, entre les deux parties de l'impulsion bipolaire et asymétrique est le paramètre que nous faisons varier dans notre étude. (Illustration réalisée grâce à Servier Medical Art, www.servier.fr).

Expérimentalement, la première partie de ce type d'impulsion électrique (carré bleu A) est une impulsion positive perméabilisante d'une durée de 5 ms (i.e. T_p) et d'intensité électrique 0,7 kV/cm (i.e. U_p). Cette impulsion positive perméabilise la membrane plasmique et induit la migration électrophorétique des molécules de plasmide jusqu'à celle-ci. Des interactions faibles et fortes de molécules de plasmide avec la membrane perméabilisée ont lieu (carré bleu B) (Figure III-12). La deuxième partie de cette impulsion électrique (carré orange C), est une impulsion négative et non perméabilisante d'une durée de 35 ms (i.e. T_n) et d'intensité électrique de 0,1 kV/cm (i.e. U_n). Cette impulsion électrique ne perméabiliserait pas la membrane plasmique mais génèreraient des forces électrophorétiques sur les molécules de plasmides dans la direction opposée à celles de la précédente. Elles pourraient décrocher les molécules de plasmides associées à la membrane de manière instable par des interactions faibles (carré orange D) (Figure III-12) *(Thèse de Goradz Pucihar, 2006)*. 10 impulsions électriques ont été appliquées pour des raisons techniques à une fréquence de 0,1 Hz (i.e. $P>2(T_n+T_p)$ et $P>T_n+T_i+T_p$). Le nombre et la fréquence de ces impulsions électriques sont respectivement de 10 et de 0,1 Hz. La variation de la durée, T_i, entre les deux parties de l'impulsion bipolaire et asymétrique nous permettra, le cas échéant, d'accéder à la durée à partir de laquelle les interactions plasmide/membrane deviennent fortes (Figure III-12).

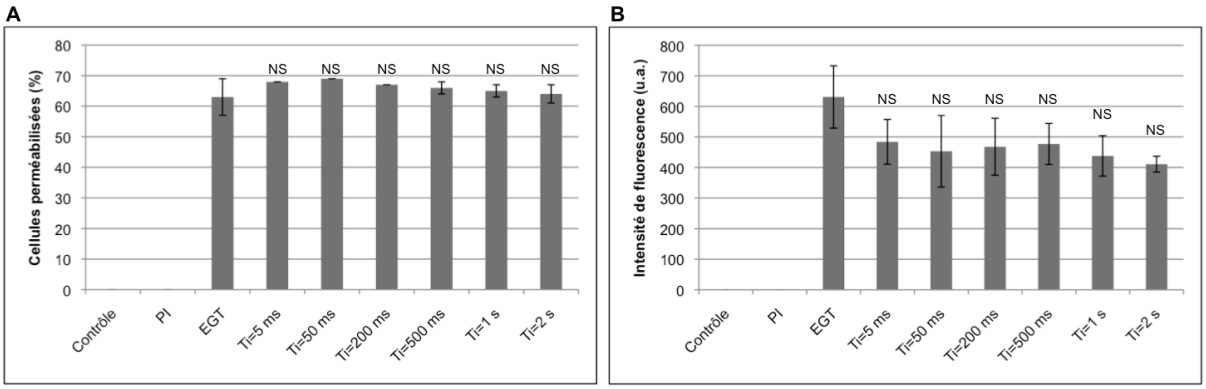

Figure III-13: Effet de T_i sur la perméabilisation des cellules CHO. Une suspension cellulaire (1.10^6 cellules/point expérimental) reprise dans du tampon de pulsation contenant 100 µM de PI. Elle est soumise soit à des impulsions électriques EGT: 10x5 ms, 0,1 Hz, à 0,7 kV/cm, soit aux impulsions électriques bipolaires et asymétriques constituées d'une impulsion positive d'une durée de 5 ms et d'intensité électrique de 0,7 kV/cm suivi d'une impulsion négative d'une durée de 35 ms et d'une intensité électrique de 0,1 kV/cm. Le nombre et la fréquence des impulsions bipolaires et asymétriques sont respectivement de 10 et de 0,1 Hz. La durée, T_i, entre les deux parties de l'impulsion bipolaire et asymétrique est le paramètre que nous faisons varier de 5 ms à 2 s dans notre étude. Après 10 minutes à 30°C, les cellules sont analysées en cytométrie de flux. Le pourcentage de cellules perméabilisées (A) et l'intensité de fluorescence associée à la perméabilisation (B) sont représentés sur ce graphique. (N=3; moyenne ± SEM).

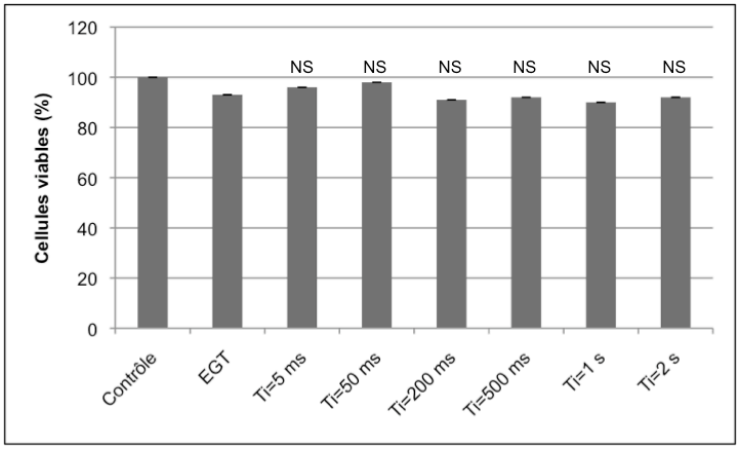

Figure III-14: Effet de T_i sur la viabilité cellulaire des cellules CHO perméabilisées. Une suspension cellulaire (1.10^6 cellules/point expérimental) reprise dans du tampon de pulsation. Elle est soumise soit à des impulsions électriques EGT: 10x5 ms, 0,1 Hz, à 0,7 kV/cm, soit aux impulsions électriques bipolaires et asymétriques constituées d'une impulsion positive d'une durée de 5 ms et d'intensité électrique de 0,7 kV/cm suivi d'une impulsion négative d'une durée de 35 ms et d'une intensité électrique de 0,1 kV/cm. Le nombre et la fréquence des impulsions bipolaires et asymétriques sont respectivement de 10 et de 0,1 Hz. La durée, T_i, entre les deux parties de l'impulsion bipolaire et asymétrique est le paramètre que nous faisons varier de 5 ms à 2 s dans notre étude. Après 10 minutes à 30°C, les cellules sont remises en culture. La survie cellulaire est révélée par spectrophotométrie 24h après électroperméabilisation. (N=3; moyenne ± SEM).

4.2. Résultats

4.2.1. Electroperméabilisation

Les cellules CHO sont soumises soit à 10 impulsions électriques bipolaires et asymétriques à la fréquence de 0,1 Hz (composées d'une impulsion positive de 5 ms à 0,7 kV/cm suivie après une durée variable T_i, d'une impulsion négative de 35 ms à 0,1 kV/cm), soit à des impulsions électriques EGT (10 x 5 ms, 0,1 Hz à 0,7 kV/cm) en présence d'iodure de propidium. Le taux et l'efficacité de perméabilisation sont déterminés par cytométrie de flux. Cette condition bipolaire a été choisie pour avoir la même charge électrique délivrée lors de chaque impulsion électrique (mais bien sûr de polarité inversé).

En absence de champ électrique, aucune perméabilisation membranaire n'est détectée (Figure III-13). En revanche, l'application d'impulsions électriques EGT induit un taux de perméabilisation de 63±6% et une efficacité de perméabilisation de 631±102 u.a (Figure III-13). Quel que soit la valeur de la durée T_i, l'application d'impulsions électriques bipolaires et asymétriques induit un taux et une efficacité de perméabilisation qui ne sont pas significativement différents des résultats obtenus avec les impulsions électriques EGT (Figure III-13).

La viabilité cellulaire est peu affectée par l'application d'impulsions électriques EGT (i.e. 93% de cellules viables) et par celle d'impulsions électriques bipolaires et asymétriques (i.e. ≥90% de cellules viables) (Figure III-14).

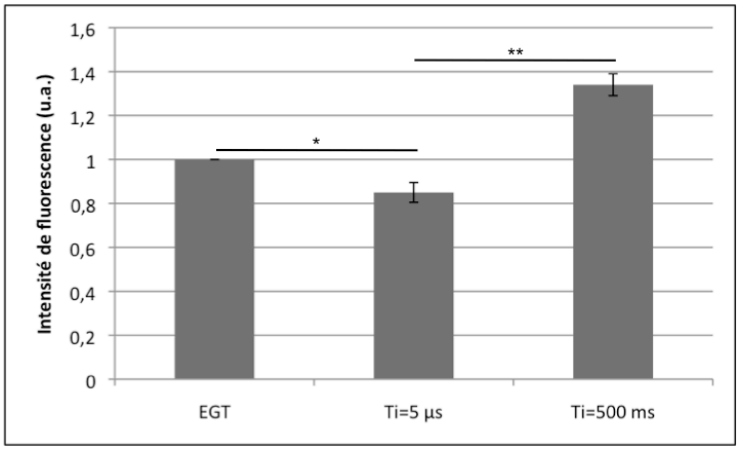

Figure III-15: Effet de T_i sur l'interaction plasmide/membrane sur des cellules CHO. Des cellules CHO sphériques (1.10^5 cellules/point expérimental) sont incubées en présence de 5 µg de plasmide peGFP-C1 marqué au TOTO-1 dans du tampon de pulsation. Elle est soumise soit à des impulsions électriques EGT: 10x5 ms, 0,1 Hz, à 0,7 kV/cm, soit aux impulsions électriques bipolaires et asymétriques constituées d'une impulsion positive d'une durée de 5 ms et d'intensité électrique de 0,7 kV/cm suivi d'une impulsion négative d'une durée de 35 ms et d'une intensité électrique de 0,1 kV/cm. Le nombre et la fréquence des impulsions bipolaires et asymétriques sont respectivement de 10 et de 0,1 Hz. La durée, T_i, entre les deux parties de l'impulsion bipolaire et asymétrique est que nous fixons à 5 µs ou à 500 ms. L'intensité de fluorescence associée à l'interaction plasmide/membrane est déterminée par le logiciel MetaMorph. ($N_{cellules}$=30; moyenne ± SEM).

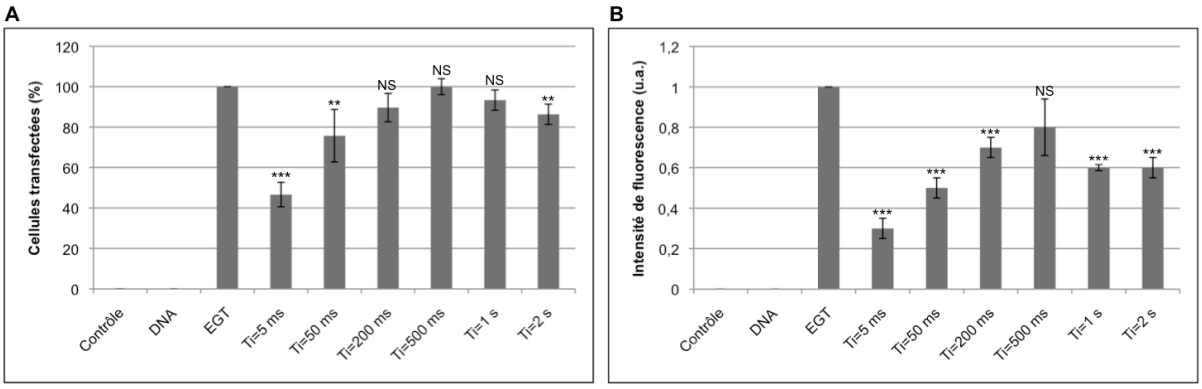

Figure III-16: Effet de T_i sur l'électrotransfert de plasmide des cellules CHO. Une suspension cellulaire (1.10^6 cellules/point expérimental) est incubée en présence de 5 µg de plasmide peGFP-C1 dans du tampon de pulsation. Elle est soumise soit à des impulsions électriques EGT: 10x5 ms, 0,1 Hz, à 0,7 kV/cm, soit aux impulsions électriques bipolaires et asymétriques constituées d'une impulsion positive d'une durée de 5 ms et d'intensité électrique de 0,7 kV/cm suivi d'une impulsion négative d'une durée de 35 ms et d'une intensité électrique de 0,1 kV/cm. Le nombre et la fréquence des impulsions bipolaires et asymétriques sont respectivement de 10 et de 0,1 Hz. La durée, T_i, entre les deux parties de l'impulsion bipolaire et asymétrique est le paramètre que nous faisons varier de 5 ms à 2 s dans notre étude. Après 10 minutes à 30°C, les cellules sont remises en culture. Le pourcentage de cellules transfectées (A) et l'intensité de fluorescence associée (B) sont détectés par cytométrie de flux 24h après électrotransfert. (N=3; moyenne ± SEM).

4.2.2. Interaction plasmide/membrane

Les cellules CHO sont soumises soit à 10 impulsions électriques bipolaires et asymétriques à la fréquence de 0,1 Hz (composées d'une impulsion positive de 5 ms à 0,7 kV/cm suivie après une durée variable T_i, d'une impulsion négative de 35 ms à 0,1 kV/cm), soit à des impulsions électriques EGT (10 x 5 ms, 0,1 Hz à 0,7 kV/cm) en présence de 5 µg de plasmide marqué au TOTO-1. L'interaction plasmide/membrane est déterminée par microscopie de fluorescence à l'échelle de la cellule unique. Les clichés sont enregistrés à la fin du train d'impulsions électriques. Des profils de fluorescence sur tout le pourtour des cellules sont tracés. L'intensité de fluorescence totale dans la zone d'interaction plasmide/membrane est calculée.

L'application d'impulsions électriques bipolaires et asymétriques avec une valeur de T_i de 5 µs permet de détecter la formation de complexes plasmide/membrane mais avec une diminution significative de la quantité de plasmide en interaction avec la membrane plasmique par rapport aux résultats obtenus avec une valeur de T_i de 500 ms (i.e. 0,85±0,05 a.u. vs 1,31±0,05 a.u.) ou pour des impulsions électriques EGT (i.e. 0,85±0,05 a.u. vs 1,31±0,05 a.u.) (Figure III-15). Une valeur de T_i de 500 ms n'a pas d'effet sur la formation des complexes plasmide/membrane.

4.2.3. Electrotransfert de plasmide

Des impulsions électriques bipolaires et asymétriques ou EGT sont appliquées à des cellules CHO en présence 5 µg de plasmide peGFP-C1. 24 heures après l'électrotransfert de plasmide, le taux et l'efficacité de transfection sont déterminés par cytométrie de flux.

A Ti court, l'application d'impulsions électriques bipolaires et asymétriques induit une diminution significative du taux et de l'efficacité de transfection par rapport aux résultats obtenus avec des impulsions électriques EGT (taux de transfection: 47±6% vs 100%; efficacité de transfection: 0,3±0,005 u.a. vs 1 u.a.) (Figure III-16). Le taux de transfection augmente significativement jusqu'à une valeur optimale de T_i de 200 ms. Pour des valeurs de T_i comprises entre 200 ms et 1 s, les taux de transfection sont comparables à celui obtenu pour des impulsions électriques EGT (i.e. ≥93±5%) (Figure III-16A). Pour une valeur de T_i de 2 s, une légère diminution mais significative du taux de transfection est observée (i.e. 86±5%). Cette dernière pourrait-être corrélée à une légère

diminution de la viabilité cellulaire des cellules transfectées. L'efficacité de transfection augmente pour atteindre un maximum de 0,8±0,14 u.a. à 500 ms. Cette efficacité de transfection n'est pas significativement différente de celle obtenue pour impulsions électriques EGT (Figure III-16B). L'efficacité de transfection diminue très légèrement pour des valeurs de T_i de 1 s (i.e. 0,6±0,015 u.a.) et 2 s (i.e. 0,6±0,05 u.a.) qui est probablement liée à une diminution de la viabilité cellulaire.

4.3. Discussion et Conclusions

Lorsque des impulsions électriques unipolaires EGT (i.e. 10 x 5 ms, 0,1 Hz, 0,7 kV/cm) sont appliquées sur des cellules, la perméabilisation est observée au niveau de la membrane face aux deux électrodes mais de manière asymétrique. La surface perméabilisée à la membrane face à l'anode est plus importante que celle face à la cathode *(Tekle et al., 1994; Gabriel et Teissié, 1997, 1999)*. La perméabilisation apparaît lorsque la valeur du potentiel transmembranaire $\Delta\Psi$ atteint la valeur critique $\Delta\Psi_c$ égale à environ 200-300 mV (Teissié et Rols, 1993).

$$\Delta\Psi = \Delta\Psi_0 + \Delta\Psi_E = \Delta\Psi_0 - fg(\lambda)rE\cos(\theta) \quad (Eq.III-5)$$

avec $\Delta\Psi_0$, différence de potentiel transmembranaire natif; $\Delta\Psi_E$, différence de potentiel transmembranaire électro-induite; f, facteur de forme; g(λ), facteur lié aux conductivités de la membrane plasmique, du cytoplasme, et du milieu extracellulaire; r, rayon de la cellule; E, intensité du champ électrique appliqué; θ, angle entre la direction du champ électrique et la normale au point M considéré sur la membrane plasmique (cf. Figure 1, page , de la revue, Escoffre et al., Mol Biotechnol., 2009).

Face à l'anode, le cosinus de l'angle θ est négatif. Les différences de potentiel transmembranaire natif et électro-induit s'ajoutent, entraînant une hyperpolarisation membranaire. Le potentiel transmembranaire $\Delta\Psi$ est décrit par l'équation suivante:

$$\Delta\Psi = \Delta\Psi_0 + fg(\lambda)rE_p \quad (Eq.III-6)$$

avec Ep, seuil de perméabilisation face à l'anode.

Face à la cathode, le cosinus de l'angle θ est positif. Les différences de potentiel transmembranaire natif et électro-induit se retranchent, entraînant une dépolarisation membranaire *(Gross et al., 1986; Tekle et al., 1994; Hibino et al., 1993)*. Le potentiel transmembranaire $\Delta\Psi$ prend la forme suivante:

$$\Delta\Psi = \Delta\Psi_0 - fg(\lambda)rE_f \quad (Eq.III-7)$$

avec E_f, seuil de perméabilisation face à la cathode.

L'hyperpolarisation de la membrane côté anode et la dépolarisation côté cathode permettent d'expliquer pourquoi le seuil de perméabilisation à la membrane face à l'anode est plus faible que celui à la membrane face à la cathode. A une intensité de champ électrique donnée, la surface perméabilisée face à l'anode est plus importante que celle face à la cathode. En revanche, l'application d'impulsions électriques bipolaires et symétriques induit une perméabilisation symétrique de la membrane plasmique *(Tekle et al., 1991; Faurie et al., 2004; Phez et al., 2005)*. Cette augmentation de la surface de perméabilisation permet d'augmenter l'efficacité de la perméabilisation membranaire *(Faurie et al., 2004; Phez et al., 2005)*.

Dans la présente étude, des impulsions électriques bipolaires et asymétriques sont appliquées aux cellules CHO. Ces impulsions électriques se décomposent en deux impulsions électriques: La première partie est une impulsion positive perméabilisante d'une durée de 5 ms et d'intensité électrique 0,7 kV/cm. La deuxième partie est une impulsion négative non perméabilisante d'une durée de 35 ms (i.e. T_p) et d'intensité électrique de 0,1 kV/cm (i.e. U_p). Cette impulsion électrique ne perméabilise pas la membrane plasmique mais génèrerait uniquement des forces électrophorétiques. Nos résultats montrent que l'application d'impulsions électriques EGT versus bipolaires et asymétriques induit un taux et une efficacité de perméabilisation comparables (Figure III-13). Ces résultats confirment que la composante négative de l'impulsion bipolaire et asymétrique ne perméabilise pas la membrane plasmique.

L'application d'impulsions électriques bipolaires et asymétriques avec une durée T_i inférieure à 500 ms induit une diminution du taux et de l'efficacité de transfection par aux impulsions électriques unipolaires EGT. Par exemple, pour une durée T_i de 5 ms, le taux et l'efficacité de transfection sont divisés respectivement d'un facteur 2 et 3 par rapport aux résultats obtenus avec des impulsions électriques unipolaires EGT (Figure III-16). Ces résultats révèlent que pour des durées T_i inférieures à 200 ms, les forces électrophorétiques générées par la composante négative (non perméabilisante) des impulsions électriques bipolaires et asymétriques, décrochent les molécules de plasmide

en interaction faible avec la membrane plasmique (Figure III-15). Par conséquent, la quantité de plasmide entrant dans les cellules et pouvant conduire à une expression est diminuée. En revanche, pour une durée T_i de 200 ms, les résultats obtenus sont comparables à ceux acquis lors de l'application d'impulsions électriques unipolaires EGT (Figure III-16). Les résultats obtenus en transfection et sur l'interaction plasmide/membrane suggèrent qu'une durée T_i de 200 ms (soit 0,2 s) est nécessaire à l'établissement d'une interaction plasmide/membrane forte non électro-dissociable, requise pour l'obtention d'une transfection efficace. Une récente étude a montré en faisant varier la polarité et la fréquence des impulsions électriques symétriques (en champ non homogène), qu'une durée de 1 s est nécessaire à l'établissement d'une interaction plasmide/membrane stable *(Faurie et al., 2010)*. Dans ce travail, la seconde impulsion conservait son caractère perméabilisant donc affectait de manière dramatique l'organisation membranaire en parallèle de la contribution électrophorétique. Notre étude (liée au développement du générateur Betatech) permet de se placer dans des conditions classiques d'électrotransfert où la membrane relaxe après l'impulsion électrique par une cinétique en 3 temps *(Pucihar et al., 2008)*. Nos résultats mettent en évidence la similitude temporelle entre la seconde phase de relaxation (i.e. retour à l'état imperméable) et celle de la formation du complexe stable plasmide/membrane. Notons que Hibino et collaborateurs avaient observé que la chute drastique de conductance électrique membranaire à la fin de l'impulsion électrique était beaucoup plus rapide (échelle de la milliseconde) et ne correspond pas à cette stabilisation *(Hibino et al., 1993)*.

Cette étude de l'effet de l'application d'impulsions bipolaires et asymétriques sur l'électrotransfert de plasmide permet une meilleure compréhension de l'interaction plasmide/membrane, étape clé du mécanisme d'électrotransfert de plasmide. Ce travail confirme la corrélation qui existe entre l'interaction plasmide/membrane et l'efficacité de transfection. Nos résultats suggèrent que l'interaction des molécules de plasmide avec la membrane perméabilisée serait un processus rapide. Les travaux avec les impulsions électriques SPHV montrent qu'elles sont créées en une centaine de microsecondes (ou moins). Cette dernière partie montre que la stabilisation du complexe plasmide/membrane s'effectue en un délai de 200 ms.

5. Effet de la topologie du plasmide sur l'interaction plasmide/membrane

5.1. Introduction

Dans les années 80 et 90, les paramètres liés aux molécules de plasmide (i.e. taille, concentration et topologie) ont été étudiés afin de comprendre les mécanismes d'électrotransfert de plasmide *in vitro*.

La taille des molécules de plasmide pouvant être transféré à l'intérieur des cellules est variable et ne constitue pas une limite comme dans le cas des vecteurs viraux. Des fragments d'ADN de plus de 65 kb ont pu être transférés dans les cellules NIH-3T3 et dans les cellules de la moelle osseuse *(Jastreboff et al., 1987)*. La taille maximale d'ADN non codant pouvant être transféré à l'intérieur des cellules est d'environ 150 à 200 kb *(Toneguzzo et al., 1986)*. La majorité des plasmides codant une molécule d'intérêt qui sont transférés dans les cellules, a une taille comprise entre 3,5 kpb et 20 kpb *(Wang et al., 2005)*. Il existe également une nouvelle génération de plasmide appelé "mini-circle" dont la taille est comprise entre 2 kpb et 3 kpb car les séquences bactériennes telles que l'origine de réplication et les gènes de résistances aux antibiotiques, ont été éliminées (*Darquet et al., 1997; Gill et al., 2009)*. L'électrotransfert *in vitro* de plasmide de petite taille est plus efficace que celui de grande taille *(Molnar et al., 2004; Wang et al., 2005)*.

La concentration de plasmide utilisée varie de 0,1 µg/mL à 100 µg/mL selon les expériences. En règle générale, plus le nombre de copies de plasmide est importante, plus le taux de cellules transfectées augmente *(Stopper et al., 1985; Andreason et Evans, 1988; Wolf et al., 1994)*. Cette dépendance est linéaire dans le cas des cellules Cos-1 *(Klenchin et al., 1991)*. Cependant, un effet toxique de certains plasmides a pu être mis en évidence lorsque des concentrations trop importantes sont utilisées. Elles entraînent une forte chute de viabilité et du taux de transfection *(Wolf et al., 1994; Winterbourne et al., 1988)*.

La topologie du plasmide a été également étudiée au sein des cellules de mammifères. En effet, le plasmide peut adopter trois conformations: superenroulé, circulaire et linéaire. La linéarisation du plasmide permet d'augmenter d'un facteur 3 à 20 l'efficacité de transfection transitoire ou stable, par rapport à celle obtenue avec la

forme circulaire ou super-enroulée *(Neumann et al., 1982; Stopper et al., 1985; Toneguzzo et al., 1986; Potter et al., 1988; Keating et al., 1990)*. Ces résultats sont compatibles avec l'hypothèse d'un mécanisme de transfert à travers des "électropores" *(Neumann et al., 1982)*. Cependant, d'autres expériences montrent que l'efficacité de transfection des cellules NIH-3T3 chute de façon brutale lorsque le plasmide est linéaire *(Xie et Tsong, 1993)*. Ces résultats s'expliquent par le fait que la linéarisation du plasmide génère des extrémités 5' et 3' libres qui rend le plasmide plus sensible à la dégradation par les exonucléases. Cependant, d'autres travaux montrent que la topologie du plasmide n'a aucune influence sur l'efficacité de transfection *(Winterbourne et al., 1988)*.

Les résultats contradictoires de la littérature et l'absence de données concernant les cellules CHO, nous ont donc incité à étudier l'effet de la topologie du plasmide sur l'interaction plasmide/membrane par vidéo-microscopie de fluorescence à l'échelle de la cellule unique et sur la transfection par cytométrie de flux.

L'ensemble des résultats obtenus dans cette étude fera l'objet d'une publication en 2010.

5.2. La publication

Effects (or not) of topology of plasmid DNA in gene electrotransfer processes

Jean-Michel Escoffre[1,2], Biliana Nikolova[3], Julien Henri[1,2], Cyril Favard[4], Laetitia Mallet[1,2], Justin Teissié[1,2], Iana Tsoneva[3] and Marie-Pierre Rols[1,2*]

[1] CNRS; IPBS (Institut de Pharmacologie et de Biologie Structurale); 205 route de Narbonne, F-31077 Toulouse, France.

[2] Université de Toulouse; UPS; IPBS; F-31077 Toulouse, France.

[3] Institute of Biophysics, Bulgarian Academy of Sciences, G. Bonchev str. Bl. 21, 1113 Sofia, Bulgaria

[4] CNRS; Institut Fresnel, UMR6133 Marseille, France.

Correspondence should be addressed to Marie-Pierre Rols & Iana Tsoneva
IPBS-CNRS UMR 5089, 205 route de Narbonne 31077 Toulouse France
Tel.: +33.5.61.17.58.11; fax: +33.5.61.17.59.94.
E-mail address: marie-pierre.rols@ipbs.fr
J-M E and B N have the same contribution

ABSTRACT

Electropermeabilization is a non-viral method that can be used to transfer plasmid DNA into cells and tissues. However and even if it is safe, this physical method remains less efficient than viral approaches. Biophysical mechanisms of gene electrotransfer are not entirely known. Contrary to small molecules that have direct and fast access to the cytoplasm, plasmid DNA is electrophoretically pushed towards the permeabilized membrane where it forms a complex before being transferred into the cytoplasm. In order to understand the biophysical mechanisms of gene electrotransfer and by this way to improve it, we investigated the dependence of plasmid DNA/membrane interaction and gene expression on the topology of plasmid DNA, i.e. linear *versus* supercoiled. Our results revealed that: i) even if plasmid DNA/membrane interactions are only slightly affected by the topology of plasmid DNA, ii) gene transfer and expression are strongly affected by it. Indeed, the linearization of plasmid DNA leads to a decrease in the transfection level.

INTRODUCTION

The permeability of cell membranes can be transiently and locally increased when external electric field pulses, over a critical intensity, are applied, a phenomenon commonly known as *electroporation* or *electropermeabilization* (1, 2). This approach is routinely used in cell and molecular biology, in biotechnology, and more recently in medicine. It is a very efficient way for cytotoxic drugs delivery in cancer cells (3-5). This process called electrochemotherapy is now accepted as a palliative clinical treatment. The use of electrotransfer for plasmid DNA delivery to cells has been widely used for many years. It has been extended to show the utility of this procedure *in vivo*. Main advantages of the controlled use of pulsed electric field are that it is a safe, rapid and non expensive procedure, equally applicable to quiescent and dividing cells. Gene electrotransfer has been performed *in vivo* on several tissue types including skin, liver, tumor, muscle, brain and spleen (6-11). Clinical trials of gene electrotransfer are under investigation (12-15). A phase I dose escalation trial of plasmid interleukin electroporation has been carried out in patients with metastatic melanoma, indicating this modality to be safe and effective (16).

Despite numerous studies, much remains unknown about the basic biophysical mechanisms (17). Performed at the single cell level, studies have yielded a phenomenological description of gene electrotransfer (18). Small and large molecules enter the cell through well defined permeabilized caps of the plasma membrane. Small molecules, such as anticancer drugs, have a direct and free access to the cytoplasm. They enter into the cell across part of the membrane facing the two electrodes via the concentration gradient difference between the exterior and cell interior by a diffusion process (19-21). In contrast, the electrotransfer of plasmid DNA only occurs in the part of the membrane facing the cathode and requires a number of consecutive steps: membrane permeabilization, electrophoretic migration of plasmid DNA towards the cell, plasmid DNA insertion into the plasma membrane, translocation across the plasma membrane, migration of plasmid DNA towards the nucleus and finally transfer of plasmid DNA across the nuclear envelope (22-26). As each of these steps may jeopardize gene expression, one may wonder if plasmid DNA molecules can play a role in that processes.

The aim of the present investigation was to study the effect of plasmid DNA topology in electrotransfer processes. Indeed, the plasmid DNA can be present in two

conformations, either supercoiled or linear. While, in standard protocols, supercoiled plasmids are generally used (16, 27), one may wonder if the topology of plasmid DNA could have any effect on the electro-mediated gene expression. It has been indeed reported contradictable results about the effect of plasmid DNA topology on the transfection efficiency (1, 28, 29). We therefore designed experiments in order to evaluate the effect of the topology of the plasmid DNA on the different steps of DNA delivery and expression. For that we used fluorescence microscopy as a tool to visualize these steps at the single cell level. Quantitative observations of plasmid DNA/membrane interaction, gene expression, and cell viability were made. Our results show that plasmid DNA under supercoiled form is more efficient for gene expression.

MATERIALS AND METHODS.

Cells: Chinese hamster ovary (CHO) cells were used. The WTT clone was selected for its ability to grow in suspension or plated on Petri dishes or on microscope glass cover slip. They were grown in MEM medium as previously described (30). Their ability to grow on a support after being maintained in suspension is a direct evidence of their viability.

Plasmid: Plasmid DNA (pEGFP-C1, 4.7 kbp) carrying the gene of the Green Fluorescent Protein gene controlled by the CMV promoter was obtained from Clonetech (Palo Alto, CA). It was purified from E. coli transfected cells by using Maxiprep DNA purification system according to Qiagen instructions (Courtaboeuf, France). This plasmid was used both for the direct visualization at the single cell level of its electrotransfer into the cells (by labeling as shown below) and for gene expression.

Plasmid linearization: 20 µg of plasmid DNA were digested by 2 µL (10 000 UIE/mL) of the restriction enzyme Stu I in buffer 2 (New England Biolabs Inc. Ipswich, MA) during 1h at 37°C. After enzymatic digestion, the enzyme was inactivated by heat (65°C) during 20 min. The digestion efficiency was verified by agarose gel electrophoresis. 0.5 µg of digested and control plasmids were put on agarose gel 1% in TAE buffer 1X (Tris 0.4M, Acetate 0.2M, EDTA 10mM, pH 8,3) and visualized under UV after ethidium bromide staining (10% v/v).

Electropulsation: Electropulsation was operated by using a CNRS cell electropulsator (Jouan, St Herblain, France), which delivered square-wave electric pulses. Stainless steel plate parallel electrodes (inter-electrode distance 4 mm) were

connected to the voltage pulse generator. A polarity inverter built in the laboratory gave inversion of the polarity between each pulse. An oscilloscope (Enertec, St. Etienne, France) monitored pulse shape.

Electrotransfection: Cells in suspension were centrifuged for 5 min at 120 g and resuspended in 100 µl of plasmid DNA containing pulsing buffer (10 mM K_2HPO_4/KH_2PO_4, 1 mM $MgCl_2$, 250 mM sucrose, pH 7.4) at a 0.5 10^6 cells/mL density. For each condition, 2 µg of pEGFP-C1 plasmid was used. 10 unipolar or bipolar rectangular pulses lasting 5 ms at 1Hz repetition frequency were applied at various amplitudes at room temperature. Cells were incubated for 10 min at room temperature and cultured in Petri dish with 2 mL of culture medium at 37°C in a 5% CO_2 incubator. 24h later, the cell monolayer was washed with PBS to remove all non-adherent cells. Cells were harvested by trypsinization, resuspended in 1 mL of PBS and analyzed by flow cytometry to evaluate both the transfection level (i.e. percentage of EGFP expressing cells) and the transfection efficiency (i.e. mean of associated fluorescence intensity). The excitation wavelength was 488 nm (argon laser) and the fluorescence of EGFP was collected in FL-1 channel (bandpass 520±42 nm). A minimum of 5×10^3 events were acquired in list mode and analyzed with Cellquest software (Becton Dickinson).

Cell viability: Viability was measured by quantifying the growth of cells over more than one generation after electropulsation (~24h) as previously described (30). Briefly, cells were pulsed and kept for 10 min at room temperature, a delay that allow the membrane to be impermeable again. They were then cultured on Petri dish with 2 mL of culture medium. Viability was measured by quantifying the number of cells, over 24h after electropulsation (more than one generation) by crystal violet staining (30).

DNA staining: Plasmid pEGFP-C1 was stained stoichiometrically with the DNA intercalating thiazole orange homodimer dye TOTO-1 (Molecular Probes, Eugene, OR) in the following manner. The pEGFP-C1 plasmid was stained with TOTO-1 dye at a DNA concentration of 1µg/µl for 60 minutes on ice. The TOTO-1 concentration was $2.3x10^{-4}$ M, to yield an average base pair to dye ratio of 5 (31).

Microscopy: For online microscopic observations, an electropulsation chamber was designed using the electrodes in contact with a microscope glass coverslip chamber (Lab-Teck II system). The electrodes were connected to the voltage generator. The chamber was placed on the stage of an inverted digitized video microscope (Leica DMIRB, Wetzlar, Germany). Cells were observed with a Leica 100x, 1.3 NA oil immersion

objective. The wavelengths were selected by using the Leica L4 filter block (450nm≤lex≤490nm; dichromatic mirror Pass Band: 515nm≤lem≤560nm) for the TOTO-1 labeled plasmid DNA. Images were recorded with the CELLscan System from Scanalytics (Billerica, Ma) equipped with a Photometrics cooled CCD camera (Princeton Instrument, inc.) (31). This digitizing set up allowed a quantitative localized analysis of the fluorescence emission along the cell membrane. Plot histograms detected local increase above the background level outside of the cells. Two characteristic parameters were used: the peak intensity and the integral under the peak. Both were directly related to the number of fluorescent molecules locally present. The light haze contributed by fluorescent-labeled structures located above and below the plane of optimal focus was mathematically reassigned to its proper places origin (Exhaustive Photon Reassignment EPR software (Scanalytics, Billerica, MA) after accurate characterization of the blurring function of the optical system (31).

Errors bars: They represent the standard error of the mean.

RESULTS

We analyzed the effect of plasmid DNA topology on cell viability, plasmid DNA/membrane interaction as well as gene transfer and expression. Cells were pulsed under electric field conditions known to induce an efficient gene expression as previously described (30, 32).

Linearization of plasmid DNA

Plasmid DNA has been linearized by using the restriction enzyme STU I that digested the plasmid DNA in uncoding part as shown in Figure 1A. The results of the digestion are shown in Figure 1B. Nearly 100 % of plasmid DNA molecules are observed to be linear.

Effect of plasmid topology on cell viability

As previously shown (30), decreased cell viability was observed after application of electric pulses. Under the present electric field conditions, 80% of cells were viable. In the presence of plasmid DNA, irrespective of its topology, additional affection of cell viability by a 20% factor was observed.

Effect of plasmid conformation on DNA/Membrane interaction

Video-microscopy at the single cell level offers direct access to the early events of plasmid DNA transfer across the electropermeabilized membrane. Images of plasmid DNA/membrane interactions were obtained by fluorescence microscopy with the TOTO-1 fluorescent labeled plasmid DNA in the minutes following pulses application. As previously described (31), fluorescent plasmid DNA interacted as "aggregates" with the permeabilized membrane. As expected, this interaction took place in membrane area facing the cathode under unipolar conditions, while it took place facing the two electrodes under bipolar conditions. This interaction was quantified at the membrane level. The percentage of positive cells (i.e. cells where plasmid DNA/membrane interaction was detected) and the fluorescence intensity (i.e. mean amount of TOTO bound to plasmid DNA interacting with cells) were determined. As shown in Figure 2, whatever the topology of plasmid DNA, 85% of cells were positive to the plasmid DNA/membrane interaction. Moreover, the polarity of electric pulses, (i.e. unipolar or “bipolar” electric pulses) did not significantly change the percentage of positive cells. Interestingly, the mean fluorescence intensity significantly decreased by 40% with the linear form under normal electric pulses delivery conditions and by 50% under bipolar conditions compared to the supercoiled form.

Effect of plasmid conformation on gene expression

Gene expression was accessed by using a plasmid carrying the DNA of the enhanced Green Fluorescent Protein. Figure 3 showed the results of gene expression measured 24h following the application of electric pulses. Whatever the topology of plasmid DNA, the transfection level was enhanced by increasing of the electric field intensity (Figure 3) as described previously for the intact form (31). However, the transfection level obtained with linear plasmid DNA was 2- to 4-fold lower than that got with supercoiled plasmid DNA (Figure 3).

The associated fluorescence intensity, related to the level of EGFP expression in the electrotransfected cells, was quantified over time (Figure 4). As under linear conditions, the percentage of transfected cells was lower, results are plotted in relative values. As shown, expression of GFP decreased along time. Namely, the expression was observed to decrease by a factor 4 in the 72 hours following plasmid DNA electrotransfer whatever the topology of plasmid DNA.

DISCUSSION

Years ago, Neumann and coworkers have shown that the efficiency of pulsed electric field induced plasmid DNA transfection of mouse L-cells is several times higher for the linear plasmid DNA than for the closed circular plasmid DNA (1). Xie and co-workers have examined electrotransfection of NIH3T3 mouse fibroblast (28). Their results indicate that cell surface binding and cell uptake of plasmid DNA did not depend on the topology of plasmid DNA. However, both the transient and the permanent expression of the plasmids were three to five times more efficient for the supercoiled DNA than for the linear DNA. More recently, by using circular and linear plasmid DNA, Glover and collaborators reported that plasmid DNA is taken up by cells equally well but circular plasmid DNA displays reduced transformation efficiency (29). Their results indicated that both exogenous plasmid DNA linearization and genomic breaks promote stable integration in a cooperative manner. All these apparently contradictory data let us to go further in the comprehension of the mechanisms of DNA electrotransfer.

According to the standard theory of electropermeabilization, the effect of the electric field is to render the cell membrane permeable. Another effect is to push DNA toward the cathode facing side of the cell leading to its insertion in it. Once into the cytoplasm, plasmid DNA has to reach the nucleus in order to gene expression occurs. DNA/membrane complex formation is a necessary condition to gene expression but not a sufficient one. It can indeed be affected by reversing the polarity and by increasing the repetition frequency of pulses (26). Recent results reveal the existence of two classes of plasmid DNA/membrane interaction: i) a metastable plasmid DNA/membrane complex from which plasmid DNA can leave and return to pulsation buffer, and ii) a stable plasmid DNA/membrane complex, where plasmid DNA cannot be removed even by applying electric pulses of reversed polarity. Only plasmid DNA belonging to the second class leads to effective gene expression (24, 26). If the first steps of gene electrotransfection, i.e. migration of the plasmid DNA towards the electropermeabilized plasma membrane and its interaction with it, are starting to be described and therefore represent guidelines to improve gene electrotransfer, the successful expression of the plasmid depends on its subsequent migration into the cell. The charge and the shape of the plasmid DNA could therefore affect these diffusion processes. One may wonder if the topology of plasmid DNA can jeopardize electrically gene delivery and gene expression success. To answer to this question, we used two topoisomers of a 4.7 kbp plasmid DNA,

(i.e. supercoiled and linear forms). Our present results reveal that plasmid DNA/membrane interaction and gene electrodelivery take place whatever the topology of the plasmid DNA. However, the amount of plasmid DNA in interaction with the membrane and transfection efficiency is lower when using linear plasmid DNA (Figure 2). These results support a mechanism where transfection efficiency is directly affected by this interaction (Figure 3).

Contour length of plasmid DNA in linear form is L_{DNA} = 1.6 μm and the effective length in supercoiled form is L_{DNA} = 0.51 μm. If one suppose that plasmid DNA passes freely through the membrane the minimal time (Δt) with drift velocity (v) is: (Δt)= $L_{DNA}/v = L_{DNA}/\mu.E_{eff,}$ where μ is the electrophoretic mobility of DNA = 1.5 $x10^{-4}cm^2.V^{-1}.s^{-1}$, E_{eff} = 0.7 $V.cm^{-1}$, 10 pulses with duration 5 ms (totally 50 ms) Δt for migration of plasmid DNA through the membrane can be calculated according to the previous work of Spassova et al. (33). It is equal to 1.5 ms for linear form and to 0.5 ms for supercoiled plasmid DNA. The diameter of linear form of plasmid DNA is in order of 2-3 nm while that of the supercoiled plasmid DNA is one order of magnitude larger (about 20-30 nm). As in the case of the interaction of DNA/cationic lipoplexes (34), formation of endocytic vesicles of plasmid DNA/lipid complexes require to create large membrane external (ext) and internal (int) surface ($S_{ext}<S_{int}$) and charge ($\sigma_{ext}<\sigma_{int}$) asymmetries. Electron microscopy failed to reveal the endosome-like formation in eukaryotic cells (35). Electrotransfection efficiency is higher in case of the supercoiled plasmid DNA (Figure 3). Altogether, these results could be explained by the following suggestions:

1. Supercoiled plasmid DNA (flexible rod form, diameter 30 nm) induces the larger electrophoretic invagination of plasma membrane and favorites the permeabilization near the adsorbed plasmid DNA.

2. The rather high diameter of adsorbed plasmid DNA in supercoiled form increases the electrical resistance of membrane and favorites the formation of bigger permeabilised percolated area near the plasmid DNA.

3. Linear forms of plasmid DNA (L_{DNA} = 1.6 μm) occupy bigger area and form some “archipelago effects” on the surface of membrane. The invagination of membrane near the adsorbed plasmid DNA will be reduced due to the lower thickness of plasmid DNA and the permeabilization will be decreased. On the other hand the casual “archipelago” spreading of linear flexible plasmid DNA on the membrane surface will decrease the percolation, motion and coalescence of pores near the plasmid DNA and

will reduce the electroporated hydrophilic permeabilized zones through which penetrate plasmid DNA.

4. The stiffened and charged macromolecules with bigger diameter could electromigrate and/or diffuse through the membrane easier. Plasmid DNA electrophoresis (of stiff macromolecules) could change the properties of electroporated area by some increases of sizes or lifetimes of pores under plasmid DNA.

The topology of plasmid DNA could therefore favorites the electropermeabilization, electrodiffusion and finally electrotransfection of cells. Moreover it can affect membrane organization leading to its deformation, a process that may be involved in its subsequent uptake into the cell. Experiments are now to be developed in that field.

ACKNOWLEDGMENTS

This work has been supported by grants to BN, IT and MPR from International Scientific Cooperation Programm the Bulgarian Academy of Sciences (Bulg. Nat. Fund (DO 02/178) to I.T) and the CNRS and Paul Sabatier University, to MPR from the Association Française contre les Myopathies (AFM), from the region Midi Pyrenees to JT. The authors want to thank Claire Millot (IPBS, Toulouse, France) for her help in cell culture.

REFERENCES

1. Neumann, E., M. Schaefer-Ridder, Y. Wang, and P. H. Hofschneider. 1982. Gene transfer into mouse lyoma cells by electroporation in high electric fields. *Embo J* 1:841-845.
2. Escoffre, J. M., D. S. Dean, M. Hubert, M. P. Rols, and C. Favard. 2007. Membrane perturbation by an external electric field: a mechanism to permit molecular uptake. *Eur Biophys J* 36:973-983.
3. Mir, L. M., L. F. Glass, G. Sersa, J. Teissie, C. Domenge, D. Miklavcic, M. J. Jaroszeski, S. Orlowski, D. S. Reintgen, Z. Rudolf, M. Belehradek, R. Gilbert, M. P. Rols, J. Belehradek, Jr., J. M. Bachaud, R. DeConti, B. Stabuc, M. Cemazar, P. Coninx, and R. Heller. 1998. Effective treatment of cutaneous and subcutaneous malignant tumours by electrochemotherapy. *Br J Cancer* 77:2336-2342.

4. Belehradek, M., C. Domenge, B. Luboinski, S. Orlowski, J. Belehradek, Jr., and L. M. Mir. 1993. Electrochemotherapy, a new antitumor treatment. First clinical phase I-II trial. *Cancer* 72:3694-3700.
5. Rols, M. P., Y. Tamzali, and J. Teissie. 2002. Electrochemotherapy of horses. A preliminary clinical report. *Bioelectrochemistry* 55:101-105.
6. Titomirov, A. V., S. Sukharev, and E. Kistanova. 1991. In vivo electroporation and stable transformation of skin cells of newborn mice by plasmid DNA. *Biochim Biophys Acta* 1088:131-134.
7. Heller, R., M. Jaroszeski, A. Atkin, D. Moradpour, R. Gilbert, J. Wands, and C. Nicolau. 1996. In vivo gene electroinjection and expression in rat liver. *FEBS Lett* 389:225-228.
8. Rols, M. P., C. Delteil, M. Golzio, P. Dumond, S. Cros, and J. Teissie. 1998. In vivo electrically mediated protein and gene transfer in murine melanoma. *Nat Biotechnol* 16:168-171.
9. Aihara, H., and J. Miyazaki. 1998. Gene transfer into muscle by electroporation in vivo. *Nat Biotechnol* 16:867-870.
10. Cemazar, M., M. Golzio, G. Sersa, M. P. Rols, and J. Teissie. 2006. Electrically-assisted nucleic acids delivery to tissues in vivo: where do we stand? *Curr Pharm Des* 12:3817-3825.
11. Mir, L. M., M. F. Bureau, J. Gehl, R. Rangara, D. Rouy, J. M. Caillaud, P. Delaere, D. Branellec, B. Schwartz, and D. Scherman. 1999. High-efficiency gene transfer into skeletal muscle mediated by electric pulses. *Proc Natl Acad Sci U S A* 96:4262-4267.
12. Gehl, J. 2008. Electroporation for drug and gene delivery in the clinic: doctors go electric. *Methods Mol Biol* 423:351-359.
13. Giardino, R., M. Fini, V. Bonazzi, R. Cadossi, A. Nicolini, and A. Carpi. 2006. Electrochemotherapy a novel approach to the treatment of metastatic nodules on the skin and subcutaneous tissues. *Biomed Pharmacother* 60:458-462.
14. Sersa, G., D. Miklavcic, M. Cemazar, Z. Rudolf, G. Pucihar, and M. Snoj. 2008. Electrochemotherapy in treatment of tumours. *Eur J Surg Oncol* 34:232-240.
15. Spugnini, E. P., G. Citro, A. D'Avino, and A. Baldi. 2008. Potential role of electrochemotherapy for the treatment of soft tissue sarcoma: first insights from preclinical studies in animals. *Int J Biochem Cell Biol* 40:159-163.

16. Daud, A. I., R. C. DeConti, S. Andrews, P. Urbas, A. I. Riker, V. K. Sondak, P. N. Munster, D. M. Sullivan, K. E. Ugen, J. L. Messina, and R. Heller. 2008. Phase I trial of interleukin-12 plasmid electroporation in patients with metastatic melanoma. *J Clin Oncol* 26:5896-5903.
17. Teissie, J., M. Golzio, and M. P. Rols. 2005. Mechanisms of cell membrane electropermeabilization: a minireview of our present (lack of ?) knowledge. *Biochim Biophys Acta* 1724:270-280.
18. Escoffre, J. M., T. Portet, L. Wasungu, J. Teissie, D. Dean, and M. P. Rols. 2009. What is (Still not) Known of the Mechanism by Which Electroporation Mediates Gene Transfer and Expression in Cells and Tissues. *Mol Biotechnol* 41:286-295.
19. Rols, M. P., and J. Teissie. 1990. Electropermeabilization of mammalian cells. Quantitative analysis of the phenomenon. *Biophys J* 58:1089-1098.
20. Puc, M., T. Kotnik, L. M. Mir, and D. Miklavcic. 2003. Quantitative model of small molecules uptake after in vitro cell electropermeabilization. *Bioelectrochemistry* 60:1-10.
21. Sun, Y., P. T. Vernier, M. Behrend, J. Wang, M. M. Thu, M. Gundersen, and L. Marcu. 2006. Fluorescence microscopy imaging of electroperturbation in mammalian cells. *J Biomed Opt* 11:024010.
22. Wolf, H., M. P. Rols, E. Boldt, E. Neumann, and J. Teissie. 1994. Control by pulse parameters of electric field-mediated gene transfer in mammalian cells. *Biophys J* 66:524-531.
23. Favard, C., D. S. Dean, and M. P. Rols. 2007. Electrotransfer as a non viral method of gene delivery. *Curr Gene Ther* 7:67-77.
24. Phez, E., C. Faurie, M. Golzio, J. Teissie, and M. P. Rols. 2005. New insights in the visualization of membrane permeabilization and DNA/membrane interaction of cells submitted to electric pulses. *Biochim Biophys Acta* 1724:248-254.
25. Hristova, N. I., I. Tsoneva, and E. Neumann. 1997. Sphingosine-mediated electroporative DNA transfer through lipid bilayers. *FEBS Lett* 415:81-86.
26. Faurie, C., M. Rebersek, M. Golzio, M. Kanduser, J. M. Escoffre, D. Pavlin, J. Teissie, D. Miklavcic, and M. P. Rols. 2010. Electrically mediated gene transfer and expression are controlled by the life-time of DNA/Membrane complex formation. *Journal of Gene Medicine* 12:117-125.

27. Golzio, M., M. P. Rols, and J. Teissie. 2004. In vitro and in vivo electric field-mediated permeabilization, gene transfer, and expression. *Methods* 33:126-135.
28. Xie, T. D., and T. Y. Tsong. 1993. Study of mechanisms of electric field-induced DNA transfection. V. Effects of DNA topology on surface binding, cell uptake, expression, and integration into host chromosomes of DNA in the mammalian cell. *Biophys J* 65:1684-1689.
29. Glover, L., and D. Horn. 2009. Site-specific DNA double-strand breaks greatly increase stable transformation efficiency in Trypanosoma brucei. *Mol Biochem Parasitol* 166:194-197.
30. Faurie, C., E. Phez, M. Golzio, C. Vossen, J. C. Lesbordes, C. Delteil, J. Teissie, and M. P. Rols. 2004. Effect of electric field vectoriality on electrically mediated gene delivery in mammalian cells. *Biochim Biophys Acta* 1665:92-100.
31. Golzio, M., J. Teissie, and M. P. Rols. 2002. Direct visualization at the single-cell level of electrically mediated gene delivery. *Proc Natl Acad Sci U S A* 99:1292-1297.
32. Kubiniec, R. T., H. Liang, and S. W. Hui. 1990. Effects of pulse length and pulse strength on transfection by electroporation. *Biotechniques* 8:16-20.
33. Spassova, M., I. Tsoneva, A. G. Petrov, J. I. Petkova, and E. Neumann. 1994. Dip patch clamp currents suggest electrodiffusive transport of the polyelectrolyte DNA through lipid bilayers. *Biophys Chem* 52:267-274.
34. Angelova, M. I., and I. Tsoneva. 1999. Interactions of DNA with giant liposomes. *Chem Phys Lipids* 101:123-137.
35. Satyabhama, S., and A. L. Epstein. 1988. Short-term efficient expression of transfected DNA in human hematopoietic cells by electroporation: definition of parameters and use of chemical stimulators. *DNA* 7:203-209.

FIGURE LEGENDS.

Figure 1: Map of the plasmid DNA and linearization efficiency.
(A) pEGFP-C1 plasmid. (B) Electrophoresis gel showing (1) markers, (2) scDNA and (3) Linear DNA. 0.5 µg of each entity have been deposit on the 1% agarose gel. Migration has been performed in TAE 1X buffer.

Figure 2: Effect of plasmid conformation on DNA/membrane interaction.
CHO cells were incubated in the presence of TOTO-1-labelled DNA (pEGFP-C1) in the pulsing buffer Train of 10 pulses of 5 ms duration was applied at 0.7 kV/cm to cells in the presence of plasmid DNA under supercoiled (1,2) or linear form (3,4). Cells were assessed 5 minutes after pulses delivery for both percentage of positive cells (cells in which DNA interacted, white bars) as well as for the amount of DNA interacted with them (black bars). 1 and 3 correspond to unipolar conditions, 2 and 4 correspond to bipolar conditions.

Figure 3: Effect of plasmid conformation on transfection.
10 pulses of 5 ms duration were applied at various field strength to cells in pulsing buffer containing a plasmid coding for the EGFP reporter gene. White symbols correspond to linear conditions; black symbols correspond to supercoiled conditions.

Figure 4: Effect of plasmid conformation on gene expression.
CHO cells were submitted to 10 pulses of 5 ms duration at 0.7 kV/cm in the presence of sc or linear plasmid DNA. Gene expression was analyzed by flow cytometry with time (up to 4 days following pulses delivery). White symbols correspond to linear conditions, black symbols correspond to supercoiled conditions. Data are reported as relative values, the references for each conditions being equal to the expression detected 1 day after pulse delivery.

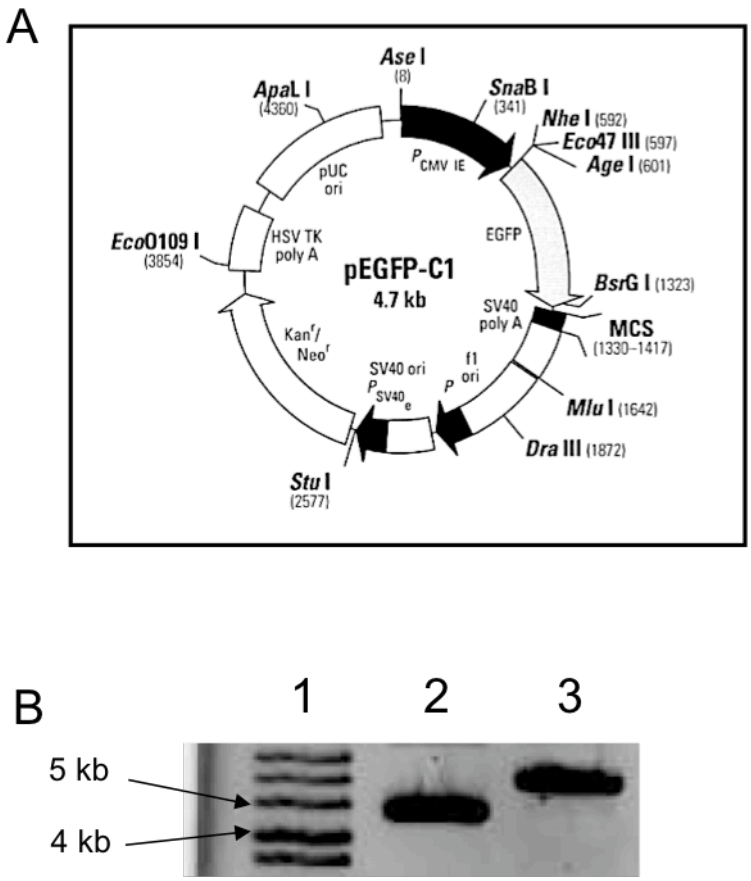
A
Ase I
(8)
SnaB I
(341)
Nhe I (592)
Eco47 III (597)
Age I (601)
ApaL I
(4360)
pUC
ori
P CMV IE
EGFP
EcoO109 I
(3854)
HSV TK
poly A
pEGFP-C1
4.7 kb
BsrG I (1323)
SV40
poly A
MCS
(1330–1417)
Kanr/
Neor
SV40 ori
P SV40
f1
ori
P
Mlu I (1642)
Dra III (1872)
Stu I
(2577)
B
1
2
3
5 kb
4 kb

Figure 1

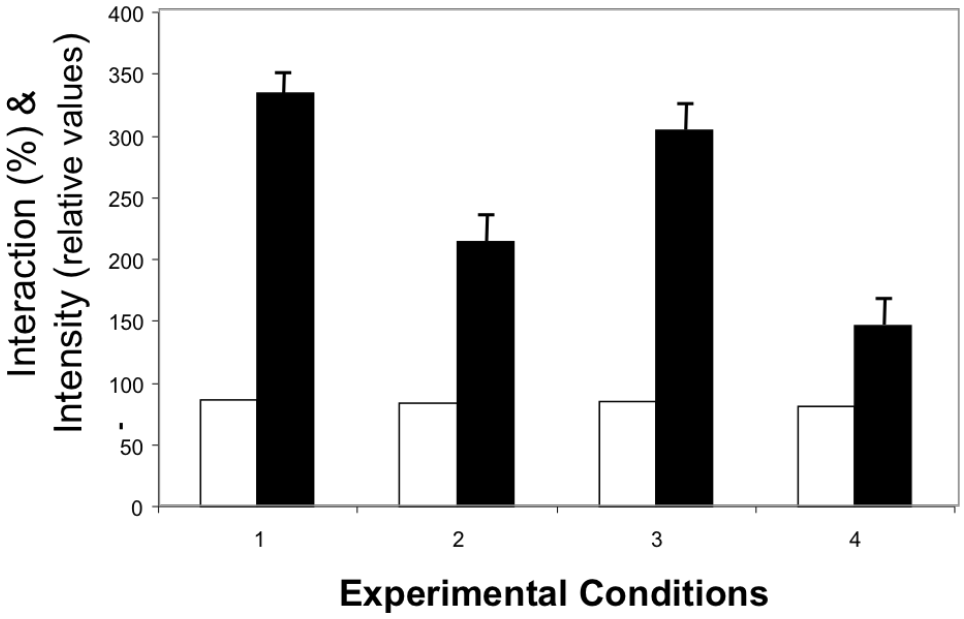
Interaction (%) &
Intensity (relative values)
400
350
300
250
200
150
100
50
0
1
2
3
4
Experimental Conditions

Figure 2

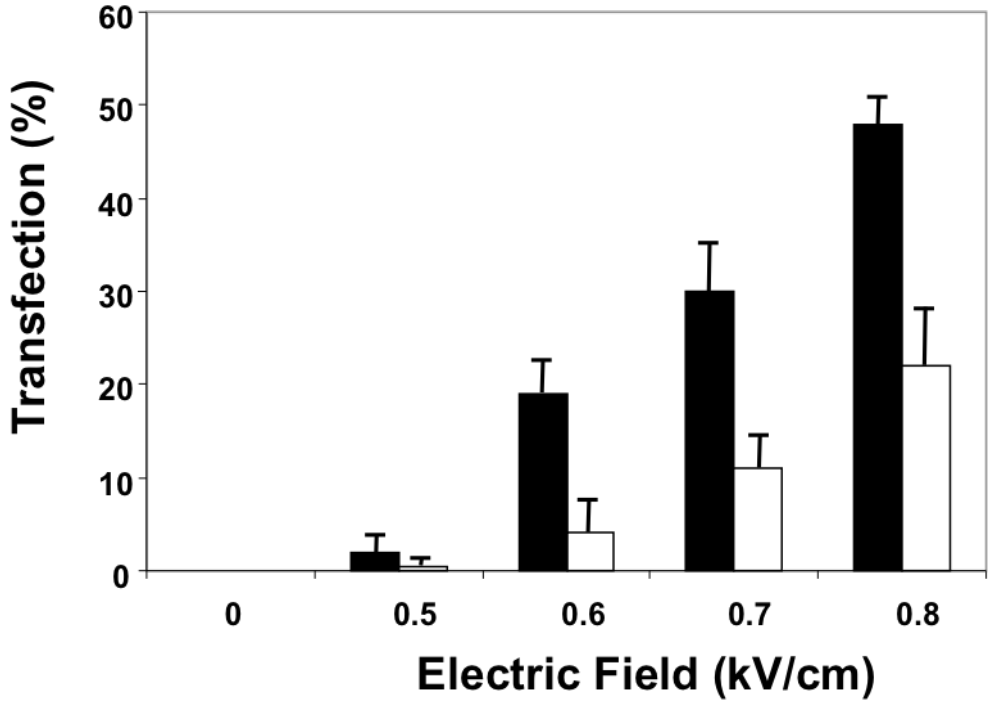
Transfection (%)
60
50
40
30
20
10
0
0
0.5
0.6
0.7
0.8
Electric Field (kV/cm)

Figure 3

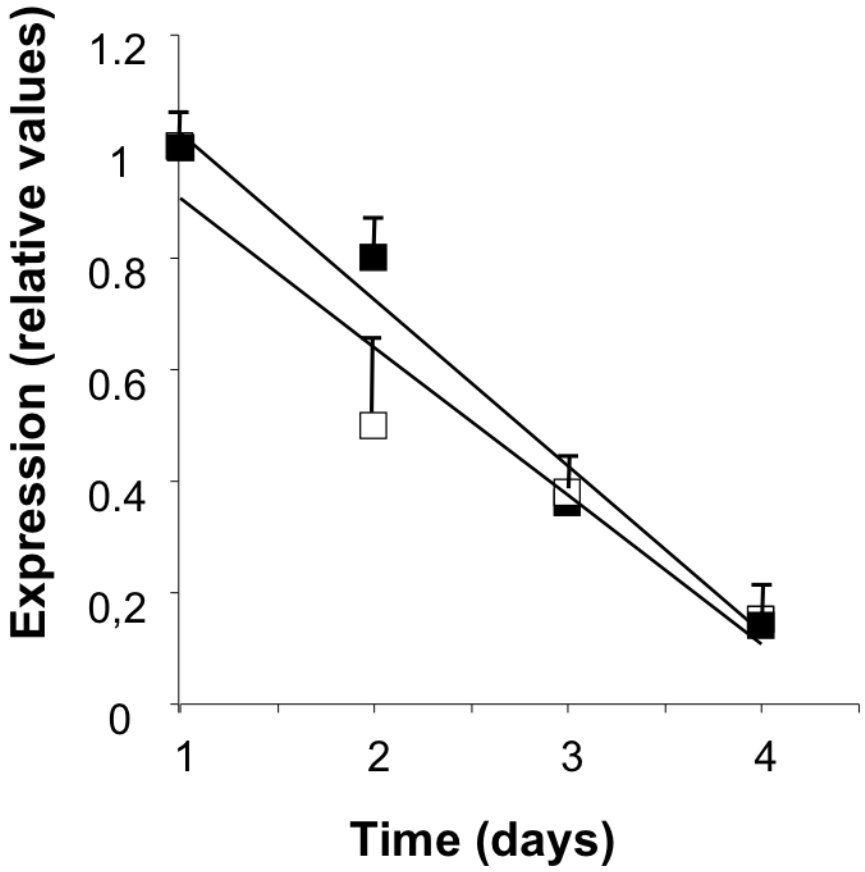

Figure 4

5.3. Discussion et Conclusions

L'objectif de ce travail consiste à étudier l'effet de la topologie du plasmide sur l'interaction plasmide/membrane et sur la transfection. Nos résultats montrent que quels que soient la topologie du plasmide (i.e. linéaire versus super-enroulé) ou les conditions électriques (i.e. unipolaire vs bipolaire), l'application d'impulsions électriques conduit à l'interaction plasmide/membrane sous la forme de complexes localisés. La quantité de plasmide en interaction avec la membrane et le taux de transfection sont plus faibles lorsque le plasmide linéaire est utilisé. En effet, l'électrotransfert de plasmide linéaire induit un taux de transfection qui est 2 à 4 fois plus faible que celui obtenu par électrotransfert de plasmide super-enroulé. Ces résultats montrent que la topologie du plasmide affecte l'interaction plasmide/membrane et l'efficacité de transfection des cellules. Cependant, nous ne pouvons pas exclure que la translocation des molécules de plasmide à travers la membrane soit différente selon la topologie du plasmide.

La topologie du plasmide affecte l'interaction plasmide/membrane et l'efficacité de transfection des cellules.

6. Etude de l'électrotransfert de plasmide sur d'autres lignées cellulaires

6.1. Introduction

Les études réalisées à l'échelle de la cellule unique ont conduit à une description phénoménologique du mécanisme de l'électrotransfert de plasmide *(Golzio et al., 2002; Pour revue, Escoffre et al., 2009)*. La perméabilisation membranaire est nécessaire mais pas suffisante pour conduire à l'expression génique. En effet, les molécules de plasmides migrent sous l'effet des forces électrophorétiques vers la surface de la cellule et interagissent avec la région membranaire faisant face à la cathode. Une seconde après l'application des impulsions électriques, cette interaction plasmide/membrane induit la formation de complexes stables et localisés *(Faurie et al., 2010)*. L'expression génique est détectée dans les heures après l'application des impulsions électriques et persiste pendant quelques jours *(Golzio et al., 2002)*. Les corrélations entre la perméabilisation membranaire, l'interaction plasmide/membrane et l'expression génique ont été démontrées sur la lignée cellulaire CHO.

L'objectif de ce travail est de déterminer si de telles corrélations existent sur d'autres lignées cellulaires: SH-SY5Y, B16-F10, C2C12, HCT-116, et ABAE. Les cellules sont transfectées dans les conditions électriques optimales de transfert de plasmide. Les taux de perméabilisation et de transfection sont déterminés par cytométrie de flux et l'interaction plasmide/membrane est visualisée par microscopie de fluorescence.

L'ensemble des résultats obtenus dans cette étude fera l'objet d'une courte publication en 2010.

6.2. La publication

DNA/membrane interaction: a key mandatory step of gene electrotransfer

Jean-Michel Escoffre[§], Yoann Gilbart[§], Marie Hubert[§], Cécile Faurie[¶], Luc Wasungu[§], Cyril Favard[♯], Muriel Golzio[§], Justin Teissié[§], Marie-Pierre Rols[§*].

[§]CNRS; IPBS (Institut de Pharmacologie et de Biologie Structurale); 205 route de Narbonne, F-31077, Toulouse, France. Université de Toulouse; UPS; IPBS; F-31077, Toulouse, France.
[¶]Cancéropole GSO Inserm U563; CHU Purpan BP 3028, 31024 Toulouse Cedex 3, France.
[♯]Institut Fresnel, Domaine Universitaire Saint Jérôme, 13397 Marseille, France
Correspondence to: Marie-Pierre Rols, CNRS; IPBS (Institut de Pharmacologie et de Biologie Structurale); 205 route de Narbonne, F-31077, Toulouse, France. Tel: +33561175811. Fax: +33561175994. Email: Rols@ipbs.fr

Direct injection of naked nucleic acids into cells and tissues can be considered as the simplest and safest method for gene delivery. However, it is generally associated with low gene expression and dramatic inter-individual variability. The controlled use of electric pulses as a safe and efficient tool to deliver plasmid DNA to target tissues and organs has been rapidly developed over the last decade. The method, called electropermeabilization (or electroporation) refers to the transient increase in the permeability of cell membranes (For review, Escoffre et al., 2007). Although the development of clinical trials, the mechanisms underlying membrane permeabilization and gene transfer are not understood (For review, Teissié et al., 2005). Elucidation of the mechanisms is of high importance for *in vitro* use in terms of efficiency and also for *in vivo* use in terms of safety. However, much remains unknown about the basic mechanisms. Several theoretical models postulate that plasmid DNA crosses the plasma membrane during electric pulse application through “electropores” (Neumann et al., 1989). However such models are not supported by experimental data. Performed at the single cell level, studies have yielded a phenomenological description of gene electrotransfer (Golzio et al., 2002; For review, Escoffre et al., 2009). Plasmid DNA indeed requires a number of consecutive steps: electrophoretic migration towards permeabilized membrane, insertion into the membrane, translocation across the

membrane, migration towards the nucleus and finally transfer across the nuclear envelope. Therefore, plasmid DNA does not enter into the cell during electric pulses but it is "trapped into" the plasma membrane. It is not homogeneously distributed on the permeabilized membrane but is present into "competent sites" whose size range from 0.1 to 0.5 µm.

These correlations between membrane permeabilization, DNA/membrane interaction and gene expression has been shown on the CHO cell line (growing both in suspension and on Petri dishes). Indeed, without permeabilization, neither DNA/membrane interaction nor gene expression can occur. Open question is whether this observation is applicable to all cell lines. If it is the case, it could be a simple and rapid way to determine which cell lines will be transfected by electric field. The topic of this letter is to give an answer to this exciting question.

For that, cells washed and culture medium was replaced by a special pulsation buffer (10 mM phosphate buffer pH 7.4, 250 mM sucrose, 1 mM $MgCl_2$). For electropermeabilization experiments, 100 µM propidium iodide was added to it. Its presence into the cells is an indicator of membrane permeabilization as already described (Golzio et al. 2004). Electropulsation was performed by applying 10 pulses, 5 ms duration, at 1 Hz frequency, and at various field intensities. Permeabilization efficiency and cell viability were analyzed 10 minutes following pulses delivery as previously described (Golzio et al. 2004). For gene transfer, cells were pulsed with 2 µg of plasmid DNA (pEGFP-C1, Clonetech). 10 pulses lasting 5 ms at a frequency of 1 Hz were applied at optimal field intensity (i.e. field intensity leading to the highest percentage of permeable and viable cells is). After a 5 min incubation, cells were cultured at 37°C during 24h. Transfection efficiency was analyzed 24h hours following the electropulsation as previously described (Golzio et al. 2004). For DNA/membrane interaction, the plasmid was stained with 2.3 10^{-4}M TOTO-1 (Molecular Probes, InvitroGen) at a DNA concentration of 1 µg/µL for 60 min on ice. Cells were incubated with 2 µg of fluorescent-labeled plasmid in pulsation buffer. Then, cells were submitted to same electric field condition as for gene transfer. DNA/membrane interaction was analyzed in the minutes following electric pulses delivery as previously described (Golzio et al. 2002).

Results of experiments performed on different cell lines having different origins and specificities are reported in Table 1. Results shows that whatever the cell line, electrical parameters can be found to allow the permeabilization of more than 50% of

the cells while preserving their viability. As already reported for CHO cells, gene expression is detected for B16F10, SH-SY5Y and ABAE cells, cell lines for which DNA/membrane interaction takes place. Therefore, there is a fair correlation between electropermeabilization, DNA/membrane interaction and gene expression in these cell lines. A recent work performed on Jurkat cells, showing the same fact (Maucksch et al. 2009). Interestingly, although HCT-116 and C2C12 cells are permeabilized, no DNA/membrane interaction neither gene expression was detected.

The take-home message of these results shows that electropermeabilization if necessary is no sufficient to induce DNA/membrane interaction and gene expression.

Acknowledgements

The authors would like to thank C. Millot for help with the cell culture and the Association Française sur les Myopathies (to MPR).

References

Escoffre JM, Portet T, Wasungu L, Teissié J, Dean D, Rols MP (2009) What is (still not) known of the mechanism by which electroporation mediates gene tranfer and expression in cells and tissues. Mol Biotechnol, 41:286-295

Escoffre JM, Dean DS, Hubert M, Rols MP, Favard C (2007) Membrane perturbation by an external electric field : a mechanism to permit molecular uptake. Eur Biophys J, 36 :973-983

Golzio M, Teissié J, Rols MP (2002) Direct visualization at the single-cell level of electrically mediated gene delivery. Proc Natl Acad Sci USA, 99:1292-1297

Golzio M, Rols MP, Teissié J (2004) In vitro and in vivo electric field-mediated permeabilization, gene transfer, and expression. Methods, 33 :126-135

Maucksch C, Bohla A, Hoffman F, Schleef M, Kumar Aneja M, Elfinger M, Hartl D, Rudolph C. (2009) Transgene expression of transfected supercoiled plasmid DNA concatemers in mammalian cells. J Gene Med., 11 :444-453

Teissié J, Golzio M, Rols MP (2005) Mechanisms of cell membrane electropermeabilization : a minireview of our present (lack of ?) knowledge. Biochim Biophys Acta, 1724 :270-280

Cell lines	Optimal electric field condition	Permeabilization (% cells)	DNA/membrane interaction	Transfection (% cells)
CHO (Chinese hamster ovary fibroblasts)	10x5ms 1Hz, 0.3 kV/cm	70%-80%	Yes	20%-40%
B16 (Murine melanoma cells)	10x5ms, 1Hz, 0.7 kV/cm	60%-70%	Yes	20-30%
C2C12 (Murine myoblasts)	10x5ms, 1Hz, 0.2 kV/cm	60%-70%	No	No
SH-SY5Y (Human neuroblastoma cells)	10x5ms, 1Hz, 0.4 kV/cm	50%-60%	Yes	5%-10%
HCT116 (Human colon cancer cells)	10x5ms, 1Hz, 0.3 kV/cm	70%-80%	No	No
ABAE (Adult Bovine Aortic Endothelial cells)	10x5ms, 1Hz, 0.25 kV/cm	70%-80%	Yes	10%-15%

Table 1: Comparison of membrane permeabilization, DNA/membrane interaction and gene expression efficiencies for different cell lines.

Optimal electric field conditions are determined for each cell line and reported (2nd column). The percentages of permeabilized and viable cells are determined (3rd column) as well as the one of transfected cells (5th column). DNA/membrane interaction is determined for some cell lines (4th column).

6.3. Discussion et Conclusions

Nos résultats montrent que les différentes lignées cellulaires sont toutes perméabilisables et potentiellement transfectables. Chaque type cellulaire a sa propre réponse vis-à-vis des impulsions électriques, du transfert du plasmide et de son expression. La perméabilisation membranaire, l'interaction plasmide/membrane et l'expression génique sont corrélées sur certaines lignées cellulaires (CHO, B16, SH-SY5Y, ABAE) qu'elles soient humaines ou murine, cancéreuses ou non. Par contre, les lignées cellulaires C2C12 et HCT-116 sont perméabilisables mais difficilement transfectable.

L'électrotransfert de plasmide est dépendant de deux facteurs. Un facteur physique, au niveau de la membrane plasmique, qui permet la perméabilisation, l'interaction et la translocation du plasmide et qui correspond à une réponse à court terme. Un facteur physiologique de la cellule qui permet le trafic intracellulaire des molécules de plasmide, l'expression génique et la survie cellulaire et qui correspond à une réponse à long terme.

Nos résultats mettent en évidence des spécificités cellulaires vis-à-vis de l'électrotransfert de plasmide. Ils confirment l'existence d'un processus multi-étapes de l'électrotransfert de plasmide dans certaines lignées cellulaires. L'électroperméabilisation demeure une étape nécessaire mais pas suffisante pour l'interaction plasmide/membrane.

PARTIE III

EFFET DE L'ELECTROPERMEABILISATION SUR LA MOBILITE LATERALE DES PROTEINES MEMBRANAIRES

Partie III. Effet de l'électroperméabilisation sur la mobilité latérale des protéines membranaires

1. Introduction

L'application d'impulsions électriques induisant la perméabilisation transitoire et réversible des cellules *(Neumann et al., 1989; Teissié et al., 2005; Escoffre et al., 2007)*, nous avons souhaité savoir si les défauts membranaires électro-induits pourraient constituer des obstacles à la diffusion de composés tels que des protéines membranaires. De plus, comme nous l'avons précédemment décrit l'électrotransfert de molécules de plasmide induit la formation de complexes plasmide/membrane *(Golzio et al., 2002; Faurie et al., 2004; Phez et al., 2005; Faurie et al., 2010)*. A ce jour, la position des molécules de plasmides dans la membrane perméabilisée n'est pas connue. Par conséquent, dans une deuxième partie, nous étudions l'effet de la présence de complexes plasmide/membrane sur la mobilité latérale d'une protéine membranaire du feuillet externe de la membrane plasmique, Rae1-eGFP *(Nomura et al., 1996)*.

Pour réaliser notre étude, nous avons utilisé une lignée de cellules CHO exprimant de manière stable la protéine membranaire Rae-1 fusionnée à la protéine fluorescent eGFP. La protéine Rae-1 est une glycoprotéine insérée dans la membrane plasmique par une ancre glycosyl-phosphatidylinositol *(Nomura et al., 1996)*. Les cellules CHO Rae1-eGFP ont été obtenues par le Pr. Bettina Couderc (Institut Claudius Regaud, Toulouse, France) et le plasmide Rae1-eGFP a été gracieusement offert par le Dr. Denis Hudrisier et le Dr. Anne Aucher (IPBS-CNRS UMR 5089, Toulouse France). Les paramètres électriques optimaux pour le transfert de plasmides dans les CHO Rae1-eGFP en adhésion sont de 10 impulsions électriques de 5 ms à une fréquence de 1 Hz et à une intensité électrique de 0,4 kV/cm. La technique de FRAP (i.e. Fluorescence Recovery After Photobleaching) est utilisée pour mesurer les temps de demi-retour de la protéine membranaire Rae1-eGFP *(Owen et al., 2009)*.

A

a

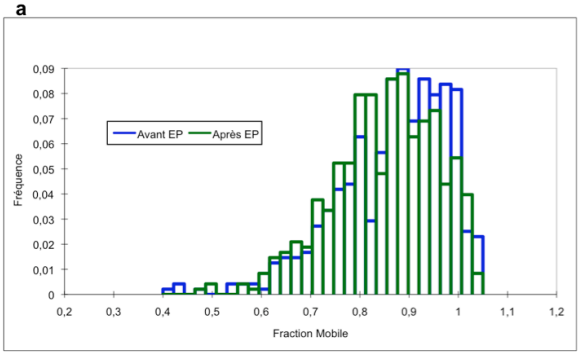

b

Variable	Observations	Obs. avec données manquantes	Obs. sans données manquantes	Minimum	Maximum	Moyenne	Ecart-type
M avant EP	478	0	478	0,415	1,047	0,868	0,111
M après EP	478	0	478	0,481	1,043	0,850	0,106

c

Test de Wilcoxon	
V	66562
Espérance	56763
Variance (V)	9015856,5
p-value(bilatérale)	0,001
alpha	0,05

d

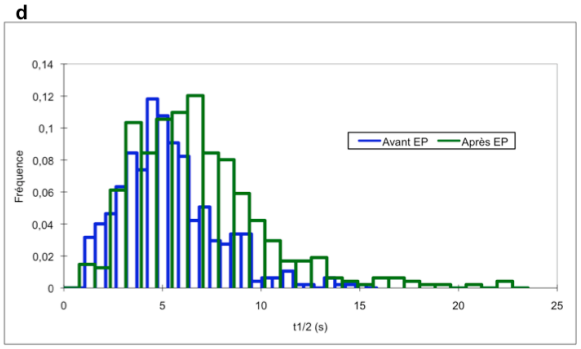

e

Variable	Observations	Obs. avec données manquantes	Obs. sans données manquantes	Minimum	Maximum	Moyenne	Ecart-type
t1/2 avant EP	474	0	474	1,155	14,850	5,287	2,415
t1/2 après EP	474	0	474	1,107	22,519	6,799	3,331

f

Test de Wilcoxon	
V	30976
Espérance	55814
Variance (V)	8790705
p-value(bilatérale)	<0,0001
alpha	0,05

B

a

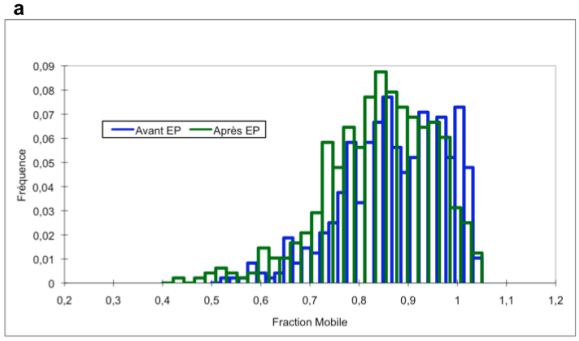

b

Variable	Observations	Obs. avec données manquantes	Obs. sans données manquantes	Minimum	Maximum	Moyenne	Ecart-type
M avant EP	480	0	480	0,525	1,045	0,875	0,104
M après EP	480	0	480	0,430	1,044	0,841	0,109

c

Test de Wilcoxon	
V	72753
Espérance	57240,5
Variance (V)	9129859,75
p-value(bilatérale)	<0,0001
alpha	0,05

d

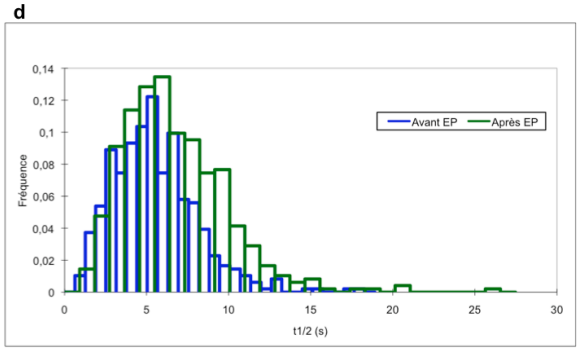

e

Variable	Observations	Obs. avec données manquantes	Obs. sans données manquantes	Minimum	Maximum	Moyenne	Ecart-type
t1/2 avant EP	483	0	483	1,025	17,906	5,490	2,566
t1/2 après EP	483	0	483	1,092	26,472	6,740	3,168

f

Test de Wilcoxon	
V	79971
Espérance	57960,6
Variance (V)	9302660,25
p-value(bilatérale)	<0,0001
alpha	0,05

Figure III-17: Effet de l'électroperméabilisation sur la mobilité latérale de la protéine membranaire Rae1-eGFP dans les régions membranaires perméabilisées face à l'anode (A) et face à la cathode (B). Des cellules CHO Rae1-eGFP adhérentes sont soumises à 10 impulsions électriques de 5 ms à une fréquence de 1 Hz et à une intensité électrique de 0,4 kV/cm sous un microscope confocal Zeiss LSM 510M. Avant et après l'application des impulsions électriques, des mesures de FRAP nous permettent de déterminer la fraction mobile, M (a-c) et le temps de demi-retour, t 1/2 (d-f). Une distribution des valeurs de M et t 1/2 obtenues avant et après électroperméabilisation est réalisée (a et d). L'ensemble des valeurs de M et de t 1/2 obtenues avant et après électroperméabilisation sont moyennés et les écart-types sont déterminés (b et e). Afin de déterminer la significativité des résultats, un test de Wilcoxon a été réalisé (c et f).

Deux régions d'intérêt de 1 µm de rayon sont définies dans les régions membranaires situées face aux électrodes (i.e. perpendiculaires aux lignes de champ électrique). Les mesures de FRAP sont réalisées avant et après l'application des impulsions électriques sur les mêmes cellules. Le temps de demi-retour ($t_{1/2}$) et la fraction mobile (M) sont déterminés *(Axelrod et al., 1976)*. Dans cette étude, nous ne cherchons pas à déterminer le coefficient de diffusion, mais cependant, celui-ci pourrait être calculé à partir de l'équation $D = \beta w^2/4t_{1/2}$ avec β, un coefficient tabulé qui est une fonction de l'efficacité de photodestruction provoquée par un faisceau Gaussien *(Yguerabide et al., 1982)*.

2. Résultats

Tous les résultats préliminaires présentés ci-dessous sont réalisés de la façon suivante: les mesures sont faites avant et après la condition d'expérience (application des impulsions électriques, application des impulsions électriques en présence des molécules de plasmide). Les résultats obtenus sont alors analysés par pair (échantillons appariés), à l'aide de tests statistiques dédiés (test statistique de Student en cas de distribution normale des valeurs; test statistique de Wilcoxon en cas de distribution quelconque). L'hypothèse de base (Ho) étant la non variabilité des deux distributions.

2.1. Electroperméabilisation

La mobilité latérale des protéines Rae1-eGFP est étudiée par FRAP dans les régions membranaires qui font face aux électrodes, i.e. anode (Figure III-17A) et cathode (Figure III-17B) avant et après l'application des impulsions électriques.

Avant l'application des impulsions électriques, la distribution des valeurs de la fraction mobile (M) (Anode: 0,868±0,111 vs Cathode: 0,875±0,104) et celle des valeurs du temps de demi-retour ($t_{1/2}$) (Anode: 5,287±2,415 s vs Cathode: 5,490±2,566) sont similaires dans les régions membranaires situées face aux électrodes (Figures III-17). En revanche, dans les 30 secondes qui suivent l'application des impulsions électriques, la distribution des valeurs de la fraction mobile se déplace vers des valeurs plus faibles ($Anode_{(-EP)}$: 0,868±0,111 vs $Anode_{(+EP)}$: 0,850±0,106; $Cathode_{(-EP)}$: 0,875±0,104 vs $Cathode_{(+EP)}$: 0,841±0,109) (Figures III-17A.a. et III-17B.a.) alors que la distribution des valeurs des temps de demi-retour tend vers des valeurs plus élevés ($Anode_{(-EP)}$: 5,287±2,415s vs $Anode_{(+EP)}$: 6,799±3,331s; $Cathode_{(-EP)}$: 5,490±2,566s vs $Cathode_{(+EP)}$: 6,740±3,168s) (Figures III-17A.d et III-17B.d.).

A

a

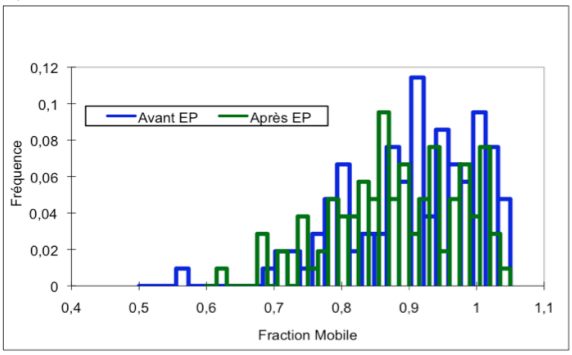

b

Variable	Observations	Obs. avec données manquantes	Obs. sans données manquantes	Minimum	Maximum	Moyenne	Ecart-type
M avant EP	105	0	105	0,568	1,047	0,907	0,095
M après EP	105	0	105	0,621	1,047	0,885	0,093

c

Test de Wilcoxon	
V	3353
Espérance	2835,5
Variance (V)	100660,25
p-value(bilatérale)	0,103
alpha	0,05

d

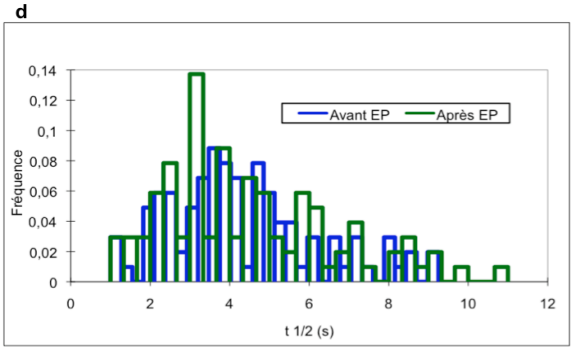

e

Variable	Observations	Obs. avec données manquantes	Obs. sans données manquantes	Minimum	Maximum	Moyenne	Ecart-type
t1/2 avant EP	102	0	102	1,107	9,155	4,332	1,889
t1/2 après EP	102	0	102	1,121	10,956	4,477	2,171

f

Test de Wilcoxon	
V	3057
Espérance	2943
Variance (V)	106438,5
p-value(bilatérale)	0,728
alpha	0,05

B

a

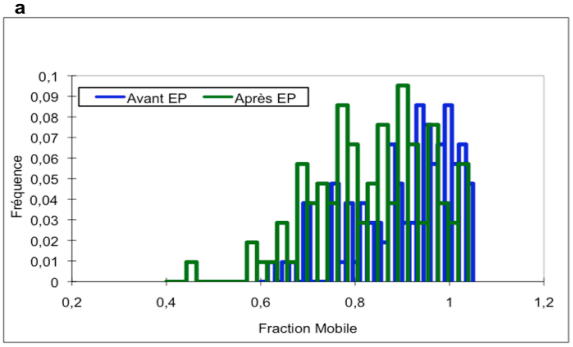

b

Variable	Observations	Obs. avec données manquantes	Obs. sans données manquantes	Minimum	Maximum	Moyenne	Ecart-type
M avant EP	105	0	105	0,618	1,048	0,910	0,102
M après EP	105	0	105	0,453	1,036	0,837	0,121

c

Test de Wilcoxon	
V	2433
Espérance	2997,5
Variance (V)	109408,75
p-value(bilatérale)	<0,0001
alpha	0,05

d

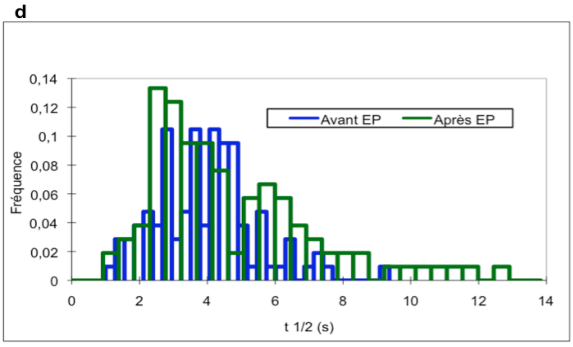

e

Variable	Observations	Obs. avec données manquantes	Obs. sans données manquantes	Minimum	Maximum	Moyenne	Ecart-type
t1/2 avant EP	105	0	105	1,210	9,266	3,950	1,485
t1/2 après EP	105	0	105	1,130	12,830	4,661	2,416

f

Test de Wilcoxon	
V	2473
Espérance	2997,5
Variance (V)	109408,75
p-value(bilatérale)	0,113
alpha	0,05

Figure III-18: Effet de l'interaction plasmide/membrane sur la mobilité latérale de la protéine membranaire Rae1-eGFP dans les régions membranaires perméabilisées face à l'anode (A) et face à la cathode (B). Des cellules CHO Rae1-eGFP adhérentes sont soumises à 10 impulsions électriques de 5 ms à une fréquence de 1 Hz et à une intensité électrique de 0,4 kV/cm, en présence de 5 µg de plasmide peGFP-C1 marqué au Cy3, sous un microscope confocal Zeiss LSM 510M. Avant et après l'application des impulsions électriques, des mesures de FRAP nous permettent de déterminer la fraction mobile, M (a-c) et le temps de demi-retour, t 1/2 (d-f). Une distribution des valeurs de M et t 1/2 obtenues avant et après électroperméabilisation est réalisée (a et d). L'ensemble des valeurs de M et de t 1/2 obtenues avant et après électroperméabilisation sont moyennés et les écart-types sont déterminés (b et e). Afin de déterminer la significativité des résultats, un test de Wilcoxon a été réalisé (c et f).

Le test statistique de Wilcoxon montre que les résultats obtenus après l'électroperméabilisation sont significativement différents de ceux obtenus avant l'électroperméabilisation. Ces variations significatives des deux distributions des valeurs de M et de $t_{1/2}$ sont observées dans les régions membranaires perméabilisées qui font face à l'anode et face à la cathode (Figures III-17A et III-17B).

2.2. Electrotransfert de plasmide

Tout d'abord, des mesures de FRAP sont réalisées dans les régions membranaires qui font face aux électrodes, i.e. anode (Figure III-18A) et cathode (Figure III-18B). Puis, Les cellules CHO Rae1-eGFP adhérentes sont électroperméabilisées en présence de 5 µg de plasmide peGFP-C1 marqué covalemment avec le fluorophore Cy-3. Enfin, des mesures de FRAP sont réalisées dans les régions membranaires perméabilisées. Etant donné que l'interaction plasmide/membrane a lieu uniquement dans la région membranaire perméabilisée face à la cathode, nous avons placé les ROI entre deux complexes plasmide/membrane.

Lorsque l'interaction plasmide/membrane a lieu, la distribution des valeurs de fraction mobile (avant EP: 0,907±0,095 vs après EP: 0,885±0,093) et celle des valeurs du temps de demi-retour (avant EP: 4,332±1,889 s vs après EP: 4,447±2,171 s) dans la région membranaire perméabilisée face à l'anode ne sont significativement pas différentes du contrôle (Figure III-18A). Si la région membranaire perméabilisée située face à la cathode est considérée, la distribution des valeurs de fraction mobile dans cette région membranaire tend significativement vers des valeurs plus faibles quand l'interaction plasmide/membrane a lieu (avant EP: 0,910±0,102 vs après EP: 0,870±0,121) (Figures III-18B.a-c). En revanche, la distribution des valeurs du temps de demi-retour ne semble pas être affectée par la présence des complexes plasmide/membrane dans cette région membranaire (avant EP: 3,950±1,485 s vs 4,661±2,416 s) (Figures III-18B.d-f).

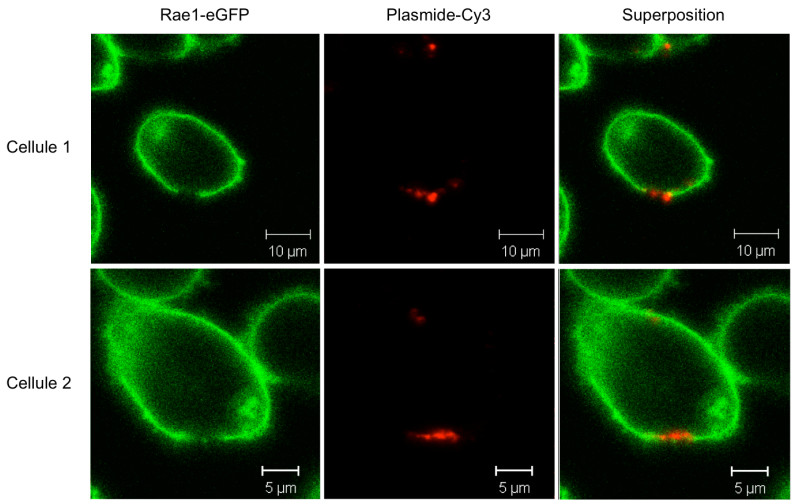

Figure III-19: Visualisation de l'interaction plasmide/membrane sur des cellules CHO Rae1-eGFP. Des cellules CHO Rae1-eGFP adhérentes sont soumises à 10 impulsions électriques de 5 ms à une fréquence de 1 Hz et à une intensité électrique de 0,4 kV/cm, en présence de 5 µg de plasmide peGFP-C1 marqué au Cy3, sous un microscope confocal Zeiss LSM 510M.

3. Discussion et conclusions

Lorsque des cellules sont soumises à des impulsions électriques, ces dernières induisent des défauts membranaires *(Teissié et al., 2005)* ou "électropores" *(Neumann et al., 1989)* qui sont à l'origine d'une perméabilisation transitoire de la membrane plasmique. Ces défauts membranaires électro-induits pourraient constituer des obstacles à la diffusion latérale des protéines membranaires.

Dans la première partie de cette étude, les résultats montrent que l'électroperméabilisation de la membrane plasmique induit une augmentation significative du temps de demi-retour et une diminution significative de la fraction mobile des protéines membranaires Rae1-eGFP. Ces données peuvent s'expliquer par le fait que les défauts membranaires électro-induits allongent artificiellement le parcours des protéines membranaires Rae1-eGFP et par conséquent leur coefficient de diffusion latérale est plus faible. Il a été montré que la présence d'obstacles impénétrables diminues le coefficient de diffusion mesuré *(Saxton et al., 1982, 1993)*. Certaines de ces protéines membranaires ne peuvent plus sortir de la zone photodétruite durant le temps de l'expérience (i.e. 40 secondes) à cause la présence d'une quantité importante de défauts membranaires électro-induits. Ceci a pour conséquence une diminution de la fraction mobile.

Lorsque des cellules sont soumises à des impulsions électriques en présence de molécules de plasmide, ces dernières viennent interagir sous la forme de complexes plasmide/membrane distincts dans la région membranaire perméabilisée face à la cathode. La présence de molécules de plasmides insérées dans la membrane plasmique perméabilisée peut perturber la mobilité latérale des protéines membranaires. Nos résultats montrent que le temps moyen de retour n'est pas significativement différent pour des protéines membranaires qui diffusent latéralement dans la région membranaire perméabilisée qui fait face à la cathode. Cependant, la diminution de la fraction mobile signifie que le nombre de protéines membranaires qui diffusent dans cette région membranaire est diminué par la présence de molécules de plasmide. Dans ce cas deux hypothèses peuvent être émises:`

(i) L'absence de variation du temps de demi-retour est siginificative, alors seul la fraction mobile décroit et dans ce cas, sachant que les molécules de plasmide présentes à la surface des cellules après électroperméabilisation ne diffusent pas du tout, deux types

de protéines peuvent êtres distinguées: Des protéines mobiles, qui ont le même coefficient de diffusion avant et après électroperméabilisation et des protéines piégées par les molécules de plasmide, qui explique la diminution de la fraction mobile. Cette hypothèse montre l'existence d'une éventuelle interaction plasmide/protéine membranaire. Elle pourra être confirmée ou non par une étude de FRET (i.e. Förster Resonnance Energy Transfer) entre les protéines Rae1-eGFP et les molécules de plasmides marquées au Cy-3 (Figure III-19).

(ii) L'absence de variation du temps de demi-retour est liée à un sous échantillonnage statistique et la tendance observée montre ici que le temps demi-retour croît même si cela n'est pas statistiquement significatif. Dans ce cas alors, les molécules de plasmide jouent le même rôle que les défauts membranaires sur la diffusion de la protéine membrane Rae-1.

Il faut noter que les effets à l'anode ne sont plus vu lors de l'électrotransfert de plasmide ceci est lié à des problèmes expérimentaux. En effet, après avoir réalisé des mesures de FRAP sur une cellule avant l'électroperméabilisation, nous appliquons des impulsions électriques en présence de molécules de plasmides fluorescents. Cependant, l'interaction plasmide/membrane n'a forcément pas lieu sur la cellule que nous avons choisi. Nous cherchons donc une cellule sur laquelle les complexes plasmide/membrane se sont formés. Par conséquent, contrairement à l'étude précédente, les mesures de FRAP sont effectuées 2 à 4 minutes après l'électroperméabilisation sur une autre cellule. Il est donc probable que les effets des défauts membranaires électro-induits sur la mobilité latérale des protéines dans la région membranaire face à l'anode se sont dissipés.

Une des perspectives à cette étude serait l'utilisation du FRAP à rayon variable. En effet, une mesure des variations de fraction mobile et de temps de demi-retour en fonction de l'espace permet d'avoir une idée sur les tailles de confinement vues par la protéine Rae-1 *(Salomé et al., 1988)*. Ce type d'étude, complété par des simulations numériques, permettrait d'avoir des informations indirectes sur la densité des défauts membranaires et éventuellement leur taille moyenne.

L'électroperméabilisation et l'interaction plasmide/membrane perturbent la mobilité latérale des protéines membranaires du feuillet externe de la membrane plasmique.

PARTIE IV

TRANSFERT DE PLASMIDE IN VITRO

PAR ÉLECTRO-SONOPORATION

Partie IV. Transfert de plasmide *in vitro* par électro-sonoporation

1. Introduction

La sonoporation est une autre méthode physique qui permet un transfert efficace et sûr de plasmides dans les cellules et les tissus *(Newman et Bettinger, 2007; Osawa et al., 2009; Delalande et al., 2009)*. Cette méthode consiste en une application rationnelle d'ondes ultrasonores en présence d'agents de contraste *(Kaddur et al., 2007)*. Sous les effets des ondes ultrasonores, les agents de contraste oscillants au contact de la membrane plasmique induisent une contrainte mécanique sur la membrane plasmique *(Tran et al., 2007; Tran et al., 2008)*. Cette contrainte induit une augmentation de la perméabilité de la membrane plasmique en créant probablement des pores membranaires et/ou en stimulant des mécanismes d'endocytose *(Meijering et al., 2009)*. Contrairement à l'électroperméabilisation, la sonoporation permet une entrée directe des molécules de plasmide dans le cytoplasme sans interaction préalable avec la membrane plasmique pendant l'application des ondes ultrasonores *(Mehier-Humbert et al., 2005)*.

Récemment, Yamashita et colloborateurs ont proposé de combiner l'électroperméabilisation avec la sonoporation afin d'augmenter l'efficacité du transfert de plasmide dans le muscle squelettique de souris *(Yamashita et al., 2002)*. Les résultats ont montré que l'électro-sonoporation induit une augmentation de l'efficacité de transfection d'un facteur 8 par rapport à l'électroperméabilisation seule et d'un facteur 6 par rapport à la sonoporation seule. Les auteurs ont suggéré que cette augmentation de l'efficacité de transfection par électro-sonoporation est liée à une diminution des dommages des tissus causés par l'électroperméabilisation *(Yamashita et al., 2002)*.

Sur la base de récents résultats obtenus sur les mécanismes biophysiques du transfert de plasmide par électroperméabilisation *(Golzio et al., 2002; Faurie et al., 2004; Faurie et al., 2009)* et par sonoporation *(Meijering et al., 2009; Tran et al., 2007; Tran et al., 2008; Deng et al., 2004),* nous avons défini comme objectif d'étudier l'efficacité de la combinaison de l'électroperméabilisation avec la sonoporation (appelé électro-sonoporation) dans le transfert de plasmide *in vitro*. Notre stratégie a consisté à

comparer l'efficacité de l'électro-sonoporation dans le transfert du plasmide peGFP-C1 dans les cellules CHO avec celles de l'électroperméabilisation et de la sonoporation seule, par cytométrie de flux et par microscopie de fluorescence.

L'ensemble des résultats obtenus dans cette étude a fait l'objet d'une publication soumise à *Ultrasound in Medicine and Biology* en janvier 2010.

2. La publication

IN VITRO GENE TRANSFER BY ELECTRO-SONOPORATION

J.M. Escoffre[1], K. Kaddur[2], M.P. Rols[1*], A. Bouakaz[2]

[1]CNRS; IPBS (Institut de Pharmacologie et de Biologie Structurale); 205 route de Narbonne, F-31077, Toulouse, France; Université de Toulouse; UPS; IPBS; F-31077, Toulouse, France.

[2]Inserm U930, CNRS ERL3106-Université François Rabelais de Tours, CHU Bretonneau, 2 bd Tonnellé, 37044 Tours Cedex 9, France.

*Corresponding author:

M.P. Rols. CNRS; IPBS (Institut de Pharmacologie et de Biologie Structurale); 205 route de Narbonne, F-31077, Toulouse, France; Université de Toulouse; UPS; IPBS; F-31077, Toulouse, France.E-mail: rols@ipbs.fr; Tel: +33561175811; Fax: +3361175994

ABSTRACT

To upregulate the expression of transfected gene, we investigated the applicability of electro-sonoporation. This approach consists of a combination of electric pulses and ultrasound assisted with gas microbubbles. Cells were firstly submitted to electrical pulses with plasmid DNA encoding eGFP and then sonoporated in presence of contrast microbubbles. 24 later, cells that received electro-sonoporationdemonstrated a 4-fold increase in transfection level (percentage of eGFP positives cells) and a 6-fold increase in transfection efficiency (associated fluorescence intensity) in comparison to cells having undergone electroporation alone. While electroporation induced the interaction of DNA with the cell membrane, sonoporation induced its direct propulsion into the cell cytoplasm and the nucleus. Sonoporation can improve the transfer of DNA in interaction with electroporated membrane by allowing its free and rapid entrance into the cells. These results demonstrate that in vitro gene transfer by electro-sonoporation could provide a new potent method for gene transfer.

Key words: Sonoporation, electroporation, ultrasound, contrast agent, gene transfer

INTRODUCTION

The controlled use of electric pulses as a safe and efficient tool to deliver plasmid DNA to target cells and tissues has rapidly evolved over the last decade (Neumann et al. 1982; Daud et al. 2008; Rosati et al. 2009). The method, called electroporation refers to the transient increase in the permeability of cell membranes (Neumann et al. 2007; Escoffre et al. 2007; Mir 2009). Despite the development of clinical trials, the biophysical mechanisms underlying membrane permeabilization and gene transfer with electroporation are still not fully understood (Teissie et al. 2005). Elucidation of these mechanisms is of high importance for *in vitro* use in terms of efficiency and also for *in vivo* use in terms of safety. Performed at the single cell level, current studies have yielded a phenomenological description of gene electrotransfer (Golzio et al. 2002; Faurie et al. 2010; Escoffre et al. 2009a). Indeed, plasmid DNA requires a number of consecutive steps before reaching the cell nucleus: membrane permeabilization, electrophoretic migration towards the cell, insertion into the permeabilized membrane, translocation across the membrane, migration towards the nucleus and finally transfer across the nuclear envelope (Golzio et al. 2002). Therefore, plasmid DNA does not enter into the cell during exposure to electric pulses but it is "trapped into" the permeabilized membrane (Faurie et al. 2004). It is not homogeneously distributed on the permeabilized membrane but is present into "competent sites" whose size range from 0.1 to 0.5 µm (Golzio et al. 2002). Recent investigation revealed the existence of two classes of plasmid DNA/membrane interaction: (i) a metastable plasmid DNA/membrane complex from which plasmid DNA can leave and return to external medium and (ii) a stable plasmid DNA/membrane complex, where plasmid DNA cannot be removed even by applying electric pulses of reversed polarity. Only plasmid DNA belonging to the second class leads to effective gene expression (Faurie et al. 2010). This DNA/membrane interaction that is a requisite step but not sufficient to get gene expression, showed clearly that the plasma membrane is a physical barrier to plasmid DNA entry.

Just like electroporation, the sonoporation is another promising physical method to deliver therapeutic genes into cells and tissues (Newmann et al. 2007; Osawa et al. 2009; Delalande et al. 2010). This method consists of the rational application of ultrasound waves in presence of gas microbubbles (Van Wamel et al. 2006; Kaddur et al. 2007; Karshafian et al. 2009). Under the effect of ultrasound waves, the oscillating

microbubbles in contact with plasma membrane induce a mechanical constraint on the cell membrane (Tran et al. 2007; Tran et al. 2008). This membrane stimulation enhances its permeability through likely the creation of membrane transient pores and likely the stimulation of endocytosis mechanisms (Meijering et al. 2009). Current studies indicate that in contrary to the electroporation, the plasmid molecules are propelled directly into the cytoplasm creating by that clusters (Mehier-Humbert et al. 2009). The combination of both physical methods as a mean to transfer molecules and genes into the cells has not been sufficiently explored. Recently, Yamashita and co-workers investigated the applicability of *in vivo* electroporation and sonoporation (electro-sonoporation) (Yamashita et al. 2002). The approach consisted of a combination of electric pulses and ultrasound waves, for gene transfer into skeletal muscle of mice. They demonstrated that mice that had undergone electro-sonoporation showed 8-fold and 1.6-fold higher gene expression level compared to mice that underwent electroporation alone and sonoporation alone, respectively. The authors suggested that the upregulation of the gene expression level induced by electro-sonoporation is the consequence of the decrease of tissue damage (Yamashita et al. 2002).

Based on the current data and the recent findings on the biophysical mechanisms of gene transfer by electroporation (Golzio et al. 2002; Faurie et al. 2010; Faurie et al. 2004) and through sonoporation (Tran et al. 2007; Tran et al. 2008; Meijering et al. 2009; Deng et al. 2004), we investigated the effectiveness of electro-sonoporation for the delivery of plasmid DNA coding eGFP protein in CHO cells. The gene delivery and expression were monitored in living cells by fluorescence microscopy and flow cytometry. This approach allowed us to address several questions: (1) Does the sonoporation with gas microbubbles improve the transfection level and efficiency of CHO cells induced by the electroporation? (2) Is any transfection improvement induced by an enhancement of the uptake of plasmid DNA aggregates induced by electroporation?

MATERIALS AND METHODS

Cell culture

Chinese hamster ovary (CHO) cells were used. The WTT clone was selected for its ability to grow in suspension or in adherence on Petri dishes or on microscope glass cover slip. The cells were grown in suspension in Eagle medium (MEM 1011, Eurobio,

Les Ulis, France) supplemented with 3.5 g/L glucose (Sigma-Aldrich, St-Louis, USA), 2.95 g/L tryptose phosphate (Sigma-Aldrich, St-Louis, USA), 8% SVF (Lonza Group Ltd, Basl, Switzerland), 0.8 mg/mL L-glutamine (Eurobio, Les Ulis, France), 100 u/mL penicillin (Sigma-Aldrich, St-Louis, USA) and 100 mg/mL streptomycine (Sigma-Aldrich, St-Louis, USA), 1X BME vitamins (Sigma-Aldrich, St-Louis, USA) (Rols et al. 1995). Their ability to grow on a support after being maintained in suspension is a direct evidence of their viability.

Plasmid DNA preparation and staining

A 4.7 kpb plasmid, pEGFP-C1 (Clonetech, Palo Alto, USA), carrying the gene of the Green Fluorescent Protein under the control of the CMV promoter, was stained stoichiometrically with the DNA intercalating thiazole orange homodimer dye TOTO-1 (Molecular Probes, Eugene, USA). The staining was carried out during 60 min on ice at a base pair to dye ratio of 5 (Rye et al. 1992; Escoffre et al. 2009b). Plasmid was prepared from transformed E. coli using Maxiprep DNA purification system according to the manufacturer's instructions (Qiagen, Chatsworth, USA).

Electroporation procedure

Electroporation was performed using a CNRS cell electropulsator (Jouan, St Herblain, France), which delivers square electric pulses. The pulse shapes were monitored using an oscilloscope (Enertec, St-Etienne, France). Stainless steel rods parallel electrodes (diameter 0.5 mm, length 10 mm, inter-electrode distance 7 mm) were connected to the voltage pulse generator. CHO cells were electropulsed by the application of millisecond electric pulses required to load macromolecules into CHO cells. Optimal excitation parameters for CHO cells were determined separately and consisted of 10 pulses lasting 5 ms at a repetition frequency of 1 Hz at 0.7 kV/cm at room temperature (Rols et al. 1992; Hui 1995).

CHO cells in the suspension were centrifuged at 120 g during 5 min. The cell pellet was resuspended in the pulsation buffer (10 mM K_2HPO_4/KH_2PO_4, 1 mM $MgCl_2$, 250 mM sucrose, pH 7.4) containing 20 µg/mL of pEGFP-C1 plasmid to a density of 5.10^6/mL. A volume of 100 µL of cell suspension was placed between the electrodes for electroporation. After electroporation, the cells were incubated during 5 minutes and then cultured in 35 mm Petri dish (Becton Dickinson Labware, Franklin Lakes, USA) with 1.5 mL of culture medium for 24h at 37°C in a 5% CO_2 incubator.

Sonoporation procedure

BR14 microbubbles (Bracco Research, Geneva, Switzerland) generously provided by Bracco Research, were used. They are composed of perfluorobutane gas encapsulated in a phospholipid monolayer. BR14 microbubbles have a mean diameter of 2.6 µm with 99 % having a diameter less than 12 µm (Schneider et al. 1997; Tsunoda et al. 2005). The microbubbles' suspension was prepared few minutes before experimentation by mixing the powder with NaCl (0.09 %) giving approximately 2.10^8 microbubbles per ml. We evaluated the effect of microbubbles concentration expressed in terms of number of bubbles per cell. US waves were generated from an unfocused single element transducer of 15 mm in diameter with a center frequency of 1 MHz (Vermon, Tours, France). The natural focal distance of the transducer was measured at 30 mm. The transducer was driven with an electrical signal generated by an arbitrary waveform generator (Agilent, Santa Clara, CA, USA) and amplified with a power amplifier (ADECE, Artannes, France). The negative peak pressure of the US wave was measured in a separate set-up with a calibrated PDVF needle hydrophone (diameter = 0.2 mm) (Precision Acoustics Ltd., Dorschester, United Kingdom).

CHO suspended cells (5.10^5 cells in 1.5 ml) were introduced in a holder containing the cell medium (Invitrogen, Cergy-Pontoise, France). The center of the plastic tube serving as a holder and containing cells was placed at the focal distance of the transducer. This tube had the following dimensions: 45 mm height, 10 mm internal width and 12 mm external width. Plasmid gene and microbubbles were added at the required concentration just before insonation. After the end of ultrasound exposure, the cells were cultured in a 35 mm Petri dish (Becton Dickinson Labware, Franklin Lakes, USA) with 1.5 mL of culture medium for 24h at 37°C in a 5% CO_2 incubator.

Electro-sonoporation procedure

The electro-sonoporation is a successive combination of electroporation and sonoporation in order to improve the transfection efficiency. The electro-sonoporation was carried out by reproducing the optimal sonoporation and electroporation conditions. CHO cells were submitted to electric pulses in presence of 20 µg/mL of pEGFP-C1 plasmid. Before the sonoporation, electropulsed cells were washed by centrifugation (120 g, 5 min) to remove the free plasmid in the bulk solution. Then, the cell pellet was resuspended in 1.5 mL of culture medium with 1% SVF before applying sonoporation.

Fluorescence microscopy

For microscopic observations, the Petri dish was placed on the stage of an inverted digitized fluorescence videomicroscope (Leica DMIRB, Wetzlar, Germany). The cells were observed with a Leica 40 times objective. The wavelengths were selected by using the Leica L4 filter block for the TOTO-1 labeled DNA and GFP-expressing cells. The images were recorded with a MetaMorph acquisition software (Version 7.04r4 © 1992-2006 Molecular Devices) equipped with a Photometrics cooled CCD camera (Princeton instrument, Inc., city and country) and a computer-controlled excitation light shutter (Leica, EL 6000, Wetzlar, Germany).

Flow cytometer

Only plated cells (i.e., viable cells) were taken into account in the assay for quantification. The cells were harvested by trypsinization and analyzed by flow cytometry to evaluate both the percentage of transfection (i.e., percentage of GFP-expressing cells) and the gene expression (i.e., mean level of fluorescence associated with this transfection).

Viability assay

Cell viability was determined by propidium iodide (PI) (Sigma-Aldrich, St-Louis, USA) exclusion. The supernatant was removed and the cells were harvested by trypsinization. Supernatant and trypsinized cells were mixed and labeled with 100 µM propidium iodide. The sample was kept in the dark at room temperature for 10 min. PI-labeled cells were analyzed by flow cytometry to evaluate the percentage of dead cells.

RESULTS

Optimal electrical and acoustical parameters for gene transfer into CHO cells.

Electroporation and sonoporation parameters were varied to obtain optimal gene transfer into CHO cells. The optimization of electroporation previously revealed that 10 electrical pulses during 5 ms at a repetition frequency of 1 Hz and at 0.7 kV/cm intensity were the optimal conditions to incorporate plasmid pEGFP-C1 into CHO cells (Faurie et al. 2002; Hui 1995; Rols et al. 1992).

The optimal exposure parameters for sonoporation were obtained by varying the acoustic parameters including acoustic pressure, exposition time, duration of pulse

repetition and number of cycles (Table 1, conditions A-G) and the concentration of BR14 microbubbles given by the number of microbubbles per cell (Table 1, condition H). Figure 1A shows direct observation of transfected cells with fluorescence microscopy. Figure 1B shows the percentage of transfected cells (i.e. transfection level) and Figure 1C, the associated fluorescence intensity (i.e. transfection efficiency) obtained following sonoporation. The results (Figures 1B and 1C) reveal that an increase in the acoustic pressure from 0.4 MPa (condition A) to 0.6 MPa (condition B), while maintaining other exposure conditions constant, induced 3-fold increase in the transfection level (9.6±0.8% vs 32.2±0.9%) and 4-fold enhancement of the transfection efficiency (279±41 vs 1336±42 a.u.). The application of acoustic pressures above 0.6 MPa caused a slight decrease of both the transfection level (24±2% at 0.7 MPa and 25,5±1.4% at 0.8 MPa) and efficiency (928±72 a.u. at 0.7 MPa and 1096±87 a.u. at 0.8 MPa). The prolongation of exposition time from 1 min (condition B) to 2 min (condition C) did not enhance the transfection level (32.3±1% vs 34.7±1.3%), nor the transfection efficiency (1336±42 a.u. vs 1444±107 a.u.). Nevertheless, the decrease of the duty cycle from 40% (condition D) to 0.02% (conditions F and G) induced a very low transfection level and a low efficiency. This was associated to alteration of cells as shown in Figure 1A (condition G). The number of BR14 microbubbles per cell is an important parameter for gene transfer by sonoporation. Indeed, a 2-fold decrease of the microbubbles concentration (conditions B and H) induced a reduction of transfection level and efficiency by 30%. Therefore, the optimal transfection level (35±1%) and transfection efficiency (1444±107 a.u.) were obtained for the following excitation parameters: acoustic pressure, 0.6 MPa; duty cycle, 40%; repetition rate, 100 µs; exposition time, 2 min and 20 BR14 microbubbles/cell.

In vitro gene transfer by electro-sonoporation

Electroporation and sonoporation were applied successively using the optimal electrical conditions (10 pulses lasting 5 ms at a frequency of 1 Hz and at 0.7 kV/cm) and the optimal acoustic conditions (0.6 MPa, 40% duty cycle for 100 µs of repetition during 2 minutes) in presence of 2 or 45 µg of pEGFP-C1. Figure 1A displays a direct observation of transfected cells with fluorescence microscopy. Figures 2B and 2C show that the transfection level and the efficiency of sonoporated cells were respectively 2-fold and 6-fold higher than those of electroporated cells (14±2% vs 7±3% and 505±280 a.u. vs 88±36 a.u.). The sonoporation alone induced twice more dead cells than the electroporation alone (5±2% vs 2.5±1%) (Figure 2D). The combination of the electroporation and sonoporation

(but without centrifugation between both procedures) induced a 3-fold and 6-fold increase of transfection level and efficiency, respectively, compared to the electroporation alone. When a centrifugation was performed between the electroporation and the sonoporation procedures to eliminate the free plasmids in the bulk solution (i.e. plasmid molecules that did not interact with the cells after electroporation), the transfection level and efficiency were 2-fold lower than those obtained by electro-sonoporation without centrifugation but still 2-fold higher than those obtained by electroporation alone. This drop was correlated with a 2-fold increase of dead cells, compared to electro-sonoporation alone (Figure 1D). When the electroporation was combined with sonoporation without BR14 microbubbles and centrifugation, the transfection level and efficiency were quite similar to those achieved with electro-sonoporation with centrifugation. However, under these conditions, the percentage of dead cells was reduced by 4.5-fold (Figure 2D). These results suggested that sonoporation improved the transfection level and efficiency obtained by electroporation while improving cell viability (Figure 2).

Trafficking of fluorescent plasmid after electro-sonoporation

To visualize the plasmid uptake, plasmids were labeled with the fluorescent marker, TOTO-1. When the CHO cells were electroporated in presence of fluorescent plasmids, DNA aggregates were visualized at the cell membrane level as previously described (Golzio et al. 2002) (see Figures 3A and 3D). This result confirms that the plasmid molecules did not enter during the application of the electric pulses and confirms the results of Golzio et al (Golzio et al. 2002). Indeed, plasmid DNA uptake has been described like a post-pulse process occurring several tens of minutes following pulse delivery (Faurie et al. 2010). At the opposite, the plasmid molecules were visualized in the cytoplasm of sonoporated cells immediately after ultrasound application (Figures 3B and 3E). This result showed that the sonoporation induced permeant structures that allowed a direct access of plasmids to cytoplasm. When, the electroporation was associated with the sonoporation, DNA aggregates were no more observed at the membrane level, but the fluorescent plasmids were visualized into the cytoplasm (Figures 3C and 3F). This data highlighted that sonoporation could be facilitated and thus accelerates the uptake of electro-induced DNA aggregates into the cytoplasm.

DISCUSSION AND CONCLUSIONS

The clinical development of gene therapy requires the development of news gene delivery methods or the improvement of existing approaches. These methods have to allow an efficient and safe gene delivery into tissues and organs.

Since the last decade, various investigations proposed the combination of different delivery methods to improve the efficiency and/or the safety of these methods. Among the non-viral methods of gene transfer, two physical methods based on the rational use of electric fields and ultrasound waves have been widely developed mainly for their easiness to use, inexpensiveness and safety. To upregulate the expression levels of transfected gene, we investigated the applicability of electro-sonoporation, which consists of a combination of electric pulses and ultrasound waves assisted with gas microbubbles, for reporter gene transfer. CHO cells that received electro-sonoporation demonstrated a 4-fold increase in transfection level and a 6-fold increase in transfection efficiency compared to CHO cells having undergone electroporation alone as shown in Figure 2. Trafficking results showed that electroporation induced the formation of plasmid DNA aggregates in the electroporated membrane, while sonoporation induced direct propulsion of the plasmid DNA into the cell cytoplasm and the nucleus (Figure 3). Electroporation process is known to be a multi-step process including the transient interaction of plasmid DNA with the electroporated membrane before its entrance into the cells. Sonoporation process is known to allow the direct and free entrance of plasmid DNA into the cells. The data reported in this study suggests that sonoporation can affect the delivery of the fluorescent plasmid DNA aggregates by allowing its free and rapid entrance into the cells (Figure 4). Therefore, transfection improvement as achieved with sonoporation after the electroporation could be ascribed to the increase of plasmid DNA accessibility into cells. These results demonstrate for the first time that *in vitro* gene transfer by electro-sonoporation could provide a new potent method for gene transfer.

Yamashita and coworkers investigated the potentiality of electro-sonoporation for *in vivo* interleukin-12 (IL-12) gene transfer (Yamashita et al. 2002). They demonstrated that mice that had undergone electro-sonoporation showed 8-fold higher serum mouse IL-12 rate compared to mice that underwent electroporation alone. Moreover, the degree of muscle damage of electroporated mice was higher than that of electro-sonoporated mice. The authors suggested that the upregulation of IL-12 expression was correlated to the reduction of tissue damage that leads to cellular death.

Nevertheless, further studies are still needed to elucidate the mechanism of the reduction of tissue damage resulting from the use of electroporation and ultrasound (Yamashita et al. 2004). However, in agreement with our results, we did not exclude that transfection improvement as achieved with sonoporation could be ascribed to the increase of plasmid DNA accessibility into muscle fibers.

Thus, using a different experimental protocol, Yamashita and coworkers described the treatment of murine orthotopic hepatocellular carcinoma (HCC) by muscle-targeted mouse interleukin-12 (mIL-12) gene transfer using *in vivo* electro-sonoporation (Yamashita et al. 2004). Their results showed that the intramuscular administration of mIL-12 gene with electro-sonoporation induced an enhancement of serum IL-12 and IFN-γ rates. This IL-12 gene therapy induced systemic tumor immunity, lymphocytic infiltration into tumors and antiangiogenetic effects that significantly prolonged of the survival periods with both growth inhibition of murine orthotopic hepatocellular carcinoma and inhibition of spontaneous lung metastasis (Yamashita et al. 2004).

In summary, our data suggested that electro-sonoporation upregulated gene expression compared to the electroporation alone. This transfection improvement as achieved with sonoporation and electroporation could be ascribed to the increase of plasmid DNA incorporation into the cells. These results demonstrated that gene transfer by electro-sonoporation might be a new strategy of gene therapy.

ACKNOWLEDGMENT

The authors would like to thank C. Millot for help with the cell culture. The Association Française sur les Myopathies (to MPR) have supported this work. JM Escoffre is the recipient of an allocation de recherche du Ministère de l'Enseignement Supérieur et de la Recherche. The authors are also grateful to the financial support of the Institut National du Cancer (INCa projet N. R07025NN) and to Bracco Research Geneva for supplying BR14 microbubbles.

REFERENCES

Daud Al, DeConti RC, Andrews S, Urbas P, Riker Al, Sondak VK, Munster PN, Sullivan DM, Ugen KE, Messina JL, Heller R. Phase I trial of interleukin-12 plasmid electroporation in patients with metastatic melanoma. J Clin Oncol 2008;26:5896-58903.

Delalande A, Bureau MF, Midoux P, Bouakaz A, Pichon C. Ultasound-assisted microbubbles gene transfer in tendons for gene therapy. Ultrasonics 2010;50:269-272.

Deng CX, Sieling F, Pan H, Cui J. Ultrasound-induced cell membrane porosity. Ultrasound Med Biol 2004;30:519-526.

Escoffre JM, Hubert M, Dean DS, Rols MP, Favard C. Membrane perturbation by an external electric field: a mechanism to permit molecular uptake. Eur Biophys J 2007;36:973-983.

Escoffre JM, Portet T, Wasungu L, Teissié J, Dean D, Rols MP. What is (still not) known of the mechanism by which electroporation mediates gene transfer and expression in cells and tissues. Mol Biotechnol 2009a;41:286-295.

Escoffre JM, Bellard E, Golzio M, Teissié J, and Rols MP. Transgene expression of transfected supercoiled plasmid DNA concatemers in mammalian cells. J Gene Med 2009b;11:1071-1073.

Faurie C, Phez E, Golzio M, Vossen C, Lesbordes JC, Delteil C, Teissie J, Rols MP. Effect of electric field vectoriality on electrically mediated gene delivery in mammalian cells. Biochim Biophys Acta 2004;1665:92-100.

Faurie C, Rebersek M, Golzio M, Kanduser M, Escoffre JM, Pavlin M, Teissie J, Micklavcic D, Rols MP. Electro-mediated gene transfer and expression are controlled by the the life-time of DNA/membrane complex formation. J Gene Med 2010;12:117-125.

Golzio M, Teissié J, Rols MP. Direct visualization at the single-cell level of electrically mediated gene delivery. Proc Natl Acad Sci USA 2002;99:1292-1297.

Hui S. Effects of pulse length and strength on electroporation efficiency (Methods Mol Biol 55). In: Animal Cell Electroporation & Electrofusion Protocols, vol. 48, J.A. Nicholoff, ed. Humana Press, Clifton, N.J., 1995, pp. 29-40.

Kaddur K, Palanchon P, Tranquart F, Pichon C, Bouakaz A. Sonopermeabilization; therapeutic alternative with ultrasound and microbubbles. J Radiol 2007;88:1777-1786.

Karshafian R, Bevan PD, Williams R, Samac S, Burns PN. Sonoporation by ultsound-activated microbubble contrast agents: effect of acoustic exposure parameters on cell membrane permeability and cell viability. Ultrasound Med Biol 2009;35:847-860.

Mehier-Humbert S, Bettinger T, Yan F, Guy RH. Ultrasound-mediated gene delivery: kinetics of plasmid internalization and gene expression. J Control Release 2005;104:203-211.

Meijering BD, Juffermans LJ, van Wamel A, Henning RH, Zuhorn IS, Emmer M, Versteilen AM, Paulus WJ, van Gilst WH, Kooiman K, de Jong N, Musters RJ, Deelman LE, Kamp O. Ultrasound and microbubbles-targeted delivery of macromolecules is regulated by induction of endocytosis and pore formation. Circ Res 2009;104:679-687.

Mir LM. Nucleics acids electrotransfer-based gene therapy (electrogenetherapy): past, current, and future. Mol Biotechnol 2009;43:167-176.

Neumann E, Shaefer-Ridder M, Wang Y, Hofschneider PH. Gene transfer into mouse lyoma cells by electroporation in high electric fields. EMBO J 1982;1:841-845.

Neumann E, Sowers AE, and Jordan CA. Electroporation and Electrofusion in Cell Biology, Plenum, (1989)

Newman CM, Bettinger T. Gene therapy progress and prospects: Ultrasound for gene transfer. Gene Ther 2007;14:465-475.

Osawa K, Okubo Y, Nakao K, Koyama N, Bessho K. Osteoinduction by microbubble-enhanced transcutaneous sonoporation of human bone morphogenetic protein-2. J Gene Med 2009;11:633-641.

Rols MP, Coulet D, Teissie J. Highly efficient transfection of mammalian cells by electric field pulses. Application to large volumes of cell culture by using a flow system. Eur J Biochem 1992;206:115-121.

Rols MP, Femenia P, Teissie J. Long-lived macropinocytosis takes place in electropermeabilized mammalian cells. Biochem Biophys Res Commun 1995;208:26-35.

Rosati M, Bergamaschi C, Valentin A, Kulkarni V, Jalah R, Alicea C, Patel V, von Gegerfelt AS, Montefiori DC, Venzon DJ, Khan AS, Draghia-Akli R, Van Rompay KK, Felber BK, Pavlakis GN. DNA vaccination in rhesus macaques induces potent immune responses and decreases acute and chronic viremia after SIVmac251 challenge. Proc Natl Acad Sci USA 2009;106:15831-15836.

Rye H, Yue S, Wemmer D, Quesada M, Haugland R, Mathies R, Glazer A. Stable fluorescent complexes of double-stranded DNA with bis-intercalating asymmetric cyanine dyes: properties and applications. Nucleic Acids Res 1992;20:1803-1812.

Schneider M, Broillet A, Bussat P, Glessinger N, Puginier J, Ventrone R, Yan F. Gray-scale liver enhancement in VX2 tumor-bearing rabbits using BR14, a new ultrasonographic contrast agent. Invest Radiol 1997;32:410-417.

Teissié J, Golzio M, Rols MP. Mechanisms of cell membrane electropermeabilization: a minireview of our present (lack of?) knowledge. Biochim Biophys Acta 2005;1724:270-280.

Tran TA, Le Guennec JY, Bougnoux P, Tranquart F, Bouakaz A. Characterization of cell membrane response to ultrasound activated microbubbles. IEEE Trans. Ultrason FerroElectr Control 2008;55:43-49.

Tran TA, Roger S, Le Guennec JY, Tranquart F, Bouakaz A. Effect of ultrasound-activated microbubbles on the cell electrophysiological properties. Ultrasound Med Biol 2007;33:158-163.

Tsunoda S, Mazda O, Oda Y, Iida Y, Akabame S, Kishida T, Shin-Ya M, Asada H, Gojo S. Imanishi J. Matsubara H. Yoshikawa T. Sonoporation using microbubble BR14 promotes pDNA/siRNA transduction to murine heart. Biochem Biophys Res Commun 2005;336:118-127.

Van Wamel A, Kooiman K, Harteveld M, Emmer M, ten Cate FJ, Versluis M, de Jong N. Vibrating microbubbles poking individual cells: drug transfer into cells via sonoporation. J Control Release 2006;112:149-155.

Yamashita YI, Shimada M, Tachibana K, Harimoto N., Tsujita E, Shirabe K, Miyazaki JI, Sugimachi K. In vivo gene transfer into muscle via electro-sonporation Hum Gene Ther 2002;13:2079-2084.

Yamashita YI, Shimada M, Minagawa R, Tsujita E, Harimoto N, Tanaka S, Shirabe K, Miyazaki JI, Maehara Y. Muscle-targeted interleukin-12 gene therapy of orthotopic hepatocellular carcinoma in mice using in vivo electrosonoporation. Mol Cancer Ther 2004;3:177-182.

Table

Table 1: Ultrasound conditions for gene delivery into CHO cells.

Sonoporation	Amp (MPa)	N (Cycles)	Repetition (µs)	Duration (min)	Bubbles (µL)
A	0.4	40	100	1	50
B	0.6	40	100	1	50
C	0.6	40	100	2	50
D	0.7	40	100	1	50
E	0.8	40	100	1	50
F	0.7	10	50 000	1	50
G	0.7	10	50 000	2	50
H	0.6	40	100	1	25

Table 2: *In vitro* gene transfer by electro-sonoporation.

Condition	Protocol
A	Without treatment
B	Sonoporation[¶] with 50 µL bubbles
C	Sonoporation[¶] without 50 µL bubbles and with 45 µg DNA
D	Sonoporation[¶] with 50 µL bubbles and 45 µg DNA
E	Sonoporation[¶] with 50 µL bubbles and 2 µg DNA
F	Electroporation[#] alone
G	Electroporation[#] with 2 µg DNA
H	Electroporation[#] followed by sonoporation[¶] with 50 µL bubbles
I	Electroporation[#] with 2 µg DNA followed by sonoporation[¶] without 50 µL bubbles
J	Electroporation[#] with 2 µg DNA followed by sonoporation[¶] with 50 µL bubbles
K	Electroporation[#] with 2 µg DNA followed by a centrifugation before sonoporation[¶] with 50 µL bubbles

[#]10 x 5ms, 1 Hz, 0.7 kV/cm. [¶]0.6 MPa, 40 cycles, 100 µs, 2 min.

Figures

Figure 1: Determination of optimal acoustic parameters for gene transfer by sonoporation into CHO cells. A suspension of CHO cells was submitted to various acoustic parameters (Table 1) in presence of BR14 microbubbles and plasmid pEGFP-C1 at final concentration of 30 µg/µL. Then, 24h after sonoporation, transfected cells were visualized by fluorescence microscopy (A). The percentage of transfected cells (B) and the associated fluorescence intensity (C) were determined by flow cytometer.

Figure 2: *In vitro* gene transfer by electro-sonoporation. A suspension of CHO cells was submitted to electroporation alone, sonoporation alone or electro-sonoporation (using conditions given in Table 2) in presence of plasmid pEGFP-C1. Then, 24h after sonoporation, transfected cells were visualized by fluorescence microscopy (A). Percentage of transfected cells (B) and the associated fluorescence intensity (C) were determined by flow cytometer. Percentage of dead cells was determined by flow cytometer after propidium iodide staining (D).

Figure 3. Tracking of fluorescent plasmid after gene transfection. pEGFP-C1 molecules were non-covalent labeled with the fluorescent probe TOTO-1. Fluorescent plasmids were transferred into cells by electroporation alone (A, D), by sonoporation (B, E) and by electro-sonoporation (C, F). The localization of fluorescent plasmids was performed using fluorescence microscopy.

Figure 4. Putative mechanism of gene transfer by electro-sonoporation. Electroporation (EP) induced the membrane permeabilization and the electrophoretic migration of plasmid membrane toward the permeabilized membrane. Plasmid DNA/membrane complexes were formed. Then, sonoporation (SN) with gas microbubbles allowed its free and rapid entrance of plasmid DNA aggregates into the cells. Therefore, transfection improvement as achieved with sonoporation after the electroporation could be ascribed to increase of DNA accessibility into CHO cells.

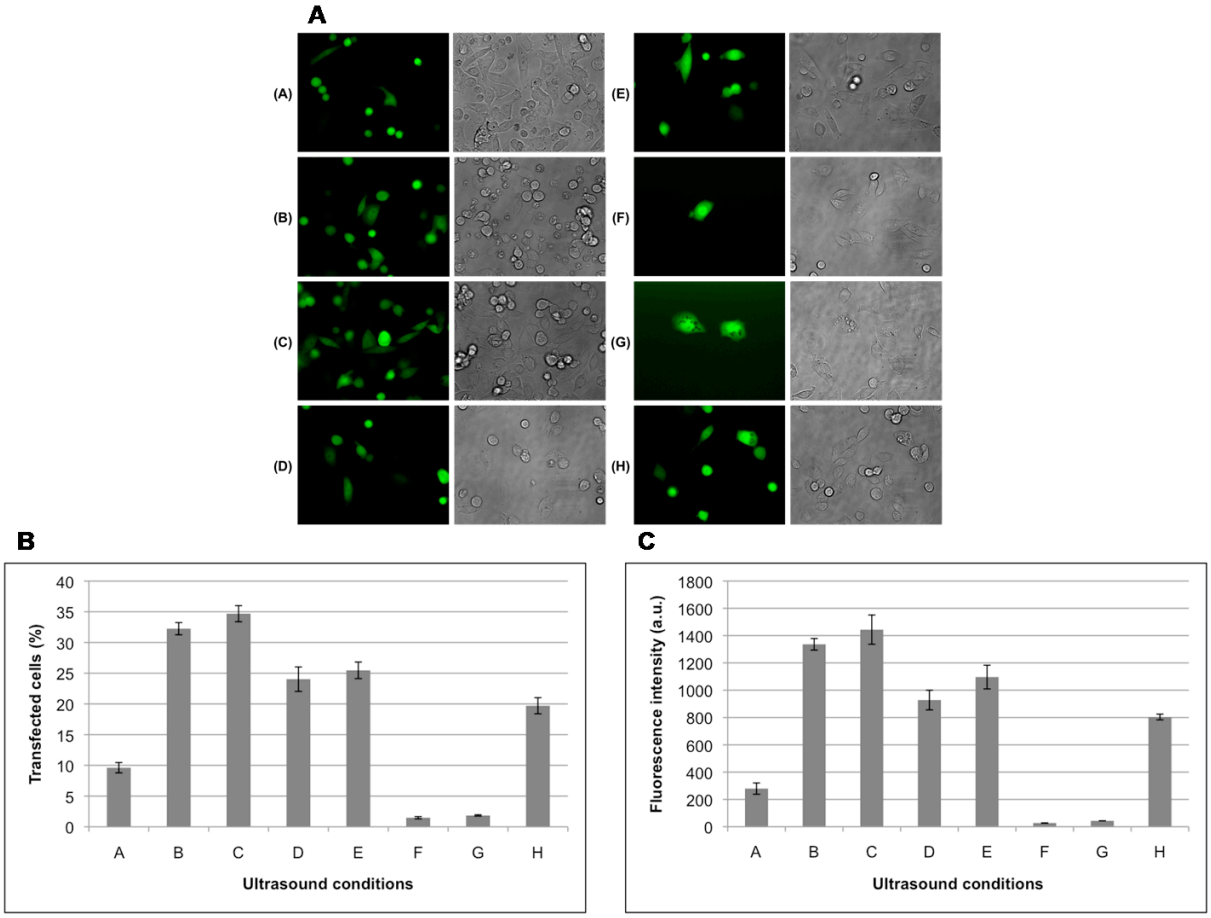
A
(A)
(B)
(C)
(D)
(E)
(F)
(G)
(H)
B
Transfected cells (%)
0
5
10
15
20
25
30
35
40
A
B
C
D
E
F
G
H
Ultrasound conditions
C
Fluorescence intensity (a.u.)
0
200
400
600
800
1000
1200
1400
1600
1800
A
B
C
D
E
F
G
H
Ultrasound conditions

Figure 1

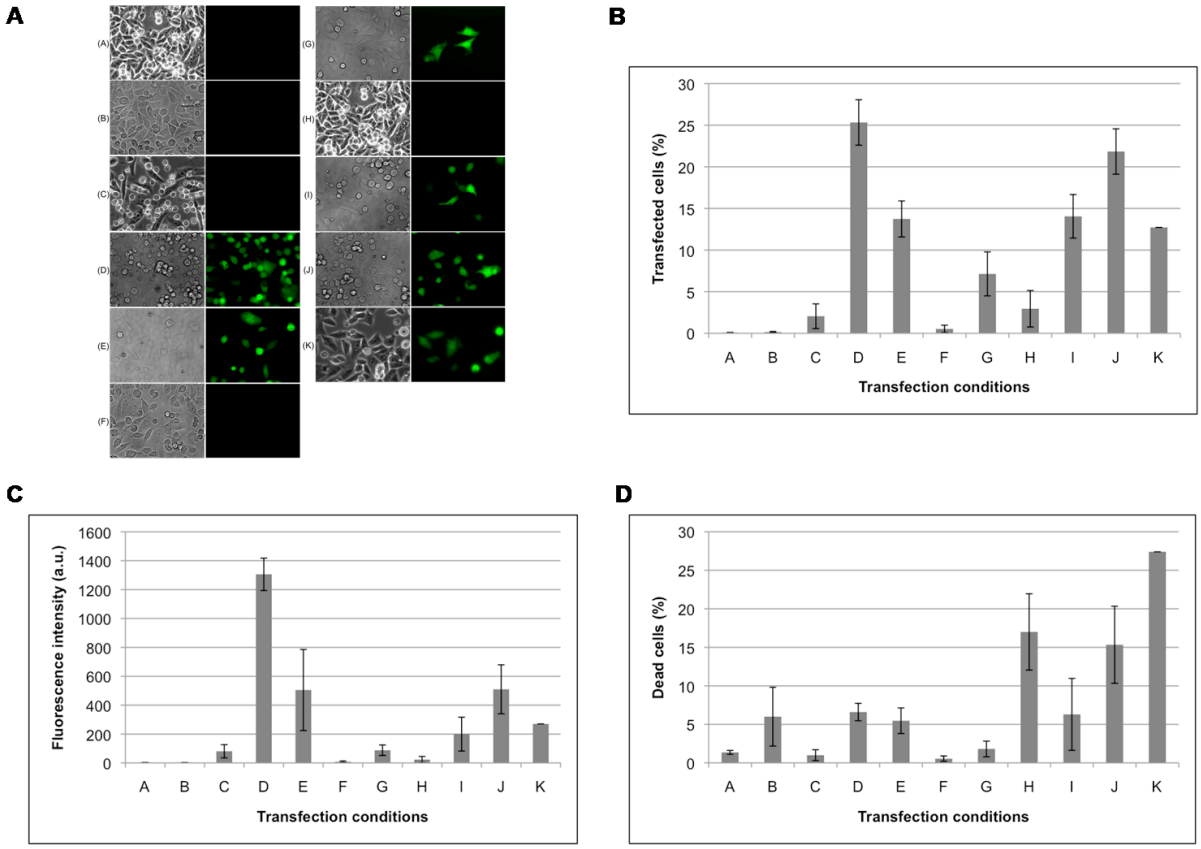
A
B
C
D
Transfected cells (%)
Transfection conditions
Fluorescence intensity (a.u.)
Dead cells (%)
A B C D E F G H I J K

Figure 2

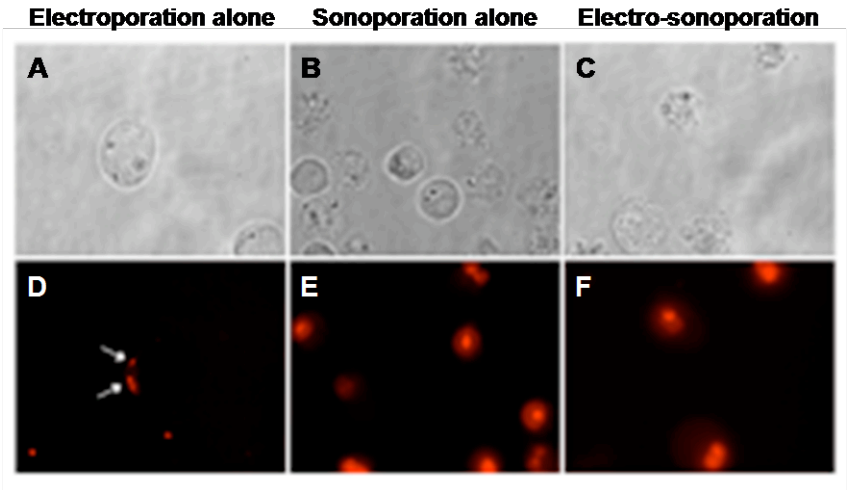
Electroporation alone
Sonoporation alone
Electro-sonoporation
A
B
C
D
E
F

Figure 3

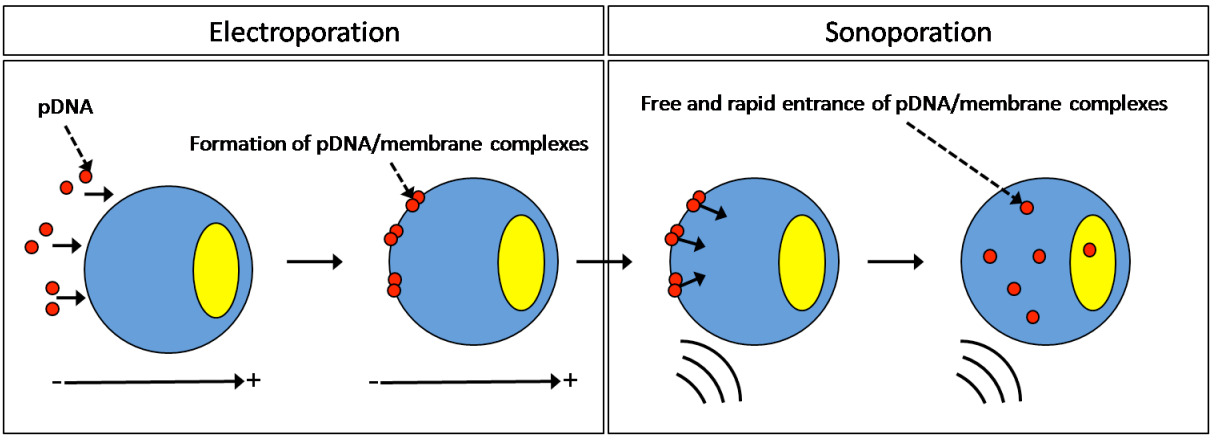
Electroporation
Sonoporation
pDNA
Formation of pDNA/membrane complexes
Free and rapid entrance of pDNA/membrane complexes
-
+
-
+

Figure 4

3. Discussion et Conclusions

Afin d'augmenter l'efficacité de transfert de plasmides, nous avons évalué la possibilité de combiner l'électroperméabilisation et la sonoporation. Cette approche a consisté à associer des impulsions électriques à des ondes ultrasonores assistées d'agents de contraste pour faciliter le transfert de plasmides dans les cellules. Nos résultats montrent que l'électro-sonoporation induit une augmentation du taux de transfection d'un facteur 4, et une augmentation de l'efficacité de transfection d'un facteur 6, par rapport aux résultats obtenus par électroperméabilisation seule (Figure III-).

En accord avec de précédents travaux, l'électroperméabilisation induit la formation de complexes plasmide/membrane localisés alors que la sonoporation ou l'électro-sonoporation induit une entrée directe des molécules de plasmides dans les cellules (Figure III-). Ces résultats montrent que la sonoporation permettrait une entrée rapide et libre des complexes plasmide/membrane électro-induits dans le cytoplasme des cellules transfectées (Figure III-). Par conséquent, l'amélioration de l'efficacité de transfection obtenue par électro-sonoporation pourrait s'expliquer pour une augmentation de l'accessibilité des molécules de plasmide dans les cellules.

Yamashita et collaborateurs ont évalué la potentialité de l'électro-sonoporation dans le transfert de plasmide codant interleukine-12 dans le muscle squelettique de souris *(Yamashita et al., 2002)*. Ils ont montré que l'électro-sonoporation induit une augmentation d'un facteur 8 du taux sérique de l'IL-12 par rapport à l'électroperméabilisation seule. Ils ont démontré que l'électro-sonoporation induit beaucoup moins de dommages musculaires que l'électroperméabilisation. Les auteurs ont suggéré que cette augmentation du taux sérique d'IL-12 est corrélée à une diminution des dommages musculaires. Les mécanismes impliqués dans la réduction des dommages musculaires par l'association des ultrasons à l'électroperméabilisation ne sont pas connus *(Yamashita et al., 2002)*. Néanmoins, au regard de nos résultats, nous pouvons supposer que cette amélioration du taux sérique d'IL-12 soit due à une augmentation de l'accessibilité des molécules de plasmide dans les fibres musculaires par sonoporation.

L'ensemble de ces résultats démontre que l'amélioration de l'efficacité de transfection obtenue par électro-sonoporation pourrait s'expliquer par une augmentation de l'accessibilité des molécules de plasmide dans les cellules. Le transfert de plasmides électro-sonoporation est une stratégie prometteuse en thérapie génique (Yamashita et al., 2002; Yamashita et al., 2004).

IV. Conclusions générales et perspectives

IV. Conclusions générales et perspectives

1. Conclusions générales

Les espoirs fondés sur les thérapies géniques et cellulaires ont stimulé, au cours de ces 25 dernières années, le développement de méthodologies de vectorisation de molécules thérapeutiques. Parmi ces méthodes, l'**électroperméabilisation** apparaît comme l'une des plus sûres et efficaces. Basée sur l'**application contrôlée d'impulsions électriques** (d'intensité en général inférieure à 1 kV/cm et de durée variable de quelques microsecondes à plusieurs millisecondes), elle permet une perte transitoire de la perméabilité sélective de la membrane plasmique *(Neumann et al., 1989)*. Il existe alors au niveau de la cellule perméabilisée des mouvements de fuite d'ions et de métabolites intracellulaires, ainsi que des mouvements d'entrée de molécules exogènes (médicaments anti-cancéreux, acides nucléiques…). Les potentialités d'application clinique de cette méthode d'électroperméabilisation sont nombreuses, aussi bien *in vitro*, qu'*ex vivo* ou *in vivo*: électrochimiothérapie, électrogénothérapie, vaccination génétique *(Escoffre et al., 2009c)*.

Les paramètres physiques (nombre, durée, fréquence et intensité) des impulsions électriques, permettent de moduler la perméabilisation (efficacité et taille des molécules électrotransférées) *(Teissié et al., 2005)*. L'intensité du champ électrique est responsable de la création de structures transitoires de perméabilisation. Le nombre et la durée interviennent sur les phases d'expansion (taille des structures transitoires de perméabilisation) et de relaxation de ces structures (durée de vie) *(Rols et Teissié, 1998a; Gabriel et Teissié, 1999)*. L'électroperméabilisation est la conséquence de la mise hors équilibre locale et réversible de la membrane.

Les phospholipides de la membrane sont la cible privilégiée du champ électrique *(Stulen, 1981; Teissié et Tsong, 1981; Lopez et al., 1988)*. La création de "pores", de 1 à 10 nm de diamètre, a été proposée mais leur existence n'a jamais encore été réellement démontrée *(Teissié et al., 2005)*. La présence de ces pores pourrait permettre d'expliquer le passage de molécules de petites tailles (comme l'iodure de propidium), par migration électrophorétique pendant l'application des impulsions électriques et par diffusion

après l'application des impulsions électriques *(Rols et Teissié, 1998a; Gabriel et Teissié, 1999; Pucihar et al., 2008)*. En revanche, ce modèle ne permet plus d'expliquer le transfert de macromolécules (>4 kDa), comme le plasmide qui apparaît comme un phénomène beaucoup plus complexe *(Golzio et al., 2002a)*.

L'électrotransfert de plasmide nécessite d'appliquer des impulsions électriques perméabilisantes et suffisamment longues. Ces paramètres doivent être optimisés. Ainsi, il est nécessaire de dépasser le seuil de perméabilisation *(Wolf et al., 1994)*. Cependant, les paramètres électriques peuvent fortement moduler l'efficacité de transfection *(Golzio et al. 2004)*. La durée de l'impulsion électrique doit être supérieure à la milliseconde, et des intensités de champ électrique trop élevées (>0,7 kV/cm) peuvent affecter la viabilité cellulaire *(Wolf et al., 1994; Rols et Teissié, 1998a)*. Plusieurs modèles ont été proposés pour expliquer le mécanisme d'électrotransfert de plasmides dans la cellule *(Escoffre et al., 2009b)*. Il apparaît clairement que le plasmide doit être présent pendant l'application du champ électrique pour qu'il y ait transfection *(Golzio et al., 2004*). Le mécanisme d'électrotransfert de plasmides se caractérise par un processus multi-étapes avec une étape d'interaction plasmide/membrane pendant l'application des impulsions électriques et une étape de translocation dans les minutes qui suivent leur application *(Golzio et al., 2002a)*. L'insertion et la translocation du plasmide ne peuvent donc pas se résumer à une simple électro-injection de la molécule dans la membrane. La membrane plasmique est un partenaire actif des premières étapes du phénomène. Ce modèle suggère aussi l'implication et l'importance de la machinerie cellulaire dans le mécanisme d'électrotransfert de plasmide.

Les travaux effectués dans ce projet de recherche ont permis d'approfondir les connaissances sur le mécanisme moléculaire et cellulaire de l'électrotransfert de plasmide avec pour objectif principal de réaliser une étude biophysique du mécanisme *in vitro*.

(i) L'application d'impulsions électriques millisecondes et perméabilisantes induit une perturbation d'ordre membranaire et une rapide translocation des phospholipides dans les régions perméabilisées. Cette translocation semble être induite par un effet direct du

champ électrique sur les dipôles des têtes des phospholipides. La translocation électro-induite des phospholipides n'est pas associée à une perte de la viabilité cellulaire.

(ii) L'existence d'un processus multi-étapes de l'électrotransfert de plasmide dans différentes lignées cellulaires a été mise en évidence. L'électroperméabilisation est une étape nécessaire et pas suffisante pour l'interaction plasmide/membrane. Une corrélation étroite entre perméabilisation membranaire, interaction plasmide/membrane et expression génique est présente dans différentes lignées cellulaires.

Pendant l'application de la première impulsion électrique, les molécules de plasmide migrent par électrophorèse et viennent interagir dans des sites distincts de la région membranaire faisant face à la cathode. La formation de complexes plasmide/membrane a lieu en une centaine de microsecondes. La durée de l'impulsion électrique joue un rôle majeur sur l'accumulation électrophorétique des molécules de plasmide au niveau de la membrane perméabilisée. L'interaction des molécules de plasmide avec la membrane perméabilisée apparaît donc comme un processus rapide. Les complexes plasmide/membrane se stabilisent en un délai de 200 ms. Un rôle distinct de l'intensité du champ électrique et du nombre d'impulsions électriques a été mis en évidence. Si l'intensité du champ électrique définit la surface membranaire où l'interaction des molécules de plasmide a lieu et de fait, le nombre de spots d'interaction, le nombre d'impulsions électriques définit la quantité de molécules de plasmide présente par complexe. De façon surprenante, le fait que l'augmentation du nombre d'impulsions électriques n'entraîne pas une augmentation du nombre de complexes indique que les sites compétents pour l'interaction des molécules de plasmide à la membrane plasmique perméabilisée sont présents dès la première impulsion électrique. Les complexes plasmide/membrane ainsi formés ne diffusent pas latéralement dans la membrane. Le cytosquelette d'actine n'est pas impliqué dans la formation de ces complexes mais pourrait être impliqué dans le transport intracellulaire des molécules de plasmides.

(iii) Les défauts membranaires électro-induits et les complexes plasmide/membranaire perturbent la mobilité latérale des protéines membranaires du feuillet externe de la membrane plasmique.

(iv) La combinaison de la sonoporation avec l'électroperméabilisation permet d'améliorer l'efficacité de transfection obtenue par l'électroperméabilisation seule. Cette

amélioration pourrait s'expliquer pour une augmentation de l'accessibilité des molécules de plasmide présentes dans les complexes plasmide/membrane par l'application d'ondes ultrasonores en présence d'agents de contraste. Le transfert de plasmides par électro-sonoporation pourrait être une stratégie prometteuse en thérapie génique.

2. Perspectives

En raison des spécificités cellulaires (HCT-116, C2C12 vs CHO, B16, SH-SY5Y, ABAE) et tissulaires (muscle squelettique vs tumeurs), une meilleure compréhension des mécanismes biophysiques impliqués dans l'électrotransfert de plasmides est requise en vue de son utilisation en clinique.

2.1. La membrane plasmique

L'interaction plasmide/membrane est un état d'équilibre qui évolue vers un piégeage irréversible des molécules de plasmide à la membrane plasmique. Ce piégeage nécessite la mise en place de structures suffisamment stable pour bloquer les molécules de plasmide à la membrane *(Phez et al., 2005; Faurie et al., 2010)*. Il est nécessaire de mieux caractériser les zones d'interaction plasmide/membrane. L'interaction plasmide/membrane se fait sous la forme d'agrégat dans des sites compétents. La nature de ces sites compétents doit être déterminée.

2.1.1. Les lipides

Les lipides semblent être une cible privilégiée du champ électrique *(Stulen, 1981; Lopez et al., 1988)*. L'interaction plasmide/membrane pourrait être favorisée selon la nature des lipides.

Au cours ce travail, nous avons pu montrer que des lignées cellulaires (e.g. C2C12, HCT-116) ne présentent pas d'interaction plasmide/membrane et ne sont pas transfectées. La composition en lipides de leurs membranes plasmiques pourra être déterminée et comparée à celle de lignées cellulaires pour lesquelles l'interaction plasmide/membrane et transfection sont détectées (e.g. CHO, B16-F10). Ces compositions seront analysées qualitativement et quantitativement par chromatographie en phase gazeuse et liquide à partir de 1 à 5 millions de cellules (Collaboration avec le plateau technique de lipidomique de l'Inserm, IFR 30).

L'utilisation de vésicules lipidiques géantes de compositions variables permettrait de tester la nature des lipides sur l'interaction plasmide/membrane *(Portet et al., 2009)*.

2.1.2. Les protéines et les oligosaccharides

A moyen terme, il pourrait être intéressant d'étudier le rôle des protéines et des oligosaccharides sur l'interaction plasmide/membrane.

Une étude de FRET (i.e. Förster Resonnance Energy Transfer) pourra être entreprise pour déterminer si une interaction physique existe entre des protéines membranaires fusionnée à l'eGFP et les molécules de plasmides marquées au Cy-3. De plus, les cellules pourraient être traitées par la trypsine, des pronases, des glycosidases (e.g. neuraminidase). Il sera nécessaire de vérifier que ces traitements n'affectent pas la viabilité cellulaire et la perméabilisation membranaire.

Le rôle des protéines sur l'interaction plasmide/membrane pourra être étudié sur des protéoliposomes géants formés par électroformation *(Girard et al., 2004)*.

2.2. Le trafic intracellulaire

Plusieurs minutes après l'interaction plasmide/membrane, les molécules de plasmides migrent dans le cytoplasme jusqu'au noyau *(Golzio et al., 2002a)*. Nous pourrons envisager une étude du trafic intracellulaire des molécules de plasmide par microscopie confocale. La colocalisation de traceurs fluorescents spécifiques d'organites intracellulaires et de plasmides fluorescents sur des cellules vivantes permettra de déterminer la voie d'entrée des molécules de plasmide et de visualiser leur migration intracellulaire. Ce travail pourra être complété par une étude dynamique du trafic intracellulaire des molécules de plasmide par suivi de particule unique (Thèse de Chrystelle Rosazza). Cette approche nous donnera de précieuses informations sur la diffusion des molécules de plasmides dans le cytoplasme et nous permettra d'envisager des stratégies pour accélérer son trafic et réduire sa dégradation.

2.3. L'enveloppe nucléaire

L'enveloppe nucléaire est une nouvelle barrière membranaire que doivent franchir les molécules de plasmide pour que leur expression ait lieu. La synchronisation des cellules en phase G2/M par l'aphidicoline permet d'augmenter l'efficacité de transfection *(Goldstein et al. 1989 ; Yorifuji et al. 1989 ; Croaker et al. 1990 ; Teshigawara*

and Katsura, 1992 ; Golzio et al. 2002b). En effet, la disparition de l'enveloppe nucléaire en phase G2/M facilite l'internalisation du plasmide dans le noyau.

2.3.1. Les séquences DTS et NLS

La présence de séquences nucléiques DTS (i.e. DNA Targeting Sequence) au sein du plasmide ou l'association de peptides NLS (i.e. Nuclear Localization Sequence) au plasmide par des interactions covalentes ou électrostatiques permettrait au plasmide de franchir l'enveloppe nucléaire par un transport actif *(Dean et al. 2005)*. Ces éléments permettraient d'améliorer l'efficacité de transfection de cellules quiescentes et capables de se diviser *(Vaughan and Dean, 2005 ; Miller and Dean, 2008).*

2.3.2. Les nsPEFs

Des travaux montrent que l'application de très courtes (10-300 ns) et très intenses (jusqu'à 300 kV/cm) impulsions électriques (i.e. nsPEF, nanosecond Pulsed Electric Field) permettent de perméabiliser les organites intracellulaires, e.g. l'enveloppe nucléaire *(Schoenbach et al., 2001; Beebe et al., 2003)*. Nous proposons d'associer des impulsions électriques EGT aux impulsions électriques nsPEF afin d'augmenter l'efficacité de transfection. L'application d'impulsions électriques EGT perméabilisera la membrane plasmique et permettra le transfert de plasmides dans le cytoplasme. Puis après un certain délai (qui sera à déterminer), l'application d'impulsions électriques nsPEF perméabilisera l'enveloppe nucléaire et facilitera le transfert des molécules de plasmides dans le nucléoplasme.

L'ensemble de ce travail de thèse montre que l'étape d'interaction plasmide/membrane est bien une étape clé du processus multi-étapes du mécanisme d'électrotransfert de plasmides. Tout paramètre qui peut altérer cette interaction module l'efficacité de transfection. Néanmoins, les étapes ultérieures de translocation membranaire, de trafic intracellulaire, de franchissement de l'enveloppe nucléaire et d'expression génique, jouent aussi un rôle essentiel dans le processus. La visualisation et la quantification du cheminement des molécules plasmides dans les différents organites intracellulaires devraient aider dans la compréhension de chacune de ces étapes.

Les études futures qui seront réalisées sur l'électrotransfert de plasmides dans les cellules et sur les sphéroïdes multi-cellulaires (Wasungu et al., 2009) devront amener des réponses pour la compréhension du mécanisme biophysique in vitro, mais devront surtout intégrer leurs résultats pour une utilisation rationnelle de l'électroperméabilisation in vivo.

V. MATÉRIEL & MÉTHODES

PARTIE I

MÉTHODES GÉNÉRALES

V. Matériel & Méthodes

Partie I. Méthodes générales

1. Cultures cellulaires

1.1. Les cellules CHO

Les cellules utilisées sont des cellules d'ovaires de hamster chinois (CHO, souche WTT). Cette lignée cellulaire partiellement transformée diffère de la souche parentale par son aptitude à être cultivée en suspension. Il est donc possible de cultiver ces cellules de deux manières différentes *(Rols et al., 1995)*:

Couche monocellulaire: dans ces conditions, les cellules sont cultivées dans des boîtes de Pétri de 35 mm (BD Falcon™, San Jose, CA), des flasks de culture ou des Labteck II (Nunc™, Thermo Fischer Scientific, Rochester, NY). Elles présentent une inhibition de contact lorsqu'elles sont à confluence.

Suspension cellulaire: dans des conditions, les cellules sont cultivées dans des flacons en verre de 0,5 L (Spinner) dans 100 mL de milieu de culture, sous agitation douce et continue (70 à 100 tours/minutes), à 37°C. La culture en suspension est effectuée après détachement des cellules en monocouche par action de la trypsine (Sigma-Aldrich® Inc., Saint-Louis, MO). Après 5 minutes d'incubation à 37°C, l'action de la trypsine est bloquée par l'ajout de milieu de culture. Les cellules sont récupérées et placées dans le spinner à raison de 0,5 10^6 cellules/mL. La densité cellulaire maintenue entre 0,5 10^6 et 1,5 10^6 cellules/mL, par dilution quotidienne, permet de garder les cellules en phase exponentielle de croissance. Une nouvelle culture est réalisée toutes les 3 ou 4 semaines à partir d'ampoules de cellules congelées.

1.2. Les cellules CHO Rae1-eGFP

Les cellules CHO Rae1-eGFP ont été données par le Pr. Bettina Couderc (Institut Claudius Regaud, Toulouse, France) et le plasmide Rae1-eGFP a été gracieusement offert par le Dr. Denis Hudrisier et le Dr. Anne Aucher (IPBS-CNRS UMR 5089, Toulouse France).

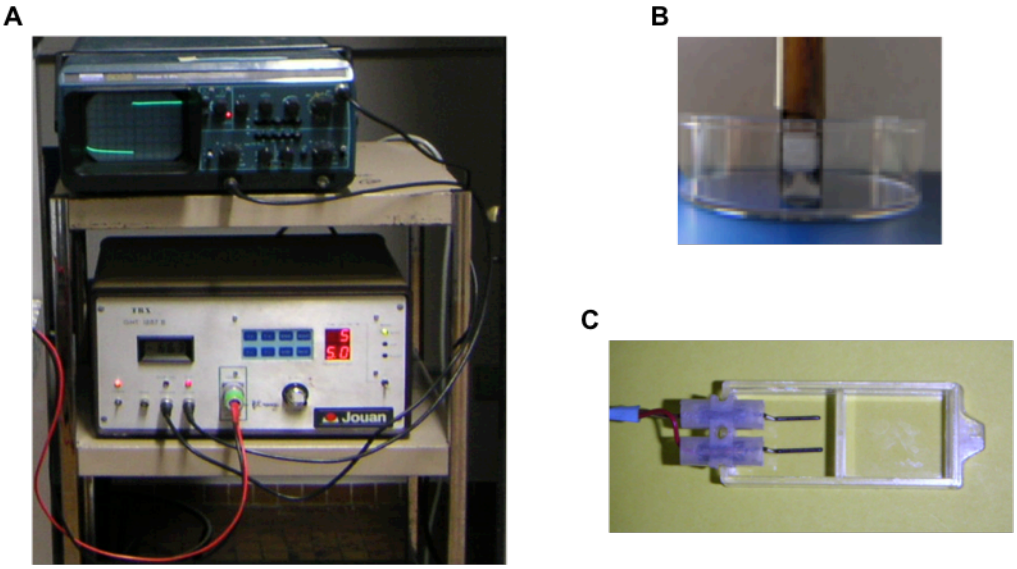

Figure VII-1: Dispositif d'électropulsation. A. L'électropulsateur : L'instrumentation expérientale est composée d'un générateur de haute tension et d'un oscilloscope. Le profil cinétique des impulsions électriques délivrées peut être visualisé sur l'écran de l'oscilloscope. **B. Les électrodes à plaque :** Les plaques à plaques ont une distance inter-électrode de 0,4 cm dans une boite de Pétri de 35 mm. **C. Les électrodes cylindriques :** Les électrodes cylindriques ont une distance inter-électrode de 0,7 cm dans un puit de Labteck *(Adapté de la thèse d'Emilie Phez, 2005)*.

Les cellules CHO sont transfectées par un plasmide codant la protéine transmembranaire Rae1 en fusion avec la protéine fluorescente eGFP. Les cellules transfectées sont cultivées sous pression de sélection au G418 (1 µg/µL) (InvivoGen, San Diego, CA). Les cellules exprimant la protéine de fusion sont sélectionnées par tri cellulaire en cytométrie de flux (FAScan; Beckman. Instruments, Inc., Fullerton, CA).

1.3. Les conditions de culture

Dans des conditions optimales de culture cellulaire, le temps de génération des cellules CHO est de l'ordre de 16-18 heures à 37°C et à 5% CO_2 dans un incubateur (Jouan, France).

Le milieu de culture utilisé est le milieu MEM 0111 (Eurobio, Les Ulis, France), complété à 8% par du sérum de veau fœtal décomplémenté (Lonza Group Ltd, Switzerland), par 3,5 g/L de D(+)-glucose (Sigma-Aldrich® Inc., Saint-Louis, MO), 2,95 g/L de bouillon de tryptose phosphate (Sigma-Aldrich® Inc., Saint-Louis, MO), 100 unités/mL de pénicilline (Sigma-Aldrich® Inc., Saint-Louis, MO), 100 mg/mL de streptomycine (Sigma-Aldrich® Inc., Saint-Louis, MO), 0,8 mg/mL de la L-glutamine (Sigma-Aldrich® Inc., Saint-Louis, MO) et enrichi en vitamines BME 100X (Sigma-Aldrich® Inc., Saint-Louis, MO). Le pH du milieu de culture est régulé à pH 7,4 par un tampon bicarbonate (bicarbonate de sodium à 3,3 g/L). La présence d'un indicateur de pH coloré, le rouge de phénol permet le contrôle visuel des variations de pH (coloration rouge orangé à pH 7-7,8). La culture en monocouche requiert une atmosphère 5% CO_2 à 37°C; l'agitation des cellules à 37°C lors de culture en suspension permet un dégagement de CO_2 suffisant pour la régulation du pH.

2. Electropulsation

2.1. Electropulsateur – TRX, GHT 1297, Jouan

L'électropulsateur est composé d'un générateur d'impulsions de haute tension (jusqu'à 1,5 kV) sous un ampérage de 8 A (TRX, GHT 1287, Jouan, France) (Figure VII-1A). Il est possible de moduler le nombre, la durée et de la fréquence des impulsions délivrées. L'intensité du champ électrique reste constante pendant la durée de l'impulsion dite à cinétique à vague carrée. Une partie du signal (V/100) est envoyée sur un oscilloscope (5026 Enertec) permettant un contrôle visuel du profil cinétique des impulsions appliquées. Des électrodes sont alors reliées au générateur. Les cellules

placées entre les électrodes, distantes de d (cm), sont soumises à un champ électrique homogène d'intensité E (V/cm) égale à E = U/d. La différence de potentiel U (V) délivrée par le générateur est liée à la résistance R (Ohm) du milieu, selon, U = R I. Le courant électrique I délivré est fixé par l'ampérage maximal par le générateur fixé à 8 A. La résistance du milieu doit donc être inférieure à U/Imax (soit U/8) afin qu'une impulsion à profil cinétique à "vague à carrée" soit correctement délivrée.

2.2. Les électrodes

Classiquement au laboratoire des électrodes constituées par deux lames en acier inoxydable, planes et parallèles sont utilisées. La distance inter-électrode d est de 4 mm (Figure VII-1B). Les électrodes cylindriques (diamètre 1 mm), adaptées pour l'étude de visualisation en microscopie de fluorescence des phénomènes d'électropulsation, sont en acier inoxydable et distantes de 7 mm (Figure VII-1C). Le champ électrique entre ces électrodes est considéré comme uniforme *(Mazères et al., 2009)*.

2.3. Le milieu de pulsation

Classiquement, le milieu de pulsation utilisé est un tampon K_2HPO_4/KH_2PO_4 10 mM, pH 7,4 (Sigma-Aldrich® Inc., Saint-Louis, MO) complété par 1 mM de $MgCl_2$ (Sigma-Aldrich® Inc., Saint-Louis, MO) et 250 mM de saccharose (Euromedex, Mundolsheim, France). Ce tampon de pulsation est iso-osmotique (320 mOsm/kg). Sa faible conductivité (1,6 mS/cm) permet de limiter l'effet Joule associé aux impulsions électriques.

3. Electroperméabilisation

Dans toutes les expériences réalisées, des cellules témoins sont utilisées. Ce témoin est le référentiel de l'étude, il correspond à un point expérimental où le champ électrique n'est pas appliqué (E = 0 kV/cm).

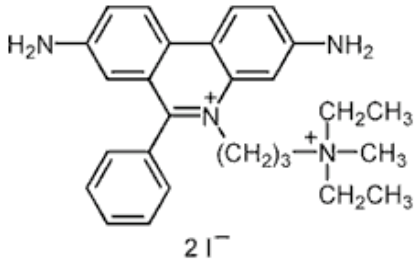

Figure VII-2: Formule chimique de l'iodure de propidium (ou PI). L'iodure de propidium est une sonde fluorescente qui se lie à l'ADN. Une fois intercalé entre les bases de l'ADN son rendement quantique de fluorescence est multiplié par 1000. Les caractéristiques spectrales de l'iodure de propidium sont : $\lambda_{max(ex)}$ = 493 nm, $\lambda_{max(em(molécule\ libre))}$ = 588 nm et $\lambda_{max(em(molécule\ liée\ à\ l'ADN))}$ = 617 nm *(Adapté de la thèse de Muriel Golzio, 1999)*.

3.1. Molécule de détection de la perméabilisation

La perméabilité membranaire est mise en évidence par l'entrée d'une petite molécule fluorescente non perméante, l'iodure de propidium ou PI (Sigma-Aldrich® Inc., Saint-Louis, MO) (Figure VII-2). Cette molécule, classiquement utilisée comme marqueur de viabilité cellulaire, pénètre dans les cellules uniquement lorsque l'intégrité membranaire de celles-ci est affectée. Les caractéristiques spectrales du PI sont: longueur d'onde maximale d'excitation, 493 nm ; longueur d'onde maximale d'émission, 588 nm (molécule libre) ; longueur d'onde maximale d'émission, 617 nm (molécule liée à l'ADN). Le rendement quantique de fluorescence de cette sonde augmente d'un facteur 1 000 lorsqu'elle s'intercale entre les bases de l'ADN. Cette caractéristique permet une observation directe de l'entrée de la sonde en microscopie de fluorescence ou en cytométrie de flux de l'échantillon sans rinçage au préalable *(Golzio et al., 2004)*.

3.2. Protocole d'électroperméabilisation des cellules

3.2.1. Cellules en suspension

Les cellules CHO en suspension dans le milieu de culture sont centrifugées 5 minutes à 120 g (Eppendorf France SARL, Le Pecq, France). Le culot cellulaire est repris par pipetage doux, dans le milieu de pulsation contenant 100 µM PI, à une densité cellulaire de 10 10^6 cellules/mL.

Les électrodes sont amenées au contact d'un support plastique (boite de pétri), 100 µL de la suspension cellulaire sont ensuite déposés entre les électrodes. Le champ électrique est appliqué sous la forme d'un train d'impulsions, en général 10 x 5 ms, 1 Hz. Les électrodes sont retirées du support, la suspension cellulaire est laissée une dizaine de minutes à 30°C afin de permettre le retour à l'état membranaire imperméable *(Rols et al., 1994)*. L'échantillon est ensuite repris dans 500 µL de tampon PBS pour l'analyse en cytométrie de flux *(Golzio et al., 2004)*.

3.2.2. Cellules en monocouches

Le milieu de culture est retiré des cellules adhérentes et remplacé par le milieu de pulsation contenant 100 µM de PI. Les électrodes sont mises en contact de la monocouche et les cellules sont électroperméabilisées comme décrit précédemment. Le

volume de milieu de suspension est ajusté au type de support plastique utilisé de telle manière à recouvrir en totalité le tapis cellulaire. Après retour de l'intégrité membranaire, la plage électropulsée peut soit être observée en microscopie de fluorescence, soit en cytométrie de flux après décollement des cellules à la trypsine *(Golzio et al., 2004)*.

Le taux de perméabilisation correspond au pourcentage de cellules perméabilisées. L'intensité de fluorescence moyenne associée au PI reflète la quantité de molécule de PI qui pénètre dans les cellules. L'efficacité de perméabilisation correspond à l'intensité de fluorescence moyenne associée au pourcentage de cellules perméabilisées.

4. Retour à l'état imperméable de la membrane

Le retour à l'état imperméable de la membrane, appelé aussi "resealing" membranaire permet généralement de déterminer la viabilité à court terme associée à la perméabilisation *(Rols et al., 1992)*. Le "resealing" a été analysé par la capacité des cellules électroperméabilisées à incorporer le PI. Pratiquement, les cellules sont électropulsées dans du milieu de pulsation. Après traitement électrique, un volume équivalent d'une solution de 200 µM de PI est ajouté à la suspension cellulaire à différents temps. Après une incubation de 10 minutes à 30°C, les cellules sont reprises dans 500 µL de tampon PBS. Les différents échantillons sont analysés par cytométrie de flux. L'intensité de fluorescence associée à l'incorporation de PI au cours du temps indique le retour à l'état imperméable de la membrane.

5. Interaction ADN/membrane

5.1. Plasmide peGFP-C1

L'utilisation de gènes rapporteurs fluorescents est un outil intéressant pour révéler la transfection aussi bien *in vitro* au niveau de la cellule isolée ou d'une population cellulaire.

Le plasmide peGFP-C1 (Clontech, Monain View, CA) portant le gène codant pour une protéine naturellement fluorescente, la "enhanced Green Fluorescent Protein" (eGFP) est le gène rapporteur choisi pour l'étude de l'électrotransfection. Ce plasmide de

4,7 kb est constitué du promoteur fort de cytomégalovirus, en aval de la séquence codante, et d'une séquence de polyadénylation de SV40 (Figure VII-3A). Des mutations géniques de la séquence codante la protéine lui confèrent les caractéristiques spectrales suivantes: longueur d'onde maximale d'excitation, 488 nm; longueur d'onde maximale d'émission, 507 nm. La eGFP est une protéine de 239 résidus aminés de poids moléculaire estimé à 27 kDa.

5.2. Production, extraction et purification du plasmide peGFP-C1

La souche DH5α de E. coli a été transformée par electroporation, par le plasmide peGFP-C1 qui lui confère une résistance à la kanamycine (30 µg/mL) pour un nombre de copies d'environ 500 par bactérie. L'extraction et la purification du plasmide peGFP-C1 sont réalisées avec le kit "Hispeed Plasmid Maxi kit" en suivant les instructions décrites par le fabricant (Qiagen, Courtaboeuf, France). La quantification et la pureté de la préparation sont déterminées par le dosage spectrophotométrique ($1,6 < DO_{260}/DO_{280} < 2$) (NanoDrop Products, Wilmington, DE) et migration électrophorétique sur gel agarose 1% (Sigma-Aldrich® Inc., Saint-Louis, MO) dans un tampon TAE 1X (Tris 0,4 M - Acetate 0,2 M - EDTA 10mM – pH 8.3) (Euromedex, Mundolsheim, France) (Figure VII-3B).

5.3. La molécule de détection de l'interaction plasmide/membrane

La visualisation de l'interaction du plasmide à la membrane est réalisée grâce à un plasmide rendu fluorescent par marquage avec le dimère de benzithiazolium-4-quinolium ou TOTO-1 (Invitrogen Corporation, Carlsbad, CA) (Figure VII-4A). La molécule fluorescente de TOTO-1 s'intercale entre les bases du plasmide avec une affinité supérieur au PI, ses caractéristiques spectrales sont: $\lambda_{max(excitation)}$ = 514 nm ; $\lambda_{max(émission)}$ = 533 nm. Le rendement quantique de fluorescence de cette sonde augmente d'un facteur 3 000 lorsqu'il est lié au plasmide *(Rye et al., 1992)*.

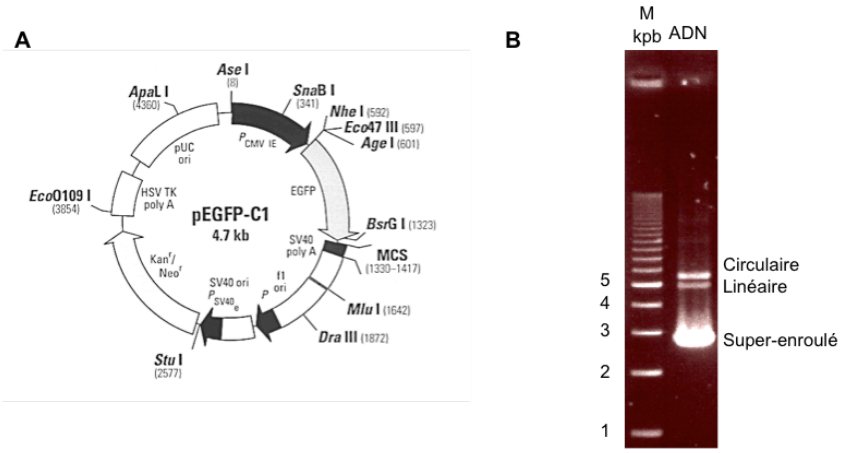

Figure VII-3: Plasmide peGFP-C1. A. Carte génétique du plasmide peGFP-C1. Le plasmide peGFP-C1 de 4,7 kb (Clontech) porte le ADNc codant pour la «enhanced Green Fluorescent Protein » (eGFP) en aval du promoteur fort CMV IE et en amont d'une séquence de polyadénylation de SV40 (SV40 polyA). L'eGFP est une protéine fluorescente de 238 acides aminés. Ses caractéristiques spectrales sont : $\lambda_{max(ex)}$ = 488 nm, $\lambda_{max(em)}$ = 507 nm. **B. Migration électrophorétique du plasmide peGFP-C1.** Migration sur gel d'agarose 1% (tampon TAE) du plasmide peGFP-C1 purifié sur colonne Qiagen (piste DNA). La piste M correspond à des marqueurs de tailles (1 kpb DNA ladder, Sigma). Trois conformations du plasmide sont observées : circulaire, linéaire, super-enroulé *(Adapté de la thèse de Muriel Golzio, 1999)*.

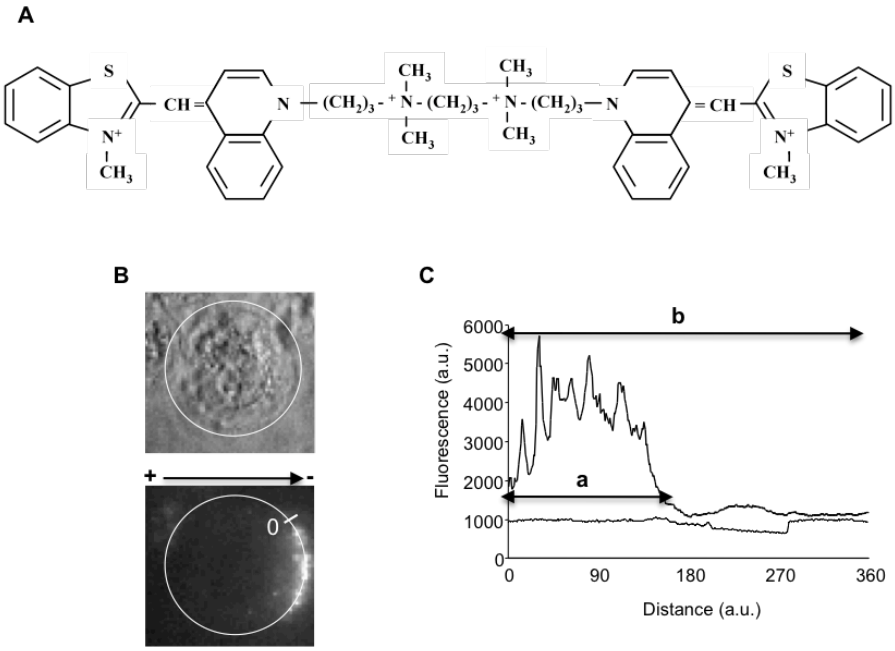

Figure VII-4: Interaction ADN/membrane. A. Formule chimique du Benzithiazolium-4-quinolium (TOTO-1). La molécule fluorescente de TOTO-1 est un intercalant de l'ADN. Ses caractéristiques spectrales sont : $\lambda_{max(ex)}$ = 514 nm, $\lambda_{max(em)}$ = 533 nm. Le rendement quantique de fluorescence de cette sonde augmente d'un facteur 3000 lorsqu'il est lié à l'ADN. **B. Visualisation de l'interaction ADN/membrane sur des cellules CHO.** Les cellules CHO sont électropulsées (10 x 5 ms, 1 Hz, 0,7 kV/cm) en présence de molécule d'ADN marquées avec le TOTO-1 (1 molécule de TOTO-1 pour 5 pb) et observées en lumière blanche (image du haut) ou en fluorescence (image du bas) 30 secondes après l'application des impulsions électriques. **C. Quantification de l'interaction ADN/membrane.** Un profil de fluorescence sur le pourtour de la cellule est représenté avant (en gris) et après (en noir) l'application des impulsions électriques. a. représente le périmètre d'interaction ADN/membrane et b. le périmètre cellulaire total. Le point 0 est le point de départ du tracé du profil de fluorescence sur le pourtour de la cellule *(Adapté de la thèse d'Emilie Phez, 2005)*.

Un récent travail montre l'utilisation de cette sonde fluorescente pour étudier le trafic intracellulaire de molécules de plasmide *(Maucksch et al., 2009)*. Suite à une lecture critique de ce travail, nous avons publié une lettre dans *Journal of Gene Medecine* expliquant que si cette méthode est une excellente sonde pour détecter l'étape d'interaction plasmide/membrane, elle n'est pas adaptée pour étudier le trafic intracellulaire des molécules de plasmide. En effet, dans des cellules fixées ou vivantes, la sonde peut se dissocier du plasmide et marquer les acides nucléiques intracellulaires. Par conséquent, la visualisation et la quantification de la biodistribution du plasmide dans les cellules sont biaisées.

THE JOURNAL OF GENE MEDICINE
J Gene Med 2009; **11**: 1071–1073.
Published online in Wiley InterScience (www.interscience.wiley.com) **DOI:** 10.1002/jgm.1384

LETTER TO THE EDITOR

Transgene expression of transfected supercoiled plasmid DNA concatemers in mammalian cells

Jean-Michel Escoffre[1,2]*
Elisabeth Bellard[1,2]
Muriel Golzio[1,2]
Justin Teissié[1,2]*
Marie-Pierre Rols[1,2]

[1]*CNRS, IPBS (Institut de Pharmacologie et de Biologie Structurale), Toulouse, France*

[2]*Université de Toulouse, UPS, IPBS, Toulouse, France*

*Correspondence to:
Jean-Michel Escoffre, Justin Teissié, CNRS, IPBS (Institut de Pharmacologie et de Biologie Structurale), 205 route de Narbonne, F-31077, Toulouse, France. E-mail: jean-michel.escoffre@ipbs.fr; justin.teissie@ipbs.fr

We read with interest the article by Maucksch *et al*. [1], who analysed transgene expression of transfected supercoiled 4.7 kb monomeric and 9.4 kb dimeric plasmid concatemer in Jurkat T cells using electroporation. The authors reported that the relative number of electrotransferred gene copies per nucleus and plasmid expression efficiency, respectively, were 1.6- and 3.5-fold higher for enhanced green fluorescent protein (EGFP)-dimer than for EGFP-monomer. However, the transfection rates considering the number of transfected cells were significantly lower for EGFP-dimer than for EGFP-monomer. Their conclusions were that more dimers were introduced in fewer cells.

The relative number of gene copies introduced in the different cellular compartments (cytoplasm and nucleus) was evaluated using a fluorescence approach, which we described some years ago [2]. This took advantage of the spontaneous binding of TOTO dyes to DNA.

Therefore, Maucksch *et al*. [1] have used noncovalent markers (SYTO-13 and TOTO-1) to determine the biodistribution of plasmids into the cells after electroporation. TOTO is virtually nonfluorescent in solution, but forms highly fluorescent complexes with double-stranded DNA (dsDNA), up to a maximum dye to DNA bp ratio of 1 : 4, with a 1000-fold fluorescence enhancement. The dsDNA–TOTO complexes are completely stable to electrophoresis on agarose and acrylamide gels [3]. However, TOTO-1 is a dye capable of bis-intercalation, although it interacts with dsDNA and ssDNA with a similar high affinity. Binding of the dye partially unwinds the DNA by distorting and elongating the helix. An external binding mode, where the dipole of the dye molecule is aligned with the DNA grooves, may be more important. TOTO-1 dye will bind to almost any sequence in dsDNA.

TOTO binding with DNA is an equilibrium, where the dye can unbind if free DNA is added (i.e. equilibrium displacement) [4]. This is indeed the case when plasmids bearing TOTO enter in the cytoplasm where free DNA is present. Furthermore, TOTO can freely leak from the cytoplasm to the nucleus (where, again, free DNA is present) in a way similar to that reported for propidium iodide [4]. TOTO labelling DNA comprises a good tool for assaying the early steps of DNA entry into cells but cannot be used to investigate the process over a long period time. If this method is used to detect plasmid/membrane interaction (Figure 1), this approach is not adapted to study the intracellular traffic of plasmid. Indeed, in living or fixed cells, the fluorescent marker can dissociate from plasmid and label intracellular nucleic acids. This comprises the traffic of TOTO. Consequently, the visualization and quantification of plasmid biodistribution into cells can be biased. In our studies, to eliminate these artefacts, we used a dye covalently bound to the plasmid after checking that the level of protein expression was not affected. Indeed, we used the covalently rhodamine-labelled plasmid (pGeneGrip; Gene Therapy Systems, San Diego, CA, USA) to observe the cell traffic of fluorescent-labelled plasmid after electroporation [2].

Golzio *et al*. [2] demonstrated that this plasmid/membrane interaction is one of the key steps for obtaining gene expression. During the application

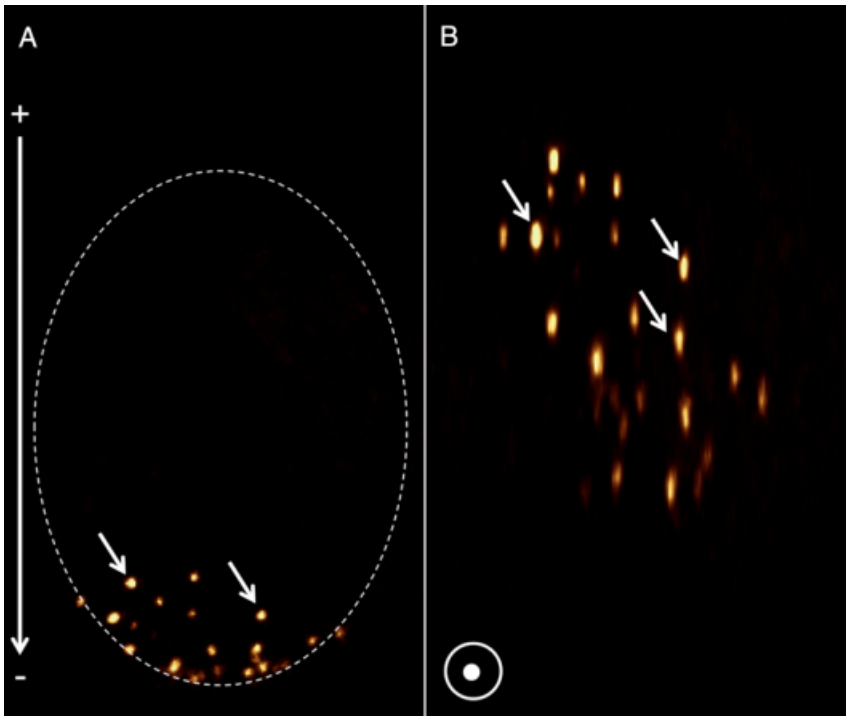

Figure 1. DNA/membrane interaction. A train of ten pulses (5 ms, 1 Hz at 0.7 kV/cm) was applied on Chinese hamster ovary (CHO) cells in the presence of pEGFP-C1 (4.7 kb) labelled with fluorescent marker, TOTO-1. The DNA/membrane interaction is observed by digitized fluorescent microscopy after deconvolution and three-dimensional reconstitution (A, top view; B, side view). White arrows indicate the DNA/membrane aggregates. The dotted line represents the perimeter of the CHO cell

of an electric pulse train, the plasma membrane is permeabilized in the regions facing the electrodes [5]. Permeabilization is necessary, but it is not a sufficient step. Indeed, plasmids are electrophoretically driven towards the cell surface and interact with the electropermeabilized side of the cell facing the cathode. The plasmid/membrane interaction results in the formation of localized aggregates (Figure 1). These complexes are formed within 1 s after the pulses. Moreover, pulses of reversed polarities cannot destroy them. Thus, this plasmid/membrane interaction is a not simple electrophoretic accumulation of plasmid DNA; instead, plasmids are trapped at the permeabilized membrane [6].

Maucksch *et al*. [1] demonstrated that a large fraction of pDNA is detected extracellularly in association with the cell membrane in most of the transfected cells, in agreement with our previous study. It is therefore surprising that the authors did not mention the work previously performed by Golzio *et al*. [2].

DNA plasmids remain trapped at the plasma membrane for up to 10 min after pulsing. Subsequently, they diffuse into the cytoplasm and are present around the nucleus 30 min later; for a review on gene electrotransfer, see Escoffre *et al*. [7]. We were unable to detect any transfer in the nucleus, meaning that the number of copies was very low, in agreement with most previous studies [8–10].

Experimental investigations [2,11] and molecular simulations [12] suggest that plasmid molecules migrate into cells by forming intermediates that involve lipid/plasmid complexes. Electric field pulses induce many defects, which cannot support direct plasmid transport (i.e. steric, entropic and image forces prevent the passage). A complex is formed between the electropermeabilized membrane and the electrophoretically-driven plasmid DNA during the application of an electric pulse train. When the electric field is switched off, structural modifications bring a slow DNA translocation into the cytoplasm. Plasmid DNA electrotransfer is not mediated by large pores as has been suggested by theoretical approaches [13–15]. The putative short-lived pore diameter cannot be considered as a limit for plasmid DNA transfer. Indeed, it was shown that very large plasmid DNA could allow expression after their electrotransfer [16].

Furthermore, we both suggested and demonstrated [17,18] that varying the pulse polarity and direction leads to an increase in the amount of plasmid in interaction with permeabilized membrane and, by doing so, improves transfection efficiency.

In conclusion, we are pleased that Maucksch *et al*. [1] were able to reproduce some of the data (plasmid/membrane interaction; cellular traffic of plasmid) that was previously obtained by our team [2] and/or other teams [8–10]. However, this is not a new finding and previous studies should be quoted [2].

Acknowledgements

Support from the region Midi-Pyrénées and Association Française contre les myopathies is acknowledged.

DOI: 10.1002/jgm

References

1. Maucksch C, Bohla A, Hoffman F, *et al*. Transgene expression of transfection surpercoiled plasmid DNA concatemers in mammalian cells. *J Gene Med* 2009; **11**: 444–453.
2. Golzio M, Teissie J, Rols MP. Direct visualization at the single-cell level of electrically mediated gene delivery. *Proc Natl Acad Sci USA* 2002; **99**: 1292–1297.
3. Rye HS, Yue S, Wemmer DE, *et al*. Stable fluorescent complexes of double-stranded DNA with bis-intercalating asymmetric cyanine: properties and applications. *Nucleic Acids Res* 1992; **20**: 2803–2812.
4. Sixou S, Teissie J. Exogenous uptake and release of molecules by electroloaded cells: a digitized videomicroscopy study. *Bioelectrochem Bioenerg* 1993; **31**: 237–257.
5. Teissie J, Golzio M, Rols MP. Mechanisms of cell membrane permeabilization: a minireview of our present (lack of?) knowledge. *Biochim Biophys Acta* 2005; **1724**: 270–280.
6. Phez E, Faurie C, Golzio M, *et al*. New insights in the visualization of membrane permeabilization and DNA/membrane interaction of cells submitted to electric pulses. *Biochim Biophys Acta* 2005; **1724**: 248–254.
7. Escoffre JM, Portet T, Wasungu L, *et al*. What is (still not) known of the mechanism by which electroporation mediates gene transfer and expression in cells and tissues. *Mol Biotechnol* 2009; **41**: 286–295.
8. Vaughan EE, DeGuilio JV, Dean DA. Intracellular trafficking of plasmids for gene therapy: mechanisms of cytoplasmic movement and nuclear import. *Curr Gene Ther* 2006; **6**: 671–681.
9. Escriou V, Carrière M, Scherman D, Wils P. NLS bioconjugates for targeting therapeutic genes to the nucleus. *Adv Drug Deliv Rev* 2003; **55**: 295–306.
10. Zanta MA, Belguise-Valladier P, Behr JP. Gene delivery: a single nuclear localization signal peptide is sufficient to carry DNA to the cell nucleus. *Proc Natl Acad Sci USA* 1999; **96**: 91–96.
11. Sukharev SI, Klenchin VA, Serov SM, *et al*. Electroporation and electrophoretic DNA transfer into cells. The effect of DNA interaction with electropores. *Biophys J* 1992; **63**: 1320–1327.
12. Tarek M. Membrane electroporation: a molecular dynamics simulation. *Biophys J* 2005; **88**: 4015–4053.
13. Krassowska W, Filev PD. Modeling electroporation in a single cell. *Biophys J* 2007; **92**: 404–417.
14. Smith KC, Neu JC, Krassowska W. Model of creation and evolution of stable electropores for DNA delivery. *Biophys J* 2004; **86**: 2813–2826.
15. Tieleman DP. The molecular basis of electroporation. *BMC Biochem* 2004; **5**: 10.
16. Molnar MJ, Gilbert R, Lu Y, *et al*. Factors influencing the efficacy, longevity, and safety of electroporation-assisted plasmid-based gene transfer into mouse muscles. *Mol Ther* 2004; **10**: 447–455.
17. Faurie C, Phez E, Golzio M, *et al*. Effect of electric field vectoriality on electrically mediated gene delivery in mammalian cells. *Biochim Biophys Acta* 2004; **1665**: 92–100.
18. Rebersek M, Faurie C, Kanduser M, *et al*. Electroporator with automatic change of electric field direction improves gene electrotransfer in vitro. *Biomed Eng Online* 2007; **2**: 6–25.

DOI: 10.1002/jgm

5.5. Protocole d'interaction plasmide/membrane

Le protocole de marquage stoechimiométrique (1 molécule de TOTO-1 / 5 pb d'ADN) est réalisé comme suit: 5 µg d'ADN plasmidique (peGFP-C1) sont mélangés avec 1,25 µL de la solution de TOTO-1 (10^{-3} M) et incubés 60 minutes à 4°C *(Rye et al., 1992)*.

Les cellules CHO en suspension dans le milieu de culture sont centrifugées 5 minutes à 120 g (Eppendorf France SARL, Le Pecq, France). Le culot cellulaire est repris par pipetage doux, dans le milieu de culture à une densité cellulaire de 0.1 10^6 cellules/mL. Chaque puits de Labteck est ensemencé avec 1 mL de la suspension cellulaire. Après une heure de culture cellulaire, le milieu de culture est aspiré puis remplacé par 500 µL de tampon de pulsation contenant 5 µg d'ADN marqué avec le TOTO-1. Les électrodes sont amenées au contact de la Lateck et le champ électrique est appliqué sous la forme d'un train d'impulsions, en général 10 x 5 ms, 1 Hz. Les cellules sont visualisées en microscopie de fluorescence avec un objectif x100 à immersion à huile. La quantification de la fluorescence moyenne, liée à l'interaction ADN/membrane, est obtenue sur la zone d'intérêt grâce au logiciel d'analyse MetaMorph. La bande de mesure est définie sur toute la longueur et la largeur de la zone d'intérêt. La fluorescence totale associée à cette bande de mesure renseigne la phase d'interaction ADN/membrane (Figure sVII-4B & VII-4C) *(Golzio et al., 2002; Faurie et al., 2004; Phez et al., 2005)*.

L'intensité de fluorescence associée au TOTO-1 lié aux molécules de plasmides en interaction avec la membrane plasmique reflète indirectement la quantité de plasmides présente dans les complexes plasmides/membrane.

6. Electrotransfection

Dans toutes les expériences réalisées, des cellules témoins sont utilisées. Ce témoin est le référentiel de l'étude, il correspond à un point expérimental où le champ électrique n'est pas appliqué (E = 0 kV/cm). L'ensemble de ces expériences est réalisé en condition stérile.

6.1. Protocole d'électrotransfection des cellules

L'entrée de l'ADN dans les cellules induite par le champ électrique s'effectue selon le même protocole que celui de l'électroperméabilisation *(Golzio et al., 2004)*.

6.1.2. Cellules en suspension

Les cellules CHO en suspension dans le milieu de culture sont centrifugées 5 minutes à 120 g (Eppendorf France SARL, Le Pecq, France). Le culot cellulaire est repris par pipetage doux dans 100 µL de tampon de pulsation contenant l'ADN à raison de 5 µg d'ADN pour 1.10^6 cellules. Les électrodes sont amenées au contact d'une boîte de Pétri, la suspension cellulaire est déposée entre les électrodes. Le champ électrique est appliqué sous la forme d'un train d'impulsions, en général 10 x 5 ms, 1 Hz. Les électrodes sont retirées du support, la suspension cellulaire est laissée 10 minutes à 37°C afin de permettre le retour à l'état membranaire imperméable. L'échantillon est ensuite repris dans 2 mL de milieu de culture, puis déposé dans des boites de Pétri de 35 mm de diamètre, et enfin placé dans l'incubateur à 37°C et à 5% CO_2 pour 24 heures *(Golzio et al., 2004)*.

6.1.3. Cellules en monocouches

Le milieu de culture est retiré des cellules adhérentes et est remplacé par le milieu de pulsation adéquat contenant l'ADN à raison de 5 µg d'ADN/essai. Le volume du tampon de pulsation est ajusté au type de support utilisé de telle manière à recouvrir en totalité le tapis cellulaire. Les électrodes sont mises en contact de la monocouche et les cellules sont électroperméabilisées comme décrit précédemment. Après 10 min, le tampon de pulsation est retiré puis remplacé par 2 mL de milieu de culture. Les cellules sont replacées dans l'incubateur à 37°C et à 5% CO_2 pour 24 heures *(Golzio et al., 2004)*.

Le taux de transfection correspond au pourcentage de cellules transfectées. L'intensité de fluorescence moyenne liée à l'expression de la protéine fluorescente eGFP reflète indirectement la quantité de plasmides entrée dans les cellules transfectées. L'efficacité de transfection correspond à l'intensité de fluorescence moyenne associée au pourcentage de cellules transfectées.

7. Viabilité cellulaire

La viabilité cellulaire à long terme associée à la transfection est basée sur la capacité des cellules électrotransfectées à adhérer à un support et à se diviser. La mesure est effectuée au-delà d'une génération soit 24 heures après l'application des impulsions électriques.

Le protocole appliqué pour réaliser cette mesure est strictement identique à celui décrit pour l'électrotransfection. La mesure de densité cellulaire est effectuée par coloration au cristal violet (Merck, Darmstadt, Germany). Le colorant diffuse librement dans des cellules et colore indifféremment le noyau et le cytoplasme des cellules. Une relation linéaire entre absorbance de la suspension colorée et le nombre de cellules a été montrée *(Gillies et al., 1986)*. Pratiquement, 24 heures après l'électrotransfection, le milieu de culture est aspiré, le tapis cellulaire est rincé deux fois avec 1 mL de tampon PBS. Les cellules sont placées sous une agitation douce (15-20 rpm) (agitateur de plaque, IKA-Vibrax, Janke & Kundel, Germany) pendant 20 minutes en présence de 1 mL de solution de cristal violet à 0,1%. L'excès de colorant est éliminé par trois rinçages successifs de 1 mL de tampon PBS. Le colorant est extrait par lyse cellulaire grâce à 1 mL d'une solution d'acide acétique à 10%. La mesure de l'absorbance est réalisée par dosage spectrophotométrique à 595 nm (Novaspec II, Pharmacia Biotech, Uppsala, Sweden) après dilution de l'échantillon dans du tampon PBS (DO_{max}<1). L'étalon interne correspond à une boîte vide qui a subi le même traitement de coloration. La DO de l'échantillon témoin (non électropulsé) correspond au 100% de survie cellulaire et devient l'échantillon de référence à l'expérience. Le pourcentage de viabilité cellulaire à long terme est alors déterminé de la façon suivante:

$$Viabilité(\%) = 100 \times \frac{DO_{échantillon}}{DO_{témoin}} \quad (Eq.VII-1)$$

8. Techniques d'analyse

8.1. Microscopie de fluorescence

Afin d'obtenir des cellules sphériques mais attachées au support, les cellules sont mises en culture 30 à 60 min au préalable dans une chambre d'observation dont le fond est constitué par une lamelle de verre adaptée pour la microscopie (Labteck system, Nunc™, Thermo Fischer Scientific, Rochester, NY). En revanche, des cellules adhérentes sont obtenues par un ensemencement des cellules 48 h avant l'expérimentation. Au moment de l'utilisation, le milieu de culture est remplacé par le milieu de culture est remplacé par le milieu de pulsation adéquat. La géométrie de ces boîtes est parfaitement adaptée pour l'utilisation des électrodes cylindriques décrites précédemment *(Mazères et al., 2009)*.

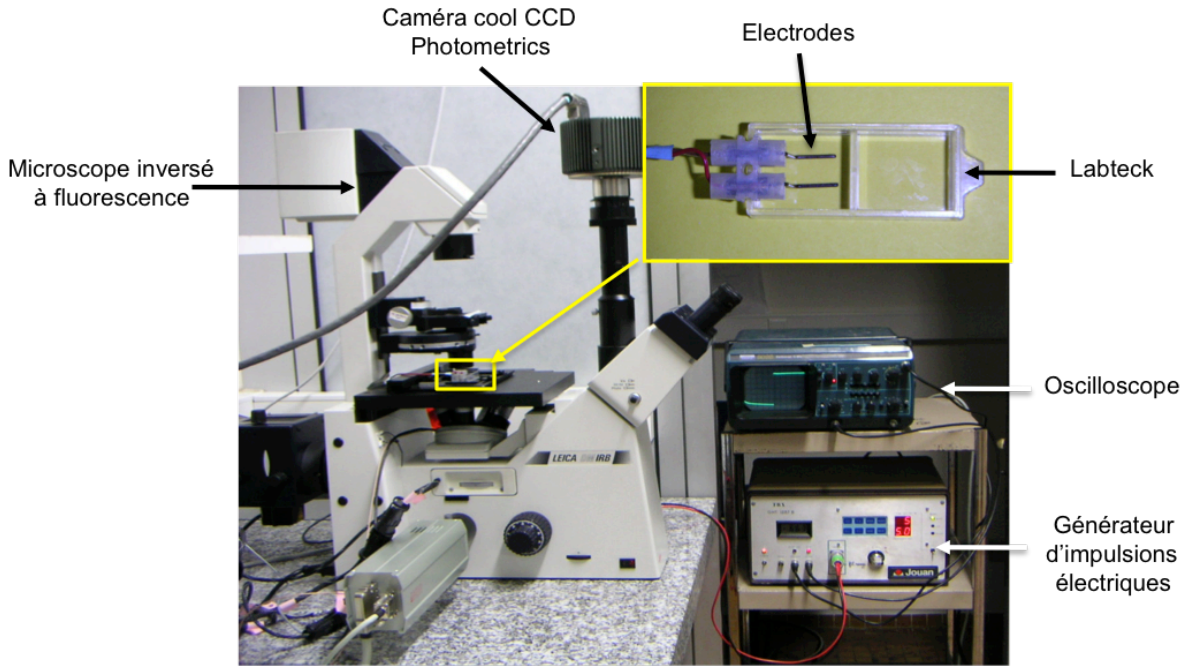

Figure VII-5: Station de vidéomicroscopie et dispositif pour l'électropulsation *(Adapté de la thèse d'Emilie Phez, 2005)*.

8.1.1. Vidéomicroscopie de fluorescence

8.1.1.1. Présentation de la station

La station de vidéomicroscopie de fluorescence se compose d'un microscope inversé à fluorescence Leica DMIRB (Leica Microsystems GmbH, Wetzlar, Germany), d'un système d'acquisition d'image (caméra CCD, contrôleur, ordinateur) et d'un système de traitement d'image (ordinateur, serveur) (Figure VII-5) *(Phez et al., 2005)*. L'obtention d'une image en vidéomicroscopie numérisée se décompose en quatre temps: acquisition, traitement, affichage et stockage.

L'acquisition se fait par une caméra CCD refroidie (Princeton Instrument Inc., Trenton, NJ) connectée au microscope qui capte les photons issus de l'échantillon fluorescent. Le détecteur convertit le signal photonique en signal électronique, le contrôleur (ST-138, Princeton instrument Inc, Trenton, NJ) découpe alors l'image en pixel (surface minimale élémentaire) et numérise (i.e. découper en pixel) le signal vidéo des intensités de lumières perçues (niveau de gris). Après traitement, l'image est transférée à l'ordinateur. L'ouverture de l'obturateur du faisceau de la lampe à mercure (EL6000, avec une lampe à mercure HXP à arc court 120 W) est contrôlée par le logiciel lors de l'acquisition. Cette installation permet ainsi une excitation contrôlée de la zone observée et évite toute photo-dégradation produite par une excitation prolongée.

La perméabilisation (entrée de PI) est visualisée avec le filtre N2.1 (515 nm < $\lambda_{max(excitation)}$ < 560 nm; $\lambda_{max(émission)}$ > 590 nm), le plasmide marqué au TOTO-1 et l'eGFP avec le filtre L4 (450 nm < $\lambda_{max(excitation)}$ < 490 nm; $\lambda_{max(émission)}$ > 515 nm) (Leica Microsystems GmbH, Wetzlar, Germany).

8.1.1.2. Acquisition et traitement de l'image

L'acquisition et le traitement des images en vidéomicroscopie de fluorescence ont été réalisés avec le logiciel MetaMorph. Ce logiciel d'acquisition d'images au cours du temps permet la réalisation de cinétique d'acquisition.

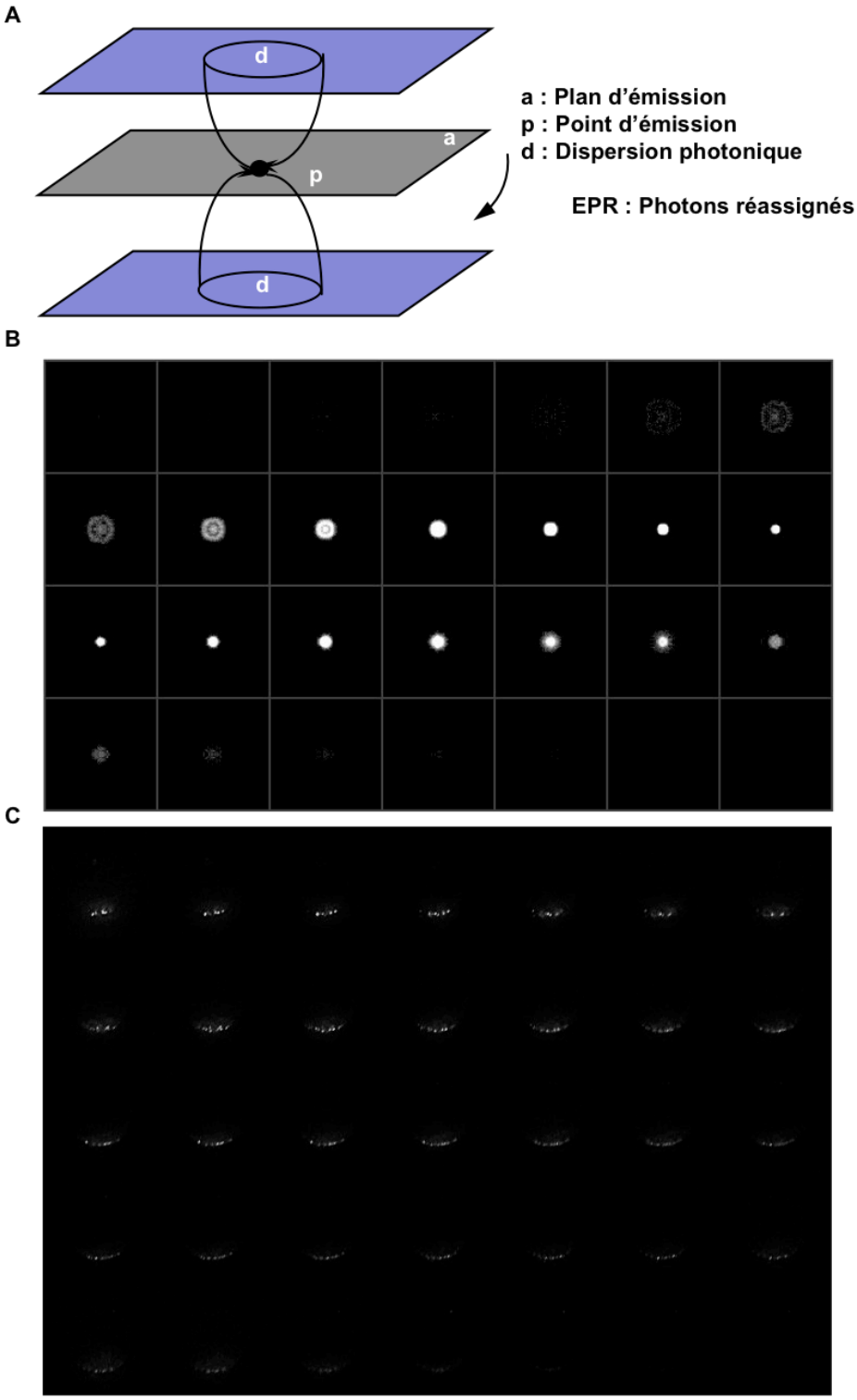

Figure VII-6: Principe de la déconvolution : A. Principe de Exhaustive Photon Reassigment (EPR) : Les photons issus du point d'émission et situés sur les plans adjacents par la dispersion photonique de l'optique du système sont réassignés par l'EPR sur leur plan d'émission d'origine en utilisant la fonction PSF comme modèle. **B. Point Spread Function :** L'objectif se déplace selon l'axe des z avec un pas de 300 nm pour l'acquisition des images (x;y). Un montage d'une série d'image en z d'une bille fluorescente de 170 nm de diamètre correspond à la PSF. **C. Déflouage d'une image :** Montage d'une série d'image en z d'une cellule CHO dont le plasmide peGFP-C1 marqué avec le fluorophore TOTO-1, est en interaction avec la membrane plasmique de la cellule. *(Adapté de la thèse de Muriel Golzio, 1999).*

Les images obtenues ont une taille de 1035 x 1317 (en résolution maximal Bin 1x1) codées sur 4096 niveaux de gris (12 bites). Il est possible d'acquérir des images (pleine taille) au cours du temps avec un délai de 1 secondes entre chaque image (temps nécessaire à l'acquisition et au traitement d'un cliché). Ce délai peut être réduit en diminuant le nombre de pixels par augmentation du binning : Bin 2x2, Bin 3x3 (ce qui entraîne une perte de résolution spatiale) ou en sélectionnant une région d'intérêt sur l'image (ROI : Region Of Interest). Le logiciel MetaMorph permet de tracer des profils sur tout le pourtour de la cellule, ou bien des profils radiaux. La fluorescence le long de ces profils est indiquée. Le périmètre d'interaction de l'ADN à la membrane, exprimé en pourcentage du périmètre cellulaire total, est décrit par l'équation suivante : (a/b) x 100, où a est le périmètre d'interaction d'ADN à la membrane et b, le périmètre cellulaire total, déterminés à partir du tracé du profil sur tout le pourtour de la cellule. La fluorescence totale dans la zone d'interaction à l'ADN à la membrane est obtenue en faisant la somme de la fluorescence par pixel de tous les pixels compris dans cette zone.

8.1.1.3. Utilisation en mode 3D

Le logiciel MetaMorph permet de réaliser l'acquisition d'images (x,y) dans le plan en z. Grâce à un piezo (Physik Instrumente GmbH & Co. KG, Karlsruhe, Germany) disposé sur l'objectif 100x (ON: 1,3, huile) (Leica Microsystems GmbH, Wetzlar, Germany), il en contrôle le déplacement en z de manière très précise. Une série de plans (x,y) est obtenue permettant ainsi une reconstitution 3D de l'objet observé grâce au module de déconvolution du logiciel MetaMorph (Figure VII-6A).

La déconvolution est un traitement mathématique permettant d'obtenir une estimation aussi fidèle que possible d'un objet biologique à partir de l'image obtenue à l'aide du détecteur, en se basant sur la connaissance des déformations infligées par le système optique. En effet, à cause de la diffraction (limitation intrinsèque de la microscopie photonique) l'image idéale d'un point en microscopie photonique n'est pas une tâche de diffraction ou fonction d'étalement du point (PSF). Cette PSF correspond à la réponse impulsionnelle du microscope pour un objectif donné. L'image de l'objet est donc une collection de PSFs qui se chevauchent créant ainsi ce flou et n'est donc qu'une "représentation" de l'objet.

Pour réaliser une PSF, on image dans les conditions de l'échantillon (milieu de montage, objectif, fluorophore…), une bille fluorescente de 0,17 µm (Invitrogen Corporation, Carlsbad, CA) dont le diamètre est inférieur à la résolution optique (Figure VII-6B). En déconvoluant l'image de l'objet avec cette PSF, on peut réassigner les signaux lumineux à leur position d'origine et ainsi restaurer l'information contenue dans le flou provoqué par le phénomène de diffraction. On peut ainsi dépasser les limites physiques de résolution de la microscopie photonique et obtenir une résolution comparable aux images acquises en microscopie confocale. Le ré-assignement des photons permet une quantification de la fluorescence sur tous les plans qui découpent l'échantillon (Figure VII-6C).

8.1.2. Microscopie confocale

Le microscope confocal ZEISS LSM 510 est un microscope inversé qui permet l'observation de matériels fixés ou vivants (Carl Zeiss SAS, Le Pecq, France). Dans sa configuration actuelle, le microscope confocal dispose d'un laser Argon permettant une excitation à 458 nm et à 488 nm et d'un laser Hélium/Néon permettant une excitation à 543 nm. Ce microscope confocal est équipé de deux photomultiplicateurs de détection confocale. Le système dispose également en mode conventionnel d'une lampe d'excitation mercure HBO 50W et de 3 jeux de filtres adaptés aux fluorophores de type eGFP et iodure de propidium pour positionner l'échantillon dans le champ d'observation de l'objectif. La numérisation des images conventionnelles est faite avec une caméra Axiocam HRm (Carl Zeiss SAS, Le Pecq, France). L'objectif utilisé en routine sur ce microscope est un objectif 63x (ON:1,4, eau). Le microscope confocal est entièrement informatisé : pilotage du microscope, acquisition des images, et traitement des images sont réalisés avec le logiciel Zeiss LSM Image Browser (Carl Zeiss SAS, Le Pecq, France). Les images de l'échantillon sont numérisées sur 8 bits (256 niveaux de gris) ou 12 bits (4096 niveaux de gris), et sont sauvegardées dans une base de données.

8.1.3. Cytométrie de flux

Le cytométrie de flux utilisé (FAScan; Beckman. Instruments, Inc., Fullerton, CA) est équipé d'un laser argon à 488 nm. L'analyse de la perméabilisation (entrée d'iodure de propidium) est effectuée sur le canal FL2 (560 nm < $\lambda_{max(émission)}$ < 600 nm) et l'analyse de la transfection (expression de l'eGFP) sur le canal FL1 (510 nm < $\lambda_{max(émission)}$ < 540 nm). Le logiciel d'acquisition et d'analyse est CellQuest. Des histogrammes

représentant le nombre de cellules comptabilisées en fonction de leur intensité de fluorescence sont obtenus (Figures VII-7 & VII-8). On peut définir deux régions : M1 et M2. Les cellules en M1 (dont l'intensité de fluorescence est faible) correspondent les cellules non perméabilisées ou n'exprimant pas l'eGFP. L'intensité de fluorescence en M1 correspond à l'autofluorescence des cellules. Les cellules en M2 (dont l'intensité de fluorescence est plus élevée) sont les cellules perméabilisées ou transfectées. L'intensité de fluorescence en M2 reflète la quantité de PI incorporé dans les cellules lors de l'électroperméabilisation ou la quantité d'eGFP exprimée suite à l'électrotransfection. En absence de champ électrique, le pourcentage de cellules en M2 est faible : 7% des cellules sont perméabilisées (ce pourcentage correspond au pourcentage de cellules mortes) et 0% des cellules transfectées. Lorsque 10 impulsions électriques de 5 ms à 0,7 kV/cm et à la fréquence de 1 Hz sont appliquées, le pourcentage de cellules fluorescentes en M2 augmente. 93% des cellules sont perméabilisées et 45% des cellules sont transfectées. La fluorescence totale par cellule passe de 30 à 636 u.a., lors de l'électroperméabilisation. La fluorescence par cellule transfectée augmente de 16 au 2265 u.a.

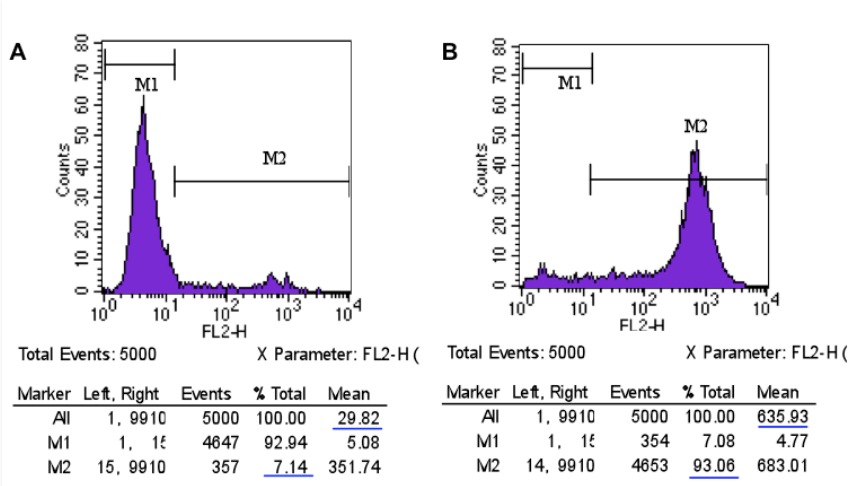

Figure VII-7: Détermination en cytométrie de flux du pourcentage de cellules perméabilisées au PI et de la fluorescence associée. Les histogrammes représentent le nombre de cellules en fonction de leur intensité de fluorescence observées sur le canal FL2 (560 nm). M1 : i.e., cellules non perméabilisées. M2 : i.e., cellules perméabilisées. Les pourcentages de cellules fluorescentes et la fluorescence moyenne des deux populations cellulaires sont surlignés dans le tableau. **A.** E = 0 kV/cm. 7,14% des cellules sont fluorescentes. La fluorescence moyenne de la population totale est de 29,82 u.a. **B.** 10 x 5 ms, 1 Hz, 0.7 kV/cm. Plus de 90% des cellules sont perméabilisées. La fluorescence moyenne est de 635,93 u.a. *(Adapté de la thèse de Muriel Golzio, 1999)*.

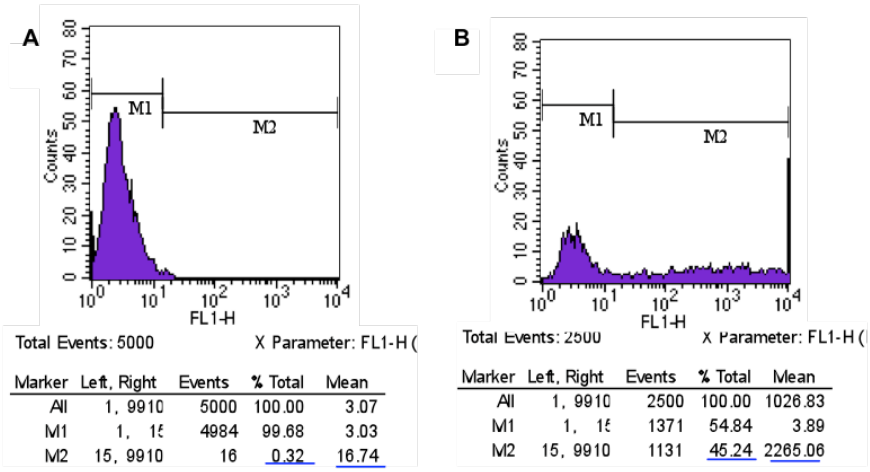

Figure VII-8: Détermination en cytométrie de flux du pourcentage de cellules exprimant l'eGFP et de la fluorescence associée. Les histogrammes représentent le nombre de cellules comptabilisées en fonction de leurs intensités de fluorescence observées sur le canal FL1 (530 nm). M1 : i.e., cellules non transfectées, M2 : i.e., cellules transfectées. Les pourcentages de cellules fluorescentes et la fluorescence moyenne des deux populations cellulaires sont surlignés dans le tableau. **A.** E = 0 kV/cm. 0,32% des cellules sont fluorescentes. La fluorescence moyenne associée à cette population est de 16,74 u.a. **B.** 10 x 5 ms, 1 Hz, 0,7 kV/cm. 45% des cellules sont transfectées. La fluorescence moyenne est de 2265,06 u.a. *(Adapté de la thèse Cécile Faurie, 2004)*.

PARTIE II

MÉTHODES SPÉCIFIQUES

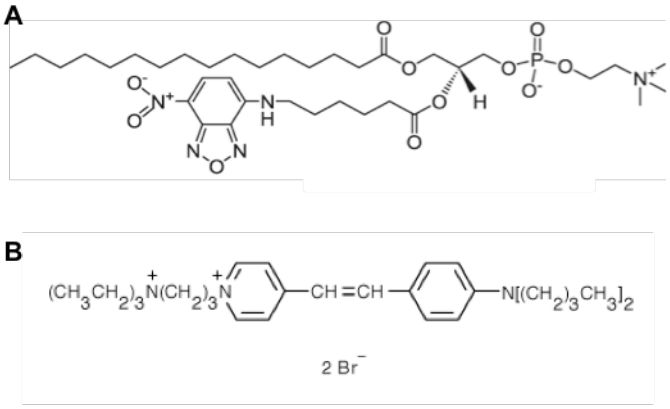

Figure VII-9: Formules chimiques du C6-NBD-PC et du FM1-43. A. Le C6-NBD-PC : Le C6-NBD-PC est un analogue de phospholipide fluorescent dont les caractéristiques spectrales sont : $\lambda_{max(ex)}$ = 470 nm, $\lambda_{max(em)}$ = 530 nm. Les acides gras sont ceux de lécithine de jaune d'œuf. **B. Le FM1-43 :** Le FM1-43 est un composé styryl lipophile dont les caractéristiques spectrales sont : $\lambda_{max(ex)}$ = 510 nm, $\lambda_{max(em)}$ = 626 nm.

Partie II. Méthodes spécifiques

1. Etude de la mobilité transverse des phospholipides

1.1. Suivi de l'internalisation du C6-NBD-PC

1.1.1. Le C6-NBD-PC

Le C6-NBD-PC est une molécule de phosphatidylcholine dont une des chaînes d'acides gras est substituée par un groupement fluorescent le N4-nitrobenzo-2-oxa-1,3-diazole (Avanti Polar Lipids Inc., Alabaster, AL) (Figure VII-9A). Ses caractéristiques spectrales sont: $\lambda_{max(excitation)}$ = 470 nm ; $\lambda_{max(émission)}$ = 530 nm. Son incorporation facilitée par une chaîne courte permet le marquage du feuillet externe de la membrane plasmique des cellules *(Julien et al., 1993)*.

1.1.2. Préparation des vésicules fluorescentes

La préparation des vésicules fluorescentes est réalisée par mélange de 10 µL d'une solution de DOPC (20 mg/mL) (Avanti Polar Lipids Inc., Alabaster, AL) à 20 µL d'une solution de C6-NBD-PC (1 mg/mL). Le film lipidique est obtenu par évaporation du chloroforme sous flux d'azote puis placé sous vide pendant une heure. Le film lipidique est resuspendu dans 10 mL de tampon PBS-Ca^{2+}/Mg^{2+} à 4°C. La solution est ensuite vortexée pendant 1 minute. Des vésicules multi-lamellaires sont ainsi obtenues. La solution de vésicules fluorescentes est soniquée pendant 7 min à 60% d'une puissance de 25 W (VibraCell, Bioblock Scientific, Illkirch, France). Des vésicules uni-lamellaires sont ainsi obtenues *(Julien et al., 1993)*.

1.1.3. Marquage des cellules

Toute la procédure de marquage se fait à une température de 4°C afin de limiter les phénomènes d'endocytose. Les cellules sont ensemencées à une densité cellulaire de 0,5 10^4 cellules dans une Labteck, 1 h avant le marquage. Après 3 rinçages successifs avec 1 mL de tampon PBS-Ca^{2+}/Mg^{2+}, elles sont mises en présence de 1 mL de suspension de vésicules fluorescentes pendant 10 minutes à 4°C. Après le marquage, les cellules sont rincées 3 fois avec du tampon de pulsation afin d'éliminer les vésicules fluorescentes en excès *(Julien et al., 1993)*.

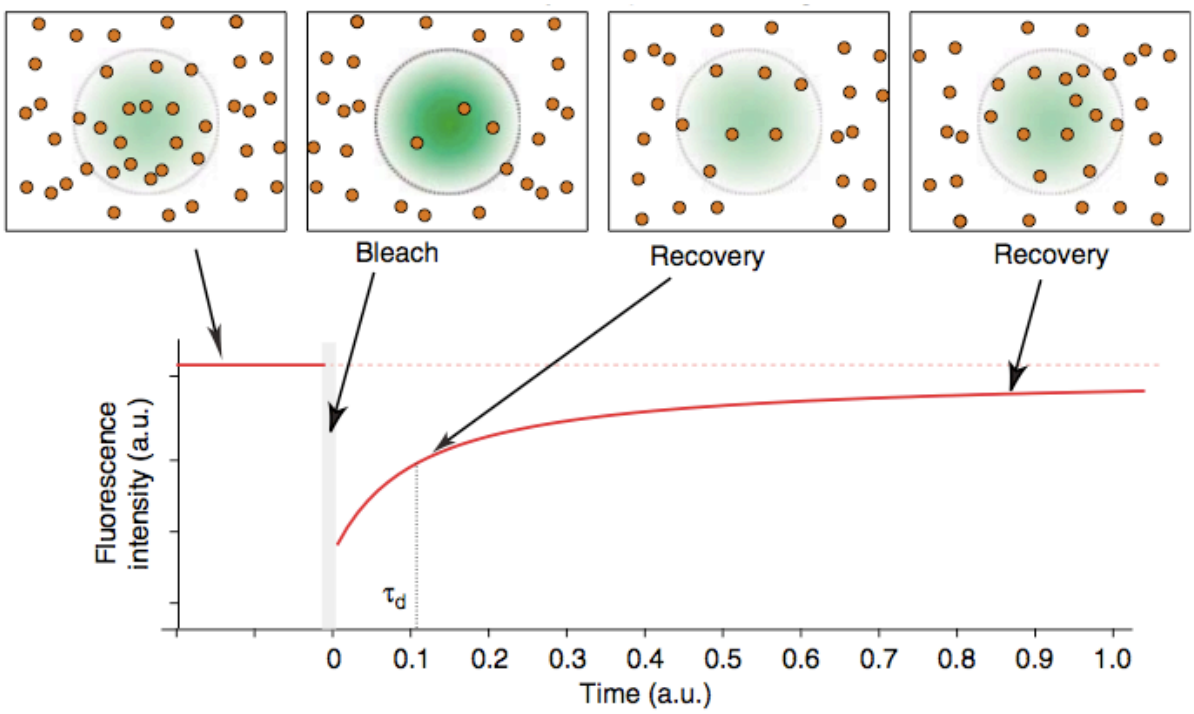

Figure VII-10: Le FRAP. L'intensité de fluorescence est enregistrée avec une faible intensité de laser dans une région d'intérêt (cercle gris). Une impulsion de haute intensité de laser est utilisé pour photodégrader la majorité des molécules fluorescentes (point rouge) présentes dans la région d'intérêt. L'intensité de fluorescence est ensuite mesurée avec une faible intensité de laser. Les molécules fluorescentes diffusent et repeuplent l'aire photodégradée. L'intensité de fluorescence de l'aire photodégradé augmente. Le temps de retour de l'intensité de fluorescence reflète le temps de diffusion des molécules fluorescentes. Si quelques molécules sont immobiles dans la région photodégradée, l'intensité de fluorescence après le retour sera plus faible qu'avant la photodégradation *(Adapté de Marguet et al., 2006)*.

1.2. Suivi de la translocation des phospholipides chargés

1.2.1. Le FM 1-43

Le FM 1-43 (Invitrogen Corporation, Carlsbad, CA) est un composé styryl lipophile utilisé dans l'étude de la membrane plasmique et dans les processus de vésiculation membranaire (Figure VII-9B). Ses caractéristiques spectrales sont : $\lambda_{max(excitation)}$ = 510 nm and $\lambda_{max(émission)}$ = 626 nm. Ce marqueur hydrosoluble, qui est non toxique pour les cellules et non fluorescent dans milieu aqueux, s'insère dans le feuillet externe de la membrane plasmique où il devient très fluorescent *(Zweifach, 2000; Gaffield et al., 2006)*.

1.2.2. Marquage des cellules

Une heure avant l'électroperméabilisation, 0,5 10^4 cellules CHO sont cultivées dans des Labteck. Les cellules sont lavées trois fois avec du tampon de pulsation et sont incubées en présence de 3 µM FM 1-43 dans du tampon de pulsation pendant 15 min à 37°C. Les cellules sont directement électroperméabilisées, en présence de la sonde FM 1-43, sans lavage *(Vernier et al., 2006)*.

2. Etude de la mobilité latérale des protéines membranaires

Le coefficient de diffusion latérale et la fraction mobile sont mesurés par Retour de Fluorescence Après Photodégradation (i.e.FRAP) en utilisant un microscope confocal Zeiss LSM 510 (Figure VII-10). Le retour de fluorescence est mesuré sur des cellules CHO Rae1-eGFP avant et après électroperméabilisation. Le laser Argon 488 nm est utilisé pour exciter la protéine eGFP. Les cellules sont observées avec un objectif x63 à immersion à eau (ON, 1.4). Après 50 images avant photodégradation (pixel time, 192 ms), deux ROI face aux électrodes de rayon w égale à 1 µm sont photodégradées et le retour de fluorescence est mesuré pendant 40 s. La durée de la photodégradation est déterminée afin que sa valeur soit inférieure ou égale à un cinquième du temps de demi-retour pour obtenir une estimation correcte du coefficient de diffusion latérale de la protéine d'intérêt, D. Les mesures expérimentales de retour de fluorescence sont normalisées et corrigées des fluctuations en z par utilisation d'une ROI comme standard interne. Le temps de demi-retour et la fraction mobile sont déterminés en ajustant les courbes de retour de fluorescence normalisé en utilisant le développement limité au

10ème ordre de l'équation modifiée donnée par Axelrod *(Axelrod et al., 1976, Causeret et al., 2005)*. Le coefficient de diffusion latérale D peut être calculé à partir de l'équation $D = \beta w^2/4t_{1/2}$ avec β une fonction de la profondeur de photodestruction (K) calibrée *(Yguerabide et al., 1982)*. L'ajustement du retour expérimental est réalisé selon une méthode de moindres carrés non linéaire (Levenberg-Marquardt) par rapport à l'expression analytique du retour de fluorescence suivante:

$$I_w(t) = \frac{1-e^{-K}}{K}(1-M) + M\sum_{n=1}^{10}\frac{(-K)^n}{n!\left(1+n+2n\frac{t}{t_{1/2}}\right)} \quad (Eq.VII-2)$$

Avec w, rayon de la ROI, K paramètre estimant la profondeur de photdestruction, M, fraction mobile et $t_{1/2}$, le temps de demi-retour.

3. Analyses statistiques

Toutes les mesures effectuées sont réalisées au moins 3 fois indépendemment et les barres d'erreurs représentées sur les graphiques représentent l'erreur standard à la moyenne (i.e. SEM).

Le test statistique est le test non paramétrique de Mann-Whitney qui permet de tester si deux échantillons ont la même moyenne. La valeur du test donne la probabilité P pour que les moyennes obtenues soient différentes. On notera * pour P<0,05 (95,5% de chance pour que les moyennes comparées soient différentes), ** pour 0,01<P<0,005 (entre 99,0 et 99,5% de chance pour que les moyennes comparées soient différentes) et *** pour P<0,001% (99,9% de chance pour que les moyennes comparées soient différentes). L'abréviation NS signifie qu'il n'y a pas de différence de moyenne entre les deux échantillons.

VI. RÉFÉRENCES BIBLIOGRAPHIQUES

VI. Références bibliographiques

Aihara, H., and Miyazaki, J.I. (1998) Gene transfer into muscle by electroporation in vivo. *Nature Biotechnol.,* **16**:867-870

Akaneya, Y., Jiang, B., and Tsumoto, T. (2005) RNAi-induced gene silencing by local electroporation in targeting brain region. *J. Neurophysiol.,* **93**:594-602

Almeida, P.F.F., Pokorny, A., and Hinderliter, A. (2005) Thermodynamics of membrane domains. *Biochim. Biophys. Acta,* **1720**:1-13

Almeida, R.F., Borst, J., Fedorov, A., Prieto, M., and Visser, A.J. (2007) Complexity of lipid domains and rafts in giant unilamellar vesicles revealed by combining imaging and microscopic and macroscopic time-resolved fluorescence. *Biophys. J.,* **93**:539-553

Andreason, G.L., and Evans, G.A. (1988) Introduction and expression of DNA molecules in eukaryotic cells by electroporation. *Biotechniques,* **6**:650-660

Axelrod, D., Koppel, D.E., Schlessinger, J., Elson, E., and Webb, W.W. (1976) Mobility measurement by analysis of fluorescence photobleaching recovery kinetics. *Biophys. J.,* **16**:1055-1069

Babiychuk, E.B., and Draeger, A. (2006) Biochemical characterization of detergent-resistant membranes: a systemic approach. *Biochem. J.,* **397**:407-416

Barteau, B., Chèvre, R., Letrou-Bonneval, E., Labas, R., Lambert, O., and Pitard, B. (2008) Physicochemical parameters of non-viral vectors that govern transfection efficiency. *Curr. Gene Ther.,* **8**:313-323.

Bartoli, M., Poupiot, J., Vulin, A., Fougerousse, F., Arandel, L., Daniele, N., Roudaut, C., Noulet, F., Garcia, L., Danos, O., and Richard, I. (2007) AAV-mediated delivery of a mutated myostatin propeptide ameliorates calpain 3 but not α-sarcoglycan defiency. *Gene Ther.,* **14**:733-740

Basse, F., Gaffet, P., Rendu, F. and Bienvenue, A. (1993) Translocation of spin-labelled phospholipids through plasma membrane during thrombin- and ionophore A23187-induced platelet activation. *Biochem.,* **82**:2337-2344

Beebe, S.J., White, J., Blackmore, P.F., Deng, Y., Somers, K., and Schoenbach, K.H. (2003) Diverse effects of nanosecond pulsed electric fields on cells and tissues. *DNA Cell Biol.,* **22**:785-796

Bell, G.I., Dembo, M., and Bongrand, P. (1984) Cell adhesion. Competition between nonspecific repulsion and specific bonding. *Biophys. J.,* **45**:1051-1064

Berezhna, S., Schaefer, S., Heintzmann, R., Jahnz, M., Boese, G., Deniz, A., and Schwille, P. (2005) New effects in polynucleotide release from cationic lipid carriers revealed by

confocal imaging, fluorescence cross-correlation spectroscopy and single particle tracking. *Biochim. Biophys. Acta,* **1669**:193-207

Bernt, K.M., Ni, S., Tieu, A.T., and Lieber, A. (2005) Assessment of a combined, adenovirus-mediated oncolytic and immunostimulatory tumor therapy. *Cancer Res.,* **65**:4343-4352

Bevers, E.M., Comfurius, P., Dekkers, D.W.C., and Zwaal, R.F.A. (1999) Lipid translocation across the plasma membrane of mammalians cells. *Biochim. Biophys. Acta,* **1439**:317-330

Bockmann, R.A., Groot, B.L., Kakorin, S., Neumann, E., and Grubmuller, H. (2008) Kinetics, statistics, and energetics of lipid membrane electroporation studied by molecular dynamics simulations. *Biophys. J.,* **95** 1837-1850

Bloquel, C., Bejjani, R., Bigey, P., Bedioui, F., Doat, M., BenEzra, D., Scherman, D., and Behar-Cohen, F. (2006) Plasmid electrotransfer of eye ciliary muscle: principles and therapeutic efficacy using hTNF-α soluble receptor in uveitis. *FASEB J.,* **20**:389-391

Brown, D.A. and London, E. (1998) Structure and origin of ordered lipid domains in biological membranes. *J. Membrane Biol.,* **164**:103-114

Carrière, M., Escriou, V., Jollet, A., Scherman, D., Azoulet, M., and Monneret, C. (2004) New synthetic glycolipids for targeted gene transfer: Synthesis, formulation in lipoplexes and specific interaction with lectin. *Drug Delivery,* **11**:351-363

Causeret, M., Taulet, N., Comunale F., Favard, C., and Gauthier-Rouvière, C. (2005) N-cadherin association with lipid rafts regulates its dynamic assembly et cell-cell junctions in C2C12 myoblasts. *Mol. Biol. Cell,* **16**:2168-2180

Cavazzana-Calvo, M., Hacein-Bey, S., de Saint Basile, G., Gross, F., Yvon, E., Nusbaum, P., Selz, F., Hue, C., Certain, S., Casanova, J.L., Bousso, P., Le Deist, F., and Fischer, A. (2000) Gene therapy of human severe combined immunodeficiency (SCID)-X1 disease. *Science,* **288**:669-672

Celec, P., Gardlik, R., Palffy, R., Hodosy, J., Stuchlik, S., and Drahovska, H. (2005) The use of transformed Escherichia coli for experimental angiogenesis induced by regulated in situ production of vascular endothelial growth factor – an alternative gene therapy. *Med. Hypotheses,* **64**:505-511

Chang, D.C., and Reese, T.S. (1990) Changes in membrane structure induced by electroporation revealed by rapid-freezing electron microscopy. *Biophys. J.,* **58**:1-12

Chapman E.R. (2002) Synaptotagmin: a Ca^{2+} sensor that tiggers exocytosis. *Nat. Rev. Mol. Cell Biol.,* **3**:498-508

Chemet, S., Desouazi, M., Hacker, D and Wurm, T. (2009) DNA delivery by micro-injection for generation of recombinant mammalian cell lines. *Methods Mol. Biol.,* **518**:1-14

Chen, S., Shohet, R.V., Frenkel P., Grayburn, P.A., and Bekeredjian, R. (2003) Optimization of ultrasound parameters of cardiac gene delivery of adenoviral or plasmid deoxyribonucleic acid by ultrasound-targeted microbubble destruction. *J. Am. Coll. Cardiol.,* **42**:301-308

Chorny, M., Polyak, B., Alferiev, I.S., Walsh, K., Friedman, G., and Levy, R.J. (2007) Magnetically driven plasmid DNA delivery with biodegradable polymeric nanoparticles. *FASEB J.,* **21**:2510-2519

Chou, P.C., Chuang, T.F., Jan, T.R., Gion, H.C., Huang, Y.C., Lei, H.J., Chen, W.Y. and Chu, R.M. (2009) Effects of immunotherapy of IL-6 and IL-15 plasmids on transmissible venereal tumor in beagles. *Vet. Immunol. Immunopath.,* **130**:25-34

Chu, G., Hayakawa, H., and Berg, P. (1987) Electroporation for the efficient transfection of mammalian cells with DNA. *Nucleic Acids Res.,* **15**:1311-1326

Chuang, Y.C., Chou, A.K., Wu, P.C., Chiang, P.H., Yu, T.J., Yang, L.C., Yoshimura, N., and Chancellor, M.B. (2003) Gene therapy for bladder pain with gene gun particle encoding pro-opiomelanocortin cDNA. *J. Urol.,* **170**:2044-2048

Cordelier, P., and Strayer, D.S. (2006) Using gene delivery to protect HIV-susceptible CNS cells: Inhibiting HIV replication in microglia. *Virus Res.,* **118**:87-97

Cordelier, P., Bienvenu, C., Lulka, H., Marrache, F., Bouisson, M., Openheim, A., Strayer, D.S., Vaysse, N., Pradayrol, L., and Buscail, L. (2007) Replication-deficient rSV40 mediate pancreatic gene transfer and long-term inhibition of tumour growth. *Cancer Gene Ther.,* **14**:19-29

Couzin, J., and Kaiser, J. (2005) As Gelsinger case ends, gene therapy suffers another blow. *Science,* **307**:1028

Croaker, G., Wass, E., and Iland, H. (1990) Electric field-mediated gene transfer in K cells: optimization of parameters affecting efficiency. *Leukemia,* **4**:502-507

Curcio, C., Khan, A.S., Spadaro, M., Quaglino, E., Cavallo, F., Forni, G., and Draghia-Akli, R. (2008) DNA immunization using constant-current electroporation affords long-term protection from autochthonous mammary carcinomas in cancer-prone transgenic mice. *Cancer Gene Ther.,* **15**:108-114

Darquet, A.M., Cameron, B., Wils, P., Scherman, D., and Crouzet, J. (1997) A new DNA vehicle for nonviral gene delivery: supercoiled minicircle. *Gene Ther.,* **4**:1341-129

Daud, A.I., DeConti, R.C., Andrews, S., Urbas, P., Riker, A.I., Sondak, V.K., Munster, P.N., Sullivan, D.M, Ugen, K.E., Messina, J.L. and Heller, R. (2008) Phase I trial of interleukin-12 plasmid electroporation in patients with metastatic melanoma. *J. Clin. Oncol.,* **26**:5896-58903

Dauty, E., Verkman, A.S. (2005) Actin cytoskeleton as the principal determinant of size-dependent DNA mobility in cytoplasm: a new barrier for non-viral gene delivery. *J. Biol. Chem.,* **280**:7823-7828

Dean, D.A., Strong, D.D., and Zimmer, W.E. (2005a) Nuclear entry of nonviral vectors. *Gene Ther.,* **12**:881-890

Delalande, A., Bureau, M.F., Midoux, P., Bouakaz, A., and Pichon, C. (2009) Ultasound-assisted microbubbles gene transfer in tendons for gene therapy. *Ultrasonics,* **50**:269-272.

Delatour, V., Helfer, E., Didry, D., Lê, .LH., Gaucher, J.F., Carlier, M.F., and Romet-Lemonne, G. (2008) Arp2/3 controls the motile behavior of N-WASP-functionalized GUVs and modulates N-WASP surface distribution by mediating transient links with actin filaments. *Biophys. J.,* **94**:4890-4905.

De Meyer, S.F., Vandeputte, N., Pareyn, I., Patrus, I., Lenting, P.J., Chuah, M.K., VandenDriessche, T., Deckmyn, H. and Vanhoorelbeke, K. (2008) Restoration of plasma von Willebrand factor deficiency is sufficient to correct thrombus formation after gene therapy for severe von Willebrand disease. *Arterioscler. Thromb. Vasc. Biol.,* **28**:1621-1626.

Demchenko, A.P., Mély, Y., Duportail, G., and Klymchenko, A.S. (2009) Monitoring biophysical properties of lipid membranes by environnement-sensitive fluorescent probes. **96**:3461-3470.

Deng, C.X., Sieling, F., Pan, H., and Cui, J. (2004) Ultrasound-induced cell membrane porosity. *Ultrasound Med. Biol.,* **30**:519-526

Deshayes, S., Morris, M.C., Divita, G., and Heitz, F. (2005) Cell-penetrating peptides: tools for intracellular delivery of therapeutics. *Cell. Mol. Life Sci.,* **62**:1839-1849

Devaux, P.F., Lopez-Montero I., and Bryde S., (2006) Proteins involved in lipid translocation in eukaryotic cells. *Chem. Phys. Lipids*, **141**:119-132.

Dietrich, A., Becherer, L., Brinckmann, U., Hauss, J., Liebert, U.G., Gütz, A. and Aust, G. (2006) Particle-mediated cytokine gene therapy leads to antitumor and antimetastatic effects in mouse carcinoma models. *Cancer Biother. Radiopharm.,* **21**:333-341

Dietrich, G., Bubert, A., Gentschev, I., Sokolovic, Z., Simm, A., and Catic, A. (1998) Delivery of antigen-encoding plasmid DNA into cytosol of macrophages by attenuated suicide Listeria monocytgenes. *Nature Biotechnol.,* **16**:181-185

Dileo, J., Miller, T.E., Chesnoy, S., and Huang, L. (2003) Gene transfer to subdermal tissues via a new gene gun design. *Hum. Gene. Ther.,* **14**:79-87

Dressler, V., Schwister, K., Haest, C.W., and Deuticke, B. (1983) Dielectric breakdown of the erythrocyte membrane enhances transbilayer mobility of phospholipids. *Biochim. Biophys. Acta,* **732**:304-307

Duchardt, F., Fotin-Mleczek, M., Schwarz, H., Fischer, R., and Brock R. (2007) A comprehensive model for the cellular uptake of cationic cell-penetrating peptides. *Traffic,* **8**:848-866

Duvshani-Eshet, M., Baruch, L., Kesselman, E., Shimoni, E., and Machluf, M. (2006) Therapeutic ultrasound-mediated DNA to cell and nucleus: bioeffects revealed by confocale and atomic force microscopy. *Gene Ther.,* **13**:163-172

Edelstein, M.L., Abedi, M.R. and Wixon, J. (2007) Gene therapy clinical trials worldwide to 2007 – an update. *J. Gene Med.,* **9**:833-842

Edidin, M., Lipids on the frontiers : a century of cell membrane bilayers. (2003) *Nature Rev. Mol. Cell Biol.,* **9**: 112-124

Eefting, D., Grimbergen, J.M., de Vries, M.R., van Weel, V., Kaijzel, E.L., Que, L., Moon, R.T., Lowik, C.W., van Bockel, J.H. and Quax, P.H. (2007) Prolonged in vivo gene silencing by electroporation-mediated plasmid delivery of small interfering RNA. *Hum. Gene Ther.,* **18**:861-869

Ellens, H., Siegel, D.P., Alford, D., Yeagle, P.L., Boni, L., Lis, L.J., Quin, P.J. and Bentz, J. (1989) Membrane fusion and inverted phases. *Biochem.,* **28**:3692-3703

Engelman, D.M. (2005) Membranes are more mosaic than fluid. *Nature,* **438**:578-580

Escoffre, J.M., Dean, D.S., Hubert, M., Rols, M.P., and Favard, C. (2007) Membrane perturbation by an external electric field: a mechanism to permit molecular uptake. *Eur. Biophys. J.,* **36**:973-983

Escoffre, J.M., Debin, A., Reynes, J.P., Drocourt, D., Tiraby, G., Hellaudais, L., Teissié, J., and Golzio, M. (2008) Long-lasting in vivo gene silencing by electrotransfer of shRNA expressing plasmid. *Tech. Cancer Res. Treat.,* **7**:1-8

Escoffre, J.M., Portet, T., Wasungu, L., Teissié, J., Dean, D., and Rols, M.P. (2009a) What is (still not) known of the mechanism by which electroporation mediates gene transfer and expression in cells and tissues. *Mol. Biotechnol.,* **41**:286-295

Escoffre, J.M., Mauroy, C., Portet, T., Wasungu, L., Rosazza, C., Gilbart, Y., Mallet, L., Bellard, E., Golzio, M., Rols, M.P., and Teissie, J. (2009b) Gene electrotransfer : From biophysical mechanisms to in vivo applications. Part 1-Biophysical mechanisms. *Biophys. Rev.,* **1**:177-184

Escoffre, J.M., Mauroy, C., Portet, T., Wasungu, L., Paganin-Gioanni, A., Golzio, M., Teissie, J., and Rols, M.P. (2009c) Gene electrotransfer : From biophysical mechanisms to in vivo applications. Part 2-In vivo developments and present clinical applications. *Biophys. Rev.,* **1**:185-191

Fantini, J., Garmy, N., Mahfoud, R., Yahi, N., (2002) Lipid rafts: structure, function ad role in HIV, Alzheimer's and prion diseases. *Expert Rev. Mol. Med.,* **20**:1-22

Faurie, C., Golzio, M., Moller, P., Teissié, J., and Rols, M.P. (2003) Cell and animal imaging of electrically mediated gene transfer. *DNA Cell Biol.,* **22**:777-783

Faurie, C., Phez, E., Golzio, M., Vossen, C., Lesbordes, J.C., Delteil, C., Teissié, J., and Rols, M.P. (2004) Effect of electric field vectoriality on electrically mediated gene delivery in mammalian cells. *Biochim. Biophys. Acta,* **1665**:92-100

Faurie, C., Rebersek, M., Golzio, M., Kanduser, M., Escoffre, J.M., Pavlin, M., Teissié, J., Miklavcic, D., and Rols, M.P. (2010) Electro-mediated gene transfer and expression are controlled by the life-time of DNA/membrane complex formation. *J. Gene Med.,* **12**:117-125

Fernandez-Botello, A., Comelles, F., Alsina, M.A., Cea, P. and Reig, F. (2008) A monolayer study on interactions of docetaxel with model lipid membranes. *J. Phys. Chem. B.,* **112**:13834-13841

Ferreira, E., Potier, E., Logeart-Avramoglou D., Salomskaite-Davalgiene, S., Mir, L.M., and Petite, H. (2008) Optimization of a gene electrotransfer method for mesenchymal stem cell transfection. *Gene Ther.,* **15**:537-544

Fischer, A., Hacein-Bey, S., Le Deist, F., Soudais, C., Di Santo, J.P., de Saint Basile, G., and Cavazzana-Calvo, M. (2000) Gene therapy of severe combined immunodeficiencies. *Immunol. Rev.,* **178**:13-20

Fox, J.E., Austin, C.D., Bayles, J.K., and Steffen, P.K. (1990) Role of membrane skeleton in preventing the shedding of coagulant-rich microvesicles from the platelet plasma membrane. *J. Cell. Biol.,* **111**:483-493

Frey, W., White, J.A., Price, R.O., Blackmore, P.F., Joshi, R.P., Nuccitelli, R., Beebe, S.J., Schoenbach, K.H. and Kolb; J.F. (2006) Plasma membrane voltage changes during nanosecond pulsed electric fiels exposure. *Biophys. J.,* **90**:3608-3615

Friedrich, U., Stachowicz, N., Simm, A., Fuhr, G., Lucas, K., and Zimmermann, U. (1998) High efficiency electrotransfection with aluminium electrodes using microsecond controlled pulses. *Bioelectrochem. Bioenerg.,* **47**:103-111

Fu, G.F., Hou, Y.Y., Fan, Y.R., Liu, W.H., and Xu, G.X. (2005) Bifidobacterium longum as an oral delivery system of endostatin for gene therapy on solid liver cancer. *Cancer Gene Ther.,* **12**:133-140

Gabriel, B., and Teissié, J. (1997) Direct observation in the millisecond time range of fluorescent molecule asymmetrical interaction with the electropermeabilized cell membrane. *Biophys. J.,* **73**:2630-2637

Gabriel, B., and Teissié, J., (1998) Fluorescence imaging in the millisecond time range of membrane electropermeabilization of single cells using a rapid ultra-low-light intensifying detection system. *Eur. Biophys. J.,* **27**:291-298

Gabriel, B., and Teissié, J., (1999) Time courses of mammalian cell electropermeabilization observed by millisecond imaging of membrane property changes during the pulse. *Biophys. J.,* **76**:2158-2165

Gaffield, M.A., and Betz, W.J. (2006) Imaging synaptic exocyosis and endocytisus with FM dyes. *Nat. Protoc.,* **1**:2916-2921

Gardlik, R., Palffy, R., Hodosy, J., Lukacs, J., Turna, J., and Celec, P. (2005) Vectors and delivery systems in gene therapy. *Med. Sci. Monit.,* **11**:RA110-121

Ghochikyan, A., Vasilevko, V., Petruschina, I., Movsesvan, N., Babikyan, D., Tian, W., Sadzikava, N., Ross, T.M., Head, E., Cribbs, D.H., and Agadjanyan, M.G. (2003) Generation and characterization of the humoral immune response to DNA immunization with a chimeric Aβ-inteleukine 4 minigene. *Eur. J. Immunol.,* **33**:3232-3241

Gill, D.R., Pringle, I.A., and Hyde, S.C. (2009) Progress and prospects: The design and production of plasmid vectors. *Gene Ther.,* **16**:165-171

Gillies R.J., Didier N., and Denton, M. (1986) Determination of cell number in monolayer cultures. *Anal. Biochem.,* **159**:109-113

Girard, P.J., Pecreaux, G., Lenoir, P., Falson, J.L., Rigaud, J.L., and Bassereau, P. (2004) A new method for the reconstitution of membrane proteins into giant unilamellar vesicles. *Biophys. J.,* **87**:419-429

Goldstein, S., Fordis, C.M., and Howard, B.H. (1989) Enhanced transfection efficiency and improved cell survival after electroporation of G2/M-synchronized cells and treatment with sodium butyrate. *Nucleic Acids Res.,* **17**:3959-3971

Golzio, M., Teissié, J., and Rols, M.P. (2002a) Direct visualization at the single-cell level of electrically mediated gene delivery. *Proc. Natl. Acad. Sci. USA,* **99**:1292-1297

Golzio, M., Teissié, J., and Rols, M.P. (2002b) Cell synchronization effect on mammalian cell permeabilization and gene delivery by electric field. *Biochim. Biophys. Acta,* **1563**:23-28

Golzio, M., Rols, M.P., and Teissie, J. (2004) In vitro and in vivo electric field-mediated permeabilization, gene transfer, and expression. *Methods,* **32**:126-135

Goyendalle, A., Vulin, A., Fougerousse, F., Leturcq, F., Kaplan, J.C., Garcia, L., and Danos, O. (2004) Rescue of dystrophic muscle through U7 snRNA-mediated exon skipping. *Science,* **306**:1796-1799

Gross, D., Loew, L.M., and Webb, W.W. (1986) Optical imaging of cell membrane potential changes induced by applied electric fields. *Biophys. J.,* **50**:339-348

Grossin, L., Cournil-Henrionnet, C., Mir, L.M., Liagre, B., Dumas, D., Etienne, S., Guingamp, C., Netter, P., and Gillet, P. (2003) Direct gene transfer into rat articular cartilage by in vivo electroporation. *FASEB J.,* **17**:829-835

Gundelfinger, E.D., Kessels, M.M., and Qualmann, B. (2003) Temporal and spatial coordination of exocytosis and endocytosis. *Nature Rev. Mol. Cell Biol.,* **4**:127-139

Gurtovenko, A.A., and Vattulainen I. (2007) Molecular mechanism for lipid flip-flops, *J. Phys. Chem. B,* **111** 13554-13559.

Haas A., (2007) The phagosomes: Compartment with a license to kill. *Traffic,* **8**:311-330

Hacein-Bey-Abina, S., Von Kalle, C., Schmidt, M., McCormack, M.P., Wulffraat, N., Leboulch, P., Lim, A., Osborne, C.S., Pawliuk, R., Morillon, E., Sorensen, R., Forster, A., Fraser, P., Cohen, J.I., de Saint Basile, G., Alexander, I., Wintergerst, U., Frebourg, T., Aurias, A., Stoppa-Lyonnet, D., Romana, S., Radford-Weiss, I., Gross, F., Valensi, F., Delabesse, E., Macintyre, E., Sigaux, F., Soulier, J., Leiva, L.E., Wissler, M., Prinz, C., Rabbitts, T.H., Le Deist, F., Fischer, A., and Cavazzana-Calvo, M. (2003a) LMO2-associated clonal T cell proliferation in two patients after gene therapy for SCID-X1. *Science*, **302**:415-419

Hacein-Bey-Abina, S., Von Kalle, C., Schmidt, M., McCormack, M.P., Wulffraat, N., Leboulch, P., Lim, A., Osborne, C.S., Pawliuk, R., Morillon, E., Sorensen, R., Forster, A., Fraser, P., Cohen, J.I., de Saint Basile, G., Alexander, I., Wintergerst, U., Frebourg, T., Aurias, A., Stoppa-Lyonnet, D., Romana, S., Radford-Weiss, I., Gross, F., Valensi, F., Delabesse, E., Macintyre, E., Sigaux, F., Soulier, J., Leiva, L.E., Wissler, M., Prinz, C., Rabbitts, T.H., Le Deist, F., Fischer, A., and Cavazzana-Calvo, M. (2003b) A serious adverse event after successful gene therapy for X-linked severe combined immunodefiency. *N. Engl. J. Med.,* **348**:255-256

Haest, C.W.M., Kamp, D., and Deuticke, B. (1997) Transbilayer reorientation of phospholipids probes in the human erythrocytes membranes. Lessons from studies on electroporated and resealing cells. *Biochim. Biophys. Acta,* **1325**:17-33

Haluska, C.K., Schröder, A.P., Didier, P., Heissler, D., Duportail, G., Mély, Y., and Marques, C.M. (2008) Combining fluorescence lifetime and polarization microscopy to discriminate phase separated domains in giant unilamellar vesicles. *Biophys. J.,* **95**:5737-5747.

Helfrich, W. (1978) Steric interaction of fluid membranes in multilayers systems. *Z. Naturforscj,* **33a**:305-315

Heller, L.C., Merkler, K., Westover, J., Cruz, Y., Coppola, D., Benson K., Daud, A., and Heller, R. (2006) Evaluation of toxicity following electrically mediated interleukin-12 gene delivery in a B16 mouse melanoma model. *Clin. Cancer Res.,* **12**:3177-3183

Heller, L.C., Jaroszeski, M.J., Coppola, D., McCray, A.N., Hickey, J., and Heller, R. (2007) Optimization of cutaneaous electrically mediated plasmid DNA delivery using novel electrode. *Gene Ther.,* **14**:275-280

Heller, R., Jaroszeski, M., Atkin, A., Moradpour, D., Gilbert, R., Wands, J., and Nicolau, C. (1996) In vivo gene electroinjection and expression in rat liver. *FEBS Lett.,* **389**:225-228

Helms, J.B. and Zurzolo, C. (2004) Lipids as targeting signals: lipid rafts and intracellular trafficking. *Traffic,* **5**:247-254

Henshaw, J.W. and Yuan, F. (2008) Field distribution and DNA transport in solid tumors during electric field-mediated gene delivery. *J. Pharm. Sci.,* **97**:691-711

Henszen, M.M., Weske, M., Schwarz, S., Haest, C.W.M., and Deuticke, B. (1997) Electric field pulses induce reversible shape transformation of human erythrocytes. *Mol. Membr. Biol.,* **14**:195-204.

Herweijer, H., and Wolff, J.A. (2007) Gene Therapy progress and prospects: Hydrodynamic gene delivery. *Gene Ther.,* **14**:99-107

Hibino, M., Itoh, H., and Kinosita, K.J. (1993) Time course of cell electroporation as revealed by microsecond imaging of transmembrane potential. *Biophys. J.,* **64**:1789-1800

Holzbach, T., Vlaskou, D., Neshkova, I., Konerding, M.A., Wortler, K., Mykhayluk, O., Gansbacher, B., Machens, H.G., Plank, C. and Giunta, R.E. (2008) Non-viral VEGF gene therapy-Magnetofection of acoustically active magnetic lipospheres ("Magnetobulles") increases tissue-survival in an oversized skin flop model. *J. Cell Mol. Med.,* in press.

Horwitz, A.F. (1981) Myoblast aminophospholipid asymmetry differs from that of fibroblasts. *FEBS Lett.,* **134**:75-78

Hristova, N.I., Angelova, M.I., and Tsoneva, I. (2002) An experimental approach for direct observation of the interaction of polyanions with sphingosine-containing giant vesicles. *Bioelectrochem.,* **58**:65-73

Hu, Q., Joshi, R.P., and Schoenbach K.H. (2005) Simulations of nanopore formation and phosphatidylserine externalization in lipid membranes subjected to a high-intensity, ultrashort electric pulse. *Phys. Rev. E Stat. Nonlin. Soft Matter Phys.*, **72**:031902.

Huang, R.Q., Qu, Y.H., Ke, W.L., Zhu, J.H., Pei, Y.Y., and Jiang, C. (2007) Efficient gene delivery targeted to the brain using a transferrin-conjugated polyethyleneglycol-modified polyaminoamine dendrimer. *FASEB J.,* **21**:1117-1125

Hui, S.W., and Stenger, D.A. (1993) Electrofusion of cells: hydridoma production by electrofusion and polyethylene glycol. *Methods Enzymol.,* **220**:212-227

Hui, S.W. (1995) Effects of pulse length and strength on electroporation efficiency. *Methods Mol. Biol., Animal cell electroporation and electrofusion.* **48**:29-41

Huttinger, C., Hirschberger, J., Jahnke, A., Kostlin, R., Brill, T., Plank, C., Kuchenhoff, H., Krieger, S. and Schillinger, U. (2008) Neoadjuvant gene delivery of feline granulocyte macrophage colony stimulating factor using magnetofection for the treatment of feline fibrosarcomas : a phase I trial. J. Gene Med., 10:655-667

Hynynen, K., McDonald, N., Vykhodtseva, N., and Jolesz, F.A. (2003) Non-invasive opening of Blood Brain Barrier by focused. *Acta Neurochir. Suppl.,* **86**:555-558

Israelachvili, J.N., Marcelja, S., and Horn, R.G. (1980) Physical principles of membrane organization. *Rev. Biophysics,* **13**:121-200

Israelachvili, J.N. (1992) Intermolecular and surface force. A. Press, ed. (London)

Israelachvili, J.N. and Wennerstrom, H. (1996) Role of hydration and water structure in biological and colloidal interactions. *Nature,* **379**:219-225

Jacobson, K., Mouristen, E.G., and Anderson, R.G.W. (2007) Lipid rafts: At a crossroad between cell biology and physics. *Nature Cell Biol.,* **9**:7-14

Jaichandran, S., Yap, S.T.P., Khoo, A.B.M., Ho, L.P., Tien, S.L. and Kon, L. (2006) In vivo liver electroporation: optimization and demonstration of therapeutic efficacy. *Hum. Gene. Ther.,* **17**:362-375

Janmey, P.A., and Kinnunen, P.K.J. (2006) Biophysical properties of lipids and dynamic membranes. *Trends Cell Biol.,* **16**:538-546

Jastreboff, M.M., Ito, E., Bertino, J.R., and Narayanan, R. (1987) Use of electroporation for high-molecular-weight DNA-mediated gene transfer. *Exp. Cell Res.,* **171**:513-517
Jérôme, V., Heider, A., Schallon, A., and Freitag, R. (2009) Exhaustive in vivo labelling of plasmide DNA with BrdU for intracellular detection in non-viral transfection of mamalian cells. *Biotechnol. J.,* **4**:1479-1487

Julien, M., Tournier, J.F., and Tocanne, J.F. (1993) Differences in the transbilayer and lateral motions of fluorescent analogs of phosphatidylcholine and phosphatidylethanolamine in the apical plasma membrane of bovine aortic endothelial cells. *Exp. Cell Res.,* 208:387-397.

Kaddur, K., Palanchon, P., Tranquart, F., Pichon, C., and Bouakaz, A. (2007) Sonopermeabilization; therapeutic alternative with ultrasound and microbubbles. *J. Radiol.,* **88**:1777-1786

Kamau, S.W., Hassa, P.O., Steitz, B., Petri-Fink, A., Hofmann, H., Hofmann-Amtenbrink, M.,von Rechenberg, B., and Hottiger, M.O. (2006) Enhancement of the efficiency of non-viral gene delivery by application of pulsed magnetic field. *Nuc. Acids Res.,* **34**:e40

Kanduser, M., Miklavcic, D., and Pavlin, M. (2009) Mechanisms involved in gene electrotransfer using high- and low-voltage pulses—an in vitro study. *Bioelectrochem.,* **74**:265-271

Kaufman, H.L., DeRafelle, G., Mitcham, J., Moroziewicz, D., Cohen, S.M., Hurst-Wicker, K.S., Cheung, K., Lee, D.S., Divito, J., Voulo, Magalese, V., Donovan, J., Dolan, K., Manson, K., Panicali, D., Wang E., Horig, H., and Marincola, F.M. (2005) Targeting the local tumor microenvironment with vaccinia virus expressing B7.1 for the treatment of melanoma. J. Clin. Invest., **115**:1903-1912

Keating, A., Horsfall, W., Howley, R., and Toneguzzo, F. (1990) Effect of different promoters on expression of genes introduced into hematopoietic and marrow stroma cells y electroporation. *Exp. Hematol.,* **18**:99-102

Kennedy, P.G.E. (1997) Potentiel use of herpes simplex virus vectors for gene therapy of neurological disorders. *Brain,* **120**:1245-1259

Khalifat, N., Puff, N., Bonneau, S., Fournier, J.B., and Angelova, M.I. (2008) Membrane deformation under local pH gradient: mimicking mitochondrial cristae dynamics. *Biophys. J.,* **95**:4924-4933

Kim, W.J., Yockman, J.W., Jeong, J.H., Christensen, L.V., Lee, M., Kim, Y.H., and Kim, S.W. (2006) Anti-angiogenic inhibition of tumour growth by systemic delivery of PEI-g-PEG/pCMV-sFlt-1 complexes in tumour-bearing mice. *J. Control. Release,* **12**:381-8

Kinosita, K.J., and Tsong, T.Y. (1977a) Hemolysis of human erythrocytes by a transient electric field. *Proc. Natl. Acad. Sci. USA,* **74**:1923-1927

Kirkham, M., and Parton, R.G. (2005) Clathrin-independent endocytosis: New insights to caveolae and non-caveolar lipid raft carriers. *Biochim. Biophys. Acta,* **1745**:273-286

Klenchin, V.A., Sukharev, S.I., Serov, S.M., Chernomordik, L.V., and Chizmadzhev, Y.A. (1991) Electrically induced DNA uptake by cells is a fast process involving DNA electrophoresis. *Biophys. J.,* **60**:804-811

Kopatz I, Remy, J.S., and Behr, J.P. (2004) A model for non-viral gene delivery: through syndecan adhesion molecules and powered by actin. *J. Gene Med.,* **6**:769-776

Kotnik, T., Miklavcic, D., and Mir, L.M. (2001b) Cell membrane electropermeabilization by symmetrical bipolar rectangular pulses. Part II. Reduced electrolytic contamination. *Bioelectrochem.,* **54**:91-95

Krassowska, W. and Filev, P.D. (2007) Modeling electroporation in a single cell. *Biophys. J.,* **92**:404-417

Kubiniec, R.T., Liang, H., and Hui, S.W. (1990) Effects of pulse length and pulse strength on transfection by electroporation. *Biotechniques,* **8**:16-20

Kurata, S., Tsukahoshi, M., Kasuya, T. and Ikawa, Y. (1986) The laser method for efficient introduction of foreingh DNA into cultured cells. *Exp. Cell. Res.,* **162**:372-378

Kuzumi, A., and Suzuki, K. (2005) Towards understanding the dynamics of membrane-raft-based molecular interactions. *Biochim. Biophys. Acta,* **1746**:234-251

Kwee, S.H., Nielsen, J.E., Celis, A., and Madsen, P.S. (1989) Permeabilization of mammalian cells in monolayer culture by electroporation at low electric field strength. *Studia Biophysica,* **130**:173-176

Larkin, J.O., Collins, C.G., Aarons, S., Tangney, M., Whelan, M., O'Reily, S., Breathmach, O., Soden, D.M., and O'Sullivan, G.C. (2007) Electrochemotherapy. Aspects of preclinical development and early clinical experience. *Annals of Surgery,* **245**:469-479.

Larsen, M.D.B., Griesenbach, U., Goussard, S., Gruenert, D.C., Geddes, D.M., Scheule, R.K., Cheng, S.H., Courvalin, P., Grillot-Courvalin, C., and Alton, E.W.F.W. (2008) Bactofection of lung epithelial cells into in vitro and in vivo using a genetically modified Escherichia coli. *Gene Ther.,* **15**:434-442

Lehrman, S., (1999) Virus treatment questioned after gene therapy death. *Nature,* **401**:517-518

Leslie, M.C., Zhao, Y.J., Lachman, L.B., Hwu, P., and Bar-Eli, M. (2007) Immunization against MUC18/MCAM, a novel antigen that drives melanoma invasion and metastasis. *Gene Ther.,* **14**:316-323

Li, L.H., Sen, A., Murphy, S.P., Jahreis, G.P., Fuji, H., and Hui, S.W. (1999) Apopotis induced by DNA uptake limits transfection efficiency. *Exp. Cell Res.,* **253**:541-550

Li, T., Tachibana, K., and Kuroki, M. (2003) Gene transfer with echo-enhanced contrast agents: Comparison between Albunex, Optison and Levovist in mice – initial results. *Radiology,* **229**:423-428

Liang, H., Purucker, W.J., Stenger, D.A., Kubiniec, R.T., and Hui, SW. (1988) Uptake of fluorescence-labeled dextrans by 10T 1/2 fibroblasts following permeation by rectangular and exponential-decay electric field pulses. *Biotechniques,* **6**:550-552

Liang, K.W., Nishikawa, M., Liu, F., Sun, B., Ye, Q., and Huang, L. (2004) Restoration of dystrophin expression in mdx mice by intravascular injection of naked DNA containing full-length dystrophin cDNA. *Gene Ther.,* **11**:901-908

Liu, F. and Huang, L. (2002) Electric gene transfer to the liver following systemic administration of plasmid DNA. *Gene Ther.,* **9**:1116-1119

Lopez, A., Rols, M.P., and Teissié, J. (1988) 31P NMR analysis of membrane phospholipids organization in viable, reversibly electropermeabilized chinese hamster ovary cells. *Biochemistry,* **27**:1222-1228

Lukacs, G.L., Haggie, P., Seksek, O., Lechardeur, D., Freedman, N., and Verkman, A.S. (2000) Size-dependent DNA mobility in cytoplasm and nucleus. *J. Biol. Chem.,* **276**:1625-1629

Luzio J.P., Pryor, D.R., Bright, N.A. (2007) Lysosomes: fusion and function. *Nature Rev. Cell Biol.,* **8**:622-632

Lyons, J.A., Sheahan, B.J., Galbraith, S.E., Mehra, R., Atkins, G.J., and Fleeton, M.N. (2007) Inhibition of angiogenesis by a Semliki Forest virus vector expressing VEGFR-2 reduces tumour growth and metastasis in mice. *Gene Ther.,* **14**:503-613

MacMahon H.T., and Gallop J.L. (2005) Membrane curvature and mechanisms of dynamic cell membrane remodelling. *Nature,* **438**:590-596

Magee, T.R., Artaza, J.N., Ferrini, M.G., Vernet, D., Zurriga, F.I., Cantini, L., Reusz-Porszasz, S., Rajfer, J., and Gonzalez-Cadavid, N.F. (2006) Myostatin short interfering hairpin RNA gene transfer increases skeletal muscle mass. *J. Gene Med.,* **8**:1171-1181

Marguet, D., Lenne, P.F., Rigneault, H., and He, H.T. (2006) Dynamics in the plasma membrane: How to combine fluidity and order. *EMBO J.,* **25**:3446-3457

Marshall, E., (1999) Gene therapy death prompts review of adenovirus vector. *Science*. **286**:2244-2245

Martin, S.J., Reutelingsperger, C.P.M., and McGahon, A.J. (1995) Early redistribution of plasma membrane phosphatidylserine is a general feature of apoptosis regardless of the initiating stimulus: inhibition by overexpression of Bcl-2 and Abl. *J. Exp. Med.,* **182**:1545-1556

Maucksch C., Bohla A., Hoffman F., Scheef M., Aneja M.K., Elfinger M., Hartl D., and Rudolph C. (2009) Transgene expression of transfected supercoiled plasmid DNA concatemers in mammalian cells. *J. Gene. Med.,* **11**:444-453

Maxfield, F.R., and Tabas, I. (2005) Role of cholesterol and lipid organization in disease. *Nature,* **438**:612-621

Mayor, S., and Pagano, R.E. (2007) Pathways of clathrin-independent endocytosis. *Nature Rev. Mol. Cell Biol.,* **8**:603-612

Mazères S., Sel D., Golzio M., Pucihar G., Tamzali Y., Miklavcic D., and Teissié J. (2009) Non invasive contact electrodes for in vivo localized cutaneous electropulsation and associated drug and nucleic acid delivery. *J. Control. Release,* **134**:125-131

Meer, G., Voelker, D.R., and Feigenson, G.W. (2008) Membrane lipids : where they are and how they behave. *Nature Rev. Mol. Cell Biol.,* **9**:112-124

Mehier-Humbert, S., Bettinger, T., Yan, F., and Guy, R.H. (2005a) Ultrasound-mediated gene delivery: Kinetics of plasmid internalization and gene expression. *J. Control. Release,* **104**:203-211

Mehier-Humbert, S., Bettinger, T., Yan, F., and Guy, R.H. (2005b) Plasma membrane poration induced by ultrasound exposure: Implication for drug delivery. *J. Control. Release,* **104**:213-222

Meijering, B.D., Juffermans, L.J., van Wamel, A., Henning, R.H., Zuhorn, I.S., Emmer, M., Versteilen, A.M., Paulus, W.J., van Gilst, W.H., Kooiman, K., de Jong, N., Musters, R.J., Deelman, L.E., Kamp, O. (2009) Ultrasound and microbubbles-targeted delivery of macromolecules is regulated by induction of endocytosis and pore formation. *Circ. Res.,* **104**:679-687

Mendez, M.A., Prudent, M., Su, B. and Girault, HH (2008) Peptide-phospholipid complex formation at liquid-liquid interfaces. *Anal. Chem.,* **80**:9499-9507

Mesojednik, S., Pavlin, D., Sersa, G., Coer, A., Kranjc, S., Grosel, A., Tevz, G., and Cemazar, M. (2007) The effect of the histological properties of tumors on translocation efficiency of electrically assisted gene delivery to solid tumors in mice. *Gene Ther.,* **14**:1261-1269

Miao, C.H., Brayman, A.A., Loeb, K.R., Ye, P., Zhou, L., Mourad, P., and Crum, L.A. (2005) Ultrasound enhances gene delivery of human factor IX plasmid. *Hum. Gene Ther.,* **16**:893-905

Miller, A.M., and Dean, D.A. (2008) Cell-specific nuclear import of plasmid DNA in smooth muscle requires tissue-specific transcription factors and DNA sequences. *Gene Ther.,* **15**:1107-1115

Mir, L.M., Bureau, M.F., Gehl, J., Rangara, R., Rouy, D., Caillaud, J.M., Delaere, P., Branellec, D., Schwartz, B., and Scherman, D. (1999) High-efficiency gene transfer into skeletal muscle mediated by electric pulses. *Proc. Natl. Acad. Sci. USA,* **96**:4262-4267

Molnar, M.J., Gilbert, R., Lu, Y., Liu, A.B., Guo, A., Larochelle, N., Orlopp, K., Lochmuller, H., Petrof, B.J., Nalbantoglu, J., and Narpati, G. (2004) Factors influencing the efficacy, longevity, and safety of electroporation-assisted plasmid-based gene transfer into mouse muscles. *Mol. Ther.,* **10**:447-455

Mosqueda-Melgar, J., Raybaudi-Massilia, R.M., and Martin-Belloso, O. (2007) Influence of treatment time and pulse frequency on Salmonella Enteritidis, Escherichia coli and Listeria monocytogenes poupulations inoculated in melon and watermelon juices treated by pulsed electric fields. *Int. J. Food Microbiol.,* **117**:192-200

Mukherjee, S., and Maxfield F.R. (2004) Membrane domains. *Annu. Rev. Cell Dev. Biol.,* **20**:839-866

Murphy, D. (2008) Production of transgenic rodents by the micro-injection of cloned DNA into fertilized one –celled eggs. *Methods Mol. Biol.,* **461**:71-109

Nabi, I.R., and Le, P.U. (2003) Caveolae/raft-dependent endocytosis. *J. Cell Biol.,* **161**:673-677

Neil, G.A., and Zimmerman, U. (1993) Electroinjection. *Methods Enzymol.,* **221**:339-361

Nemunaitis, J., Cunningham, C., Senzer, N., Kuhn, J., Cramm, J., and Litz C. (2003) Pilot trial of genetically modified, attenuated Salmonella expressing the E. coli cytosine deaminase gene in refractory cancer patients. *Cancer Gene Ther.,* **10**:737-744

Neumann, E., Schaefer-Ridder, M., Wang, Y., and Hofschneider, P.H. (1982) Gene transfer into mouse lyoma cells by electroporation in high electric fields. *EMBO J.,* **1**:841-845

Neumann, E., Sowers, A.E., and Jordan, C.A. (1989) Electroporation and electrofusion in cell biology. *Plenum*.

Neumann, E., Kakorin, S., and Toensing, K. (1999) Fundamentals of electroporative delivery of drugs and genes. *Bioelectrochem. Bioenerg.,* **48**:3-16

Newman, C.M.H. and Bettinger, T. (2007) Gene therapy progress and prospects: Ultrasound for gene transfer. *Gene Ther.,* **14**:465-475

Niethammer, A.G., Xiang, R., Becker, J.C., Wodrich, H., Pertl, U., and Karsten, G. (2002) A DNA vaccine against VEGF receptor 2 prevents effective angiogenesis and inhibits tumor growth. *Nature Med.,* **8**:1369-1375

Ohlfest, J.R., Freese, A.B., and Largaespada, D.A. (2005) Nonviral vectors for cancer gene therapy: Prospects for integrating vectors and combination therapies. *Curr. Gene Ther.,* **5**:629-641

Osawa, K., Okubo, Y., Nakao, K., Koyama, N., and Bessho, K. (2009) Osteoinduction by microbubble-enhanced transcutaneous sonoporation of human bone morphogenetic protein-2. *J. Gene Med.,* **11**:633-641.

Pakhomov, A.G., Bowman, A.M., Ibey, B.L., Andre, F.M., Pakhomova, O.N., and Schoenbach, K.H. (2009) Lipid nanopores can form a stable, ion channel-like conduction pathway in cell membrane. *Biochem. Biophys. Res. Commun.,* **385**:181-186

Palffy, R., Gardlik, R., Hodosy, J., Behuliak, M., Resko, P., Radvansky, J., and Celec, P. (2006) Bacteria in gene therapy: bactofection versus alternative gene therapy. *Gene Ther.,* **13**:101-105

Park, T.G., Jeong, J.H., and Kim, S.W. (2006) Current status of polymeric gene delivery systems. *Adv. Drug Deliv. Rev.,* **58**:467-486

Parker, A.L., Newman, C., Briggs, S., Seymour, L., and Sheridan, P.J. (2003) Nonviral gene delivery: Techniques and implications for molecular medicine. *Expert Rev. Mol. Med.,* **5**:1-15

Parton, R.G., and Richards, A.A. (2003) Lipid rafts and caveolae as portals for endocytosis: New insights and common mechanisms. *Traffic,* **4**:724-738

Parton, R.G., and Simons, K. (2007) The multiple faces of caveolae. *Nature Rev. Mol. Cell Biol.,* **8**:185-194

Pelkmans, L., and Helenius, A. (2002) Endocytosis via caveolae. *Traffic,* **3**:311-320

Peng, B., Zhao, Y., Xu, L. and Xu, Y. (2007) Electric pulses applied prior to intramuscular DNA vaccination greatly improve the vaccine immunogenicity. *Vaccine,* **25**:2064-2073

Phez, E., Faurie, C., Golzio, M., Teissié, J., and Rols, M.P. (2005) New insights in the visualization of membrane permeabilization and DNA/membrane interaction of cells submitted to electric pulses. *Biochim. Biophys. Acta,* **1724**:248-254

Pichon, C., Gonçalves, C., and Midoux, P., (2001) Histidine-rich peptides and polymers for nucleic acids delivery. *Adv. Drug Deliv. Rev.,* **53**:75-94

Piknova, B., Pérochon, E., and Tocanne, J.F. (1993) Hydrophobic mismatch and long-range protein/lipid interactions in bacteriorhodopsin/phosphatidylcholine vesicles. *Eur. J. Biochem.,* **218**:385-396

Pitard, B. (2002) Supramolecular assemblies of DNA delivery systems. *Som. Cell Mol. Gen.,* **27**:5-15

Portet T, Camps I Febrer F, Escoffre JM, Favard C, Rols MP, and Dean DS (2009) Visualization of lipid expulsion during the shrinkage of giant vesicles under electropulsation. *Biophys. J.,* **96**:4109-4121

Potter, H. (1988) Electroporation in biology: methods, applications, and instrumentation. *Anal. Biochem.,* **174**:361-373

Pringle, I.A., McLachlan, G., Collie, D.D.S., Summer-Jones, S.G., Lawton, A.E., Tennant, P., Baker, A., Gordon, C., Blundell, R., Varathalingam, A., Davies, L.A., Schmid, R.A., Cheng, S.H., Porteous, D.J., Gill, D.R., and Hyde, S.C. (2007) Electroporation enhances reporter gene expression following delivery of naked plasmid DNA to the lung. *J. Gene Med.,* **9**:369-380

Pucihar, G., Kotnik, T., Miklavcic D., and Teissié, J. (2008) Kinetics of transmembrane transport of small molecules into electropermeabilized cells. *Biophys. J.,* **95** 2837-2848.

Raper, S.E., Chirmule, N., and Lee, FS. (2003) Fatal systemic inflammatory response syndrome in a ornithine transcarbamylase deficient patient following adenoviral gene transfer. *Mol. Genet. Metab.,* **80**:148-158

Rols, M.P., and Teissié, J. (1990a) Electropermeabilization of mammalian cells – Quantitative analysis of the phenomenon. *Biophys. J.,* **58**:1089-1098

Rols, M.P., and Teissié, J. (1990b) Control of electric field induced cell membrane permeabilization by membrane order. *Biochemistry,* **29**:2960-2966

Rols, M.P., and Teissié, J., (1992) Experimental evidence for the involvement of the cytoskeleton in mammalian cell electropermeabilization. *Biochim. Biophys. Acta,* **1111**:45-50

Rols, M.P., Delteil, C., Serin, G. and Teissié, J. (1994) Temperature effects on electrotransfection of mammalian cells. *Nucleic Acids Res.,* **22**:540

Rols, M.P., Femenia, P., and Teissié, J. (1995) Long-lived macropinocytosis takes place in electropermeabilized mammalian cells. *Biochem. Biophys. Res. Comm.,* **208**:26-35

Rols, M.P., and Teissié, J. (1998a) Electropermeabilization of mammalian cells to macromolecules: Control by pulse duration. *Biophys. J.,* **75**:1415-1423

Rols, M.P., Delteil, C., Golzio, M., Dumond, P., Cros, S., and Teissié, J. (1998b) In vivo electrically mediated protein and gene transfer in murine melanoma. *Nature Biotechnol.,* **16**:168-171

Rothman, J.E., and Lenard, J. (1977) Membrane asymmetry. *Science,* **195**:743-753

Rye H.S., Yue S., Wemmer D.E., Quesada M.A., Haugland R.P., Mathies R.A., and Glazer A.N. (1992) Stable fluorescent complexes of double-stranded DNA with bis-intercalating asymmetric cyanine dyes: properties and applications. *Nucleic Acids Res.,* **20**:2803-2812

Saito, T., and Nakatsuji, N. (2001) Efficient gene transfer into embryonic mouse brain using in vivo electroporation. *Dev. Biol.,* **240**:237-246

Salomé, L, Cazeils, J.L., Lopez, A., and Tocanne, J.F. (1998) Characterization of membrane domains by FRAP experiments at variable observation areas. *Eur. Biophys. J.,* **27**:391-402

Santini, M.T., Indovina, P.L., Cantafora, A. and Blotta, I. (1990) The cesium induced delay in myoblast membrane fusion is accompanied by changes in isolated membrane lipids *Biochim. Biophys. Acta,* **1023**:298-304

Saxton, M.J. (1982) Lateral diffusion in an archipelago. Effects of impermeable patches on diffusion in a cell membrane. *Biophys. J.,* **39**:165-173.

Saxton, M.J., (1993) Lateral diffusion in an archipelago. Single-particle diffusion. *Biophys. J.,* **64**:1766-1780.

Scherer, F., Anton, M., Schillinger, U., Henke, J., Bergemann, C., Krüger, A., Gänsbacher, B., and Plank, C. (2002) Magnetofection: enhancing and targeting gene delivery by magnetic force in vitro and in vivo. *Gene Ther.,* **9**:102-109

Schoenbach, K.H., Beebe, S.J., and Buescher, E.S. (2001) Intracellular effect of ultrashort electrical pulses. *Bioelectromagnetics,* **222**:440-448

Schote, U., and Seelig, J. (1998) Interaction of the neuronal marker dye FM1-43 with lipid membranes. Thermodynamics and lipid ordering. *Biochim. Biophys. Acta,* 1415:135-146

Schwarz, S., Deuticke, B., and Haest, C.W.M., (1999) Passive transmembrane redistributions of phospholipids as a determinant of erythrocyte shape change. Studies on electroporated cells. *Mol. Membr. Biol.,* **16**:247-255.

Schwister, K., and Deuticke, B. (1985) Formation and properties of aqueous leaks induced in human erythrocytes by electrical breakdown. *Biochim. Biophys. Acta,* **816**:332-348

Seelig, J. (1987) Phospholipid head groups as sensors of electric charge in membranes. *Biochemistry,* **26**:7535-7541

Sersa, G., Miklavcic, D., Cemazar, M., Rudolf, Z., Pucihar, G., and Snoj, M. (2008) Electrochemotherapy in treatment of tumours. *EJSO,* **34**: 232-240

Shechter, E (2000) Biochimie et Biophysique des membranes – Aspects structuraux et fonctionnels. 2ème Edition. Dunod.

Shen, H., Kanoh, M., Liu, F., Maruyama, S., and Asano, Y. (2004) Modulation of immune system by Listeria monocytogenes-mediated gene transfer into mammalian cells. *Microbiol. Immunol.,* **48**:329-337

Shibata, M.A., Moritomo, J., and Otsuki, Y. (2002) Suppression of murine mammary carcinoma growth and metastasis by HSVtk/GCV gene therapy using in vivo electroporation. *Cancer Gene Ther.,* **9**:16-27

Sibarita, J.B. (2005) Deconvolution microscopy. *Adv. Biochem. Engin/Biotechnol.,* **95**:201-243

Shimokawa, T., Okumura, K., and Ra, C. (2000) DNA induces apoptosis in electroporated huma promonocytic cell line U937. *Biochem. Biophys. Res. Commun.,* **270**:94-99

Simons, K., and Ikonen, E. (1997) Functional rafts in cell membranes. *Nature*, **387**:569-572

Simons, K., and Toomre, D. (2000) Lipid rafts and signal transduction. *Nature Rev. Mol. Cell Biol.,* **1**:31-41

Simons, K., and Vaz, W.L.C. (2004) Model systems, lipid rafts, and cell membranes. *Annu. Rev. Biophys. Biomol. Struct.,* **33**:269-295

Smith, K.C., Neu, J.C. and Krassowka, W. (2004) Model of creation and evolution of stable electropores for DNA delivery. *Biophys. J.,* **86**:2813-2826

Starke-Peterkovic, T., Turner, N., Vitha, M.F., Waller, M.P., Hibbs, D.E., and Clarke, R.J. (2006) Cholesterol effect on the dipole potential of lipid membranes. *Biophys. J.,* **90**:4060-4070

Stopper, H., Zimmerann, U., and Wecker, E. (1985) High yields of DNA-transfer into mouse L-cells by electropermeabilization. *Z. Naturforschung,* **40c**:929-932

Stulen, G. (1981) Electric field effects on lipid membrane structure. *Biochim. Biophys. Acta,* **640**:621-627

Suda, T. and Liu, D. (2007) Hydrodynamic gene delivery: its principles and applications. *Mol. Ther.,* **15**:2063-2069

Sukharev, S.I., Klenchin, V.A., Serov, S.M., Chernomordik, L.V., and Chizmadzhev, Y.A. (1992) Electroporation and electrophoretic DNA transfer into cells. The effects of DNA interaction with electropores. *Biophys. J.,* **63**:1320-1327

Takehara, T., Uemura, A., Tatsumi, T., Suzuki, T., Kimura, R., Shiotani, A., Ohkawa, K., Kanto, T., Hiramatsu, N and Hayashi, N. (2007) Natural killer cell-mediated ablation of

metastatic liver tumors by hydrodynamic injection of IFN-γ gene to mice. Int. J. Cancer, **15**:1252-1260

Tang, H., Kawabata, A., Takemoto, M., Yamanishi, K. and Mori, Y. (2008) Human herpesvirus-6 infection induces the reorganization of membrane microdomains in target cells, which are required for virus entry. *Virology,* **378**:265-271

Tarek, M. (2005) Membrane electroporation: A molecular dynamics simulation. *Biophys. J.,* **88**:4045-4053

Teissié, J., and Tsong, T.Y. (1981) Electric field induced transient pores in phospholipids bilayer vesicles. *Biochemistry,* **20**:1548-1554

Teissié, J. (1987) Polar head molecular packing of dipalmitoylglycerophosphocholine in the gel state: A fluorescence investigation. *Biochemistry,* **26**:840-846

Teissié, J., and Rols, M.P. (1993) An experimental evaluation of the critical potential difference inducing cell membrane electropermeabilization. *Biophys. J.,* **65**:409-413

Teissié, J., Golzio, M., and Rols, M.P. (2005) Mechanisms of cell membrane electropermeabilization: A minireview of our present (lack of ?) knowledge. *Biochim. Biophys. Acta,* **1724**:270-280

Teissié, J. (2007) Biophysical effects of electric fields on membrane water interfaces: a mini review. *Eur. Biophys. J.,* **36**:967-972

Teissié, J., Escoffre, J.M., Rols, M.P., and Golzio, M. (2008) Time dependence of electric field effects on cell membranes. A review for critical selection of pulse duration for therapeutical applications. *Radiol. Oncol.,* **42**:196-206

Tekle, E., Astumian, R.D., and Chock, P.B. (1990) Electro-permeabilization of cell membranes: effect of the resting membrane potential. *Biochem. Biophys. Res. Commun.,* **172**:282-287

Tekle, E., Astumian, R.D., and Chock, P.B. (1991) Electroporation by using oscillating electric field: An improved method for DNA transfection of NIH 3T3 cells. *Proc. Natl. Acad. Sci. USA,* **88**:4230-4234

Tekle, E., Astumian, R.D., and Chock, P.B. (1994) Selective ans asymmetric molecular transport across electroporated cell membranes. *Proc. Natl. Acad. Sci. USA,* **91**:11512-11516

Teruel, M.N. and Meyer T. (1997) Electroporation-induced formation of individual calcium entry sites in the cell body and processes of adherent cells, *Biophys. J.,* **73**:1785-1796.

Teshigawara, K., and Katsura, Y. (1992) A simple and efficient mammalian gene expression system using an EBV-based vector transfected by electroporation in G2/M phase. *Nucleic Acids Res.,* **20**:2607

Tieleman, D.P. (2004) The molecular basis of electroporation. *BMC Biochem.,* **5**:1-12

Titomirov, A.V., Sukharev, S. and Kistanova, E. (1991) In vivo electroporation and stable transformation of skin cells of newborn mice by plasmid DNA. *Biochim. Biophys. Acta Report,* **1088**:131-134

Tocanne, J.F., and Teissié, J. (1990) Ionization of phospholipids and phospholipids-supported interfacial lateral diffusion of protons in membrane model systems. *Biochim. Biophys. Acta,* **1031**:111-142

Toneguzzo, F., Hayday, A., and Keating, A. (1986) Electric field-mediated DNA transfer: transient ans stable gene expression in human and mouse lymphoid cells. *Mol. Cell Biol.,* **6**:703-706

Toti, F., Satta, N., Fressinaud, E., Meyer, D., and Freyssinet, J.M. (1996) Scott syndrome characterized by impaired transmembrane migration of procoagulant phosphatidylserine and hemorrhagic complications, is an inherited disorder. *Blood,* **87**:1409-1415

Tran, T.A., Roger, S., Le Guennec, J.Y., Tranquart, F., and Bouakaz, A. (2007) Effect of ultrasound-activated microbubbles on the cell electrophysiological properties. *Ultrasound Med. Biol.,* **33**:158-163

Tran, T.A., Le Guennec, J.Y., Bougnoux, P., Tranquart, F., and Bouakaz, A. (2008) Characterization of cell membrane response to ultrasound activated microbubbles. *IEEE Trans. Ultrason FerroElectr. Control.,* **55**:43-49

Triozzi, P.L., Allen, K.O., Carlisle, R.R., Craig, M., Lobuglio, A.F., and Conry, R.M. (2005)Phase I study of the intratumoral administration of recombinant canarypox viruses expressing B7.1 and interleukin 12 in patients with metastatic melanoma. *Clin. Cancer Res.,* **11**:4168-4175

Ugen, K.E., Kutzler, M.A., Marrero, B., Westover, J., Coppola, D., Weiner, D.B. and Heller, R., (2006) Regression of subcutaneous B16 melanoma tumors after intratumoral delivery of an IL-15-expressing plasmid followed by in vivo electroporation. *Cancer Gene Ther.,* **13**:969-974

Vaha-Koskela, M.J.V., Kuusinen, T.I., Holmlund-Hampf, J.C., Furu, P.T., Heikkila, J.E., and Hinkanen, A.E. (2007) Semliki Forest Virus vectors expressing transforming growth factor beta inhibit experimental autoimmune encephalomyelitis in Balb/c mice. *Biochem. Biophys. Res. Comm.,* **355**:776-781

Vandermeulen, G., Staes, E., Vanderhaeghen, M.L., Bureau, M.F., Scherman, D., and Préat, V. (2007) Optimisation of intradermal DNA electrotransfer for immunisation. *J. Control. Res.,* **124**:81-87

Vaughan, E.E., and Dean D.A. (2005) Intracellular trafficking of plasmids during transfection is mediated by microtubules. *Mol. Ther.,* **13**:422-428

Vera, M., and Fortes, P. (2004) Simian virus-40 as a gene therapy vector. *DNA Cell Biol.,* **23**:271-282

Verkleij, A.J., Leunissen-Bijvelt, J., De Kruijiff, B., Hope, M. and Culluis, P.R. (1984) Non-blayer structures in membrane fusion. *CIBA Found Symp.,* **103**:45-59

Vernier, P.T., Sun, Y., and Gundersen, M.A. (2006) Nanoelectropulse-driven membrane perturbation and small molecule permeabilization. *BMC Cell Biol.,* **19**:7-37

Vernier, P.T., Ziegler, M.J., Sun, Y., Gundersen, M.A., and Tieleman, D.P. (2006) Nanopore-facilitated, voltage-driven phosphatidylserine translocation in lipid bilayers in cells and in silico. *Phys. Biol.,* **3**:233-247
Vernier, P.T. and Ziegler M.J. (2007) Nanosecond field alignment of head group and water dipoles in electroporating phospholipid bilayers. *J. Phys. Chem. B*, **111**:12993-12996.

Waehler, R., Russel, S.J., and Curiel, D.T. (2007) Engineering targeted viral vectors for gene therapy. *Nature Rev. Genet.,* **8**:573-587

Wang, X.D., Tang, J.G., Xie, X.L., Yang, J.C., Shuai, L., Ji, J.G., and Gu, J. (2005) A comprehensive study of optimal conditions for naked plasmid DNA transfer into skeletal muscle by electroporation. *J. Gene Med.,* **7**:1235-1245

Wang, M. and Hajishengallis, G. (2008) Lipid raft-dependent upake, signalling and intracellular fate of Porphyromonas gingivalis in mouse macrophages. *Cell Microbiol.,* **10**:2029-2042

Wells, D.J. (2004) Gene therapy progress and prospects: Electroporation and other physical methods. *Gene Ther.,* **11**:1363-1369

Winterbourne, D.J., Thomas, S., Hermon-Taylor, J., Hussain, I., and Johnstone, A.P. (1988) Electric shock-mediated transfection of cells. *Biochem. J.,* **251**:427-434.

Wolf, H., Rols, M.P., Boldt, E., Neumann, E., and Teissie, J. (1994) Control by pulse parameters of electric field-mediated gene transfer in mammalian cells. *Biophys. J.,* **66**:524-531

Wolff, J.A., Malone, R.W., Williams, P., Chong, W., Acsadi, G., Jani, A., and Felgner, P.L. (1990) Direct gene transfer into mouse muscle in vivo. *Science,* **247**:1465-1468

Xenariou, S., Griesenbach, U., Ferrari, S., Dean, P., Scheule, R.K., Cheng, S.H., Geddes, D.M., Plank, C., and Alton, E.W.F.W. (2006) Using magnetic forces to enhance non-viral gene transfer airway epithelium in vivo. *Gene Ther.,* **13**:1545-1552

Xie, T.D., and Tsong, T.Y. (1993) Study of mechanisms of electric field-induced DNA transfection. V. Effects of DNA topology on surface binding, cell uptake, expression, and integration into host chromosomes of DNA in the mammalian cell. *Biophys. J.,* **65**:1684-1689

Yamaji-Hasegawa, A., and Tsujimoto, M. (2006) Asymmetric distribution of phospholipids in biomembranes. *Biol., Pharm., Bull.,* **29**:1547-1553

Yamashita, Y.I., Shimada, M., Tachibana, K., Harimoto, N., Tsujita, E., Shirabe, K., Miyazaki, J.I., and Sugimachi, K. (2002) In vivo gene transfer into muscle via electro-sonporatoin. *Hum. Gene Ther.,* **13**:2079-2084

Yorifuji, T., Tsuruta, S., and Mikawa, H. (1989) The effect of cell synchronization on the efficiency of stable gene transfer by electroporation. *FEBS Letters,* **245**:201-203

Yguerabide, J., Schmidt, J.A., Yguerabide, E.E. (1982) Lateral mobility in membranes as detected by fluorescence recovery after photobleaching. *Biophys. J.,* **40**:69-75

Zachowski, A. (1993) Phospholipids in animal eukaryotic membranes: transverse asymmetry and movement. *Biochem. J.,* **294**:1-14

Zagon, I.S., Sassani, J.W., Malefyt, K.J., and MacLaughin, P.J. (2006) Regulation of corneal repair by particle mediated gene transfer of opioid growth factor receptor complementary DNA. *Arch. Ophthalmol.,* **124**:1620-4

Zallen, D.T. (2000) US gene therapy in crisis. *TIG,* **16**:272-275

Zanta, M.A., Belguise-Valladier, P., and Behr, J.P. (1999) Gene delivery: A single nuclear localization signal peptide is sufficient to carry DNA to the cell nucleus. *Proc. Natl. Acad. Sci. USA,* **96**:91-96

Zeira, E., Manevitch, A., Manevitch, Z., Kedar, E., Gropp, M., Daudi, N., Barsuk, R., Harati, M., Yotvat, H., Troilo, P.J., Griffiths, T.G., Pacchione, S.J., Roden, D.F., Niu, Z., Nussbaum, O., Zamir, G., Papo, O., Hemo, Izhack, H., Lewis, A. and Galun, E. (2003) Femtosecond infrared laser – an efficient and safe in vivo gene delivery system for prolonged expression. *Mol. Ther.,* **8**:342-350

Zeira, E., Manevitch, A., Manevitch, Z., Kedar, E., Gropp, M., Daudi, N., Barsuk, R., Harati, M., Yotvat, H., Troilo, P.J., Griffiths, T.G., Pacchione, S.J., Roden, D.F., Niu, Z., Nussbaum, O., Zamir, G., Papo, O., Hemo, Izhack, H., Lewis, A. and Galun, E. (2007) Femtosecond laser: a new intradermal DNA delivery method for efficient, long-term gene expression and genetic immunization. *FASEB J.,* **21**:00-00

Zerbib, D., Amalric, F., and Teissié, J. (1985) Electric field mediated transformation : Isolation and characterization of a TK^+ subclone. *Biochem. Biophys. Res. Comm.,* **129**: 611-618

Zhang, G., Gao, X., Song, YK., Vollmer, R., Stolz, D.B., and Gasiorowski, J.Z. (2004) Hydroporation as the mechanism of hydrodynamic delivery. *Gene Ther.,* **11**:675-682

Zhang, X., Divangahi, M., Ngai, P., Santosuosso, M., Millar, J., Zganiacz, A., Wang, J., Bramson, J., and Xing, Z. (2007) Intramuscular immunization with a monogenic plasmid DNA tuberculosis vaccine: Enhanced immunogenicity by electroporation and co-expression of GM-CSF transgène. *Vaccine,* **25**:1342-1352

Zimmermann, D., Terpitz, U., Zhou, A., Reuss, R., Muller, K., Sukhorukov, V.L., Gessner, P., Nagel, G., Zimmermann, U., and Bamberg, E. (2006) Biophysical characterization of electrofused giant HEK293-cells as a novel electrophysiological expression system. *Biochem. Biophys. Res. Commun.,* **348**:673-681

Zweifach, A. (2000) FM1-43 reports plasma membrane phospholipid scrambling in T-lymphocytes. *Biochem. J.,* **349**:255-260

VII. PUBLICATIONS

VII. Publications

Les publications, les revues et les chapitres de livre rédigés au cours de ma thèse et auxquels j'ai apporté mon soutien technique et/ou scientifique, mais qui ne sont pas présentés dans ce mémoire, sont les suivantes.

PARTIE I

ÉLECTROPERMÉABILISATION DE VÉSICULES GÉANTES

Partie I. Electroperméabilisation de vésicules géantes

Portet T, Mauroy C, Démery V, Houles T, **Escoffre JM**, Dean DS, and Rols MP (2010) Destabilizing giant liposomes with electric fields: An overview of current applications. CRAS (Submitted Review).

Portet T, Camps I Febrer F, **Escoffre JM,** Favard C, Rols MP, and Dean DS (2009) Visualization of lipid expulsion during the shrinkage of giant vesicles under electropulsation. Biophys. J., 96:4109-4121 (Article).

Destabilizing Giant Liposomes with Electric Fields: An Overview of Current Applications

Thomas Portet[† a,b], Chloé Mauroy[† b], Vincent Démery [a], Thibault Houles [b], Jean-Michel Escoffre [b], David S. Dean [a] and Marie-Pierre Rols[‡ b].

[a] *Laboratoire de Physique Théorique, CNRS UMR 5152, Université Paul Sabatier, Toulouse, FRANCE.*
[b] *Institut de Pharmacologie et de Biologie Structurale, CNRS UMR 5089, Université Paul Sabatier, Toulouse, FRANCE.*

[†] TP and CM contributed equally to this review. [‡] Corresponding author: MPR.

Received *****; accepted after revision +++++

Abstract

This review presents an overview of the effects of electric fields on Giant Unilamellar Vesicles (GUVs). The application of electrical fields leads to three basic phenomena (i) shape changes (ii) membrane breakdown (iii) uptake of molecules. We describe how some of the above observations can be used to measure a variety of physical properties of lipid membranes, or to advance our understanding of the phenomena of electropermeabilization. We also present results on how electropermeabilization and other liposome responses to applied fields are affected by lipid composition and by the presence of molecules of therapeutic interest in the surrounding solution.

To cite this article: A. Name1, A. Name2, C. R. Physique 6 (2005).

Résumé

Déstabilisation de liposomes géants par des champs électriques :
Un tour d'horizon des applications actuelles

Cette revue dresse un état de la connaissance des effets de champs électriques sur des vésicules unilamellaires géantes (GUVs). L'application de champs électriques donne lieu à trois classes de phénomènes (i) des changements de forme (ii) un bouleversement de la membrane (iii) l'entrée de molécules. Nous expliquons comment ces phénomènes peuvent être utilisés pour mesurer diverses caractéristiques de la membrane lipidique, ou comment ils peuvent aider à améliorer notre compréhension de l'électroperméabilisation. Nous présentons aussi des nouveaux résultats concernant l'influence de la composition lipidique de la membrane ou la présence de molécules d'intérêt thérapeutique dans le milieu de pulsation.

Pour citer cet article : A. Name1, A. Name2, C. R. Physique 6 (2005).

Key words: Giant Unilamellar Vesicle ; Electric field ; Deformation ; Poration ; Fusion ; Applications ; Methods *Mots-clés :* Vésicule Unilamellaire Géante ; Champ électrique ; Déformation ; Poration ; Fusion ; Applications ; Méthodes

Email address: rols@ipbs.fr (Marie-Pierre Rols[‡]).

1. Introduction

Our conception of the role of lipid molecules in biological membranes has dramatically evolved over the past few decades. The lipid membrane was first considered as a purely passive barrier and a substrate to house membrane proteins which carried out the biological functions of the cell membrane. However it is now widely accepted that lipids play an active role in a number of biological processes. Their physico-chemical properties, confered by their structure and their amphiphilic nature, have consequences well beyond their self-assembly and ability to form a barrier. However, the study of the behavior of lipid molecules in a complex environment, such as a living cell, turns out to be a very difficult task due to the presence of other cell constituents such as the cytoskeleton and organelles, and also because of the large number of different lipid species present. Another source of complexity emerges from the presence of various membrane proteins and the cell glycocalyx.

Fortunately, we are now able to form cell-sized artificial membranes with well controlled compositions . These objects are called Giant Unilamellar Vesicles (GUVs), and are also referred to as giant vesicles or giant liposomes. Their study has become increasingly popular in chemistry, biology and physics laboratories. Their primary interest is probably their size which, being of the order of several micrometers, allows their direct observation *via* optical microscopy techniques. During the eighties, Angelova and Dimitrov developed an efficient protocol for GUV production known as electroformation [1], which was later shown to indeed produce *unilamellar* vesicles [2]. Due to the ease of their fabrication and their rich phenomenology, artificial vesicles have received an ever growing interest from the scientific community, as attested by the increasing number of studies using GUVs as membrane model systems. We anticipate that this tendancy could even accelerate in the future, as a number of obstacles in the preparation of giant liposomes under physiological conditions have recently been overcome [3,4,5,6].

This paper has for aim the introduction of the various phenomena that occur when GUVs are subjected to electric fields. Dimova *et al* have written comprehensive reviews about the effects of electric fields on GUVs [7,8] and about the physics of GUVs in general [9]. The present paper is a natural sequel to these articles. Being a review paper, it naturally suffers from a certain subjectivity and is obviously not exhaustive, however we hope it will be of use to newcomers in the field or to people familiar with Dimova's reviews and who wish to know about the most recent developments. It is organized in the following way: we first describe results on the influence of electric fields on giant liposomes, along with their theoretical explanations when they exist. We then describe some applications resulting from these behaviors. In addition, we present some preliminary results on the effect of lipid composition and the presence of poloxamers on the electropermeabilization of GUVs. Some results on the electromediated uptake of DNA by GUVs are also described.

2. Some effects of electric fields on giant vesicles

Both DC pulses and AC fields can strongly destabilize giant vesicles and influence their behavior. Depending on the parameters of the applied field, giant vesicles can porate, fuse, deform, or even exhibit domain motion in the case of multicomponent liposomes. The purpose of this section is to present these phenomena.

2.1. *Deformation*

To our knowledge, the deformation of giant vesicles by electric fields (or electrodeformation) was first extensively studied by Kummrow and Helfrich in the early nineties [10]. The authors applied sinusoidal AC electric fields of $\sim$1 kHz frequency and amplitudes ranging up to 100 V/cm, and found that spherical liposomes deformed into prolate ellipsoids oriented in the field direction, the degree of deformation increasing with the magnitude of the applied field. This type of deformation had already been predicted earlier [11]. Monitoring the relative area dilation of the membrane yielded an experimental estimate for the bending rigidity k_c of the lipid bilayer (see subsection 3.1). A few years later, Mitov *et al* explained theoretically and observed experimentally a prolate to oblate shape transition when increasing the field frequency above a few kHz [12]. However, these experiments were limited to vesicles in pure water (internal-external conductivity ratio $x = \lambda_{in}/\lambda_{out} \approx 1$), and to AC field frequencies in the kHz range. An extensive study of the influence of the media's electrical conductivities ($x > 1$ or $x < 1$) in a wider range of frequencies f (from 10^2 to 10^8 Hz) was published fifteen years later [13]. In [13] Aranda *et al* observed that GUVs could attain oblate, prolate or spherical shapes upon varying x or f, and were able to construct a morphological *phase* diagram describing four different transitions whose characteristic frequencies depend on the

conductivity ratio x. At high frequencies (several MHz), all vesicles were found to adopt spherical shapes. At low frequencies ($f <$ a few kHz), all vesicles deformed into prolate ellipsoids, as predicted in [11]. The prolate to oblate transition happens at intermediate frequencies for $x < 1$, *i.e.* when there is more salt outside the liposomes than inside. Another transition of this type could also be triggered at a fixed frequency f by varying x, for example by adding pure water to the sample and thus increasing the conductivity ratio. These behaviors can be qualitatively understood if one considers the motion of ions and the distance they travel in presence of an AC electric field. If the field frequency is large they are virtually immobile, while if the frequency is lowered they can be pushed against the membrane and then modify the vesicle shape. Nevertheless, at that time there was no theory able to fully describe these four transitions as a function of f and x. Winterhalter and Helfrich's theory [11] did not account for the recovery of the spherical shape at high frequencies, and Mitov's theory could not either [12]. An analytical theory explaining all the features in the morphological diagram of [13] was finally developed in [14]. In this approach, vesicle shape was determined by balancing electric, hydrodynamic, bending and tension stresses exerted on the membrane. This force balance approach also provides information about the kinetics of liposome deformation, unlike former theories based on energy minimization [11,12].

Winterhalter and Helfrich's model also predicted that DC pulses should deform spherical vesicles into prolate ellipsoids too [11]. However, DC pulses usually have durations of the order of several tens or hundreds of microseconds, or at most of some milliseconds. Imaging at such high rates is impossible with classical video cameras, so if one wants to get insight at what happens *during* an electric pulse application, one has to work with a fast imaging setup allowing image acquisition at several thousands frames per second. This approach was first applied by Riske and Dimova , and they indeed found that GUVs deformed into prolate ellipsoids upon the application of electric pulses of 50–300 μs duration and 1–3 kV/cm amplitude [15]. They worked with salt-free solutions, but still at a conductivity ratio of $x \sim 1.3$, meaning that the solution inside the vesicle was more conductive that the outer one. Later, when the same authors wanted to work in conditions closer to physiological ones and to investigate the role of salts in the exterior medium, it was somewhat surprisingly found, that vesicles subjected to electric pulses in salt solutions always adopted cylindrical shapes, irrespective of their ionic content (and thus of the conductivity ratio)[16]. This finding still lacks a quantitative theoretical explanation.

2.2. *Electropermeabilization*

Electric pulses may also have much more dramatic effects on lipid bilayers than simple deformation. They can sufficiently disrupt the membrane as to allow the uptake of otherwise nonpermeant molecules such as Propidium Iodide, plasmid DNA or cisplatin. Depending on the field strength used this can occur in a reversible manner and without affecting cell viability [17]. This process, called electropermeabilization, has led to biomedical applications in the fight against cancer, or in the field of gene therapy [18,19]. Despite its increasing popularity among physicians, biologists and oncologists, no one knows for sure what really happens when subjecting a living cell to a permeabilizing electric pulse. Uptake mechanisms are triggered by the electric potential difference across the membrane $\Delta\psi$ induced by the field and seem to be dependent on the size and charge of the transfered compounds. No consensus exists on the way the membrane reorganizes at the molecular level and this question still remains a challenge. Here again, GUVs are convenient tools to investigate these questions. Some studies have been performed, and have shown that giant vesicles can indeed become permeabilized by DC electric pulses. By coupling electropermeabilization and the micropipette aspiration technique, it was shown that the critical membrane voltage $\Delta\psi_c$ required for breakdown ranged from 1.1 to 1.8 V depending on membrane composition [20]. It was also observed that a macropore of several micrometers size could be induced [21]. It was later shown by Tekle *et al* that the mechanism of pore formation is asymmetric [22]. A macropore is formed on the cathode-facing side of the vesicle, whereas the presence of many smaller pores on the other hemisphere can be inferred from the size decrease of the liposome following pulse application. This phenomenon of GUVs shrinkage during electropulsation was then extensively studied by our team [23]. By applying a sequence of long (5 ms) electric pulses, we found that vesicles shrank, down to a critical radius beyond which their size no longer changed. We identified three mechanisms for the lipid loss: formation of macropores on the cathode-facing side as already reported [22], formation of tubular structures on the anode facing side, and formation of small vesicles at both poles. These three features should probably not be considered as distinct mechanisms. Macropore and tubules formation probably reflect the same phenomena, as they were found to occur together. Small vesicles expulsion can be understood as another way of expelling lipids, and may under certain conditions be more energetically favorable than tubule formation. While assuming that the area lost per pulse was proportional to the permeabilized area (the area on the vesicle where the induced transmembrane voltage $\Delta\psi = (3/2)RE\cos(\theta)$ exceeded the critical transmembrane voltage $\Delta\psi_c$, R

denoting the radius of the vesicle, E the pulse amplitude and θ the angle with respect to the field direction), we were able to analytically predict the decrease of the GUV radius as a function of the number of applied pulses. We fitted our experimental data with the appropriate formula, and finally obtained the values of $\Delta\psi_c$ for DOPC and EggPC vesicles, 0.85 and 1 V respectively. Later on, we conducted the same experiments with liposomes of another composition: DOPC/Sphingomyelin/Cholesterol (2/2/1, mol/mol/mol) [unpublished results]. We found $\Delta\psi_c \approx 0.4$ V for this composition closer to the actual lipidic composition of a real cell membrane. This finding is interesting, as to our knowledge, such a low value for permeabilization threshold of GUVs has never previously been found. Typical values are about 1 V for giant liposomes containing a single phosphatidylcholine, or a simple two component mixture, while typical critical transmembrane voltages are about 0.2 V for many cell types [24]. Our results thus indicate that the reason for this discrepancy with respect to the case of simple model membranes may be due to the presence of several lipid phases. Macropore formation was also studied by Riske and Dimova [15]. The pulses they applied were shorter and more intense than ours, but could still cause macropore formation. It was shown that poration of the vesicles affected the membrane relaxation dynamics, and that the initial membrane tension had a strong influence on the critical potential difference for porating the GUV. Another recent study reported that the presence of anionic lipid species in the membrane could cause vesicle bursting, whereas simple phosphatidylcholine membranes usually reseal after a permeabilizing electric pulse [25].

2.3. *Motion of domains*

Increasing the membrane complexity by addition of different phospholipids and cholesterol leads to phenomena that can not be observed in single component GUVs. Staykova *et al* managed to monitor the motion of liquid ordered domains in giant vesicles made of DOPC/DPPC/Cholesterol (different molar ratios were explored) subjected to AC electric fields of ∼500 V/cm amplitude in the kHz frequency range [26]. They report that this movement had characteristic features depending on the field parameters, and that it was caused by the inhomogeneous surface tension induced by the field because of the chamber geometry. It was the first time this phenomenon of induced charge electro-osmosis was observed and studied on a lipid membrane.

2.4. *Fusion*

Membrane fusion is a key process of life. It is one of the most common ways for molecules to enter or exit cells. The process of fusion occurs in a variety of important biological processes such as nerve signal transmission provided by the fusion of synaptic vesicles to the outer membranes of nerve cells. Other processes where fusion occurs are intracellular trafficking [27,28] and viral infection by membrane-enclosed viruses [29,30].

However, membrane fusion does not occur spontaneously because of large energetic barriers in biological membranes. These energetic barriers are caused by Van der Waals, electrostatic and steric repulsions and by strong hydration [31,32]. To promote membrane fusion it is essential to overcome these barriers. In biological membrane systems this process occurs *via* fusion proteins [33,34] in a multistep process. For most viruses, a fusion event is achieved in two steps. First, fusion proteins recognise a site for fusion on the membrane of the host cell. Then, the hydrophobic domain of the fusion protein inserts itself into the membrane of the host cell.

Studies of the fusion pathway have shown two important types of intermediate structures in the fusion mechanism: hemifusion structures and fusion pores [35]. Hemifusion structures form a connection between outer leaflets but not between inner leaflets which remain distinct. They are transient structures that either dissociate to give two independent membranes or induce fusion pores [35]. Fusion pores are connections between both outer and inner leaflets, they form an aqueous connection between the two aqueous compartments. The propensity to obtain these two intermediates depends on lipid composition, as fusion depends on the ability of the membrane to bend into these states and thus on the spontaneous curvature and bending rigidity of the associated monolayers and bilayers [36]. Obviously another condition to induce fusion is the establishment of a sufficiently close inter-bilayer proximity. As hydration forces contribute to the repulsion between membranes, the fusogenic state can be induced via bilayer dehydration [37]. In biological systems dehydration can be induced by calcium ions that neutralize the negatively charged phospholipid head groups, reducing electrostatic repulsion between membranes, and/or help the formation of Ca^{2+}-phosphate bridges between opposing bilayers [38]. Dehydration can also be induced by the application of an electric field on membrane systems, which can rearrange the interfacial water molecule network [39].

Electrofusion is a very convenient way to control, both spatially and temporally, fusion events. It is thus possible to trigger and observe the whole fusion process to study the underlying mechanisms. To occur, electrofusion requires two conditions: (a) electropermeabilization and (b) contact between lipid membranes. When the two membranes are close enough and lipid perturbation is high enough, fusion occurs; for cells this was demonstrated by Zimmermann in 1982 [40]. It has been shown that membrane fusion can be obtained, not only by pulsing cells already in close contact, but also by bringing them into close contact after their permeabilization [41,42,43]. Electropermeabilized membranes are thus fusogenic. For a better understanding of the fundamental processes involved in membrane fusion, lipid vesicles are often used as model systems [44,17]. An AC field can be used to align vesicles in the field direction and bring two vesicles into contact. A subsequent application of a DC pulse induces the permeabilization of the two vesicles and if permeabilization is induced in the contact area fusion is induced. Membrane fusion is a fast process. It has been shown that the fusion process occurs within two stages [45]. The first stage is the opening of the fusion neck with an average expansion velocity of about 2 cm/s. In the second stage, the neck-expansion velocity slows down until complete opening of the fusion neck. In the absence of salt, the fusion typically occurs at several contact points of the vesicles. In the case of several contact points (more than two), the coalescence of these fusion necks can lead to small vesicles enclosed in the contact zone [45]. In the presence of salt in the solution outside of the vesicles, the DC pulse induces vesicles deformation and the vesicles are pushed together and form a flat contact zone. As no enclosed vesicles are observed, one may infer that only one fusion neck or a small number of such necks has been formed.

In summary, it is possible to control and observe vesicle fusion by the method of electrofusion. Vesicle fusion has applications that we will discuss in subsection 3.3.

3. Some applications

In the last section, we have reviewed the various possible responses of GUVs subjected to different kinds of electric fields. These phenomena have led to applications, which we describe in this section. We first describe how shape analysis of giant liposomes in an AC field can allow the measurement of the lipid bilayer bending rigidity k_c. Then we show how electric pulses can be used to efficiently load GUVs with non permeant molecules. In subsection 3.3, we highlight some applications of membrane fusion. Finally we explain how to measure the edge or line tension γ of lipid membranes, and how electric fields can be employed to improve the current measurement methods.

3.1. *Measuring bending rigidities*

The bending rigidity k_c is a material property of lipid membranes introduced by Helfrich in his theory of the elasticity of lipid bilayers [49]. It has the dimensions of energy and, roughly speaking, can be related to the energy price one has to pay in order to bend a membrane. It plays a role in the control of the membrane shape, in the determination of the amplitude of thermal fluctuations, or in the modulation of membrane proteins activity, and thus being able to measure it is of interest in the understanding of various biological events. Here we will just describe the k_c measurement method based on electrodeformation. There exist other ways of measuring bending rigidities which are described in the review of Marsh [46].

Bending rigidity measurements *via* electrodeformation were first carried out by Kummrow and Helfrich [10]. Giant vesicles were exposed to AC fields of a few kHz frequency and $\sim$100 V/cm amplitude, and shapes were recorded while increasing the field amplitude. The liposomes deformed gradually into a more and more elongated prolate ellipsoid, and also changed their apparent surface area due to the flattening of thermal fluctuations. The basic idea of the method is first to calculate the lateral tension σ induced by the field using the relation $\sigma(c_1+c_2)_e-(T_{rr})_e=\sigma(c_1+c_2)_p$, where c_1 and c_2 are the principal curvatures of the ellipsoid, T_{rr} is the stress exerted on the outer surface of the vesicle by the field which gives rise to the deformation and the flattening of undulations, and the subscripts e and p indicate that the associated quantities are calculated at the equator and the poles of the vesicle, respectively. The relative area change α is given by $(k_BT/8\pi k_c)\ln(\sigma/\sigma_0)$; one can easily see that fitting a straight line to the logarithmic plot of α as a function of σ leads to a determination of k_c and of the vesicle's initial tension σ_0. This method was later applied by Gracià *et al* in order to study the influence of cholesterol on the rigidity of membranes of various compositions [47]. The authors also employed another measurement method for k_c based on the analysis of membrane fluctuations (see [48] for example). It was found

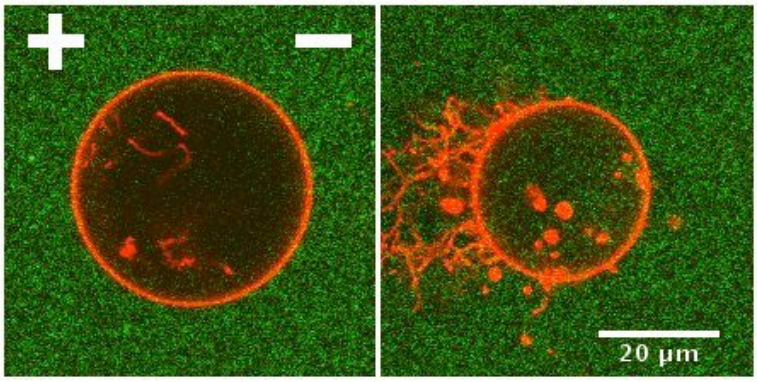

Figure 1. Confocal microscopy image of a DOPC GUV fluorescently labeled with Rhodamine-PE (red) in presence of plasmid DNA labeled with TOTO (green). One can see on the left image that there is no DNA present inside the liposome before electric treatment, and on the right one that after electropermeabilization the vast majority of electrotransfered DNA is under free form and not enclosed in endocytosis-like vesicles. Tubules and small vesicles associated with lipid loss, as described in 2.2, can also be observed. Field polarity is indicated on the left picture.
Image obtenue par microscopie confocale d'un GUV de DOPC marqué à la Rhodamine-PE (rouge) en présence d'ADN plasmidique marqué au TOTO (vert). On peut voir sur l'image de gauche qu'il n'y a pas d'ADN dans le liposome avant application des impulsions électriques, et sur l'image de droite qu'après l'électroperméabilisation la grande majorité de l'ADN transféré est présent sous forme libre, et non dans des vésicules d'endocytose. On peut aussi observer les tubules et petites vésicules associés à la perte de lipides décrits en section 2.2. La polarité du champ est indiquée sur l'image de gauche.

that the electrodeformation method leads to slightly lower values k_c than the fluctuation method (as noted in[10]). Nevertheless, both methods give the same trends and reproducible results. The results suggest that the effect of cholesterol addition on the membrane bending rigidity is concentration dependent, but is also higly influenced by the lipid type to which cholesterol is added. An important point to keep in mind is that the electrodeformation method using the theoretical analysis described above cannot be applied if one works in salt solutions or with charged lipid species.

3.2. *Loading vesicles*

As previously stated, DC pulses are useful tools to enable the entry of nonpermeant molecules into cells. They can thus also enable one to load a vesicle with compounds of interest. This has applications in drug delivery, where lipid vesicles play the role of cargo carriers, but is also of interest in fundamental research, for example when trying to understand the nature of the DNA/membrane interaction occuring during cell electropermeabilization [50]. As far as we know, two papers focusing on the electromediated DNA uptake by liposomes have been published to date. In [51], the authors applied a single electric pulse of 12.5 kV/cm amplitude and 300 μs duration to large unilamellar vesicles ($\sim$100 nm size, two orders of magnitude smaller than GUVs) composed of DPPC/cholesterol (7/3, mol/mol) in presence of high molecular mass DNA of size similar to that of the plasmid DNA usually employed in gene transfer protocols. They claim that the uptake mechanism took place *via* the electrostimulated formation of endosome-like vesicles rather than *via* electropores. These conclusions were questioned ten years later by Lurquin and Athanasiou, who found that DNA could enter DPPC GUVs under free form by a mechanism involving electro-induced membrane pores [52]. They used longer pulses (12 ms) of smaller amplitude (1500 V/cm), but which caused greater induced transmembrane voltages than those of Chernomordik *et al* [51].

In order to resolve these conflicting results, we carried out DNA loading experiments on DOPC GUVs. Our results clearly favor the second mechanism involving DNA entry *via* electropores. As can be seen on Fig. 1, showing a vesicle before (left panel) and after (right panel) electric treatment (15 pulses of 5 ms duration, 370 V/cm amplitude and 0.33 Hz frequency), plasmid DNA stays trapped inside the vesicle, mostly under free form and not in endocytosis-like vesicles. Tubules and small vesicles associated with lipid loss and vesicle shrinkage, as described in 2.2, can also be observed. These small vesicles may contain some DNA, but DNA entry under free form is the predominant mechanism. Using confocal microscopy, we were able to quantify the amount of DNA entering the liposome after each pulse, and are currently developing a theoretical model able to account for the increase of DNA concentration inside the GUV [53].

3.3. *Applications of fusion*

As membrane fusion induces a mixing of the lipids initially present in each membrane and a mixing of the aqueous compartments, electrofusion could be used to introduce molecules into a membrane or into an aqueous compartment. In the case of the fusion of two vesicles having different lipid compositions, it is possible to produce multicomponent vesicles of well-defined composition [54,7]. This provides the possibility of studying the dynamics of domain formation and stability. When giant vesicles are prepared directly with a multicomponent lipid mixture, the compositions of the different vesicles are dispersed about the composition of the initial lipid mixture. Electrofusion of two vesicles each made of different components thus allows one to obtain vesicles with a well specified composition. Fusing two vesicles of non-miscible lipid composition produces micro-domains in the resulting vesicle's membrane.

The fusion of two vesicles of different content is a realization of a microreactor. It has been shown that two vesicles can encapsulate one ore more reagent molecules [55]. When electrofusion is induced between these two vesicles, the contents of the two vesicles are mixed and a chemical reaction between the two reagent molecules can occur. This method needs one condition to be efficient: the lipid membranes of the two compartments have to be impermeable to the reactants. The first use of vesicles as microreactors was demonstrated with a chemical reaction between the calcium sensitive fluorescent dye fluo-3 and Ca^{2+} [55]. A batch of vesicles was loaded with fluo-3 and another was loaded with Ca^{2+}. The two types of containers were mixed, electrofusion was induced and fluorescence enhancement due to the formation of a complex between fluo-3 and Ca^{2+} was observed. The method of electrofusion provides a promising tool for studying and following one chemical reaction at a time where spatial and temporal localization can be precisely controlled. Furthermore, the small volume used in this technique could also provide a general chemical or biochemical delivery system.

Based on this previous experiment, electrofusion has been used as a method for nanoparticle synthesis in vesicles [56]. In this case, one vesicle is loaded with Na_2S and the other one with $CdCl_2$. The application of an AC field allows the bringing of vesicles into contact, DC pulse application then induces fusion and as a consequence mixing of the two compartments. Fluorescence in the interior of the resulting vesicles indicates the formation of CdS nanoparticles. Thanks to this approach it is possible to observe and monitor the whole reaction with an optical microscope. This experiment suggests that nanoparticles could be synthesized in biological compartments even without the intervention of macromolecules.

3.4. *Measuring edge/line tensions*

The hydrocarbon chains of lipids are hydrophobic and the energy cost per unit length for leaving the hydrophobic core of a membrane in contact with water is called the line or edge tension γ. It is often hypothesized that for large edges the lipid heads can bend over the edge to make the edge hydrophilic, however there is still an edge tension due to the bending energy associated with this lipid rearrangement. The edge tension is a lipid material property and depends on the external medium. It is the edge tension that makes a membrane patch embedded in an aqueous environment spontaneously bend to form a vesicle, and it also generates the force driving pore closure in lipid bilayers [57,58]. Roughly speaking, the higher the edge tension, the faster the pore closes and one can deduce γ from the evaluation of the corresponding pore closure times.

We put this idea into practice while studying the influence of a poloxamer molecule on EggPC GUVs. It was seen in [59] that poloxamers could modify lipid membrane properties under electric pulses. We explored the effect of the presence of poloxamer in the surrounding solution. Using poloxamer L64 at concentrations of 2.5 and 5 g/L, we first observed no effect on giant liposomes at rest. Then we applied porating electric pulses of 5 ms duration and $\sim$500 V/cm amplitude to these liposomes, and using a fast EMCCD camera we were able to measure the size of the pores and their closure time. We saw no difference of the pore size between liposomes with or without poloxamer, regardless of the concentration. A study of pore closure shows a strong effect: the average measured closure time without poloxamer is 0.2 s while it is 0.4 s with poloxamer, and we did not detect any effect of the concentration of poloxamer. Pore closure is thus twice as slow with poloxamer, and this seems to indicate that L64 reduces the edge tension of EggPC membranes, hence helping to maintain the membrane in a permeabilized state. Since the above results come from very few measurements (6 without poloxamer and 2 for each poloxamer concentration) they are only preliminary and still need to be corroborated.

It is possible to go beyond these qualitative observations and to accurately measure edge tension values. Harbich and Helfrich observed open cylindrical EggPC giant vesicles in AC fields and then deduced a value of 20 pN for γ [60]. Zhelev and Needham obtained values in the same range [21] for SOPC and SOPC/cholesterol (1/1, mol/mol)

liposomes while coupling the electroporation technique and micropipette aspiration. A more recent edge tension measurement method emerged from the theoretical work by Brochard-Wyart *et al* [61]. Considering a spherical vesicle of size R, it was shown that in the limit corresponding to experiments on giant vesicles, a pore of radius r spent the vast majority of its lifetime in a so-called slow closure stage during which the quantity $R^2 \ln(r)$ decreased linearly with time, the coefficient of proportionality being equal to $(-2\gamma/3\pi\eta_0)$, where η_0 denotes the external medium viscosity. The same group later applied this method to pure DOPC GUVs and also to systems containing cholesterol or a surfactant, opening pores *via* intense visible light illumination. Adding glycerol to the aqueous solutions caused slowing down of the dynamics, and they were thus able to measure the pore size during the slow closure stage using classical fluorescence microscopy. They obtained values of γ for their different vesicle compositions, and found that cholesterol caused an increase of γ whereas the surfactant led to a decrease [62]. The main problem of this approach is that glycerol influences the lipid bilayer organization, and that fluorescent dyes embedded in the membrane behave as impurities and may hence lead to inaccurate edge tension measurements. We thus proposed an improvement of Brochard-Wyart's method based on the application of an electric pulse to porate the vesicle and on ultrafast phase contrast imaging to monitor pore size evolution [63]. This method is easy to implement, requires little equipment, and does not suffer from the drawbacks related to the presence of glycerol and fluorescent dye.

4. Conclusions

Giant vesicles provide a useful model system for measuring a variety of physical properties of lipid membranes and for improving our understanding of the electropermeabilization and electrofusion phenomena. In this review, we have tried to summarize the presently known effects of electric fields on giant vesicles and some of their practical applications, and to present current research topics covered by our group. Subjecting GUVs to DC pulses or alternating AC fields can destabilize the lipid bilayer, inducing different behavior such as deformation of the vesicles, poration, motion of domains or fusion. An outline of these various behaviors and their applications is presented in Fig. 2.

It is now known that the deformation of the vesicles depends not only on the frequency and the intensity of the applied field but also on the solutions conductivities. Furthermore the deformations are not exactly the same depending on the presence or not of salt in the external medium and on the shape of the applied electric field (AC or DC). By monitoring the relative area dilatation of the membrane, it is possible to estimate the lateral tension of the vesicle σ_0 and the bending rigidity k_c of the lipid bilayer.

Electric pulses have more dramatic consequences than just deformation. With suitable parameters for the electric field it is possible to electropermeabilize the membrane. This effect can lead to exchange of molecules between the inside and the outside of the vesicle. If the electropermeabilization is strong enough, membrane macropores can be visualized *via* optical microscopy. When a sequence of pulses is used, such observations are in general accompanied with loss of lipid membrane material and a subsequent GUV size decrease allowing the determination of a critical transmembrane voltage. Moreover, by monitoring the evolution of the pore radius it is possible to measure another lipid material property, the edge or line tension γ.

When two vesicles are in close contact, electropermeabilizing them with suitably chosen electric field parameters can induce their fusion. This electrofusion method allows the control and observation of vesicle fusion, and is thus useful for insertion of molecules into the membrane or for mixing different chemicals in the resulting vesicle, thus giving a microreactor.

Acknowledgements

We acknowledge financial support from the Institut Universitaire de France, ANR-PCV (project CMIDT-139888), and the Association Française contre les Myopathies. We thank our colleagues C. Favard, J. Tessié, L. Wasungu, N. Mignet, M. Bureau and D. Scherman for many useful discussions and interactions on the subjects discsussed in this review.

References

[1] M. I. Angelova and D. S. Dimitrov, Liposome electroformation, Faraday Discuss. Chem. Soc. 81 (1986) 303.

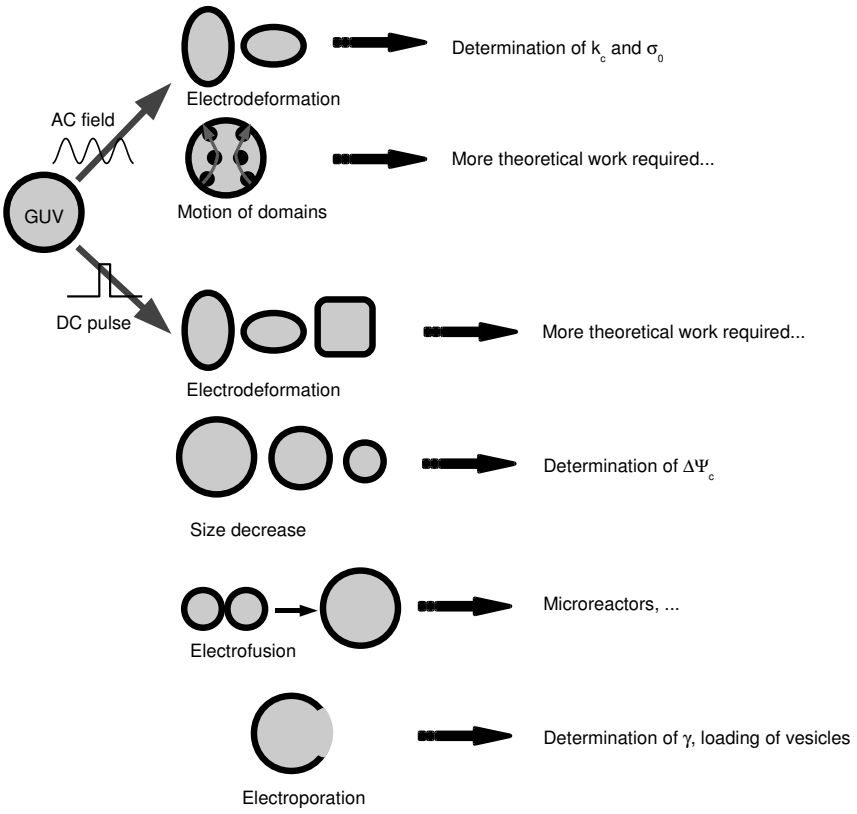

Figure 2. Diagram summarizing the influence of electric fields on giant lipid vesicles and their practical applications. The mention "More theoretical work required..." means that the current understanding of the phenomenon does not allow to design practical applications yet, and that deeper knowledge is still needed to fully exploit this effect of the electric field.
Schéma récapitulant l'influence des champs électriques sur des vésicules lipidiques géantes et leurs applications pratiques. La mention "More theoretical work required..." indique que notre compréhension des phénomènes mentionnés est pour le moment limitée, et qu'une connaissance approfondie est requise pour nous permettre de concevoir des applications.

[2] N. Rodriguez et al., Giant vesicles formed by gentle hydration and electroformation: a comparison by fluorescence microscopy, Colloids Surf. B 42 (2005) 125.

[3] D.J. Estes and M. Mayer, Giant liposomes in physiological buffer using electroformation in a flow chamber, Biochim. Biophys. Acta 1712 (2005) 152.

[4] L.-R. Montes et al., Giant unilamellar vesicles electroformed from native membranes and organic lipid mixtures under physiological conditions, Biophys. J. 93 (2007) 3548.

[5] T. Pott et al., Giant unilamellar vesicle formation under physiologically relevant conditions, Chem. Phys. Lip. 154 (2008) 115.

[6] K.S. Horger et al., Films of agarose enable rapid formation of giant liposomes in solutions of physiologic ionic strength, J. Am. Chem. Soc. 131 (2009) 1810.

[7] R. Dimova et al., Giant vesicles in electric fields, Soft Matter 3 (2007) 817.

[8] R. Dimova et al., Vesicles in electric fields: Some novel aspects of membrane behavior, Soft Matter 5 (2009) 3201.

[9] R. Dimova et al., A practical guide to giant vesicles. Probing the membrane nanoregime via optical microscopy, J. Phys.: Condens. Matter 18 (2006) S1151.

[10] M. Kummrow and W. Helfrich, Deformation of giant lipid vesicles by electric fields, Phys. Rev. A 44 (1991) 8356.

[11] M. Winterhalter and W. Helfrich, Deformation of spherical vesicles by electric fields, J. Colloid Interface Sci. 122 (1988) 583.

[12] M. D. Mitov et al., Electric-field-dependent thermal fluctuations of giant vesicles, Phys. Rev. E 48 (1993) 628.

[13] S. Aranda et al., Morphological transitions of vesicles induced by alternating electric fields, Biophys. J. 95 (2008) L19.

[14] P. M. Vlahovska et al., Electrohydrodynamic model of vesicle deformation in alternating electric fields, Biophys. J. 96 (2009) 4789.

[15] K. A. Riske and R. Dimova, Electro-deformation and poration of giant vesicles viewed with high temporal resolution, Biophys. J. 88 (2005) 1143.

[16] K. A. Riske and R. Dimova, Electric pulses induce cylindrical deformations on giant vesicles in salt solutions, Biophys. J., 91 (2006) 1778.

[17] E. Neumann et al., Electroporation and electrofusion in cell biology, Plenum, New York, 1989.

[18] M. Belehradek et al., Electrochemotherapy, a new antitumor treatment. First clinical phase I-II trial, Cancer 72 (1993) 3694.

[19] J.-M. Escoffre et al., What is (still not) known of the mechanism by which electroporation mediates gene transfer and expression in cells and tissues, Mol. Biotechnol. 41 (2009) 286.

[20] D. Needham and R. M. Hochmuth, Electro-mechanical permeabilization of lipid vesicles; Role of membrane tension and compressibility, Biophys. J. 55 (1989) 1001.

[21] D.V. Zhelev and D. Needham, Tension stablized pores in giant vesicles: determination of pore size and pore line tension, Biochim. Biophys. Acta. 1147 (1993) 89.

[22] E. Tekle et al., Asymmetric pore distribution and loss of membrane lipid in electroporated DOPC vesicles, Biophys. J. 81 (2001) 960.

[23] T. Portet et al., Visualization of membrane loss during the shrinkage of giant vesicles under electropulsation, Biophys. J. 96 (2009) 4109.

[24] J. Teissié and M.-P. Rols, An experimental evaluation of the critical potential difference inducing cell membrane electropermeabilization, Biophys. J. 65 (1993) 409.

[25] K.A. Riske et al., Bursting of charged multicomponent vesicles subjected to electric pulses, Soft Matter 5 (2009) 1983.

[26] M. Staykova et al., Membrane flow patterns in multicomponent giant vesicles induced by alternating electric fields, Soft Matter 4 (2008) 2168.

[27] G. Eitzen, Actin remodeling to facilitate membrane fusion, Biochim. Biophys. Acta 1641 (2003) 175.

[28] J.C. Hay, Calcium: a fundamental regulator of intracellular membrane fusion?, EMBO Rep. 8 (2007) 236.

[29] M. Kielian and F.A. Rey, Virus membrane-fusion proteins: more than one way to make a hairpin, Nat. Rev. Microbiol. 4 (2006) 67.

[30] W. Weissenhorn et al., Virus membrane fusion, FEBS Lett. 581 (2007) 2150.

[31] C.A. Helm et al., Role of hydrophobic forces in bilayer adhesion and fusion, Biochemistry 31 (1992) 1794.

[32] Y. Kozlovsky and M.M. Kozlov, Stalk model of membrane fusion: solution of energy crisis, Biophys. J. 82 (2002) 882.

[33] C.M. Carr and P.S. Kim, A spring-loaded mechanism for the conformational change of influenza hemagglutinin, Cell 73 (1993) 823.

[34] Y.G. Yu et al., Insertion of a coiled-coil peptide from influenza virus hemagglutinin into membranes, Science 266 (1994) 274.

[35] B.R. Lentz et al., Protein machines and lipid assemblies: current views of cell membrane fusion, Curr. Opin. Struct. Biol. 10 (2000) 607.

[36] L.V. Chernomordik and M.M. Kozlov, Protein-lipid interplay in fusion and fission of biological membranes, Annu. Rev. Biochem. 72 (2003) 175.

[37] B.R. Lentz, Polymer-induced membrane fusion: potential mechanism and relation to cell fusion events, Chem. Phys. Lip. 73 (1994) 91.

[38] A. Jeremic et al., Calcium drives fusion of SNARE-apposed bilayers, Cell. Biol. Int. 28 (2004) 19.

[39] A. Lopez et al., 31P NMR analysis of membrane phospholipid organization in viable, reversibly electropermeabilized Chinese hamster ovary cells, Biochemistry 27 (1988) 1222.

[40] U. Zimmermann, Electric field-mediated fusion and related electrical phenomena, Biochim. Biophys. Acta 694 (1982) 227.

[41] A.E. Sowers, A long-lived fusogenic state is induced in erythrocyte ghosts by electric pulses, J. Cell. Biol. 102 (1986) 1358.

[42] J. Teissié and M.P. Rols, Fusion of mammalian cells in culture is obtained by creating the contact between cells after their electropermeabilization, Biochem. Biophys. Res. Commun. 140 (1986) 258.

[43] M.P. Rols and J. Teissié, Ionic-strength modulation of electrically induced permeabilization and associated fusion of mammalian cells, Eur. J. Biochem. 179 (1989) 109.

[44] L.K. Tamm et al., Membrane fusion: a structural perspective on the interplay of lipids and proteins, Curr. Opin. Struct. Biol. 13 (2003) 453.

[45] C. Haluska et al., Time scales of membrane fusion revealed by direct imaging of vesicle fusion with high temporal resolution, Proc. Natl. Acad. Sci. U.S.A. 103 (2006) 15841.

[46] D. Marsh, Elastic curvature constants of lipid monolayers and bilayers, Chem. Phys. Lip. 144 (2006) 146.

[47] R.S. Gracià et al., Effect of cholesterol on the rigidity of saturated and unsaturated membranes determined from fluctuation and electrodeformation analysis on giant vesicles, Soft Matter, in press.

[48] M. B. Schneider et al., Thermal fluctuations of large quasi-spherical bimolecular phospholipid-vesicles, J. Phys. 45 (1984) 1457.

[49] W. Helfrich, Elastic properties of lipid bilayers: theory and possible experiments, Z. Naturforsch 28c (1973) 693.

[50] M. Golzio et al., Direct visualization at the single-cell level of electrically mediated gene delivery, Proc. Natl. Acad. Sci. U.S.A. 99 (2002) 1292.

[51] L. V. Chernomordik et al., Electrostimulated uptake of DNA by liposomes, Biochim. Biophys. Acta 1024 (1990) 179.

[52] P. F. Lurquin and K. Athanasiou, Electric field-mediated DNA encapsulation into large liposomes, Biochem. Biophys. Res. Commun. 267 (2000) 838.

[53] T. Portet et al., Electromediated DNA uptake into giant unilamellar vesicles, In preparation.

[54] K.A. Riske et al., Electrofusion of model lipid membranes viewed with high temporal resolution, Biophys. Rev. Lett. 4 (2006) 387.

[55] D.T. Chiu et al., Chemical transformations in individual ultrasmall biomimetic containers, Science 283 (1999) 1892.

[56] P. Yang et al., Nanoparticle formation in giant vesicles: synthesis in biomimetic compartments, Small 5 (2009) 2033.

[57] P. Fromherz et al., From discoid micelles to spherical vesicles; the concept of edge activity, Faraday Discuss. Chem. Soc. 81 (1986) 39.

[58] O. Sandre et al., Dynamics of transient pores in stretched vesicles, Proc. Natl. Acad. Sci. U.S.A. 96 (1999) 10591.

[59] V. Sharma et al., Poloxamer 188 decreases susceptibility of artificial lipid membranes to electroporation, Biophys. J. 71 (1996) 3229.

[60] W. Harbich and W. Helfrich, Alignment and opening of giant lecithin vesicles by electric fields, Z. Naturforsch. 34a (1979) 1063.

[61] F. Brochard-Wyart et al., Transient pores in stretched vesicles: role of leak-out, Physica A 278 (2000) 32.

[62] E. Karatekin et al., Cascade of transient pores in giant vesicles: line tension and transport, Biophys. J. 84 (2003) 1734.

[63] T. Portet and R. Dimova, A new method for measuring edge tensions: effect of membrane composition, Submitted to Biophys. J.

Visualization of Membrane Loss during the Shrinkage of Giant Vesicles under Electropulsation

Thomas Portet,[†‡] Franc Camps i Febrer,[†] Jean-Michel Escoffre,[†] Cyril Favard,[§] Marie-Pierre Rols,[†] and David S. Dean[‡*]

[†]Institut de Pharmacologie et de Biologie Structurale, Centre National de la Recherche Scientifique, UMR 5089, and [‡]Laboratoire de Physique Théorique, Centre National de la Recherche Scientifique, UMR 5152, Université Paul Sabatier, Toulouse, France; and [§]Institut Fresnel, Centre National de la Recherche Scientifique, UMR 6133, Marseille, France

ABSTRACT We study the effect of permeabilizing electric fields applied to two different types of giant unilamellar vesicles, the first formed from EggPC lipids and the second formed from DOPC lipids. Experiments on vesicles of both lipid types show a decrease in vesicle radius, which is interpreted as being due to lipid loss during the permeabilization process. We show that the decrease in size can be qualitatively explained as a loss of lipid area, which is proportional to the area of the vesicle that is permeabilized. Three possible modes of membrane loss were directly observed: pore formation, vesicle formation, and tubule formation.

INTRODUCTION

Electropermeabilization is a commonly used physical method in which electric pulses are applied to cells and vesicles, and has been widely reviewed in the literature (1–7). An effect of major importance is that, under certain circumstances, the electric pulses can induce the transient permeabilization of the cell plasma membrane. This permeabilization manifests itself via the crossing of the cell membrane by molecules that would normally not be able to permeate the cell membrane. When subjected to sufficiently large electric fields, vesicle membranes become permeable to small molecules (8,9) and flat membranes show a marked increase in their electrical conductance (10). Small molecules appear to cross the permeabilized membranes via simple diffusion. However, complex processes, such as electrophoresis and direct interactions with the membrane, come into play for larger molecules such as DNA. Electropermeabilization is now regularly employed as a delivery method for a large variety of molecules such as drugs, antibodies, oligonucleotides, RNA, and DNA (6,9,11–13). Initial studies were carried out in vitro on cells in culture, but as the technique has developed, an increasing amount of data has been obtained in vivo on tissues (14–16); this method is being adapted to the clinical context (17,18). Clearly the method has a huge potential in the fields of cancer treatment and gene therapy, offering, in some cases, more efficient, more controllable, and safer treatment protocols (when compared to viral transfection methods, for example). From a purely physical point of view, the application of an electric field to a lipid membrane has two notable effects. The first is a mechanical one in which the stresses caused by the field can deform the membrane; for instance, causing a spherical vesicle to deform into an ellipsoidal or cylindrical one (19–22). This deformation can be thoroughly understood in terms of a macroscopic continuum description of the cell membrane in terms of its bulk electrical and mechanical properties. The second phenomenon of electropermeabilization is much less well understood. Despite its increasing popularity as a therapeutic method, there are still many open questions about the underlying physical mechanisms involved in electropermeabilization. Indeed, at the simplest level, the basic structural changes induced by the field on the membrane structure are still to be fully understood. A number of physical theories have been put forward to explain the phenomenon of electropermeabilization. Historically, the first explanations of electropermeabilization were based on classical continuum theories, which predict dielectric breakdown of the membrane at a critical field strength (23–28). The main problem with such theories is that, although predicting a dielectric/mechanical breakdown transition, they do not provide a description of the physical state of the permeabilized membrane. Currently, the most popular explanation for electropermeabilization is that pores are formed because of a local increase in the surface tension due to the electric field (29–33). This increase in surface tension energetically favors the formation of pores, which is otherwise energetically defavored by their line tension. A similar theory was first introduced to explain the rupture of soap films (34). In this theory, the pores can become stabilized in a hydrophobic-to-hydrophilic pore transition via the rearrangement of the lipids at the pore edges. Because the permeabilization is explained by the formation of pores, the phenomenon described by this theory is referred to as electroporation. Recently, numerical simulations have confirmed that pores can be induced by strong electric fields (35–41); typically, the systems simulated are small, and no significant lipid loss during pore formation has been reported.

Submitted May 29, 2008, and accepted for publication February 20, 2009.

*Correspondence: dean@irsamc.ups-tlse.fr

Editor: Petra Schwille.

0006-3495/09/05/4109/13 $2.00

doi: 10.1016/j.bpj.2009.02.063

When discussing the phenomenon of electropermeabilization, we must distinguish between two key stages of the process:

Step 1. The physical change induced in the membrane by the field (in the absence of molecules to be transported).

Step 2. The interaction of the molecules that are to be transported with the modified membrane.

At the simplest level, combination of Steps 1 and 2 can be observed experimentally as a transport phenomenon using marked molecules or via conductivity experiments. In this article, we demonstrate that Step 1 can be indirectly detected via a change in the size of giant liposomes under electropulsation and an associated direct visualization of the expulsion of lipids from the liposomes. Concretely we study the effect of a series of permeabilizing pulses, well separated in time, on the size of giant unilamellar vesicles (GUVs). In the experiments, the radius of the GUV is measured after each pulse and we find that each GUV studied shows, on average, a decrease in its radius down to a critical radius beyond which its size no longer changes. This decrease in size points to the fact that, during the physical processes leading to electropermeabilization, lipids are lost from the vesicle—thus leading to a reduction in their size.

Our experiments are not a direct study of permeabilization; however, they constitute an indirect method of studying electropermeabilization that is relatively straightforward to carry out and interpret in terms of simple physical models that are relatively well established. From an experimental point of view, the crucial advantage of using GUVs is that their composition can be varied and controlled, and in addition, their membrane is not subjected to internal mechanical constraints, as is the case for living cells with cellular cytoskeletons. Furthermore, their size is similar to that of mammalian cells, which allows a direct visualization by an optical microscope.

Lipid loss during electropermeabilization seems likely as if, for instance, pores are formed the lipids near the edges of these pores will be subject to strong variations in the local electric potential and the electric field. Charges and dipole moments on lipids will interact strongly with the electric field and variations of the electric field, respectively. The forces involved may well be capable of tearing lipids from the membrane structure. However, our experiments suggest that the mechanism of lipid loss is a collective one, which involves the formation of small structures such as tubules and vesicles as well as pores. A simple comparison of electrostatic (dipole electric field interaction) energy and hydrophobic free energy suggests that individual lipids cannot be removed from the membrane.

The phenomenon of lipid loss due to an applied field has previously been studied in Tekle et al. (42) but from quite a different point of view (in that study, the effect of single pulses was examined). DOPC vesicles of sizes of ~20 μm were subjected to pulsed electric fields of ~1 kV/cm and duration 700 μs. The vesicles were observed using a standard fluorescent microscope and at the cathode-facing side, single pores of the size of ~7 μm were observed. Such pores were, however, seldom found on the anode-facing side. However, it was inferred that this side was also permeabilized but that the pores responsible were too small to be observed. In the experiments, it was also noted that up to 14% of the vesicle surface could be lost during the process of pore formation/permeabilization.

TABLE 1 Abbreviations used

a	Membrane thickness.
a_e	Membrane electrical thickness.
A	Area of the vesicle.
A_p	Permeabilized area.
C	Constant depending on R, a, and the various conductivities of the problem.
$DiIC_{18}$	1,1′-dioctadecyl-3,3,3′,3′-tetramethylindocarbocyanine perchlorate.
DOPC	1,2-Dioleoyl-*sn*-glycero-3-phosphocholine.
EggPC	L-α-Phosphatidylcholine (egg, chicken).
E	Magnitude of the applied electric field.
l	Length of the hydrocarbon chain.
N_c	Number of pulses needed to enter the shrinking regime.
p	Dipole moment of the PC headgroup.
PR	Preshrinking regime.
q	Probability that one pulse induces a transition from the pre-shrinking to the shrinking regime.
R_c	Critical radius.
λ	Fraction of the permeabilized area lost per pulse.
Rhodamine PE	L-α-Phosphatidylethanolamine-*n*-(Egg Lissamine Rhodamine PE).
$R(n)$	Radius of the vesicle after n pulses.
W_c	Rescaled critical radius, $R_c/R(0)$
SR	Shrinking regime.
$W(n)$	Rescaled radius of the vesicle after n pulses, $R(n)/R(0)$
$\Delta\Psi$	Transmembrane voltage.
$\Delta\Psi_0$	Initial transmembrane voltage induced by the first pulse at the poles of the liposomes.
$\Delta\Psi_c$	Critical transmembrane voltage n: number of pulses.
θ	Angle on the cell surface with respect to the direction of the applied field.
θ_c	Critical angle.
Σ_0	Initial surface tension.
Σ_{el}	Surface tension induced by the electric field.
Σ_{lys}	Lysis tension.
ε_m	Membrane dielectric constant.
ρ	Effective radius of the lipid hydrocarbon tail viewed as a cylinder.
μ	Lipid tail hydrophobic free energy per unit of area.

See Table 1 for a list of terms and parameters used in this article.

EXPERIMENTAL SETUP

We decided to work with two different lipids. However, we wanted phospholipids with identical head groups to obtain the same dipole behavior. Thus, we used DOPC and EggPC, purchased from Avanti Polar Lipids (Alabaster, AL). The formation medium is an aqueous solution with 240 mM sucrose. The pulsation buffer is an aqueous solution of 260 mM glucose

that also contains 1 mM phosphate buffer KH_2PO_4/K_2HPO_4 (Merck, Darmstadt, Germany) to impose a physiological pH of 7.4, and 1 mM sodium chloride (Prolabo, Briare, France) to achieve an electrical conductivity in the range of a few hundreds of μS/cm. Conductivities of internal and external solutions are measured with an HI 8820 conductimeter (Hanna Instruments, Lingolsheim, France), and have the values $\sigma_i \approx 15$ μS/cm and $\sigma_e \approx 460$ μS/cm, respectively. The osmolarities are 285 mOsm/kg for the formation medium, and 305 mOsm/kg for the pulsation buffer. These measurements were performed with an Osmomat 030 osmometer (Gonotec, Berlin, Germany). The different refractive indexes of the internal and external media yields a contrast which enables the vesicles to be visualized using a microscope, and the density difference allows the sedimentation of the vesicles on the bottom of the chamber, thus reducing their distance from the objective. EggPC liposomes are visualized by phase contrast, and DOPC liposomes by fluorescence microscopy. We worked with two different dyes (Rhodamine PE (Avanti Polar Lipids) and $DiIC_{18}$ (Molecular Probes, Eugene, OR)) without any noticeable change in our experimental results. The vesicle formation method employed here is electroformation, as described in Angelova and Dimitrov (43). We chose this technique because it is simple, easily reproducible, and has a good yield. Furthermore, a large amount of the produced vesicles is unilamellar, as demonstrated in Rodriguez et al. (44).

Electroformation

Lipid solution

The lipids are diluted in chloroform, at a mass concentration of 0.5 mg/mL. For DOPC vesicles, the fluorescent probe is added at 0.005 mg/mL. This preparation and the following steps can be performed at room temperature, because the gel-phase/liquid-phase transition temperature of the lipids used is much lower.

Formation chamber

The chamber is made of two glass layers covered with Indium Tin Oxide to ensure the electrical conductivity of the surface. The two layers are separated by an adhesive silicone joint of 1 mm width. The connection with the generator (model 128, AC Exact; Hillsboro, OR) is maintained by two wires, each one soldered on a small copper strip stuck on the ITO slide. Then, 15 μL of lipid solution is deposited on the conducting sides of the glass slides. The deposition is carried out slowly and at constant rate in a chamber held at 4°C to slowly evaporate the chloroform and then the slides are dried under vacuum for a couple of hours to entirely remove the remaining solvent molecules.

Finally, the slides are sealed together, and the chamber is filled with the formation medium.

Voltage application

We apply a sinusoidal voltage of 25 mV peak to peak at 8 Hz. The voltage is increased by 100 mV steps every 5 min, up to a value of 1225 mV. It is maintained under these conditions overnight. Next, we apply a square wave of same amplitude at 4 Hz for 1 h to detach the liposomes from the slides.

Electropulsation

Pulsation chamber

The chamber where the GUVs are subjected to the electric field is composed of a glass slide and a coverslip. Two parallel copper strips of thickness 70 μm are stuck on the slide at a distance of 1-cm apart. The coverslip is then stuck onto the slide and strips with heated parafilm. The chamber is 1-cm long (between electrodes), 2.6-cm wide (width of the coverslip), and 250-μm high (value estimated via measurements with a microscope). We first introduce 60 μL of pulsation buffer between the slide and the coverslip, while taking care of filling the whole chamber to ensure the conductivity of our medium. Next, we add 5 μL of our GUV preparation. Capillarity phenomena prevent the solution from leaking out of the chamber.

The electrode thickness is about the size of our biggest liposomes, which represents only a quarter of the chamber height. We could not a priori be certain of the homogeneity of the field. However, we solved numerically Laplace's equation with the finite element software Comsol Multiphysics (Comsol, Burlington, MA) for the case of our geometry. We found that the field was almost homogeneous in the bottom part of the chamber between the electrodes, and that the size and shape of the permeabilized area were not significantly different from that computed for a geometry with much bigger electrodes (data not shown).

Pulsation method

Electropulsation is carried out using a CNRS cell electropulsator (Jouan, St. Herblain, France), which delivered square-wave electric pulses. An oscilloscope (Enertec, St. Etienne, France) is used to monitor the pulse shape and amplitude. The process of electropulsation is performed directly under the microscope. For the phase contrast visualization, we used an inverted epifluorescence microscope (Leica model No. DM IRB; Leica Microsystems, Wetzlar, Germany) equipped with a camera (Princeton model No. RTE/CCD-1317-K/0; Princeton Instruments, Trenton, NJ) and a 40× Leica phase contrast objective, and an inverted confocal microscope (Zeiss model No. LSM 510; Carl Zeiss, Jena, Germany) with a 63× Zeiss objective for fluorescence imaging. Excitation at 543 nm was provided by a HeNe laser, and emission filter was a 560-nm long-pass. The pulse duration was not set to a few hundreds of microseconds as in the literature (21,22,42), but to 5 ms, because this value is commonly used for gene transfer protocols in mammalian cells (9). In most cases, we apply pulses at 0.5 Hz. However, we sometimes have to interrupt the pulse train for a few seconds to recenter the image on the liposome of interest. Indeed, the observed vesicle does not always stay immobile. It often experiences a translational motion toward the positive electrode, because of which we sometimes have to modify the centering. This displacement was always directed toward the anode, irrespective of the net electric charge of the fluorescent probe that we used (negative for Rhodamine PE and positive for $DiIC_{18}$). As we will see later, the direction of this motion is coherent with the sign of the ζ-potentials of the vesicles, which does not depend on the type of dye chosen. Due to the need to recenter the image from time to time, the frequency of the pulses is not constant over a whole experiment, but we checked that this did not affect our results. The time delay between two consecutive pulses is of the same order of magnitude, ranging from 2 s to a few tens of seconds. This duration seems to be much longer than the time needed by the vesicle to relax after one pulse, therefore it does not matter if pulses are separated by 2 or 20 s. Direct observation showed that vesicles were distorted rapidly after the pulse application, but as far as the eye could see, there was no visible size or shape change between two consecutive pulses. The pulse amplitude is chosen according to the rule $ED = (4/3)\Delta\Psi_0 = Const$ (see details later for this choice), where E denotes the amplitude of the electric field, and D the initial diameter of the GUV. The constant is chosen to be 1.7 V. This choice means that at the beginning of every experiment the potential difference drop, $\Delta\Psi_0$, across the GUV membrane at the poles facing the electrodes is theoretically (see later) equal to ~1.3 V; this value is well beyond the value of 200 mV typically cited as the permeabilization threshold for Chinese hamster ovary cells (45,46) and of the order of that cited for artificial vesicles and other cell types (3,26,47). In the pulsation chamber, the distance between the electrodes is 1 cm and so the potential applied between the electrodes is $1.7/D$ V, where D is measured in centimeters or conveniently $17/D$ kV if we measure D in μm. The idea behind this large choice of initial transmembrane potential $\Delta\Psi_0$ is that the field will initially permeabilize the membrane and continue to do so until the vesicle size becomes significantly smaller than the initial one. We note that our protocol yields initial transmembrane potentials that are slightly lower but of the same order as those in the experiments of Tekle et al. (42), which varied between 1.4 and 2.5 V.

The experimental strategy is simple. We focus on a liposome and we measure its initial diameter. We then tune the voltage amplitude according

to the rule described above, and we apply a pulse train until the GUV does not shrink anymore. We acquire one image between two consecutive pulses (~1 s after each pulse), so we are sure that the vesicle has experienced an electric pulse between two consecutive values of the diameters we measure. Image processing tasks are performed with ImageJ (National Institutes of Health, Bethesda, MD).

ζ-Potentials measurements

We measured the average ζ-potentials of our GUVs by photon correlation spectroscopy (Zetasizer 3000 HS; Malvern, Worcestershire, United Kingdom), using the following method. We diluted 1 mL of the GUV solution obtained after electroformation in 2 mL of a special buffer containing 240 mM sucrose, 1.5 mM phosphate buffer, and 1.5 mM sodium chloride. Vesicles are thus suspended in a medium containing 1 mM sodium chloride, 1 mM phosphate buffer, and 240 mM sucrose. This composition is the same as that of our pulsation medium, except for the 260 mM glucose replaced by 240 mM sucrose to avoid sedimentation of the vesicles, which would make the measurement impossible. We then split the 3 mL into two samples, on which we performed two series of 10 measurements each.

THEORY

The basic theory that explains electroporation is based on the modeling of the vesicle electrode system in terms of a weakly conductive cell membrane of conductivity denoted by σ_m, with external and internal media of much higher conductivities denoted by σ_e and σ_i, respectively. We denote by R the radius of the vesicle assumed spherical, and which stays spherical throughout the experiments. In our experiments, R lies typically between 10 and 100 μm. The thickness of the vesicle membrane is denoted by a and typically has the value of 4 nm. In the steady state, which is achieved on timescales much shorter than the time over which the pulse is applied, the electric potential Ψ obeys Laplace's equation, and if θ denotes the angle on the cell surface with respect to the direction of the applied field, which is of magnitude E, then the potential drop across the membrane at that point is given by (see (1) for instance for a detailed derivation)

$$\Delta\Psi = -CRE\cos(\theta), \tag{1}$$

where C is a constant depending on R, a, and the various conductivities of the problem. In the limits where $\sigma_m << \sigma_i$, $\sigma_m << \sigma_e$, and $a << R$, the constant C becomes very simple and takes the value $C = 3/2$. For the parameters of the experiments carried out here, we are close to the limit where C takes this limiting value. The most important point for our analysis here is that C is independent of R. We thus find that, for a thin membrane, the electric field inside the membrane and normal to its surface, denoted by E_n, is given by

$$E_n(\theta) = \frac{CRE\cos(\theta)}{a}. \tag{2}$$

Equation 2 demonstrates that there is a huge amplification of the externally applied field across the membrane. This huge electric field internal to the membrane causes structural changes. Whether this structural change corresponds to the formation of pores, dielectric breakdown, or the formation of defects or vesicles, is still open to debate. However, in experiments where permeabilization is measured either via conductivity measurements of planar membranes or by direct optical observation of the entry of marker molecules, a consensus exists that permeabilization occurs locally in the membrane when the magnitude of the potential drop across the membrane $\Delta\Psi$ exceeds a certain threshold $\Delta\Psi_c$, which is estimated to be ~0.25–1.0 V (3,26,45–47). This corresponds to a field within the membrane of ~50–250,000 kV/m (for a membrane of thickness 4 nm). This critical threshold is seemingly quite universal, being largely independent of cell and vesicle composition. There is an alternative though largely equivalent physical explanation of field-induced breakdown of the membrane. The effect of a local potential drop $\Delta\Psi$ across the membrane is to induce a local electrical surface tension Σ_{el}, which can be computed via the Maxwell stress tensor and is given by $\Sigma_{el} = \varepsilon_m\Delta\Psi^2 a/2a_e^2$, where ε_m is the dielectric constant of the membrane, a is its thickness, and a_e its electrical thickness (7,26). If the initial surface tension of the membrane is Σ_0, then, upon applying the field, the total tension is $\Sigma = \Sigma_0 + \Sigma_{el}$. The tension of rupture of a lipid membrane is called the lysis tension Σ_{lys} and thus, when the local tension Σ exceeds Σ_{lys}, we expect the membrane to be destabilized. This formulation is strictly equivalent to the existence of a critical value of the local electric field in the membrane at which breakdown will occur. However, in this formulation we see that $\Delta\Psi_c$ will depend on the initial surface tension of the vesicle Σ_0. Indeed, such a dependence on Σ_0 has been reported experimentally (21). In terms of the initial and lysis tension, the critical potential is given by

$$\Delta\Psi_c = \sqrt{\frac{2a_e^2}{\epsilon_m a}(\Sigma_{lys} - \Sigma_0)}, \tag{3}$$

and thus, we see that the value of the applied field required to affect the membrane will depend on the initial tension of the vesicle. In our study, we are interested in the mechanism of lipid loss, and the $\Delta\Psi_c$ that induces lipid loss does not necessarily correspond to that necessary to induce permeabilization; however, it is reasonable to expect that the two critical potentials have the same order of magnitude. Studies of electropermeabilization phenomena show that the critical potential depends on the duration of the applied pulse, the critical potential being smaller for longer pulses (11). This means that the underlying physical mechanisms rely on activated processes such as nucleation events for first-order phase transitions. This means that an applied pulse may have no effect with some probability, and this probability should decrease with the amplitude and duration of the pulse. In our experimental setup, the liposomes are visibly under an initial tension, and we expect that there is some distribution of initial tensions even for vesicles of the same composition and similar sizes. The critical potential for each vesicle should therefore be expected to vary.

As we are looking at vesicles, we can neglect any possible modification of the transmembrane potential due to cellular activity and thus assume that it is given purely by Eq. 1. Assuming that the mechanical and electric membrane thickness a and a_e remains constant, there is a critical transmembrane potential drop beyond which the membrane becomes permeabilized or susceptible to lipid loss. Clearly, at fixed electric field parameters (amplitude and duration), a cell can no longer be permeabilized when its radius is smaller than a certain critical radius R_c, beyond which no part of the cell is permeabilized. We thus expect that the permeabilization and thus, vesicle shrinkage will stop once the vesicle has this critical radius. The region where the magnitude of $\Delta\Psi$ is maximal is clearly that facing the electrodes, corresponding to $\theta = 0$ and $\theta = \pi$, and so these are the last points where the membrane is permeabilizable. The value of R_c is thus given by

$$\Delta\Psi_c = CER_c. \tag{4}$$

If we are in the situation where $R > R_c$, then about the pole at $\theta = 0$ the region where θ is between 0 and θ_c is permeabilized and θ_c is given by

$$\theta_c = \arccos\left(\frac{\Delta\Psi_c}{CRE}\right). \tag{5}$$

This region gives one-half of the total permeabilized area of the vesicle, which we denote by A_p. We thus find that

$$\frac{1}{2}A_p = 2\pi\int_0^{\theta_c} R^2\sin(\theta)d\theta = 2\pi R^2\left(1-\frac{R_c}{R}\right). \tag{6}$$

Now we consider how the area loss upon a pulsation can be related to the physical parameters of the system. The simplest idea is to assume that the area lost is simply proportional to the permeabilized membrane area. This does not presuppose the mechanism of lipid loss; we simply assume that, in the region where the field exceeds the critical value, the membrane structure is altered. This alteration can be interpreted as a form of dielectric breakdown, and where it occurs, we assume that lipids can be effectively lost from the membrane surface.

If n denotes the number of pulses, treating n as a continuous variable, we can write that, on average,

$$\frac{dA}{dn} = -\lambda A_p, \tag{7}$$

that is to say, the average area lost per pulse is simply proportional to the area where the critical membrane potential (or equivalently surface tension) is exceeded. Note that we should really use a discrete difference equation rather than the continuous one above; however, we have, numerically, checked that the difference behavior is insignificant when compared to the typical experimental errors. Now if we assume that $\Delta\Psi_c$ remains constant throughout the experiment, Eq. 7 can be solved using $A = 4\pi R^2$ to obtain

$$R(n) = R_c + (R(0) - R_c)\exp\left(-\frac{\lambda}{2}n\right). \tag{8}$$

Thus, we expect an exponential decay to the critical value of R_c, as given by Eq. 4. If we define the dimensionless variable

$$W(n) = \frac{R(n)}{R(0)}, \tag{9}$$

then $W(n)$ obeys

$$W(n) = W_c + (1 - W_c)\exp\left(-\frac{\lambda}{2}n\right), \tag{10}$$

and W_c is the asymptotic value of W after a large number of pulses have been applied and beyond which the vesicle is no longer permeabilizable; it is given by

$$W_c = \frac{R_c}{R(0)} = \frac{\Delta\Psi_c}{CER(0)}. \tag{11}$$

Now, in the experiments, if we choose to apply fields E such that $ER(0)$ is constant, then if $\Delta\Psi_c$ and C are constant we find that

$$W_c = \frac{\Delta\Psi_c}{\Delta\Psi_0}, \tag{12}$$

where $\Delta\Psi_0$ is the initial experimentally imposed potential drop at the poles of the cells and is by construction (i.e., via the choice of E) the same for all vesicles. With this choice of E, all plots of W as a function of the number of pulses n should collapse onto the same curve if $\Delta\Psi_c$ remains constant during the experiment and if it is the same for all vesicles. All plots will have $W(0) = 1$, and should attain the asymptotic value W_c after the same characteristic number of pulses (as we have assumed that λ is independent of R).

We stress here that, if $ER(0)$ is taken to be constant, then the normal component of the electric field within the membrane is the same for every vesicle studied at the beginning of each experiment and thus, independently of any theory used to analyze the results, we are always looking at systems where the local electric fields in the membranes are the same.

Clearly three sources of additional complexity are neglected in the above analysis:

1. The surface tension will fluctuate during the permeabilization/lipid loss process.
2. The local electric field seen by the vesicles will fluctuate due to the presence of other vesicles (48).
3. We shall see in the section on experimental results that several mechanisms can be involved in the process of lipid loss (pore, vesicle, and tubule formation) and clearly, the choice of a single fitting parameter for lipid loss per permeabilized area λ is another simplification. Indeed, λ should be interpreted as an average area loss

parameter due to the (at least) three visualized mechanisms of lipid expulsion.

The initial surface tension (which will have some distribution about an average value) will also play a role in the initiation of the permeabilization and lipid loss process. The extent to which the vesicle retains a memory of this initial tension, is an important point. If, after each pulse, it had the same tension, then the distribution of the values of W_c would be a direct reflection of this initial surface tension distribution. However, it is likely that the tension will vary after each pulse and indeed, that the tension is a dynamical variable. Our experimental results imply that the reduction of the radius is due to expulsion of lipid from the main vesicle, but that some expelled lipid is still in contact with the main vesicle (as in the case of tubules). These attached lipids will constitute a reservoir, which will modify the effective surface tension of the main vesicle, and this tension itself will evolve if the system has not had time to equilibrate between pulses. We conclude that, in fitting the data with the simple model presented here, we should find a scatter in the resulting values of λ and W_c due to points 1–3, mentioned above.

EXPERIMENTAL RESULTS

Observations and data fitting

The existence of the critical radius R_c was confirmed by the two following observations:

Observation 1. After a sufficiently large number of pulses had been applied, all the vesicles we could find in our sample had sizes lower than the one of the initial liposome of interest.

Observation 2. We noticed that a liposome that had reached its critical radius could experience another shrinkage if the field magnitude was increased.

We should mention that we sometimes saw vesicles disintegrating, and thus we could not observe the size stabilization. We only kept data corresponding to shrinking and stabilizing GUVs, and we finally gathered 51 data sets for DOPC and 47 for EggPC. Another fact that must be mentioned is the following. In some cases, the size diminution did not begin immediately after the first pulse. We had to apply several electric pulses before being able to detect radius decrease. A possible explanation for this fact is that, like the permeabilization process, the mechanism for lipid loss requires a change in the physical state of the membrane—the formation of defects or pores, for example. The effect of the field is therefore twofold; it allows for the formation of defects, and once defects are present, the field, along with the presence of the defects, allows for lipid loss. We may assume that the creation of defects is an activated process, and at each pulse, the membrane develops defects with some probability q. Note that we assume it is only the defect creation process that has this probabilistic nature (once the vesicle size has begun to decrease, lipids are expelled after each pulse as long as the vesicle radius is $>R_c$). To describe this phenomenon, we suppose that one vesicle can be found either in a preshrinking (no defects) or in a shrinking (with defects) regime (preshrinking regime, i.e., PR or shrinking regime, i.e., SR, respectively), the transition to the SR after a pulse being a stochastic event occurring with constant probability q, independent of the number of pulses applied before. This hypothesis of a random event is legitimate because our model should incorporate the intrinsic stochastic nature of permeabilization processes (3). The fact that q does not depend on n is justified if we assume that a vesicle having experienced a harmless pulse recovers the same state it had in the PR. Within this modified framework, the former expression of the scaled variable $W(n)$ (Eq. 10) now reads

$$W(n) = \mathrm{H}(N_c - n - 1) + \mathrm{H}(n + 1 - N_c)\left[W_c^{\mathrm{fit}} + \left(1 - W_c^{\mathrm{fit}}\right)\exp\left(-\frac{\lambda^{\mathrm{fit}}}{2}n\right)\right], \quad (13)$$

where H denotes a Heaviside function taking the value 1 for a positive argument and 0 otherwise, and N_c the critical number of pulses needed before entrance in the SR. This means that the fitted curve will be constant up until N_c, and then decay exponentially after $n = N_c$. We have denoted the critical value of W_c given by the fit as W_c^{fit} and the effective value of λ estimated from fitting is denoted by λ^{fit}. In terms of our theory, we expect the average value of W_c^{fit} to be concentrated at W_c with fluctuations around this value. All fits were performed with the formula given by Eq. 13, so we obtained values of N_c, W_c^{fit}, and λ^{fit} for each of the 51 DOPC data sets. With assumptions described above, the random variable N_c should follow a geometric (discrete and memory-less) distribution. We checked this by plotting the normalized histogram of N_c, and as Fig. 1 shows, the values of N_c are well fitted by a geometric distribution of the form

$$\mathrm{Probability}(N_c = n) = q(1-q)^{n-1}. \quad (14)$$

The shown fit yields the value $q = 0.33$, which means that N_c has the average value $\langle N_c \rangle = 1/q = 3$. In Fig. 2, we present four examples of data sets (*crosses*) and associated fits (*full lines*). Diamond marks correspond to the images shown later in Figs. 5 and 6 depicting the different mechanisms of lipid loss (see details below). Except for liposome C that immediately starts to shrink, we can clearly identify the PRs, the SRs, and the stabilization of sizes. Detailed information about pulse spacing for data from Fig. 2, which is not constant over a whole experiment because of the lateral motion of the vesicles, can be found in Table S1 in the Supporting Material.

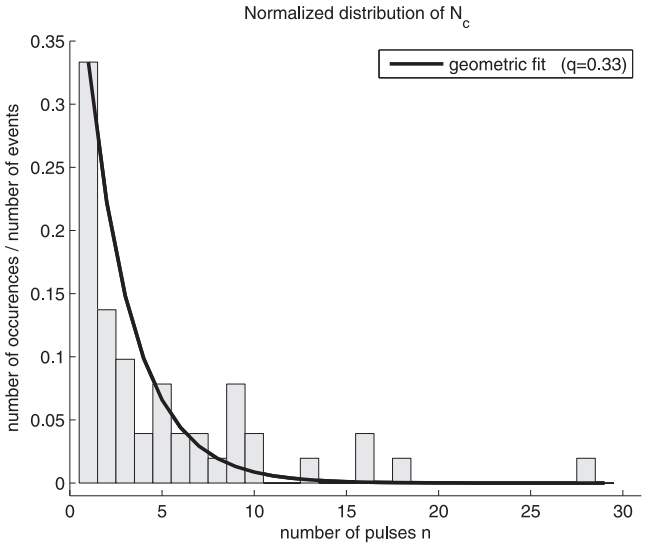

FIGURE 1 Normalized distribution of the values of N_c obtained after fitting of experimental data for DOPC vesicles. Solid line is a fit to a geometric distribution of the form given in Eq. 14, yielding the value $q = 0.33$.

Quantitative analysis—DOPC

As a first step in our data analysis, we can take the average of all the experimental curves and then carry out a fit; this yields the values $\lambda = 0.16$ and $W_c = 0.65$. The fit also yields the number of pulses necessary to put the liposome in the active state, where lipid loss can be induced, to be $N_c = 1.73$. The experimental data was also examined to see whether there was any correlation between the fitted value of W_c and λ with the initial vesicle radius $R(0)$. No appreciable correlation was seen, thus validating our hypothesis that the vesicle shrinkage can be well described in terms of the rescaled (dimensionless) quantity $W(n)$. A second way to estimate the parameters of the model is to fit λ and W_c for each curve individually to obtain $\langle \lambda^{fit} \rangle$, $\langle W_c^{fit} \rangle$, and $\langle N_c \rangle$, with the average value of the fitting parameters averaged over the individual experiments. The values obtained were $\langle \lambda^{fit} \rangle = 0.25$, $\langle W_c^{fit} \rangle = 0.58$, and $\langle N_c \rangle = 4.99$. This value of $\langle N_c \rangle$ agrees well with that of 3, estimated by the geometric distribution fit to the histogram of the fitted values for N_c.

Figs. 3 and 4 show the histograms of λ^{fit} and W_c^{fit}, respectively. As mentioned in the section called Theory, in fitting the data with our simple model we should expect to see variation in the values of λ and W_c obtained due to fluctuations of the surface tension (both initial and during the permeabilization process), local electric field, and possibly the effective number of defects created after the N_c pulses needed to enter into the permeabilized state. We note that it has been demonstrated in the literature (21,22) that the critical potential necessary to induce permeabilization is indeed dependent on the surface tension.

Quantitative analysis—EggPC

The experiments with EggPC were performed first and at that time, we had not yet made the considerations about the PR and the SR. We only kept data sets corresponding to immediately shrinking vesicles, therefore in this section $N_c = 1$ for each liposome. Despite this simplification, we did the same data processing as that described for DOPC. The fit on the average of all experimental curves yields the values $\lambda = 0.27$ and $W_c = 0.77$. The values of the fitting parameters averaged over the individual experiments are $\langle \lambda^{fit} \rangle = 0.31$ and $\langle W_c^{fit} \rangle = 0.69$.

About the anode-directed motion of the vesicles

The translational motion we observed was always directed toward the anode, suggesting that the GUVs could carry a net negative charge, even with a positively charged fluorescent dye. We checked this by measuring the ζ-potential of the vesicles in a medium with ionic composition equivalent to that of our pulsation medium, the sugar composition being different to avoid vesicle sedimentation making the measure impossible. We examined four different types of vesicles: EggPC alone, DOPC alone, DOPC labeled with Rhodamine PE, and DOPC labeled with $DiIC_{18}$. We did not use EggPC vesicles with a fluorescent dye, because our experiments

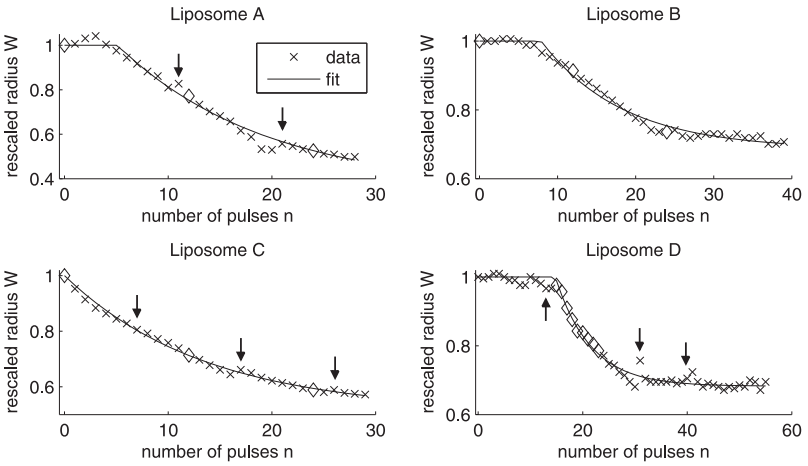

FIGURE 2 Examples of experimental data and corresponding fits for DOPC liposomes. (*Top left*) Liposome A; fit results are $N_c = 6$, $\lambda = 0.13$, and $W_c^{fit} = 0.35$. (*Top right*) Liposome B; fit results are $N_c = 9$, $\lambda = 0.19$, and $W_c^{fit} = 0.69$. (*Bottom left*) Liposome C; fit results are $N_c = 1$, $\lambda = 0.15$, and $W_c^{fit} = 0.51$. (*Bottom right*) Liposome D; fit results are $N_c = 16$, $\lambda = 0.30$, and $W_c^{fit} = 0.68$. Pulse magnitudes are 290, 360, 235, and 300 *V*/cm, respectively. Pulse duration is 5 ms. Arrows, if present, indicate data just before which we had to recenter the image on the liposome of interest. There is thus a time interval of $\approx$10 s before the indicated point, instead of 2 s as in all other cases.

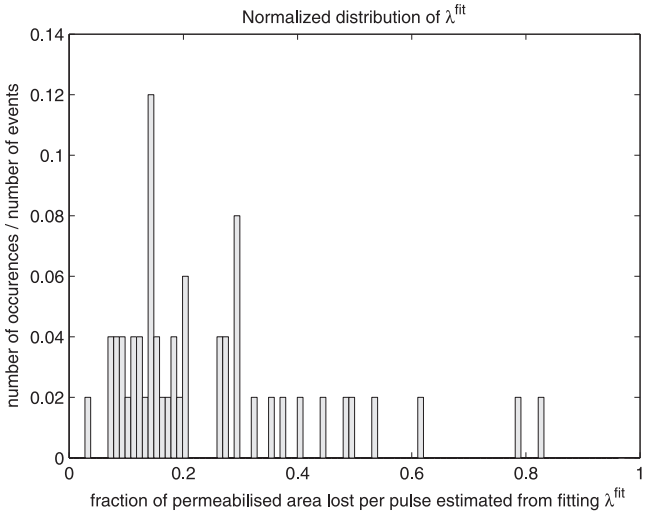

FIGURE 3 Distribution of the values of λ^{fit} obtained after data fitting for DOPC liposomes.

involving EggPC were performed via phase contrast microscopy, without any probe.

For all four vesicle compositions, we find an average ζ-potential of ~ -20 mV, a value in agreement with that found in Carvalho et al. (49) for DOPC GUVs, and whose sign is consistent with our observations. This corresponds to a negligible negative surface charge for the GUVs, <1 elementary charge per thousand of lipids. This residual electric charge possibly due to lipid impurities manifests itself only via the anode-directed motion of the vesicles, because of the large magnitude of the applied electric field.

About the initial pH asymmetry

Internal and external media of our GUVs were not at the same pH conditions (6.6 and 7.4, respectively). It was thus questionable whether this pH asymmetry had any significant influence in our experiments. The answer is no, based on the three following arguments. First, it is true that local pH gradients can induce the formation of tubular structures (50). However, such gradients have a magnitude of ~4 pH units, much higher than our 0.8 pH units. Second, as can be seen on our phase contrast images (data not shown), GUVs become permeabilized during pulsation, and experience a mixing of their internal and external media. Thus, the initial pH asymmetry should disappear after a few permeabilizing pulses. Third, the observation that the vesicles are stable and do not exhibit any shape changes until the electric field is applied corroborates the fact that the initial pH asymmetry of our GUVs has no significant effect.

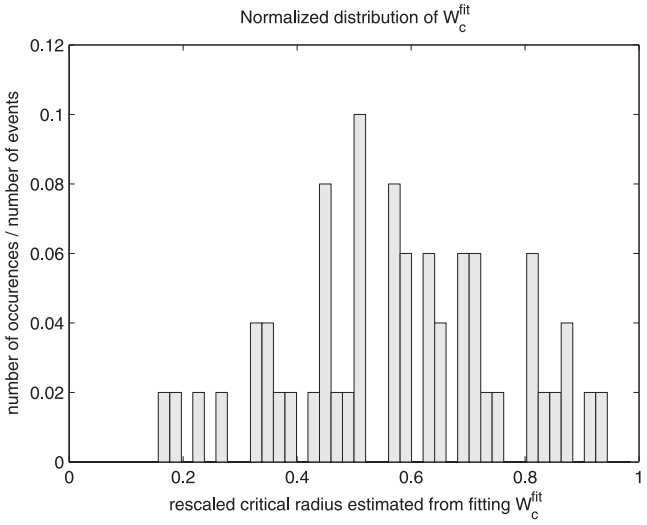

FIGURE 4 Distribution of the values of W_c^{fit} obtained after data fitting for DOPC liposomes.

Mechanisms of lipid loss

One of the most fascinating aspects of the experiments is the wide variety of mechanisms of lipid loss that can be observed. Three different mechanisms of lipid loss are observed when the lipids are fluorescently marked, as is the case on our experiments on DOPC liposomes (these observed mechanisms do not show any appreciable dependence on the probe employed). (We emphasize here that the term ''lipid loss'' implies loss of lipid from the bulk spherical part of the vesicle; the lipid ejected appears, in most cases, to remain attached to or close to the parent vesicle.)

The three basic mechanisms are shown in Figs. 5 and 6. Images were taken with the confocal microscope.

The first and most frequent mechanism is the formation of small vesicles at both the anode-and cathode-facing poles. Those vesicles are mainly thrown out of the GUVs, but some of them were also driven inside the GUVs. Liposomes A and C of Fig. 5 lost their lipids in such a manner (Movie S1 in the Supporting Material shows that mechanism for another GUV). Interestingly, a similar phenomenon has been reported when high-frequency alternating electric fields are applied to sea urchin eggs (51)—firstly, the cell is deformed and elongated by the field; and secondly, this cell splits into two smaller cells and a number of much smaller vesicles.

The second phenomenon we could observe (see photographs for liposome B in Fig. 5) was the creation of lipid tubules on the exterior of the anode-facing hemisphere (Movie S2 shows that mechanism for liposome B). DOPC molecules expelled from the membrane rearranged in the form of tubular structures, whose lengths grew with the number of applied pulses. These structures initiated from the pole facing the positive electrode and remained attached to the vesicle. However, they then appeared to diffuse away from the pole toward the equator (while remaining attached to the membrane) and appeared to cover most of the anode-facing hemisphere, as shown in Fig. 5. We also saw on the cathode-facing side of Fig. 6 that tubules can grow on the interior surface of the liposome. These structures also diffuse toward the equatorial regions, the number and size of tubules,

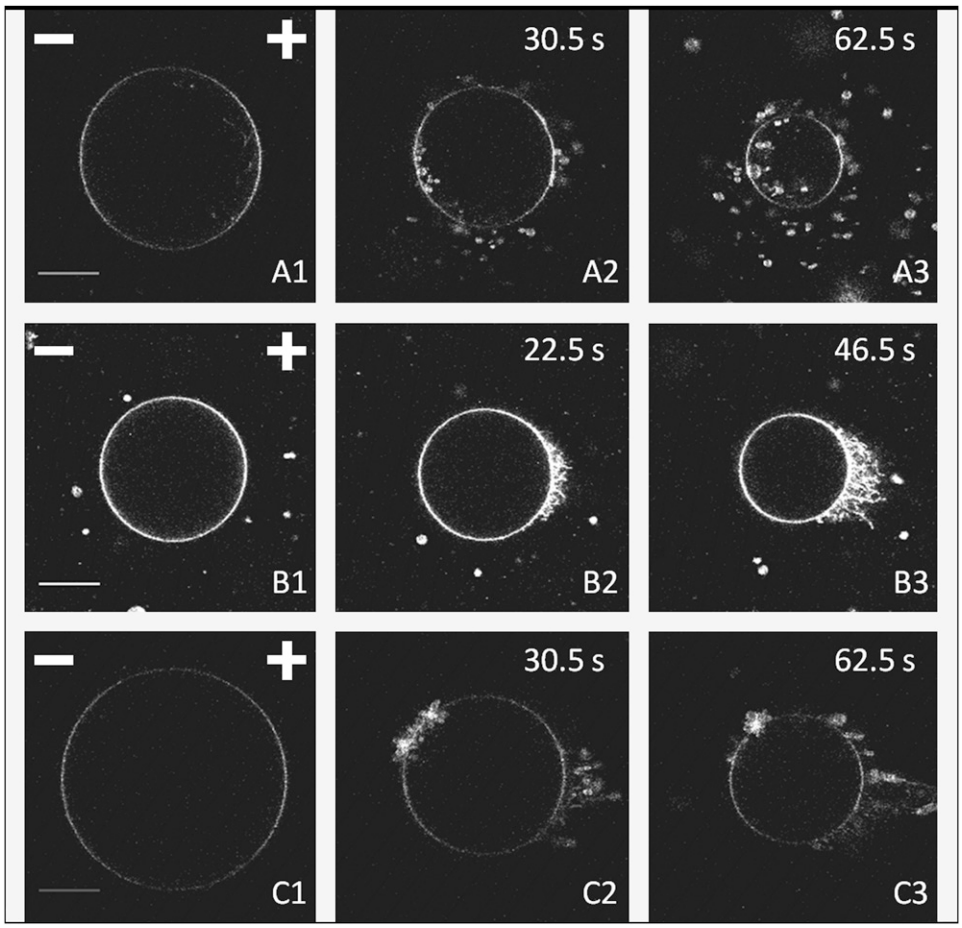

FIGURE 5 Images of liposomes A, B, and C, composed of DOPC and labeled with Rhodamine PE, at times indicated by the diamonds in Fig. 2, corresponding to 0, 12, and 24 applied pulses. Liposomes A and C lose lipids by formation of vesicles, and liposome B by formation of tubules. Scalebars (20-μm length) and positions of the electrodes appear in the first photograph of each vesicle. Pulse magnitudes are 290, 360, and 235 V/cm, respectively. Pulse duration is 5 ms. Times in upper-right corners indicate when images were acquired, the time origin being the onset of the first pulse. No time indication means that the picture was taken before the first pulse.

however, being smaller. This mechanism of tubule formation appears to be stronger on the anode-facing hemisphere.

Finally, we also noticed the presence of pores on the cathode-facing hemisphere (as did (42)). This was a quite rare observation, but it is normal because our acquisition times were of a few hundreds of milliseconds, the same order of magnitude as the lifetimes of such pores (42). Liposome D, which has entered the SR after 16 pulses, is found to have pores after 16 and 18 pulses, as shown by images D2 and D4 of Fig. 6. On the next images, we can see the beginning of the formation of the tubular structures described previously. We thus conclude that those two mechanisms could occur together for a same vesicle. The fact that we detected only a few GUVs exhibiting pore formation is certainly due to the too-low acquisition speed of our experimental setup. Recently, it has been shown that pore formation can be induced in vesicles by solubilizing the membrane (52), and that this process of pore formation is also associated with membrane loss and thus, vesicle shrinkage. An animation of the shrinkage of liposome D associated with pores and tubules formation is available in Movie S3.

The eventual long-term evolution of the structures described above (after pulsation has been stopped) varied from one experiment to another. The small vesicles, in most cases, diffused away from the liposome and the vesicle radius stayed constant. However, the behavior of the tubular structures exhibited wide variation. Some of the tubules broke away from the GUV and diffused away, sometimes forming vesicles and sometimes not. Other tubules remained attached to the vesicles, exhibiting polymerlike fluctuations. In some cases, they were reabsorbed into the GUV membrane after a time of approximately minutes. In fact, the eventual fate of tubules was strongly dependent on their environment, notably on whether other vesicles came in contact with them or not. In the cases where tubules were reabsorbed, the volume of the vesicle they were attached to increased, and the final state of the vesicle was often nonspherical, and appeared to be under little tension (in agreement with the idea that the attached lipids act as reservoir of lipid for the main vesicle).

DISCUSSION

Giant liposomes subjected to pulsed DC electric fields diminish in size and lose lipids via several observable mechanisms—vesicle ejection, tubule formation, and pore formation. This is quite different to what is observed in living cells, which tend to swell under electroporation (53–56). The experiments, along with the associated model, provide us

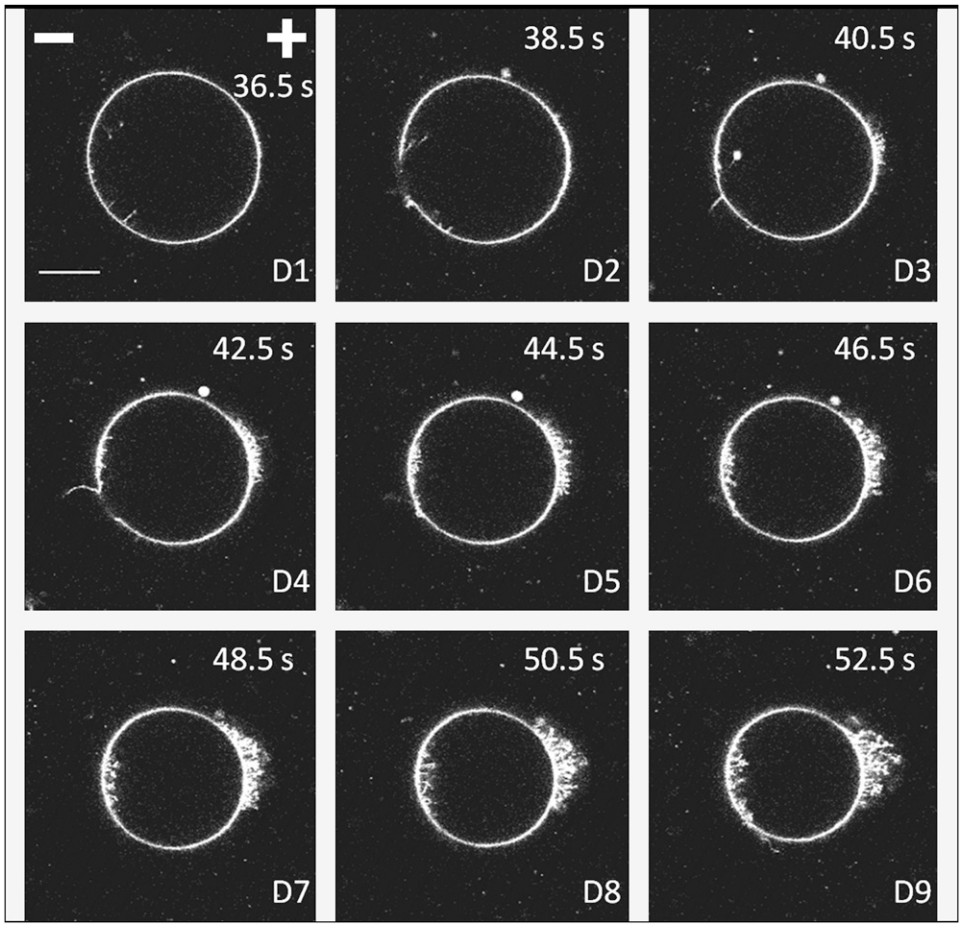

FIGURE 6 Images of liposome D, composed of DOPC and labeled with Rhodamine PE, at times indicated by the diamonds in Fig. 2. Image D1 is acquired after 15 pulses, D2 after 16 pulses, D3 after 17 pulses, etc. We can see pores on pictures D2 and D4 on the cathode-facing hemisphere. Scalebar (20 μm length) and position of the electrodes appear in the first photograph. Pulse magnitude and duration are 300 V/cm and 5 ms. Times in upper-right corners indicate when images were acquired, the time origin being the onset of the first pulse.

with the following picture of lipid loss due to applied pulses. The lipid loss proceeds by a two-stage process. First, if the applied field is high enough, a membrane passes from an inactive state where it has no induced defects to one where defects are present. We have seen that this process is of an exponential character reminiscent of radioactive decay. Secondly, for DOPC composed vesicles, once defects are present the membrane loss per pulse is $\sim\lambda \approx 0.20$ of the area in which the transmembrane potential exceeds the critical value, denoted here by $\Delta\Psi_c$. From our estimate $W_c = 0.65$ obtained by fitting the average of all curves, we find that, on average, $\Delta\Psi_c = W_c \times \Delta\Psi_0 = 0.65 \times 1.3$ V ≈ 0.85 V. If we use the average value of $\langle W_c^{fit} \rangle$ obtained by fitting the individual curves, we obtain $\Delta\Psi_c \approx 0.75$ V.

These values of $\Delta\Psi_c$ are to be compared with those reported for certain cell membranes $\Delta\Psi_c \approx 1$ V (3,47) and tension free vesicles (1-stearoyl-2-oleoyl phosphatidylcholine and dioleoyl phosphatidyglycerol) (26), where $\Delta\Psi_c \approx 1.1$ V. Similar results apply for EggPC but in this case, $\lambda \approx 0.29$ and there is thus, with comparison to DOPC, more lipid loss per unit area of where the critical transmembrane potential is exceeded. The estimated value of W_c obtained by fitting the average of all curves is 0.77, which gives a critical transmembrane voltage of 1 V. The estimate from the average values obtained over individual fits yields a value of 0.69 for W_c, thus leading to a critical transmembrane voltage $\Delta\Psi_c \approx 0.89$ V.

Recently numerical simulations have provided much insight into the membrane organization occurring during the membrane permeabilization process (35–41). The picture emerging is one where the strong electric field present in the membrane causes water molecules (via their dipole interaction with the applied field) to penetrate into the membrane. There is an initial formation of so-called hydrophobic pores because the water molecules are in proximity to the hydrophobic core of the membrane. Subsequently, the lipid head dipoles reorient to form hydrophilic pores where the lipid heads line the inside of the pore. The mechanism behind this reorientation involves hydrophobic effects and electrostatic effects. For example, dipole moments that are oriented normal to the membrane surface (which is roughly the case for DOPC) are favorably aligned on one side of the membrane but not on the other. This means that, on the side where they are well oriented, the field keeps them straight toward the normal. However, on the side where they are maloriented, they can lower their energy by turning in toward the core of the membrane. This tendency to turn inside the membrane lowers their electrostatic energy and

aids the formation of hydrophilic pores. The same effect is clearly present before water penetration into the bilayer core, and helps to form defects that favor penetration by water molecules. This explains why formation appears to be initiated from a particular membrane side in electrically neutral membranes. However, in numerical simulations, lipid loss from the membrane is not generally observed during pore formation and pore resealing. This could be because the timescales over which the simulations are carried out are too short. Indeed, it is difficult to see, if we accept the above image of the pore formation mechanism, how lipid loss to the extent observed in our experiments can be explained by such processes. The main differences between the experiments here and numerical simulations is that the system here is much larger and that the pores formed are an order-of-magnitude larger than those seen in simulations (which can be interpreted as prepores). We have seen that vesicle formation seems to make a major contribution to the observed lipid loss, and there is presumably a minimal size that a vesicle can have (for thermodynamic and mechanical reasons); thus, if the simulated system contains less lipids than required to build a vesicle of minimal size, then lipid loss by vesiculization cannot be observed. Another possible mechanism for lipid loss is that lipid headgroup dipoles, which are maloriented, instead of turning into the membrane to be better oriented, are simply expelled from the membrane. This expulsion will increase the free energy of the lipid due to hydrophobic interactions but lower the electrostatic energy. The hydrophobic component of the free energy increase could be lowered by the formation of small vesicles into which these expelled lipids could be incorporated. We recall that, in smaller vesicles, the electrostatic energy of maloriented lipid headgroup dipoles is much smaller due to the scaling with R, the vesicle radius, of the potential drop across the membrane. The idea that single lipids can be extracted due to the field turns out to be unrealistic. The dipole moment p of the PC headgroup is ~20 Debye (see (57) and references therein), which means that the maximal electrostatic energy of a maloriented dipole is $\sim E_{\mathrm{D}} \approx p(\Delta\Psi/a)$, where $\Delta\Psi$ is the potential drop across the membrane. However, the hydrophobic energy of a lipid tail placed in water is given by $E_{\mathrm{hydro}} \approx 2\pi\rho l\mu$, where l is the total length of the hydrocarbon chain and ρ is its effective radius (viewed as a cylinder). Clearly, the tail length is approximately related to the membrane thickness by $l \approx a/2$. The term μ is a hydrophobic free energy per unit of area and takes a value of ~40 mJ/m^2 (58). The effective cylindrical radius of the lipid hydrocarbon tail is estimated at 0.8 nm (there is, of course, really two tails each of radius ~0.4 nm (58)). Equating these two energies yields a critical transmembrane potential beyond which lipids can be torn out directly by the field as

$$\Delta\Psi^* \approx \frac{\pi a^2 \rho\mu}{p} \approx 24\ V. \tag{15}$$

This value of $\Delta\Psi^*$ is to be compared with the value given typically for the critical potential drop across the membrane necessary to achieve permeabilization which, as previously mentioned, is ~200 mV for a wide range of membrane types. In addition, the electric field seen by the lipid heads is only the amplified one if we assume that the head region is of low conductivity, having a value close to that cited for the total membrane conductivity. We thus conclude that, for permeabilization seen in the range of voltages of our experiments, a simple mechanism of tearing out lipids is unlikely to occur (although this mechanism could conceivably play a role when high intensity short pulses are applied). The conclusion of the above estimation is that lipids must be ejected together in structures that minimize their hydrophobic energy such as micelles, tubules, and vesicles, as is indeed seen in our experimental results.

There is a clear asymmetry in our observations of lipid loss, in agreement with the observations of Tekle et al. (42); when we observed pore formation, it was on the cathode-facing side of the liposome. However, the anode-facing side was the one where the formation of tubules was favored. The mechanism of symmetry breaking could well be related to the anisotropic dielectric structure of the membrane due to the behavior of its lipid components.

Another interesting feature of our results is that the vesicle does not always lose lipid material from the first pulse onwards. This implies that the vesicle needs to be in a particular state (induced by the field with some probability) to enter into the shrinking regime (SR). The difference between the SR and preshrinking regime is unclear, but one could speculate that, in the SR, the membrane has defects that facilitate the loss of lipids. The number and nature of defects created at the inception of the SR is presumably stochastic in nature and could be responsible for the variations in the parameter λ seen in our experiments. The continued application of pulses then leads to a number of visible modes of membrane loss, vesicle formation, tubule formation, and pore formation. In the context of applied DC pulses, only pore formation had been previously reported (42). Vesicle formation due to alternating fields has been reported (51), but the underlying physics appears quite different, as, in the presence of AC fields, the formation of small vesicles occurs via the fission of the initial cell into two similar-sized daughter cells. Perhaps the most striking phenomenon is that of tubule formation, which leads to a hairlike structure of tubules around the liposome. Thus repeated application of short DC pulses leads to the shrinkage of artificial vesicles and a rich phenomenology of lipid structure formation. As a final comment, the phenomenon of lipid loss observed here seems to support aspects of the phase transition model of electropermeabilization (59). In this model, the electric field can induce a transition from a state where the bilayer is thermodynamically stable to one where smaller units, for example micelles, are thermodynamically preferred. The fact that the lipid loss process is not always immediately

initiated when $N_c \neq 1$, supports the first-order nature of the transition.

SUPPORTING MATERIAL

One table and three movies are available at http://www.biophysj.org/biophysj/supplemental/S0006-3495(09)00660-2.

We thank Emilie Phez and Justin Teissié for useful discussions on this work. We also thank Émile Perez and Plamen Kirilov from the Laboratoire des Intéractions Moléculaires et Reactivité Chimique et Photochimiique in Toulouse for allowing us to use their facilities to measure the ζ-potentials of our vesicles. Our group belongs to the Centre National de la Recherche Scientifique consortium CellTiss.

We acknowledge financial support from the Association Française contre les Myopathies, the Institut Universitaire de France, and the contracts ANR Cemirbio and DGA REI2 (0624034).

REFERENCES

1. Neumann, E., A. E. Sowers, and C. A. Jordan. 1989. Electroporation and Electrofusion in Cell Biology. Plenum Press, New York.
2. Weaver, J. C. 1995. Electroporation theory. Concepts and mechanisms. *Methods Mol. Biol.* 55:3–28.
3. Weaver, J. C., and Y. A. Chizmadzhev. 1996. Theory of electroporation: a review. *Bioelectrochem. Bioenerg.* 41:135–160.
4. Teissié, J., M. Golzio, and M.-P. Rols. 2005. Mechanisms of cell membrane electropermeabilization: a minireview of our present (lack of?) knowledge. *Biochim. Biophys. Acta.* 1724:270–280.
5. Escoffre, J.-M., D. S. Dean, M. Hubert, M.-P. Rols, and C. Favard. 2007. Membrane perturbation by an external electric field: a mechanism to permit molecular uptake. *Eur. Biophys. J.* 36:973–983.
6. Favard, C., D. S. Dean, and M.-P. Rols. 2007. Electrotransfer as a nonviral method of gene delivery. *Curr. Gene Ther.* 7:67–77.
7. Dimova, R., K. A. Riske, S. Aranda, N. Bezlyepkina, R. L. Knorr, et al. 2007. Giant vesicles in electric fields. *Soft Matter.* 3:817–827.
8. Neumann, E., and K. Rosenheck. 1972. Permeability changes induced by electric impulses in vesicular membranes. *J. Membr. Biol.* 10:279–290.
9. Rols, M.-P. 2006. Electropermeabilization, a physical method for the delivery of therapeutic molecules into cells. *Biochim. Biophys. Acta.* 1758:423–428.
10. Robello, M., and A. Gliozzi. 1989. Conductance transition induced by an electric field in lipid bilayers. *Biochim. Biophys. Acta.* 982:173–176.
11. Rols, M.-P., and J. Teissié. 1998. Electropermeabilization of mammalian cells to macromolecules: control by pulse duration. *Biophys. J.* 75:1415–1423.
12. Golzio, M., J. Teissié, and M.-P. Rols. 2002. Direct visualization at the single-cell level of electrically mediated gene delivery. *Proc. Natl. Acad. Sci. USA.* 99:1292–1297.
13. Antov, Y., A. Barbul, H. Mantsur, and R. Korenstein. 2005. Exposure of cells to pulsed low electric fields enhances adsorption and uptake of macromolecules. *Biophys. J.* 88:2206–2223.
14. Belehradek, M., C. Domenge, B. Luboinski, S. Orlowski, J. Belehradek, Jr, et al. 1993. Electrochemotherapy, a new antitumor treatment. First clinical phase I–II trial. *Cancer.* 72:3694–3700.
15. Gehl, J., T. Sorensen, K. Nielsen, P. Raskmark, S. Nielsen, et al. 1999. In vivo electroporation of skeletal muscle: threshold, efficacy and relation to electric field distribution. *Biochim. Biophys. Acta.* 1428: 233–240.
16. Sersa, G., D. Miklavcic, M. Cemazar, Z. Rudolf, G. Pucihar, et al. 2008. Electrochemotherapy in treatment of tumors. *Eur. J. Surg. Oncol.* 34:232–240.
17. Gilbert, R., M. Jaroszeski, and R. Heller. 1997. Novel electrode designs for electrochemotherapy. *Biochim. Biophys. Acta.* 1334:9–14.
18. Gothelf, A., L. Mir, and J. Gehl. 2003. Electrochemotherapy: results of cancer treatment using enhanced delivery of bleomycin by electroporation. *Cancer Treat. Rev.* 29:371–387.
19. Winterhalter, M., and W. Helfrich. 1988. Deformation of spherical vesicles by electric fields. *J. Colloid Interface Sci.* 122:583–586.
20. Kummrow, M., and W. Helfrich. 1991. Deformation of giant lipid vesicles by electric fields. *Phys. Rev. A.* 44:8356–8360.
21. Riske, K. A., and R. Dimova. 2005. Electro-deformation and poration of giant vesicles viewed with high temporal resolution. *Biophys. J.* 88: 1143–1155.
22. Riske, K. A., and R. Dimova. 2006. Electric pulses induce cylindrical deformations on giant vesicles in salt solutions. *Biophys. J.* 91:1778–1786.
23. Crowley, J. 1973. Electrical breakdown of bimolecular lipid membranes as an electromechanical instability. *Biophys. J.* 13:711–724.
24. Abidor, I., V. Arakelyan, L. Chernomordik, Y. A. Chizmadzhev, V. Pastushenko, et al. 1979. Electric breakdown of bilayer membranes I: The main experimental facts and their qualitative description. *Bioelectrochem. Bioenerg.* 6:37–52.
25. Pastushenko, V., Y. Chizmadzhev, and V. Arekelyan. 1979. Electric breakdown of bilayer membranes II. Calculation of the membrane lifetime in the steady-state diffusion approximation. *Bioelectrochem. Bioenerg.* 6:53–62.
26. Needham, D., and R. M. Hochmuth. 1989. Electro-mechanical permeabilization of lipid vesicles—role of membrane tension and compressibility. *Biophys. J.* 55:1001–1009.
27. Isambert, H. 1998. Understanding the electroporation of cells and artificial bilayer membranes. *Phys. Rev. Lett.* 80:3404–3407.
28. Sens, P., and H. Isambert. 2002. Undulation instability of lipid membranes under an electric field. *Phys. Rev. Lett.* 88:128102–128105.
29. Powell, K., and J. Weaver. 1986. Transient aqueous pores in bilayer membranes: a statistical theory. *Bioelectrochem. Bioenerg.* 15:211–227.
30. Glaser, R., S. Leikin, L. Chernomordik, V. Pastushenko, and A. Sokirko. 1988. Reversible electrical breakdown of lipid bilayers and formation and evolution of pores. *Biochim. Biophys. Acta.* 940:272–287.
31. Barnett, A., and J. C. Weaver. 1991. Electroporation: a unified, quantitative theory of reversible electrical breakdown and mechanical rupture in artificial planar bilayer membranes. *Bioelectrochem. Bioenerg.* 25: 163–182.
32. Neu, J., and W. Krassowska. 2003. Modeling postshock evolution of large electropores. *Phys. Rev. E Stat. Nonlin. Soft Matter Phys.* 67: 021915–021926.
33. Neu, J., K. Smith, and W. Krassowska. 2003. Electrical energy required to form large conducting pores. *Bioelectrochem. Bioenerg.* 60:107–114.
34. Derjaguin, B., and Y. Gutop. 1961. Theory of the breakdown (rupture) of free films. *Kolloidn Zh.* 24:370–374.
35. Tieleman, D. P. 2004. The molecular basis of electroporation. *BMC Biochem.* 5:10.
36. Leontiadou, H., A. Mark, and S. Marrink. 2004. Molecular dynamics simulations of hydrophilic pores in lipid bilayers. *Biophys. J.* 86:2156–2164.
37. Tarek, M. 2005. Membrane electroporation: a molecular dynamics simulation. *Biophys. J.* 88:4015–4053.
38. Hu, Q., R. P. Joshi, and K. H. Schoenbach. 2005. Simulations of nanopore formation and phosphatidylserine externalization in lipid membrane subjected to high intensity, ultra-short electric pulse. *Phys. Rev. E Stat. Nonlin. Soft Matter Phys.* 72:031902.
39. Hu, Q., S. Viswanadham, R. P. Joshi, K. H. Schoenbach, S. J. Beebe, et al. 2005. Simulations of transient membrane behavior in cells subjected to a high intensity, ultra-short electric pulse. *Phys. Rev. E Stat. Nonlin. Soft Matter Phys.* 71:031914.
40. Tieleman, D. P. 2006. Computer simulations of transport through membranes: passive diffusion, pores, channels and transporters. *Clin. Exp. Pharm. Phys.* 33:893–903.

41. Wohlert, J., W. den Otter, O. Edholm, and W. J. Briels. 2006. Free energy of a trans-membrane pore calculated from atomist molecular dynamics simulations. *J. Chem. Phys.* 124:154905–154914.

42. Tekle, E., R. D. Astumian, W. A. Friauf, and P. B. Chock. 2001. Asymmetric pore distribution and loss of membrane lipid in electroporated DOPC vesicles. *Biophys. J.* 81:960–968.

43. Angelova, M. I., and D. S. Dimitrov. 1986. Liposome electroformation. *Faraday Discuss. Chem. Soc.* 81:303–311.

44. Rodriguez, N., F. Pincet, and S. Cribier. 2005. Giant vesicles formed by gentle hydration and electroformation: a comparison by fluorescence microscopy. *Colloids Surf. B.* 42:125–130.

45. Teissié, J., and M.-P. Rols. 1993. An experimental evaluation of the critical potential difference inducing cell membrane electropermeabilization. *Biophys. J.* 65:409–413.

46. Gabriel, B., and J. Teissié. 1997. Direct observation in the millisecond time range of fluorescent molecule asymmetrical interaction with the electropermeabilized cell membrane. *Biophys. J.* 73:2630–2637.

47. Tsong, T. Y. 1991. Electroporation of cell membranes. *Biophys. J.* 60: 297–306.

48. Pavlin, M., N. Pavselj, and D. Miklavcic. 2002. Dependence of induced transmembrane potential on cell density, arrangement, and cell position inside a cell system. *IEEE Trans. Biomed. Eng.* 49:605–612.

49. Carvalho, K., L. Ramos, C. Roy, and C. Picart. 2008. Giant unilamellar vesicles containing phosphatidylinositol(4,5)biphosphate: characterization and functionality. *Biophys. J.* In press.

50. Khalifat, N., N. Puff, S. Bonneau, J.-B. Fournier, and M. Angelova. 2008. Membrane deformation under local pH gradient: mimicking mitochondrial crystal dynamics. *Biophys. J.* In press.

51. Marszalek, P., and T. Tsong. 1995. Cell fission and formation of mini cell bodies by high frequency alternating electric field. *Biophys. J.* 68:1218–1221.

52. Rodriguez, N., S. Cribier, and F. Pincet. 2006. Transition from long- to short-lived transient pores in giant vesicles in an aqueous medium. *Phys. Rev. E.* 74, 061902.1–10.

53. Kinosita, K., and T. Tsong. 1977. Formation and resealing of pores of controlled sizes in human erythrocyte membrane. *Nature.* 268:438–441.

54. Abidor, I., A. Barbul, D. Zhelev, P. Doinov, I. Bandrina, et al. 1993. Electrical properties of cell pellets and cell electrofusion in a centrifuge. *Biochim. Biophys. Acta.* 1152:207–218.

55. Abidor, I., L. Li, and S. Hui. 1994. Studies of cell pellets: II. Osmotic properties, electroporation, and related phenomena: membrane interactions. *Biophys. J.* 67:427–435.

56. Golzio, M., M. Mora, C. Raynaud, C. Delteil, J. Teissié, et al. 1998. Control by osmotic pressure of voltage-induced permeabilization and gene transfer in mammalian cells. *Biophys. J.* 74:3015–3022.

57. Pasenkiewicz-Gierula, M., Y. Takaoka, H. Miyagawa, K. Kitamura, and A. Kusumi. 1999. Charge pairing of headgroups in phosphatidylcholine membranes: a molecular dynamics simulation study. *Biophys. J.* 76: 1228–1240.

58. Israelachvili, J. 2000. Intermolecular and Surface Forces, 2nd Ed. Academic Press, San Diego, CA.

59. Sugàr, I. P. 1979. A theory of the electric field-induced phase transition of phospholipid bilayers. *Biochim. Biophys. Acta.* 556:72–85.

PARTIE II

ÉLECTROTRANSFERT DE PLASMIDES

Partie II. Electrotransfert de plasmides

1. In vitro

Escoffre JM, Teissie J, and Rols MP (2010) Gene transfer: How can the biological barriers be overcome? J. Membr. Biol., (Submitted Review).

Faurie C, Rebersek M, Golzio M, Kanduser M, **Escoffre JM,** Pavlin M, Phez E, Teissie J, Miklavcic D, and Rols MP (2010) Time-dependence of DNA/membrane complex formation in electrically mediated gene transfer. J. Gene Med., 12:117-125 (Article).

Wasungu L, **Escoffre JM,** Valette A, Teissie J, and Rols MP (2009) Use of a 3D in vitro spheroid model as a way to study the mechanisms of electroporation. Int. J. Pharm., 379:278-284 (Article).

Teissie J, **Escoffre JM,** Rols MP, Golzio M (2008) Time dependence of electric field affects on cell membranes. A review for a critical selection of pulse duration for therapeutic applications. Radiol. Oncol., 42:196-206 (Review).

GENE TRANSFER: HOW CAN THE BIOLOGICAL BARRIERS BE OVERCOME?

Journal:	*Journal of Membrane Biology*
Manuscript ID:	Draft
Manuscript Type:	Special Issue
Date Submitted by the Author:	
Complete List of Authors:	Escoffre, Jean-Michel; CNRS, IPBS Teissié, Justin; CNRS, IPBS Rols, Marie-Pierre; CNRS, IPBS UMR5089
Keywords:	membrane transport mechanisms, Membrane Structure, membrane biophysics, Electrical aspects/Membrane Structure

GENE TRANSFER: HOW CAN THE BIOLOGICAL BARRIERS BE OVERCOME?

Jean-Michel Escoffre[¶], Justin Teissié[¶], and Marie-Pierre Rols[¶*].

[¶]CNRS; IPBS (Institut de Pharmacologie et de Biologie Structurale); 205 route de Narbonne, F-31077, Toulouse, France; Université de Toulouse; UPS; IPBS; F-31077, Toulouse, France.

*Correspondence: Marie-Pierre Rols, CNRS; IPBS (Institut de Pharmacologie et de Biologie Structurale); 205 route de Narbonne, F-31077, Toulouse, France; Université de Toulouse; UPS; IPBS; F-31077, Toulouse, France. Tel +33561175811. Fax +33561175900. Email rols@ipbs.fr

Abstract

Physical methods represent a promising approach for the safe delivery of therapeutic plasmid DNA in genetic and acquired human diseases. However, their development in clinics is limited by their low efficacy. At the cellular level, efficient gene transfer is dependent on several factors including extracellular matrix, plasmid DNA uptake and the nucleocytoplasmic transport. This paper reviews the main barriers that plasmid DNA encounters from the extracellular environment towards the interior of cell and the different strategies developed to overcome these biological barriers. Diffusional and metabolic fences of the extracellular matrix and the cytoplasm affect plasmid DNA uptake. These barriers reduce the number of intact plasmids that reach the nucleus. Nuclear uptake of plasmid DNA further requires either an increase of nuclear permeability, or an active nuclear transport via the nuclear pore. A better understanding of the cellular and molecular basis of the physical gene transfer process may provide strategies to overcome those obstacles that highly limit the efficiency and the use of the gene delivery methods.

Keywords: Gene therapy, physical methods, extracellular matrix, plasma membrane, cytoplasm, nucleus.

Introduction

The clinical development of gene therapy requires the use of safe and efficient methods that deliver a therapeutic gene to target cells where gene expression can be achieved. A gene delivery method has to overcome several obstacles: (1) it should first protect the transgene against the degradation by the nucleases present in the intracellular matrix and ought to increase the transgene diffusion through the extracellular matrix (McMahon et al 2001; Bureau et al 2004; Mesojednilk et al 2007). (2) Then, it should bring the transgene across the plasma membrane of target cells (Stephens and Pepperkok 2001). (3) Next, it has to facilitate the intracellular migration of transgene until the nucleus and limit the transgene degradation by intracellular nucleases (Lukacs et al 2000). (4) Finally, delivery methods should bring the transgene across the nuclear envelope (Vaughan et al 2006) (Figure 1).

In general, recombinant viral vectors have been used preferentially in clinical trials due to their high gene delivery efficiency and their ability to induce high-level and long-lasting gene expression in various tissues (Gardlik et al 2005; Waehler et al 2007). The efficiency of these vectors lies in the infectious properties of virus that are controlled by viral proteins. Nevertheless, these same proteins could induce specific immune responses that would limit the ability to re-administer the viral vector and inhibit the efficiency of gene transfer (Lehrmann 1999; Marshall 1999). Moreover, retrovirus or lentivirus derived vectors could evoke insertional mutations during their integration into the host genome (Hacein-Bey-Abina et al 2003a, 2003b). In addition, previous works showed that recombination events could lead to the formation of replication competent viruses (Broeke and Burny 2003).

In contrast, plasmid DNA molecules are just covalent closed circles of double-stranded DNA with no associated proteins. Plasmid DNA molecules are simpler, easier to mass-produce and potentially safer than viral vectors (Wells et al., 2004). Low immunogenicity and lack of integration of plasmid DNA make it a highly attractive molecule for gene therapy provided that an efficient, safe and targeted delivery can be achieved (Wells et al., 2004).

In this review, we will describe the different barriers encounter by plasmid DNA during gene transfer and we propose various strategies to overcome these physico-chemical barriers. Then, we will discuss the mechanisms, the advantages and limitations of physical gene delivery approaches that are shown to be active for *ex vivo* and *in vivo* gene delivery.

1. Extracellular matrix

The space which surrounds the cells, called the extracellular space, contains a set of macromolecules, polysaccharides or glycosaminoglycanes, fibrous proteins, salts and water, known as the extracellular matrix (ECM) (Berrier and Yamada, 2007). The glycosaminoglycanes are negatively charged and are the hyaluronic acid, the chondroitin sulfate, the dermatan sulfate, the heparan, heparin and keratin. The main proteins of structure are collagen and the elastin as well as the proteins of adhesion, fibronectin and laminin (Berrier and Yamada, 2007 ; Kass et al., 2007). According to its composition, the extracellular matrix can take various aspects, liquid like interstitial liquid or the synovial liquid rich in polysaccharide, gelatinous as the tendons rich in fibrous proteins, solid like the bone rich in calcium phosphate (Berrier and Yamada, 2007). The basal membrane which separates epithelial tissue from conjonctive tissue constitutes a kind of ECM. The components of the ECM are synthesized and secreted by cells such as fibroblasts and chondroblastes and broken up by enzymes called matrix metalloproteinases (Stamenkovic, 2003 ; Berrier and Yamada, 2007).

To reach the plasma membrane of target cells, the plasmid DNA must diffuse through the ECM without being degraded by the extracellular nucleases (Bureau et al 2004). Compared to the small molecules, diffusion, distribution, degradation and uptake of plasmid DNA into cells have been investigated to a much smaller extent. Previous works showing that the delivery of macromolecules such as plasmid DNA to cells in target tissues such as skeletal muscles (Bureau et al., 2004), tumours (Netti et al., 2000 ; Pluen et al., 2001 ; Alexandrakis et al., 2004), skin (Vandermulen et al., 2007), and respiratory tissues (Walther et al., 2005), is affected by the amount of nucleases, which

degrade plasmid DNA, and by the amount of ECM components, such as collagen (Netti et al., 2000 ; Pluen et al., 2001) and hyaluronic acid (Alexandrakis et al., 2004). Consequently, in order to increase the efficiency of gene transfer, some strategies have been developed to increase the diffusion of plasmid DNA and to limit its degradation into the target tissues. The main strategy to increase the diffusion and distribution of plasmid DNA into the tissue consisted in controlled and partial degradation of ECM by using enzymes such as hyaluronidase and collagenase. This approach is efficient into skeletal muscle (Favre et al., 2000 ; MacMahon et al 2001 ; Mennuni et al., 2002 ; Molnar et al., 2004 ; Schertzer et al., 2006 ; Evans et al., 2008), liver (Dubensky et al 1984) and tumours (Kuriyama et al., 2001 ; Mesojednik et al 2007) but inefficient in skin (Vandermeulen et al., 2007). Indeed, some works showed that the pretreatment with hyaluronidase induced a 10- to 25-fold increase of gene expression in mice and rabbit skeletal muscle after i.m. injection and electroporation compared to without pretreatment (MacMahon et al 2001 ; Mennuni et al., 2002 ; Molnar et al., 2004 ; Schertzer et al., 2006). Dubensky and collaborators proposed to combine hyaluronidase with collagenase into liver and spleen by injecting calcium phosphate-precipitated plasmid DNA. Their results showed that these organs were more homogeneously transfected than without enzymatic treatment (Dubensky et al 1984).

To limit the degradation of plasmid DNA, the main approach was to protect the plasmid DNA by using chemical formulation or to inhibit the exogenous DNAses. Nicol and collaborators showed that plasmid DNA formulated with poly-L-glutamate induced a 4- to 12-fold increase of gene expression in skeletal muscle after i.m. injection and electroporation in comparison to saline injection alone (Nicol et al., 2002). Others works showed that the plasmid DNA formulated with poloxamers such as SP1017 increased gene expression by about 10-fold and maintained higher gene expression into skeletal muscle after i.m. injection compared with naked DNA (Riera et al., 2004). These data suggested that chemical formulation might enhance plasmid DNA uptake by protecting the plasmid DNA to degradation by nucleases (Lemieux et al., 2000). The second approach consisted in the use of nuclease

inhibitors such as aurintricarboxylic acid (ATA) (Walther et al., 2005). Previous works showed that the in vitro and in vivo co-administration of ATA with the naked plasmid DNA was able to improve transfer efficiencies in respiratory tissues and skin of mice, pigs and macaques (Glasspool-Malone et al., 1999, 2000, 2002). For example, Walther and collaborators demonstrated that jet-injection of plasmid containing ATA led to a 3-fold increase in gene expression into human colon tumours compared to jet-injection without ATA (Walther et al., 2005).

2. Plasma membrane

The cell membrane is a physical barrier that separates the intracellular components from the extracellular environment. It contains two main classes of molecules, proteins and lipids. Cell membrane hinders the free diffusion of plasmid DNA between cell cytoplasm and external medium (Stephens and Pepperkok, 2001).

Direct injection of naked plasmid DNA into a tissue is a simple and safe method available to achieve gene delivery and expression. Previous works suggested that the mechanism involved in the gene transfer could be based on the interaction between plasmid DNA and specific or non-specific receptors on the plasma membrane and their internalization into the target cells (Budker et al 2000).

The proof of concept has been reported by Wolff and collaborators that obtained gene expression into mouse muscle for sixty days (Wolff et al 1990). Local injection of plasmid DNA has also been shown to facilitate gene delivery into tumour xenografts (Kawase et al 2003), liver (Andre et al 2006), brain (Schwartz et al 1996), skin (Choate et al 1996), heart (Ardehali et al 1995), thyroid (Sikes et al 1994) and tendons (Jayankura et al 2003).

The main limitations of this delivery method are low-levels of transgene expression, inter-individual heterogeneities and its limited distribution. These limitations could reflect the low diffusion and the degradation of plasmid DNA in the extracellular matrix and in the cytoplasm of cells. In order to improve the efficiency of plasmid DNA delivery, physical methods have been developed

(Stephens and Pepperkok, 2001). The general principle of physical methods is based on the transient disruption of cell membrane in order to facilitate DNA uptake (Table 1).

2.1. Electroporation

The application of controlled electric field pulses induces the transient and localized cell membrane permeabilization (Neumann and Rosenheck, 1972; Escoffre et al 2007), a process that can be used for the enhancement of gene uptake into cells of naked plasmid DNA (Neumann et al 1982; Golzio et al 2005 ; Escoffre et al., 2009). The transfection efficiency depends on electric field parameters such as number (up to 10), duration (~ ms) and strength (~ V/cm) of electric pulses. These parameters are controlled and can be adjusted according to cells and tissues (Golzio et al 2005). Theoretical models have been proposed to explain the mechanism of this reversible membrane electropermeabilization and its potentiality to allow the access of non-permeant molecules inside the cells. Nevertheless, the molecular definition of the transient permeable structures is not yet known (Teissie et al 2005). Indeed, two hypotheses are defended: the first hypothesis suggests that plasmid DNA moves through large and hydrophilic pores without interaction between plasmid DNA and plasma membrane. The size of these pores was estimated at between 1 and 10 nm. Plasmid DNA access directly into the cytosol (Krassowka et al 2007 ; Smith KC et al 2004 ; Tieleman et al 2004 ; Neumann et al 1982). The second hypothesis proposes a plasmid DNA/plasma membrane interaction (Golzio et al 2002; Sukharev et al 1992; Tarek 2005). This interaction is the result of electrophoretic accumulation of plasmid DNA with permeabilized membrane.. Membrane translocation and intracellular migration occur after the electric field application (Golzio et al 2002).

A wide range of tissues have been transfected by electroporation including skin (Titomirov et al 1991 ; Vandermeulen et al 2007), kidney (Isaka et al 2005), lung (Zhou et al 2007), liver (Heller et al 1996 ; Liu and Lang 2002), muscle (Aihara et al 1998 ; Mir et al 1999), joints (Bloquel et al 2007), heart (Dean 2005), spleen (Tupin et al 2003), brain (Saito and Nakatsuji 2001), eyes

(Bloquel et al 2006) and tumours (Rols et al 1998 ; Goto et al 2000). This approach consists in local or systemic injection of plasmid DNA solution following controlled application of electric field. Only the tissue placed between the electrodes is transfected (Escoffre et al., 2008). In most works, electroporation increases the gene expression by a 100- to 1000-fold compared to the simple injection of plasmid DNA. Moreover, electrotransfection decreases the inter-individual variability compared to direct injection of plasmid DNA (Mir et al 1999). In addition, electrotransfection can achieve long-lasting expression into tissues. Indeed, gene expression was detected from nine months to one year into skeletal muscle (Mir et al 1999). To improve the transfection efficiency by electrotransfection, factors such as the size and concentration of plasmid DNA, electrode shape, number, orientation and duration of the electric field pulses have been optimized (Mir et al 1999; Faurie et al 2003 ; Faurie et al 2004). Previous works showed that the in vivo biodistribution of plasmid DNA was slowed down by the complex organization of tissues like skeletal muscle or tumours (Bureau et al 2004; Mesojednik et al 2007). Nevertheless, the treatment of tissues with hyaluronidase and/or collagenase prior to injection of plasmid DNA induced the partial degradation of extracellular matrix (MacMahon et al 2001). This treatment improved the plasmid DNA diffusion into the tissues and limited the nuclease degradation of plasmid DNA. For consequence, the gene transfection was enhanced (MacMahon et al 2001). In addition, the application of electric pulses with different polarities and orientations allowed to increase gene transfection by enhancing the plasmid DNA/membrane interaction around the cells (Faurie et al 2003; Faurie et al 2004). Pre-clinical studies showed the therapeutic potentiality of this gene transfer method in the treatment of monogenic diseases such as muscular atrophy (Lesbordes et al 2002), β-thalassemy (Payen et al 2001) and ischemic limbs (Nishikage et al 2004). Moreover, recent works showed that the electrotransfection of vaccine DNA into muscle or skin, increased the immune response compared to direct injection of vaccine plasmid (Dupuis et al 2000 ; Widera et al 2000 ; Babiuk et al 2002 ; Dayball et al 2003). Potent immune responses against bacterial (Zhang et al 2007) and viral infections (Hirao et al 2008) and cancer (Kalat et al 2002 ;

Buchan et al 2005 ; Curcio et al 2008) were obtained by electrotransfection of vaccine plasmid into muscle or skin tissues. Then, the expression of suicide gene, cytokines, antiangiogenic factors, antitumor suppressors such as, thymidine-kinase/ganciglovir (Shibata et al 2002), Il-12 (Heller et al 2006), and p53 (Grosel et al 2006) are under investigation for cancer gene therapy.

2.2. Sonoporation

The sonoporation is a physical method of genes delivery into cells and tissues by using ultrasound exposure in the presence of microbubbles (Newman and Bettinger 2007 ; Karshafian et al., 2009). Ultrasound frequencies used for gene delivery are near range of imaging ultrasound frequencies. Therefore, the microbubbles are the same than the ones used for ultrasound contrast imaging. The transfection efficiency depends on the acoustic pressure, the duty cycle and the time exposure of cells to ultrasounds (Duvshani-Eshet et al 2006). Ultrasound exposure is necessary but not sufficient to deliver genes into cells. In addition, the nature of microbubbles, their lifetime and their concentration are involved in the transfection efficiency (Li et al 2003). The mechanism of DNA uptake into cells is not very clear but some work suggests that the sonoporation induced the creation of pores in the plasma membrane. Imaging studies showed that the microbubbles interacted with the plasma membrane (van Wamel et al 2004). Under ultrasound exposure, the microbubbles induced mechanic constraints on the plasma membrane and increased the membrane permeability by the creation of pores (Tran et al 2006 ; Postema et al 2004). Mehier-Humbert and collaborators demonstrated that the size of these pores is inferior or equal to 75 nm for rat mammary carcinoma cells (Meiher-Humbert et al 2005a). The kinetics of plasmid internalization and gene expression showed that sonoporation allowed a rapid and direct transfer of naked DNA into the cell cytoplasm probably via ultrasound-induced pores in the membrane. The kinetics of protein expression was significantly faster for sonoporation than lipofection, the mechanism of which requires endocytosis (Mehier-Humbert et al 2005b).

The sonoporation is simple and efficient method to transfer genes into skin (Yoon et al., 2009) skeletal muscle (Li et al 2005), cardiac muscle (Condo et al 2004), liver (Miao et al 2005) and tumour (Suzuki et al 2008). In addition, Hynynen and collaborators showed that intracranial sonoporation induced a transient permeabilization of blood-brain barrier of rabbit (Hynynen et al 2003). The sonoporation is a non-invasive method to deliver therapeutic genes in the treatment of neurodegenerative diseases and brain cancer. This method has a promising future in the treatment of cardiac diseases. For example, Condo et al demonstrated that the sonoporation may enable myocardial hepatocyte growth factor gene transfer with a systemic administration of naked plasmid, which enhances angiogenesis, limits infarction size, and prevents left ventricular remodeling after myocardial infarction in rat model (Condo et al 2003). In addition, Hauff et al led the proof of concept to transfer therapeutic gene into tumours. The delivery of suppressor gene p16 into human pancreatic adenocarcinoma by sonoporation induced 2-fold decrease of growth tumour after three treatments (Hauff et al 2005).

2.3. Hydrodynamic injection

Hydrodynamic injection is based on a rapid injection of large volume of plasmid DNA solution via the tail vein (eg 5 µg plasmid DNA in 5 to 8s in 1.6 mL to 1.8 mL saline solution for a 20 g mouse). Transfection efficiency of the hydrodynamic injection is determined by the combined effect of a large volume and high injection speeds. This procedure induced gene transfer in highly perfused internal organs, especially the liver (Herweijer and Wolff, 2007).

Previous work has attempted to explain the mechanisms involved in hydrodynamic gene transfer. Budker et al suggested that plasmid DNA crossed the plasma membrane of hepatocytes by receptor-mediated pathway (Budker et al 2000). Whereas, Zhang et al have demonstrated that hydrodynamic injection induced a transient irregularity of heart function and a rapid increase in vena cava pressure (Zhang et al 2004). Hydrodynamic injection enlarged liver fenestrae and enhanced the membrane permeability of the hepatocytes. At the cell level, their data suggested that hydrodynamic gene delivery is

accomplished by the generation of membrane pores in the hepatocytes. This mechanism could allow direct entry of plasmid DNA into cytoplasm without endocytosis (Zhang et al 2004 ; Andre et al 2007).

Such simple and efficient method for gene delivery has been used to express therapeutic proteins such as fetal liver kinase-1 (Yazawa et al 2006) and IFN-γ (Takehara et al 2007) in mouse or rat models of liver diseases. Moreover, hydrodynamic injection is used to deliver genes into muscle tissues in the temporarily isolated limbs of primates and isolated limb perfusion (Zhang et al 2001). This procedure is performed via the arterial and venous routes. Transfection efficiency is higher than a simple intramuscular injection and only, muscles of perfused limb are transfected (Herweijer and Wolff 2007). Previous works demonstrated high efficiency delivery of a dystrophin plasmid to dystrophic murine model (Liang et al 2004).

The translation of hydrodynamic injection for gene therapy in human clinic supposed to inject up to 8 L (ie 10% of body weight) of saline solution at a high rate. Human body would not tolerate this high volume. Nevertheless, to overcome this obstacle, balloon catheter-based (Eastman et al 2002) and occlusion-assisted infusion (Alino et al 2007) could be used for gene delivery by hydrodynamic injection in future clinical applications.

2.4. Gene gun

Gene gun is a nonviral method whose principle is based on the bombardment of small gold particles coated with plasmid DNA accelerated by using pressurized gas on tissues. Ballistic gene delivery allows direct penetration through the plasma membrane into the cytoplasm and even the nucleus, bypassing the endosomal pathway (Cheng et al 1993).

Gene gun is a simple and efficient method to deliver genes into skin (Gaffal et al 2007), mucosa (Wang et al 2003), and interne organs after surgery such as liver (Chang et al 2008). Various work reported the use of gene gun to introduce plasmid DNA encoding antigens such as $A\beta_{42}$ (Ghochikyan et al 2003) or cytokines such as IL-4 (Ghochikyan et al 2003), IL-12 (Dietrich et al

2006) for genetic vaccination and immunotherapy against infectious diseases and cancer.

The main limitation of gene gun is the shallow penetration of plasmid DNA into the tissue (ie few millimetres). Nevertheless, Dileo and collaborators adjusted a new gene gun that allowed shooting microparticles under high pressure (Dileo et al 2003). Thus, subcutaneous tissues such as muscle and tumours could be transfected and long-lasting expression could be achieved. Another limitation is the little knowledge of the becoming and clearance of these gold particles *in vivo*.

2.5. Laser beam gene transduction

In 1986, Kurata et al demonstrated that the application of a laser beam on culture cells incubated with plasmid DNA solution increased the transfection efficiency. The mechanism involved in the plasmid DNA uptake could be membrane pores that allow direct transfer into the cytoplasm without endocytosis (Kurata et al 1986).

Femtosecond laser beam transduction system is a safe and efficient method of intradermal (Zeira et al., 2007 ; Tsen et al., 2009), intratumoral (Tsen et al., 2009) and intramuscular (Zeira et al., 2003) nonviral gene delivery in mice. Indeed, Zeira et al reported that gene delivery into muscle could be enhanced by application of a femtosecond infrared laser (5s at 30 mW). The gene transfer was more efficient than a simple intramuscular injection and gene expression was detected for 100 days without tissue damages (Zeira et al 2003). The same group showed the use of laser beam gene transfer in genetic vaccination against hepatitis B virus (HBV) surface antigen (HBsAg). High titers of HBsAg-specific antibodies were detected lasting 210 days and the activation of Th1 and Th2 immune responses were induced (Zeira et al 2007).

The main limitation of this method is the focus depth of laser beam. Indeed, the laser was focused to 2 mm under the mouse skin (Zeira et al 2003). The translation of this method in human clinic requires a high power of penetration of laser beam. The use of laser beam in gene therapy seems to be limited to the muscle and skin tissues.

2.6. Magnetofection

The magnetofection rests on the delivery of paramagnetic nanoparticles coated with plasmid DNA into cells or tissues under the effect of strong magnetic fields. There was negligible transfection with paramagnetic nanoparticles in the absence of magnetic fields (Scherer et al 2002 ; Kamau et al 2006). Previous evidence suggested that paramagnetic nanoparticles entered via endocytosis pathway. Nevertheless, Chorny et al demonstrated that the use of large sized of paramagnetic nanoparticles (ie 375 nm of diameter) exhibited higher transfection rates than small sized of nanoparticles (ie 185 and 240 mm of diameter). This result can be explained by the fact that the internalization large sized of paramagnetic nanoparticles escaped lysosomal pathway and released DNA next to the nucleus (Chorny et al 2007).

Application of magnetic fields following local injection of plasmid DNA enhanced *in vivo* reporter gene transfer to the gastrointestinal tract and vasculature of the ear (Scherer et al 2002). In therapeutic strategy for the treatment of cystic fibrosis, Xenariou et al showed that the magnetofection can enhance the reporter gene transfer into the airway epithelium *in vivo* (Xenariou et al 2006). Recently, Huntinger et al., demonstrated that feGM-CSF applied by magnetofection is safe and feasible approach to treatment feline fibrosarcomas in veterinary oncology (Huttinger et al., 2008). Nevertheless, it would seem that the improvement of transfection efficiency induced by the magnetofection is not as high as the improvement induced by the other physical methods.

2.7*. Jet-injection*

In 1982, Furth et al., developed the jet-injection that allows gene transfer into different tissue types with deeper penetration of the applied naked DNA (Furth et al., 1982). The physical method is based on the use of jets with high velocity exerting force to penetrate skin and underlying tissues leading to the efficient transfection of the jet-injected areas (Furth et al., 1995). Indeed, low-volume jet injection employed uses compressed air to inject solutions of 3 to 10 µL containing naked or formulated DNA at high speed (>300 m/s) into desired tissue. The energy of this high-speed liquid allows the jet to precisely penetrate

into tissue associated with a spread distribution of the liquid allowing a more effective penetration of the targeted area (Walther et al., 2001). The variation in pressure setting has an influence on the penetration depths and transfer efficiencies and therefore allows the adaptation of the jet-injection to the specific application (Walther et al., 2001). The mechanism involved in the plasmid DNA uptake is unknown but probably a membrane disruption took place (Walther et al., 2004).

The jet-injection increased the transfection efficiency into muscle (Furth et al., 1995 ; Cartier et al., 2000), skin (Furth et al., 1995 ; Sawamura et al., 1999 ; Heansler et al., 1999), and tumours (Walther et al., 2001, 2002, 2005, 2006, 2008 ; Stein et al., 2008 ; Cartier et al., 2000). The transgene expression produced by the jet-injection covers broad areas associated with deep penetration of 5 to 10 mm within the jet-injected tissue (Walther et al., 2004). In vivo application of jet-injection is not associated with tissue damage or significant reactions at injection sites (Furth et al., 2005). This method can achieve transfer efficiencies that are comparable to gene gun and electroporation (Furth et al., 1992 ; Furth et al., 1995). The main applications are the cancer gene therapy and DNA vaccination. Indeed, Stein et al., led the proof of concept to complete in vivo reversal of multidrug resistance phenotype by jet-injection of anti-MDR1 short hairpin RNA-encoding plasmid DNA. Two jet-injections of anti-MDR1 shRNA vectors into the tumors, combined with two intravenous administrations of doxorubicin were sufficient to induce a decrease of tumor growth (Stein et al., 2008). Recently, Walther et al., published the first results of phase I clinical trial, which evaluated safety, feasibility and efficiency of nonviral intratumoral jet-injection gene transfer in patients with skin metastases from melanoma and breast cancer. These results showed that intratumoral jet-injection of plasmid DNA led to efficient reporter gene expression in all patients. No side effects were experienced, supporting safety and applicability of this novel physical method (Walther et al., 2008).

2.8. Plasma

Recently, Jaroszeski and Connolly developed plasma-mediated gene delivery. This approach rests on the ions deposit on the cells and tissues surface by using DC plasmas. The results showed that in vitro plasma-mediated delivery of tracer molecules occurred in a dose dependent manner with the optimum condition increasing delivery by up to 60% relative to control. Plasma exposure caused no adverse affects cell viability (Connolly et al., 2009). The same team investigated the use of a plasma-mediated gene delivery into murine skin in vivo. This delivery method included injecting the dermis with plasmid DNA and then exposing the outer skin surface to direct current helium plasma to increase DNA plasmid uptake into cells. This method did not require physical contact between the skin and an electrical source. No involuntary muscle contractions were observed during plasma treatment, and no skin damages were observed post-treatment. Gene expression was dependent upon plasma exposure time, polarity and DNA dose. Maximum expression levels were 20-fold higher than control samples that received DNA injections alone. Thus, Jaroszeski et al., demonstrated the feasibility of plasma based delivery and that it could potentially compete with other DNA delivery methods for the skin (Jaroszeski et al., 2009). Plasma-mediated gene delivery has future in human clinic for genetic vaccination.

2.9. Combination of physical methods

The prospects of nonviral delivery methods lie in the combination of various nonviral delivery methods to improve the transfection efficiency and the development of strategies to overcome physical obstacles such as extracellular matrix and nuclear uptake.

Indeed, Yamashita et al. investigated the efficiency of a combination of electroporation and ultrasound (called electro-sonoporation) as a new potent nonviral gene transfer method into mouse skeletal muscle using naked plasmid DNA encoding luciferase gene as the marker of the local protein expression, and mouse interleukin-12 gene as the marker of systemic secretion of therapeutic protein. This work demonstrated that luciferase activity and serum mIL-12 in mice that had undergone electro-sonoporation were twofold higher

after gene transfer than were those in mice having undergone electrotransfection alone (Yamashita et al 2002). The electro-sonoporation of IL-12 plasmid DNA into skeletal muscle could be used to stimulate or induce anti-tumoral immune response. Moreover, Habib et al., proposed the same approach to transfer human thrombopoietin plasmid DNA into skeletal muscle to treat thrombocytopaenia, which are one clinical frequently encountered in patients with chronic liver failure or cancer following treatment with chemotherapy. This combination induced a 2.5- and 5-fold increase of thrompopoietin compared sonoporation or electroporation alone, respectively. This increase is correlated with platelets production (Habib et al., 2004).

Then, Holzbach et al., investigated the potential of magnetofection of magnetic liposphere (called magnetobubbles) containing VEGF-165 encoding plasmid DNA, and sonoporation, on survival and perfusion of ischemic skin flaps. The magnetic field maintained the magnetobubbles at ischemic skin flaps level. Then, the ultrasounds induced the gene transfer. The results showed an increased flap survival of 50% and a significant increase of flap perfusion compared without ultrasound or without magnetic field. The safe combination magnetofection-sonoporation is equally efficient as adenoviral transduction (Holzbach et al., 2008).

3. Cytoplasm and nuclear envelope

3.1. Cytoplasm

Enclosed within the plasma membane, the cytoplasm contains organelles, which are filled with liquid that is kept separate from the rest of the cytoplasm by others intracellular membranes. The part of the cytoplasm that is not held within organelles is called the cytosol. This cytosol is a complex mixture of cytoskeleton filaments (e.g. actin microfilaments and microtubules) dissolved molecules, and water that fills much of cell volume. The cytosol can be considered as a gel, with a fibers network dispersed through water (Lechardeur and Lukacs, 2006). The mesh-like structure of the cytoskeleton, the presence of organelles and the high protein concentration impose an intensive molecular crowding of the cytoplasm which limits the diffusion of large

sized macromolecules (Lechardeur and Lukacs, 2002). The translational mobility of macromolecule smaller than 500-750 kDa is only 3-4 fold slower than in water, but it is markedly impeded for larger molecules (Seksek et al., 1997). Mobility of plasmid DNA is negligible in the cytoplasm of microinjected myotubes (Dowty et al., 1995) and HeLa cells (Lukacs et al., 2000). Thus, the DNA becomes sensitive to degradation by the intracellular enzymes. Previous works revealed that 50% of plasmid DNA is eliminated in 12h from HeLa and COS cells and in 4h from myotubes (Lechardeur et al., 1999 ; Pollard et al., 2001). In the cases of tissues, radiolabelled plasmid DNA indeed progressively leave muscles and is degraded as soon as 5 min after plasmid injection (Bureau et al., 2004).

3.2. Nuclear Envelope

Beside cytoplasm, the nuclear envelope represents the last physical barrier to the gene expression (Miller and Dean, 2009). While molecules smaller than 40 kDa can diffuse through the nuclear pore complexes, larger molecules must carry a specific targeting signal, the nuclear localization sequence to cross the nuclear enveloppe (Miller and Dean, 2009). The significant size of plasmid DNA (2-10 MDa) makes it unlikely that the nuclear entry occurs by passive diffusion (Lukacs et al., 2000). Dividing cells are more transfectable than quiescent ones, suggesting than plasmid DNA enter the nucleus after disassembly of nuclear envelope during mitosis (Miller and Dean, 2009). Indeed, cell synchronization affects gene delivery by physical methods reinforcing the statement that the disappearance of the nuclear enveloppe facilitates direct access of plasmid DNA to the expression machinery (Chida et al., 1998 ; Golzio et al., 2002).

3.3. Strategies

New challenges are to overcome the limiting steps represented to the cytoplasm crowding and the transfer through nuclear envelope. One possibility is that plasmid DNA become cargo on cytoskeletal motors much like viruses do, and move to the nucleus in a directed fashion (Vaughan et al., 2006). Indeed, the presence of DNA nuclear targeting sequence (DTS) in the plasmid DNA is

specifically recognized by cytosolic proteins carrying nuclear localization sequence. Thus, it increased the intracellular migration mediated by microtubules network and nuclear uptake by using active transport machineries of target cells (Vaughan et al 2006). Dean et al., demonstrated that the transfection efficiency is improved when plasmid DNA carried DTS are transferred in dividing and quiescent cells and tissues by microinjection (Vaughan et al., 2006) and electroporation (Vaughan et al., 2006 ; Zhou et al., 2007). Moreover, the same team showed that given DNA nuclear targeting sequences can be used to restrict DNA nuclear import to specific cell types providing a new, novel means of cell targeting for gene therapy (Miller et al., 2008). Indeed, they demonstrated that the Smooth Muscle Cells-specific DNA nuclear targeting sequence from the Smooth Muscle Gamma Actin promoter drives nuclear accumulation of plasmids and subsequent gene expression exclusively in the smooth muscle cell layer of the vessel wall in the intact vasculature of rats using electropulsation mediated delivery (Miller et al., 2008 ; Young et al., 2008). In the same idea, an approach consisted in complexing plasmid DNA with NLS-peptides by electrostatic interactions, in attaching these peptides in a random and covalent way to the plasmid DNA and in attaching NLS-peptides in specific site to the plasmid by using PNAs (Dean et al., 2005). Indeed, NLS-plasmid DNA complexes enhance transfection efficiency mediated by electroporation (Mir and Piedrahita, 2004 ; Collins et al., 2007), and sonoporation (Duvshani-Eshet et al., 2008).

Alternatively, it has been shown that the nuclear uptake of macromolecules such as plasmid DNA can be enhanced significantly by addition of the amphiphilic molecule trans-cyclohexane-1,2-diol (TCHD) (Ribbeck and Gorlich, 2002 ; Lentacker et al., 2008). The mechanism by which TCHD causes nuclear localization of macromolecules can be explained based on the recent finding that the inner channel of the nuclear pore complexes is filled with a hydrogel. This hydrogel is build-up by cross-linked nucleoporins. The cross-links are formed between hydrophobic phenylalanine-glycine repeats present in the nucleoporins. TCHD causes a temporary, non-selective gating of the pore by inducing a disruption of the hydrophobic interactions between the

hydrophobic repeats of the nucleoporins. Such a disruption is expected to increase the mesh-size of the hydrogel present in the NPC and hence nuclear entry of macromolecules that are otherwise excluded from the nucleus. It is important to mention that the effect of TCHD is reversible and does not cause damage to the nuclear pores (Ribbeck and Gorlich, 2002). To improve gene transfer mediated by sonoporation, Lentacker et al., proposed to treat the target cells by the TCHD. Thus, they induced a 2 fold-increase of transfection efficiency (Vandenbroucke et al., 2007 ; Lentacker et al., 2008).

Another alternative could come from nanosecond pulsed electric fields (NsPEFs). Recent works suggested the benefit of the nanosecond pulsed electric fields (NsPEFs), called supra-electroporation, in gene transfer (Gowrishankar et al 2006). This approach consists in applying intense and short electric pulses, ie 10-300 kV/cm lasting tens of ns in order to induce the permeabilization of intracellular organelles such as the nucleus (Tekle et al 2005). The authors reorted that when nsPEFs (ie 10 ns, 150 kV/cm) were applied after classical electroporation pulses (ie 3.5 ms, 0.3 kV/cm) transfection efficiency was increased by 3-fold compared to classical electroporation, only (Beebe et al 2003).

Conclusions

Adverse effects associated with virus-mediated gene therapy trials have stimulated efforts to improve the efficiency of physical vectors. The way borrowed by the DNA plasmid during the gene transfer is not a right and direct way but a sown way of obstacles. The additive effect of extracellular and cellular obstacles, accounting for the poor gene transfer efficiency of physical delivery systems, has been largely determined. At the cellular level, the trafficking of plasmid DNA between the extracellular environment and the nucleus and gene expression are prevented by both physico-chemical and metabolic barriers. Thus, improvements in gene transfer protocols to overcome these obstacles, will allow to achieve safe and efficient therapeutic transgene expression for future clinical applications such as genetic vaccination and cancer gene therapy.

Acknowledgements

Many thanks are due to the financial supports from the CNRS, the Association Française sur les Myopathies, the ANR “Cemirbio”, the ANR “CMIDT” and the Région Midi-Pyrénées.

JME was the recipient of a PhD fellowship of the French government

References

Aihara H, and Miyazaki JI. (1998). Gene transfer into muscle by electroporation in vivo. *Nature Biotechnol,* 16:867-70.

Alexandrakis G, Brown EB, Tong RT, McKee TD, Campbell RB, Boucher T et al. (2004). Two-photon fluorescence correlation microscopy reveals the two-phase nature of transport in tumors. Nat. Med., 10 :203-207

Alino SF, Herrero MJ, Noguera I, Dasi F, Sanchez M. (2007). Pig liver gene therapy by non-invasive interventionist catheterism. *Gene Ther,* 14:334-43.

Andre FM, Cournil-Henrionnet C, Vernerey D, Opolon P, Mir LM. (2006). Variability of naked DNA expression after direct local injection: the influence of the injection speed. *Gene Ther,* 13:1619-27

Ardehali A, Fyfe A, Laks H, Drinkwater DC Jr, Qiao JH, Lusis AJ. (1995). Direct gene transfer into donor hearts at the time of harvest. *J Thorac Cardiovasc Surg,* 109:716-19; Discussion 719-20.

Babiuk S, Baca-Estrada ME, Foldvari M, Storms M, Rabussay D, Widera G, Babiuk LA. (2002). Electroporation improves the efficacy of DNA vaccines in large animals. *Vaccine,* 20:3399-408.

Beebe SJ, White J, Blackmore PF, Deng Y, Somers K, Schoenbach KH. (2003). Diverse effects of nanosecond pulsed electric fields on cells and tissues. *DNA Cell Biol,* 22:785-96.

Berrier AL, Yamada KM. (2007). Cell-Matrix adhesion. J Cell Physiol., 213:565-573

Bloquel C, Bejjani R, Bigey P, Bedioui F, Doat M, BenEzra D, Scherman D, Behar-Cohen F. (2006). Plasmid electrotransfer of eye ciliary muscle: principles and therapeutic efficacy using hTNF-α soluble receptor in uveitis. *FASEB J,* 20:389-91.

Bloquel C, Denys A, Boissier MC, Apparailly F, Bigey P, Scherman D, Bessis N. (2007). Intra-articular electrotransfer of plasmid encoding soluble TNF receptor variants in normal and arthritic mice. *J Gene Med,* 9:986-93.

Broeke AV, and Burny A. (2003). Retroviral Vector Biosafety: Lessons from sheep. *J Biomed Biotechnol,* 2003:9-12.

Buchan S, Gronevik E, Mathiesen I, King CA, Stevenson FK, Rice J. (2005). Electroporation as a "prime/boost" strategy for naked DNA vaccination against a tumor antigen. *J Immunol,* 174:6292-8

Budker V, Budker T, Zhang G, Subbotin V, Loomis A, Wolff JA. (2000). Hypothesis: naked plasmid DNA is taken up by cells in vivo by a receptor-mediated process. *J Gene Med,* 2:76-88.

Bureau MF, Naimi S, Torero Ibad R, Seguin J, Georger C, Arnould E, Maton L, Blanche F, Delaere P, Scherman D. (2004). Intramuscular plasmid DNA electrotransfer. Biodistribution and degradation. *Biochim Biophys Acta,* 1676:138-48

Cartier R, Ren SV, Walther W, Stein U, Lewis A, Schlag PM, Li M, Furth PA. (2000). In vivo gene transfer by low-volume jet-injection. Anal. Biochem., 282 :262-265

Chang ML, Chen JC, Yeh CT, Chang MY, Liang CK, Chiu CT, Lin DY, Liaw YF. (2008). Gene gun bombardment with DNA-coated gold particles is a potential alternative to hydrodynamics-based transfection for delivering genes into superficial hepatocytes. *Hum Gene Ther,* 19:391-5

Cheng L, Ziegelhoffer PR, and Yang NS. (1993). In vivo promoter activity and transgene expression in mammalian somatic tissues evaluated by using particle bombardment. *Proc Natl Acad Sci USA,* 90:4455-9.

Chida K, Sueyoshi R, Kuroki T. (1998). Efficient and stable gene transfer following microinjection into nuclei of synchronized animal cells progressing from G1/S boundary to early S phase. Biochem Biophys Res Commun., 249:849-852

Choate KA, and Khavari PA. (1997). Direct cutaneous gene delivery in a human genetic skin disease. *Hum Gene Ther,* 8:1659-65.

Chorny M, Polyak B, Alferiev I.S, Walsh K, Friedman G, Levy RJ. (2007). Magnetically driven plasmid DNA delivery with biodegradable polymeric nanoparticles. *FASEB J,* 21:2510-9.

Connolly R, Lopez G, Wegerif GD, Hoff AM, Jaroszeski MJ. (2009). Effects of plasma mediated molecular delivery. XXth International Symposium on Bioelectrochemistry and Bioenergetics, Romania.

Collins E, Birchall JC, Williams JL, Gumbleton M. (2007). Nuclear localisation and pDNA condensation in non-viral gene delivery. J. Gene Med., 9:265-274

Curcio C, Khan AS, Spadaro M, Quaglino E Cavallo F, Forni G, Draghia-Akli R. (2008). DNA immunization using constant-current electroporation affords long-term protection from autochthonous mammary carcinomas in cancer-prone transgenic mice. *Cancer Gene Ther,* 15:108-14

Dayball K, Millar J, Miller M, Wan YH, Bramson J. (2003). Electroporation enables plasmid vaccines to elicit CD8+ T cell responses in the absence of CD4+ T cells. *J Immunol,* 171:3379-84.

Dean DA. (2005). Nonviral gene transfer to skeletal, smooth, and cardiac muscle in living animals. *Am J Physiol Cell Physiol,* 289:233-45.

Dietrich A, Becherer L, Brinckmann U, Hauss J, Liebert UG, Gutz A, Aust G. (2006). Particle-mediated cytokine gene therapy leads to antitumor and antimetastatic effects in mouse carcinoma models. *Cancer Biother Radiopharm,* 21:333-41.

Dileo J, Miller TE, Chesnoy S, Huang L. (2003). Gene transfer to subdermal tissues via a new gene gun design. *Hum Gene Ther,* 14:79-87.

Dowty ME, Williams P, Zhang G, Hagstrom JE, Wolff JA. (1995). Plasmid DNA entry into postmitotic nuclei of primary rat myotubes. Proc Natl Acad Sci USA, 92:4572-4576

Dubensky TW, Campbell BA, Villarreal LP. (1984). Direct transfection of viral and plasmid DNA into the liver or spleen of mice. Proc. Natl. Acad. Sci. USA, 81:7529-7533

Dupuis M, Denis-Mize K, Woo C, Goldbeck C, Selby MJ, Chen M, Otten GR, Ulmer JB, Donnelly JJ, Ott G, MacDonald DM. (2000) Distribution of DNA vaccines determines their immunogenicity after intramuscular injection in mice. *J Immunol,* 165:2850-8.

Duvhani-Eshet M, Baruch L, Kesselman E, Shimoni E, Machluf M. (2006). Therapeutic ultrasound-mediated DNA to cell and nucleus: bioeffects revealed by confocal and atomic force microscopy. Gene Ther, 13:163-72.

Eastman SJ, Baskin KM, Hodges BL, Chu Q, Gates A, Dreusicke R, Anderson S, Scheule RK. (2002). Development of catheter-based procedures for transducing the isolated rabbit liver with plasmid DNA. Hum. *Gene Ther,* 13:2065-77.

Escoffre JM, Dean DS, Hubert M, Rols MP, Favard C. (2007). Membrane perturbation by an external electric field: a mechanism to permit molecular uptake. *Eur Biophys J,* 36:973-83

Escoffre JM, Debin A, Reynes JP, Drocourt D, Tiraby G, Hellaudais L, Teissie J, Golzio M. (2008). Long-lasting in vivo gene silencing by electrotransfer of shRNA expressing plasmid. Technol Cancer Res Treat., 7:109-116

Escoffre JM, Portet T, Wasungu L, Teissié J., Dean D, Rols MP. (2009). What is (still not) known of the mechanism by which electroporation mediates gene transfer and expression in cells and tissues. Mol Biotechnol., 41:286-295

Evans V, Foster H, Graham IR, Foster K, Athanasopoulos T, Simons JP, Dickson G, Owen JS. (2008). Human apolipoprotein E expression from mouse skeletal muscle by electrotransfer of nonviral DNA (plasmid) and pseudotyped recombinant adeno-associated virus (AAV2/7). Hum. Gene. Ther., 19:569-578.

Faurie C, Golzio M, Moller P, Teissie J, Rols MP. (2003). Cell and animal imaging of electrically mediated gene transfer. *DNA Cell Biol,* 22:777-83

Faurie C, Phez E, Golzio M, Vossen C, Lesbordes JC, Delteil C, Teissie J, Rols MP. (2004). Effect of electric field vectoriality on electrically mediated gene delivery in mammalian cells. *Biochim Biophys Acta,* 1665:92-100

Favre D, Cherel Y, Provost N, Blouin V, Ferry N, Moullier P, and Salvetti A. (2000). Hyaluronidase enhances recombinant adeno-associated virus (rAAV)-mediated gene transfer in the rat skeletal muscle. Gene Ther., 7:1417-1420

Furth PA, Shamay A, Wall RJ, Hennighausen L. (1992). Gene transfer into somatic tissues by jet injection. Anal Biochem., 205:365-368

Furth PA, Shamay A, Hennighausen L. (1995). Gene transfer into mammalian cells by jet injection. Hybridoma, 14:149-152

Gaffal E, Schweichel D, Tormo D, Steitz J, Lenz J, Basner-Tschakarjan E, Limmer A, Tuting T. (2007). Comparative evaluation of CD8+ CTL responses following gene gun immunization targeting the skin with intracutaneous injection of antigen-transduced dendritic cells. *Eur J Cell Biol,* 86:817-26.

Gardlik R, Palffy R, Hodosy J, Lukacs J, Turna J, Celec P. (2005). Vectors and delivery systems in gene therapy. *Med Sci Monit,* 11:RA110-21.

Ghochikyan A, Vasilevko V, Petruschina I, Movsesyan N, Babikyan D, Tian W, Sadzikava N, Ross TM, Head E, Cribbs DH, Agadjanyan MG. (2003). Generation and characterization of the humoral immune response to DNA immunization with a chimeric Aβ-interleukine 4 minigene. *Eur J Immunol,* 33:3232-41

Golzio M, Teissie J, Rols MP. (2002). Cell synchronization effect on mammalian cell permeabilization and gene delivery by electric field. Biochim Biophys Acta, 1563:23-28

Golzio M, Rols MP, and Teissie J. (2004). In vitro and in vivo electric field-mediated permeabilization, gene transfer, and expression. *Methods,* 32:126-35.

Goto T, Nishi T, Tamura T, Dev SB, Takeshima H, Kochi M, Yoshizato K, Kuratsu J, Sakata T, Hofmann GA, Ushio Y. (1999). Highly efficient electro-gene therapy of solid tumor by using an expression plasmid for the herpes simplex virus thymidine kinase gene. *Proc Natl Acad Sci USA,* 97:354-9.

Gowrishankar TR, Esser AT, Vasilkoski Z, Smith KC, Weaver JC. (2006). Microdosimetry for conventional and supra-electroporation in cells with organelles. *Biochem Biophys Res Comm,* 341:1266–76.

Greenleaf W.J, Bolander ME, Sarkar G. (1998). Artificial cavitation nuclei significantly enhance acoustically induced cell transfection. *Ultrasound Med Biol,* 24:587-95.

Grosel A, Sersa G, Kranjc S, Cemazar M. (2006). Electrogene therapy with p53 of murine sarcomas alone or combined with electrochemotherapy using cisplatin. *DNA Cell Biol,* 25:674-83.

Habib N, Havlik R, Jiao L, Kiri A, Jensen S, Nicholls J, Sarraf C, Goldspink G, Davies A, Slavik L, Wood C, Tiraby M, Drocourt D, Reynes JP, Smadja C, Tiraby JG. (2004). Combination of optison with ultrasound and electroporation increases albumin and thrompoietin transgene expression whilst elongation factor promoter prolongs ist duration. Gene Ther Mol Biol., 8:1-8

Hacein-Bey-Abina S, Von Kalle C, Schmidt M, McCormack MP, Wulffraat N, Leboulch P, Lim A, Osborne CS, Pawliuk R, Morillon E, Sorensen R, Forster A, Fraser P, Cohen JI, de Saint Basile G, Alexander I, Wintergerst U, Frebourg T, Aurias A, Stoppa-Lyonnet D, Romana S, Radford-Weiss I, Gross F, Valensi F, Delabesse E, Macintyre E, Sigaux F, Soulier J, Leiva LE, Wissler M, Prinz C, Rabbitts TH, Le Deist F, Fischer A, Cavazzana-Calvo M. (2003a). LMO2-associated clonal T cell proliferation in two patients after gene therapy for SCID-X1. *Science*, 302:415-9.

Hacein-Bey-Abina S, Von Kalle C, Schmidt M, Le Deist F, Wulffraat N, McIntyre E, Radford I, Villeval JL, Fraser CC, Cavazzana-Calvo M, Fischer A. (2003b). A serious adverse event after successful gene therapy for X-linked severe combined immunodefiency. *N Engl J Med,* 348:255-6.

Hauff P, Seemann S, Reszka R. (2005). Evaluation of gas-filled microparticles and sonoporation as gene delivery systems: feasibility study in rodent tumor models. *Radiology,* 236:572-8.

Heansler J, Verdelet C, Sanchez V, Girerd-Chambaz Y, Bonnin A, Trannoy E, Krishnan S, Meulien P. (1999). Intradermal DNA immunization by using jet-injectors in mice and monkeys. Vaccine, 17:628-638.

Heller L, Merkler K, Westover J, Cruz Y, Coppola D, Benson K, Daud A, Heller R. 2006. Evaluation of toxicity following electrically mediated interleukin-12 gene delivery in a B16 mouse melanoma model. *Clin Cancer Res,* 12:3177-83.

Heller R, Jaroszeski M, Atkin A, Moradpour D, Gilbert R, Wands J, Nicolau C. (1996). In vivo gene electroinjection and expression in rat liver. *FEBS Lett,* 389:225-8.

Herweijer H, and Wolff JA. (2007). Gene Therapy progress and prospects: Hydrodynamic gene delivery. *Gene Ther,* 14:99-107.

Hirao LA, Wu L, Khan AS, Satishchandran A, Draghia-Akli R, Weiner DB. (2008). Intradermal/cutaneous immunization by electroporation improves plasmid vaccine delivery and potency in pigs an rhesus macaques. *Vaccine,* 26:440-8

Holzbach T, Vlaskou D, Neshkova I, Konerding MA, Wortler K, Mykhaylyk O, Gansbacher B, Machens HG, Plank C, Giunta RE. (2008). Non-viral VEGF gene therapy – Magnetofection of acoustically active magnetic liposphere (Magnetobubbles) increases tissue-survival in an oversized skin flap model. J Cell Mol Med.,

Huttinger C, Hirschberger J, Jahnke A, Kostlin R, Brill T, Plank C, Kuchenhoff H, Krieger S, Schillinger U. (2008). Neoadjuvant gene delivery of feline granulocyte-macrophage colony-stimulating factor using magnetofection for the treatment of feline fibrosarcomas: a phae I trial. J. Gene Med. 10:655-667.

Hynynen K, McDannold N, Vykhodtseva N, Jolesz FA. (2003). Non-invasive opening of BBB by focused ultrasound. *Acta Neurochir Suppl,* 86:555-8.

Isaka Y, Yamada K, Takabatake Y, Mizui M, Miura-Tsujie M, Ichimaru N, Yazawa K, Utsugi R, Okuyama A, Hori M, Imai E, Takahara S. (2005). Electroporation-mediated HGF gene transduction protected the kidney against graft injury. *Gene Ther,* 12:815-20.

Jaroszeski MJ, Connolly R, Wegerif GD, Lopez G, Ugen K, Hoff AM. (2009). Plasma based method for augmenting DNA delivery to skin. XXth International Symposium on Bioelectrochemistry and Bioenergetics, Romania.

Jayankura M, Boggione C, Frisén C, Boyer O, Fouret P, Saillant G, Klatzmann D. (2003). In situ gene transfer into animal tendons by injection of naked DNA and electrotransfer. *J Gene Med,* 5:618-624

Kalat M, Kupcu Z, Schuller S, Zalusky D, Zehetner M, Paster W, Schweighoffer T. (2002). In vivo plasmid electroporation induces tumor antigen-specific CD8+ T-cell responses and delays tumor growth in a syngeneic mouse melanoma model. *Cancer Res,* 62:5489-94

Kamau SW, Hassa PO, Steitz B, Petri-Fink A, Hofmann H, Hofmann-Amtenbrink M, von Rechenberg B, Hottiger MO. (2006). Enhancement of the

efficiency of non-viral gene delivery by application of pulsed magnetic field. *Nuc Acids Res,* 34:e40.

Karshafian R, Bevan PD, Williams R, Samac S, Burns PN. (2009). Sonoporation by ultrasound-activated microbubble contrast: effect of acoustic exposure parameters on cell membrane permeability and cell viability. Ultrasound Med Biol., 35:847-860.

Kass L, Erler JT, Dembo M, Weaver VM. (2007). Mammary epithelial cell: influence of extracellular matrix composition and organization during development and tumorigenesis. Int J Biochem Cell Biol., 39:1987-1994

Kawase J, (2003). *Pharm Sci*, 92:1295-304

Kondo I, Ohmori K, Oshita A, Takeuchi H, Fuke S, Shinomiya K, Noma T, Namba T, Kohno M. (2004). Treatment of acute myocardial infarction by hepatocyte growth factor gene transfer. *J Am Coll Cardiol,* 44:644-53.

Krassowka W, and Filev PD. 2007. Modeling electroporation in a single cell. *Biophys J,* 92:404–17.

Kurata S, Tsukahoshi M, Kasuya T, Ikawa Y. (1986). The laser method for efficient introduction of foreingh DNA into cultured cells. *Exp Cell Res,* 162:372-8.

Kuriyama N, Kuriyama H, Julin CM, Lamborn KR and Israel MA. (2001). Protease pretreatment increases the efficacy of adenovirus-mediated gene therapy for the treatment of an experimental glioblastoma model. Cancer Res., 61:1805-1809

Lechardeur D, Sohn KJ, Haardt M, Joshi PB, Monck M, Graham RW, Beatty B, Squire J, O'Brodovich H, Lukacs GL. (1999). Metabolic instability of plasmid DNA in the cytosol : A potential barrier to gene transfer. Gene Therapy, 6:482-497

Lechardeur D, and Lukacs GL. (2002). Intracellular barriers to non-viral gene transfer. Current Gene Therapy, 2:183-194.

Lechardeur D, and Lukacs GL. (2006). Nucleocytoplasmic transport of plasmid DNA : A perilous journey from the cytoplasm to the nucleus. Hum Gene Ther., 17:882-889

Lehrman S. (1999). Virus treatment questioned after gene therapy death. *Nature,* 401:517-8

Lemieux P, Guérin N, Paradis G, Proulx R, Chistyakova L, Kabanov A, and Alakhov V. (2000). A combination of poloxamers increases gene expression of plasmid DNA in skeletal muscle. Gene Ther., 7:987-991

Lentacker I, Vandenbroucke RE, Lucas B, Demeester J, Smedt SC, Sanders NN. (2008). New strategies for nucleic acid delivery to conquer cellular and nuclear membranes. Journal of Controlled Release, 132:279-288

Lesbordes JC, Bordet T, Haase G, Castelnau-Ptakhine L, Rouhani S, Gilgenkrantz H, Kahn A. (2002). In vivo electrotransfer of the cardiotrophin-1 gene into skeletal muscle slows down progression of motor neuron degeneration in pmn mice. *Hum Mol Genet,* 11:1615-25

Li T, Tachibana K, and Kuroki M. (2003). Gene transfer with echo-enhanced contrast agents: comparison between Albunex, Optison, and Levovist in mice-initial results. *Radiology,* 229:423-8.

Liang KW, Nishikawa M, Liu F, Sun B, Ye Q, Huang L. (2004). Restoration of dystrophin expression in mdx mice by intravascular injection of naked DNA containing full-length dystrophin cDNA. *Gene Ther,* 11:901-8.

Liu F, and Huang L. (2002). Electric gene transfer to the liver following systemic administration of plasmid DNA. *Gene Ther,* 9:1116-9.

Lukacs GL, Haggie P, Seksek O, Lechardeur D, Freedman N, Verkman GL. (2000). Size-dependent DNA mobility in cytoplasm and nucleus. *J Biol Chem,* 275:1625-9.

McMahon JM, Signori E, Wells KE, Fazio VM, Wells DJ. (2001). Optimization of electrotransfer of plasmid into skeletal muscle by pretreatment with hyaluronidase – increased expression with reduced muscle damage. *Gene Ther,* 8:1264-70.

Marshall E. (1999). Gene therapy death prompts review of adenovirus vector. *Science,* 286: 2244-5.

Meiher-Humber S, Bettinger T, Yan F, Guy RH. (2005b). Ultrasound-mediated gene delivery: Kinetics of plasmid internalization and gene expression. *J Control Release,* 104:203-11.

Meiher-Humber S, Bettinger T, Yan F, Guy RH. (2005a). Plasma membrane poration induced by ultrasound exposure: Implication for drug delivery. *J Control Release,* 104:213-22.

Mennuni C, Calvaruso F, Zampaglione I, Rizzuto G, Rinaudo D, Dammassa E, Ciliberto G, Fattori E, La Monica N. (2002). Hyaluronidase increases electrogene transfer efficiency in skeletal muscle. Hum. Gene Ther., 13:355-365

Mesojednik S, Pavlin D, Sersa G, Coer A, Kranjc S, Grosel A, Tevz G, Cemazar M. (2007). The effect of the histological properties of tumors on translocation efficiency of electrically assisted gene delivery to solid tumors in mice. *Gene Ther,* 14:1261-9

Miao CH, Brayman AA, Loeb KR, Ye P, Zhou L, Mourad P, Crum LA. (2005). Ultrasound enhances gene delivery of human factor IX plasmid. *Hum Gene Ther,* 16:893-905.

Miller AM, Dean DA. (2009). Tissue-specific and transcription factor-mediated nuclear entry of DNA. Adv Drug Deliv Rev., 61:603-613

Miller AM, Dean DA. 2008. Cell-specific nuclear import of plasmid DANN in smooth muscle requires tissue-specific transcription factors and DNA sequences. Gene Ther., 15:1107-1115

Mir B, Piedrahita JA. (2004). Nuclear localization signal and cell synchrony enhance gene targeting efficiency in primary fetal fibroblasts. Nucleic Acids Res., 32:e25

Mir LM, Bureau MF, Gehl J, Rangara R, Rouy D, Caillaud JM, Delaere P, Branellec D, Schwartz B, Scherman D.(1999). High-efficiency gene transfer into skeletal muscle mediated by electric pulses. *Proc Natl Acad Sci USA,* 96:4262-7.

Molnar MJ, Gilbert R, Lu Y, Liu AB, Guo A, Larochelle N, Orlopp K, Lochmuller H, Petrof BJ, Nalbantoglu J, and Karpati G. (2004). Factors influencing the efficacy, longevity, and safety of electroporation-assisted plasmid-based gene transfer into mouse muscles. Mol Ther., 10:447-455

Netti PA, Berk DA, Swartz MA, Grodzinsky AJ, Jain RK. (2000). Role of extracellular matrix assembly in interstitial transport in solid tumors. Cancer Res., 60:2497-2503

Neumann E, Schaefer-Ridder M, Wang Y, Hofschneider PH. (1982). Gene transfer into mouse lyoma cells by electroporation in high electric fields. EMBO J, 1:841-5.

Neumann E, and Rosenheck K. (1972). Permeability changes induced by electric impulses in vesicular membranes. J Membr Biol, 10:279-90.

Newmann CMH, and Bettinger T. 2007. Gene therapy progress and prospects: Ultrasound for gene transfer. *Gene Ther,* 14:465-75.

Nicol F, Wong M, MacLaughlin FC, Perrard J, Wilson E, Nordstrom JL, and Smith LC. (2002). Poly-L-glutamate, an anionic polymer, enhances transgene expression for plasmids delivered by intramuscular injection with in vivo electroporation. Gene Ther., 9 :1351-1358

Nishikage S, Koyama H, Miyata T, Ishii S, Hamada H, Shigematsu H. (2004). In vivo electroporation enhances plasmid-based gene transfer of basic fibroblast growth factor for the treatment of ischemic limb. *J Surg Res,* 120:37-46

Payen E, Bettan M, Rouyer-Fessard P, Beuzard Y, Scherman D. (2001). Improvement of mouse β-thalassemia by electrotransfer of erythropoietin cDNA. *Exp Hemato.,* 29:295-300

Pluen A, Boucher Y, Ramanujan S, McKee TD, Gohongi T, di Tomaso E, Brown EB, Izumi Y, Campbell RB, Berk DA, Jain RK. (2001). Role of tumor-host interactions in interstitial diffusion of macromolecules: cranial vs subcutaneous tumors. Proc. Natl. Acad. Sci. USA, 98:4628-4633

Pollard H, Toumaniantz G, Amos JL, Avet-Loiseau H, Guihard G, Behr JP, Escande D. (2001). Ca2+-sensitive cytosolic nucleases prevent efficient delivery to the nucleus of injected plasmids. J Gene Med., 3:153-164

Postema M, van Wamel A, Ten Cate FJ, de Jong N. (2004) High-speed photography during ultrasound illustrated potential therapeutic applications of microbubbles. *Med Phys,* 32:3707-11.

Ribbeck K, Gorlich D. (2002). The permeability barrier of nuclear pore complexes appears to operate via hydrophobic exclusion. EMBO J., 21:2664-2671

Riera M, Chillon M, Aran JM, Cruzado JM, Torras J, Grinyo JM, Fillat C. (2004). Intramuscular SP1017-formulated DNA electrotransfer enhances transgene expression and distributes hHGF to different rat tissues. J Gene Med., 6:111-118

Rols MP, Delteil C, Golzio M, Teissie. (1998). In vivo electrically mediated protein and gene transfer in murine melanoma. *Nature Biotechnol,* 16:168-71.

Saito T, and Nakatsuji N. 2001. Efficient gene transfer into embryonic mouse brain using in vivo electroporation. *Dev Biol,* 240:237-46.

Sawamura D, Ina S, Itai K, Meng X, Kon A, Tamai K, Hanada K, Hashimoto I. (1999). In vivo gene introduction into keratinocytes using jet-injection. Gene Ther., 6:1785-1787

Scherer F, Anton M, Schillinger U, Henke J, Bergemann C, Krüger A, Gänsbacher B, Plank C. (2002). Magnetofection: enhancing and targeting gene delivery by magnetic force in vitro and in vivo. *Gene Ther,* 9:102-9.

Schertzer JD, Plant DR, Lynch GS. (2006). Optimizing plasmid-based gene transfer for investigating skeletal muscle structure and function. Mol. Ther., 13:795-803

Schwartz B, Benoist C, Abdallah B, Rangara R, Hassan A, Scherman D, Demeneix BA.(1996). Gene transfer by naked DNA into adult mouse brain. *Gene Ther,* 3:186-96.

Seksek O, Biwersi J and Verkman AS. (1997). Translational diffusion of macromolecules-sized solutes in cytoplasm and nucleus. J Cell Biol., 138:131-142.

Shibata MA, Moritomo J, and Otsuki Y. (2002). Suppression of murine mammary carcinoma growth and metastasis by HSVtk/GCV gene therapy using in vivo electroporation. *Cancer Gene Ther,* 9:16-27.

Sikes ML, O'Malley BW Jr, Finegold MJ, Ledley FD. (1994). In vivo gene transfer into rabbit thyroid follicular cells by direct DNA injection. *Hum Gene Ther,* 5:837-44.

Smith KC, Neu JC, and Krassowska W. (2004). Model of creation and evolution of stable electropores for DNA delivery. *Biophys J,* 86:2813–26.

Stamenkovic I. (2003). Extracellular matrix modelling: the role of matrix metalloproteinases. J Pathol., 200:448-464

Stein U, Walther W, Stege A, Kaszubiak A, Fichtner I, Lage H. (2007). Complete in vivo reversal of the multidrug resistance phenotype by jet-injection of anti-MDR1 short hairpin RNA-encoding plasmid DNA. Mol Ther., 16:178-186

Stephens DJ, and Pepperkok R. (2001). The many ways to cross the plasma membrane. *Proc Natl Acad Sci USA,* 98:4295-8.

Sukharev SI, Klenchin VA, Serov SM, Chernomordik LV, Chizmadzhev YuA. (1992). Electroporation and electrophoretic DNA transfer into cells. The effect of DNA interaction with electropores. *Biophys J,* 63:1320–7.

Suzuki R, Takizawa T, Negishi Y, Utoguchi N, Sawamura K, Tanaka K, Namai E, Oda Y, Matsumura Y, Maruyama K. (2008). Tumor specific ultrasound enhanced gene transfer in vivo with novel liposomal bubbles. *J Control Release,* 125:137-44.

Takehara T, Uemura A, Tatsumi T, Suzuki T, Kimura R, Shiotani A, Ohkawa K, Kanto T, Hiramatsu N, Hayashi N. (2007). Natural killer cell-mediated ablation of metastatic liver tumors by hydrodynamic injection of IFN-γ gene to mice. *Int J Cancer,* 15:1252-60.

Tarek M. (2005). Membrane electroporation: a molecular dynamics simulation. *Biophys J,* 88:4015–53.

Teissié J, Golzio M, and Rols MP. (2005). Mechanisms of cell membrane electropermeabilization: A minireview of our present (lack of ?) knowledge. *Biochim Biophys Acta,* 1724:270-80.

Tekle E, Oubrahim H, Dzekunov SM, Kolb JF, Schoenbach KH, Chock PB. (2005). Selective field effects on intracellular vacuoles and vesicle membranes with nanosecond electric pulses. *Biophys J,* 89:274–84.

Tieleman DP. 2004. The molecular basis of electroporation. *BMC Biochem,* 5:10

Titomirov, A.V., Sukharev, S., and Kistanova, E. (1991) In vivo electroporation and stable transformation of skin cells of newborn mice by plasmid DNA. Biochim Biophys Acta. 1088:131-134

Tran TA, Roger S, Le Guennec JY, Tranquart F, Bouakaz A. (2006). Effect of ultrasound-activated microbubbles on the cell electrophysiological properties. *Ultrasound Med. Biol,* 33:158-163.

Tsen SW, Wu CY, Meneshian A, Pai SI, Hung CF, Wu TC. (2009). Femtosecond laser treatment enhances DNA transfection efficiency in vivo. J. Biomed. Sci., 16:36

Vandenbroucke RE, Lucas B, Demeester J, Smedt SC, Sanders NN. (2007). Nuclear accumulation of plasmid DNA can be enhanced by non-selective gating of the nuclear pore. Nucleic Acids Research, 35:e86

Vandermeulen G, Staes E, Vanderhaeghen ML, Bureau MF, Scherman D, Préat V. (2007). Optimisation of intradermal DNA electrotransfer for immunisation. *J Control Res,* 124:81-7.

van Wamel A, Bouakaz A, Versluis M, de Jong N. 2004. Micromanipulation of endothelial cells: ultrasound-microbubble-cell interaction. *Ultrasound Med Biol,* 30:1255-8.

Vaughan EE, DeGiulio JV, and Dean DA. (2006). Intracellular trafficking of plasmids for gene therapy mechanisms of cytoplasmic movement and nuclear import. *Curr Gene Ther,* 6:671-81.

Waehler R, Russel SJ, and Curiel DT. (2007). Engineering targeted viral vectors for gene therapy. *Nature Rev Genet,* 8:573-87.

Walther W, Stein U, Fichtner I, Malcherek L, Lemm M, Schlag PM. (2001). Nonviral in vivo gene delivery into tumors using a novel low volume jet-injection technology. Gene Ther., 8:173-180

Walther W, Stein U, Fichtner I, Voss C, Schmidt T, Schleef M, Nellessen T, Schlag PM. (2002). Intratumoral low-volume jet-injection for efficient nonviral gene transfer. Mol Biotechnol., 21:105-115

Walther W, Stein U, Siegel R, Fichtner I, Schlag PM. (2005a). Use of the nuclease inhibitor aurintricarboxylic acid (ATA) for improved non-viral intratumoral in vivo gene transfer by jet-injection. J Gene Med., 7:477-485

Walther W, Stein U, Fichtner I, Kobelt D, Aumann J, Arlt F, Schlag PM (2005). Nonviral jet-injection gene transfer for efficient in vivo cytosine deaminase suicide gene therapy of colon carcinoma. Mol Ther., 12:1176-1184

Walther W, Minow T, Martin R, Fichtner I, Schlag PM, Stein U. (2006). Uptake, biodistribution, and time course of naked plasmid DNA trafficking after intratumoral in vivo jet injection. Hum Gene Ther., 17:611-624

Walther W, Siegel R, Kobelt D, Knosel T, Dietel M, Bembenek A, Aumann J, Schleef M, Baier R, Stein U, Schlag PM. (2008). Novel jet-injection technology for nonviral intratumoral gene transfer in patients with melanoma and breast cancer. Clin Cancer Res., 14:7545-7553

Wang J, Murakami T, Yoshida S, Matsuoka H, Ishii A, Tanaka T, Tobita K, Ohtsuki M, Nakagawa H, Kusama M, Kobayashi E. (2003). Predominant cell-mediated immunity in the oral mucosa: gene gun-based vaccination against infectious diseases. *J Dermatol Sci,* 31:203-10.

Wells DJ. (2004). Gene therapy progress and prospects: Electroporation and other physical methods. Gene Ther., 11:1363-1369

Widera G, Austin M, Rabussay D, Goldbeck C, Barnett SW, Chen M, Leung L, Otten GR, Thudium K, Selby MJ, Ulmer JB. (2000). Increased DNA vaccine delivery and immunigenicity by electroporation in vivo. *J Immunol,* 164:4635-40.

Wolff JA, Malone RW, Williams P, Chong W, Acsadi G, Jani A, Felgner PL. 1990. Direct gene transfer into mouse muscle in vivo. *Science,* 247:1465-8.

Xenariou S, Griesenbach U, Ferrari S, Dean P, Scheule RK, Cheng SH, Geddes DM, Plank C, Alton EW. (2006). Using magnetic forces to enhance non-viral gene transfer airway epithelium in vivo. *Gene Ther,* 13:1545-52.

Yamashita Y, Shimada M, Tachibana K, Harimoto N, Tsujita E, Shirabe K, Miyazaki J, Sugimachi K. (2002). In vivo gene transfer into muscle via electro-sonoporation. *Hum. Gene Ther.,* 13:2079-2084

Yazawa H, Murakami T, Li HM, Back T, Kurosaka K, Suzuki Y, Shorts L, Akiyama Y, Maruyama K, Parsoneault E, Wiltrout RH, Watanabe M. (2006). Hydrodynamics-based gene delivery of naked DNA coding fetal liver kinase-1 gene effectively suppresses the growth of pre-existing tumours. *Cancer Gene Ther.,* 13:993-1001.

Yoon CS, Jung HS, Kwon MJ, Lee SH, Kim CW, Kim MK, Lee M, Park JH. (2009). Sonoporation of the minicircle-VEGF(165) for wound healing of diabetic mice. Pharm. Res. 26 :794-801

Young JL, Zimmer WE, Dean DA. (2008). Smooth muscle-specific gene delivery in the vasculature based on restriction of DNA nuclear import. Exp Biol Med., 233 :840-848.

Zhang G, Gao X, Song YK, Vollmer R, Stolz DB, Gasiorowski JZ, Dean DA, Liu D. (2004). Hydroporation as the mechanism of hydrodynamic delivery. *Gene Ther,* 11:675-82.

Zhang G, Budker V, Williams P, Subbotin V, Wolff JA. (2001). Efficient expression of naked DNA delivered intraarterially to limb muscles of nonhumans primates. *Hum Gene Ther,* 12: 427-38

Zhang X, Divangahi M, Ngai P, Santosuosso M, Millar J, Zganiacz A, Wang J, Bramson J, Xing Z. (2007). Intramuscular immunization with a monogenic plasmid DNA tuberculosis vaccine: Enhanced immunogenicity by electroporation and co-expression of GM-CSF transgene. *Vaccine,* 25:1342-52

Zhou R, Dean DA. (2007). Gene transfer of interleukine 10 to the murine cornea using electroporation. Exp Biol Med., 232:362-369

Zeira E, Manevitch A, Manevitch Z, et al. (2007). Femtosecond laser: a new intradermal DNA delivery method for efficient, long-term gene expression and genetic immunization. *FASEB J,* 21:3522-33

Zeira E, Manevitch A, Manevitch Z, Kedar E, Gropp M, Daudi N, Barsuk R, Harati M, Yotvat H, Troilo PJ, Griffiths TG 2nd, Pacchione SJ, Roden DF, Niu Z, Nussbaum O, Zamir G, Papo O, Hemo I, Lewis A, Galun E. (2003). Femtosecond infrared laser – an efficient and safe in vivo gene delivery system for prolonged expression. *Mol Ther,* 8:342-50.

Zhou R, Norton JE, Zhang N, Dean DA. (2007). Electroporation-mediated transfer of plasmids to the lung results in reduced TLR9 signaling and inflammation. *Gene Ther,* 14:775-80.

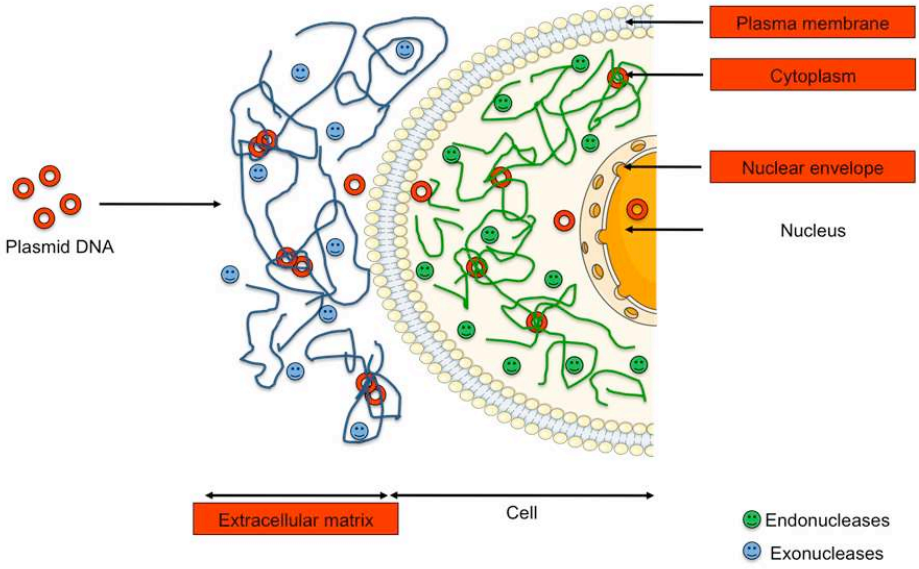

Schematic representation of biological barriers to gene transfer.
1. Extracellular matrix restricts the diffusional mobility of plasmid DNA.
2. Exonucleases degrade actively plasmid DNA.
3. Plasma membrane prevents the plasmid DNA uptake.
4. The cytoskeleton and molecular crowding restrict the diffusional mobility of plasma DNA in the cytoplasm.
5. Cytosolic endonucleases degrade actively plasmid DNA.
6.Translocation efficiency of plasmid in the nucleus is restricted by the nuclear envelope.

254x190mm (96 x 96 DPI)

Methods	DNA injection	Tissue	Mechanism	Advantages	Limitations	Future clinical applications
Local injection	Intratissue	Skin, Muscle, Tumour, Liver, Brain, Heart, Thyroid, Tendons	Pore	Simplicity, Safety	Low efficiency, Access to interne organs	Genetic vaccination
Electroporation	Topical, Intratissue	Skin, Muscle, Kidney, Lung, Liver, Joints, Heart, Spleen, Brain, Eyes, Tumour	Pore	High efficiency, Safety	Access to interne organs	Genetic vaccination, Cancer gene therapy
Sonoporation	Topical, Systemic	Muscle, Liver, Heart, Tumour, Bone	Pore	Good efficiency, Safety	Transfection efficiency	Cardivascular diseases, Cancer gene therapy
Hydrodynamic injection	Systemic, Intravascular	Liver, Muscle	Pore	High efficiency, Safety	Translation to human body	Genetic vaccination, Cancer gene therapy
Gene gun	Topical	Skin, Mucosa	Membrane disruption	Good efficiency, Safety	Weak tissue penetration, Fate of particle	Genetic vaccination
Laser beam gene transduction	Topical	Skin, Muscle	Pore	Good efficiency	Weak tissue penetration	Genetic vaccination
Magnetofection	Topical	Gastrointestinal tract, Vasculature of ear, Airway epithelium	Endocytosis, Membrane disruption	High efficiency in vitro	Low efficiency in vivo, Fate of particle, Safety	Cancer gene therapy
Jet-Injection	Topical, Intratissue	Skin, Muscle, Tumour	Membrane disruption	High efficiency, Safety	Access to interne organs	Genetic vaccination, Cancer gene therapy
Plasma	Topical	Skin	Membrane disruption	Low efficiency	Weak tissue penetration	Genetic vaccination

Table 1

Characteristics of physical gene delivery systems.

THE JOURNAL OF GENE MEDICINE
J Gene Med 2010; **12**: 117–125.
Published online 25 November 2009 in Wiley InterScience (www.interscience.wiley.com) **DOI:** 10.1002/jgm.1414

RESEARCH ARTICLE

Electro-mediated gene transfer and expression are controlled by the life-time of DNA/membrane complex formation

Cécile Faurie[1,2,4]
Matej Rebersek[3]
Muriel Golzio[1,2]
Masa Kanduser[3]
Jean-Michel Escoffre[1,2]
Mojca Pavlin[3]
Justin Teissie[1,2]
Damijan Miklavcic[3]
Marie-Pierre Rols[1,2]*

[1]*CNRS, Institut de Pharmacologie et de Biologie Structurale, Toulouse, France*

[2]*Université de Toulouse, UPS, Institut de Pharmacologie et de Biologie Structurale, Toulouse, France*

[3]*University of Ljubljana, Faculty of Electrical Engineering, Ljubljana, Slovenia*

[4]*Present address: Centre de Référence des Pathologies Plaquettaires – Plateforme Technologique d'Innovation Biomédicale, Hôpital Xavier Arnozan, Pessac, France*

*Correspondence to:
Marie-Pierre Rols, Institut de Pharmacologie et de Biologie Structurale-CNRS UMR 5089, 205 route de Narbonne 31077, Toulouse, France. E-mail: marie-pierre.rols@ipbs.fr

Received: 22 June 2009
Revised: 21 August 2009
Accepted: 7 October 2009

Abstract

Background Electroporation is a physical method used to transfer molecules into cells and tissues. Clinical applications have been developed for antitumor drug delivery. Clinical trials of gene electrotransfer are under investigation. However, knowledge about how DNA enters cells is not complete. By contrast to small molecules that have direct access to the cytoplasm, DNA forms a long lived complex with the plasma membrane and is transferred into the cytoplasm with a considerable delay.

Methods To increase our understanding of the key step of DNA/membrane complex formation, we investigated the dependence of DNA/membrane interaction and gene expression on electric pulse polarity and repetition frequency.

Results We observed that both are affected by reversing the polarity and by increasing the repetition frequency of pulses. The results obtained in the present study reveal the existence of two classes of DNA/membrane interaction: (i) a metastable DNA/membrane complex from which DNA can leave and return to external medium and (ii) a stable DNA/membrane complex, where DNA cannot be removed, even by applying electric pulses of reversed polarity. Only DNA belonging to the second class leads to effective gene expression.

Conclusions The life-time of DNA/membrane complex formation is of the order of 1 s and has to be taken into account to improve protocols of electro-mediated gene delivery.

Keywords electroporation; gene delivery; electric field; pulse repetition frequency; electropermeabilization; membrane

Introduction

The cell plasma membrane acts as a selective barrier that regulates the exchange of molecules between the cell and the external medium. Therefore, the delivery of therapeutic molecules such as DNA into living cells and tissues represents an outstanding challenge in molecular biology and medicine. Delivery can be achieved using biological vectors such as viruses or using chemical approaches. However, the use of these methods in the field of gene therapy is limited because of their lack of efficiency and/or safety [1]. A physical approach, electropermeabilization also named electroporation,

was introduced in the 1970s and was subsequently developed in the 1980s for gene delivery [2]. This method has been used with increasing popularity [3–6]. Applications have been successfully developed for antitumor drug delivery [7–9] and the transfer of genes [4,10–14]. Electrochemotherapy is accepted in a number of countries as a palliative treatment and clinical trials of gene electrotransfer are under investigation [15–18]. A phase I dose escalation trial of plasmid interleukin electroporation was carried out in patients with metastatic melanoma. Biopsies showed plasmid dose proportional increases in interleukin-12 protein levels as well as marked tumor necrosis and lymphocytic infiltrate, indicating that this modality is safe, effective and titrable [19].

Despite numerous studies, much remains unknown about the basic mechanisms of how DNA enters cells [20]. Several theoretical models postulate that DNA crosses the plasma membrane during electric pulse application through 'electropores' [2,21–23]. However, such models are not supported by experimental data [24,25]. They necessitate the creation of pores that have never experimentally been observed. Performed at the single cell level, studies have yielded a phenomenological description of gene electrotransfer. Small and large molecules enter the cell through well-defined permeabilized caps of the plasma membrane. Small molecules enter the cell across part of the membrane facing the two electrodes via the concentration gradient difference between the exterior and cell interior by a diffusion process [26–28]. By contrast, the introduction of DNA only occurs in the part of the membrane facing the cathode and requires a number of consecutive steps: electrophoretic migration of DNA towards the cell, DNA insertion into the membrane, translocation across the membrane, migration of DNA towards the nucleus and, finally, transfer of DNA across the nuclear envelope [29–32]. Therefore, DNA does not enter into the cell during electric pulses but it is 'trapped into' the plasma membrane. Its presence inside the cytoplasm is only detected several minutes after pulse application [33]. The electric field induces a key reaction between the membrane under the electrical stress and the DNA, which is electrophoretically accumulated at the interface, leading to its insertion [29,34–36]. The present study aimed to characterize the interaction of the DNA with the membrane. Indeed, the plasmid DNA has two possibilities: either to penetrate into the cell or to return into the bulk [29]. However, in our previous model [33], the plasmid was assumed to move only towards the cytoplasm, and we therefore changed the electric field orientation to evaluate the role of the electropermeabilized caps and the DNA electrophoretic migration [37]. This was achieved by studying, at the single cell membrane level, the role of the electromigration of plasmid DNA towards (or from) the membrane, as well as the kinetics of DNA interaction with the membrane during the process of its entrance into the cells. We have designed experiments where the direction of electric field could be alternated in a way that each consecutive pulse was delivered with reversed polarity. If the interaction of the DNA with the cell membrane is transient, it must be affected by changing the pulse polarity at various pulse repetition frequencies. Quantitative observations of DNA/membrane interactions were made as a function of pulse polarity and repetition frequency. The results obtained support the existence of two classes of DNA interaction with the plasma membrane: one leading to a metastable DNA/membrane complex from which the DNA can escape and go back to external medium and the other leading to a stable DNA/membrane complex, where the plasmid cannot be removed, even by applying electric pulses of reversed polarity. These results have to be taken into account for protocols of electro-mediated gene delivery.

Materials and methods

Cells

Chinese hamster ovary (CHO) cells were used. The WTT clone was selected for its ability to grow in suspension or plated on Petri dishes or on microscope glass cover slip. They were grown in minimal essential medium as previously described [37]. Their ability to grow on a support after being maintained in suspension comprises direct evidence of their viability.

Plasmid

A 4.7-kb plasmid (pEGFP-C1) carrying the green fluorescent protein (GFP) gene controlled by the cytomegalovirus promoter was obtained from Clonetech (Palo Alto, CA, USA). It was purified from *Escherichia coli* transfected cells using the Maxiprep DNA purification system according to the manufacturer's instructions (Qiagen, Courtaboeuf, France). This plasmid was used both for the direct visualization at the single cell level of its electrotransfer into the cells (by labeling as shown below) and for gene expression.

Electropulsation

Electropulsation was performed using a new system of electroporator developed at the University of Ljubljana. This electroporator delivers between one and 32 square-wave electric pulses of 80–400 V amplitude, with a duration of 10 s to 1 ms, and a pulse repetition frequency in the range 0.1–5000 Hz. A particularity of this electroporator is an embedded electrode commutator. This commutator applies one of three possible states to each of the electrodes: positive, negative or high impedance state; thus, the electric field direction between the electrodes can be changed. Electrode state change is accomplished within 12 ms. Therefore, for bipolar pulses lasting 1 ms,

DOI: 10.1002/jgm

the maximum repetition frequency, corresponding to the minimum time required for switching the electrodes, is 76.9 Hz. The electrodes were designed as cylindrical rods made of stainless steel allowing delivery of electric field in different directions and, at the same time, providing a relatively homogeneous electric field distribution [38]. In the present study, two opposite electrodes, 5 mm apart (diameter 3.5 mm), were used for the delivery of either unipolar or bipolar pulses. Six electric pulses lasting 1 ms were applied at 0.8 kV/cm; these parameters allowed high permeabilization and transfection efficiencies at the same time as preserving cell viability.

Electropermeabilization

Cells in suspension were centrifuged for 5 min at 120 *g* and resuspended in 100 l of pulsing buffer (10 mM K_2HPO_4/KH_2PO_4 buffer, 1 mM $MgCl_2$, 250 mM sucrose, pH 7.4) at a 0.5×10^6 cells/ml cell density.

Penetration of propidium iodide (100 M, in pulsing buffer) was used to monitor permeabilization. Six unipolar or bipolar rectangular pulses lasting 1 ms at various repetition frequencies were applied at 400 V amplitude (e.g. at a 800 V/cm voltage to distance ratio) at room temperature. Accordingly, cells that had already been pulsed were diluted in 1 ml of phosphate-buffered saline (PBS) buffer and analysed 10 min after the application of pulses by flow cytometry (Becton Dickinson FACScan; Becton-Dickinson Biosciences, Franklin Lakes, NJ, USA) to determine both the percentage of fluorescent cells (i.e. the percentage of permeabilized cells) and the level of fluorescence associated with this permeabilization (i.e. the efficiency of permeabilization). In all experiments, cells treated exactly the same way apart from being exposed to electric pulses were used as control cells. Cells were resuspended in 1 ml of buffer and analysed by flow cytometry, gating with the scatters (forward scatter and side scatter) to exclude debris. The excitation wavelength was 488 nm (argon laser) and the fluorescence of intracellular propidium iodide was collected in FL-2 channel (bandpass 585 ± 42 nm). A minimum of 5×10^3 events were acquired in list mode and analysed with Cellquest software (Becton Dickinson).

Cell viability

Viability was measured by quantifying the growth of cells over more than one generation after application of electric pulses (approximately 24 h) as previously described [37]. Briefly, cells were pulsed as above in absence of propidium iodide and kept for 10 min at room temperature, with the delay allowing the membrane to become impermeable again. They were then cultured on Petri dish with 2 ml of culture medium. Viability was measured by quantifying the number of cells over 24 h after electropulsation (more than one generation) by crystal violet staining.

Electrotransfection

Cells in suspension were centrifuged for 5 min at 120 *g* and resuspended in 100 l of plasmid DNA containing pulsing buffer at a 0.5×10^6 cells/ml density. For each condition, 4 g of pEGFP-C1 plasmid was used. As in the electropermeabilization protocol, six unipolar or bipolar rectangular pulses lasting 1 ms at various repetition frequencies were applied at a 400 V amplitude (800 V/cm voltage to electrode distance ratio) at room temperature. Cells were incubated for 10 min at room temperature and cultured in Petri dish with 2 ml of culture medium at 37 °C in a 5% CO_2 incubator. Twenty-four hours later, the cell monolayer was washed with PBS to remove all non-adherent cells. Cells were harvested by trypsinization, resuspended in 1 ml of PBS and analysed by flow cytometry to evaluate both the percentage of fluorescent cells (i.e. the percentage of GFP expressing cells) and the mean level of fluorescence associated with GFP expressing cells (i.e. the efficiency of gene expression). The excitation wavelength was 488 nm (argon laser) and the fluorescence of GFP was collected in FL-1 channel (bandpass 520 ± 42 nm). A minimum of 5×10^3 events were acquired in list mode and analysed with Cellquest software (Becton Dickinson).

DNA staining

Plasmid pEGFP-C1 was stained stoichiometrically with the DNA intercalating thiazole orange homodimer dye TOTO-1. The pEGFP-C1 plasmid was stained with TOTO-1 dye at a DNA concentration of 1 g/ l for 60 min on ice. The TOTO-1 concentration was 2.3×10^{-4} M, yielding an average base pair to dye ratio of 5 [33]. TOTO-1 was obtained from Molecular Probes (Eugene, OR, USA).

Microscopy

For on line microscopic observations, an electropulsation chamber was designed using the electrodes in contact with a microscope glass coverslip chamber (Lab-Tek I system; Nunc I1, Dutsher SA, Brumath, France). The electrodes were connected to the voltage generator. The chamber was placed on the stage of an inverted digitized video microscope (DMIRB; Leica, Wetzlar, Germany). Cells were observed with a Leica ×100, 1.3 NA oil immersion objective. The wavelengths were selected using the Leica L4 filter block ($450 \text{ nm} \leq \lambda_{ex} \leq 490$ nm; dichromatic mirror pass band: $515 \text{ nm} \leq \lambda_{em} \leq 560$ nm) for the TOTO-1-labeled DNA. Images were recorded with the CELLscan System from Scanalytics (Billerica, MA, USA) equipped with a Photometrics cooled charge-coupled device camera (Princeton Research Instruments, Inc., Princeton, NJ, USA) [33]. This digitizing set up allowed a quantitative localized analysis of the fluorescence emission along the cell membrane. Plot histograms

DOI: 10.1002/jgm

detected local increase above the background level outside of the cells. Two characteristic parameters were used: the peak intensity and the integral under the peak. Both were directly related to the number of fluorescent molecules locally present. The light haze contributed by fluorescent-labeled structures located above and below the plane of optimal focus was mathematically reassigned to its proper places origin (Exhaustive Photon Reassignment EPR software; Scanalytics) after accurate characterization of the blurring function of the optical system [33].

Statistical analysis

Errors bars represent the standard error of the mean. The statistical significance of differences between the means of unipolar and bipolar was evaluated by an unpaired Student's *t*-test. All statistics tests were two sided (NS, not significant; $^{*}p < 0.05$; $^{**}p < 0.01$; $^{***}p < 0.005$).

Results

We analysed the effect of electric pulses polarity and repetition frequency on membrane permeability, gene transfer and expression by affecting the DNA plasma membrane interaction. Cells were pulsed under electric field conditions of strength, number and duration that were known from previous studies to lead to efficient gene expression [37,39]. The use of the new square-wave pulse generator [38] made it possible to deliver repeated pulses at various frequencies with normal or reversed polarities (i.e. unipolar or bipolar pulses, respectively).

In the present study, we compared the effect of a train of six unipolar or bipolar rectangular electrical pulses lasting 1 ms delivered with a delay between pulses varying from 12 ms to 10 s (corresponding to a pulse repetition frequency of 76.9 Hz to 0.1 Hz, respectively).

Effect of pulse repetition frequency on membrane permeabilization

The results obtained regarding the uptake of propidium iodide into cells submitted to unipolar or bipolar electric pulses as a function of repetition frequency are shown in Figure 1. The percentage of permeabilized cells was not affected when frequency of pulse repetition was increased, regardless of the polarity used (unipolar or bipolar) (Figure 1A). Almost 80% of cells were propidium iodide positive (i.e. permeabilized).

The associated fluorescence intensity, related to the number of molecules incorporated into the electropermeabilized cells, was not dramatically affected. Indeed, it only slightly decreased above 1 Hz under unipolar conditions, whereas it did not significantly change under bipolar conditions (Figure 1B).

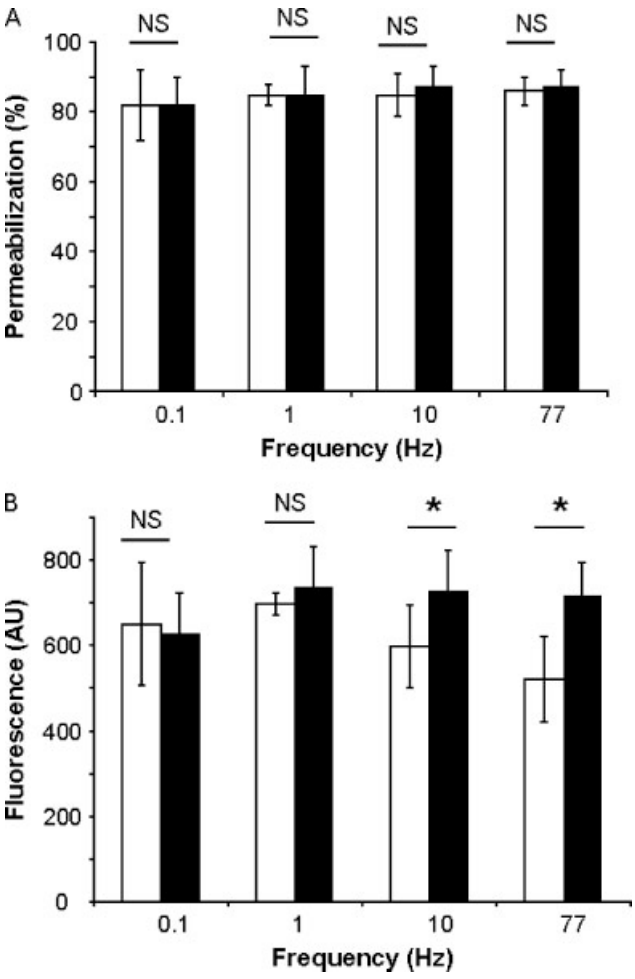

Figure 1. Effect of unipolar and bipolar pulse frequency on CHO cell permeabilization. (A) Percentage of permeabilized cells. (B) Mean fluorescence intensity associated with pulsed cells. Train of six pulses of 1 ms in duration at 400 V were applied as a unipolar (white symbol) and bipolar train (black symbol) to cells in pulsing buffer containing propidium iodide. Permeabilization was quantified by flow cytometry

Effect of pulse repetition frequency on cell viability

Cell viability was decreased when increasing the pulse repetition frequency, regardless of whether the pulses in the train were unipolar or bipolar (Figure 2). Under unipolar conditions, 60% of cells were viable at 0.1 Hz, although this percentage decreased to 25% of survival at 10 Hz to reach a plateau. The same profile was observed under bipolar conditions. No significant difference was observed between unipolar and bipolar conditions.

Effect of pulse repetition frequency on DNA/membrane interaction

Videomicroscopy at the single cell level offers direct access to the early events of DNA transfer across the electropermeabilized membrane. Images of DNA/membrane

DOI: 10.1002/jgm

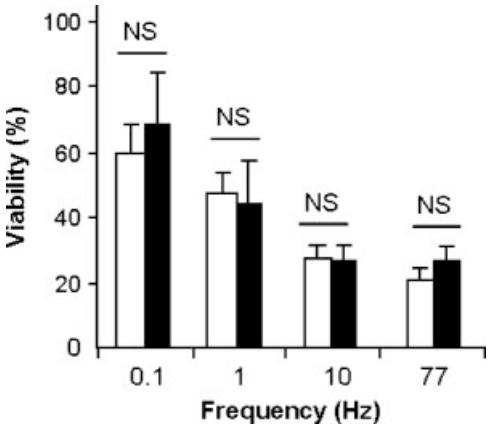

Figure 2. Effect of unipolar and bipolar pulse frequency on CHO cell viability. Train of six pulses of 1 ms in duration was applied at 400 V to cells. Cell survival was assessed by cristal violet staining 24 h after electropulsation. White symbols, unipolar conditions; black symbols, bipolar conditions

interactions were obtained by fluorescence microscopy with the TOTO-1 fluorescent-labeled plasmid DNA in the minutes after pulse application. As previously described [33], and as shown in Figure 3, DNA interacted as 'aggregates' only with the electropermeabilized part of the membrane facing the cathode under unipolar conditions. In bipolar conditions, DNA interacted on both sides of the cell surface facing the electrodes [37]. DNA does not enter the cell during electric pulses but it is 'trapped into' the membrane. Its presence inside the cytoplasm is only detected minutes after pulses delivery. Therefore, the interaction of plasmid DNA at the membrane level can be quantified. Moreover, as shown in Figure 3, the amount of DNA interacting with the membrane varied according to the pulse repetition frequency. The quantitative analysis of micrographs obtained under unipolar and bipolar conditions was performed as reported in Figure 4. Two distinct pieces of information were obtained: the percentage of positive cells (corresponding to the cells that DNA interacted with) and the fluorescence intensity (corresponding to the mean amount of DNA interacting with cells). Forty-seven percent of cells were positive under 0.1 Hz unipolar conditions. When increasing the frequency, this percentage increased by a factor of two to reach 92% at 10 Hz and decreased to 80% for higher frequencies. At the same time, a quantitative fluorescence analysis was performed to determine the quantity of DNA interacting with the permeabilized membrane. The mean fluorescence increased with increase in frequency up to a factor of four. However, under bipolar conditions, the percentage of cells interacting with DNA decreased from 78% to 40% (a factor of two) when the pulse repetition frequency was larger than 1 Hz. Under those bipolar conditions, the fluorescence slightly increased from 0.1 Hz to 10 Hz and then decreased with further increases in pulse repetition frequency.

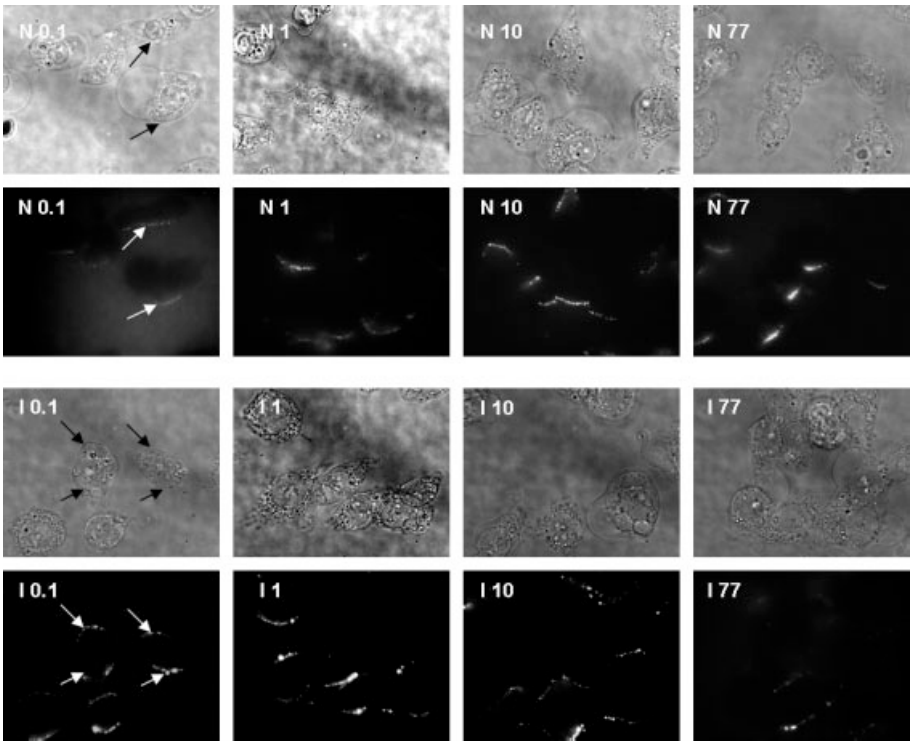

Figure 3. Effect of pulse polarities on DNA/membrane interaction. CHO cells were incubated in the presence of TOTO-1-labeled DNA (pEGFP-C1) in the pulsing buffer. Six pulses of 1 ms in duration at 400 V were applied to cells for unipolar and bipolar pulses sequences at a 0.5 Hz pulse repetition frequency. The time exposure of the camera was set at 1 s. Images of cells where DNA interacts with are given under phase contrast and fluorescence for different pulse frequencies (i.e. 0.1, 1, 10 and 77 Hz). N, normal conditions; I, inverted conditions. White arrows show DNA/membrane complexes, black arrows show the corresponding areas under phase contrast

DOI: 10.1002/jgm

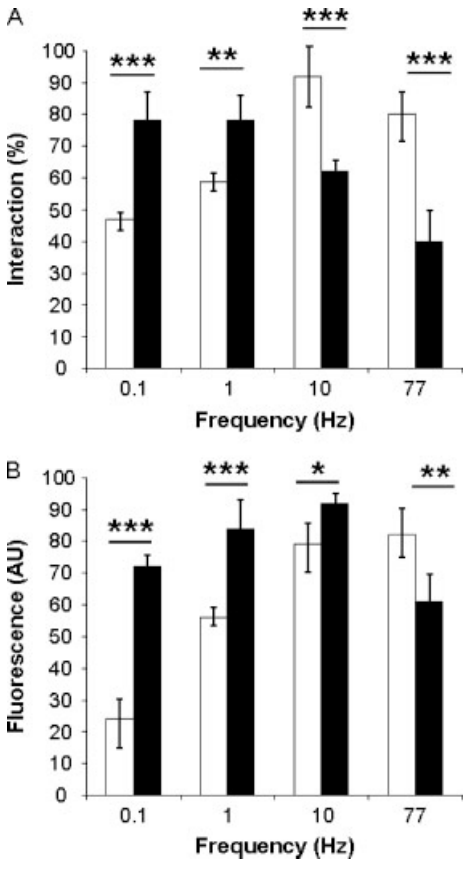

Figure 4. Effect of pulse polarities on DNA/membrane interaction. CHO cells were incubated in the presence of TOTO-1-labeled DNA (pEGFP-C1) in the pulsing buffer. Six pulses of 1 ms in duration at 400 V were applied to cells for unipolar and bipolar pulses sequences at a 0.5 Hz pulse repetition frequency. The time exposure of the camera was set at 1 s. Percentage of cells where DNA interacts with (A) as well as the mean fluorescence level of labeled DNA associated with their membrane (B) were quantified. White symbols, unipolar conditions; black symbols, bipolar conditions

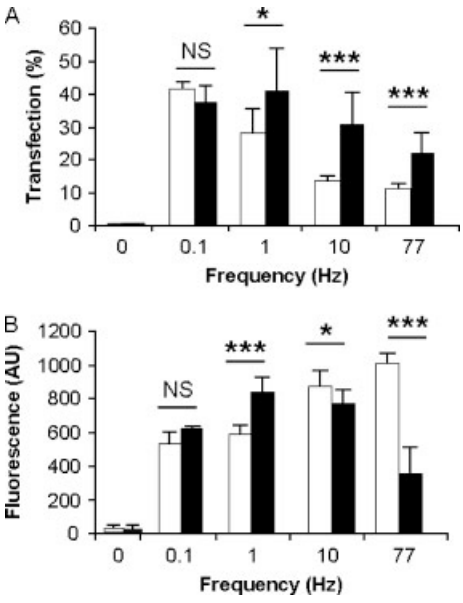

Figure 5. Effect of a train of unipolar and bipolar pulses with a different repetition frequency on CHO cell gene expression. (A) Percentage of electrotransfected cells. (B) Associated mean fluorescence level of GFP expressing cells. Six pulses of 1 ms in duration were applied at 400 V to cells in pulsing buffer containing a plasmid coding for the GFP reporter gene. GFP expression was detected 24 h after electric treatment by flow cytometry. White symbols, unipolar conditions; black symbols, bipolar conditions

Effect of pulse repetition frequency on gene expression

Gene expression was accessed by using a plasmid carrying the GFP gene. The results of GFP expression, measured 24 h after pulse application, in cells submitted to electric pulses of the same or reversed polarity as a function of repetition frequency are shown in Figure 5. The percentage of transfected cells was 40% at 0.1 Hz under unipolar conditions (Figure 5A). The increase of pulse repetition frequency significantly decreased the percentage of transfected cells to 10% at 77 Hz. The same profile was observed under bipolar conditions, with approximately 40% of transfected cells at 0.1 Hz and a slight but significant decrease to 25% at 77 Hz (Figure 5A).

The associated fluorescence intensity, related to the level of GFP expression in the electrotransfected cells, has a more complex behaviour (Figure 5B). With respect to a pulse repetition frequency larger then 1 Hz, the GFP expression was observed to increase up to two times under unipolar conditions (Figure 5B). Under bipolar conditions, however, pulse repetition frequency values of approximately 1 Hz appear to be optimal for the gene expression. Outside this apparent optimum (i.e. pulse repetition frequencies higher or lower than 1 Hz), GFP expression was decreased (Figure 5B).

Discussion

To be of use clinically, gene delivery methods have to be safe and efficient. For that, it is a necessity to be able to control each step of the DNA delivery process. Electroporation shows promise in that field because proofs of concept of its *in vivo* use and, more recently, of its first clinical trial have been published [12,19,40]. The method is safe because DNA is specifically delivered to the cells and organs in between the electrodes. However, compared to viral methods, it is less efficient because higher quantities of plasmid DNA are required. To better understand the mechanism involved in electro-mediated DNA transport across the cell membrane, and therefore to improve efficiency of the method, we designed experiments where the direction of the electric field was reversed between each consecutive electric pulse that was applied. The electric field was thus either delivered in a single direction (unipolar conditions), or its direction was reversed between consecutive pulses (bipolar conditions). The pulses were delivered (and the polarity changed in bipolar conditions) with different delays between pulses

DOI: 10.1002/jgm

by varying pulse repetition frequencies, so that we were able to experimentally determine the characteristic time of DNA plasma membrane association and the consequences in gene expression. Electric pulse parameters (i.e. pulse intensity, number and duration) were chosen in a regime where both membrane permeabilization (Figure 1) and cell viability (Figure 2) were not significantly affected by the pulse polarities. Indeed, under these experimental conditions, 80% of cells were permeabilized irrespective of the pulse repetition frequency. The cell viability decreased with an increasing pulse repetition frequency, in agreement with previous studies [41].

Under unipolar conditions, increasing the pulse repetition frequency (i.e. decreasing the delay between electric pulses) directly enhances the amount of DNA interacting with electropermeabilized membrane (Figure 4B). This increase was directly correlated with an increase in gene expression (Figure 5B), showing a direct relationship between the two phenomena. However, as far as the percentage of cells is concerned, the data appear to be contradictory. It would be expected that an increase in the number of cells with DNA interacting with the membrane would have a higher number of transfected cells. However, as shown Figure 4A, even if the number of cells increased with pulse frequency up to 10 Hz, the number of cells that expressed the reporter gene decreased with pulse frequency (Figure 5A). These results are a direct illustration of the complexity of gene delivery phenomena. If DNA interaction with the membrane is a necessary condition to obtain gene expression, it is not a sufficient condition. One possible explanation to explain these data is the loss in cell viability. Cell viability was indeed shown to decrease by increasing the pulse repetition frequency (Figure 2) as a direct effect of electric field application. Moreover, under given pulses parameters, this can also be the result of a high number of DNA molecules interacting with the membrane and/or entering cells; the toxicity of DNA in electroporated cells has been previously shown to be concentration-dependent [42].

Under bipolar conditions, the effects of pulse repetition frequency are biphasic: (i) for frequencies below 1 Hz, the same effects as those observed under unipolar conditions were observed, but (ii) for frequencies above 1 Hz, the opposite effects were observed. Namely, under bipolar conditions, increasing the pulse repetition frequency (and decreasing the delay between pulses) and pulse inversion resulted in a reduction of the quantity of DNA interacting with the membrane (Figure 4B), which was also accompanied by a decrease in gene expression (Figure 5B), but still showing a direct correlation between the two phenomena. Moreover, in that case, there was a fair agreement between the percentage of cells with DNA interacting with the membrane (Figure 4A) and expressing GFP (Figure 5A) and the efficiencies (Figures 4B and 5B). All these data can be interpreted by considering that, under bipolar conditions, a short delay between pulses (i.e. high pulse repetition frequency) prevents the formation of a stable DNA/membrane complex by uncoupling DNA with the membrane, leading to a decrease in gene expression. The results obtained show that a delay of approximately 1 s, corresponding to the breaking point of the curve, is necessary for DNA to form this stable complex with the membrane. This delay indeed varies from 0.1 s to 1 s (i.e. 10 Hz and 1 Hz as shown in Figure 4B and Figures 4A, 5A and 5B, respectively).

From a mechanism point of view, the present stusy provides new insight into the mechanisms of DNA electrotransfer by addressing one of the key steps of the process, namely DNA/membrane complex formation. It demonstrates the existence of two classes of DNA/membrane interactions: (i) a metastable DNA/membrane complex from which the DNA can leave and return to external medium as a result of electrophoretic stress (caused by the reversal of the electric field direction within less than 1 s after the previous pulse) and (ii) a stable DNA/membrane complex, where the plasmid cannot be removed even by applying electric pulses of reversed polarity. Only DNA belonging to the second class may be effective for gene expression. This suggest the formation of anchoring points/structures within the cell surface, allowing DNA not to be desorbed to form the stable complex with the membrane. DNA takes an order of seconds to become trapped in them. Electro-mediated gene transfer and expression can therefore be described as a complex process with different successive steps, with time scales that can be considered to range from s to days (Table 1).

Table 1. Kinetics of the different steps involved in DNA electro-mediated delivery into cells

Time scale	Steps involved in DNA electro-mediated delivery	Reference
Microsecond*	Plasma membrane permeabilization	Kinosita and Tsong (1979) Neumann *et al*. [2]
Millisecond*	Electrophoretic migration of DNA towards the membrane DNA/membrane complex formation	Wolf *et al*. [29] Hristova *et al*. [32] Golzio *et al*. [33]
Second	Conversion of the metastable form of the DNA/membrane complex to a stable one	Present study
Minute	DNA translocation/diffusion across the membrane	Eynard *et al*. [35]
Hour	DNA migration towards the nucleus	Bertling *et al*. (J Biochem Biophys Methods, 1987)
Day	Gene expression	Rols and Teissié (Biophys J, 1998) Kubiniec *et al*. [39]

*Electric field applied.

DOI: 10.1002/jgm

These data highlight the role of plasmid DNA migration towards the membrane and the importance of designing pulse parameters for electric field-mediated gene delivery applications. It is possible that, when keeping all the pulse parameters constant, pulse duration and number, as well as pulse intensity, alter gene expression. Gene expression will be improved by increasing the number of interaction sites between plasmid DNA and the cell membrane. This can be carried out either by applying electric pulses of reversed polarity or by changing electric field direction [38]. However, the delay between pulses (i.e. pulse repetition frequency) will have to be carefully chosen to insure DNA/membrane complex formation. Optimization of the electric pulses parameters (direction, frequency) has already demonstrated an improvement of the electroporation method in the field of its clinical applications. For example, in electrochemotherapy experiments, reversing the pulse polarity and changing the electric field orientation was associated with an improvement of tumor eradication [43,44]. Because a train of electric pulses with repetition frequency of 1 Hz is usually applied to the tumors, each pulse in the train excites the underlying nerves and provokes muscle contractions. Therefore, for patients involved in electrochemotherapy, the use of pulses with a repetition frequency higher than the frequency of tetanic contraction would represent a reduced number of muscle contractions and the associated unpleasant sensations [45]. Indeed, this is what is presently carried out, as reported in a recent clinical study [46] that supports the results of the ESOPE study [47] where 5 kHz repetition frequency of electric pulses were used. Electrochemotherapy also gives excellent results in veterinary medicine [48]. A very recent study performed on dogs confirms that electroconvulsive threapy comprises an easy, effective and safe local treatment for tumors. It represents an alternative treatment to surgery, specifically for smaller nodules in which a complete response with long duration can be obtained after only one treatment session, or when the nodule is unresectable because of the location [49]. The possibilities for the clinical use of pulses with a high repetition frequency in electro-mediated gene transfer and expression are now considered. However, as far as the DNA electrotransfer process is concerned, the data obtained in the present study demonstrate that the frequency of the pulses when applied under inverted polarities should be carefully adjusted to lead to efficient gene expression. Moreover, as shown in the present study, the correlation between the percentage of transfected cells and the efficiency of expression (i.e. level of expression) can be highly affected by electric field parameters, depending on the way that the electric pulses (polarity, frequency) are applied and most likely also on the amount of electrotransfered plasmid DNA. The DNA concentration has to be adjusted to lead to a high expression level without any severe cell damage. Once again, the DNA concentration will have to be adjusted to each cell type and tissue. For gene therapy applications, one therefore has to optimize the electrotransfer method to favor either the percentage of positive cells and/or the amount of gene expression. Accordingly, a reporter gene such as GFP is a convenient method that can be used *in vivo* in combination with more global detection such as Luciferase activity [50]. This will be particularly important in tissues where new constraints are present, such as the high cell density and the environment of cells in specific organs. One can expect that, in the near future, by improving our knowledge of all the steps involved in DNA electrotransfer, which comprises a process that is more complex than simply pushing DNA through electropores, we will be able to define new protocols (based on a refinement of electric pulses parameters) that will lead not only to a safer method, but also one of the more efficient gene therapy protocols.

Acknowledgements

This work was supported by grants from the Fondation pour la Recherche Médicale to C.F.; from the International Exchange from the Paul Sabatier University in Toulouse to C.F. and M.P.R.; from the Association Française contre les Myopathies (AFM) to M.P.R.; from the region Midi Pyrenees to J.T.; from the French-Slovenian Scientific Cooperation (PROTEUS and PICS Programs) to D.M. and J.T.; and from the Slovenian Research Agency (ARRS) to D.M., M.R. and M.P. The authors want to thank Claire Millot (IPBS, Toulouse, France) for her help with the cell culture and David S. Dean (LPT, Toulouse, France) for his helpful comments on the manuscript.

References

1. Hacein-Bey-Abina S, *et al*. Sustained correction of X-linked severe combined immunodeficiency by ex vivo gene therapy. *N Engl J Med* 2002; **346**: 1185–1193.
2. Neumann E, *et al*. Gene transfer into mouse lyoma cells by electroporation in high electric fields. *EMBO J* 1982; **1**: 841–845.
3. Heller LC, Heller R. In vivo electroporation for gene therapy. *Hum Gene Ther* 2006; **17**: 890–897.
4. Cemazar M, *et al*. Electrically assisted nucleic acids delivery to tissues in vivo: where do we stand? *Curr Pharm Des* 2006; **12**: 3817–3825.
5. Gehl J. Electroporation: theory and methods, perspectives for drug delivery, gene therapy and research. *Acta Physiol Scand* 2003; **177**: 437–447.
6. Giraud P, *et al*. Effects of electrochemotherapy on cutaneous metastases of human malignant melanoma. *Int J Radiat Oncol Biol Phys* 1996; **36**: 1285.
7. Mir LM, *et al*. Effective treatment of cutaneous and subcutaneous malignant tumours by electrochemotherapy. *Br J Cancer* 1998; **77**: 2336–2342.
8. Belehradek M, *et al*. Electrochemotherapy, a new antitumor treatment. First clinical phase I–II trial. *Cancer* 1993; **72**: 3694–3700.
9. Rols MP, Tamzali Y, Teissie J. Electrochemotherapy of horses. A preliminary clinical report. *Bioelectrochemistry* 2002; **55**: 101–105.
10. Titomirov AV, Sukharev S, Kistanova E. In vivo electroporation and stable transformation of skin cells of newborn mice by plasmid DNA. *Biochim Biophys Acta* 1991; **1088**: 131–134.
11. Heller R, *et al*. In vivo gene electroinjection and expression in rat liver. *FEBS Lett* 1996; **389**: 225–228.
12. Rols MP, *et al*. In vivo electrically mediated protein and gene transfer in murine melanoma. *Nat Biotechnol* 1998; **16**: 168–171.
13. Aihara H, Miyazaki J. Gene transfer into muscle by electroporation in vivo. *Nat Biotechnol* 1998; **16**: 867–870.

14. Mir LM, *et al*. High-efficiency gene transfer into skeletal muscle mediated by electric pulses. *Proc Natl Acad Sci USA* 1999; **96**: 4262–4267.
15. Gehl J. Electroporation for drug and gene delivery in the clinic: doctors go electric. *Methods Mol Biol* 2008; **423**: 351–359.
16. Giardino R, *et al*. Electrochemotherapy a novel approach to the treatment of metastatic nodules on the skin and subcutaneous tissues. *Biomed Pharmacother* 2006; **60**: 458–462.
17. Sersa G, *et al*. Electrochemotherapy in treatment of tumours. *Eur J Surg Oncol* 2008; **34**: 232–240.
18. Spugnini EP, *et al*. Potential role of electrochemotherapy for the treatment of soft tissue sarcoma: first insights from preclinical studies in animals. *Int J Biochem Cell Biol* 2008; **40**: 159–163.
19. Daud AI, *et al*. Phase I trial of interleukin-12 plasmid electroporation in patients with metastatic melanoma. *J Clin Oncol* 2008; **26**: 5896–5903.
20. Teissie J, Golzio M, Rols MP. Mechanisms of cell membrane electropermeabilization: a minireview of our present (lack of?) knowledge. *Biochim Biophys Acta* 2005; **1724**: 270–280.
21. Sukharev SI, *et al*. Electroporation and electrophoretic DNA transfer into cells The effect of DNA interaction with electropores. *Biophys J* 1992; **63**: 1320–1327.
22. de Gennes PG. Passive entry of a DNA molecule into a small pore. *Proc Natl Acad Sci USA* 1999; **96**: 7262–7264.
23. Krassowska W, Filev PD. Modeling electroporation in a single cell. *Biophys J* 2007; **92**: 404–417.
24. Kennedy SM, *et al*. Quantification of electroporative uptake kinetics and electric field heterogeneity effects in cells. *Biophys J* 2008; **94**: 5018–5027.
25. Gowrishankar TR, Weaver JC. Electrical behavior and pore accumulation in a multicellular model for conventional and supra-electroporation. *Biochem Biophys Res Commun* 2006; **349**: 643–653.
26. Rols MP, Teissie J. Electropermeabilization of mammalian cells. Quantitative analysis of the phenomenon. *Biophys J* 1990; **58**: 1089–1098.
27. Puc M, *et al*. Quantitative model of small molecules uptake after in vitro cell electropermeabilization. *Bioelectrochemistry* 2003; **60**: 1–10.
28. Sun Y, *et al*. Fluorescence microscopy imaging of electroperturbation in mammalian cells. *J Biomed Opt* 2006; **11**: 024010.
29. Wolf H, *et al*. Control by pulse parameters of electric field-mediated gene transfer in mammalian cells. *Biophys J* 1994; **66**: 524–531.
30. Favard C, Dean DS, Rols MP. Electrotransfer as a non viral method of gene delivery. *Curr Gene Ther* 2007; **7**: 67–77.
31. Phez E, *et al*. New insights in the visualization of membrane permeabilization and DNA/membrane interaction of cells submitted to electric pulses. *Biochim Biophys Acta* 2005; **1724**: 248–254.
32. Hristova NI, Tsoneva I, Neumann E. Sphingosine-mediated electroporative DNA transfer through lipid bilayers. *FEBS Lett* 1997; **415**: 81–86.
33. Golzio M, Teissie J, Rols MP. Direct visualization at the single-cell level of electrically mediated gene delivery. *Proc Natl Acad Sci USA* 2002; **99**: 1292–1297.
34. Golzio M, *et al*. Control by osmotic pressure of voltage-induced permeabilization and gene transfer in mammalian cells. *Biophys J* 1998; **74**: 3015–3022.
35. Eynard N, *et al*. Electrotransformation mechanism of procaryotic and eucaryotic cells: a recent development. *Bioelectrochem Bioenerg* 1997; **44**: 103–110.
36. Golzio M, Teissie J, Rols MP. Control by membrane order of voltage-induced permeabilization, loading and gene transfer in mammalian cells. *Bioelectrochemistry* 2001; **53**: 25–34.
37. Faurie C, *et al*. Effect of electric field vectoriality on electrically mediated gene delivery in mammalian cells. *Biochim Biophys Acta* 2004; **1665**: 92–100.
38. Rebersek M, *et al*. Electroporator with automatic change of electric field direction improves gene electrotransfer in-vitro. *Biomed Eng Online* 2007; **6**: 25.
39. Kubiniec RT, Liang H, Hui SW. Effects of pulse length and pulse strength on transfection by electroporation. *Biotechniques* 1990; **8**: 16–20.
40. Mir LM. Application of electroporation gene therapy: past, current, and future. *Methods Mol Biol* 2008; **423**: 3–17.
41. Vernhes MC, Cabanes PA, Teissie J. Chinese hamster ovary cells sensitivity to localized electrical stresses. *Bioelectrochem Bioenerg* 1999; **48**: 17–25.
42. Shimokawa T, Okumura K, Ra C. DNA induces apoptosis in electroporated human promonocytic cell line U937. *Biochem Biophys Res Commun* 2000; **270**: 94–99.
43. Cemazar M. Treatment of a tumor model with ECT using $4 + 4$ electrode configuration. In *Electrically Mediated Delivery of Molecules to Cells*, Jaroszeski MJ, Heller R, Gilbert RA (eds). Humana Press: Totowa, 1996; 259–264.
44. Sersa G, *et al*. Changing electrode orientation improves the efficacy of electrochemotherapy of solid tumors in mice. *Bioelectrochem Bioenerg* 1996; **39**: 61–66.
45. Zupanic A, Ribaric S, Miklavcic D. Increasing the repetition frequency of electric pulse delivery reduces unpleasant sensations that occur in electrochemotherapy. *Neoplasma* 2007; **54**: 246–250.
46. Quaglino P, *et al*. Electrochemotherapy with intravenous bleomycin in the local treatment of skin melanoma metastases. *Ann Surg Oncol* 2008; **15**: 2215–2222.
47. Marty M, *et al*. Electrochemotherapy – an easy, highly effective and safe treatment of cutaneous and subcutaneous metastases: results of ESOPE (European Standard Operating Procedures of Electrochemotherapy). *Eur J Cancer Suppl* 2006; **4**: 3–13.
48. Cemazar M, *et al*. Electrochemotherapy in veterinary oncology. *J Vet Intern Med* 2008; **22**: 826–831.
49. Kodre V, *et al*. Electrochemotherapy compared to surgery for treatment of canine mast cell tumours. *In Vivo* 2009; **23**: 55–62.
50. Cemazar M, *et al*. Control by pulse parameters of DNA electrotransfer into solid tumors in mice. *Gene Ther* 2009; **16**: 635–644.

DOI: 10.1002/jgm

International Journal of Pharmaceutics 379 (2009) 278–284

Contents lists available at ScienceDirect

International Journal of Pharmaceutics

journal homepage: www.elsevier.com/locate/ijpharm

A 3D *in vitro* spheroid model as a way to study the mechanisms of electroporation

L. Wasungu[a,b], J.-M. Escoffre[a,b], A. Valette[b,c], J. Teissie[a,b], M.-P. Rols[a,b,*]

[a] CNRS, IPBS (Institut de Pharmacologie et de Biologie Structurale), 205 route de Narbonne, F-31077 Toulouse, France
[b] Université de Toulouse, UPS, IPBS, F-31077 Toulouse, France
[c] CNRS, LBCMCP (Laboratoire de Biologie Cellulaire et Moléculaire du Contrôle de la Prolifération), 118 route de Narbonne, F-31062 Toulouse, France

ARTICLE INFO

Article history:
Received 30 January 2009
Received in revised form 19 March 2009
Accepted 27 March 2009
Available online 5 April 2009

Keywords:
Electroporation
DNA
Spheroid
Electropermeabilization
Confocal microscopy
Delivery

ABSTRACT

Electropermeabilization is a physical method to deliver molecules into cells and tissues. Clinical applications have been successfully developed for antitumoral drug delivery and clinical trials for gene electrotransfer are currently underway. However, little is known about the mechanisms involved in this transfer. The main difficulties stem from the lack of single cell models which reliably replicate the complex *in vivo* environment. In order to increase our understanding of the DNA electrotransfer process, we exploited multicellular tumor spheroids as an *ex vivo* model of tumor. We used confocal microscopy to visualize the repartition of permeabilized cells in spheroids subjected to electric pulses. Our results reveal that even if cells can be efficiently permeabilized with electric fields, including those cells present inside the spheroids, gene expression is by contrast limited to the external layers of cells. Taken together, these results, in agreement with the ones obtained in tumors, indicate that the spheroid model is more relevant to an *in vivo* situation than cells cultured as monolayers. They validate the spheroid model as a way to study electro-mediated gene delivery processes.

1. Introduction

The delivery of therapeutic molecules into cells and tissues remains a major challenge in pharmacology. This is because the plasma membrane of the cell acts as a selective barrier that hinders the uptake of small as well as large hydrophilic molecules into cells. Therefore, efficient and safe delivery methods are essential to overcome this barrier. Delivery of DNA can be achieved by taking advantages of natural vectors such as viruses. However efficient, their use is limited due to their lack of safety (Hacein-Bey-Abina et al., 2002). For the past 20 years a huge variety of non-viral methods, including chemical and physical vectors, have been developed. In recent years, significant efforts have been made to use the potential of nanotechnology in drug delivery (Hamidi et al., 2008; Brigger et al., 2002). Amongst physical methods, electropermeabilization, also named electroporation, which was introduced in the 1970s, has been further developed in the 1980s for drug and gene delivery (Neumann et al., 1982; Kinosita and Tsong, 1979). The method, based on the transient permeabilization of the plasma membrane by applying electric field pulses, has been used with increasing popularity (Heller and Heller, 2006; Cemazar et al., 2006b; Gehl, 2003; Giraud et al., 1996). Applications such as electrochemotherapy, have been successfully developed for antitumoral drug delivery (Mir et al., 1998; Belehradek et al., 1993; Rols et al., 2002) as well as others for the transfer of genes (Titomirov et al., 1991; Heller et al., 1996; Rols et al., 1998; Aihara and Miyazaki, 1998; Cemazar et al., 2006b; Mir et al., 1999). At present, electrochemotherapy is accepted in a number of countries as a palliative treatment (Gehl, 2008). Clinical trials of gene electrotransfer are currently under investigation. A phase I dose escalation trial of plasmid interleukin electroporation has been carried out in patients with metastatic melanoma and has shown encouraging results (Daud et al., 2008). However, one has to notice that even if *in vitro* electrotransfer is usually efficient in almost all cell lines, *in vivo* gene delivery and expression faces some problems. For instance in tumors, efficiency remains low with only a few percent of transfected cells (Rols et al., 1998). Those cells are in addition only found at the periphery of the tumors (Mesojednik et al., 2007).

The mechanisms behind the improved gene delivery *in vivo* remain largely unknown. A better understanding of these mechanisms, and their efficiencies in overcoming obstacles for *in vivo* delivery, is critical to the improvement and advancement of this therapeutic strategy. While the mechanism of membrane permeabilization and pore formation is still a subject of continuous debate, it is accepted that the driving force behind electropermeabilization is the applied field-induced transmembrane voltage

* Corresponding author at: CNRS, IPBS (Institut de Pharmacologie et de Biologie Structurale), 205 route de Narbonne, F-31077 Toulouse, France.
Tel.: +33 5 61 17 58 11; fax: +33 5 61 17 59 94.
E-mail address: marie-pierre.rols@ipbs.fr (M.-P. Rols).

0378-5173/$ – see front matter © 2009 Elsevier B.V. All rights reserved.
doi:10.1016/j.ijpharm.2009.03.035

(Teissie et al., 2005). The transmembrane voltage depends on the shape and orientation of the cells and the microenvironment surrounding the cells (Valic et al., 2003; Kotnik and Miklavcic, 2000). Moreover, electromediated drug delivery depends on the nature of the drugs themselves. Small molecules enter the cell across part of the membrane facing the two electrodes by a diffusion process (Rols and Teissie, 1990; Puc et al., 2003; Sun et al., 2006). In contrast, the introduction of DNA is much more complicated. The electric field induces a key reaction between the electropermeabilized membrane and the DNA which is electrophoretically accumulated at the interface. DNA does not enter into the cell during electric pulses but it is first "trapped into" the plasma membrane before entering the cell a long time after pulses application (Golzio et al., 2002). These dependences lead to spatially heterogeneous cellular uptake of solutes into tumors during electroporation, making it difficult to achieve a uniform cellular delivery of genes to tissues (Henshaw and Yuan, 2008). Studies performed on cells in culture, even if instructive, are of limited use when relating to cells within a tissue environment since in the former, delivered molecules have direct access to these cells. Indeed, in tissues, the diffusion of molecules is impaired with large molecules such as DNA having no direct or free access to the entire cell population. Thus, an abiding limitation of studies performed in animals is the lack of reductionist experimental approaches which at a single cell level reliably mirror the ongoing processes at an organ level.

The aim of the present study was to increase our understanding of the DNA electrotransfer process. Our adopted strategy used a 3D *in vitro* spheroid model as a way to study the mechanisms of electropermeabilization. To this end, we exploited multicellular tumor spheroids as an *ex vivo* model of tumor. Upon growth, spheroids display a gradient of proliferating cells (Sutherland, 1988). These proliferating cells are located in the outer cell-layers and the quiescent cells are located more centrally. When the central cells become deprived in oxygen and glucose, cell death and necrosis occur. This cell heterogeneity is similar to that found in avascular microregions of tumors. They can be used to evaluate tumor response to therapeutic agent and are useful to identify new markers of the response to endocrine treatment and to investigate the effects of drugs combination (Truchet et al., 2008). We used confocal microscopy to visualize the repartition of permeabilized cells in spheroids submitted to electric pulses. Our results reveal that despite small molecules, such as propidium iodide, being efficiently transferred into cells, including cells present in the center of the spheroids, transfer and expression was limited to the external layers of cells in agreement with the ones obtained in tumors.

2. Materials and methods

2.1. Cells

The HCT 116 cell line was derived from a human colorectal carcinoma and the LPB cell line was derived from methylcholanthrene-induced C57Bl/6 mouse sarcoma. They were selected for their ability to grow plated on Petri dishes and to form spheroids. HCT 116 cells were grown in DMEM media (Gibco) containing 4.5 g/l glucose, L-glutamine and pyruvate and supplemented with 10% (v/v) of heat inactivated fetal calf serum, 100 U/ml penicillin and 100 mg/ml streptomycin. LPB cells were maintained in Eagle's minimum essential medium (EMEM; Gibco-Invitrogen, Carlsbad, CA, USA) with 10% fetal calf serum (Gibco), penicillin (100 units/ml) (Gibco-Invitrogen), streptomycin (100 mg/ml, Gibco-Invitrogen) and L-glutamine (0.58 mg/ml; Eurobio, France) in a 5% CO_2 humidified incubator at 37 °C (Jouan, St. Herblain, France). LPB cells were transduced with viral vectors to stably express eGFP (Cemazar et al., 2006a). To that purpose, a retro viral vector, MFG-eGFP, encoding the eGFP under the control of 50 long terminal repeat (LTR) was used. 293T cells, generously provided by the Genethon (Evry, France), were transiently transfected using the calcium phosphate co-precipitation protocol with pMDG encoding VSV-G protein, pGagPol encoding gag and pol and MFG-eGFP. Virus containing supernatants was collected 36–72 h after transfection, filtered and concentrated to titers of 1–5109 colony forming units (c.f.u.)/ml. LPB cells were plated in 35 mm culture dish 24 h prior transduction. On day 0 cells were transduced with viral vectors at a MOI of 100:1. After transduction (48 h) cells were harvested for FACS analysis on a Becton–Dickinson FACScan to select LPB cells stably expressing eGFP.

2.2. Generation of spheroids

The hanging-drop method has been adapted to produce spheroids of similar diameter (Del Duca et al., 2004). Drops (20 μl) containing 500 cells were suspended on the lid of agar coated 24-well dishes containing 500 μl of culture media. After the 72 h required for cell aggregation, the spheroids were transferred to the bottom of the well containing 500 μl of culture medium. Multicellular spheroids were then allowed to grow for 10 days and the spheroids used in the experiments sized in average around 500 μm of diameter.

2.3. Plasmid extraction

A 4.7 kb plasmid (pEGFP-C1) containing the gene coding for the Green Fluorescent Protein under control of the CMV promoter was obtained from Clonetech (Palo Alto, CA). It was purified from *Escherichia coli* transfected cells by using Maxiprep DNA purification system according to Qiagen instructions (Courtaboeuf, France).

2.4. Electropulsation

Electropulsation was achieved by using a CNRS cell electropulsator (Jouan, St Herblain, France) which delivered square-wave electric pulses. An oscilloscope (Enertec, St. Etienne, France) monitored pulse shape. Stainless steel flat parallel electrodes (1 cm length, 1 cm width) were used.

2.5. Electropermeabilization

Spheroids were resuspended in 200 μl of pulsing buffer (10 mM K_2HPO_4/KH_2PO_4 buffer, 1 mM $MgCl_2$, 250 mM sucrose, pH 7.4). Permeabilization was performed on Petri dish by application of long electric pulses required to transfer genes and to load macromolecules into cells. Penetration of propidium iodide (100 μM, in pulsing buffer) was used to monitor permeabilization (Golzio et al., 2002). Ten pulses lasting 5 ms at a frequency of 1 Hz were applied at a given electric field intensity at room temperature, conditions known to induce efficient and transient cell permeabilization (Rols and Teissie, 1998).

2.6. Electrotransfection

Spheroids were resuspended in plasmid DNA containing pulsing buffer. For each condition, 10 μg of pEGFP-C1 plasmid was used. As with the electropermeabilization protocol, 10 pulses lasting 5 ms were applied at various pulses amplitude. Spheroids were incubated for 5 min at room temperature and cultured in agar coated wells of 24-wells plate with 500 μl of culture medium at 37 °C in a 5% CO_2 incubator for 24 h.

2.7. Confocal microscopy

Spheroids were observed with a Zeiss LSM 510 confocal microscope. For the GFP fluorescence, samples were excited with an Argon laser set at a 488 nm wavelength and emission was collected through a band pass filter from 500 nm to 530 nm. PI fluorescence was excited with a Helium–Neon laser set at 543 nm wavelength and emitted light was collected through a 560–615 nm band pass filter. Several sections of the spheroid were imaged until the loss of fluorescent signal. Images represent the compilation of all the optical slices in a 3D projection.

3. Results

In an attempt to gain insight into the process of drug delivery mediated by applied electric pulses, we used multicellular spheroids as a way to explore the mechanisms of electrotransfer at the single cell level on an *ex vivo* tumor model. According to our previous works, electric pulses were applied in the millisecond time range. Such conditions are known to allow transfer of macromolecules (Rols and Teissie, 1998). Propidium iodide was used as a marker of membrane permeabilization. A plasmid coding for the GFP was used to detect DNA delivery and gene expression with time. In the present study, we used confocal microscopy as a convenient tool to image the spatial distribution of those molecules which have been taken up by live cells, i.e. without any fixation or slicing of the sample.

3.1. Electropermeabilization of multicellular spheroids

Electropermeabilization in the presence of propidium iodide of spheroids from LPB cells, constitutively expressing GFP, allowed for the study of both the entry of external molecules (propidium iodide) and the release of internal molecules (GFP). Spheroids were subjected to 10 electric pulses lasting 5 ms at the following intensities: control (0 kV/cm), 0.1 kV/cm, 0.3 kV/cm and 0.5 kV/cm. As shown in Fig. 1, control spheroids showed heterogeneous expression of GFP in the cells. No detection of propidium iodide was present indicating the absence of dead cells. Application of electric pulses led to a decrease of the green intensity associated to the GFP with a concomitant increase of the red fluorescence associated with propidium iodide uptake. At 0.1 kV/cm, only a few cells were permeabilized. At 0.3 kV/cm, more than 50% of the cells had taken up propidium iodide. At 0.5 kV/cm, practically the entire cell population was permeabilized to propidium iodide. The fluorescent pictures are a 3D compilation of confocal slices and allowed for the visualization of cells up to a depth of 140 μm. Permeabilized cells appeared to be homogeneously distributed in the core of the spheroids, at least in the regions where their detection has been performed.

3.2. Electrotransfer of gene to multicellular spheroids

Spheroids from HCT116 cells were transfected by electropermeabilization in the presence of a plasmid coding for the green fluorescent protein (GFP). Electro-gene transfer was performed by

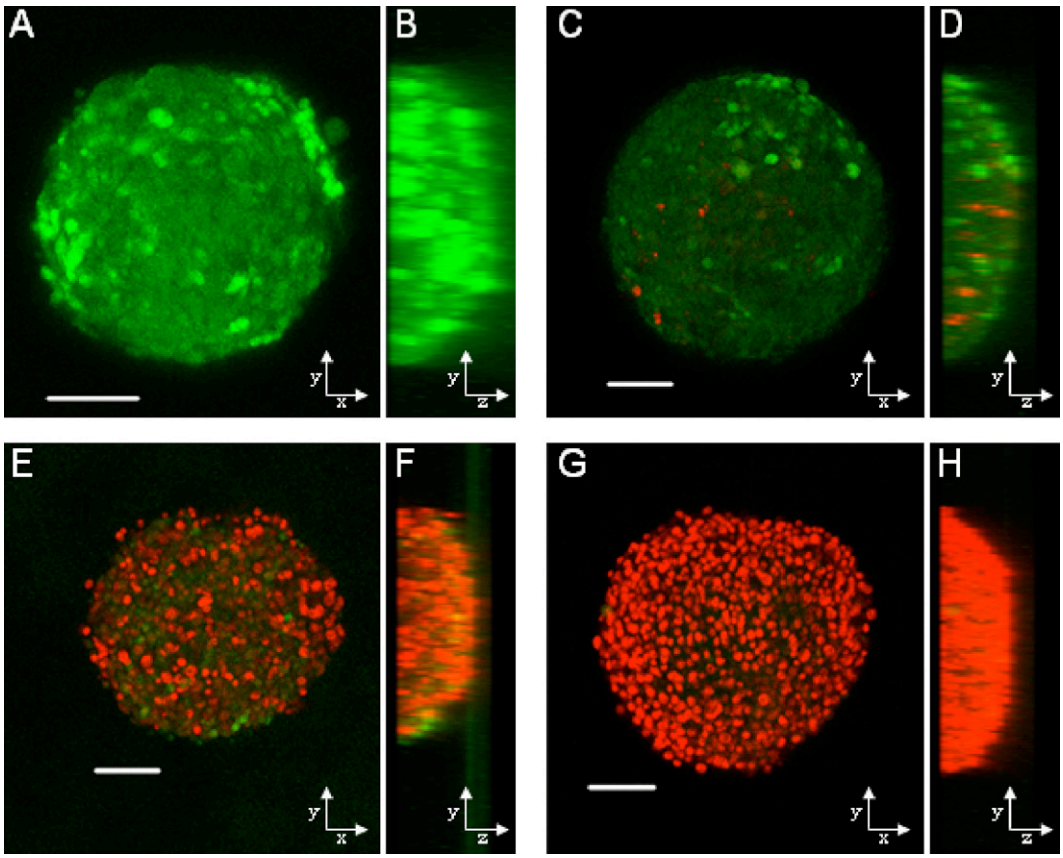

Fig. 1. Electropermeabilization of LPB spheroids with propidium iodide. Spheroids from LPB cells constitutively expressing the GFP (green fluorescence) were electropermeabilized (red fluorescence). Electropermeabilization was performed as described in Section 2 and three different intensities were tested: control (A and B); 0.1 kV/cm (C and D); 0.3 kV/cm (E and F) and 0.5 kV/cm (G and H). The fluorescent images are a 3D compilation of 15 optical slices of up to 140 μm depth in total. A, C, E and G show the image in the *X*–*Y*-axis of the 3D compilation with B, D, F and H showing the image in the *Z*-axis. The scale bars represent 200 μm. (For interpretation of the references to color in this figure legend, the reader is referred to the web version of the article.)

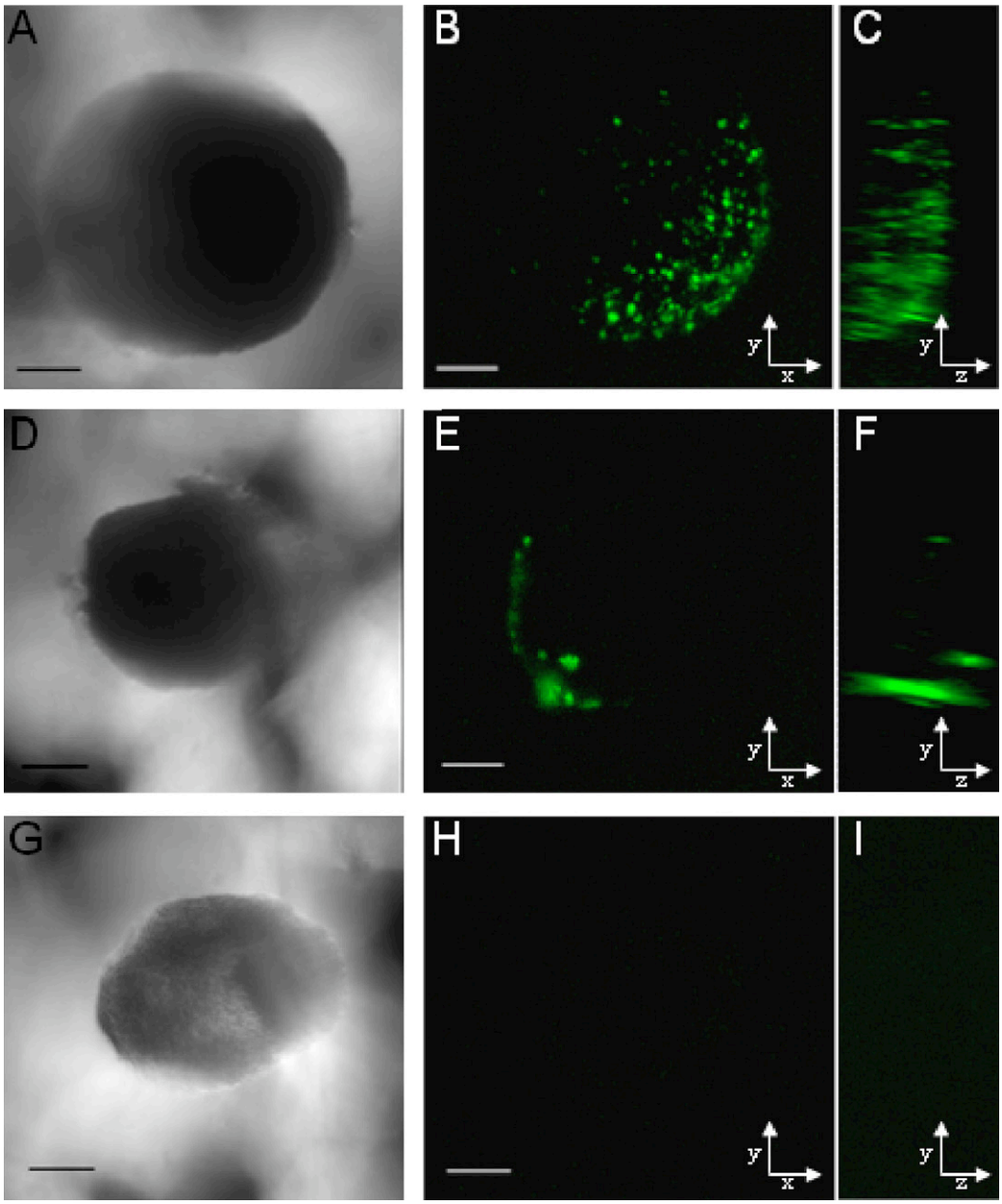

Fig. 2. Electro-gene transfer of multicellular spheroids. Spheroids from HCT116 cells were transfected by electropermeabilization with a plasmid coding for the green fluorescent protein (GFP). The efficiency of expression and its distribution were analyzed by confocal microscopy 24 h after transfection. Electro-gene transfer was performed as described in Section 2 and three intensities were tested for the applied electric field: 0.3 kV/cm (A–C); 0.5 kV/cm (D–F) and 0.8 kV/cm (G–I). A, D and G show transmitted light images of the spheroid with B, C, E, F, H and I being the respective fluorescent images. The fluorescent images are a 3D compilation of confocal slices of up to 460 μm, 550 μm and 380 μm in depth for the first, second and third spheroid respectively. B, E, and H are in the *X*–*Y*-axis with C, F, and I showing images in the corresponding *Z*-axis. The scale bars represent 100 μm.

applying 10 electric pulses lasting 5 ms at the following intensities: 0.3 kV/cm, 0.5 kV/cm and 0.8 kV/cm. The expression efficiency and the distribution of the GFP protein were analyzed by confocal microscopy 24 h after electric pulses application. Fluorescent pictures are a 3D compilation of confocal slices up to 460 μm, 550 μm and 380 μm in depth for the three electric pulse conditions, respectively. As shown in Fig. 2, gene expression could be detected. The highest efficiency was obtained at 0.3 kV/cm electric pulses intensity. Under this condition, few cells were transfected. However, in contrast to propidium iodide uptake experiments, increasing the pulse intensity did not result in any increase in transfection efficiency. The percentage of green cells dramatically decreased at 0.5 kV/cm and no cells expressing the GFP protein could be detected at 0.8 kV/cm. This observation correlated well with a decrease in cell viability as observed by an arrest of the spheroid growth following application of electric pulses above 0.4 kV/cm (data not shown). A striking observation is that transfected cells were not homogeneously distributed into the spheroids. Indeed, they appeared to be only localized in the outer layers of the spheroids. Also of note was that expression was only detected in one cap of the spheroids. This result was consonant with those obtained in cells *in vitro* where only one pole of the cells, the one facing the negative electrode was competent for DNA delivery (Fig. 3A).

4. Discussion

In this study, we used multicellular tumor spheroids of LPB and HCT116 cancer cells as a tissue model to assess the distribution

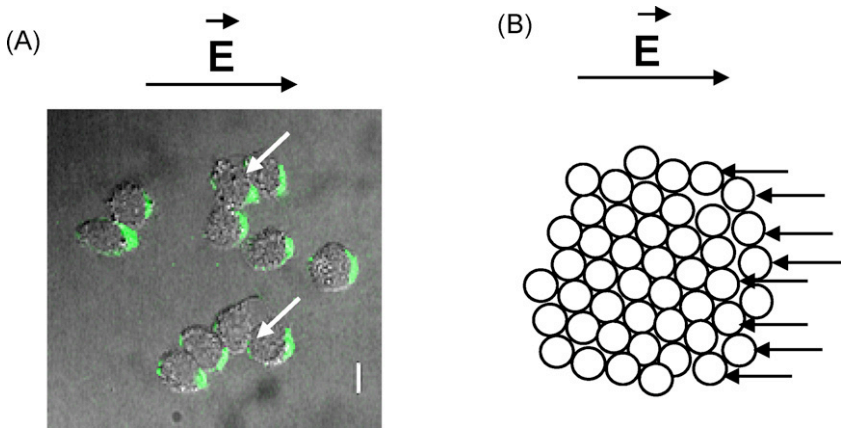

Fig. 3. DNA transfer in cells and spheroids. (A) Image of cells subjected to electric field in the presence of fluorescent plasmid DNA taken 1 min following pulses application as in Faurie et al. (2004). White arrows indicate areas of contact between cells where DNA cannot interact with. (B) Schematic representation of cells in a spheroid and their potential interaction with plasmid DNA (black arrows indicate the direction of DNA diffusion movement in an electric field).

of molecular uptake in a multicellular environment as a function of electric field strength. These experiments were undertaken to gain an understanding of, as well as to compare the differences and similarities of responses between cells in a multicellular environment and cells in culture when submitted to electric pulses. Molecular uptake was consistently dependent on the size of the molecules to be delivered. Propidium iodide (MW: 668 Da) uptake could be observed in spheroids for field strengths of 0.3 kV/cm and higher, with the percentage of permeabilized cells increasing with an increase in field intensity. The method was highly efficient since practically the entire cell population was permeabilized. No clear difference could be detected between cells at the periphery of the tumor model and the cells located deeper within the spheroid's core. Moreover, uptake of exogenous propidium iodide correlated well with a decay in GFP intensity that could be due to a release of internal GFP molecules (MW: 27 kDa). Such data are in good agreement with data obtained *in vitro* in cells cultured in monolayer or in suspension (Rols and Teissie, 1990). In contrast, differences could be observed in the case of the uptake of macromolecules as plasmid DNA (MW: 3 MDa). Gene expression was lower for cells within the spheroids than for cells in culture, with only a limited number of cells expressing the reporter gene. Moreover, transfected cells were heterogeneously distributed, being only located in the first outer proliferating cell layers at one particular pole of the spheroids. Such a well defined localization of transfected cells reaffirms what was observed with cells in culture (Fig. 3), where only the cap facing the cathode is susceptible to gene transfer as previously reported (Golzio et al., 2002). Moreover, as shown by the arrow in Fig. 3A, close contacts between cells may act as physical barriers that limit the diffusion of plasmid DNA and therefore its access to cells present in the core of the spheroid as drawn in Fig. 3B. Taken together, these results indicate that the spheroid model is more relevant to an *in vivo* situation than cells in culture validating the spheroid model as a useful tool to study electro-mediated gene delivery processes.

Studies using spheroids as models that mimic *in vivo* situations have been reported by others groups working on gene delivery using different vectors. Grill and collaborators studied the interactions between tumor and adenoviruses using multicellular spheroids grown from primary brain tumor material. Using reporter genes expressed by replication-defective adenoviruses, they showed that infection was restricted to the first layer of cells (Grill et al., 2002). Using a replication-competent adenovirus, they showed that transgene expression in the spheroid was considerably enhanced and that viral spreading deep into the 3D structure took place. They concluded that organotypic spheroids offer a versatile *in vitro* system for studying distribution, spread, and oncolysis by adenoviruses in a clinically relevant model. In a study combining non-viral methods for gene delivery, Mellor and collaborators showed that PEI-mediated transfection was limited to cells at the MCTS periphery. Using fluorescent PEI, it was found that complexes could only penetrate the outer 3–5 proliferating cell layers of the MCTS, sparing the deeper quiescent cells. This 'resistance' to transfection observed in quiescent cells was overcome through the use of electroporation. However, despite the improved efficacy of electroporation in quiescent tissue, the gene expression was still confined to the outer regions of MCTS. The results suggest that limited access to central regions of an MCTS remain a significant barrier to gene delivery (Mellor et al., 2006). Clearly a prominent feature of solid neoplasms, the avascular regions represent a major obstacle to achieving widespread gene delivery into tumors. Various strategies could potentially improve the tissue penetration of vectors such as PEI for example, by using a receptor-mediated approach to increase membrane-association and endocytic uptake of polyplexes. Alternatively, disruption of tight junctions between adjacent tumor cells is a further option. Transfection of MCTS, using either PEI or electroporation to deliver the pDNA, resulted in transfection of only a small proportion (<5%) of total cells (Mellor et al., 2006). The higher levels of reporter gene expression and increased efficacy in quiescent cells afforded by electroporation make it a promising strategy for tumor gene therapy. However, full exploitation of this approach will only be possible by improving access to the deeper, avascular areas of solid tumors. The extracellular reservoir of molecules, and thus the efficiency of tumor electrochemotherapy, has been improved by pre-exposure of tumor tissue to the drug. Important discrepancy between *in vitro* conventional monolayer cultures and *in vivo* tissues is the three-dimensional environments (e.g., cell–cell and cell–ECM, extracellular matrix, interactions) for the cells. Han et al. (2007) showed that a reporter gene was expressed even at the inner region of MCTS where necrosis was considered to be developed; small spheroids have a relatively weak structure due to their immature development of cell–cell and cell–ECM interactions. In contrast, large spheroids have a heterogeneous structure consisting of outer layers of viable cells and a solid core of necrotic or hypoxic cells, resembling a monolayer cell culture where the cells adhere to the hard substrate. Such morphological differences between small and large spheroids may account for their different sensitivities against polyplex-induced cytotoxicity. Canatella and collaborators reported that molecule uptake progressively decreased for cells located deeper within a spheroid's interior. Overall reduced levels of uptake were explained by locally reduced electric field strength within spheroids due to spatially heterogeneous electrical properties and a reduced extracellular reservoir of solute within spheroids

due to dense packing of cells. The dependence of uptake on radial position within spheroids was explained by an extracellular solute concentration gradient during transient diffusional lag times and the observation that cell size decreased for cells located deeper within spheroids, which in turn led to smaller cell volumes and smaller transmembrane voltages (Canatella et al., 2004). These observations suggest that tissue electroporation could be enhanced by using larger field strengths than those used for cell suspensions (Canatella et al., 2004). However, as shown in the present work, increasing electric field strength induced cellular damage resulting in a decrease in gene expression (Fig. 2). Another interest of the spheroid model is related to junctions that exist between cells as well as the extracellular matrix (ECM) that makes it closer to the tissues reality than cells with high density such as cell pellet obtained by centribugation (Pucihar et al., 2007). In such situation, the influence of cell density on cell membrane electropermeabilization has been investigated on dense cell suspensions which represent a simple model for studying electropermeabilization of tissues. Permeabilization decrease was proposed to be due to the changes in the local electric field, which led to a decrease in the amplitude of the induced transmembrane voltage. Other barriers can exist that hinder pDNA transfer and therefore expression (Bureau et al., 2004). Other strategies have been therefore investigated to modify tissue ECM for improving interstitial pDNA transport during electric field application. Muscle pretreated with hyaluronidase was shown to result in a fivefold increase in reporter gene expression (Molnar et al., 2004). In tumors, the distance of DNA electrophoresis was correlated with tissue collagen content. Pretreatment of tumors with collagenase has led to an increase in the efficiency of gene delivery with adenovirus vectors (Henshaw and Yuan, 2008). However, the ECM modification may facilitate tumor metastasis since matrix metalloproteinase expression has been associated with metastasis.

Such observations lead us to propose methodological solutions based on electric field parameters to improve DNA delivery. The intratumoral electric field, which determines the efficiency of electric field-mediated drug and gene delivery, is significantly lower from the applied field (Mossop et al., 2006). Based on analytical and numerical models of the local electric field distribution, the applied voltage can be chosen specifically to achieve adequate electric field inside the target tissue while minimizing damages of the surrounding tissue (Corovic et al., 2007). However, in the case of irregularly shaped tissue structures, such as bulky tumors, electric field homogeneity is almost impossible to be achieved with current electrode arrangements. The use of conductive gels, matched to the conductivity of the tissues, has been proposed to fill dead spaces between plate electrodes gripping the tissue so that the electric field distribution becomes less heterogeneous (Ivorra et al., 2008). However, electric field strength if too high can damage the cells. Another alternative we can propose is to change the way electric pulses are delivered. Usually, electric pulses are applied in one direction. We previously showed that changing the polarity and direction of electric pulses increased transfection of cells in cultures and also cells in tissues, where both increases in the area of muscle as the local gene expression were obtained (Faurie et al., 2003; Faurie et al., 2004). The fraction of transfected cells can indeed be increased by changing the electric field direction between electrical pulses without affecting the cell viability (Rebersek et al., 2007). When cells are in clusters, which is representative of tissues, only the first layers of cells facing negative electrode can be transfected (Fig. 3B). Applying electric field pulses under different directions can therefore help DNA to interact with permeabilized cells all around the tumors. The problem of the access of DNA to the internal layers of cells still remains. A possible solution is the application of very low intensity but long pulses to electrophoretically push the DNA towards the center of the tumors, before applying standard electric pulses.

As a general conclusion, all these data suggest that the spheroid can be considered as a good model to study the mechanisms of electro-mediated molecules delivery. Furthermore, this approach lends itself to the philosophy of the 3R's which promotes reliable alternatives to animal experiments in an attempt to reduce the numbers of animals used.

Acknowledgements

This work has been supported by grants to MPR from the Association Française contre les Myopathies (AFM) and from the region Midi-Pyrénées for a general support to gene therapy (grant to JT). The authors would like to thank Professor B. Couderc (ICR, Toulouse, France) for providing LPB cell line encoding for GFP. They also would like to thank Dr. J.D. Swinny for the proof reading of this manuscript.

References

Aihara, H., Miyazaki, J., 1998. Gene transfer into muscle by electroporation in vivo. Nat. Biotechnol. 16, 867–870.
Belehradek, M., Domenge, C., Luboinski, B., Orlowski, S., Belehradek Jr, J., Mir, L.M., 1993. Electrochemotherapy, a new antitumor treatment. First clinical phase I-II trial. Cancer 72, 3694–3700.
Brigger, I., Dubernet, C., Couvreur, P., 2002. Nanoparticles in cancer therapy and diagnosis. Adv. Drug Deliv. Rev. 54, 631–651.
Bureau, M.F., Naimi, S., Torero Ibad, R., Seguin, J., Georger, C., Arnould, E., Maton, L., Blanche, F., Delaere, P., Scherman, D., 2004. Intramuscular plasmid DNA electrotransfer: biodistribution and degradation. Biochim. Biophys. Acta 1676, 138–148.
Canatella, P.J., Black, M.M., Bonnichsen, D.M., Mckenna, C., Prausnitz, M.R., 2004. Tissue electroporation: quantification and analysis of heterogeneous transport in multicellular environments. Biophys. J. 86, 3260–3268.
Cemazar, M., Golzio, M., Escoffre, J.M., Couderc, B., Sersa, G., Teissie, J., 2006a. In vivo imaging of tumor growth after electrochemotherapy with cisplatin. Biochem. Biophys. Res. Commun. 348, 997–1002.
Cemazar, M., Golzio, M., Sersa, G., Rols, M.P., Teissie, J., 2006b. Electrically-assisted nucleic acids delivery to tissues in vivo: where do we stand? Curr. Pharm. Des. 12, 3817–3825.
Corovic, S., Pavlin, M., Miklavcic, D., 2007. Analytical and numerical quantification and comparison of the local electric field in the tissue for different electrode configurations. Biomed. Eng. Online 6, 37.
Daud, A.I., Deconti, R.C., Andrews, S., Urbas, P., Riker, A.I., Sondak, V.K., Munster, P.N., Sullivan, D.M., Ugen, K.E., Messina, J.L., Heller, R., 2008. Phase I trial of interleukin-12 plasmid electroporation in patients with metastatic melanoma. J. Clin. Oncol. 26, 5896–5903.
Del Duca, D., Werbowetski, T., Del Maestro, R.F., 2004. Spheroid preparation from hanging drops: characterization of a model of brain tumor invasion. J. Neurooncol. 67, 295–303.
Faurie, C., Golzio, M., Moller, P., Teissie, J., Rols, M.P., 2003. Cell and animal imaging of electrically mediated gene transfer. DNA Cell Biol. 22, 777–783.
Faurie, C., Phez, E., Golzio, M., Vossen, C., Lesbordes, J.C., Delteil, C., Teissie, J., Rols, M.P., 2004. Effect of electric field vectoriality on electrically mediated gene delivery in mammalian cells. Biochim. Biophys. Acta 1665, 92–100.
Gehl, J., 2003. Electroporation: theory and methods, perspectives for drug delivery, gene therapy and research. Acta Physiol. Scand. 177, 437–447.
Gehl, J., 2008. Electroporation for drug and gene delivery in the clinic: doctors go electric. Methods Mol. Biol. 423, 351–359.
Giraud, P., Bachaud, J.M., Teissie, J., Rols, M.P., 1996. Effects of electrochemotherapy on cutaneous metastases of human malignant melanoma. Int. J. Radiat. Oncol. Biol. Phys. 36, 1285.
Golzio, M., Teissie, J., Rols, M.P., 2002. Direct visualization at the single-cell level of electrically mediated gene delivery. Proc. Natl. Acad. Sci. U.S.A. 99, 1292–1297.
Grill, J., Lamfers, M.L., van Beusechem, V.W., Dirven, C.M., Pherai, D.S., Kater, M., van Der Valk, P., Vogels, R., Vandertop, W.P., Pinedo, H.M., Curiel, D.T., Gerritsen, W.R., 2002. The organotypic multicellular spheroid is a relevant three-dimensional model to study adenovirus replication and penetration in human tumors in vitro. Mol. Ther. 6, 609–614.
Hacein-Bey-Abina, S., Le Deist, F., Carlier, F., Bouneaud, C., Hue, C., De Villartay, J.P., Thrasher, A.J., Wulffraat, N., Sorensen, R., Dupuis-Girod, S., Fischer, A., Davies, E.G., Kuis, W., Leiva, L., Cavazzana-Calvo, M., 2002. Sustained correction of X-linked severe combined immunodeficiency by ex vivo gene therapy. N. Engl. J. Med. 346, 1185–1193.
Hamidi, M., Azadi, A., Rafiei, P., 2008. Hydrogel nanoparticles in drug delivery. Adv. Drug Deliv. Rev. 60, 1638–1649.
Han, M., Bae, Y., Nishiyama, N., Miyata, K., Oba, M., Kataoka, K., 2007. Transfection study using multicellular tumor spheroids for screening non-viral polymeric gene vectors with low cytotoxicity and high transfection efficiencies. J. Control. Release 121, 38–48.

Heller, L.C., Heller, R., 2006. In vivo electroporation for gene therapy. Hum. Gene. Ther. 17, 890–897.
Heller, R., Jaroszeski, M., Atkin, A., Moradpour, D., Gilbert, R., Wands, J., Nicolau, C., 1996. In vivo gene electroinjection and expression in rat liver. FEBS Lett. 389, 225–228.
Henshaw, J.W., Yuan, F., 2008. Field distribution and DNA transport in solid tumors during electric field-mediated gene delivery. J. Pharm. Sci. 97, 691–711.
Ivorra, A., Al-Sakere, B., Rubinsky, B., Mir, L.M., 2008. Use of conductive gels for electric field homogenization increases the antitumor efficacy of electroporation therapies. Phys. Med. Biol. 53, 6605–6618.
Kinosita Jr, K., Tsong, T.Y., 1979. Voltage-induced conductance in human erythrocyte membranes. Biochim. Biophys. Acta 554, 479–497.
Kotnik, T., Miklavcic, D., 2000. Analytical description of transmembrane voltage induced by electric fields on spheroidal cells. Biophys. J. 79, 670–679.
Mellor, H.R., Davies, L.A., Caspar, H., Pringle, C.R., Hyde, S.C., Gill, D.R., Callaghan, R., 2006. Optimising non-viral gene delivery in a tumour spheroid model. J. Gene Med. 8, 1160–1170.
Mesojednik, S., Pavlin, D., Sersa, G., Coer, A., Kranjc, S., Grosel, A., Tevz, G., Cemazar, M., 2007. The effect of the histological properties of tumors on transfection efficiency of electrically assisted gene delivery to solid tumors in mice. Gene. Ther. 14, 1261–1269.
Mir, L.M., Bureau, M.F., Gehl, J., Rangara, R., Rouy, D., Caillaud, J.M., Delaere, P., Branellec, D., Schwartz, B., Scherman, D., 1999. High-efficiency gene transfer into skeletal muscle mediated by electric pulses. Proc. Natl. Acad Sci. U.S.A. 96, 4262–4267.
Mir, L.M., Glass, L.F., Sersa, G., Teissie, J., Domenge, C., Miklavcic, D., Jaroszeski, M.J., Orlowski, S., Reintgen, D.S., Rudolf, Z., Belehradek, M., Gilbert, R., Rols, M.P., Belehradek Jr, J., Bachaud, J.M., Deconti, R., Stabuc, B., Cemazar, M., Coninx, P., Heller, R., 1998. Effective treatment of cutaneous and subcutaneous malignant tumours by electrochemotherapy. Br. J. Cancer 77, 2336–2342.
Molnar, M.J., Gilbert, R., Lu, Y., Liu, A.B., Guo, A., Larochelle, N., Orlopp, K., Lochmuller, H., Petrof, B.J., Nalbantoglu, J., Karpati, G., 2004. Factors influencing the efficacy, longevity, and safety of electroporation-assisted plasmid-based gene transfer into mouse muscles. Mol. Ther. 10, 447–455.
Mossop, B.J., Barr, R.C., Henshaw, J.W., Zaharoff, D.A., Yuan, F., 2006. Electric fields in tumors exposed to external voltage sources: implication for electric field-mediated drug and gene delivery. Ann. Biomed. Eng. 34, 1564–1572.
Neumann, E., Schaefer-Ridder, M., Wang, Y., Hofschneider, P.H., 1982. Gene transfer into mouse lyoma cells by electroporation in high electric fields. EMBO J. 1, 841–845.
Puc, M., Kotnik, T., Mir, L.M., Miklavcic, D., 2003. Quantitative model of small molecules uptake after in vitro cell electropermeabilization. Bioelectrochemistry 60, 1–10.
Pucihar, G., Kotnik, T., Teissie, J., Miklavcic, D., 2007. Electropermeabilization of dense cell suspensions. Eur. Biophys. J. 36, 173–185.
Rebersek, M., Faurie, C., Kanduser, M., Corovic, S., Teissie, J., Rols, M.P., Miklavcic, D., 2007. Electroporator with automatic change of electric field direction improves gene electrotransfer in vitro. Biomed. Eng. Online 6, 25.
Rols, M.P., Delteil, C., Golzio, M., Dumond, P., Cros, S., Teissie, J., 1998. In vivo electrically mediated protein and gene transfer in murine melanoma. Nat. Biotechnol. 16, 168–171.
Rols, M.P., Tamzali, Y., Teissie, J., 2002. Electrochemotherapy of horses. A preliminary clinical report. Bioelectrochemistry 55, 101–105.
Rols, M.P., Teissie, J., 1990. Electropermeabilization of mammalian cells. Quantitative analysis of the phenomenon. Biophys. J. 58, 1089–1098.
Rols, M.P., Teissie, J., 1998. Electropermeabilization of mammalian cells to macromolecules: control by pulse duration. Biophys. J. 75, 1415–1423.
Sun, Y., Vernier, P.T., Behrend, M., Wang, J., Thu, M.M., Gundersen, M., Marcu, L., 2006. Fluorescence microscopy imaging of electroperturbation in mammalian cells. J. Biomed. Opt. 11, 024010.
Sutherland, R.M., 1988. Cell and environment interactions in tumor microregions: the multicell spheroid model. Science 240, 177–184.
Teissie, J., Golzio, M., Rols, M.P., 2005. Mechanisms of cell membrane electropermeabilization: a minireview of our present (lack of ?) knowledge. Biochim. Biophys. Acta 1724, 270–280.
Titomirov, A.V., Sukharev, S., Kistanova, E., 1991. In vivo electroporation and stable transformation of skin cells of newborn mice by plasmid DNA. Biochim. Biophys. Acta 1088, 131–134.
Truchet, I., Jozan, S., Baron, S., Frongia, C., Balaguer, P., Richard-Foy, H., Valette, A., 2008. Estrogen and antiestrogen-dependent regulation of breast cancer cell proliferation in multicellular spheroids: influence of cell microenvironment. Int. J. Oncol. 32, 1033–1039.
Valic, B., Golzio, M., Pavlin, M., Schatz, A., Faurie, C., Gabriel, B., Teissie, J., Rols, M.P., Miklavcic, D., 2003. Effect of electric field induced transmembrane potential on spheroidal cells: theory and experiment. Eur. Biophys. J. 32, 519–528.

Radiol Oncol 2008; 42(4): 196-206. *doi:10.2478/v10019-008-0016-2*

review

Time dependence of electric field effects on cell membranes. A review for a critical selection of pulse duration for therapeutical applications

Justin Teissié [1,2], Jean Michel Escoffre[1,2], Marie Pierre Rols[1,2], Muriel Golzio[1,2]

[1] *CNRS; IPBS (Institut de Pharmacologie et de Biologie Structurale); 205 route de Narbonne, F-31077 Toulouse, France;*
[2] *Université de Toulouse; UPS; IPBS; F-31077 Toulouse, France*

Background. *Electropulsation is one of the non-viral methods successfully used to transfer drugs and genes into living cells in vitro as in vivo. This approach shows promise in field of gene and cellular therapies. This presentation first describes the temporal factors controlling electropermeabilization to small molecules (< 4kDa) and then the processes supporting DNA transfer in vitro. The description of in vitro events brings our attention on the processes occurring before (s), during (ms) and after electropulsation (ms to hours) of DNA and cells. They all appear to be multistep events with well defined kinetics. They cannot be described as just punching holes in a lipid matrix in a two states process.*

Conclusions. *The faster events (may be starting on the ns time scale) appear to be under the control of the external field while the slower ones are linked to the cell metabolism. Investigating the associated collective molecular reorganization by fast kinetics methods and molecular dynamics simulation will help in their safe developments for the in vivo processes and their present and potential clinical applications.*

Key words: electropulsation; electropermeabilization; electrotransfection; electroporation

Introduction

The application of electric field pulses to cells leads to the transient permeabilization of the membrane (electropermeabilization).[1] This phenomenon brings new properties to the cell membrane: it becomes permeabilized, fusogenic and exogenous membrane proteins can be inserted. It has been used to introduce a large variety of molecules into many different cells *in vitro*.[2,3] Clinical applications of the electropermeabilization are now under development as a results of the EU Cliniporator and Esope programs. A local antitumoral drug delivery to patients (a method called electrochemotherapy) is under clinical trial.[4-8] Transdermal drug delivery is obtained *in vivo*.[9] More recently, electropermeabilization has been also used to transfer DNA *in vivo,* into the skin, liver, melanoma and skeletal muscle cells.[10-15] It

Received 27 August 2008
Accepted 13 October 2008

Correspondence to: Dr. Justin Teissié, IPBS Université de Toulouse UMR 5089 CNRS, 205 route de Narbonne, 31077 Toulouse, France. Phonel: +33(0)5 61 17 58 12; Fax: +33(0)5 61 17 59 94; Email: justin.teissie@ipbs.fr

has the main advantages of being easy to use, fast, reproducible and safe.

While during 30 years due to technological limits, pulse duration was always larger than 1 microsecond, the recent availability of high voltage (tens of kV) nanosecond long pulse generators opens the way to a new approach. Very fast perturbations under strong fields are induced in the membrane organization.[16,17] A new field of development is now present for electropermeabilization and promising results for clinical applications were reported.

One of the limiting problems remains that very few is known on the physicochemical mechanisms supporting the reorganisation of the cell membrane. The molecular target of the field effect remains unclear.

The present review focuses on the critical role played by the pulse duration in the electropermeabilization to small molecules (< 4kDa) and on its support to the processes associated to DNA transfer *in vitro*. Pulse durations are easy to adjust for an optimization of the clinical target: electrochemotherapy, irreversible electropermeabilization or gene therapy as suggested as a final conclusion.

Electropermeabilization

Theory of membrane potential difference modulation.

An external electric field modulates the membrane potential difference.[18] From the physical point of view, a cell can be described as a spherical capacitor which is charged by the external electrical field. The transmembrane potential difference induced by the electric field, $\Delta\Psi i$ is a complex function $g(\lambda)$ of the specific conductivities of the membrane (λ_m), the pulsing buffer (λ_{out}) and the cytoplasm (λ_{cyt}), the membrane thickness and the cell size. Thus,[1]

$$\Delta\Psi i = f.\ g(\lambda).\ r.\ E.\cos\theta \qquad [1]$$

in which θ designates the angle between the direction of the normal to the membrane at the considered point on the cell surface and the field direction, E the field intensity, r the radius of the cell and f, which is a shape factor (a cell being a spheroid). Therefore, $\Delta\Psi i$ is not uniform on the cell surface. It is maximum at the positions of the cell facing the electrodes. These physical predictions were checked experimentally by videomicroscopy by using the potential difference sensitive fluorescent probes.[19-21]

The pulse duration plays a critical role when shorter than the capacitive loading time of the membrane. In the previous part of the paper, it was considered that the pulse was long enough to bring the potential steady state value. The loading time τ_{load} brings a limit in this description.[1]

$$\Delta\Psi i = f.\ g(\lambda).\ r.\ E.\cos\theta\ (1 - \exp(-t / \tau_{load})) \qquad [2]$$

Assumming that the membrane is a true dielectric with no electric leak, the loading time. τ_{load}, is given by

$$\tau_{load} = rC_m\ (1/2\lambda_{out} + 1/\lambda_{cyt}) \qquad [3]$$

C_m is the membrane capacitance, λ_{out} and λ_{cyt}, respectively, the conductance of the external buffer and of the cytoplasm. τ_{load} is longer for larger cells in a heterogeneous population. Longer pulses are needed to reach the asymptotic electrically induced transmembrane voltage value (Eq. 1). A key assumption in this physical description is that the electric pulse is a sharp square wave.[22] This description is under the assumption that the cell is a sphere. A more complex description is needed for spheroidal cells and their orientation relative to the field has to be taken into account.[23,24]

The membrane leakiness affects the loading time of the membrane when the field is applied.[1] Its physical definition is given in [26] by:

$$\tau = r\,Cm\,(\lambda_{cyt} + 2\lambda_{out}) / (2\,\lambda_{cyt}\lambda_{out} + r\lambda_m\,(\lambda_{cyt} + 2\,\lambda_{out})/d) \qquad [4]$$

As λ_m is dependent on the membrane leakiness, the loading time of the membrane will decrease with an increase in the membrane leakiness. The pulse duration plays a more critical role in such a case. But under physiological conditions, where λ_{out} is larger than 10 mS/cm, as λ_{cyt} is about 4 mS/cm, τ_{load} is always of the order of 1 μs for mammalian cells

Critical parameters affecting electropermeabilization

Effects of the electric field parameters. When the resulting transmembrane potential difference $\Delta\Psi$(*i.e.* the sum between the resting value of cell membrane $\Delta\Psi o$ and the electroinduced value $\Delta\Psi i$) reaches threshold values close to 250 mV, membranes become permeable.[25-26]

Permeabilization is controlled by the field strength. Field intensity larger than a critical value (Ep) must be applied to the cell suspension. From Eq. [1], permeabilization is first obtained for θ close to 0 or π. Ep is such that:

$$\Delta\Psi perm = f\,g\,(\lambda)\,r\,Ep \qquad [5]$$

Parts of the cell surface facing the electrodes are affected. The extent of the permeabilized surface of a spherical cell, Aperm, is given by:

$$Aperm = Atot\,(1 - Ep/E)/2 \qquad [6]$$

where Atot is the cell surface and E is the applied field intensity. Increasing the field strength (decreasing Ep/E) will increase the part of the cell surface, which is brought to the electropermeabilized state. This critical value of the transmembrane potential will be reached after a longer delay for the edges of the cap due to the loading time. But this delay remains always in the μs time scale. This will affect the mechanism of electropermeabilization only for a very short pulse duration.

These theoretical predictions were assayed on cell suspension by measuring the leakage of metabolites (ATP)[27] or observed at the single cell level by digitised fluorescence microscopy.[28,29] The experimental results are in agreement with the predictions. The field strength must be larger than the threshold value Ep to induce permeabilization. The permeabilized part of the cell surface is a linear function of the reciprocal of the field intensity. Permeabilization, due to structural alterations of the membrane, remained restricted to a cap on the cell surface when short lived pulses (microseconds) are applied. The area affected by the electric field depends also on the shape (spheroid) and on the orientation of the cell with the electric field lines.[24] If a train of 10 pulses is applied at a frequency of 1 Hz, it is observed that long pulses (more than 1 ms) slightly larger than Ep bring a permeabilization on two caps on the cell surface, each facing one electrode.

Experimental results obtained either by monitoring conductance changes on cell suspension[34] or by fluorescence observation at the single cell level microscopy[28,29] shows that the local level of permeabilization is strongly controlled by the pulse duration.[27,28]

As an electrical current is flowing, Joule heating is taking place. The temperature of the sample increases as a linear function of the pulse duration and of the square of the field intensity. I*n vitro*, this deleterious by-effect is controlled by using a low ionic content pulsing buffer to deliver a limited amount of energy. This of course cannot be controlled by that means *in vivo* but the tissue can be considered as a heat sink.

Sieving of electropermeabilization

Electropermeabilization allows a post-pulse free-like diffusion of small molecules (up to 4 kDa) whatever their chemical nature. There is a size limit for permeabilization and the process for macromolecules is described in the second part of the text. Polar small compounds cross easily the electropermeabilized membrane. But the most important feature is that this membrane organisation is long-lived in cells. Diffusion is observed during the seconds and minutes following the ms pulse. Most of the exchange takes place after the pulse.[28,29] Resealing of the membrane defects and of the induced permeabilization is a first order process, which appears to be controlled by protein reorganisation. For a given cell, the resealing time (reciprocal of k) is a function of the pulse duration but not of the field intensity as checked by digitised videomicroscopy.[27] A precise analysis shows that several resealing processes are acting, two are very fast (ms, <s) while the last one remains present during several minutes at room temperature.[30] Resealing of membrane defects is a metabolic process under control of the energy reserves of the cell.[31] One can take advantage of this slow resealing to deliver the successive pulses at a 1kHz frequency to reduce the duration of the treatment in ECT.[32]

These observations are in agreement with a model where the target of the field is under the control of the pulse duration. Due to their internal flexibility (mainly at the level of the polar heads), phospholipids are sensitive to short pulses. Their change in configuration brings an effect on the membrane proteins. The transmembrane ionic exchange induces a secondary effect on the cell organization. When long pulses are applied, they can induce long range reorganization (an electrophoretic drift of polar membrane components) and a direct effect on more rigid dipoles such as those associated with membrane proteins. Long pulses are not acting only on phospholipids but may affect directly the organization of membrane proteins.[33] Of course, the transmembrane exchange will be larger as the density of membrane defects will be increased.

Loading of macromolecules is a more complex mechanism, that will be described in details later.

Associated transmembrane exchange

Molecular transfer of small molecules (<4kDa) across the permeabilized area is mostly driven by the concentration difference across the membrane. Electrophoretic contribution to the transmembrane exchange during the pulse affects the loading of polar compounds.[29,30] Free diffusion of low weight polar molecules after the pulse can be described by using the Fick equation on its electropermeabilized part.[27] It plays the most important contribution to the loading. This gives the following expression for a given molecule S and a cell with a radius r:

$$\Phi(S) = 2\pi r^2 P_S \Delta S X(N, T) (1 - Ep/E) \exp(-k(N, T) t) \quad [7]$$

where $\Phi(S)$ is the flow at time t after the N pulses of duration T (the delay between the pulses being short compared to t), P_S is the permeability coefficient of S across the permeabilized membrane and ΔS is the concentration gradient of S across the membrane. Ep depends on r (size). Permeabilization remains present for a longer time when cells are kept at low temperature. The cytoskeletal integrity plays also a major role.[33]

Cellular responses

Reactive oxygen species (ROS) are generated at the permeabilized loci, depending

on the electric field parameters.[35] These ROS can affect the viability. The amount of ROS is increased with an increase in pulse duration. Long pulses may therefore be toxic for cells.

When a cell is permeabilized, a transient osmotic swelling may result leading to an entrance of water into the cell. This increase of cell volume can lead to the rupture of the membrane.[36,37] This swelling is under the strong control of the pulse duration. Using μs pulse does not trigger swelling (with the exception of red blood cells, the so called osmotic swelling) [38] while a twofold increase in volume was reported when using ms pulses.

There is a loss of the bilayer membrane asymmetry of the phospholipids.[39]

Carry-home messages on permeabilization

When cells are submitted to short lived electric field pulses, a free exchange of hydrophilic molecules takes place across the membrane. A leakage of cytosolic metabolites into the cytoplasm is obtained. Nevertheless, cell viability can be preserved under controlled electric field conditions. More drastic electric conditions affect strongly the cell viability. This effect is cell specific and some strains are weakly resistant to the electric trauma. Bringing them to a reversible permeabilized state needs a careful tuning of the electric parameters. The exchange of the hydrophilic compounds is strongly controlled by the pulse duration. Indeed the pulse duration plays a decisive role in the level of loading as it controls i) the density of permeabilized defects (X in Eq. 7) ii) the life time of these defects (k in Eq. 4).[40] Short pulses will induce few short lived defects and a very limited loading (that cannot even be detected in many conditions). A larger loading (leakage) of the cytoplasmic content will occur with long pulses. The cell viability will be preserved more when using short pulses.

Clinical applications are supported either by the loading of therapeutic compounds (bleomycin)[5-7] or by irreversible permeabilization (IRE).[41.]Electrochemotherapy is obtained by a low number of successive short lived pulses (100 μs) while IRE requires a much longer treatment. A delay between pulses as short as 1 ms can be observed to reduce the pain of the patient.

DNA electrotransfer

Gene expression is obtained after applying electric pulses to a cell DNA mixture. No transfected cells were detected in absence of electric field, in absence of DNA, or when DNA was added after the pulses.[42,43]

Electrotransfection was only detected for electric field values leading to permeabilization. Transfection threshold values were the same as the ones for cell permeabilization when pulses lasting ms were applied.[44.]

Events during electropulsation: Membrane –DNA interaction

Field strength is observed to have a critical role. Cell membrane must be permeabilized for plasmid-membrane interaction to occur. Plasmids interact only with the permeabilized cell surface. It is accumulated by the field associated electrophoretic drag as shown by fluorescence microscopy.[45] But no free plasmid diffusion into the cytoplasm is detected while this was proposed in older works.[42] No plasmid membrane interaction occurs if the nucleic acids are added after electropermeabilizing cells as proposed in.[19,38] Negatively charged DNA molecules migrate when submitted to an electric field.[43,46] But, electrophoretic DNA accumulation by itself is not enough to

bring transmembrane transfer and gene expression whatever the pulse duration.

Under permeabilizing field conditions, the pulse duration plays a critical role in the formation of the plasmid-cell complex. The complex between the plasmid and the cell surface is detected only when the pulse duration is at least 1 ms. This suggests that the density of defects is critical in the interaction between DNA and the permeabilized membrane.

Furthermore, this interpretation is supported by the observation that the DNA content in the complex, determined by the local fluorescence emission, is under the control of the field strength and the pulse duration.[45]

The reaction time of the DNA pushed against the part of the cell surface under the permeabilizing stress of the external field is increased by a longer pulse duration. This again is involved in the positive role of the pulse duration in gene electrotransfer.

This contribution of the pulse duration to the plasmid-membrane interaction has already been illustrated by a complex dependence of the gene expression.[43] The associated gene expression Expr is shown to obey the following equation:

$$Expr = K\ N\ T^{2.3}\ (1 - Ep/E)\ f(DNA) \qquad [8]$$

as long as the cell viability is not affected to a large extent by the pulse duration.[45] All parameters are as described above, K being a constant. The dependence on the plasmid concentration (ADN) is rather complex as high levels of plasmids appear to be toxic.[47]

A very recent on line videomicroscopy study showed that plasmid DNA was trapped in the electropermeabilized membrane where it forms aggregates.

The practical conclusion is that *in vitro* an effective transfer is obtained by using long pulses in order to drive the DNA towards the permeabilized area of the membrane by electropermeabilization but with a low field strength to preserve the cell viability.[44,48] Nevertheless, the transfection was obtained with short strong pulses in the pioneering experiments [18] and with stem cells.[49]

Events after electropulsation

The main conclusion of the observations during the pulse is that plasmids do not cross the membrane during that step, even if the membrane is permeabilized (for small molecules). They form complexes at the permeabilized membrane level. More than 2 s appears to be needed to get a stable DNA membrane complex after a 5 ms pulse.[66]

Cell electroassociated DNA remains accessible to DNAaseI, a double–strand nucleic acid degrading enzyme, up to 60 s after the pulsation in the case of CHO cells.[3] The DNA aggregates, which are anchored in the membrane after the electric field application, remain sensitive to the degrading action of the externally post pulse added nucleases, which are known not to cross the membrane

High field nanosecond field pulses cellular effect

Under classical electropulsation conditions (micro-millisecond duration, a few kV/cm magnitude), the transmembrane voltage change is only present on the plasma membrane. The interior of the cell is shielded from the external field by the plasma membrane. The electrical behaviour of the cell is different under strong HV nanosecond lasting pulses. A fast charging capacitive effect is present.[50] Two membrane capacitances, C_1 for the outer cell plasma membrane and C_2 for the inner organelle membrane, are being charged by currents from the exter-

nal voltage source. Charging of the external capacitance induces a transient voltage across the cytoplasm.[52] It results a charging of the organelle capacitance. As the size of the organelle is very small and the conductivity of the cytoplasm is higher than that of the external buffer, the charging time of the organelle capacitor is much faster than that of the plasma membrane capacitor.[51] The electric field induced transmembrane permeabilizing voltage is reached for the organelle as well for the plasma membrane.[52] As soon as the plasma membrane is electropermeabilized, it is short circuited and only a fraction of the external field remains present on the organelles.[50,51]

Another consequence of ultrashort pulses is the induction of an electrodeformation of the cell (electrostretching). The magnitude of this stress is high under low conductivities conditions. It brings an electrostretching of the membrane. This is supposed to contribute to the expansion step in the electropermeabilization. The induction of the force is very fast and is transiently present in the nanosecond range when a low conductivity buffer is present. The effect is not present when the buffer conductivity is close to the one of the cytoplasm.[53,54] This stretching effect can be present only when the rise time of the electric pulse is very fast (ns). This is not the case with pulse generators routinely used nowadays. But this effect should be kept in mind with the new developments of ns HV pulse generators.

As a consequence, organelles can be electropermeabilized by nanosecond long pulses. This is indeed what is observed. Cytoplasmic stored Calcium pools are observed to be released by nanosecond pulses. Permeabilization of organelles can be used to trigger apoptosis and cell death without direct leak from the cytoplasm. This was proposed as an approach to destroy tumor cells.[52,55-58] Preclinical studies of drug free tumor eradication were reported.[59,60]

The nuclear enveloppe can be permeabilized. Therefore, a new strategy for plasmid transfer is present. In a first step, millisecond pulses are used to introduced plasmids in the cytoplasm as classically described. After a 30 min incubation, a nanosecond high strength field is applied to induce the destabilization of the nucleus membrane and to facilitate the nuclear transfer of the plasmid and its expression. A significant increase of expression can be apparently obtained.[61]

This new methodology is a "hot" field of investigations where encouraging results have been published. But it is not yet a mature field as "classical" electropulsation.

Conclusions

"Classical" Electropermeabilization processes can be followed from microseconds up to days. Kinetic studies of electropermeabilization led to a description in 5 steps:

1- "*Induction step*"- the field induced the membrane potential difference increase which gave local defects (may be due to kinks in the lipid chains) when it reached a critical value (about 200 mV). A mechanical stress was present with a magnitude that depends on the buffer composition. This can be detected in less than 1 nanosecond but a limit is given by the charging time of the membrane. Molecular dynamic simulation suggests that it is much faster [62] in agreement with the nanosecond experiments (μs to ns due to the pulse generator).

2- "*Expansion step*"- These defects expanded as long as the field was present and with a strength larger than a critical value. Again an electromechanical stress remained present. This may be due to a "coalescence" process (μs to ms)

3- "*Stabilisation step*"- As soon as the field intensity was lower than the threshold value, that is mentioned in step 1, stabilisa-

Table 1. Operating parameters for the *in vitro* applications of electropulsation on mammalian cells

Applications	Duration	Field strength	Number of pulses
Electrochemotherapy (ECT)	100 μs	1.3 kV/cm	8
Electrotransfection (EGT)	5 to 10 ms	0.5 to 0.8 kV/cm	8
Eradication (IRE)	300 μs	1.5 kV/cm	3 x 10
Nanopulse eradication (nsIRE)	60 ns	12 kV/cm	200

tion processes were taking place within a few milliseconds, which brought the membrane to the permeabilized state for small molecules (ms).

4- "*Resealing step*"- A slow resealing was then occurring on a scale of seconds and minutes. It was a first order process. It is driven by the cellular metabolism (s to min).

5- "*Memory effect* "- Some changes in the membrane properties remained present on a longer time scale (hours) but the cell behaviour was finally back to normal.

Experiments showed that the mechanism of DNA transfer was different from what was observed for electropermeabilization (transfer of small molecules). Indeed, experimental results led to the conclusion that plasmids had to be present during electropulsation but crossed the electropulsed membrane in the minutes following it. No gene transfer was detected with a post-pulse DNA addition. These results were obtained on bacteria, yeast and mammalian cells.[37,63,64]

We proposed a model in which Electrotransfection appears as a multistep process [43] and brought its direct experimental evidence.[45.]

During the pulse,

i- electropermeabilization takes place (μs)
ii- plasmids are electrophoretically driven into contacts with the cell surface (ms)
iii- a metastable complex is formed between plasmids and the localised electropermeabilized part of the cell membrane (ms).
iv- a stable complex results (s)
v- long after the pulse, plasmids left the complex and diffused in the cytoplasm (min)
vi- a small fraction crossed the nuclear envelope to be expressed (h).

This interaction between plasmids and electropermeabilized membrane is strongly controlled by the pulse duration (always on the ms time scale). Additive effects of successive pulses are obtained. Only the localised part of the cell membrane brought to the permeabilized state by the external field is competent for the transfer.[43]

Practical consequences

Electropermeabilization is one of the non-viral methods successfully used to transfer genes into living cells *in vitro* as *in vivo*. It has the main advantages of being easy to perform, fast, reproducible and safe. This approach appears promising for gene therapy and is a clinical routine for drug delivery. A careful choice of the pulse duration and delays between the successive steps of electropulsation is needed to get successful applications (Table 1).[65] This remains linked to phenomenological conclusions. Its further developments need a better understanding of the basic effects induced at the membrane, cellular and tissue levels by electrical events and the plasmid entry in the cell.

Acknowledgements

This work was supported by the CNRS, the AFM (Association française pour les myopathies), the région Midi Pyrénées and the Proteus Slovenia-CNRS exchange program.

The authors wish to thank their colleagues: L. Mir in Villejuif (France), D. Miklavcic, T. Kotnik, M. Cemazar, G. Sersa and G. Pucihar, all from Ljubljana (Slovenia) and E. Neumann in Bielefeld (Germany) for so many helpful discussions.

References

1. Neumann E, Sowers AE, Jordan CA. Electroporation and electrofusion in cell biology. York: Plenum press; 1989.

2. Orlowski S, Mir LM. Cell electropermeabilization: a new tool for biochemical and pharmacological studies. *Biochim Biophys Acta* 1993; **1154:** 51-63.

3. Eynard N, Rols MP, Ganeva V, Galutzov B., Sabri N, Teissié J. Electrotransformation pathways of procaryotic and eucaryotic cells: recents developments. *Bioelectrochem Bioenerg* 1997; **44:** 103-10.

4. Mir LM, Roth C, Orlowski S, Quintin Colonna F, Fradelizi D, et al. Systemic antitumor effects of electrochemotherapy combined with histoincompatible cells secreting interleukin-2. Systemic antitumor effects of electrochemotherapy combined with histoincompatible cells secreting interleukin-2. J Immunother Emphasis Tumor Immunol 1995; **17:** 30-8 .

5. Cemazar M, Sersa G. Electrotransfer of therapeutic molecules into tissues.*Curr Opin Mol Ther* 2007; **9:** 554-62.

6. Sersa G, Miklavcic D, Cemazar M, Rudolf Z, Pucihar G, Snoj M. Electrochemotherapy in treatment of tumours. *Eur J Surg Oncol* 2008; **34:** 232-40.

7. Mir LM, Gehl J, Sersa G, Collins CG, Garbay JR, Billard V, et al. Standard operating procedures of the electrochemotherapy: Instructions for the use of bleomycin or cisplatin administered either systemically or locally and electric pulses delivered by the CliniporatorTM by means of invasive or non-invasive electrodes *Eur J Cancer 2006;* **42(Suppl 4):** 14-25.

8. Mir LM, Glass LF, Sersa G, Teissie J, Domenge C, Miklavcic D, et al. Effective treatment of cutaneous and subcutaneous malignant tumours by electrochemotherapy. *Br J Cancer* 1998; **77:** 2336-42.

9. Prausnitz MR, Bose VG, Langer R, Weaver JC. Electroporation of mammalian skin: a mechanism to enhance transdermal drug delivery. *Proc Natl Acad Sci USA* 1993; **90:** 10504-8.

10. Titomirov A, Sukarev S, Kistanova E. In vivo electroporation and stable transformation of skin cells of newborn mice by plasmid DNA. *Biochim Biophys Acta* 1991; **1088:** 131-4.

11. Heller R, Jaroszeski M, Atkin A, Moradpour D, Gilbert R, Wands J, et al. In vivo gene electroinjection and expression in rat liver. *FEBS Lett* 1996; **389:** 225-8.

12. Rols MP, Delteil C, Golzio M, Dumond P, Cros S, Teissie J. In vivo electrically mediated protein and gene transfer in murine melanoma. *Nat Biotechnol* 1998; **16:** 168-71.

13. Aihara H, Miyazaki J. Gene transfer into muscle by electroporation in vivo. *Nat Biotechnology* 1998; **16:** 867-70.

14. Mir LM, Bureau MF, Rangara R, Schwartz B, Sherman D. Long-term, high level in vivo gene expression after electric pulse- mediated gene transfer into skeletal muscle. *C R Acad Sci III* 1998; **321:** 893-9.

15. Muramatsu T, Nakamura A, Park M. In vivo electroporation: A powerful and convenient means of nonviral gene transfer to tissues of living animals. [Review]. *Int J Mol Med* 1998; **1:** 55-62.

16. Pliquett U, Joshi RP, Sridhara V, Schoenbach KH. High electrical field effects on cell membranes. *Bioelectrochemistry* 2007; **70:** 275-82.

17. Pakhomov AG, Kolb JF, White JA, Joshi RP, Xiao S, Schoenbach KH. Long-lasting plasma membrane permeabilization in mammalian cells by nanosecond pulsed electric field (nsPEF). *Bioelectromagnetics* 2007; **28:** 655-63.

18. Neumann E, Schaefer-Ridder M, Wang Y, Hofschneider PH. Gene transfer into mouse lyoma cells by electroporation in high electric fields. *EMBO J* 1982; **1:** 841-5.

19. Gross D, Loew LM, Webb WW. Optical imaging of cell membrane potential changes induced by applied electric fields. *Biophys J* 1986; **50:** 339-48.

20. Lojewska Z, Farkas DL, Ehrenberg B, Loew LM. Analysis of the effect of medium and membrane conductance on the amplitude and kinetics of membrane potentials induced by externally applied electric fields. *Biophys J* 1989; **56:** 121-8.

21. Hibino M, Shigemori M, Itoh H, Nagayama K, Kinosita K jr. Membrane conductance of an electroporated cell analyzed by submicrosecond imaging of transmembrane potential. *Biophys J* 1991; **59:** 209-20.

22. Kotnik T, Pucihar G, Rebersek M, Miklavcic D, Mir LM. Role of pulse shape in cell membrane electropermeabilization. *Biochim Biophys Acta* 2003; **1614:** 193-200.

23. Pucihar G, Kotnik T, Valic B, Miklavcic D. Numerical determination of transmembrane voltage induced on irregularly shaped cells. *Ann Biomed Eng* 2006; **34:** 642-52.

24. Valic B, Golzio M, Pavlin M, Schatz A, Faurie C, Gabriel B, et al. Effect of electric field induced transmembrane potential on spheroidal cells: theory and experiment. *Eur Biophys J* 2003; **32:** 519-28.

25. Teissié J, Tsong TY. Electric field induced transient pores in phospholipid bilayer vesicles. *Biochemistry* 1981; **20:** 1548-54.

26. Teissié J, Rols MP. An experimental evaluation of the critical potential difference inducing cell membrane electropermeabilization. *Biophys J* 1993; **65:** 409-13.

27. Rols MP, Teissie J. Electropermeabilization of mammalian cells. Quantitative analysis of the phenomenon. *Biophys J* 1990; **58:** 1089-98.

28. Gabriel B, Teissie J. Direct observation in the millisecond time range of fluorescent molecule asymmetrical interaction with the electropermeabilized cell membrane. *Biophys J* 1997; **73:** 2630-7.

29. Gabriel B, Teissie J. Time courses of mammalian cell electropermeabilization observed by millisecond imaging of membrane property changes during the pulse. *Biophys J* 1999; **76:** 2158-65.

30. Pucihar G, Kotnik T, Miklavic D, Teissie J. Kinetics of transmembrane transport of small molecules into electropermeabilized cells. *Biophys J* 2008; **95:** 2837-48.

31. Rols MP, Delteil C, Golzio M, Teissie J. Control by ATP and ADP of voltage-induced mammalian-cell-membrane permeabilization, gene transfer and resulting expression. *Eur J Biochem* 1998; **254:** 382-8.

32. Pucihar G, Mir LM, Miklavcic D. The effect of pulse repetition frequency on the uptake into electropermeabilized cells in vitro with possible applications in electrochemotherapy. *Bioelectrochemistry* 2002; **57:** 167-72.

33. Teissie J, Rols MP. Manipulation of cell cytoskeleton affects the lifetime of cell membrane electropermeabilization. *Ann N Y Acad Sci* 1994; **720:** 98-110.

34. Kinosita K Jr, Tsong TY. Voltage-induced conductance in human erythrocyte membranes. *Biochim Biophys Acta* 1979; **554:** 479-97.

35. Gabriel B, Teissie J. Generation of reactive-oxygen species induced by electropermeabilization of Chinese hamster ovary cells and their consequence on cell viability. *Eur J Biochem* 1994; **223:** 25-33.

36. Kinosita K Jr,Tsong TY. Hemolysis of human erythrocytes by transient electric field. *Proc Natl Acad Sci USA* 1977; **74:** 1923-7.

37. Golzio M., Mora MP, Raynaud C, Deltei C, Teissie J, Rols MP. Control by osmotic pressure of voltage-induced permeabilization and gene transfer in mammalian cells. *Biophys J* 1998; **74:** 3015-22.

38. Tsong TY. Electroporation of cell membranes. *Biophys J* 1991; **60:** 297–306.

39. Haest CW, Kamp D, Deuticke B. Transbilayer reorientation of phospholipid probes in the human erythrocyte membrane. Lessons from studies on electroporated and resealed cells. *Biochim Biophys Acta* 1997; **1325:** 17-33.

40. Rols MP, Teissie J. Electropermeabilization of mammalian cells to macromolecules: control by pulse duration. *Biophys J* 1998; **75:** 1415-23.

41. Al-Sakere B, Andre F, Bernat C, Connault E, Opolon P, Davalos RV, et al. Tumor ablation with irreversible electroporation. *PLoS ONE* 2007; **2(11):** e1135.

42. Klenchin VA, Sukharev SI, Serov SM, Chernomordik LV, Chizmadzev YuA Electrically induced DNA uptake by cells is a fast process involving DNA electrophoresis. *Biophys J* 1991; **60:** 804-11.

43. Wolf H, Rols MP, Boldt E, Neumann E, Teissie J. Control by pulse parameters of electric field-mediated gene transfer in mammalian cells. *Biophys J* 1994; **66:** 524-31.

44. Rols MP, Teissie J. Electropermeabilization of mammalian cells to macromolecules: control by pulse duration. *Biophys J* 1998; **75:** 1415-23.

45. Golzio M, Teissie J, Rols MP. Direct visualization at the single-cell level of electrically mediated gene delivery. *Proc Natl Acad Sci U S A* 2002; **99:** 1292-7.

46. Neumann E, Werner E, Sprafke A, Kruger K. Electroporation phenomena. Electrooptics of plasmid DNA and of lipid bilayer vesicles. In: Jennings BR, Stoylov SP, editors. Colloid and molecular electro-optics. Bristol: IOP publishing LTD; 1992. p. 197-206.

47. Rols MP, Coulet D, Teissie J. Highly efficient transfection of mammalian cells by electric field pulses. Application to large volumes of cell culture by using a flow system. *Eur J Biochem* 1992; **206:** 115-21.

48. Kubiniec RT, Liang H, Hui SW. Effects of pulse length and pulse strength on transfection by electroporation. *Biotechniques* 1990; **8:** 16-20.

49. Ferreira E, Potier E, Logeart-Avramoglou D, Salomskaite-Davalgiene S, Mir LM, Petite H. Optimization of a gene electrotransfer method for mesenchymal stem cell transfection. *Gene Ther* 2008; **15:** 537-44.

50. Frey W, White JA, Price RO, Blackmore PF, Joshi RP, Nuccitelli R, et al. Plasma membrane voltage changes during nanosecond pulsed electric field exposure. *Biophys J* 2006; **90:** 3608-15.

51. Kotnik T, Miklavcic D. Theoretical evaluation of voltage inducement on internal membranes of biological cells exposed to electric fields. *Biophys J* 2006; **90:** 480-91.

52. Tekle E, Oubrahim H, Dzekunov SM, Kolb JF, Schoenbach KH, Chock PB. Selective field effects on intracellular vacuoles and vesicle membranes with nanosecond electric pulses. *Biophys J* 2005; **89:** 274-84.

53. Muller KJ, Sukhorukov VL, Zimmermann U. Reversible electropermeabilization of mammalian cells by high-intensity, ultra-short pulses of submicrosecond duration. *J Membr Biol* 2001; **184**: 161-70.

54. Sukhorukov VL, Mussauer H, Zimmermann U. The effect of electrical deformation forces on the electropermeabilization of erythrocyte membranes in low- and high-conductivity media. *J Membr Biol* 1998; **163:** 235-45.

55. Beebe SJ, Fox PM, Rec LJ, Willis LK, Schoenbach KH. Nanosecond high intensity pulsed electric fields induce apoptosis in human cells. *FASEB J* 2003; **30:** 286–292.

56. Vernier TP, Sun YH, Marcu L, Craft CM, Gundersen MA. Nanoelectropore-induced phosphatidylserine translocation. *Biophys J* 2004; **86:** 4040–8.

57. Brown FD, Rozelle AL, Yin HL, Balla T, Donaldson JG. Phosphatidylinositol 4,5-bisphosphate and Arf-regulated membrane traffic. *J Biol Chem* 2001; **154:** 1007–17.

58. White JA, Blackmore PF, Schoenbach KH, Beebe SJ. Stimulation of capacitative calcium entry in HL-60 cells by nanosecond pulsed electric fields. *J Biol Chem* 2004; **279:** 22964–72.

59. Nuccitelli R, Pliquet U, Chen X, Ford W, James Swanson R, Beebe SJ, et al. Nanosecond pulsed electric fields cause melanomas to self-destruct. *Biochem Biophys Res Commun* 2006; **343:** 351-60.

60. Garon EB, Sawcer D, Vernier PT, Tang T, Sun Y, Marcu L, et al. .In vitro and in vivo evaluation and a case report of intense nanosecond pulsed electric field as a local therapy for human malignancies. *Int J Cancer* 2007; **121:** 675-82.

61. Beebe SJ, White J, Blackmore PF, Deng Y, Somers K, Schoenbach KH. Diverse effects of nanosecond pulsed electric fields on cells and tissues. *DNA Cell Biol* 2003; **22:** 785-96.

62. Tarek M. Membrane electroporation: a molecular dynamics simulation. *Biophys J* 2005; **88:** 4045-53.

63. Eynard N, Sixou S, Duran N, Teissie J. Fast kinetics studies of Escherichia coli electrotransformation. *Eur J Biochem* 1992; **209:** 431-6.

64. Ganeva V, Galutzov B, Teissie J. Fast kinetic studies of plasmid DNA transfer in intact yeast cells mediated by electropulsation. *Biochem Biophys Res Commun* 1995; **214:** 825-32.

65. Lebar AM, Sersa G, Kranjc S, Groselj A, Miklavcic D. Optimisation of pulse parameters in vitro for in vivo electrochemotherapy. *Anticancer Res* 2002; **22:** 1731-6.

66. Phez E, Faurie C, Golzio M, Teissié J, Rols MP. New insights in the visualization of membrane permeabilization and DNA/membrane interaction of cells submitted to electric pulses. *Biochim Biophys Acta* 2005; **1724:** 248-54.

2. In vivo

Escoffre JM, Paganin-Gioanni A, Golzio M, Rols MP and Teissie J (2010) Gene electrotransfer: From basic processes to preclinical applications. Adv. Elec. Tech. Biol. Med. (Accepted Book Chapter).

Escoffre JM, Debin A, Reynes JP, Drocourt D, Tiraby G, Hellaudais L, Teissie J, and Golzio M (2008) Long-lasting in vivo gene silencing by electrotransfer of shRNA expressing plasmid. Technol. Cancer Res. Treat., 7:1-8 (Article).

Paganin-Gioanni A, **Escoffre JM,** Mazzolini L, Rols MP, Teissie J, and Golzio M (2007) In vivo imaging of siRNA electrotransfer and silencing in different organs. IFMBE Proceedings, 16:624-627 (Book Chapter).

14

Gene Electrotransfer: From Basic Processes to Preclinical Applications

Jean-Michel Escoffre
Université de Toulouse

Aurélie Paganin-Gioanni
Université de Toulouse

Elisabeth Bellard
Université de Toulouse

Muriel Golzio
Université de Toulouse

Marie-Pierre Rols
Université de Toulouse

Justin Teissié
Université de Toulouse

14.1 Introduction

Plasmid-DNA-based gene transfer is an elegant strategy for gene therapy because it suppresses the need for a biological (viral) vector, although its use is limited by the lack of efficient and safe delivery methods (Gill et al., 2009). When compared with viral vector, the advantages include the absence of immunogenicity and integration into the host genome (Gill et al., 2009). One physical method that has emerged as a way to improve the *in vivo* delivery of plasmid DNA is electropermeabilization (or electroporation). Since its first demonstration 25 years ago (Neumann et al., 1982), this method is now routinely used for *in vitro* transfection (Escoffre et al., 2009; Mir, 2009). The application of controlled electric pulses causes a transient permeabilization of the plasma membrane and thus allows exogenous
AQ1 molecules to enter the cells (Teissié et al., 2005; Escoffre et al., 2008). *In vivo*, electropermeabilization is efficient for enhanced plasmid DNA delivery and expression (Heller et al., 1996; Rols et al., 1998). *In vivo*, electropermeabilization is effective on many tissues: skeletal muscle (Aihara and Miyazaki, 1998; Mir et al., 1999), liver (Heller et al., 1996), skin (Vandermeulen et al., 2007), brain (Kondoh et al., 2000), testis (Huang et al., 2000), and tumor (Rols et al., 1998). The use of *in vivo* gene electrotransfer has seen tremendous growth, including the initiation of clinical trials (Daud et al., 2008; Horton et al., 2008; Gehl, 2008).

Gene expression levels, patterns, and kinetics after *in vivo* gene electrotransfer can be controlled by modifying electrode configurations, electrical parameters, tissue features, and plasmid constructs (Heller and Heller, 2006). The resulting flexibility in *in vivo* expression is a distinct advantage of electropulsation. Most of these parameters should be carefully selected to obtain specific gene expression associated for desired therapeutic benefit. The increased use of *in vivo* gene electrotransfer has established its potential for many therapeutic applications such as cancer therapy and DNA vaccination. Useful information on *in vivo* gene electrotransfer can be found in several recent reviews (Heller and Heller, 2006; Mir, 2009).

This chapter focuses on the basic processes involved in preclinical application of gene electrotransfer. The biophysical mechanisms of electrically mediated gene transfer will first be described. The relative contributions of physical and biochemical parameters on the efficiency and safety of *in vivo* gene electrotransfer will also be delineated.

14.2 Biophysical Considerations

14.2.1 Present Knowledge on the *In Vitro* Electrotransfer

Gene electrotransfer to mammalian cells is obtained by mixing cells and plasmids in a biocompatible buffer, then by applying a well-controlled electric field pulse train (shape of pulses; choice of field strength, E; pulse duration, T; number of pulses, N; pulse repetition frequency, f), and finally bringing the mixture in a culture medium (Neumann et al., 1982; Klenchin et al., 1991; Wolf et al., 1994). Gene electrotransfer is applicable whatever the cell types (bacteria, yeast, and mammalian cells) (Golzio et al. 1998; Eynard et al., 1992; Ganeva et al., 1995).

14.2.1.1 Electric Field Strength Effects

Gene electrotransfer is only detected for electric field values leading to membrane permeabilization ($E_c > E_p$). Transfection threshold values (E_t) are the same as the ones for cell permeabilization (E_p) when milliseconds pulses are applied (Rols and Teissié, 1998). Field strength is observed to have a critical role. Plasmid molecules, negatively charged, migrate when submitted to an electric field (Neumann et al., 1992; Wolf et al., 1994). In the "low" electric field regime (i.e. $E_c < E_p$), no membrane permeabilization occurs and plasmid simply electrophoretically flows along the cell membrane toward the anode. However, above the critical permeabilizing field value ($E_c > E_p$), two main processes occur: (1) plasma membrane is permeabilized (μs); and (2) plasmid undergoes the electrophoretic migration (ms) and interacts with permeabilized membrane (Golzio et al., 2002; Teissié et al., 2008).

14.2.1.2 Timescale

No free plasmid diffusion into the cytoplasm is detected though it was proposed in older reports (Klenchin et al., 1991). The biophysical structure of the plasmid/membrane complex has to be elucidated. In the minutes following pulse applications, plasmids leave the complex and diffuse in the cytoplasm. Then, plasmids can be observed at the nucleus surface a few hours after electropulsation, but only a small fraction crosses the nuclear envelope to be expressed (Golzio et al., 2002). These intracellular steps remain rather poorly understood, as already mentioned (Teissié et al., 2008).

Under permeabilizing field conditions, the pulse duration plays a critical role in the formation of the plasmid/membrane complexes. These complexes are easily detected when the pulse duration is at least about 1 ms. Furthermore, this interpretation is supported by the observation that the plasmid content in the complex is under the control of the field strength (E), the number of successive pulses (N), and the pulse duration (T) (Golzio et al., 2002). The time for reaction with the membrane of the plasmid dragged against permeabilized membrane under the electrophoretic migration is increased by long pulse durations. This again is involved in the positive role of the pulse duration in gene electrotransfer.

This contribution of the pulse duration to the plasmid/membrane interaction has already been illustrated by a complex dependence of the gene expression (Wolf et al., 1994). The practical conclusion is that *in vitro* an effective transfer is obtained by using long pulses in order to drive the plasmid toward the permeabilized membrane but with low field strength to preserve the cell viability (Kubiniec et al., 1990; Rols and Teissié, 1998). But one should keep in mind that plasmids must be mixed with cells before the application of electric pulses.

14.2.1.3 Biological Parameters

The dependence on the plasmid concentration is rather complex. Expression levels increase with the plasmid concentrations. But high levels of plasmids appear to be toxic (Rols et al., 1992).

Because there are different physical barriers and heterogeneous geometries within tissue, *in vitro* pseudo-tissue models such as dense cell suspensions (Pucihar et al., 2007) and multicellular tumor spheroid (Canatella et al., 2004; Wasungu et al., 2009) have been developed to understand the biophysical processes of electropermeabilization and gene transfer in tissues. These studies showed a perturbation of local electrical field on dense cell suspensions (Susil et al., 1998; Pavlin et al., 2002), affecting both permeabilization and gene expression (Pucihar et al., 2007) and a hindrance to gene delivery (Wasungu et al., 2009) related to the self-organization of cells in pseudo-tissues. Indeed, close contacts between cells and extracellular matrix (1) modify the electric field distribution and (2) act as physical barriers that limit the diffusion of DNA plasmid (steric hindrance) and therefore its access to cells present in the core of the tissue. The systematic comparison of biophysical studies from isolated cells to 3D spheroid model allows the development and the optimization of *in vivo* gene electrotransfer procedures.

AQ2

14.2.2 *In Vivo* Gene Electrotransfer

14.2.2.1 Electropulsation Protocols

The increased use of *in vivo* gene electrotransfer is related to both the efficiency and the flexibility (i.e. easy to perform, fast, reproducible, and safe) of this physical method. Plasmid DNA has been successfully delivered to both internal and surface tissues and organs (Heller and Heller, 2006). Because the gene expression characteristics (i.e., level and duration) can be varied by meticulous selection of electrical parameters, the selection of those parameters is important to achieve a compatible profile of gene expression with a therapeutic benefit. In agreement with *in vitro* mechanism of gene electrotransfer, these electrical parameters have to be adapted to induce cell permeabilization within the tissue, electrophoresis of plasmid molecules, and no damage to the tissue. Seven different protocols of electropulsation have been reported to obtain suitable gene expression into tissues (Table 14.1). Appropriate electrical parameter selection is dependent on the tissue being targeted. One should notice that in most protocols, the voltage term (V) while inaccurate is used for the field. This "V" terminology will be retained.

14.2.2.1.1 Long Pulse and Medium Voltage (LPMV)

As for *in vitro* protocols, the use of square-wave long and medium pulses is the most popular pulse design for *in vivo* gene electrotransfer. The first successful efficient gene transfer in melanoma tumors was obtained with electric pulses of a few ms duration (Rols et al., 1998). Low and long field strength pulses are shown to induce high and long gene expression in skeletal muscle (Aihara and Miyazaki, 1998; Mir et al., 1999; Lucas and Heller, 2001), skin (Pedron-Mazoyer et al., 2007), and liver (Suzuki et al., 1998). As with *in vitro* results, DNA plasmid had to be present during the electric pulses. The application of long and low pulses induced the tissue permeabilization and localized electrophoresis of DNA plasmid within the target tissues. Muscle damage may be present. Interestingly, a pulse duration control of the delivered voltage was demonstrated to reduce muscle damage while maintaining the same level of gene transfection (Cukjati et al., 2007).

TABLE 14.1 *In Vivo* Gene Electrotransfer Protocols

References	No. of Pulses	Shape, Polarity	Electric Field	Pulse Length (ms)	Frequency (Hz)	Tissue
Aihara and Miyazaki (1998) and Draghia-Akli et al. (1999)	4–6	Square, monopolar (alternate polarity)	60–400 V/cm	50	1	Skeletal muscle
Rols et al. (1998), Mir et al. (1999), and MacMahon et al. (2001)	8–10	Square, monopolar	100–200 V/cm	20	1–8	Skeletal muscle, melanoma
Mathiesen (1999) and Rizzuto et al. (1999)	8,000–10,000	Square, bipolar	100 V/cm	0.2	1000	Skeletal muscle
Vicat et al. (2000) and Heller et al. (1996)	5	Square, monopolar	1600 V/cm	0.1	1	Skeletal muscle, liver
Bureau et al. (2000) and Satkauskas et al. (2002, 2005) Pavselj and Préat (2005)	HV: 1–8 LV: 1–16	Square, monopolar	HV: 800 V/cm LV: 60–100 V/cm	HV: 0.01–0.5 LV: 50–800	HV: 1 LV: 5–100	Skeletal muscle, liver, skin, tumor
Liu et al. (2007) and Simon et al. (2008)	1–9	Alternating current sine wave	10–30 V/cm	100–900	60	Skeletal muscle, liver, skin, tumor
Khan et al. (2005) and Hirao et al. (2008)	2–3	Square, monopolar	0.1–0.5 A[a]	20–52	1	Skeletal muscle

[a] Current.

14.2.2.1.2 Short Pulses and High Voltage (SPHV)

In hepatocellular carcinoma, high expression is obtained with short and high field strength pulses (Heller et al., 1996). Vicat and collaborators showed that short and high field strength pulses also induced high gene expression in the skeletal muscle. Gene electrotransfer with short and high field strength pulses was reported to provide sustained and long-lasting gene expression (Vicat et al., 2000), a conclusion in conflict with a later observation (Lucas and Heller, 2001) where short expression was associated to the use of short pulses.

14.2.2.1.3 High Voltage and Low Voltage (HVLV)

The studies on mechanisms of gene electrotransfer *in vitro* highlighted that electrically mediated delivery included a permeabilizing component that permeabilized the plasma membrane and an electrophoretic component that facilitated transport of molecules to the permeabilized membrane. These studies suggested that this delivery method should include *in vivo* two basic components that could be obtained by combining two pulse types (Mir, 2009). This combination includes a short and high field strength pulse (i.e., permeabilizing component), followed by long and low field strength pulses (i.e., electrophoretic component). This hypothesis was evaluated for gene transfer to skeletal muscle (Bureau et al., 2000; Durieux et al., 2002; Satkauskas et al., 2002, 2005, André et al., 2008), tumor, skin (Pavselj and Préat, 2005), and liver (André et al., 2008; Cemazar et al., 2009). The combined pulses allow for the use of pulsing parameters, which could reduce potential discomfort from the electropulsation procedure. A large range of LV strengths can be used to obtain a significant luciferase gene expression in muscles Additional variables that should be considered include pulse number (the LV can be a train of pulses) and pulse frequency (which was always 1 Hz).

14.2.2.1.4 Short Pulse and High Frequency (SPHF)

An alternative approach, which consisted of applying short bipolar pulses (0.2 ms) at high repetition frequency (100–1000 Hz), was found to be also effective (Mathiesen, 1999; Rizzuto et al., 1999, 2000). Rizzuto and collaborator demonstrated that high-frequency trains of electric pulses cause less damage than single long pulses for the same cumulative pulse duration (Rizzuto et al., 1999; Zampaglione et al., 2005). On the basis of previous studies, bipolar pulses should be chosen for future applications, as they do not in fact cause a net movement of charges and thus side effects such as electrochemical effects should be reduced. SPHF electropulsations are a safe and efficient method to erythropoietin gene transfer into skeletal muscles of mice (Rizzuto et al., 1999, 2000; Mennuni et al., 2002; Cappelletti et al., 2003; Fattori et al., 2005), rabbit (Fattori et al., 2005; Zampaglione et al., 2005), and nonhuman primates (Fattori et al., 2005; Zampaglione et al., 2005) in preclinical trials of anemia related to kidney failure. Moreover, this electropulsation procedure is successfully used in preclinical development of genetic vaccination against tumors (Cipriani et al., 2008; Dharmapuri et al., 2009; Peruzzi et al., 2009). This protocol opens a new field for basic research, as the electrophoretic long range drift of DNA is not present. The bipolar field gives only a local movement on the submillisecond timescale.

14.2.2.1.5 Alternating Current Sine Waves (ACSW)

Currently, all commercial electropulse generators are designed to provide direct current (DC) square-wave pulses, which cause membrane permeabilization and are believed to be critical also for providing the electrophoretic force needed for DNA movement to the cell membrane (Bureau et al., 2000; Miklavcic et al., 2000; Satkauskas et al., 2002, 2005). Typically, achieving high levels of gene expression using the traditional DC square-wave pulses requires electric field strengths, prone to result in irreversible tissue damage (Muramatsu et al., 1998; Durieux et al., 2004; MacMahon and Wells, 2004). Studies in human volunteers on electroporation of skin (Wallace et al., 2001) and muscle (Tjelle et al., 2006) have shown that the high field strength of DC square-wave pulses at 1 Hz leads to an augmented sensation of pain. Liu and collaborators showed that efficient *in vivo* gene transfer is achieved using the low and safe pulses of ACSW with a frequency of 60 Hz (Liu et al., 2007). Compared with traditional DC square-wave pulses, the ACSW pulses used in this study established no net electrophoretic force but resulted in higher gene transfer efficiency, supporting their previous finding that electrophoretic forces are not involved in gene electrotransfer *in vivo* (Liu et al., 2006). Importantly, the field strength required to obtain high level of gene transfer was with less toxicity observed than with conventional DC square-wave pulses.

14.2.2.1.6 Constant-Current Electroporation (CCV)

Conventional electropulsation technologies are based upon constant-voltage concepts. Due to decreases in the tissue resistance during the electropermeabilization process, a clamped voltage pulse brings an increase in the current flowing through the tissue during the duration of the pulse and may result in loss of the perfect square-wave function, tissue damage, and reduced plasmid transfer and expression (Gehl and Mir, 1999; Gehl et al., 1999). Previous studies focused that the tissue resistance varies from subject to subject, from tissue to tissue within the same animal and during the electropermeabilization due to cellular uptake of the formulation volume (Khan et al., 2005). The constant-current electropulsation setup is able to measure the tissue resistance before, between, and during the electric field pulses and adjust the voltage to account for these individual changes. This feature allows the device to maintain a true constant-current delivery and a square wave through the tissue during electropermeabilization, preventing heating of tissue (Bloquel et al., 2004) and consequently reducing tissue damage and pain, as well as contributing to the overall increase in plasmid transfer and expression (Fattori et al., 2005; Khan et al., 2005). Constant-current electropulsation is a very efficient technology to develop DNA vaccination on small and high animals (Curcio et al., 2008; Draghia-Akli et al., 2008; Hirao et al., 2008).

14.2.2.2 Applicator Types

The choice of applicator types used for electropermeabilization is a crucial step in an efficient and safe gene transfer. A key parameter of gene electrotransfer is the local electric field strength. As the field results from a voltage applied between two electrodes, the electrode configuration is obviously controlling the field distribution and resulting transfection efficiency (Gehl and Mir, 1999). Electrode configurations for therapeutic purposes are parallel plates, contact wires, contact plates, needle pairs, and needle arrays (Gilbert et al., 1997; Jaroszeski et al., 1997; Ramirez et al., 1998; Mazères et al., 2009). Electrode configuration controls electric field distribution in tissue. However, due to its anatomy and its electrical properties, the tissue reacts to the applied external electric field. If the applied external electric field is high enough, local permeabilization of the tissue occurs, i.e., electric field distribution strongly controls permeabilization (Miklavcic et al., 1998). But if the local electric field is too high, an irreversible local alteration of cell membrane occurs. This may result in local burns. In gene therapy, it is very important to obtain a large volume of permeabilized tissue, within the tissue being subjected to electropulsation while preserving cell viability. A safe approach in the design of optimal electrode configuration is to compute the electric field distribution in tissues by means of numerical modeling. Modeling of electric field distribution in tissue is difficult due to heterogeneous material properties of tissue and its shape (Mossop et al., 2006; Pavselj and Miklavcic, 2008). Therefore, tissue electrical heterogeneity was never taken into account in the simulation, (Gowrishankar and Weaver, 2003). Due to the swelling, the volume fraction was affected (Deng et al., 2003). Such a geometrical change should affect the field distribution in tissue and the value of the field at the cell level in the tissue (Pavlin et al., 2002). Numerical modeling on homogeneous phantom tissues has been successfully used and also validated by comparison between computed and measured consequences of electric field distribution (Miklavcic et al., 1998, 2000). Electropermeabilization induces a membrane conductance change as previously described (Kinosita and Tsong, 1979; Abidor et al., 1994) and observed in tissue (Miklavcic et al., 2000). A precise simulation of the time-dependent field distribution in the tissue is clearly needed for different electrode geometries to optimize this electro-technical aspect of the biological treatment (Pucihar et al., 2009).

14.2.2.2.1 Plate Parallel Electrodes

Plate parallel electrodes are the most frequently used in gene electrotransfer of different kinds of tissues such as skeletal muscle and tumor. Their limit is that the tissue must be pinched between the electrodes. These electrodes offer the advantages that electric pulses can be applied transcutaneously and that electric field between the electrodes is quite homogeneous (Gehl et al., 1999). Nevertheless, these electrodes have two main limitations: (1) the small gap between the electrodes, which is limited by the electrical power of electropulsators and (2) high field at the contact of the electrode with the skin, which can induce electrical burns.

14.2.2.2.2 Needle Electrodes

The needle electrodes enable deeper penetration of the electric field into the tissue. The electric field distribution is not homogenous resulting in higher field intensity around the needles bringing local tissue necrosis. The heterogeneous field distribution is under the control of the diameter of each electrode (Miklavcic et al., 2000). Furthermore, a syringe electrode device for simultaneous injection and electropermeabilization showed that lower electric field strength compared to plate electrodes is required for the same transfection efficiency, also reducing the muscle wound (Liu and Huang, 2002).

14.2.2.2.3 New Designs

Therefore, new electrodes are designed and tested to minimize tissue damages (Babiuk et al., 2003; Dona et al., 2003). Spatula electrodes used for electropermeabilization of mouse skeletal muscle were shown to induce less tissue damage compared to plate and needle electrodes (Dona et al., 2003). Needle-free

patch and Meander contact electrodes were proved to be effective and safe for gene delivery in the skin (Babiuk et al., 2003). Wire contact electrodes are highly user friendly for the treatment of large skin surfaces (Mazères et al., 2009).

14.3 Biological Aspects

14.3.1 Design of Plasmid Vectors

Plasmid DNA molecules are covalent closed circles of double-stranded DNA with no associated proteins. Plasmid DNA molecules are simpler, easier to mass-produce, and potentially safer than viral vectors (Gill et al., 2009). Low immunogenicity and lack of integration of plasmid DNA make them a highly attractive molecule for gene therapy provided that an efficient, safe, and targeted delivery can be achieved (Gill et al., 2009).

14.3.1.1 Plasmid Sequences

Huge constructs (3.5–20 kbp) can be electrotransferred but the size of the plasmid also has a role in effectiveness of gene electrotransfer (Wang et al., 2005). Injection of small plasmids alone and in combination with electropulsation induced better transfection efficiency compared to larger plasmid (Molnar et al., 2004; Wang et al., 2005). The relationship between the plasmid size and transfection efficiency was linear (Bloquel et al., 2004). Moreover, a new form of supercoiled plasmid DNA, called minicircle (1.5–3 kbp), has been developed, without any bacterial sequences and antibiotic resistance markers (Darquet et al., 1997; Gill et al., 2009). The bacterial sequences contain unmethylated bacterial CG dinucleotides, which are immunostimulator motives decreasing the duration of gene expression. A reduction or elimination of CpGs from plasmid DNA (CpG-free plasmid) leads to improvements in the level and persistence of gene expression (Hyde et al., 2008).

14.3.1.2 Nuclear Targeting

The mechanism, by which DNA migrates toward and into the nucleus in *in vivo* conditions by electropermeabilization, still has to be elucidated. To overcome the limitations regarding the migration of the plasmid inside the nucleus, several approaches have been used. One example is the inclusion of sequence that binds to transcription factor (TF) to facilitate intracellular trafficking and nuclear import. A region of smooth muscle γ-actin (SMGA) promoter that contains a number of smooth muscle-specific TF-binding sites have been shown to improve the nuclear uptake of plasmid DNA and also dramatically increases gene expression in vivo (Miller and Dean, 2008). When plasmid DNA containing the SMGA sequence was electrotransferred, gene expression was specifically detected into rat smooth muscle vasculature compared to plasmid DNA with SV40 sequence (Young et al., 2008).

14.3.1.3 Promoters

Promoter selection is crucial to the level and persistence of gene expression in different tissues. The preference for viral promoters (Vandermeulen et al., 2009), capable of high-level but often short-lived gene expression, has recently shifted toward selecting constitutively expressing (Matsuda and Cepko, 2007) or tissue-specific endogenous promoters (Durieux et al., 2005). Use of the human poly-ubiquitin C promoter has resulted in sustained expression in the mouse lung, following the delivery of naked plasmid DNA through electroporation (Gazdhar et al., 2006). Tissue-specific promoters may offer improved specificity and safety for gene electrotransfer (Durieux et al., 2005). For example, skin-specific promoters are used to restrict the expression of DNA vaccine to specific cell types (Vandermeulen et al., 2009). The use of plasmids with tissue-specific promoter resulted in significant, but very low protein expression, as compared to that obtained with ubiquitous and strong promoter, e.g., CMV and CAG promoters, plasmids. Nevertheless, for the success of gene therapy in clinics, it is essential to develop gene regulation systems (Rubenstrunk et al., 2005; Matsuda and Cepko, 2007).

Rubenstrunk and collaborators reported a regulation strategy based on the murine metallothionein promoter in a plasmid context using electric pulses delivery as an inducer (Rubenstrunk et al., 2005).

14.3.2 Injection and Biodistribution of Plasmid Vectors

Plasmid solutions should reach the target tissue localized between the electrodes, where electric pulses are applied. Gene expression depends on the amount of injected plasmid (range of plasmid amount: 20–100 μg) (Mathiesen, 1999; Mir et al., 1999) and on the volume of injection (Dupuis et al., 2000). For preclinical applications, different routes of injection are defined on the target: intramuscular (i.m.), intradermal (i.d.), intratumoral (i.t.), and intravenous (i.v.) (Lucas et al., 2002). The volume of injection is limited by the size of the target to avoid a dramatic and damaging tissue swelling. The injection speed is seldom taken into account. A recent work suggested that the injection speed is a key parameter to gene delivery into skeletal muscle and liver (André et al., 2006). In case of mice skeletal muscle, injection speed of 1.5 μL/s is associated with a high-level expression (Golzio et al., 2004). The delay between injection and electropulsation depends on the tissue. In the case of murine B16 melanoma tumors, a short delay (<1 min) leads to a high level of transfection (Rols et al., 1998). Whereas, in murine skeletal muscle, a delay between a few seconds and 4 h does not change the transfection efficiency (Satkauskas et al., 2001).

The space, which surrounds the cells, called extracellular space, contains several macromolecules, polysaccharides, or glycosaminoglycanes, fibrous proteins, salts, and water, called extracellular matrix (ECM). This ECM forms a structured gel (Berrier and Yamada, 2007). The presence of ECM into the tissue does not perturb the distribution of electric field but limits the diffusion, the electrophoretic movement, and the distribution of plasmids into the target tissue (Cappelletti et al., 2003; Henshaw and Yuan, 2008). Previous works show that delivery of plasmid DNA to cells in the target tissue such as skeletal muscles (Bureau et al., 2004), tumors (Netti et al., 2000; Pluen et al., 2001; Alexandrakis et al., 2004), skin (Vandermeulen et al., 2007), and respiratory tissues (Walther et al., 2005), is affected by the amount of nucleases, which degrade plasmid DNA, and by the amount of ECM components such as collagen (Netti et al., 2000; Pluen et al., 2001) and hyaluronic acid (Alexandrakis et al., 2004). Consequently, in order to increase the efficiency of gene transfer, some strategies have been developed to increase diffusion of plasmid DNA and to limit its degradation into the target tissues. The main strategy to increase the diffusion and distribution of plasmid DNA into the tissue consisted in controlled degradation of ECM by using enzymes such as hyaluronidase and collagenase. This approach is more efficient in the gene transfer into skeletal muscle (MacMahon et al., 2001; Mennuni et al., 2002; Molnar et al., 2004; Schertzer et al., 2006; Evans et al., 2008) and tumors (Mesojednik et al., 2007) but inefficient in skin (Vandermeulen et al., 2007). Indeed, some works showed that the pretreatment with hyaluronidase induced a 10- to 25-fold increase of gene expression in mice and rabbit skeletal muscle after i.m. injection and electropulsation compared to without pretreatment (MacMahon et al., 2001; Mennuni et al., 2002; Molnar et al., 2004; Schertzer et al., 2006). To limit the degradation of plasmid DNA, the main approach was to protect the plasmid DNA by using chemical formulation or to inhibit the exogenous DNAses. Nicol and collaborators showed that plasmid DNA formulated with poly-L-glutamate induced a 4- to 12-fold increase of gene expression in skeletal muscle after i.m. injection and electropulsation in comparison to saline injection alone (Nicol et al., 2002). Other works showed that the plasmid DNA formulated with poloxamers such as SP1017 increased gene expression by about 10-fold and maintained higher gene expression into skeletal muscle after gene electrotransfer compared with naked DNA alone (Riera et al., 2004). These data suggested that chemical formulation might enhance plasmid DNA expression by protecting the plasmid DNA from degradation by nucleases (Lemieux et al., 2000). The second approach consisted in the use of nuclease inhibitors such as aurintricarboxylic acid (ATA) (Glasspool-Malone and Malone, 2002).

14.4 Preclinical Applications

14.4.1 Production of Ectopic Proteins

The skeletal muscle is the preferred target for gene electrotransfer. Indeed, the skeletal muscle has interesting physiological properties being multinucleated (i.e., high number of expression machineries) and presenting long-lived fibers (i.e., long-lasting gene expression), which open several applications in gene therapy (Aihara and Miyazaki, 1998; Mir et al., 1999). Moreover, its rich vascularization makes muscle a secreting organ of therapeutic proteins (Trollet et al., 2008). Indeed, i.m. electrotransfer of plasmid encoding erythropoietin (EPO) induces the production of EPO therapeutic doses to treat the anemia related to kidney diseases (Rizzuto et al., 1999, Hojman et al., 2007). In the same way, TGFR-β2 receptor and VEGF-164 factor expressions treat respectively, the lung injury and fibrosis (Yamada et al., 2007) and diabetic neuropathy (Murakami et al., 2006).

Gene electrotransfer allowed the development of antitumoral immunotherapies. Indeed, electrotransfer of plasmid encoding suicide gene (e.g., ePNP/fludarabine) (Deharvengt et al., 2007), cytokines (e.g., IL-12) (Daud et al., 2008), antiangiogenesis factors (e.g., vasostatin) (Jazowiecka-Rakus et al., 2006), and tumor suppressors (e.g., p53) (Kusumanto et al., 2007) into skeletal muscle or tumors stimulated or activated the immune responses against the tumors. This immunotherapy induced a decrease of tumor growth and limited the tumor recovery and metastasis progression.

14.4.2 DNA Vaccination

Gene electrotransfer allowed the development of genetic electrovaccination. Genetic vaccination results from a direct injection of plasmid encoding vaccinal protein into the muscle or the skin (Wolff et al., 1990; Rice et al., 2008). This protein induces the host response and activates the immune system. Compared to gene therapy, genetic vaccination requires only low and transient gene expression in a few cells (Rice et al., 2008). Several works showed that gene electrotransfer increases the immune response against the antigen compared to the injection alone (Dupuis et al., 2000; Widera et al., 2000; Babiuk et al., 2002; Dayball et al., 2003). The electrovaccination allowed the development of genetic vaccines against bacterial infections such as *Mycobacterium tuberculosis* (Zhang et al., 2007) and viral infections such as HIV (Martinon et al., 2009). Recently, electrovaccination showed its efficiency to induce immune response against tumors (Kalat et al., 2002; Buchan et al., 2005; Curcio et al., 2008; Seo et al., 2009). Improvement and modulation of the immune response induced by DNA vaccines are observed by boosting DNA vaccine expression with plasmid encoding cytokines such as interleukine-12 (Hirao et al., 2009). An open question is the putative positive effect of muscle fiber electrodamages that may play a role of adjuvants (Widera et al., 2000; Chiarella et al., 2008).

14.5 Conclusions

This chapter attempts to evaluate the contributions of different parameters on the efficiency of nucleic acid delivery by electropulsation. A rather fair control of gene electrotransfer can be obtained by selecting appropriate physical as well as biochemical parameters, and optimization can be performed in order to obtain highly efficient expression both *in vitro* and *in vivo* for preclinical studies. At the present state of our knowledge, no negative consequence of gene electrotransfer has been reported *in vivo*. Even if clinical protocols now are under trial (Daud et al., 2008), other experimental studies (such as preclinical research on pets: dog, cat, and horse) are needed to evaluate other potential side effects.

Acknowledgments

This contribution was supported by grants from Region Midi-Pyrénées, ANR Cemirbio, DGA (REI2), and AFM.

References

Abidor IG, Li LH, Hui SW (1994) Studies of cell pellets: II. Osmotic properties, electroporation, and related phenomena: Membrane interactions. *Biophys J* 67:427–435.

Aihara H, Miyazaki JI (1998) Gene transfer into muscle by electroporation in vivo. *Nat Biotechnol* 16:867–870.

André FM, Cournil-Henrionnet C, Vernerey D, Opolon P, Mir LM (2006) Variability of naked DNA expression after direct local injection: The influence of the injection speed. *Gene Ther* 13:1619–1627.

André FM, Gehl J, Sersa G, Préat V, Hojman P, Eriksen J et al. (2008) Efficiency of high- and low-voltage pulse combinations for gene electrotransfer in muscle, liver, tumor and skin. *Hum Gene Ther* 19:1261–1271.

Alexandrakis G, Brown EB, Tong RT, McKee TD, Campbell RB, Boucher T et al. (2004) Two-photon fluorescence correlation microscopy reveals the two-phase nature of transport in tumors. *Nat Med* 10:203–207.

Babiuk S, Baca-Estrada ME, Foldvari M, Storms M, Rabussay D, Widera G, Babiuk LA (2002) Electroporation improves the efficacy of DNA vaccines in large animals. *Vaccine* 20:3399–3408.

Babiuk S, Baca-Estrada ME, Foldvari M, Baizer L, Stout R, Storms M et al. (2003) Needle-free topical electroporation improves gene expression from plasmids administrated in porcine skin. *Mol Ther* 8:992–998.

Berrier AL, Yamada KM (2007) Cell-matrix adhesion. *J Cell Physiol* 213:565–573.

Buchan S, Gronevik E, Mathiesen I, King CA, Stevenson FK, Rice J (2005) Electroporation as a "prime/boost" strategy for naked DNA vaccination against a tumor antigen. *J Immunol* 174:6292–6298.

Bloquel C, Fabre E, Bureau FM, Scherman D (2004) DNA electrotransfer for intracellular and secreted proteins expression: New methodological developments and applications. *J Gene Med* 6(suppl 1):s11–s23.

Bureau FM, Gehl J, Deleuze V, Mir LM, Scherman D (2000) Importance of association between permeabilization and electrophoretic forces for intramuscular DNA electrotransfer. *Biochim Biophys Acta* 1474:353–359.

Canatella PJ, Black MM, Bonnichsen DM, Mckenna C, Prausnitz MR (2004) Tissue electroporation: Quantification and analysis of heterogeneous transport in multicellular environments. *Biophys J* 86:3260–3268.

Cappelletti M, Zampaglione I, Rizzuto G, Ciliberto G, La Monica N, Fattori E (2003) Gene electro-transfer improves transduction by modifying the fate of intramuscular DNA. *J Gene Med* 5:324–332.

Cemazar M, Golzio M, Sersa G, Hojman P, Kranjc S, Mesojednik S, Rols MP, Teissié J (2009) Control of pulse parameters of DNA electrotransfer into solid tumors in mice. *Gene Ther* 16:635–644.

Chiarella P, Massi E, De Robertis M, Sibilio A, Parrella P, Fazio VM, Signori E (2008) Electroporation of skeletal muscle induces danger signal release and antigen-presenting cell recruitment independently of DNA vaccine administration. *Expert Opin Biol Ther* 8:1645–1657.

Cipriani B, Fridman A, Bendtsen C, Dharmapuri S, Mennuni C, Pak I et al. (2008) Therapeutic vaccination halts disease progression in BALB-neuT mice: The amplitude of elicited immune response is predictive of vaccine efficacy *Hum Gene Ther* 19:670–680.

Cukjati D, Batiuskaite D, André F, Miklavcic D, Mir LM (2007) Real time electroporation control for accurate and safe *in vivo* non-viral gene therapy. *Bioelectrochemistry* 70:501–507.

Curcio C, Khan AS, Spadaro M, Quaglino E, Cavallo F, Forni G, Draghia-Akli R (2008) DNA immunization using constant-current electroporation affords long-term protection from autochthonous mammary carcinomas in cancer-prone transgenic mice. *Cancer Gene Ther* 15:108–114.

Darquet AM, Cameron B, Wils P, Scherman D, Crouzet J (1997) A new DNA vehicle for nonviral gene delivery: Supercoiled minicircle. *Gene Ther* 4:1341–1349.

Daud AI, DeConti RC, Andrews S, Urbas P, Riker AI, Sondak VK et al. (2008) Phase I trial of interleukin-12 plasmid electroporation in patients with metastatic melanoma. *J Clin Oncol* 26:5896–5903.

Dayball K, Millar J, Miller M, Wan YH, Bramson J (2003) Electroporation enables plasmid vaccines to elicit CD8+ T cell responses in the absence of CD4+ T cells. *J Immunol* 171:3379–3384.

Deharvengt S, Rejuba S, Wack S, Aprahamian M, Hajri A (2007) Efficient electrogene therapy for pancreatic adenocarcinoma treatment using the bacterial purine nucleoside phosphorylase suicide gene with fludarabine. *Int J Oncol* 30:1397–1406.

Deng J, Schoenbach KH, Buescher ES, Hair PS, Fox PM, Beebe SJ (2003) The effects of intense submicrosecond electrical pulses on cells. *Biophys J* 84:2709–2714.

Dharmapuri S, Aurisicchio L, Neumer P, Verdirame M, Ciliberto G, La Monica N (2009) An oral TLR7 agonist is a potent adjuvant of DNA vaccination in transgenic mouse tumor models. *Cancer Gene Ther* 16:462–472.

Dona M, Sandri M, Rossini K, Dell'Aica I, Podhorska-Okolow M, Carraro U (2003) Functional in vivo gene transfer into the myofibers of adult skeletal muscle. *Biochem Biophys Res Commun* 312:1132–1138.

Draghia-Akli R, Khan AS, Brown PA, Pope MA, Wu L, Hirao L, Weiner DB (2008) Parameters for DNA vaccination using adaptive constant-current electroporation in mouse and pig models. *Vaccine* 26:5230–5237.

Dupuis M, Denis-Mize K, Woo C, Goldbeck C, Selby MJ, Chen M et al. (2000) Distribution of DNA vaccines determines their immunogenicity after intramuscular injection in mice. *J Immunol* 165:2850–2858.

Durieux AC, Bonnefoy R, Manissolle C, Freyssenet D (2002) High-efficiency gene electrotransfer into skeletal muscle: Description and physiological applicability of a new pulse generator. *Biochem Biophys Res Commun* 296:443–450.

Durieux AC, Bonnefoy R, Russo T, Freyssenet D (2004) In vivo gene electrotransfer into skeletal muscle: Effects of plasmid DNA on the occurrence and extent of muscle damage. *J Gene Med* 6:809–816.

Durieux AC, Bonnefoy R, Freyssenet D (2005) Kinetic of transgene expression after electrotransfer into skeletal muscle: Importance of promoter origin/strength. *Biochim Biophys Acta* 1725:403–409.

Escoffre JM, Portet T, Wasungu L, Teissié J, Dean D, Rols MP (2009) What is (still not) known of the mechanism by which electroporation mediates gene transfer and expression in cells and tissues. *Mol Biotechnol* 41:286–295.

Evans V, Foster H, Graham IR, Foster K, Athanasopoulos T, Simons JP, Dickson G, Owen JS. 2008. Human apolipoprotein E expression from mouse skeletal muscle by electrotransfer of nonviral DNA (plasmid) and pseudotyped recombinant adeno-associated virus (AAV2/7). *Hum Gene Ther* 19:569–578.

Eynard N, Sixou S, Duran N, Teissié J (1992) Fast kinetics studies of Escherichia coli electrotransformation. *Eur J Biochem* 209:431–436.

Fattori E, Cappelletti M, Zampaglione I, Mennuni C, Arcuri M, Rizzuto G, Costa P, Perretta G, Ciliberto G, La Monica N (2005) Gene electro-transfer of an improved erythropoietin plasmid in mice and non-human primates. *J Gene Med* 7:228–236.

Ganeva V, Galutzov B, Teissié J (1995) Fast kinetics studies of plasmid DNA transfer in intact yeast cells mediated by electropulsation. *Biochem Biophys Res Commun* 214:825–832.

Gazdhar A, Bilici M, Pierog J, Ayuni EL, Gugger M, Wetterwald A, Cecchini M, Schmid RA (2006) In vivo electroporation and ubiquitin promoter-a protocol for sustained gene expression in the lung. *J Gene Med* 8:910–918.

Gehl J (2008) Electroporation for drug and gene delivery in the clinic: Doctors go electric. *Methods Mol Biol* 423:351–359.

Gehl J, Mir LM (1999) Determination of optimal parameters for in vivo gene transfer by electroporation, using a rapid in vivo test for cell permeabilization. *Biochem Biophys Res Commun* 261:377–380.

Gehl J, Sorensen TH, Nielsen K, Raskmark P, Nielsen SL, Skovsgaard T, Mir LM (1999) In vivo electroporation of skeletal muscle: Threshold, efficacy and relation to electric field distribution. *Biophys Biochim Acta* 1428:233–240.

Gilbert RA, Jaroszeski MJ, Heller R (1997) Novel electrode designs for electrochemotherapy. *Biochim Biophys Acta* 1334:9–14.

Gill DR, Pringle IA, Hyde SC (2009) Progress and prospects: The design and production of plasmid vectors. *Gene Ther* 16:165–171.

Glasspool-Malone J, Malone RW (2002) Enhancing direct in vivo transfection with nuclease inhibitors and pulsed electrical fields. *Methods Enzymol* 346:72–91.

Golzio M, Mora MP, Raynaud C, Delteil C, Teissié J, Rols MP (1998) Control by osmotic pressure of voltage-induced permeabilization and gene transfer in mammalian cells. *Biophys J* 74:3015–3022.

Golzio M, Teissié J, Rols MP (2002) Direct visualization at the single-cell level of electrically mediated gene delivery. *Proc Natl Acad Sci USA* 99:1292–1297.

Golzio M, Rols MP, Teissié J (2004) In vitro and in vivo electric-field-mediated permeabilization, gene transfer, and expression. *Methods* 33:126–135.

Gowrishankar TR, Weaver JC (2003) An approach to electrical modelling of single and multiple cells. *Proc Natl Acad Sci USA* 100:3203–3208.

Heller LC, Heller R (2006) In vivo electroporation for gene therapy. *Hum Gene Ther* 17:890–897.

Heller R, Jaroszeski M, Atkin A, Moradpour D, Gilbert R, Wands J, Nicolau C (1996) In vivo gene electroinjection and expression in rat liver. *FEBS Lett* 389:225–228.

Henshaw JW and Yuan F (2008) Field distribution and DNA transport in solid tumors during electric field-mediated gene delivery. *J Pharm Sci* 97:691–711.

Hirao LA, Wu L, Khan AS, Hokey DA, Yan J, Dai A, Betts MR, Draghia-Akli R, Weiner DB (2008) Combined effects of IL-12 and electroporation enhances the potency of DNA vaccination in macaques. *Vaccine* 26:3112–3120.

Hojman J, Gissel H, Gehl J (2007) Sensitive and precise regulation of haemoglobin after gene transfer of erythropoietin to muscle tissue using electroporation. *Gene Ther* 14:950–959.

Horton HM, Lalor PA, Rolland AP (2008) IL-2 plasmid electroporation: From preclinical studies to phase clinical trial. *Methods Mol Biol* 423:361–372.

Huang Z, Tamura M, Sakurai T, Chuma S, Saito T, Nakatsuji N (2000) In vivo transfection of testicular germ cells and transgenesis by using the mitochondrically localized jellyfish fluorescent protein gene. *FEBS Lett* 487:248–251.

Hyde SC, Pringle IA, Abdullah S, Lawton AE, Davies LA, Varathalingam A et al. (2008) CpG-free plasmids confer reduced inflammation and sustained pulmonary gene expression. *Nat Biotechnol* 26:549–551.

Jaroszeski MJ, Gilbert RA, Heller R (1997) In vivo antitumor effects of electrochemotherapy in a hepatoma model. *Biochim Biophys Acta* 1334:15–18.

Jazowiecka-Rakus J, Jarosz M, Szala S (2006) Combination of vasostatin gene therapy with cyclophosphamide inhibits growth of B16(F10) melanoma tumours. *Acta Biochim Pol* 53:199–202.

Kalat M, Kupcu Z, Schuller S, Zalusky D, Zehetner M, Paster W, Schweighoffer T (2002) In vivo plasmid electroporation induces tumor antigen-specific CD8+ T-cell responses and delays tumor growth in a syngeneic mouse melanoma model. *Cancer Res* 62:5489–5494.

Khan AS, Pope MA, Draghia-Akli R (2005) Highly efficient constant-current electroporation increases in vivo plasmid expression. *DNA Cell Biol* 24:810–818.

Kinosita K Jr, Tsong TY (1979) Voltage-induced conductance in human erythrocyte membranes. *Biochim Biophys Acta* 554:479–497.

Klenchin VA, Sukharev SI, Serov SM, Chernomordik LV, Chizmadzev YuA (1991) Electrically induced DNA uptake by cells is a fast process involving DNA electrophoresis. *Biophys J* 60:804–811.

Kondoh T, Motooka Y, Bhattacharjee AK, Kokunai T, Saito N, Tamaki N (2000) In vivo gene transfer into the periventricular region by electroporation. *Neurol Med Chir* 40:618–622.

Kubiniec RT, Liang H, Hui SW (1990) Effects of pulse length and pulse strength on transfection by electroporation. *Biotechniques* 8:16–20.

Kusumanto YH, Mulder NH, Dam WA, Losen M, De Baets MH, Meijer C, Hospers GA (2007) Improvement of in vivo transfer of plasmid DNA in muscle: Comparison of electroporation versus ultrasound. *Drug Deliv* 14:273–277.

Lemieux P, Guérin N, Paradis G, Proulx R, Chistyakova L, Kabanov A, Alakhov V. 2000. A combination of poloxamers increases gene expression of plasmid DNA in skeletal muscle. *Gene Ther* 7:987–991.

Liu F, Huang L (2002) Electric gene transfer to the liver following systemic administration of plasmid DNA. *Gene Ther* 9:1116–1119.

Liu F, Heston S, Shollenberger LM, Sun B, Mickle M, Lovell M, Huang L (2006) Mechanism of in vivo DNA transport into cells by electroporation: Electrophoresis across the plasma membrane may not be involved. *J Gene Med* 8:353–361.

Liu F, Sag D, Wang J, Shollenberger LM, Niu F, Yuan X, Li SD, Thompson M, Monahan P (2007) Sine-wave current for efficient and safe in vivo gene transfer. *Mol Ther* 15:1842–1847.

Lucas ML, Heller R (2001) Immunomodulation by electrically enhanced delivery of plasmid DNA encoding IL-12 to murine skeletal muscle. *Mol Ther* 3:47–53.

Lucas ML, Heller L, Coppola D, Heller R (2002) IL-12 plasmid delivery by in vivo electroporation for the successful treatment of established subcutaneaous B16.F10 melanoma. *Mol Ther* 5:668–675.

MacMahon JM, Wells DJ (2004) Electroporation for gene transfer to skeletal muscles: Current status. *BioDrugs* 18:155–165.

MacMahon JM, Signori E, Wells KE, Fazio VM, Wells DJ (2001) Optimisation of electrotransfer of plasmid into skeletal muscle by pretreatment with hyaluronidase-increased expression with reduced muscle damage. *Gene Ther* 8:1264–1270.

AQ3 Martinon F, Kaldma K, Sikut R, Culina S, Romain G, Tuomela M et al. (2009) Persistent immune responses induced by a HIV DNA vaccine delivered in association with electroporation in the skin of nonhuman primates. *Hum Gene Ther* 20:1291–1307.

Mathiesen I (1999) Electropermeabilization of skeletal muscle enhances gene transfer in vivo. *Gene Ther* 6:508–514.

Matsuda T, Cepko CL (2007) Controlled expression of transgenes introduced by in vivo electroporation. *Proc Natl Acad Sci USA* 104:1027–1032.

Mazères S, Sel D, Golzio M, Pucihar G, Tamzali Y, Miklavcic D, Teissié J (2009) Non invasive contact electrodes for in vivo localized cutaneous electropulsation and associated drug and nucleic acid delivery. *J Control Release* 134:125–131.

Mennuni C, Calvaruso F, Zampaglione I, Rizzuto G, Rinaudo D, Dammassa E, Ciliberto G, Fattori E, La Monica N (2002) Hyaluronidase increases electrogene transfer efficiency in skeletal muscle. *Hum Gene Ther* 13:355–365.

Mesojednik S, Pavlin D, Sersa G, Coer A, Kranjc S, Grosel A, Tevz G, Cemazar M. 2007. The effect of the histological properties of tumors on translocation efficiency of electrically assisted gene delivery to solid tumors in mice. *Gene Ther* 14:1261–1269.

Miklavcic D, Beravs K, Semrov D, Cemazar M, Demsar F, Sersa G (1998) The importance of electric field distribution for effective in vivo electroporation of tissues. *Biophys J* 74:2152–2158.

Miklavcic D, Semrov D, Mekid H, Mir LM (2000) A validated model of in vivo electric field distribution in tissues for electrochemotherapy and for DNA electrotransfer for gene therapy. *Biochim Biophys Acta* 1523:73–83.

Miller AM, Dean DA (2008) Cell-specific nuclear import of plasmid DNA in smooth muscle requires tissue-specific transcription factors and DNA sequences. *Gene Ther* 15:1107–1115.

Mir LM (2009) Nucleic acids electrotransfer-based gene therapy (electrogenetherapy): Past, current, and future. *Mol Biotechnol* 43:167–176.

Mir LM, Bureau MF, Gehl J, Rangara R, Rouy D, Caillaud JM, Delaere P, Branellec D, Schwartz B, Scherman D (1999) High-efficiency gene transfer into skeletal muscle mediated by electric pulses. *Proc Natl Acad Sci USA* 96:4262–4267.

Molnar MJ, Gilbert R, Lu Y, Liu AB, Guo A, Larochelle N et al. (2004) Factors influencing the efficacy, longevity, and safety of electroporation-assisted plasmid-based gene transfer into mouse muscles. *Mol Ther* 10:447–455.

Murakami T, Arai M, Sunada Y, Nakamura A (2006) VEGF 164 gene transfer by electroporation improves diabetic sensory neuropathy in mice. *J Gene Med* 8:773–781.

Muramatsu T, Nakamura A, Park HM (1998) In vivo electroporation: A powerful and convenient means of nonviral gene transfer to tissues of living animals. *Int J Mol Med* 1:55–62.

Neumann E, Schaefer-Ridder M, Wang Y, Hofschneider PH (1982) Gene transfer into mouse lyoma cells by electroporation in high electric fields. *EMBO J* 1:841–845.

Neumann E, Werner E, Sprafke A, Kruger K (1992) Electroporation phenomena. Electrooptics of plasmid DNA and of lipid bilayer vesicles. In: Jennings BR, Stoylov SP, eds., *Colloid and Molecular Electro-Optics*. Bristol, U.K.: IOP publishing Ltd., pp. 197–206.

Netti PA, Berk DA, Swartz MA, Grodzinsky AJ, Jain RK (2000) Role of extracellular matrix assembly in interstitial transport in solid tumors. *Cancer Res* 60:2497–2503.

Nicol F, Wong M, MacLaughlin FC, Perrard J, Wilson E, Nordstrom JL, Smith LC (2002) Poly-L-glutamate, an anionic polymer, enhances transgene expression for plasmids delivered by intramuscular injection with in vivo electroporation. *Gene Ther* 9:1351–1358.

Pavlin M, Pavselj N, Miklavcic D (2002) Dependence of induced transmembrane potential on cell density, arrangement, and cell position inside a cell system. *IEEE Trans Biomed Eng* 49:605–612.

Pavselj N, Miklavcic D (2008) Numerical modeling in electroporation-based biomedical applications. *Radiol Oncol* 42:159–168.

Pavselj N, Préat V (2005) DNA electrotransfer into the skin using a combination of one high- and one low-voltage pulse. *J Control Release* 106:407–415.

Pedron-Mazoyer S, Plouet J, Hellaudais J, Teissié J, Golzio M (2007) New anti angiogenesis developments through electro-immunization: Optimization by in vivo optical imaging of intradermal electro gene transfer. *Biochim Biophys Acta* 1770:137–142.

Peruzzi D, Mori F, Conforti A, Lazzaro D, De Rinaldis E, Ciliberto G, La Monica N, Aurisicchio L (2009) MMP11: A novel target antigen for cancer immunotherapy. *Clin Cancer Res* 15:4104–4113.

Pluen A, Boucher Y, Ramanujan S, McKee TD, Gohongi T, di Tomaso E et al. 2001. Role of tumor-host interactions in interstitial diffusion of macromolecules: Cranial vs subcutaneous tumors. *Proc Natl Acad Sci USA* 98:4628–4633.

Pucihar G, Kotnik T, Teissié J, Miklavcic D (2007) Electropermeabilization of dense cell suspensions. *Eur Biophys J* 36:173–185.

Pucihar G, Miklavcic D, Kotnik T (2009) A time-dependent numerical model of transmembrane voltage inducement and electroporation of irregularly shaped cells. *IEEE Trans Biomed Eng* 56:1491–1501.

Ramirez LH, Orlowski S, An D, Bindoula H, Dzodic R, Ardouin P et al. (1998) Electrochemotherapy on liver tumours in rabbits. *Br J Cancer* 77:2104–2111.

Rice J, Ottensmeier CH, Stevenson FK (2008) DNA vaccines: Precision tools for activating effective immunity against cancer. *Nat Rev Cancer* 8:108–120.

Riera M, Chillon M, Aran JM, Cruzado JM, Torras J, Grinyo JM, Fillat C (2004) Intramuscular SP1017-formulated DNA electrotransfer enhances transgene expression and distributes hHGF to different rat tissues. *J Gene Med* 6:111–118.

Rizzuto G, Cappelletti M, Malone D, Savino R, Lazzaro D, Costa P et al. (1999) Efficient and regulated erythropoietin production by naked DNA injection and muscle electroporation. *Proc Natl Acad Sci USA* 96:6417–6422.

Rizzuto G, Cappelletti M, Malone D, Mennuni C, Wiznerowicz M, De Martis A, Maione D, Ciliberto G, La Monica N, Fattori E (2000) Gene electrotransfer results in a high-level transduction of rat skeletal muscle and corrects anemia of renal failure. *Hum Gene Ther* 11:1891–1900.

Rols MP, Teissié J (1998) Electropermeabilization of mammalian cells to macromolecules: Control by pulse duration. *Biophys J* 75:1415–1423.

Rols MP, Coulet D, Teissié J (1992) Highly efficient transfection of mammalian cells by electric field pulses. Application to large volumes of cell culture by using a flow system. *Eur J Biochem* 206:115–121.

Rols MP, Delteil C, Golzio M, Dumond P, Cros S, Teissié J (1998) In vivo electrically mediated protein and gene transfer in murine melanoma. *Nat Biotechnol* 16:168–171.

Rubenstrunk A, Trollet C, Orsini C, Scherman D (2005) Positive in vivo heterologous gene regulation by electric pulses delivery with metallothionein I gene promoter. *J Gene Med* 7:1565–1572.

Satkauskas S, Bureau MF, Mahfoudi A, Mir LM (2001) Slow accumulation of plasmid in muscle cells: Supporting evidence for a mechanism of DNA uptake by receptor-mediated endocytosis. *Mol Ther* 4:317–323.

Satkauskas S, Bureau MF, Puc M, Mahfoudi A, Scherman D, Miklavcic D, Mir LM (2002) Mechanisms of in vivo DNA electrotransfer: Respective contributions of cell electropermeabilization and DNA electrophoresis. *Mol Ther* 5:133–140.

Satkauskas S, André F, Bureau MF, Scherman D, Mikkavcic D, Mir LM (2005) Electrophoretic component of electric pulses determines the efficacy of in vivo DNA electrotransfer. *Hum Gene Ther* 16:1194–1201.

Schertzer JD, Plant DR, Lynch GS (2006) Optimizing plasmid-based gene transfer for investigating skeletal muscle structure and function. *Mol Ther* 13:795–803.

Seo SH, Jin HT, Park SH, Youn JI, Sung YC (2009) Optimal induction of HPV DNA vaccine-induced CD8(+) T cell responses and therapeutic antitumor effect by antigen engineering and electroporation. *Vaccine* 27:5906–5912.

AQ4 Susil R, Semrov D, Miklavcic D (1998) Electric field induced transmembrane potential depends on cell density and organization. *Electromagn Biol Med* 17:391–399.

Suzuki T, Shin BC, Fujikura K, Matsuzaki T, Takata K (1998) Direct gene transfer into rat liver cells by in vivo electroporation. *FEBS Lett* 425:436–440.

Teissié J, Golzio M, Rols MP (2005) Mechanisms of cell membrane electropermeabilization: A minireview of our present (lack of ?) knowledge. *Biochim Biophys Acta* 1724:270–280.

Teissié J, Escoffre JM, Golzio M, Rols MP (2008) Time dependence of electric field effects on cell membranes. A review for a critical selection of pulse duration for therapeutical applications. *Radiol Oncol* 42:196–206.

Tjelle TE, Salte R, Mathiesen I, Kjeken R, Scheerlinck JP, Karlis J (2006) A novel electroporation device for gene delivery in large animals and humans. *Vaccine* 24:4667–4670.

Trollet C, Scherman D, Bigey P (2008) Delivery of DNA into muscle for treating systemic diseases: Advantages and challenges. *Methods Mol Biol* 423:199–214.

Vandermeulen G, Staes E, Vanderhaeghen ML, Bureau, MF, Scherman D, Préat V (2007) Optimisation of intradermal DNA electrotransfer for immunisation. *J Control Res* 124:81–87.

Vandermeulen G, Richiardi H, Escriou V, Ni J, Fournier P, Schirrmacher V, Scherman D, Préat V (2009) Skin-specific promoters for genetic immunization by DNA electroporation. *Vaccine* 27:4272–4277.

Vicat JM, Boisseau S, Jourdes P, Lainé M, Wion D, Bouali-Benazzouz R, Benabid AL, Berger F (2000) Muscle transfection by electroporation with high-voltage and short-pulse currents provides high-level and long-lasting gene expression. *Hum Gene Ther* 11:909–916.

Wallace MS, Ridgeway B, Jun Z, Schulteis G, Rabussay D, Zhang L (2001) Topical delivery of lidocaine in healthy volunteers by electroporation, electroincorporation, or iontophoresis: An evaluation of skin anesthesia. *Reg Anesth Pain Med* 26:229–238.

Walther W, Stein U, Siegel R, Fichtner I, Schlag PM. 2005. Use of the nuclease inhibitor aurintricarboxylic acid (ATA) for improved non-viral intratumoral in vivo gene transfer by jet-injection. *J Gene Med* 7:477–485.

Wang XD, Tang JG, Xie XL, Yang JC, Shuai L, Ji JG, Gu J (2005) A comprehensive study of optimal conditions for naked plasmid DNA transfer into skeletal muscle by electroporation. *J Gene Med* 7:1235–1245.

Wasungu L, Escoffre JM, Valette A, Teissié J, Rols MP (2009) A 3D in vitro spheroid model as a way to study the mechanisms of electroporation. *Int J Pharm* 379:278–284.

Widera G, Austin M, Rabussay D, Goldbeck C, Barnett SW, Chen M et al. (2000) Increased DNA vaccine delivery and immunogenicity by electroporation in vivo. *J Immunol* 164:4635–4640.

Wolf H, Rols MP, Boldt E, Neumann E, Teissié J (1994) Control by pulse parameters of electric field-mediated gene transfer in mammalian cells. *Biophys J* 66:524–531.

Wolff JA, Malone RW, Williams P, Chong W, Acsadi G, Jani A, Felgner PL (1990) Direct gene transfer into mouse muscle in vivo. *Science* 247:1465–1468.

Young JL, Zimmer WE, Dean DA (2008) Smooth muscle-specific gene delivery in the vasculature based on restriction of DNA nuclear import. *Exp Biol Med* 233:840–848.

Zampaglione I, Arcuri M, Cappelletti M, Ciliberto G, Perretta G, Nicosia A, La Monica N, Fattori E (2005) In vivo DNA gene electro-transfer: A systematic analysis of different electrical parameters. *J Gene Med* 7:1475–1481.

Zhang X, Divangahi M, Ngai P, Santosuosso M, Millar J, Zganiacz A, Wang J, Bramson J, Xing Z (2007) Intramuscular immunization with a monogenic plasmid DNA tuberculosis vaccine: Enhanced immunogenicity by electroporation and co-expression of GM-CSF transgène. *Vaccine* 25:1342–1352.

Author Queries

[AQ1] The following references are not listed in the reference list: Escoffre et al. (2008), Mossop et al. (2006), Bureau et al. (2004), Yamada et al. (2007), Hirao et al. (2009); Draghia-Akli et al. (1999), Simon et al. (2008)

[AQ2] The year in Wasungu et al. (2009) has been changed as per the reference list.

[AQ3] Please check for the inserted volume number and page range in Martinon et al. (2009).

[AQ4] Please check for the inserted journal title in Susil et al. (1998).

Technology in Cancer Research and Treatment
ISSN 1533-0346
Volume 7, Number 2, April 2008

Long-lasting *In vivo* Gene Silencing by Electrotransfer of shRNA Expressing Plasmid

www.tcrt.org

Jean-Michel Escoffre, M.Sc.[1]
Arnaud Debin, Ph.D.[2]
Jean-Paul Reynes, Ph.D.[2]
Daniel Drocourt, Ph.D.[2]
Gérard Tiraby, D.Sc.[2]
Laëtitia Hellaudais[1]
Justin Teissie, D.Sc.[1,*]
Muriel Golzio, Ph.D.[1]

[1]IPBS Universite P Sabatier/CNRS
UMR 5089, 205 route de Narbonne
31077 Toulouse, France
[2]CAYLA – InvivoGen
5 rue Jean Rodier
31400 Toulouse, France

RNA interference appears as a promising tool for therapeutic gene silencing. A key limit is the delivery of the siRNA. A safe approach is to use a physical method such as *in vivo* electropulsation with contact electrodes. Getting a long lived silencing can be better approached by using the *in situ* expression of shRNA. This is presently obtained by using co-electrotransfer of specific plasmids coding for expression and silencing of a fluorescent protein. Using a non invasive fluorescence imaging assay, electrodelivery in mouse muscles is observed to induce complete silencing over more than two months in a specific way. The proper choices of the plasmids (sequence and relative amounts) and of the electric pulsing conditions appear as key parameters in the successful silencing.

Key words: Plasmids; Gene electrotransfer; GFP; Muscle; Silencing; and shRNA.

Introduction

RNA interference (RNAi) is rapidly becoming an important tool for studying gene functions and holds promise for the development of therapeutic gene silencing (1). RNAi is a post-transcriptional process triggered by the delivery of double-stranded RNA (dsRNA) that induces gene silencing in a sequence-specific manner (2). An efficient gene silencing required a safe and efficient delivery, a stability of the silencing agent and long lived effects (3). RNA interference can be achieved by using chemically synthesized siRNA (small interfering RNA) or shRNA (short hairpin RNA) expressing plasmid.

Previous works showed that the delivery of chemically synthesized siRNA resulted in strong and sequence-specific inhibition of gene expression *in vitro* (4, 5) and *in vivo* (6, 7). However, chemically synthesized siRNAs had several drawbacks beside their expensive cost such as a transient gene expression silencing due to their short lived stability *in vivo* (8). To overcome these limitations, the delivery of shRNA expression cassettes appeared as a more suitable approach. The development of these expression cassettes required safe and efficient *in vivo* targeted delivery methods. Viral vectors have been reported as highly efficient methods for shRNA delivery to several tissues (9, 10). Unfortunately, viral proteins could induce specific immune responses that could limit the ability to re-administer the viral vectors (11, 12). Moreover, the viral vectors, like retrovirus or lentivirus could evoke insertional mutations during their integration into the host genome (13, 14). In contrast, DNA plasmids were composed entirely of covalently closed circles of double-stranded DNA with no associated proteins. Commercially available efficient, highly transfectable and simple-to-use plasmids have been designed such as psiRNA™ and pCpG-siRNA™. These plasmids were designed by inserting a DNA frag-

[*]Corresponding Author:
Justin Teissie, D.Sc.
Email: justin.teissie@ipbs.fr

ment of approximately 50 mer, which after transcription from the human H1 or 7SK RNA polymerase III promoter, generated short RNAs with a hairpin structure (shRNAs) (15, 16). shRNAs were more stable than chemically synthesized siRNAs and their expression within the cells, allowed long-lasting silencing of target gene expression (17). Nevertheless, gene delivery with plasmid vectors is highly inefficient if DNA plasmids are not associated with chemical or physical methods. DNA plasmids are more suitable for large volume production and quality control than viral vectors. Moreover, the most advantages of DNA plasmid are lack of integration and low immunogenicity. Plasmid DNA could be a highly attractive molecule for gene therapy when it is associated with safe, efficient, and targeted delivery method (18, 19).

During the 90's, *in vivo* electrotransfer appeared as a promising tool for exogenous drugs delivery. Moreover, this non viral method offered the advantages as reduction of toxicity, safety, and friendly use (20). *In vivo* electrotransfer allowed efficient delivery of DNA plasmids and others larges molecules like proteins (21) and antisense oligonucleotides (22). DNA plasmid can be easily delivers to the skin and liver but skeletal muscle has recently attracted a lot of attention, muscle being considered as a first choice cellular factory. Indeed, expression of the episomal plasmid could be long lived in muscle tissue (23, 24). Indeed, a wide range of tissues have been targeted including skin (25), liver (26), lung (27), skeletal (23, 24) and cardiac muscle (28), kidney (29), joints (30), brain (31), and retina (32). Delivery was targeted to the volume of tissue localized between the electrodes, where the electric field is applied (33, 34).

In living animals, the quantitative follow-up of reporter gene expression is very important to monitor the therapeutic gene expression in targeted tissues and to assess the effectiveness of delivery methods. *In vivo* optical imaging is a noninvasive method that can detect and follow the reporter gene activity on the same animal as a function of time (35, 36). Indeed, working on the same animal brings a reduction of the number of experimental animals and increases the accuracy of statistical analysis. Exogenous gene expression of fluorescent proteins such as enhanced green fluorescent protein (eGFP) can be detected directly on living animals by means of a fluorescence stereomicroscope coupled to a cooled charged-coupled device camera (CCD camera).

In this study, we investigated the effectiveness of electrotransfer for the targeted delivery of DNA plasmid coding for shRNA in adult mice using tibialis cranialis muscle as a model system. The resulting gene silencing is monitored in living animals by time-lapse fluorescence imaging. Silencing of gene expression was observed over a two-month period.

Materials and Methods

Animals

All animal studies were conducted in accordance with the principles and procedures outlined by the European convention for the protection of vertebrate animals used for experimentation. Seven to 10 weeks old Balb/c female mice were used in this study (IFFA CREDO, France).

Plasmids

pCLEF14-EGFP plasmid contains enhanced green fluorescent protein cDNA under the control of the elongation factor 1α (EF1α) promoter (InvivoGen, France see www.invivogen.com/).

pUC18 plasmid contains the cDNA of sub-unit α of LacZ under the control of the pLac promoter (InvivoGen, France).

psiRNA25-EGFP or psiRNA25-SCR (InvivoGen, France): psiRNA25 is an RNA polymerase III-based plasmid that contains the human 7SK RNA Pol III promoter. The DNA fragments coding for scramble shRNA (SCR) or shRNA against eGFP (EGFP) mRNA are designed by a siRNA design algorithm of InvivoGen, named siRNA Wizard (//www.sirnawizard.com/). DNA sequence of eGFP shRNA (relative position to ATG), GCAAGCTGACCCTGAAGTTCA**CCACC**TGAACTTCAGGGTCAGCTTGC and DNA sequence of scramble shRNA, GCATATGTGCGTACCTAGCAT**TCAAGAG**ATGCTAGGTACGCACATATGC (Loop in bold).

pCpG76-EGFP ou pCpG76-SCR (InvivoGen, France): pCpG76 is a plasmid that combines a CpG-free plasmid backbone with shRNA expression cassette of psiRNA25 plasmids. In the expression cassette, mCMV enhancer sequence is added on upstream of 7SK promoter. This plasmid is designed for long lasting expression of shRNA *in vivo* as the plasmid does not induce inflammatory responses (37) and gene silencing by methylation in vertebrates hosts (38).

Plasmids (see Table I) were produced in the Cayla facility. Identity was confirmed by agarose gel. Contamination with RNA was not observed and the majority of plasmids was present as covalently closed circles.

In vivo Electrotransfer

Two days before the experiments, the hair on leg was removed with hair removal lotion (Nair, France). During the electrotransfer, animals were anesthetized by intraperitoneal injection of physiologic saline (10 mL/kg) containing Xylasine (1 mg/mL) and Ketamine (5 mg/mL).

Table I
The different constructs used in this study are presented in this table.

	pCLEF14-EGFP	pUC	psiRNA25-EGFP or SCR	pCpG76-EGFP or SCR
Coding sequence	EGFP protein	Sub-unit α of Lac Z protein	shRNA against EGFP mRNA or scramble shRNA	shRNA against EGFP mRNA or scramble shRNA
CpG motif	Yes	Yes	Yes	No
Enhancer /promoter	No enhancer EF1α Promoter	No enhancer pLac promoter	No enhancer 7SK promoter	mCMV enhancer 7SK promoter

In total, 5 μg of pCLEF14-EGFP (1 μg/μL) in PBS are mixed with 10 μg (Ratio target/shRNA, 1/2), 25 μg (Ratio target/shRNA, 1/5), 50 μg (Ratio target/shRNA, 1/10) of pUC18 or plasmid expressing shRNA. The DNA mix was adjusted to a 25 μL final volume with PBS. The plasmid solution was injected slowly (about 15s) with a Hamilton syringe through a 26G needle (Hamilton, Bonaduz, Switzerland) into tibialis cranialis muscles in anesthetized mice.

Within 1 min after the intra-muscular injection of plasmids, electrical field pulses were applied to the muscle. A 6 mm gap is maintained between plates, which were 10 × 10 mm × mm each (.1 cm^2).The injected leg was held steady and the electrodes (IGEA, Italy) were applied to the lateral sides of the hind limb. The fixed 6 mm gap distance between the electrodes allowed to maintain contact with the skin surface. Electrode jelly (Comepa, St Denis, France) was used on the electrode plates to ensure good electrical contact. Electrode position can be easily changed by a rotation of the electrode set around the muscle. A 90º rotation brings a direction of the field in a perpendicular direction, so called crossed directions. Electric pulses of 120 V were applied in two sets of four rectangular wave pulses of crossed directions, lasting 20 ms at 1 Hz using a Jouan electropulsator (CNRS, France) (24, 39) (Fig. 1). All parameters were set from the control keyboard of the Jouan generator but could be obtained with other suitable square wave pulse generators. Pulse shape was monitored online with an oscilloscope (Enertec, St-Etienne, France) to control the accurate delivery.

Non Invasive Animal Fluorescent Imaging

The eGFP expression in the mouse muscle was detected directly on the anaesthetized animal by digitalized stereomicroscopy (40). Fluorescent muscle fibers were observed through the skin. This procedure allows to monitor reporter gene expression on the same animal by time-lapse fluorescence imaging.

A stereo fluorescence microscope (Leica MZFL III, Germany) was used for visualization using the ×0.8 magnification. The whole muscle was observed as a 12 bits 1.3 M pixels image with a cooled CCD Camera (Roper Coolsnap fx). The MetaVue software (Universal, USA) drives the camera and allowed image analysis from a Dell computer. The fluorescence excitation was obtained with a Mercury Arc Lamp (HBO, Osram, Germany) and either the GFP or the G filters (Leica). The GFP fluorescence from the muscle was quantitatively evaluated at different days and thereafter with weekly intervals until the GFP fluorescence was no longer detectable. A dark image (no incident light), a light map with the GFP filter (using a reference fluorescent sample (Chroma, USA), images of muscle through the GFP filter and the G (red) filter were taken. The picture of muscle with G filter (autofluorescence signal) was subtracted from the image of muscle with GFP filter. The resulting image was divided by the image of light map corrected from the dark signal. This operation allowed to suppress the autofluorescence and the dark signal from the image of muscle through the GFP filter. The correction brought by the light map allowed to take into account the fluctuations of mercury arc lamp and the optical defects of the microscope. On the resulting image, the tibialis cranialis muscle was located and gated to give the region of interest (ROI) (Fig. 2). The mean fluorescence in the gated area (whole muscle) was quantitatively estimated.

Statistical Analysis

Four to six legs were treated for each condition. Differences between mean fluorescence levels measured in our experiments were statistically evaluated by using an unpaired Student t-test using the Prism software (version 4.02, Graphpad).

Results

Gene Electrotransfer and Expression

Mice muscle were electrotransferred with 5 μg of pCLEF14-EGFP plasmid. Expression (GFP emission) was detected 24 hours after electropulsation. The whole muscle imaging method allowed the detection of fluorescent fibers during more than 72 days.

Except the muscle contraction during the field pulse, no side effect was associated to the treatment as previously reported (41).

Gene Silencing in Mice

Mice muscle were electropulsed with a mixture of pCLEF14-EGFP plasmid and pUC18, psiRNA25-EGFP, psiRNA25-SCR, pCpG76-EGFP, or pCpG76-SCR at various ratios (1:2, 1:5, and 1:10) with a constant amount of

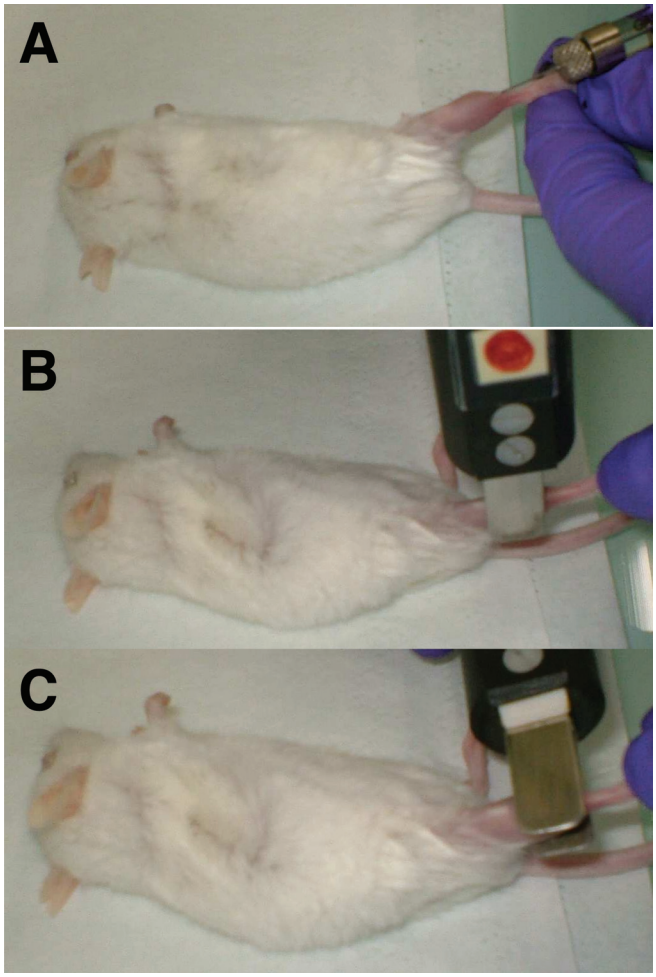

Figure 1: Experimental procedure. The animal is under anesthesia during all the experimental procedure. (**A**) The plasmid solution (25 µl) is injected in the tibialis muscle. The mouse leg was previously shaved. (**B**) The electrodes are set around the leg and four electric pulses of 120 V lasting 20 ms at 1 Hz are applied. (**C**) The electrode set is turned to a perpendicular position around the leg. Four electric pulses of 120 V lasting 20 ms at 1 Hz are delivered.

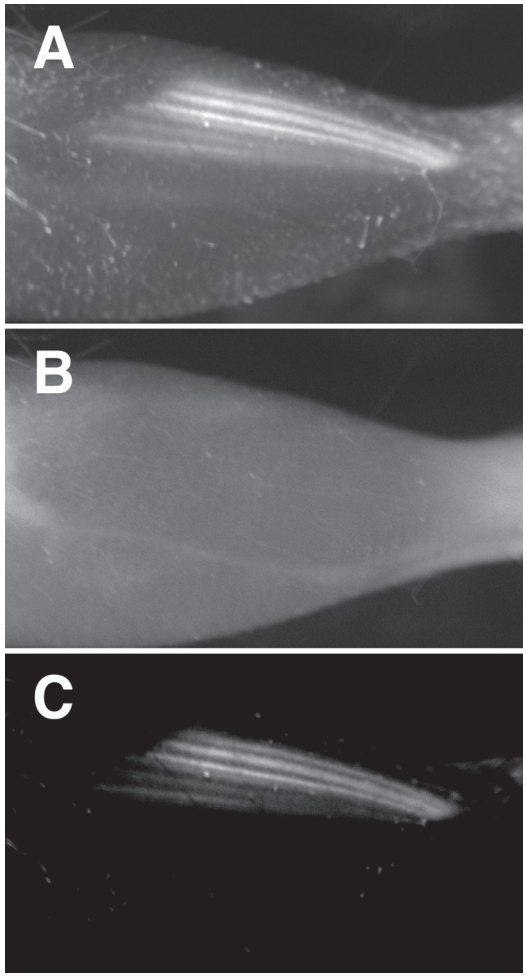

Figure 2: Whole muscle fluorescence imaging. (**A**) The electrotransfected muscle is observed by fluorescence stereomicroscopy with the gfp filter. GFP and autofluorescent emissions are detected. (**B**) The same muscle is observed with the G filter. Only the autofluorescence emission is detected. (**C**) After the correction protocol (see ***Materials and Methods***), only the GFP emission is detected and quantified.

pCLEF14-EGFP plasmid (5 µg) achieved by varying the quantity of shRNA expressing plasmid to evaluate the efficiency of these different plasmids.

The co-transfer of pCLEF14-EGFP plasmid and pCpG76-EGFP or psiRNA25-EGFP plasmid in a ratio 1:2 induced a partial silencing of GFP expression during the first 23 days (Fig. 3). However, after the day 23, GFP expression was no detected until day 72. When anesthetised mice were electropulsed after injection of pCLEF14-EGFP plasmid mixed with control plasmid (psiRNA25-SCR, pCpG76-SCR, pUC18), GFP expression was detected 24h after electrotransfer. GFP fluorescence was quantified by time-lapse fluorescence imaging on the same animal. Fluorescence was present only in the tiabialis cranialis muscle that was electropulsed. It remained detectable during a long period (more than 70 days). When the pCLEF14-EGFP plasmid was co-introduced with pCpG76-SCR and whatever the ratio between these two plasmids, the GFP expression was higher than the co-introduction with pUC18 or psiRNA25-SCR plasmid during 70 days. A specific enhancing effect in expression (fluorescence) was associated with the pCpG construct after co-introduction with the EGFP coding plasmid.

Promoters of shRNA Plasmid

psiRNA25 and pCpG76 are RNA polymerase III-based plasmids that contains the human 7SK RNA Pol III promoter. In a series of *in vitro* previous experiments aimed to compare the strength of the human 7SK, H1, and U6 promoters, InvivoGen found that the best silencing efficiencies of various target genes was consistently obtained with the 7SK promoter (see invivogen website). When we co-transferred of pCLEF14-EGFP-v01 and shRNA plasmid bearing either 7SK or H1 promoter in the muscle mice by electropulsation,

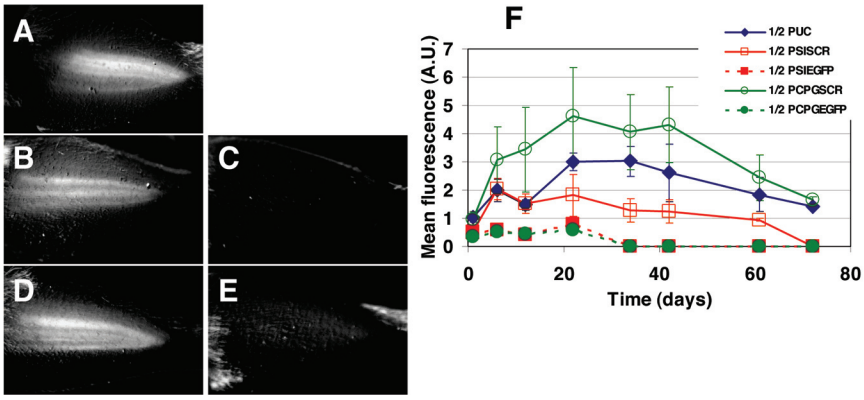

Figure 3: Co-transfection: Plasmid Ratio GFP/shRNA 1/2. Whole muscle imaging on day 4 after co-transfer with pUC18 (**A**), psiRNA25-SCR (**B**) and psiRNA25-EGFP (**C**), pCpG76-SCR (**D**), and pCpG76-EGFP (**E**) plasmids. Mean fluorescence changes after the different treatments pUC18 (♦), psiRNA25-SCR (□) and psiRNA25-EGFP (■), pCpG76-SCR (○) and pCpG76-EGFP (●) plasmids (+/- SD) where plotted as a function of time (**F**). N = 4 muscles.

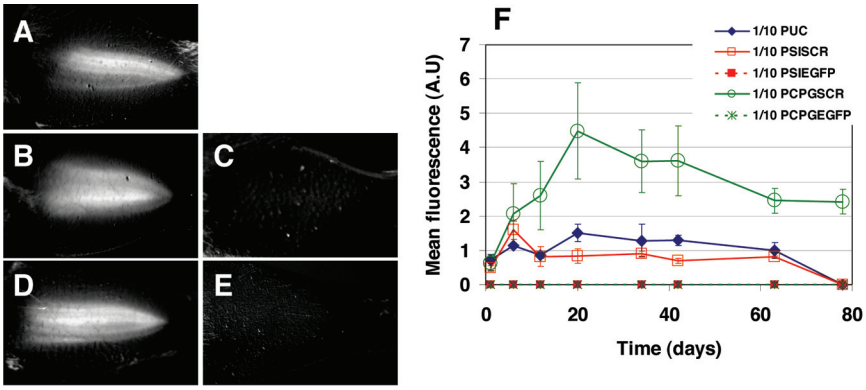

Figure 4: Co-transfection: Plasmid Ratio GFP/shRNA 1/10. Whole muscle imaging on day 4 after co-transfer with pUC18 (**A**), psiRNA25-SCR (**B**) and psiRNA25-EGFP (**C**), pCpG76-SCR (**D**), and pCpG76-EGFP (**E**) plasmids. Mean fluorescence changes after the different treatments pUC18 (♦), psiRNA25-SCR (□) and psiRNA25-EGFP (■), pCpG76-SCR (○) and pCpG76-EGFP (●) plasmids (+/- SD) where plotted as a function of time (**F**). N = 4 muscles.

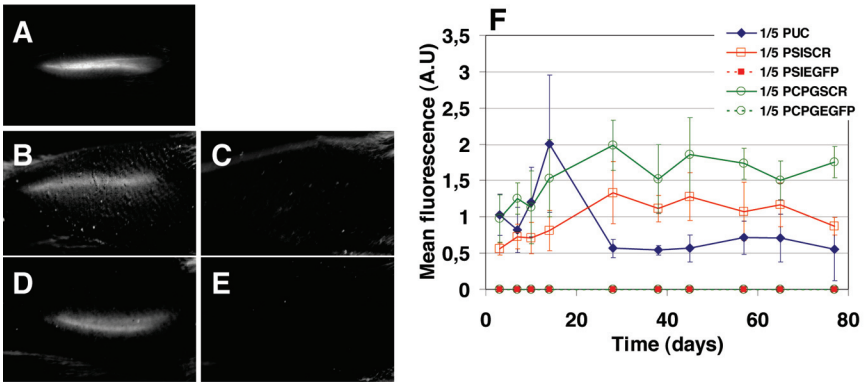

Figure 5: Co-transfection: Plasmid Ratio GFP/shRNA 1/5. Whole muscle imaging on day 6 after co-transfer with pUC18 (**A**), psiRNA25-SCR (**B**) and psiRNA25-EGFP (**C**), pCpG76-SCR (**D**), and pCpG76-EGFP (**E**) plasmids. Mean fluorescence changes after the different treatments pUC18 (♦), psiRNA25-SCR (□) and psiRNA25-EGFP (■), pCpG76-SCR (○) and pCpG76-EGFP (●) plasmids (+/- SD) where plotted as a function of time (**F**). N = 6 muscles.

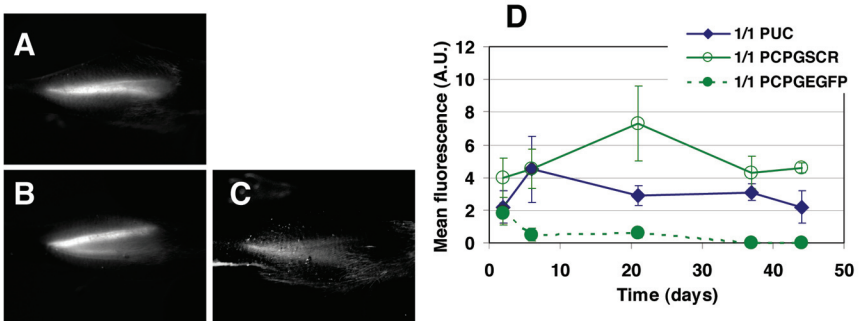

Figure 6: Co-transfection: Plasmid Ratio GFP/shRNA 1/1. Whole muscle imaging on day 7 after co-transfer with pUC18 (**A**), pCpG76-SCR (**B**), and pCpG76-EGFP (**C**) plasmids. Mean fluorescence changes after the different treatments pUC18 (♦), pCpG76-SCR (○), and pCpG76-EGFP (●) plasmids (+/- SD) where plotted as a function of time (**D**). N = 6 muscles.

we observed that again the shRNA plasmid with 7SK induced the best silencing efficiency *in vivo* (Data not shown).

Dose Effect on Silencing

When we increased by 2.5 or 5 fold the amount of pCpG76-EGFP or psiRNA25-EGFP plasmid keeping constant the amount of pCLEF14-EGFP plasmid (5:1 or 10:1 ratio), GFP expression was not detected during the 78 days (Figs. 4 and 5). This indicated that gene silencing in muscle was dose-dependent, detectable within 24 hours and complete only three days after the electrotransfer. The specificity of the silencing was present with these higher doses The co-introduction of pCpG76-SCR or psiRNA25-SCR plasmid and pCLEF14-EGFP plasmid at 5:1 and 10:1 ratio did not induce a GFP fluorescence decrease. The enhancing effect of the pCpG76-SCR plasmid was present but was not increased by the increase in the dose of injected plasmids.

In another set of experiments, pCLEF14-EGFP plasmid and different forms of "silencing" plasmids were co-electrotransferred (ratio 1:1). GFP expression silencing was present but at a limited extend up to day 33 (Fig. 6). Then complete silencing was present. Again an enhancing effect in expression was present with the pCpG76-SCR plasmid as compared with the pUC18.

Discussion

Since its discovery (42), the number of application of RNA interference has increased dramatically. RNA interference appeared as an exciting tool to identify news target genes and was proposed as a new therapeutic strategy (43). These two applications required long-term silencing of genes.

In this study, we demonstrated that long-term silencing of exogenous gene *in vivo*, by electrically-mediated delivery of shRNA expressing plasmids, was possible.

We showed that by intramuscular electrotransfer of plasmid expressing GFP protein, in combination with non invasive animal fluorescence imaging, we were able to monitor and quantify the expression of exogenous delivered GFP for at least 70 days. This confirmed that electrotransfer was safe, easy to implement, and allowed a localized delivery. Long lived gene expression of electrotransfered plasmid has been already reported when using similar pulsing conditions (23, 24). The main reason of this long gene expression is known to be linked to the physiology of muscle tissue. Indeed, the myofibers were quiescent structures with long life time. Consequently, the DNA plasmid was maintained under episomal form and long lasting expression was detected in skeletal muscle Gene delivery to skeletal muscle was a promising strategy for the treatment of muscle disorders and for the systemic secretion of therapeutic proteins. In the present case, we were expecting a long term expression of the shRNA. This is indeed the case.

Non invasive fluorescence imaging enabled real-time, non-invasive monitoring of GFP expression *in vivo* on the same mice. Consequently, the total number of mice used could be reduced significantly and the statistic power increased (35, 36). This approach complied with the recommendations on the use of laboratory animals in experimental research (3Rs rule). Therefore, fluorescence imaging was an interesting and reliable method to follow and quantify the silencing effect of psiRNA25 and pCpG76 plasmids over time.

In this study, we showed that by intramuscular electrotransfer of shRNA expressing plasmid, we were able to knock down the exogenous expression of co-transferred transgene for at least 70 days in mice muscle. This effect was dose-dependent and sequence specific because no silencing effect occurred with the scramble shRNA coding plasmid. shRNA expressing plasmid induced more efficient and long-lasting gene silencing than chemically synthetic siRNA. Indeed, two groups reported the delivery of chemically synthesized siRNA in mice muscles by electrotransfer. These works showed the maximal duration of gene silencing to be, respectively, 7 and 11 days (40, 43). The longest silencing effect was obtained with a protocol rather similar to the one of the present study. The present study shows that complete silencing was obtained for a 6 to 7 times longer period by using properly designed shRNA coding plasmids. It suggested that the stability of the chemical form was less than that of the plasmid. The onset of silencing with low amount of shRNA vectors was later than with siRNA. This could be due to the need of a critical level of expressed shRNA to induce the silencing. This is in agreement with the long delay observed with the very low amount of plasmids (1/1 ratio reported in Fig. 6). Of course silencing is present at once with high amounts of siRNA or shRNA plasmids.

Using a different experimental protocol (shorter pulse duration, unidirectional pulses, different mice, 50 μg of plasmid) and pHippy siRNA plasmid, Eefting *et al*. investigated Luciferase silencing by siRNA expression (45). Silencing was highly present only with a high dose of the "silencing" construct (1:9 ratio). Complete silencing was not obtained. Silencing was progressive and the highest level was observed only after 30 days but remained present thereafter. No inflammatory reaction was detected. In our approach, we observed a complete gene silencing three days after electrotransfer with 1/5 and 1/10 ratio. The difference in the observations may be explained by the choice in the "silencing" plasmids. Expression after electrotransfer is known to be controlled by the choice in the promoter (46, 47).

In addition, we observed that the co-transfer of pCLEF14-EGFP and pCpG76-SCR plasmid induced higher GFP

expression than the co-transfer of pCLEF14-EGFP and psiRNA25-SCR or pUC18. No significant dose effect was observed. This suggested either that pCpG76-SCR was a better DNA carrier than other plasmids or more likely that the other constructs induced a reduction of the expression. CpG motifs may be immunostimulatory elements leading to a rapid decline of transgene expression *in vivo* (48).

Endogeneous gene silencing was partially achieved in muscles on Toll-like receptor by Eefting *et al*. More interestingly, shRNA coding for myostatin silencing were electrotransfered in rat muscles by a different protocol where 100 µg of shRNA coding plasmids were injected into rat tibialis anterior or contralateral muscles (47). Resulting changes were assayed two weeks after the electrotreatment. RT-PCR and Western blotting were used to determine myostatin expression. Muscle fiber sizes were measured to assay the physiological response. Protein expression was reduced only by 50%. Expression of transgenes decreased by half after 28 days. The procedure was associated to a protocol using needle electrodes known to be rather damaging for the muscle. This is known to induce a negative effect on expression (50-52).

In conclusion, the present study demonstrated that under electrical conditions shown to give a high level in plasmid expression, electrically-mediated of small amount of pCpG™ and psiRNA™ plasmid-based delivery of shRNA resulted in long lived silencing of GFP expression for at least 70 days in mice muscles. The prolonged knock-down effect after a single intramuscular electrotransfer suggests that this physical delivery method is suitable for targeted gene therapy of muscular dystrophies, myostatin being proved to be a target gene (52).

Acknowledgements

This work was supported by grants from AFM, Region Midi Pyrenees and the CNRS CEA IPA program.

References

1. Cheng, J. C., Moore, T. B., Sakamoto, K. M. RNA interference and human disease. *Molecular Genetics and Metabolism 80*, 121-128 (2003).
2. Dykxhoorn, D. M., Novina, C. D., Sharp, P. A. Killing the messenger: short RNAs that silence gene expression. *Nature Reviews Molecular Cell Biology 4*, 457-467 (2003).
3. Walters, D. K., Jelinek, D. F. The effectiveness of double-stranded short inhibitory RNAs (siRNAs) may depend on the method of transfection. *Antisense Nucleic Acid Drug Development 12*, 411-418 (2002).
4. Elbashir, S. M., Lendeckel, W., Tuschl, T. RNA interference is mediated by 21 and 22 nucleotides RNAs. *Genes Development 15*, 188-200 (2001).
5. Elbashir, S. M., Harborth, J., Lendeckel, W., Yalcin, A., Weber, K., Tuschl, T. Duplexes of 21 nucleotides RNAs mediate RNA interference in cultured mammalian cells. *Nature 411*, 494-498 (2001).
6. Golzio, M., Mazzolini, L., Moller, P., Rols, M. P., Teissie, J. Inhibition of gene expression in mice muscle by in vivo electrically mediated siRNA delivery. *Gene Therapy 12*, 246-251 (2005).
7. Contreras, J. L., Vilatoba, M., Eckstein, C., Bilbao, G., Thompson, J. A., Eckhoff, D. E. Caspase-8 and caspase-3 small interfering RNA decreases ischemia/reperfusion injury to the liver in mice. *Surgery 136*, 390-400 (2004).
8. Ryther, R. C. C., Flynt, A. S., Philips, J. A., Patton, J. G. siRNA therapeutics; big potential from small RNAs. *Gene Therapy 12*, 5-11 (2005).
9. Tiscornia, G., Singer, O., Ikawa, M., Verna, I. A general method for gene knockdown in mice by using lentiviral vectors expressing small interfering RNA. *Proc Natl Acad Sci USA 100*, 1844-1848.
10. Uchida, H., Tanaka, T., Sasaki, K., Kato, K., Dehari, H., Ito, Y., Kobune, M., Miyagischi, M., Taira, K., Tahara, H., Hamada, H. Adenovirus-mediated transfer of siRNA against surviving induced apoptosis and attenuated tumor cell growth *in vitro* and *in vivo*. *Molecular Therapy 10*, 162-171 (2004).
11. Lehrman, S. Virus treatment questioned after gene therapy death. *Nature 401*, 517-518 (1999).
12. Marshall, E. Gene therapy death prompts review of adenovirus vector. *Science 286*, 2244-2245 (1999).
13. Hacein-Bey-Abina, S., Von Kalle, C., Schmidt, M., McCormack, M. P., Wulffraat, N., Leboulch, P., Lim, A., Osborne, C. S., Pawliuk, R., Morillon, E., Sorensen, R., Forster, A., Fraser, P., Cohen, J. I., de Saint Basile, G., Alexander, I., Wintergerst, U., Frebourg, T., Aurias, A., Stoppa-Lyonnet, D., Romana, S., Radford-Weiss, I., Gross, F., Valensi, F., Delabesse, E., Macintyre, E., Sigaux, F., Soulier, J., Leiva, L. E., Wissler, M., Prinz, C., Rabbitts, T. H., Le Deist, F., Fischer, A., Cavazzana-Calvo, M. LMO2-associated clonal T cell proliferation in two patients after gene therapy for SCID-X1. *Science 302*, 415-419 (2003).
14. Hacein-Bey-Abina, S., Von Kalle, C., Schmidt, M., Le Deist, F., Wulffraat, N., Macintyre, E., Radford, I., Villeval, J. L., Fraser, P., Cavazzana-Calvo, M , Fischer, A. A serious adverse event after successful gene therapy for X-linked severe combined immunodeficiency. *New England Journal of Medecine 348*, 255-256 (2003).
15. Czauderna, F., Santel, A., Hinz, M., Durieux, B., Arnold, W., Klippel, A., Kaufmann, J. Inductible shRNA expression for application in a prostate cancer mouse model. *Nucleic Acids Research 31*, e127 (2003).
16. Ill, C. R., Chiou, H. C. Gene therapy progress and prospects: recent progress in transgene and RNAi expression cassettes. *Gene Therapy 12*, 795-802 (2005).
17. Scherr, K. J., Morgan, M. A., Eder, M. Gene silencing mediated by small interfering RNAs in mammalian cells. *Current Medicinal Chemistry 10*, 245-256 (2003).
18. Wells, D. J. Gene therapy progress and prospects: electroporation and other physical methods. *Gene Therapy 11*, 1363-1369 (2004).
19. Vorhies, J. S., Nemunaitis, J. Nonviral delivery vehicles for use in short hairpin RNA-based cancer therapies. *Expert Rev Anticancer Ther 7*, 373-382 (2007).
20. Golzio, M., Rols, M. P., Teissie, J. *In vitro* and *in vivo* electric field-mediated permeabilization, gene transfer and expression. *Methods 32*, 126-135.
21. Rols, M. P., Delteil, C., Golzio, M., Dumond, P., Cros, S., Teissie, J. *In vivo* electrically mediated protein and gene transfer in murine melanoma. *Nature Biotechnology 16*, 168-171 (1998).
22. Faria, M., Spiller, D. G., Dubertret, C., Nelson, J. S., White, M. R., Scherman, D., Helene, C., Giovannangeli, C. Phosphoramidate oligonucleotides as potent antisense molecules in cells and *in vivo*. *Nature Biotechnology 19*, 40-44 (2001).
23. Aihara, H., Miyazaki, J. I. Gene transfer into muscle by electroporation *in vivo*. *Nature Biotechnology 16*, 867-870 (1998).
24. Mir, L. M., Bureau, F. B., Gehl, J., Rangara, R., Rouy, D., Caillaud, J. M., Delaere, P., Branellec, D., Schwartz, B., Scherman, D. High-efficiency gene transfer into skeletal muscle mediated by electric pulses. *Proc Natl Sci USA 96*, 4262-4267 (1999).
25. Pedron-Mazoyer, S., Plouët, J., Hellaudais, L., Teissie, J., Golzio, M. New anti-angiogenesis developments through electro-immunization:

optimization by *in vivo* optical imaging of intradermal electrogenetransfer. *Biochim Biophys Acta 1770*, 137-142 (2007).
26. Heller, R., Jaroszeski, M., Atkin, A., Moradpour, D., Gilbert, R., Wands, J., Nicolau, C. *In vivo* gene electroinjection and expression in rat liver. *FEBS Lett 389*, 225-228 (1996).
27. Pringle, I. A., McLachlan, G., Collie, D. D., Sumner-Jones, S. G., Lawton, A. E., Tennant, P., Baker, A., Gordon, C., Blundell, R., Varathalingam, A., Davies, L. A., Schmid, R. A., Cheng, S. H., Porteous, D. J., Gill, D. R., Hyde, S. C. Electroporation enhances reporter gene expression following delivery of naked plasmid DNA to the lung. *J Gene Med 9*, 369-380 (2007).
28. Harrison, R. L., Byrne, B. J., Tung, L. Electroporation-mediated gene transfer in cardiac tissue. *FEBS Lett 435*, 1-5 (1998).
29. Isaka, Y., Yamada, K., Takabatake, Y., Mizui, M., Miura-Tsujie, M., Ichimaru, N., Yazawa, K., Utsugi, R., Okuyama, A., Hori, M., Imai, E., Takahara, S. Electroporation-mediated HGF gene transfection protected the kidney against graft injury. *Gene Therapy 12*, 815-820 (2005).
30. Khoury, M., Bigey, P., Louis-Plence, P., Noel, D., Rhinn, H., Scherman, D., Jorgensen, C., Apparailly, F. A comparative study on intra-articular versus systemic gene electrotransfer in experimental arthritis. *Gene Therapy 8*, 1027-1036 (2006).
31. Wang, H., Ko, C. H., Koletar, M. M., Ralph, M. R., Yeomans, J. Casein kinase I epsilon gene transfer into the suprachiasmatic nucleus via electroporation lengthens circadian periods of tau mutant hamsters. *Eur J Neuroscience 25*, 3359-3366 (2007).
32. Matsuda, T., Cepko, C. L. Electroporation and RNA interference in the rodent retina *in vivo* and *in vitro*. *Proc Natl Acad Sci USA 101*, 16-22 (2004).
33. Cemazar, M., Golzio, M., Sersa, G., Rols, M. P., Teissié, J. Electrically-assisted nucleic acids delivery to tissues *in vivo*: where do we stand? *Current Pharmaceutical Design 12*, 3817-3825 (2006).
34. Heller, L. C., Heller, R. *In vivo* electroporation for gene therapy. *Hum Gene Ther 17*, 890-897 (2006).
35. Golzio, M., Rols, M. P., Gabriel, B., Teissie, J. Optical imaging of in vivo gene expression: a critical assessment of the morphology and associated technologies. *Gene Therapy 11*, S85-S91 (2004).
36. Yang, M., Baranov, E., Li, X. M., Wang, J. W., Jiang, P., Li, L., Moossa, A. R., Penman, S., Hoffman, R. M. Whole-body and intravital optical imaging of angiogenesis in orthotopically implanted tumors. *Proc Natl Acad Sci USA 98*, 2616-2621 (2001).
37. Bauer, S., Kirschning, C. J., Hacker, H., Redecke, V., Hausmann, S., Akira, S., Wagner, H., Lipford, G. B. Human TLR9 confers responsiveness to bacterial DNA via species-specific CpG motif recognition. *Proc Natl Acad Sci USA 98*, 9237-9242 (2001).
38. Chevalier-Mariette, C., Henry, I., Montfort, L., Capgras, S., Forlani, S., Muschler, J., Nicolas, J. F. CpG content gene silencing in mice : evidence from novel transgenes. *Genome Biology 4*, R53 (2003).
39. Faurie, C., Golzio, M., Moller, P., Teissié, J., Rols, M. P. Cell and animal imaging of electrically mediated gene transfer. *DNA Cell Biol 22*, 777-783 (2003).
40. Bogdanov, A., Weissleder, R. *In vivo* imaging of gene delivery and expression. *Trends Biotechnology 20*, S11-S18 (2003).
41. Golzio, M., Mazzolini, L., Moller, P., Rols, M. P., Teissié, J. Inhibition of gene expression in mice muscle by *in vivo* electrically mediated siRNA delivery. *Gene Therapy 12*, 246-251 (2005).
42. Fire, A., Xu, S., Montgomery, M. K., Kostas, S. A., Driver, S. E., Mello, C. C. Potent and specific genetic interference by double-stranded RNA in Caenorhabditis elegans. *Nature 391*, 806-811 (1998).
43. Kim, K. N. RNA interference in functional genomics and medicine. *J Korean Med Sci 18*, 309-318 (2003).
44. Kishida, T., Asada, H., Gojo, S., Ohashi, S., Shin-Ya, M., Yasutomi, K., Terauchi, R., Takahashi, K. A., Kubo, T., Imanishi, J., Mazda, O. Sequence-specific gene silencing in murine muscle induced by electroporation-mediated transfer of short interfering RNA. *J Gene Med 6*, 105-110 (2004).
44. Eefting, D., Grimbergen, J. M., de Vries, M. R., van Weel, V., Kaijzel, E. L., Que, I., Moon, R. T., Löwik, C. W., van Bockel, J. H., Quax, P. H. Prolonged *in vivo* gene silencing by electroporation-mediated plasmid delivery of small interfering RNA. *Human Gene Therapy 18*, 861-869 (2007).
45. Durieux, A. C., Bonnefoy, R., Freyssenet, D. Kinetic of transgene expression after electrotransfer into skeletal muscle: importance of promoter origin/strength. *Biochim Biophys Acta 1725*, 403-409 (2005).
46. Fabre, E. E., Bigey, P., Orsini, C., Scherman, D. Comparison of promoter region constructs for in vivo intramuscular expression. *J Gene Med 8*, 636-645 (2006).
47. Yew, N. S. Controlling the kinetics of transgene expression by plasmid design. *Adv Drug Deliv Rev 57*, 769-780 (2005).
48. Magee, T. R., Artaza, J. N., Ferrini, M. G., Vernet, D., Zuniga, F. I., Cantini, L., Reisz-Porszasz, S., Rajfer, J., Gonzalez-Cadavid, N. F. Myostatin short interfering hairpin RNA gene transfer increases skeletal muscle mass. *J Gene Med 8*, 1171-1181 (2006).
49. Donà, M., Sandri, M., Rossini, K., Dell'Aica, I., Podhorska-Okolow, M., Carraro, U. Functional *in vivo* gene transfer into the myofibers of adult skeletal muscle. *Biochem Biophys Res Commun 312*, 1132-1138 (2003).
50. Durieux, A. C., Bonnefoy, R., Busso, T., Freyssenet, D. *In vivo* gene electrotransfer into skeletal muscle: effects of plasmid DNA on the occurrence and extent of muscle damage. *J Gene Med 6*, 809-816 (2004).
51. Leroy-Willig, A., Bureau, M. F., Scherman, D., Carlier, P. G. *In vivo* NMR imaging evaluation of efficiency and toxicity of gene electrotransfer in rat muscle. *Gene Ther 12*, 1434-1443 (2005).
52. Patel, K., Amthor, H. The function of myostatin and strategies of myostatin blockade-new hope for therapies aimed at promoting growth of skeletal muscle. *Neuromuscular Disorders 15*, 117-126 (2005).

Received: Needed; Revised: Needed;
Accepted: Needed

In vivo imaging of siRNA electrotransfer and silencing in different organs

A. Paganin-Gioanni[1], J.M. Escoffre[1], L. Mazzolini[2], M.P. Rols[1], J. Teissié[1]and M. Golzio[1]

[1] IPBS-CNRS, UMR5089 , Toulouse, France
[2] ISTMT, CNRS, Toulouse, France

Abstract—**RNA interference (RNAi)-mediated gene silencing approaches appear very promising for therapies based on the targeted inhibition of disease-relevant genes. The major hurdle to the therapeutic development of RNAi strategies remains however the efficient delivery of the RNAi-inducing molecules, the short interfering RNAs (siRNAs) and short hairpin RNAs (shRNAs), to the target tissue. In this study we have investigated the contribution of electrically-mediated delivery of siRNA and/or shRNA into muscles or tumors stably expressing a green fluorescent protein (EGFP) target reporter gene. The silencing of EGFP gene expression was quantified over time by fluorescence imaging in the living animal. Our study indicate that electric field can be used as an efficient method for RNAi delivery and associated gene silencing into cells of muscle and solid tumors in vivo.**

Keywords— **Electroporation, RNA interference, imaging, siRNA, ShRNA.**

I. Introduction

Since its discovery[1], RNA interference has been described and extensively characterized in a number of organisms [2-4]. The identification of the short interfering RNAs (siRNAs) involved in this process and their use for sequence specific gene silencing has offered a new approach for molecular therapeutics by taking advantages of the progress in genomics[5, 6].

This development requires, however, new safe and efficient *in vivo* siRNA delivery methods [7]. SiRNAs appear as a very promising new therapeutical agent but besides the problem of delivery, an unanswered problem is to know how long its effect lasts after a single dose delivery [8]. Most recently published *in vivo* results were obtained by « hydrodynamic transfection ». This stringent approach (injection within a few seconds in the tail vein of a volume one tenth the mass of the animal) appears to bring siRNA (and DNA) delivery mainly targeted to the liver [9-13]. Other methods were described where a systemic or a localized (portal vein injection) delivery was obtained by adding different chemical compounds to the siRNA solution [14-17]. SiRNA gene silencing could be obtained *in vivo* on reporter as well as endogenous genes. Delivery remains a critical issue for the development of siRNA as an effective therapeutic [7]. More recently, fluorescently labelled siRNA were injected IV or IP in mice being complexed with cationic lipid liposomes [16]. Rather high amounts (100 µg) were injected in this experiment. Clearly the need for a delivery method suitable for targeting a broad range of tissues remains required. The demonstration in 1998 of drug and plasmid electrotransfer and gene expression in tumours [18, 19] led to the proposal that *in vivo* electropulsation was a promising tool for exogenous agents delivery [20]. Furthermore it was observed that a very efficient *in vivo* electroloading of large molecules other than plasmids was obtained for proteins [19], dextran [21], and antisense oligonucleotides [22]. Electrically mediated gene transfer had been shown to be effective on many tissues: liver [23], skin [24], muscle [21, 25] and heart [26]. Delivery is targeted to the volume where the field pulse is applied, *i.e.* under the control of the electrode localization. This technology allows delivery to almost all tissues, after a small surgery when needed. Impressive results were described in the case of muscles where treatment with non-invasive contact electrodes brought a long lasting expression of therapeutical genes [27].

Recent developments in optical imaging provide continuous monitoring of gene delivery and expression in living animals [28]. Indeed, reporter gene activity can be accurately followed of the same animal as a function of time with no adverse effects either on the reporter gene product or on the animal itself. This increases the statistical relevance of a study, while decreasing the number of animals required. Exogenous gene expression of fluorescent reporter proteins such as GFP can be detected by the associated emission using a highly sensitive CCD camera**.**

II. Materials and methods

A. siRNAs

All siRNAs were purchased from Qiagen Xeragon (Germantown, MD, USA). The egfp22 siRNA (sense: 5' r(GCA AGC UGA CCC UGA AGU UCA U), antisense: 5' r(GAA CUU CAG GGU CAG CUU GCC G)) is directed against GFPmRNA. The P76 siRNA (sense: 5'r (GCG GAG UGG CCU GCA GGU A)dTT, antisense: 5' r(UAC CUG CAG GCC ACU CCG C)dTT) is directed against an unrelated human mRNA and shows no significant homology to mouse transcripts. It was used as a control for specificity of

T. Jarm, P. Kramar, A. Županič (Eds.): Medicon 2007, IFMBE Proceedings 16, pp. 624–627, 2007

the siRNA construct. ShRNA were provided by Cayla InvivoGen.

B. In vivo Electropulsation

Saline solution (*i.e.* PBS containing 40 units of the RNAse inhibitor RNAsin^R (Promega, Madison, WI) and either egfp22 or p76-siRNA were slowly injected (about 15s) with a Hamilton syringe through a 26G needle (Hamilton, Bonaduz, Switzerland) into the muscle or the tumor, under anesthesia (with or without plasmid pEGFPC1). In control conditions, the volume of siRNA was replaced by the siRNA suspension buffer to keep the injection conditions similar. 30s after injection, an electric pulsation was applied. Plate parallel electrodes (length 1 cm, width 0.6 mm, interelectrode distance 6 mm) (IGEA, Carpi, Italy) were fitted around the muscle or the tumor. The skin was previously shaved with a cream (Veet). A good electric contact was obtained between the skin and the electrodes using a conducting paste (Eko-gel, Egna, Italy). The tissue was electropulsed with selected parameters using the PS 10 CNRS Electropulsator (Jouan, St Herblain, France). Square waved pulses were delivered. Voltage, pulse duration and frequency of pulses were all pre-set on the Electropulsator depending on the tissue (see legend of the figures). All parameters were monitored on line with an oscilloscope (Metrix, Annecy, France).

C. Non invasive stereomicroscopy fluorescence imaging in live animals:

GFP expression in the tissue cells was detected directly through the skin on the anaesthetized animal by digitized fluorescence stereomicroscopy. This procedure allowed the observation of GFP expression on the same animal during several days. High magnification images were obtained with an epifluorescence stereomicroscope using the 0.8 magnification (Leica MZFL III, Germany) and a cooled CCD camera (Roper Coolsnap fx). A 15-mm^2 part of the animal was observed, which was suitable to observe the treated tissue. Camera was driven by the MetaVue software 2.6 (Universal, USA) from a Dell computer. The exposure time was set at 1 s. with no binning. The fluorescence excitation was obtained with a Mercury Arc lamp (HBO, Osram, Germany) and a GFP filter (Leica) for emission. The GFP fluorescence was quantitatively evaluated at different days. A transmission picture and a picture with GFP filter were taken on each tissue.

From the transmission picture, the tissue was located and manually gated to give the region of interest (ROI). On the picture taken with the GFP filter, the mean fluorescence in the gated area was quantitatively estimated. Another ROI was defined next to the non treated part of the tissue to determine the mean fluorescence background on the skin and normal tissue. Numerical values obtained by Metavue analysis software were transferred to Microsoft Excel and used for data analysis. To quantify the knockdown induced by the delivery of the siRNAs, the fluorescence intensity of the tissue on day 0 (*i.e.* before the treatment) was set as the 100% value for each animal and the " relative fluorescence on day X" values were in reference to this initial value. This allowed to get rid of the observed variations in the initial GFP fluorescence of tissue between the different animals.

III. Results

A. Electrotransfer of siRNA in muscles

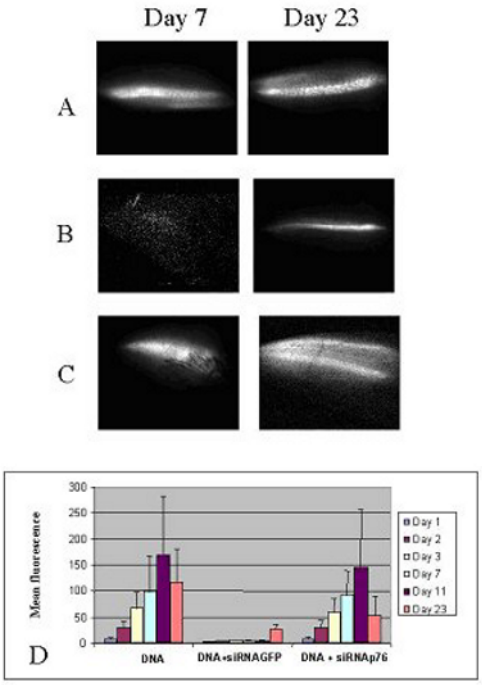

Fig. 2: RNA interference in 9 weeks old C57Bl/6 mouse leg muscle. Representative images of the GFP fluorescence from the mouse leg (Each image is 1 cm wide).
A- GFP expression resulting from plasmid alone electrotransfer as observed on days 7 and 23 in the same leg.
B- GFP expression silencing as observed on days 7 and 23 in the same leg when the plasmid was cotransfered with the specific egfp22 siRNA.
C- GFP expression remained unaffected when an unrelated siRNA (p76) was cotransfered with the plasmid.
D- Changes in the mean fluorescence emission with time.
Sample standard deviations are shown. (n=4)

Plasmid electrotransfer and expression in muscles are known to be very efficient. Up to 70-80 % of the fibers can be transfected after injection of 25 µg of a GFP coding plasmid and by using adequate electrical conditions. Emission of the green protein was high 7 days after the electrical treatment. When the specific siRNA was electro-transferred (DNA +AntiGFP), significant decrease of the GFP expression was observed. Our fluorescence analyses also led us to conclude that inhibition of gene expression lasts more than 11 days. SiRNA delivery therefore occurs in almost all fibers.

B. Electrotransfer of shRNA in muscles

Inhibition of GFP expression was observed by the decreased of fluorescence emission in the muscle after co-transfection of a plasmid encoding GFP and the plasmid encoding shRNA. The use of shRNA leads to a stronger inhibition of the GFP expression (more than 50 days) than synthetic siRNA.

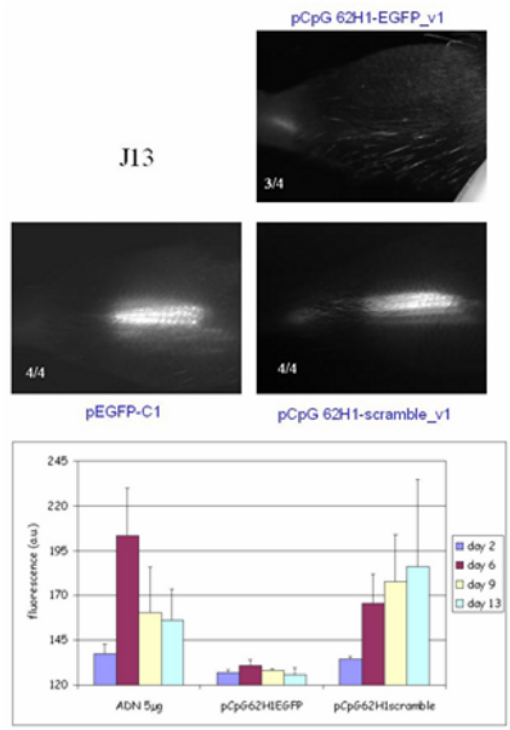

Fig. 3: RNA interference in 9 weeks old C57Bl/6 mouse leg muscle. Representative images of the GFP fluorescence from the mouse leg (Each image is 1 cm wide).
A- GFP expression resulting from plasmid alone electrotransfer as observed on days 13. GFP expression silencing was observed when the plasmid pEGFPC1 was co-transferred with the specific pCpG 62H1 EGFP_v1 shRNA (ratio 1/10, respectively). GFP expression remained unaffected when an unrelated pCpG 62H1 EGFP_v1 was cotransfered with the plasmid.
B- Changes in the mean fluorescence emission with time. Sample standard deviations are shown. (n=4)

C. SiRNA transfer in tumors

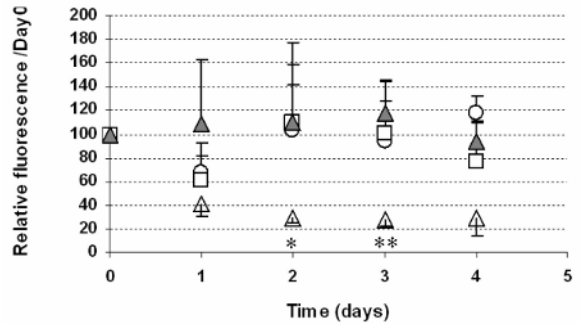

Fig. 4: Time dependence of mean fluorescence intensity of the B16F10 GFP tumors
Time dependence of mean fluorescence intensity of B16F10 GFP tumors in control untreated tumors and in tumors treated with; electric field : PBS + EP (❍), unrelated siRNA : p76 + EP (□), 12 µg of egfp22 siRNA alone : AntiGFP - EP (▲) and egfp22 siRNA electro-transferred : AntiGFP + EP (△) . On each animal, the mean fluorescence of the tumor was evaluated on a relative scale using the observation just before the treatment as a reference. (N= number of mice per group; for days 1 and 2: 7<N<9, days 3 and 4: 4<N<5). Differences in fluorescence levels between AntiGFP – EP and AntiGFP + EP conditions were statistically compared by used an unpaired t-test two-sided using the KyPlot software. * P<0.05 and ** P<0.01 were plotted when observed.

In vivo imaging was used to follow fluorescent tumors and fluorescence intensity as a function of time. GFP fluorescence emission was quantified by digital imaging. Tumor growth was not affected by the treatment (neither siRNA intra-tumoral injection nor electric pulses i.e. EP). When the specific siRNA was electro-transferred (AntiGFP + EP), significant decrease of the GFP expression was observed within 2 days following the treatment. As shown in the pictures of the figures 1 and 2, the fluorescence associated to the tumor disappeared in the treated group (AntiGFP + EP) whereas the fluorescence remained the same in the different control groups.

IV. Conclusions

In this study, we defined an experimental system allowing visualizing and quantifying the down regulation of a expressed EGFP reporter gene in muscles and subcutaneous B16-F10 mouse melanoma tumors using non invasive *in vivo* fluorescence imaging. This allowed us to follow *in situ* the kinetics of siRNA-mediated inhibition of gene expression, the topology of the effect and to test the impact

of electrical treatment on the establishment of gene knock-down.

Acknowledgment

This work was supported by grants from the CNRS ("Imagerie du petit animal" program), the EU cliniporator project, the Region Midi-Pyrenées, the AFM and the ARC (Association pour la Recherche sur le Cancer).

References

1. Fire A *et al.* Potent and specific genetic interference by double-stranded RNA in Caenorhabditis elegans. *Nature* 1998; **391:** 806-811.
2. Denli AM, Hannon GJ. RNAi: an ever-growing puzzle. *Trends Biochem Sci* 2003; **28:** 196-201.
3. Hutvagner G, Zamore PD. RNAi: nature abhors a double-strand. *Curr Opin Genet Dev* 2002; **12:** 225-232.
4. Hannon GJ. RNA interference. *Nature* 2002; **418:** 244-251.
5. McManus MT, Sharp PA. Gene silencing in mammals by small interfering RNAs. *Nat Rev Genet* 2002; **3:** 737-747.
6. Sioud M. Therapeutic siRNAs. *Trends Pharmacol Sci* 2004; **25:** 22-28.
7. Zamore PD, Aronin N. siRNAs knock down hepatitis. *Nat Med* 2003; **9:** 266-267.
8. Herweijer H, Wolff JA. Progress and prospects: naked DNA gene transfer and therapy. *Gene Ther* 2003; **10:** 453-458.
9. Song E *et al.* RNA interference targeting Fas protects mice from fulminant hepatitis. *Nat Med* 2003; **9:** 347-351.
10. McCaffrey AP *et al.* RNA interference in adult mice. *Nature* 2002; **418:** 38-39.
11. McCaffrey AP *et al.* Inhibition of hepatitis B virus in mice by RNA interference. *Nat Biotechnol* 2003; **21:** 639-644.
12. Lewis DL *et al.* Efficient delivery of siRNA for inhibition of gene expression in postnatal mice. *Nat Genet* 2002; **32:** 107-108.
13. Zender L *et al.* Caspase 8 small interfering RNA prevents acute liver failure in mice. *Proc Natl Acad Sci U S A* 2003; **100:** 7797-7802.
14. Verma UN *et al.* Small interfering RNAs directed against beta-catenin inhibit the in vitro and in vivo growth of colon cancer cells. *Clin Cancer Res* 2003; **9:** 1291-1300.
15. Sorensen DR, Leirdal M, Sioud M. Gene silencing by systemic delivery of synthetic siRNAs in adult mice. *J Mol Biol* 2003; **327:** 761-766.
16. Sioud M, Sorensen DR. Cationic liposome-mediated delivery of siRNAs in adult mice. *Biochem Biophys Res Commun* 2003; **312:** 1220-1225.
17. Bertrand JR *et al.* Comparison of antisense oligonucleotides and siRNAs in cell culture and in vivo. *Biochem Biophys Res Commun* 2002; **296:** 1000-1004.
18. Mir LM *et al.* Effective treatment of cutaneous and subcutaneous malignant tumours by electrochemotherapy. *Br J Cancer* 1998; **77:** 2336-2342.
19. Rols MP *et al.* In vivo electrically mediated protein and gene transfer in murine melanoma. *Nat Biotechnol* 1998; **16:** 168-171.
20. Potts RO, Chizmadzhev YA. Opening doors for exogenous agents. *Nat Biotechnol* 1998; **16:** 135.
21. Mathiesen I. Electropermeabilization of skeletal muscle enhances gene transfer in vivo. *Gene Ther* 1999; **6:** 508-514.
22. Faria M *et al.* Phosphoramidate oligonucleotides as potent antisense molecules in cells and in vivo. *Nat Biotechnol* 2001; **19:** 40-44.
23. Heller R *et al.* In vivo gene electroinjection and expression in rat liver. *FEBS Lett* 1996; **389:** 225-228.
24. Glasspool-Malone J, Somiari S, Drabick JJ, Malone RW. Efficient nonviral cutaneous transfection. *Mol Ther* 2000; **2:** 140-146.
25. Aihara H, Miyazaki J. Gene transfer into muscle by electroporation in vivo. *Nat Biotechnol* 1998; **16:** 867-870.
26. Harrison RL, Byrne BJ, Tung L. Electroporation-mediated gene transfer in cardiac tissue. *FEBS Lett* 1998; **435:** 1-5.
27. Rizzuto G *et al.* Efficient and regulated erythropoietin production by naked DNA injection and muscle electroporation. *Proc Natl Acad Sci U S A* 1999; **96:** 6417-6422.
28. Yang M *et al.* Whole-body and intravital optical imaging of angiogenesis in orthotopically implanted tumors. *Proc Natl Acad Sci U S A* 2001; **98:** 2616-2621.
29. Takahashi, Y., et al., Gene silencing in primary and metastatic tumors by small interfering RNA delivery in mice: quantitative analysis using melanoma cells expressing firefly and sea pansy luciferases. J Control Release, 2005. **105**(3): p. 332-43.
30. Akaneya, Y., B. Jiang, and T. Tsumoto, RNAi-induced gene silencing by local electroporation in targeting brain region. J Neurophysiol, 2005. **93**(1): p. 594-602.
31. Golzio, M., et al., Inhibition of gene expression in mice muscle by in vivo electrically mediated siRNA delivery. Gene Ther, 2005. **12**(3): p. 246-51.
32. Shoji, M., et al., RNA interference during spermatogenesis in mice. Dev Biol, 2005. **282**(2): p. 524-34.
33. Tao, J., et al., Inhibiting the growth of malignant melanoma by blocking the expression of vascular endothelial growth factor using an RNA interference approach. Br J Dermatol, 2005. **153**(4): p. 715-24.

Author: Golzio Muriel
Institute: IPBS - CNRS
Street: 205 route de narbonne
City: Toulouse
Country: France
Email: Muriel.golzio@ipbs.fr